Rare Earth Elements

Hosted by

PROCEEDINGS OF THE 52nd CONFERENCE OF METALLURGISTS (COM),
Hosting by MATERIALS SCIENCE TECHNOLOGY CONFERENCE (MS&T)
OCTOBER 27 to 31, 2013, MONTRÉAL, QUÉBEC, CANADA

Rare Earth Elements

Editors

Ian M. London
Avalon
Toronto, Canada

John R. Goode
Toronto, Canada

Georgiana Moldoveanu
Toronto, Canada

Mandeep S. Rayat
Toronto, Canada

Symposium Organized by the Hydrometallurgy Section of the Metallurgy and Materials Society of the Canadian Institute of Mining, Metallurgy and Petroleum

A Publication of The
Canadian Institute of Mining, Metallurgy and Petroleum
1250 - 3500 de Maisonneuve Blvd. West
Westmount, Québec, Canada H3Z 3C1
http://www.metsoc.org

ISBN: 978-1-926872-20-9
Printed in Canada

If you are interested in purchasing a copy of this book
call: (514) 939-2710, ext. 1327

Foreword

Significant and accelerating advancements continue in rare earth resource development, processing and applications technology, all of which go towards enhancing the quality of life. The application technologies, be they in the areas of renewable energy production, energy storage, demand-side energy efficiency, hybrid vehicles, tablet computers, smartphones, digital displays or lasers, all rely on materials made possible by the elements of the lanthanide group (commonly referred to as “rare earths”). Consumer and policy-driven demand for these advanced technology products has strained the supply of available rare earths. The rare earth supply chain, from mine to final product, however is complex and relatively long, and faces a number of unique challenges particularly outside of China, as it is only now emerging or re-emerging. It is therefore critically important to conduct research in all steps of the supply chain, from geology, extraction, separation and refining, to final product design, lifecycle management and recycling. It is also important to understand the economic and environmental issues related to meeting the demand for rare earth-based materials. Success will be significantly facilitated through national and multinational collaboration. This second Rare Earth Elements (REE) Symposium at the Conference of Metallurgists, building on the success of the inaugural REE Symposium held in September 2012, provides a collaborative forum to share ideas and technical advances, as well as to discuss these critical and timely issues.

The response to this new symposium has exceeded our expectations. The proceedings volume contains fifty-one peer-reviewed papers from academia, government and industry from 16 countries. Complementing papers from Canada and the United States are significant contributions from China, Germany, Japan, Korea, Belgium, the UK and elsewhere. The Symposium provides an opportunity for authors and delegates from around the world and across all aspects of the rare earth supply chain to meet their colleagues and discuss common interests and concerns.

With the interest generated by the importance of the subject area, two international Rare Earth organizations will be holding meetings concurrently with the REE Symposium in Montreal. The eight-country member International Rare Metals Working Group, chaired by the Korea Institute of Industrial Technology, will be convening its annual meeting, and the Rare Earth Technology Alliance, the US-based international member industry association under the auspices of the American Chemical Council will be holding its quarterly meeting. Technical papers from members of these respected organizations have been integrated into the Symposium program.

The papers in these proceedings have been laid out in six thematic categories: Rare Earth Element Industry Overview, Mineralogy and Beneficiation of Rare Earth Resources, Hydrometallurgy of Rare Earth Mineral Concentrates, Rare Earth Element Separation, Rare Earth Elements in Advanced Materials, and Recycling of Rare Earth Elements, reflecting the structure of this year’s full three-and-a-half day Symposium.

This symposium, and the proceedings volume, were made possible through the determined effort to formulate an informative program by the Organizing Committee and the preparation of quality manuscripts by the authors. Once manuscripts were received, the tasks of refereeing, editing and indexing the various submissions were assumed by the editors, who are indebted to the authors for their efforts in preparing the papers and their understanding of the need for a consistently formatted volume. The Symposium program and the production of this volume was a significant undertaking over a period of twelve months, under the guidance of an eight-person Organizing Committee comprising of Ian London (Co-Chair), Mandeep Singh Rayat (Co-Chair), John Goode, In-Ho Jung, Georgiana Moldoveanu, Dimitri Psaras, Niels Verbaan, and Jack Zhang. Engaging with individual authors, committee members contributed a generous amount of time in structuring the Symposium and reviewing each paper. This team was also fortunate in engaging and being supported by a cadre of other internationally-based reviewers. The editors applaud and thank all of our colleagues.

The Organizing Committee of this second Rare Earths Symposium at COM 2013 sincerely thank all the authors, speakers and participants and looks forward to continued collaboration in advancing the needed supply chains and our collective desire to improve the quality of life.

Ian M. London
John R. Goode
Georgiana Moldoveanu
Mandeep S. Rayat
Editors

Editors' Biographies

Ian M. London has been actively engaged in the rare earth/rare metals sector for seven years. In addition to addressing market and project development initiatives, Ian established Avalon's University Outreach Initiative and Corporate Social Responsibility Roadmap in 2011. Ian was also one of the original editors for *RareMetalBlog* and *RareMetalApps.* Ian chaired the Organizing Committee for the inaugural REE Symposium at COM12. Ian brings an extensive career in corporate management, international marketing and project management. His 40 years of industry experience includes terms as President & CEO of Ontario Hydro International Inc. and CEO of Process Products Limited. Ian has served on several new technology and alternative energy company boards. Ian has been sought after speaker on the emerging rare earth sector and corporate social sustainability. Ian earned his Metallurgical Engineering degree from McGill University and an MBA from the Schulich School of Business.

John R. Goode is an independent metallurgical consultant who has worked on many rare earths projects. John graduated from the Royal School of Mines, London, UK in 1963. He then emigrated to Canada and joined Falconbridge Nickel Mines. After spending two years in Canada he returned to the UK and worked for two years at the Avonmouth lead-zinc smelter owned by Rio Tinto Zinc. He then transferred to Elliot Lake, Canada where he spent six years in thorium, rare earth and uranium development and operations. In 1976 John joined Kilborn Engineering where he completed numerous gold, uranium and base metal projects. He also worked on several rare earth projects including Denison's 1986 yttrium plant, a new separation plant at Molycorp's Mountain Pass operation, evaluation of the Strange Lake project, and Due Diligence studies on several Chinese plants. In 1994 John joined Barrick and spent four years in China. He returned to Canada in 1998 and established a metallurgical consultancy.

Georgiana Moldoveanu has been Postdoctoral Fellow in the Department of Chemical Engineering and Applied Chemistry at the University of Toronto since 2009. As a senior member of the Aqueous Process Engineering and Chemistry Group she manages research projects focused in three areas: rare earths hydrometallurgy, gypsum scale control in industrial streams and water purification via forward osmosis. Georgiana graduated in 1993 from the University of Bucharest (Romania) with a B.Sc. in Chemistry and worked for three years as a formulation chemist at the Centre for Macromolecular Materials and Membranes. She then pursued post-graduate studies at McGill University, where she earned her M.Eng (1999) and Ph.D (2005) in Metallurgical and Material Engineering.

Mandeep Singh Rayat graduated from the Schulich School of Business at York University in 2011 with an MBA degree. While pursuing his MBA, Mandeep served as President of the Natural Resources Opportunities Club, a student club which exposes business students to the opportunities in the natural resource industries. He started working for Avalon Rare Metals shortly after completing his MBA, playing a key role in the development of Avalon's first Annual Corporate Sustainability Report and assisting in Avalon's University outreach programs. Mandeep also has bachelors' degrees in Chemical Engineering and Economics from the University of Western Ontario (1999) and a master's degree in Chemical Engineering from the University of Toronto (2002).

Symposium Organizing Committee

Ian M. London, Avalon Rare Metals, Toronto, Canada (Co-Chair)
Mandeep Singh Rayat, Toronto, Canada (Co-Chair)
John Goode, J.R. Goode and Associates, Toronto, Canada
In-Ho Jung, McGill University, Montreal, Canada
Georgiana Moldoveanu, University of Toronto, Canada
Dimitri Psaras, Molycorp, USA
Niels Verbaan, SGS Mineral Services, Lakefield, Canada
Jack Zhang, Saskatchewan Research Council, Canada

The Organizing Committee would also like to thank the following individuals for lending their assistance in reviewing the papers contained in this publication:

Rene du Preez, Mintek, South Africa
Joe Ferron, HydroProc Consultants, Canada
Gareth Hatch, Technology Metals Research, USA
Sunil Jayasekera, SJ Mets Consulting Pty Ltd, Australia
Marthie Kotze, Mintek, South Africa
Ron Molnar, MetNetH20, Peterborough, Canada
Edgar Peek, Molycorp, Canada
Olga Yahorava, Mintek, South Africa

Table of Contents

Rare Earth Elements

RARE EARTH ELEMENT INDUSTRY OVERVIEW

MINERALOGY AND BENEFICIATION OF RARE EARTH RESOURCES

HYDROMETALLURGY OF RARE EARTH MINERAL CONCENTRATES

RARE EARTH ELEMENT SEPARATION

RARE EARTH ELEMENTS IN ADVANCED MATERIALS

RECYCLING OF RARE EARTH ELEMENTS

Rare Earth Element Industry Overview

THE CRITICAL MATERIALS INSTITUTE

Alexander H. King[1] and Roderick G. Eggert[2]

Critical Materials Institute
[1]The Ames Laboratory, Ames, IA 50011-3020, U.S.A.
[2]Division of Economics & Business, Colorado School of Mines, Golden, CO 80401 U.S.A.

Keywords: Rare Earths, Yttrium, Neodymium, Europium, Terbium, Dysprosium, Lithium, Tellurium

Abstract

In January of 2013, the U.S. Department of Energy announced the establishment of a new Energy Innovation Hub, to be known as the Critical Materials Institute, or CMI. Led by the Ames Laboratory, CMI has three other DOE national laboratories, eight universities, and eight corporations as partner institutions. Its mission is to eliminate materials criticality as an impediment to the commercialization of clean energy technologies for today and tomorrow.

Introduction

Rare earths are sold as oxides, elemental metals, and in other forms, and although they are not traded through an open commodities market, public attention was drawn to rapid price increases for many of the rare earth elements, beginning in 2010. As prices rose to astronomical levels – eventually reaching more than 10 times their pre-2010 levels for some elements – concerns emerged concerning the needs for these elements, and the security and stability of their supply. Metals that had previously been the province of a few technical specialists began to be discussed in the popular media, and political attention soon followed.

Concerns about the rare earths were further heightened in September of 2010, when a dispute over fishing rights and the control territorial waters resulted in the arrest of a Chinese fishing boat captain by the Japanese coastguard. China retaliated by cutting off exports of rare earths to Japan, resulting in the emergence of the term “rare earth diplomacy.” It was widely reported that the late Chinese leader, Deng Xiaoping, had commented that while the Middle East has oil, China dominates the rare earths [1].

Starting late in 2010, hearings were held on the rare earths by various committees in the U.S. Congress, and the term “critical material” came into widespread use. A number of reports emerged on the topic and it was recognized that the rare earths were indeed archetypal “critical materials” but were possibly not the only ones that needed to be considered [2-10]. In the spring of 2011 President Obama’s budget request to Congress included funds for an Energy Innovation Hub for Critical Materials, and following an open competition, the funds for the hub were awarded to a team led by the Ames Laboratory, in January 2013.

Critical Materials

A critical material is a substance used in modern technology, which is subject to supply risk and for which there are no easy substitutes. The materials that fall within this definition are not fixed. Lists of critical materials vary with location, because industrial needs and materials sources tend to be localized: distinct differences can therefore be seen between the lists of critical materials produced by studies conducted for different governments, as seen in references 2-10. Critical materials lists also vary with time, as supply and demand vary: sources of materials can cease to be available for a number of reasons, and new sources can emerge, while demand can be altered quite radically by the demise of old technologies or the emergence of new ones. Even within a particular region at a particular time, any list of critical materials will depend on who compiles it: an automotive manufacturer will have a different list than an electronics manufacturer, although there will be overlaps.

There have been critical materials for nearly as long as there have been man-made materials, and some historians now believe that criticality of copper may have contributed to the end of the bronze age and the ensuing collapse of the ancient Greek civilization. Other critical materials have emerged from time to time, and the 20th Century case of cobalt provides an instructive example. In the early 1970's the central African nation of Zaire was the dominant source. Cobalt was used in superalloys and had emerging uses in magnets following the development of Sm-Co as a permanent magnet material. In 1978, a revolt overtook the mining province of Katanga, cutting off supplies of cobalt and several other materials. The price history of cobalt before, during and after the revolution can be seen in Figure 1: decades of price instability are common in the aftermath of materials criticality events.

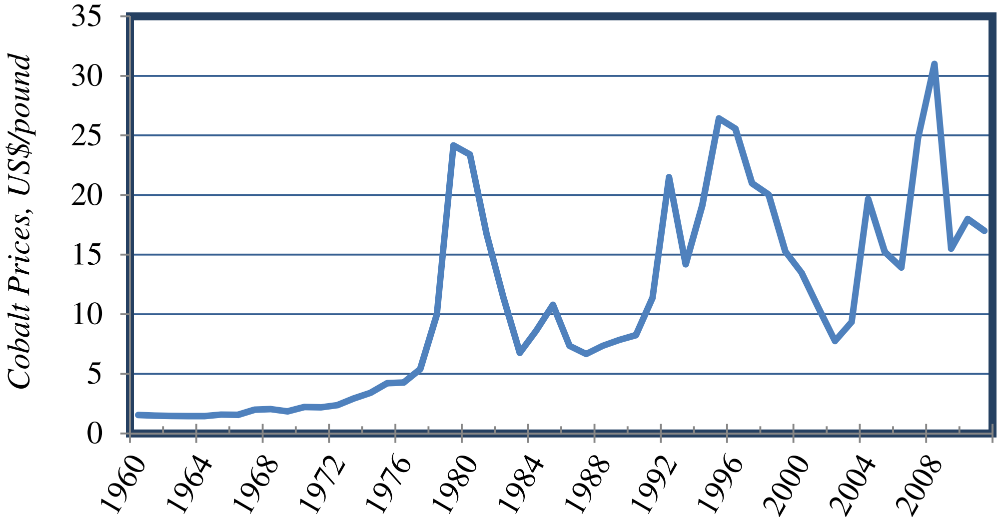

Figure 1. Annual average prices of cobalt from 1960 to 2011. Note the price spike associated with the Katangan revolt of 1978, and severe price instability that continues today.

Critical Materials for Clean Energy Technologies

The Critical Materials Institute was established to assure secure supplies of materials needed for clean energy technologies in the USA, over the next ten to fifteen years. Its initial program addresses seven elements identified as either “critical” or “near critical” over this timeframe, in the Critical Materials Strategy developed by the US Department of Energy [8]. These include five of the rare earths: yttrium, neodymium, europium, terbium and dysprosium, in addition to lithium and tellurium.

These elements are widely applied in modern technologies, as illustrated by the partial list of their uses in Table I. They have uses beyond clean energy and may therefore be of concern to constituencies other than DOE. The rare earths, in particular, are subject to supply risk primarily because one country – China – dominates the world’s supply. Until very recently, China provided as much as 97% of the world’s industrial rare earth supplies. There are no easy substitutes for the rare earths in most of their applications because they impart highly specialized properties to magnets, phosphors and other specialized applications, largely enabled by the effects of the 4f electrons that define the lanthanide series.

Table I. Principal Uses in Clean Energy Technologies of the Materials Addressed by CMI.

	Photovoltaic Films	**Wind Turbines**	**Vehicles**		**Lighting**
MATERIAL	*Coatings*	*Magnets*	*Magnets*	*Batteries*	*Phosphors*
Lithium				◆	
Tellurium	◆				
Yttrium					◆
Neodymium		◆	◆	◆	
Europium					◆
Terbium					◆
Dysprosium		◆	◆		

The CMI Approach

CMI is one of DOE’s five Energy Innovation Hubs. These are integrated research centers that combine basic and applied research with engineering to accelerate scientific discovery in critical energy issue areas. Leadership is vested in scientists who are given the authority to assign funds where they are most effectively used and the funding level was initially set at $20M - $25M per year, for 5 years, renewable for an additional five.

CMI deploys a strategy with three fundamental pillars, or focus areas, tied together by a fourth crosscutting area that provides underlying research germane to two or more of the pillar focus areas. The three pillars of the CMI strategy are:

- Diversifying supply;
- Developing substitute materials;

- Driving reuse, recycling, and more efficient use of materials in manufacturing.

The Institute brings together world-class expertise across all of these areas in addition to basic physics and chemistry, along with advanced lifecycle and economic analysis. With such broad needs, our research team is dispersed over 18 partnering institutions as illustrated in Figure 2, and maintaining the integrated team approach is one of CMI's major challenges.

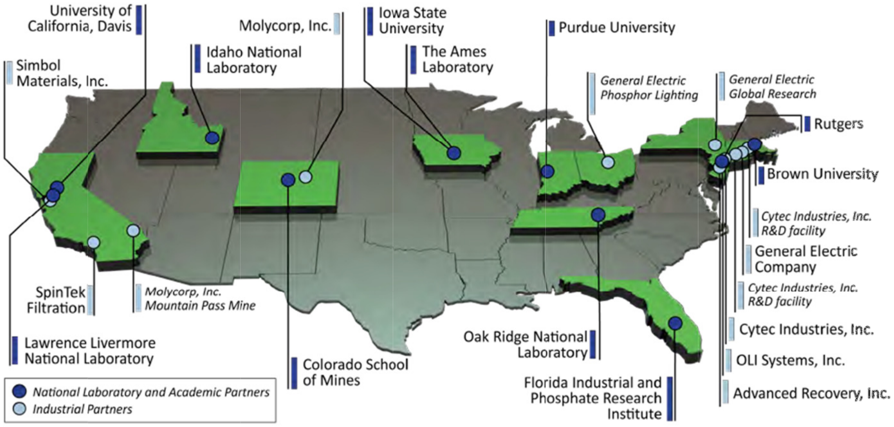

Figure 2. The geographic distribution of CMI participating institutions.

A second challenge revolves around matching the CMI research program to the timescale of materials criticality events. As seen in Figure 1, and also reflected in the 2010 rare earth price spike, the initial emergence of criticality is reflected by a price excursion that typically lasts three or four years, although prices tend to remain unstable for decades to follow. In crafting responses to criticality events, we note that:

- Diversifying sources is often taken to mean mine development, which takes at least 10 years, *when a known resource already exists*;

- Deploying a substitute material in an existing product takes an average of 4 years, *when there is an existing option* – which is not the case for any of the materials addressed by CMI;

- Development and deployment of *new* substitute materials takes an average of 18 years.

The timescales for conventional responses to materials criticality events are clearly not commensurable with the timescales over which criticality emerges, with the result that technologies that rely upon the affected materials may not survive in the marketplace.

A case in point is the choice of technologies for electricity generation using wind-turbines. The most efficient and reliable wind turbine technology for utility-scale units (750kW and up) utilizes direct-drive generators, which are enabled by high-strength Nd-Fe-B permanent magnets, (which also contain significant amounts of Dy). Alternative technologies use less powerful magnets and increased generator rotation rates enabled by gearboxes, or use induction-type generators, which have no permanent magnets, but are much larger. Various hybrid technologies also exist. The high failure-rate of wind-turbine gearboxes increases their operating costs, but do not completely offset their cost advantage over comparable direct-drive turbines, whose price is dominated by the cost of the magnet materials. The result is that (according to data provided by the American Wind Energy Association) only 223 of the 33,000 utility-scale wind turbines installed so far in the U.S. are direct-drive units. Anecdotal information suggests that direct-drive units command a much larger market share in China.

CMI houses lifecycle and economic analysis functions that have the specific role of guiding the research emphasis in pursuit of reducing the criticality of any particular material, in the interest of providing manufacturers with viable options in a timely manner. For example, it is recognized that demand for europium and terbium is partly driven by the adoption of high-efficiency fluorescent lighting technologies including compact fluorescent bulbs and T5 long-tube lamps. These technologies are expected to give way to LEDs in ten to fifteen years, so the current bulge in demand will level off or decline at that point. As we seek solutions to the criticality of Eu and Tb, then, short-term solutions are preferred over longer-term ones, and we have a strong focus on recycling, and no direct effort to diversify supply, since the development of new conventional mines is a decade-long effort. In other cases, where we see continued long-term growth in demand, such as lithium and neodymium, our efforts focus more heavily on matters related to the diversification of supply. The Critical Materials Institute focuses on producing workable solutions on a schedule that is relevant to the projected demand for the materials in question.

The Research Program

The Critical Materials Institute has started work on 35 discrete projects, each of which has a specific target for deployment and a timescale determined by considerations like the ones described above. The timescales range from very short (3 years) to quite long (10 years) but in each case, the timescale relates to projections for needs that are addressed by the individual projects.

Work on source diversification focuses on developing technologies that can lower the cost of existing mineral processing and improve the economics of existing sources by finding new uses for by-products. We are also looking at methods for accessing unconventional sources in the form of existing mineral streams such as phosphate processing. Some of these projects have the fastest anticipated impact, among the CMI program.

In the area of materials substitution, CMI is working toward new magnet materials with reduced rare earth content, and also on enabling the spring magnet concept through novel manufacturing methods. We are developing new red and green phosphors, to replace europium and terbium, and we are developing new methodologies for materials design, linking computation and experimentation in a novel framework.

To drive more efficient use, reuse and recycling of materials, CMI is developing methods for recycling rare earths from available streams such as lamp phosphors and magnets, and tellurium from solar cells. It is also developing new separations technologies including supercritical fluids, membrane solvent extraction, electro-recycling, pyroprocessing and bioleaching.

Supporting all of the other scientific work, CMI has a crosscutting research function, to develop basic scientific knowledge and databases germane to all of the other projects, environmental assessments, and supply-chain, lifecycle and economic analysis. As noted above, the economic aspects of this work guide and direct of all of our projects.

Every project that we undertake has a commercialization plan and is monitored by technology transfer experts. If conditions change sufficiently to affect the viability of its commercialization plan, then a project will be redirected or possibly terminated, even if it is producing outstanding science.

In addition to the CMI's research projects and commercialization efforts, the hub provides outreach efforts that include education programs, coordination with other U.S. funded critical materials efforts, and an information service called the Critical Materials Information Center. An industrial affiliates program provides input into the CMI research directions, access to CMI results and licensing opportunities for CMI-developed technologies.

In its initial five-year funding period, CMI aims to deliver four major outcomes:

1. Assured materials supply chains for clean energy manufacturing in the U.S.;
    a. By solving current critical materials issues;
    b. By identifying and averting future criticality issues;
2. Assured supplies of technical talent and expertise;
3. Provision of critical materials information to researchers, producers & OEMs;
4. Coordination of Federal critical materials research efforts for maximum impact.

Acknowledgements

This work is supported by the Advanced Manufacturing Office of the U.S. Department of Energy, through contract number DE-AC02-07CH11358.

References

1. Bradsher, K., "Amid Tension, China Blocks Vital Exports to Japan," *New York Times*, Sept. 22, 2010.

2. *Minerals, Critical Minerals, and the U.S. Economy* U.S. National Research Council, (Washington, DC, National Academies Press, 2008).

3. *Critical Elements for New Energy Technologies*, (Cambridge, MA, MIT Energy Initiative, 2010).

4. *Critical Raw Materials for the EU*, (Brussels, European Commission, 2010).

5. *Critical Materials Strategy*, (Washington DC, U.S. Department of Energy, 2010).

6. *Energy Critical Elements: Securing Materials for Emerging Technologies*, (Washington, DC, American Physical Society & Materials Research Society, 2011).

7. *Risk List 2011*, (London, British Geological Survey, 2011).

8. *Critical Materials Strategy*, (Washington DC, U.S. Department of Energy, 2011).

9. Grasso, V.B., “Rare Earth Elements in National Defense: Background, Oversight Issues, and Options for Congress”, (Congressional Research Service, 2012).

10. Silberglitt, R., J.T. Bartis, B.G. Chow, D.L. and K. Brady “Critical Materials: Present Danger to U.S. Manufacturing” (Rand Corporation, 2013).

11. Waldbaum, J.C., *From Bronze to Iron: The Transition from the Bronze Age to the Iron Age in the Eastern Mediterranean*, (Göteborg, Sweden, Paul Aströms Förlag, 1978).

12. Waldbaum, J.C., “The First Archaeological Appearance of Iron,” *The Coming of the Age of Iron*, ed. T.A. Wertime and J.D. Mulhy, (New Haven, Conn.: Yale University Press, 1980), 69-98.

CURRENT KOREAN R&D AND INVESTMENT STRATEGIES IN RESPONSE TO REE DEMAND & SUPPLY CONCERNS

Taek-Soo Kim[1,*], Hong Jun Chae[1], Bum Sung Kim[1], Ryan T. Ott[2] and In-Ho Jung[3]

[1]Korea Institute for Rare Metals (KIRAM) & Korea Institute of Industrial Technology
(KITECH), Songdo-Dong, Yeonsu-Gu, Incheon 406-840, South Korea
[2]Ames Laboratory, 105 Metals Development, lowa State University, Ames 50011-3020, USA
[3]McGill University, 3610 University Street, Montreal, Quebec H3A 2B2, Canada

Keywords: Rare Earth Elements, Rich Korea1140, KIRAM, KITECH

Abstract

Rare metals have become a critical issue due to their dramatic increase in industrial use as well as their rarity. Depending on the ratio of the demand and supply of each rare metal element in a nation, the number and specific criticality of each rare metal is defined differently. For example, in Korea 35 elements are deemed critical, whereas 33 elements are considered critical in the USA. Since the rare metals become critical in a way of rarity, each nation have and are making efforts to assure themselves of supply-demand solutions.

In 2010, Korea launched a ten-year, industry-wide initiative based on the Rare Metals Strategy announced in 2009. The initiative includes three main courses of actions: securing the elements through exploration and recycling systems, promoting R&D activity on the material value chain by supporting government and enterprises, and establishing the infrastructure to support rare metal industries.

As the results of the plan, the Korean Institute for Rare Metals (KIRAM) was established, and funded USD 15 million R&BD programs were launched for five years from 2010. -. One of the important actions taken by KIRAM was to organize a global network as well as a domestic network on rare metals. The global network was launched in April 2011 in Incheon, Korea with the aim of exchanging the international cooperation on rare metals and the establishment of international committee. Eight countries, including Canada, China, Germany, Indonesia, Japan, USA, UK and Korea are involved. For the domestic network, rare metals industries, urban mining societies and publicly supported authorities are being coordinated to develop industrial technology on rare metal.

This paper will discuss some of the trends and Korea’s strategies related to rare metals R&D in industry and academia.

Introduction

Rare metals are defined as metals which are rare in the earth crust and also are difficult to extract from ores. In addition to their rarity, the mal-distribution of natural resources is a critical point in global materials flow. Even though the difficulties in accessibility to rare metal natural resources may be similar with that of fossil fuels, the aggregate requirements for rare metals have increased as the global economics grows. It has been said that we are now in the rare metal and clean technology age.

Rare metals have been referred to as the “vitamins of industry” and their importance in industry has been recognized for some time. Consumers have become highly dependent on products that cannot be made without using rare metals, and as such, rare metals supply and demand solutions are becoming “the lifeline of industry”.

Examples of rare metals include Indium, Chromium, Tungsten, Cobalt, Manganese, Molybdenum, Vanadium and the Rare Earths, as shown in Table I. These rare metals are essential materials for the high performance and high functionality of industrial products, and are key resources for mainstream industries.

The number of rare metals are deemed to critical vary by country. For example, Korea has identified 35, while Japan and the United States have identified 31 and 33 respectively. The primary reason for the differences is attributed to the industrial demand and the availability of supply. Although the quantity of any one element may be very rare on earth, it cannot be deemed a ‘rare’ metal if the demand is also rare. On the other hand, if the ratio of demand of any one metal to its supply is quite high, whatever the quantity is, it has to be a rare metal. For example, some elements are needed only at relatively low intensity (e.g. platinum in catalysts or tellurium in photovoltaic films), but may be extremely rare in the earth's crust. Other elements, like indium or silver which may be somewhat more common, are needed in much larger quantities. Still others, such as neodymium or lithium, which may be relatively common, are rarely concentrated by mineralogical processes. Moreover, some elements may be particularly rare in one country, but are found in economically viable deposits in another country, and as such may raise geopolitical issues should demand for them escalate. Others rare metals are only produced in very limited quantities as co-products with other extraction operations so that their supply may not necessarily respond to demand.

The importance of securing rare metal supply or better, supply-demand balance is different for and dependent on each country. Depending on the balance between the supply and demand of each country, the number of rare metals is distinguished by economic and political circumferences of that country.

This paper discusses strategies and R&D trends on rare metals using present and future industrial data.

Trends of Rare Metal Industry

Figure 1 shows, as a typical example, the applications of various rare metals in the automotive industry, especially for a hybrid car, which is (or will be) equipped with various electronic components. It is seen that the rare metals such as Ni, Li, Co and rare earth metals (Nd and Dy) are used for batteries and motors. Some other element like In are used in displays.

Figure 2 shows the main stream industries in Korea… present and future. Although it would be common by many countries, Korea is trying to develop three areas -- energy-environment products, transportation and information-based technology (IT). In order to maximize the effect of these efforts, the government and industries concerned about ensuring its capability and capacity for the final production, which includes ensuring raw element supply grows and competitive.

Figure 2 also shows different technology categories, its core rare metals and the important rare metals required. For instance, the technology categories include photovoltaic powder generation, wind-mill powder generation and fuel cell technology with its energy-environmental benefits. Transportation technology, green car and ship/ocean-related industries are actively developing. Light emitting diodes (LEDs), semiconductor and display were declared primary components in the IT category. These industries clearly demonstrate where and why many rare metals are absolutely necessary, and are defined as the critical materials in Korea. These include In, Ga, Te, REEs, for the energy related product; REEs, Li, Ni, Mo, V and W for transportation; and Ga, In, As, Y, Eu, Tb and Ni for IT.

Figure 3 shows the consumption of rare metals in an area as the photovoltaic power generation, its several technology platforms with their respective composition profiles. From the left, the structure of Si based cell, CIGS cell and CdTe cell are seen. Considering the quantity and composition, as well as the production plans for each cell type, the consumption for each rare metal, such as In, Ca and Se, can be anticipated (bottom right). The demand increases continually, suggesting the need to establish and secure the supply system.

Table II is another example of why Korea is making an effort to assure the stronger supply and demand balances of rare metals, since it has significant impact on where our industries are headed in the future. Korea has identified six key strategic divisions, including energy/environment, transportation, new IT, convergence, biotechnology and knowledge service. These divisions are again divided into 22 main target industries. For example, the convergence area contains four main industries such as robotics, advanced materials/nano-based convergence, IT-based convergence and broadcasting/communication. In order to develop these industries, various rare metals are needed to provide for the parts such as semiconductors, antennas, sensors, displays, and batteries. Again, Korea is willing to pioneer and build growing industries and identifying the relativeness between the industry and the rare metals necessary for these strategies.

In order to systemize and assure its rare metal needs, the Government of Korea announced a main strategy related to resource, industry and value chain. This strategy has been framed under the banner ‘RICH Korea 1140’, as shown in Figure 4. Among the 35 designated rare metals, Korea has determined its focus will be on 11 key elements (Figure 5) and their core 40 technologies. In developing the strategy, industries were initially systematically analyzed and compared domestically and globally, along with their planned short, mid and long term goals. A detailed process for assuring the adequate availability of the rare metals, included as securing resource, developing R&D and establishing infrastructure was conducted. This process was driven by of the principles shown in Figure 6.

As shown in Figure 7, the Korean Government also understands that the rare metals industry is built upon the value chain principle. As such, Korea not only considers the importance of production or natural resources, but also all requirements, capabilities and capacities within the value chain. The rare metal-related strategy was and continues to be developed, with full consideration of natural resources, materials processing, final producing, and recycling process at the same time. In addition, supply shortage, climate change economy and environmental impacts are taken into account.

In order to conduct the rare metal program proposed by government and industries, the Korea Institute of Industrial Technology (KITECH) was established by the Ministry of Knowledge Economy, under the aegis of KIRAM. As shown in Table III, KIRAM serves three main functions: infra-structuring, supports enterprises and facilitates global cooperation. For infra-structuring activities, as a first step, KITECH established and updated a full information service system for rare metal. A pilot scale Research & Business Development (R&BD) facilitie designed for rare metals was also constructed to serve as a bridge or technology interface between universities and industry. Education on the rare metals, directed at young people, especially for middle and high school students, as well as industry personnel is also an important core activity.

Believing that rare metal supply and demand is the commonly shared concern worldwide, KIRAM initiated the International Rare Metals R&D Workshop as a focal point for international cooperation, with the participating from eight key countries. The goal of the group is to facilitate collaborative research projects and to seek forms of standardization, both domestically and internationally.

As a detailed step for real action of rare metals industry development, the Korean government has also launched several key R&D program in conjunction with industry, institutes and universities, as shown in Table III. The development program for rare metals is carried out in three main areas: mining and smelting, extraction and recycling, and materialization including a substitution technology. On occasion, finding a single R&D theme to support the plan of main and future industries has proven to be challenging

Summary

The subject of rare metals has become a hot industrial and strategic issue due to its core role in current and emerging technologies, particularly in light if their rarity. The rarity of rare metals is determined not only by their occurrence in the earth's crust, but also the balance between their demand and supply. Assuring solutions has been launched along various lines, including exploration of new ore bodies, recycling, and substitution. At present, Korea is working to develop its rare metal-related industries by considering the value chain principle. It has also reached out seeking international cooperation as the rare metals opportunities and challenges have a global dimension.

Effectively addressing the rare metal challenges are imperative to minimizing the climate change, and providing a sustainable opportunity to future generations.

Table I. Definition of Rare Metals in Korea [1]

	Class	Elements	Type number
Rare Metal	Alkali/Alkaline earth metals	Li, Mg, Cs, Be, Sr, Ba	6
	Semimetal elements	Ge, P, As, Sb, Bi, Se, Te, Sn, Si	9
	Iron group elements	Co, Ni	2
	Boron group elements	B, Ga, In, Tl, Cd	5
	High melting point metals	Ti, Zr, Hf, V, Nb, Ta, Cr, Mo, W, Mn, Re	11
	Rare earth metals	REE : 17Species	1
	Platinum group elements	Ru, Rh, Os, Pd, Ir, Pt	1
Total			35

Table II. Necessity of Rare Metals in Future Considering the Core Industry Trend [2-3]

Class	Target industry	Introduction of target industry	Relation with rare metals industry	Rare Metals
Energy/ Environment	Clean energy	Synthesis of brown coal and subbituminous coal to produce synthesis of green fuel	Core technology of FT process with catalyst of rare metals	Co, Ni, Ru
	Ocean Bio-fuels	Usage of marine plants to produce bio-ethanol	Chemical reaction of bio mass catalyst	Ni
	Solar cell	The original technology of third generation of solar cell, Mass production of third generation solar cell	Energy conversion system	In(TCO), Ga, Se, Si, Cd, Te
	Collection of CO_2 Recycling of CO_2	Collection and recycling of CO_2 from industry	Recycling of CO_2, Chemical reaction of rare metals catalyst	Ti, Zr
	Generation of fuel cell	Usage of hydrogen fuel to produce clean energy	Fuel cell of rare metals	Ni, Y, Zr, La, Sr, Ga, Cr, Mn Sm, Co
	Nuclear power plant	Nuclear power generation industry	Plant structure materials of nuclear power generation	Ni, Co, Mo, W, Ti, Cr
Transportation system	Green car	Low-carbon green car, Electric car, Hydrogen fueled car	Drive motor, Battery, Fuel cell	REE, Li, Co, Ni, Fuel cell
	Ship/Ocean system	High value ship, Marine structure, Mobile harbor	Steel materials of Ship/Marine structure	Ni, Cr, W, Mo, V
New IT	Semiconductor	System semiconductor, New-generation memory	High-purity Rare Metals	Rare Metals
	Display	Smart display: Flexible, Self-luminous, 2nd display	High-purity Rare Metals	In, Mo, Nd
	Next-generation wireless communication	Mobile device	Fusion of mobile communication for hardware	Semiconductor, Display
	LED Lamp	High efficiency, Eco-friendly, High value : Lamp industry	Rare metals of LED	Ga, As, In, Pt

	RFID-USN	Distribution, Circulation, Production management, Ubiquitous computing	Tag, Antennas, Sensor, Independent source	Ni, Ag, Sensor, MPG
Fusion of new industry	Robot	Intelligent robot industry	Semiconductor, Sensor, Battery	Battery, Sensor
	New materials/ Fusion of nano-materials	New materials: NT-based, IT, BT, E2T Fusion technology	Function of new materials	Rare Metals
	Fusion of IT system	IT network of national infrastructures	Dependent on IT hardware	Semiconductor, Display, Sensor, Battery
	The convergence of Broadcasting and media	Fusion of Broadcast-Communication, Virtuous circle based on Service-Network-Mobile industries	Multi-function of mobile industry, High performance of mass information flow	Semiconductor, Display, Sensor, Battery
Bio	New medicine and equipment	Development of new drugs, Development of IT-medical equipment	Location tracing, Sensor technology of IT-Self diagnosis	Sensor, Semiconductor, Battery
Knowledge service	Software	Software development	Voice, Gesture, Haptic, etc., Input information hardware of new concept	Sensor, Semiconductor, battery, Display
	Design	High value of product for design	Creation of value product with generic technology	Mold, Design industry
	Health care	Medical equipment, Health service	Medical equipment, IT-based service	Sensor, Semiconductor, Wireless communication, Battery
	Culture technology	Development of high-tech CT from environment of digital convergence	Culture technology(CT), IT fusion of interactive communication	IT, Sensor, Battery

Table III. R&D Status of Domestic Rare Metals [4]

	Technology	Title	Support
Exploring & Mining	Mining & Smelting	1. Concentrating and smelting for domestic rare metals	
		2. Exploration of rare metal ores in Korea	
		3. Reaching and separating technology for REE - Ores for Domestic (Monazites) and overseas (Monazite & Bastnaesites) - Infrastructures for the production	
		4. Study on the Exploring of Rare Metals (Mo, Sn)	KETEP
		5. The origin of domestic uranium mine for the evaluation of distribution and endowed property technology development	KETEP
		6. Progress in the exploration of industry technology	
		7. Securing of fundamental technology on dissolution/leaching and purification relating to REE smelting	KORES
		8. Domestic patents related to REE smelting	
		9. Development of magnesium extraction and purification technology for enhancement of lithium recovery from Bolivia Uyuni brine	KIGAM
		10. Development of Lithium Carbonate manufacturing technology from Bolivia Uyuni brine	KORES
		11. Study on development of the collection and recovery technology from REE ore	
Urban mines	Extraction & Recycling	1. Study on the extraction and purification of rare metals from CRT & LCD monitors	SMBA
		2. Development of the extraction and purification technology of rare metals using liquid chromatography method	KEIT
		3. Extraction of valuable metals from electronic waste (e-waste) and enrichment facilities technology	SMBA
		4. Development of conversion technology of from disposal/bad magnet to high quality magnet	KEIT
		5. Recycling technology of Mg scrap in steel industry	KETEP
		6. Development of secondary battery material using recovered and recycled nickel	KETEP
		7. Development of the recycling technology for by-product titanium chip and the applied technology of precious metal oxides in coating electrode	KETEP
		8. Recycling of ferronickel slag and high value-added technology	KETEP
		9. Development of recycling of sawing dust silicon crystal	KETEP
		10. Development of new recycling technology of rare metals from urban mine	KETEP
		11. Collection of rare metals from Si-based waste module and development of high purification technology	KETEP

Materials technology	Materials	1. Development of Nd permanent magnets using anisotropic	KEIT
		2. Development of high-purified raw materials for platinum group (Ru, Ir)	KETEP
		3. Fabrication of light conversion nano-materials for energy conservation and development of applied technology	KETEP
		4. Development of spherical oxide nano particles less than 100 nm with high purity and homogeneity	SMBA
		5. Development of magnetic materials for Motor	KEIT
		6. Development of MRI 4-channel 10 KW high-frequency power amplifier using permanent magnet	SMBA
		7. Design of PM generator for wind turbine and development of origin technology	KEIT
		8. Development of hybrid electric power source and power transfer core component	KEIT
		9. Development of automatic feeding device using the permanent magnet-based hybrid gripper	SMBA
		10. Development of mass synthesis technology for metal oxide nano powder	SMBA
		11. The recycling and high purification technology of Te	KEIT
		12. Ultra high-purification technology of rare metals (Pt, Ru, Mo, Nb)	KIGAM
		13. Synthesis of functional Nano magnetic particles	KIMS
		14. Technology of cobalt metallization using eco-environment smelting process	KIGAM
		15. Fabrication technology of high-efficiency catlytic for alternative/reduction of platinum	KIST
		16. Commercialization study relating to functional material	KIGAM

* Korea Institute of Energy Technology Evaluation and Planning “KETEP”, Korea Resources Corporation “KORES”, Korea Institute of Geoscience and Mineral Resources “KIGAM”, Korea Evaluation Institute of Industrial Technology “KEIT”, Korea Institute of Science and Technology “KIST”, Korea Institute of Materials Science “KIMS”, Small and Medium Business Administration “SMBA”

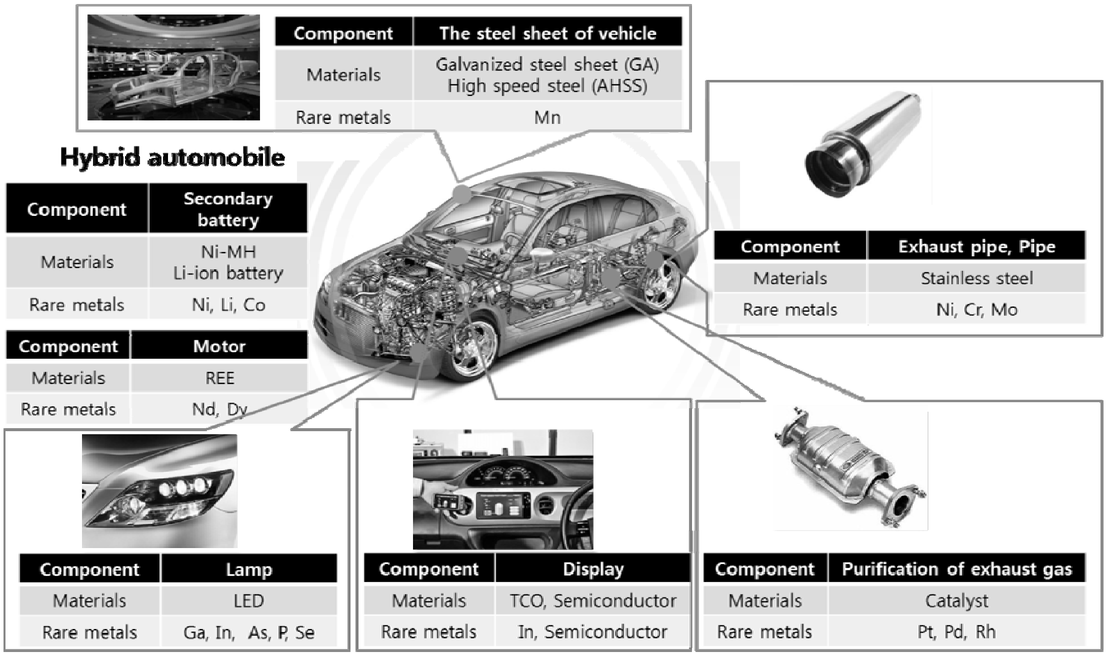

Component	The steel sheet of vehicle
Materials	Galvanized steel sheet (GA) High speed steel (AHSS)
Rare metals	Mn

Component	Secondary battery
Materials	Ni-MH Li-ion battery
Rare metals	Ni, Li, Co

Component	Motor
Materials	REE
Rare metals	Nd, Dy

Component	Exhaust pipe, Pipe
Materials	Stainless steel
Rare metals	Ni, Cr, Mo

Component	Lamp
Materials	LED
Rare metals	Ga, In, As, P, Se

Component	Display
Materials	TCO, Semiconductor
Rare metals	In, Semiconductor

Component	Purification of exhaust gas
Materials	Catalyst
Rare metals	Pt, Pd, Rh

Figure 1. Usage of rare metals in automotive [1, 4].

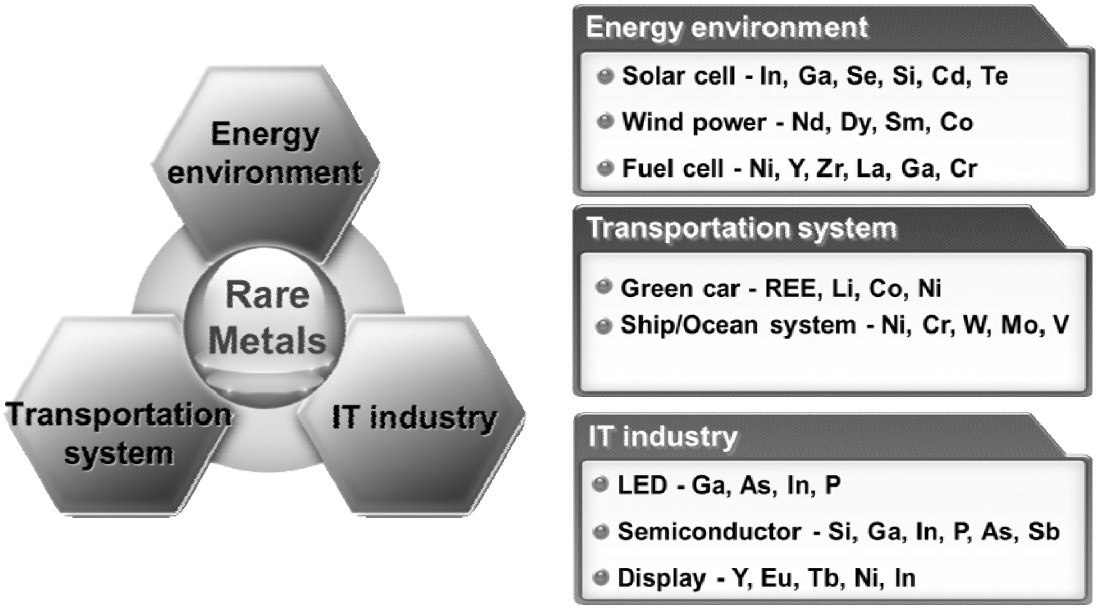

Energy environment

- Solar cell - In, Ga, Se, Si, Cd, Te
- Wind power - Nd, Dy, Sm, Co
- Fuel cell - Ni, Y, Zr, La, Ga, Cr

Transportation system

- Green car - REE, Li, Co, Ni
- Ship/Ocean system - Ni, Cr, W, Mo, V

IT industry

- LED - Ga, As, In, P
- Semiconductor - Si, Ga, In, P, As, Sb
- Display - Y, Eu, Tb, Ni, In

Figure 2. Future core industries with a role of rare metals [1, 4].

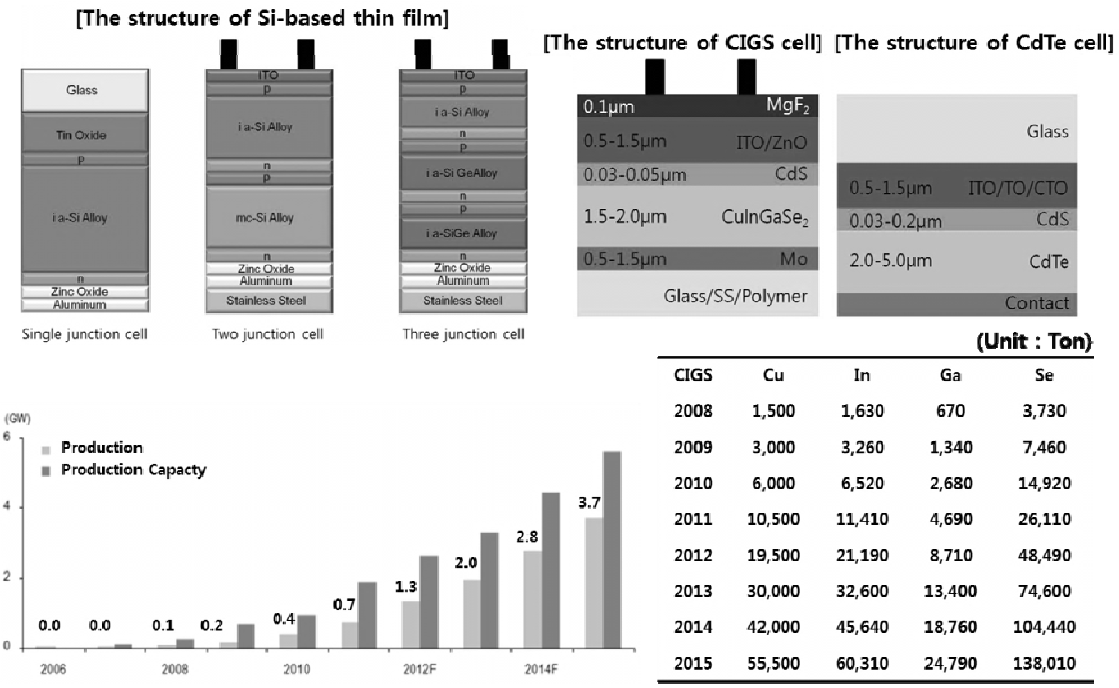

(Unit : Ton)

CIGS	Cu	In	Ga	Se
2008	1,500	1,630	670	3,730
2009	3,000	3,260	1,340	7,460
2010	6,000	6,520	2,680	14,920
2011	10,500	11,410	4,690	26,110
2012	19,500	21,190	8,710	48,490
2013	30,000	32,600	13,400	74,600
2014	42,000	45,640	18,760	104,440
2015	55,500	60,310	24,790	138,010

Figure 3. An Example of rare metals usage in solar cells estimated considering the product structure and market trend [1, 4].

Figure 4. Main strategy of rare metals assurance [1, 4].

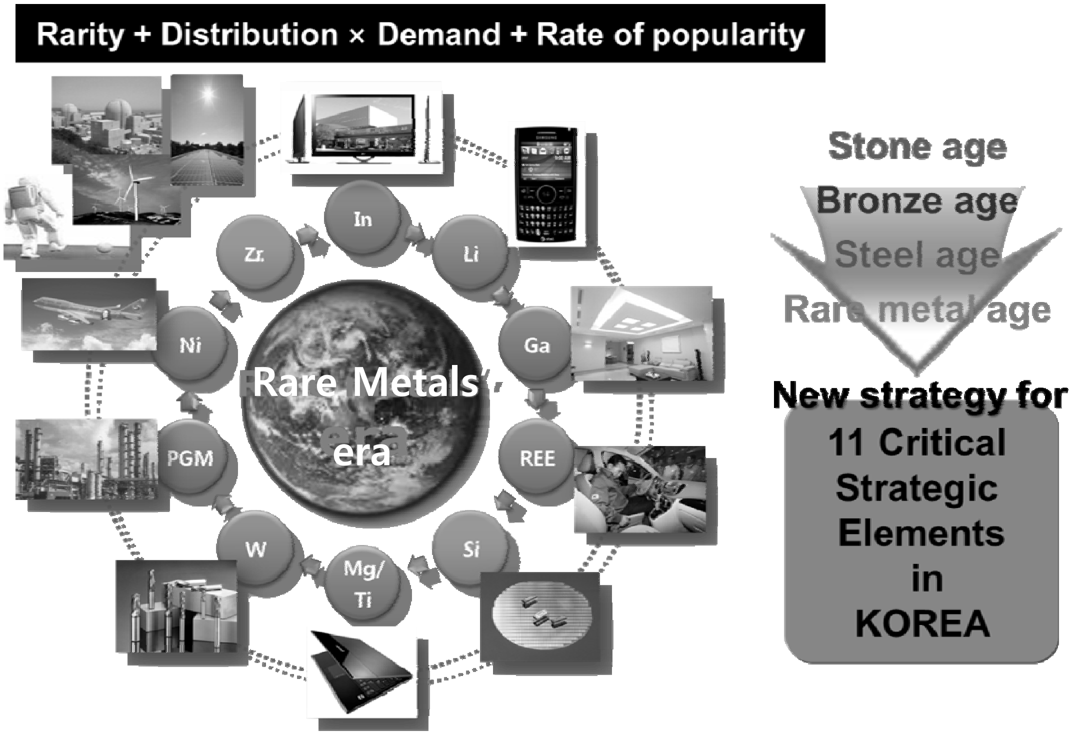

Figure 5. 11 Core rare metals chosen by several factors [1, 4].

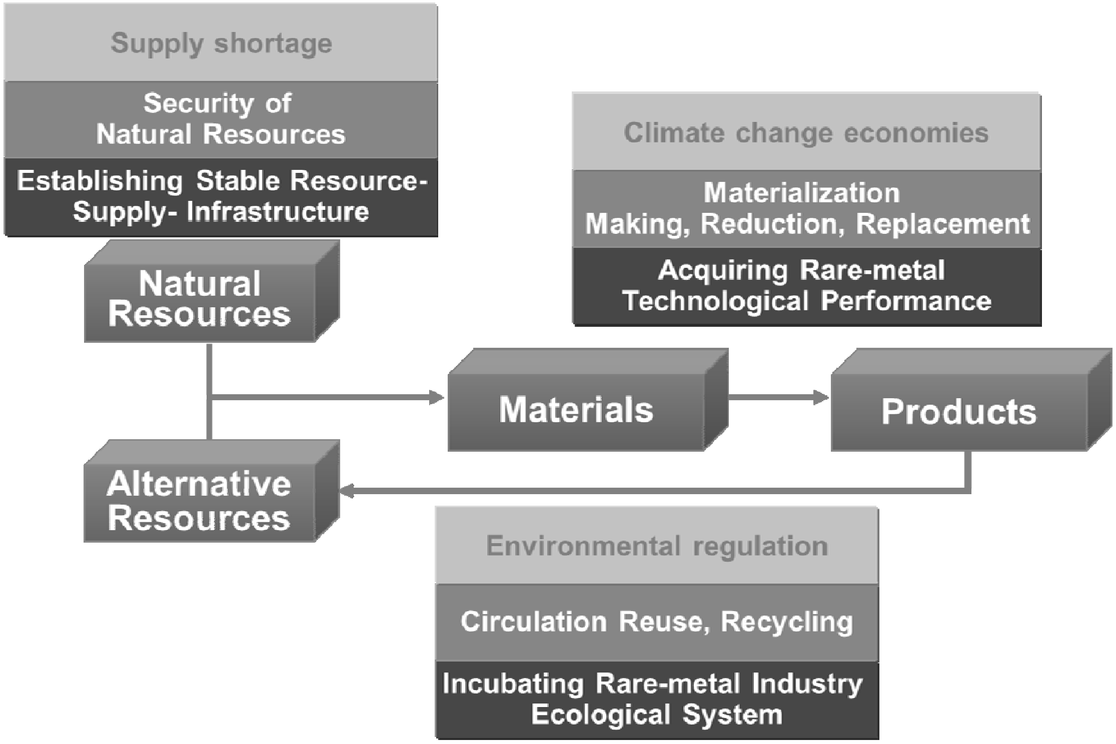

Figure 6. Principles of rare metals development on value chain [1, 4].

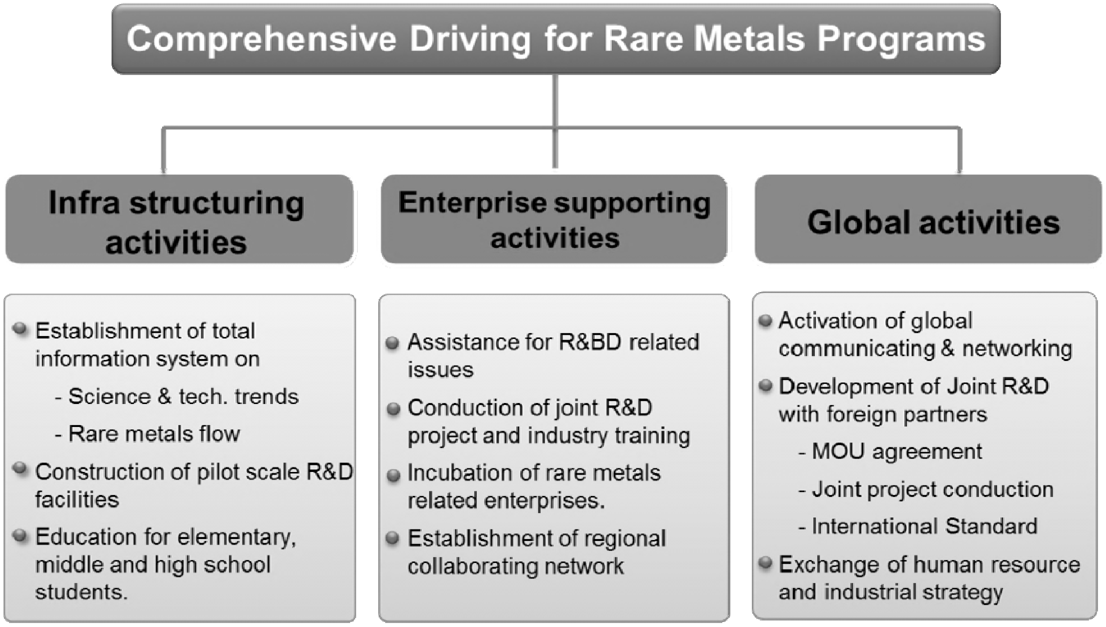

Figure 7. The Activities done and doing by KIRAM [1, 4].

References

1. http://www.kiram.re.kr
2. http://www.mke.go.kr
3. http://www.mcst.go.kr
4. Kim, T-S., “Strategy and Research and Development for Rare Metals Driven in Korea”, Critical Minerals 2013 (4-5 Jun 2013, Perth, Western Australia).

REALIZING CANADA'S RARE EARTH ELEMENTS RESOURCE POTENTIAL: R&D PERSPECTIVE

Janice Zinck[1]

[1]CanmetMINING, Natural Resources Canada, 555 Booth Street, Ottawa, Canada,
janice.zinck@nrcan.gc.ca

Keywords: Rare Earth Elements (REE), Critical Metals, Processing, Mineralogy, Characterization, Resources, Leaching, Separation, Toxicity, Environment, Network

Abstract

Rare earth elements (REE) are resources of strategic importance to Canada. However this emerging REE industry requires new and complex metallurgical research to be able to effectively and environmentally develop Canadian REE deposits. Due to the critical nature of these metals and the need for metallurgical research and development (R&D) across this emerging industry there is a strong national role. To address this need CanmetMINING is undertaking research to advance technological innovation for Canadian REE projects. Following a gaps analysis, several research projects were initiated including mineralogical characterization of Canadian rare earth ores, physical separation techniques to produce high grade REE concentrates, evaluation of leaching and separation processes for REE ores, and investigation of the chemistry and toxicity of REE leachates. The paper discusses these research gaps and recent advances in these areas, as well as additional work being undertaken in the area of certified reference materials and regulatory requirements for radioactive residuals.

Introduction

While Canada currently has little domestic direct or manufacturing demand for the rare earths, it has or controls not only more deposits of rare earths than any other country, but also significant operational expertise in processing rare-earth ores to high-purity metals [1]. Canada has an enormous opportunity to play an important niche role in the world market for rare earth elements (REE). The country's geological endowment coupled with its world-class expertise in mining and processing, position it to be a major player in the emerging rare earths industry through fulfilling national and international downstream supply chains. According to the Canadian Chamber of Commerce "Canada's rare earth deposits can offer a substantial competitive advantage" and while there are numerous rich deposits in the country as of mid 2013 Canada was not a REE producing nation [2].

Currently, Canada is a an importer of light rare earth elements or LREE (glass/stone polishing, fluid cracking catalysts) and an importer of REE-containing components (automobiles, electric/hybrid vehicles, wind turbines, aerospace applications) and roughly within the next decade Canada will be a future producer of heavy rare earth elements or HREE.

Figure 1 portrays the processes to bring a natural resource project to fruition. The time frame can take years, even decades, and cost may vary from $50 million to 1 plus billion dollars depending on the many variables in bringing a mine into production. Canada's industry is emerging and several companies are projecting production within five to ten years (Table I). However, several challenges must be addressed to achieve such success.

Challenges for Success

Canadian geology, exploration know-how, mining experience, regulatory infrastructure and investment climate all strongly support a potentially prosperous REE industry in Canada. However, some issues could impact its success. In particular, there is a deficiency of qualified personnel and laboratories especially in the areas of mineralogy, chemistry, and metallurgy.

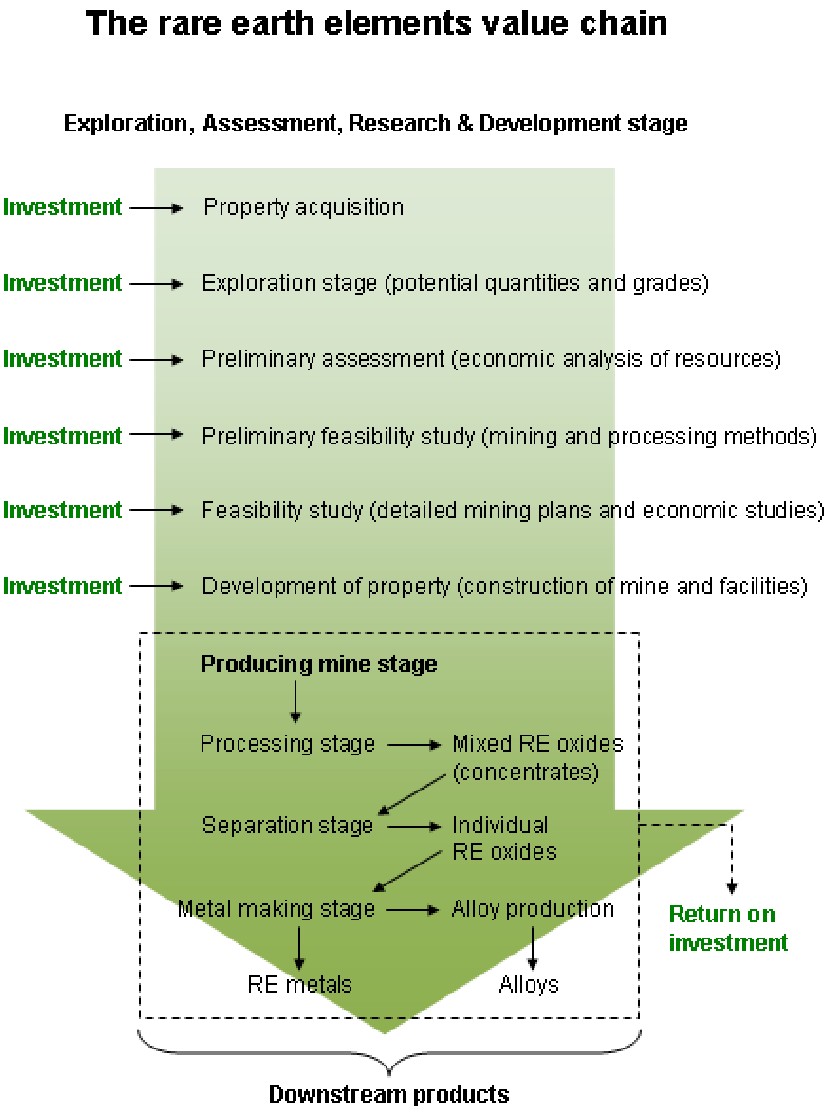

Figure 1. Rare earth element investment and supply chain. The supply chain is highlighted by the dashed box.

Insufficient skills and facilities could result in metallurgical testing delays that could ultimately delay production schedules [3]. Furthermore there is the lack of any downstream processing facilities or direct end-users of REE in Canada, to support the development of primary REE production. In other words, there is the lack of an existing value chain in Canada. While this is a current challenge, it presents an opportunity for the creation of an REE value chain in Canada.

Table I. Canadian Rare Earth Projects at Various Stages (Feasibility, Pre-feasibility, etc.)

Project/Owner	**Target Year**	**% HREE**
Avalon Rare Metals	2016 - 2017	28%
Commerce Resources	> 2020	10%
GéoMéga Resources	> 2020	2%
Great Western Minerals	2020	4%
Matamec Exploration	2018 - 2019	32%
Search Minerals	2019 - 2020	20%
Orbite Aluminae	2014	5%
Pele Mountain Resources	2018 - 2019	15%
Quest Rare Minerals	2018 - 2019	38%
Rare Earth Minerals	> 2020	10%

Some additional challenges for Canadian and other resource companies are the infrastructure, climate, the profile of REE in the investment community, and trade barriers. Canadian REE projects are located across the country in differing climates, geography and geology (Figure 2).

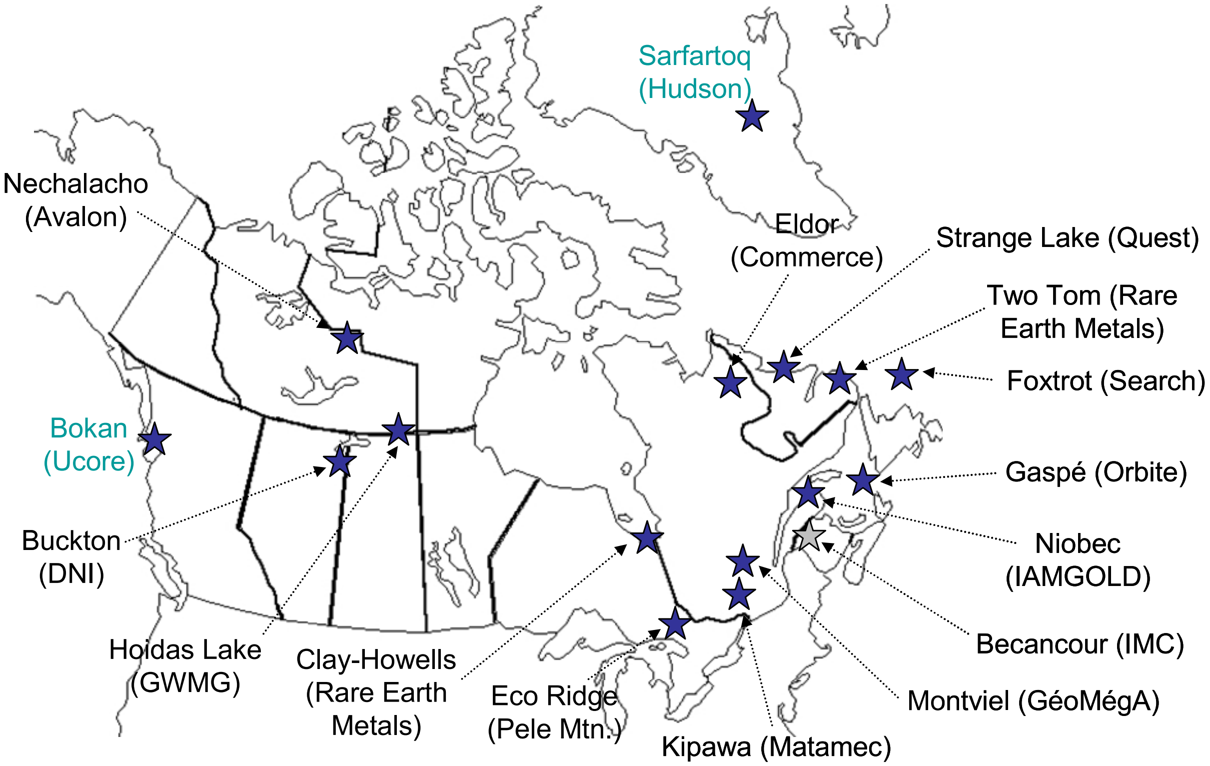

Figure 2. Selected more advanced Canadian rare earth projects. Note Bokan and Sarfartoq are not Canadian deposits but are owned by Canadian companies.

The sprint to be first to demonstrate economic viability of an advanced REE project is to attract off-take commitments and strategic investment. It is a competitive business and effectively the players are competing both for market share and for capital. The Canadian REE industry is clearly advancing its resource developments to secure a solid market position and the industry as with most other prospective projects around the world strives to manage capital and operating expenditures and increase efficiency and effectiveness. The three most important factors in this race are heavy rare earth balance, grade and mineralogy, which translate into ease of processing and extraction.

Several intellectual and physical infrastructural gaps need to be addressed: better metallurgical processes for these complex ores; improved extraction and processing activities to meet environmental standards; development of highly qualified people to meet capacity shortfalls for Canadian mining companies and research facilities; coordination of technical and scientific REE information, and, a policy framework to address the importance of critical materials (such as REE) for the Canadian economy.

It is worth reiterating that the demand for critical metals, including REE and other strategic metals are expected to exceed supply within 10-15 years. In particular, there will likely be global market deficiencies in neodymium, europium, terbium, dysprosium and yttrium.

Technological Challenges

Over the past 15 years, research and knowledge have evolved regarding the characteristics and uses of rare earth elements such that many of these materials have become indispensible in the manufacture of advanced technological equipment with a particular focus on clean-energy applications such as wind turbines and hybrid/electric cars. Most consumer electronic devices require REE and new technologies being developed for water purification, desalination, magnetic refrigeration, and more energy-efficient light bulbs will need REE as well. Canada currently relies upon the import of REE-containing components for the manufacture of key products in many industries. Thus, while the sector directly involved in REE is worth roughly $2 billion (130 000 tonnes), its indirect value throughout the global economy may be measured in trillions of dollars.

While grades and tonnage govern the success of other commodity projects, in the rare earth industry, metallurgy is often the determining factor. As noted earlier, one of the greatest challenges facing the Canadian and international rare earth industry is the cost of processing of rare earth ores and the lack of existing processing and refining infrastructure in Canada.

Rare earth elements are difficult to separate from one another once they have been liberated from REE-bearing minerals. At the atomic level, the lanthanide elements have a similar outer electronic structure, with this structure shielding the so-called 4f electrons within the atom [4]. The presence and incremental filling of these electron orbitals are key characteristics of the lanthanides. This unique structure leads to REE ions that are very similar in size to each other. It is this similarity in ionic radii across the group, not the adjacency of their atomic numbers, which gives rise to the similar chemical properties associated with each of the REEs. This makes them difficult to separate, even with the use of intensive processes such as solvent extraction (SX).

Aspects or rare earth mineralogy, mineral processing, hydrometallurgy and environmental management are further discussed below.

Mineralogy

According to experts [5] mineralogy is the most important factor in rare earth processing as it controls the metallurgy. If the mineralogy is not well understood, then the metallurgy will be flawed and inefficient. Upfront mineralogical assessments can identify important mineralogical associations, in turn leading to correct metallurgical planning and providing early predictions in beneficiation test work [6]. Despite more than 200 known REE-bearing minerals, only three are considered to be the principal REE mineral ores most feasible for the extraction of rare earth metals: bastnaesite $(Ce,La,Y)CO_3F$, monazite $(Ce,La,Nd,Th)PO_4$ and xenotime (YPO_4) [7].

Considering the structural, morphological and compositional diversity of REE minerals, and the complexity of natural (e.g. weathering) and engineered (e.g. physical concentration, leaching) REE fractionation and enrichment mechanisms, mineralogical characterization is a key component at all steps ranging from exploration to production. Detailed characterization of the chemical, structural, textural, morphological, and surface properties of REE minerals within a deposit and a thorough understanding of the evolution of these properties are the basis for the identification of efficient concentration and extraction processes. To stimulate and support REE development efforts in Canada, Natural Resources Canada is focussing on providing such critical information for important REE deposit types. Specifically, the work is directed at characterization of REE accessory minerals and the reactive processes associated with leaching, as well as the distribution and nature of REE carriers in ion-adsorption REE. This research is being achieved through the development of robust mineralogical characterization approaches that will take advantage of the respective strengths of advanced micro-analytical techniques [8]. Recent advances at CanmetMINING include the correlation of mineralogy and leaching behaviour as well the development of ion implants as an efficient X-ray microanalysis of heavy rare earth elements.

Mineral Processing

The minerals containing REE are extensively dispersed and inter-grown with several oxide, carbonate and phosphate minerals. Consequently they are very difficult to liberate at coarse grinding and are thus difficult to separate without special methods and reagents to obtain high grade rare earth mineral concentrates. Although the REE in the same mineralogical class have similar behaviours, the minerals in which they occur vary in their chemical and mineralogical nature. Therefore, unlike base metal sulphide minerals, there are no reagents that may be applied across the board for efficient flotation. Due to the relatively low volume of annual production, the chemical industry does not invest in the development of specific collectors (chemicals) for flotation of individual REE minerals. The relatively low metal recovery and concentrate grade during processing may be attributed to the lack of selectivity of the reagents (chemicals) used in flotation, which are not synthesized particularly for REE minerals. The overall processing challenges and issues to be resolved through systematic research and innovations may be summarized as follows [3]:

- Lack of mineral specific collectors and or depressants to selectively separate minerals from ores into individual concentrates and tails;
- Lack of sufficient understanding of individual REE mineral physical and chemical behaviours (responses) to develop efficient processing flowsheets;
- Achieving high separation efficiencies with low reagent, water and energy consumption; and
- Producing high grade concentrates to reduce high consumption of acids and hydroxides required to dissolve all RE elements before extraction.

The separation of REE-bearing minerals requires complex unit operations, often consisting of crushing, grinding (with minimum fine creation), classification, gravity separation and/or magnetic separation, before or after bulk or selective flotation of valued minerals. Innovative approaches are needed to close or at least narrow the key technological gaps related to physical separation (gravity and magnetic) followed by flotation [3]. Some specific options include:

- The development of generic grinding schemes that allow the liberation of individual REE minerals at coarse grind, thereby reducing the amount of hard-to-float ultrafine REE mineral particles;
- Rejection of sterile host rocks after crushing with emerging ore-sorting technologies that are gaining greater acceptance and will allow more efficient processing of ores containing one or multiple RE minerals;
- Development of a collector mixing strategy to maximize RE minerals recovery by flotation; and
- Appropriate testing of RE minerals flotation for development of the most efficient flowsheet.

Generic/conceptual flowsheets for the separation of REE minerals from the gangue by flotation are not available in the literature. In comparison, such generic flowsheets exist for the down stream extraction processes. In general, there have been no breakthroughs in the development of uniquely suited collectors for efficient flotation of major REE minerals although extensive testing of various combinations of chemicals were made by the Chinese to activate the rare-earth metal bearing minerals while depressing the accompanying rock forming minerals of lesser values.

A wide range of technology combinations employed by Canadian REE projects including ore pre-concentration plus magnetic separation, low intensity magnetic separation plus high intensity magnetic separation, flotation and magnetic separation in parallel, gravity separation plus magnetic separation and flotation, magnetic separation plus flotation and gravity separation, flotation alone and no physical separation. Overall recoveries vary from 70% to 93% total rare earth oxides (TREO) in concentrates ranging from 25% to 45% [9].

Improving the recovery of REE minerals translates into (a) maximizing the utilization of non-renewable and rare resources, a challenge that requires further refinement of existing technologies and the development of new ones, and (b) maximizing the removal of thorium (Th) and uranium (U)-bearing minerals (which almost always coexist with REE minerals) from the tailings, thereby improving the environmental performance of the operations. This equally requires a very innovative approach to processing, specifically by flotation, where the desirable final concentrate grade is higher than 60% TREO, to render the downstream hydrometallurgical treatment flowsheet less complex, more economic, and more environmentally efficient. If the concentrate is not free of some of the gangue minerals, subsequent roasting with sulphuric acid could generate harmful gases such as hydrofluoric acid, sulphur dioxide, etc. and voluminous slag; a slag that is sometimes radioactive.

CanmetMINING has recently commissioned a physical separation pilot plant and has completed work to improve recovery and quality of concentrate produced through flotation in combination with other physical separation options. Work is also focussing on decreasing impurities and gangue minerals reporting to the concentrate

Hydrometallurgy

By far the most challenging processing step is that of REE hydrometallurgy and specifically, separation. Mechanical and pyrometallurgical methods have high-energy demands and consequently high costs. Furthermore, dust collecting and/ or gas cleaning systems are required, and they are not as versatile as hydrometallurgical processes. Hydrometallurgical processes generally consist of different steps of pre-treatment, in order to improve metal dissolution rates in the aqueous phase, followed by leaching, concentration and/or purification and finally recovery of different metals from the leach solution. In the leaching step either an acid or a base can be used depending on the material being treated. The most commonly used hydrometallurgical concentration and purification methods in the mining industry today are precipitation, liquid- liquid extraction (LLE), solvent extraction and ion exchange (IX). For the final recovery step precipitation and electrolysis are often used. Solvent extraction followed by electrowinning has, for example, become quite popular for copper and nickel recovery in the mining industry. In zinc refineries, iron and cadmium are precipitated as residues after which zinc is recovered using electrowinning [10]. Hydrometallurgical extraction technologies applied to the mineral concentrates are different from those applied to the adsorbed ion types.

Metals separation from the concentrate involves an initial process of chemically dissolving the minerals. Cracking is a complete chemical dissolution of the REE minerals. Cracking may require roasting for effective chemical attack. Inadvertently, other rock minerals that were not successfully separated at the physical concentration step will also dissolve contributing to increased chemical consumption and complication of the metal extraction processes. The amount of chemical required depends on the purity of the concentrate. Because each concentrate produced from each ore deposit is unique, the chemical separation process and its complexity are also unique. The solution containing the dissolved metals is further manipulated to yield mixed but simpler rare earth compounds. The mixed rare earth compounds are further refined to produce separate metals with more than 99.9% purity depending on applications. It is for this reason that a wealth of knowledge has to be generated through extensive research to produce these uniquely strategic metals.

There remain numerous research gaps in rare earth hydrometallurgy that must be addressed to better understand and develop the process metallurgical flowsheets needed. Studies on rare earth complexation chemistry in both aqueous and organic phases are needed and will allow for the invention of new chemicals, complexing agents for dissolving the REE elements from ores and will also lead to innovations in highly efficient SX (separation) systems.

Leaching is an unavoidable step for the production of REE. The practice and research in REE leaching are primarily focused on acid leach. Although roasting is not a hydrometallurgy process, it has been an important step in the overall hydrometallurgy process for the destruction of REE-bearing ores. At least four major processes that have been active in REE production in China are using roasting as the pretreatment step before leach. These processes could provide opportunities for Canadian ores. These processes are: concentrated sulphuric acid roasting; intensified concentrated sulphuric acid roasting; CaO-NaCl roasting; and Na_2CO_3 roasting. Alkaline leaching has become the major process in China for processing hard rock type (rather than ion-adsorbed) REE ores. Many other processes also exist [3].

Among the many topics in this area, the separation of U and Th from REE is of special importance in Canada. Liquid membrane permeation (LMP) has been an efficient technology in recovering REE from the leaching solutions. Such technology is not new in the hydrometallurgy world, but requires further study for REE applications.

In the production of high purity products, the extraction chromatography technology appeared to be a new and effective method. This method has been applied by some Chinese producers and may be applicable in Canada for high purity production.

Developments in the solvent extraction field can be used in REE production and will largely increase the economics and environmental rating of the process. Some options include: microwave intensified SX, ultrasound intensified SX, magnetic intensified SX, froth flotation SX and certainly the very attractive centrifuge SX technologies.

Environmental Aspects

There are several environmental issues related to REE production. The most significant issue is that many primary REE deposits contain significant amount of radioactive elements, mainly thorium and to a lesser extent uranium. This and other environmental issues associated with REE production are summarized in Table II [11].

There are limited data on the toxicological and epidemiological properties of rare earth elements. In addition, as metallurgical processes have yet to be finalized for Canadian projects the effluent and waste aspects of REE processing are not well understood.

Table II. Summary Table of Pollutants, Impacted Environmental Media, Emission Sources, and Activity Associated with REE Mining, Processing, and Recycling [11]

Activity	**Emission Source(s)**	**Primary Pollutant of Concern**
Mining (surface and underground)	Overburden Waste rock Sub-ore stockpile Ore stockpile	Radiologicals Metals Mine influenced water, acidic drainage, neutral drainage Dust and associated pollutants
Processing	Crushing/grinding	Dust
	Tailings Tailings impoundment Processing effluents	Radiologicals Metals Turbidity Organics Dust and associated pollutants
Recycling	Collection	Transportation pollutants
	Dismantling and separation Scrap Waste Landfill	Dust and associated pollutants Volitile organic compounds (VOCs) Metals Organics
	Processing	Dust and associated pollutants Volitile organic compounds (VOCs) Dioxins Metals Organics

Other Research Needs

The literature identifies several other areas where more work is needed to help establish a sustainable REE industry in Canada [3].

- Reference materials: The availability of credible rare earth element reference materials has been identified as a potential area for further work. Development of these reference materials would provide industry with a standard reference for reporting and analytical purposes.

- Recycling: The recovery of REE from end-of-life high-tech products is a priority in countries such as Japan and Europe that have no, or limited primary REE resources. The development of recycling options is constrained by a lack of efficient collection systems, the challenge of effective and safe disassembly and treatment.

The Canadian REE Research Network

There is an opportunity for Canada to coordinate and collaborate on REE research**.** A proposed Canadian REE research network would provide a permanent space where Canadian stakeholders interested in rare earth elements R&D could share information about their REE-related work. This network would seek synergies and stimulate research partnerships and help to maximize innovation in REE processing. This approach would optimize the use of Canadian REE-related R&D efforts, and would provide opportunities for discussion and coordination of these Canadian R&D activities. The overall goal of the network would be to focus and further strengthen Canada's R&D capacity for REE. In addition it would help inform the Government of Canada vis-à-vis ongoing liaison with international bodies concerning REE. Further, the network would track Canadian REE research activities, which would be accessible through an inventory of REE projects. It would also provide reference materials to the REE community to facilitate collaboration and accelerate innovation. As of July 2013, the Network was in the early stages of framing its mission and priorities and establishing an industry-academia-government executive committee or board to provide oversight and guidance so that the resulting organization is effective, relevant and beneficial. In addition, a web presence has been established at www.ree-etr.ca. This site will serve as a portal for the network to exchange and disseminate information and get updates on the network progress and activities.

Conclusions

Canada has the world's majority of reserves, 51% of the total rare earth oxides (TREO) and 59% of the HREO (heavy rare earth oxides) outside of China. Couple this with its expertise in chemical and metallurgical processing and its experience in mining, Canada will soon be a REE producing nation. To achieve this however technological challenges must be overcome with the REE community working collectively and efficiently.

Acknowledgements

The author would like to express her appreciation to NRCan colleagues Robert Sinclair, Yves Thibault, Tesfaye Negeri, Chen Xia, Maureen Leaver, Melissa Desforges, Rory Cameron and Sean Langley for their input to NRCan's REE research program. The Canadian REE industry is also acknowledged for its input and ongoing guidance.

References

1. Lifton, J. "Canada and Critical Rare-Earth Metals" (Technology Metals Research, January 23, 2011). http://www.techmetalsresearch.com/2011/01/canada-and-critical-rare-earth-metals/

2. Kremmidas, T., "Canada's Rare Earth Deposits Can Offer a Substantial Competitive Advantage" (Canadian Chamber of Commerce, April 2012).

3. Natural Resources Canada. "The Rare Earth Elements Project: R&D Gaps Analysis" (Minerals and Metals Sector, April 2012).

4. Hatch, G. 2012. Rare-Earth Terminology – A Refresher on the Basics (Resource Investor, December 13, 2012). http://www.resourceinvestor.com/2012/12/13/rare-earth-terminology-a-refresher-on-the-basics#.Uc3TbhOBlVA.email.

5. Mariano, A. "Technology Metals Summit" (Panel Discussion, April 2013).

6. Thompson, Wendy et al. "Mineralogical Studies in Assisting Beneficiation of Rare Earth Element Minerals from Carbonatite Deposits" (Proceedings of the 10th International Congress for Applied Mineralogy (ICAM) edited by Maarten A.T.M. Broekmans) 665-672.

7. Gupta, C.K., and N. Krishnamurthy. *Extractive Metallurgy of Rare Earths*. (CRC Press, 2004).

8. Thibault, Y. “Mineralogical characterization applied to the development of Rare Earth Elements resources”, (Project statement of work, CanmetMINING, Natural Resources Canada, April 2012).

9. Negeri, T. “Physical Separation of Re-Minerals (A Short Review)” Presentation at the Natural Resources Canada hosted Rare Earth Elements Workshop June 25-26, 2013.

10. KTH Royal Institute of Technology. “Separation of rare earth metals” (School of Chemical Science and Engineering, March 2013.)

11. Environmental Protection Agency. “Rare Earth Elements: A Review of Production, Processing, Recycling, and Associated Environmental Issues” (EPA Office of Research and Development. December 2012. EPA 600/ R-12/572)http://nepis.epa.gov/Adobe/PDF/P100EUBC.pdf

RESOURCES AND EXPLOITATION OF RARE EARTH ORE IN CHINA

Ruan Chi[1]; Zhigao Xu[1]; Junxia Yu[1]; Zhengyan He[2]

[1] School of Chemical Engineering & Pharmacy,
Wuhan Institute of Technology, Wuhan 430073, China;

[2] School of Minerals Processing and Bioengineering, Central South University, Changsha, 410083, China

Keywords: Exploitation; Rare Earth Ore; Endogenic Deposit; Exogenic Deposit; Processing Techniques

Abstract

As the major rare earth supplier in the world, China is very rich in the mineral resources. The distributions and characteristics of endogenic and exogenic rare earth deposits are concretely described. The important endogenic rare earth deposits, dominated by light rare earths, are located in Baiyunebo, Weishan and Sichuan Mianning, and most of the exogenic rare earth deposits, concentrated in heavy rare earths, are weathered crust elution-deposited rare earth deposits. Exploitation and utilization value of different rare earth ores are compared in detail and the various processing techniques are discussed according to different mineral species, components and structures.

Introduction

It is an indisputable global consensus that rare earths are not rare. Rare earth deposits are found in 37 countries and distributed in Asia, Europe, Africa, Oceania, North America and South America. The main rare earth countries are China, United States of America, Australia, Russia, Brazil, Canada, South Africa, Greenland, Mongolia, Kazakhstan, Kyrgyzstan, Malaysia and India which possess many large scale or super-large scale rare earth deposits [1]. According to the report of the US Geological Survey in 2011, the proved rare earth resources in the world is about 110 million tonnes (REO) in which China is 55 million tonnes, the former Soviet Union is 19 million tonnes and the United States of America is 13 million tonnes. China issued its White Paper on Rare Earths in 2012 and claimed that China accounts for 23% of the total RE reserves of the world. The rare earth mines are mainly distribute in Inner Mongolia, Jiangxi, Guangdong, Guizhou, and Sichuan etc. Most light rare earth ores are in the north, and most heavy rare earth ores are in the south. The principal exploited rare earth ores are the Baiyunebo, Sichuan Mianning, Shandong Weishan, and the weathered crust elution-deposited rare earth ore [2]. Among them, Baiyunebo is the richest rare earth resources [3]. With years of endeavor, China has become the biggest rare earth producer, user and exporter [4].

The application of rare earth makes a great contribution to the development of industry, but the exploiting of rare earth also brings serious resource and environment problems. For the past few years, many measures have been taken on the mining, producing and exporting of rare earth to protect the resources and environment and achieve the sustainable and healthy development of the rare earth industry.

Main Rare Earth Deposits in China and the RE Partitioning

The Mineral Type Rare Earth Ore

The Baiyuneboite Rare Earth Ore in Inner Mongolia: Baiyunebo rare earth deposit is a large multi-metal deposit containing iron, rare earth and niobium etc. The orebody consists of west deposit, main deposit, high magnetic deposit, east deposit, east Jie Le Gele, dulahala and the east contact zone going from west to the east. Baiyunebo rare earth deposits derive from the metamorphic sedimentation (hydrothermal replacement) and the composition of the ores is quite complex containing 170 kinds of minerals. About 17 elements are found in the minerals including iron, rare earth, niobium, thorium, calcium fluoride, potassium, phosphorus, sulphur and scandium etc [5] The same element can exist in several forms or even more than a dozen of minerals, so the mineral species are multiplied and also with a relatively complicated structure. The minerals are intimately associated with each other in sub-sieve size ranges. Therefore, Baiyunebo deposit is a unique large multi-metal deposit that is rich in iron, rare earth and niobium all over the world. The reserve of rare earth at Baiyunebo is first and the reserves of niobium and thorium are second in the world [6].

The reserves of iron ore in Baiyunebo deposit are as follows: 716 million tonnes in main deposit and east deposit, 912 million tonnes in West deposit. The prospective reserve of REO is 135 million tonnes, industrial reserve is 43.5 million tonnes which occupies 83% of the national one (52 million tonnes). The prospective reserve of Nb_2O_5 and ThO_2 is 6.6 and 2.2 million tonnes, respectively.

More than 90% of the rare earth elements in Baiyunebo ores are present as independent ore phase, and about 4~7% are distributed in the iron ore and fluorite. Light rare earth occupies 88.5~92.4% of the total rare earth oxide, while the yttrium group elements are rare. Therefore, Baiyuneboite is a typical light rare earth ore with a high ratio of $\sum CeO_2/\sum Y_2O_3$ (27.11~64.41).

Bastnaesite, Bunsite, Cebaite, Huangheite, Carbocerine, Barium-parisite and Cryptolite etc., are the primary rare earth minerals in Baiyunebo, and the dominated bastnaesite and monazite, whose ratio is 6:4~7:3, accounts for 73.14~96.05% of the rare earth minerals. The particle size of rare earth mineral is between 0.01~0.07 mm and almost 70~80% are below 0.04 mm. The mixed rare earth ore contains other useful minerals such as magnetite, hematite, colombite and fluorite. The main gangue minerals are beloeilite, crocidolite, biotite, calcite, dolomite, barite, apatite, pyrite, feldspar, and quartz, etc.

Sichuan Liangshan Rare Earth Ore: Rare earth resources are relatively rich in Sichuan. Maoniuping rare earth ore with a high industrial value is located in the rare earth metallogenic belt with a length of 150 km in Liangshan. The rare earth reserve is about 2 million tonnes and mainly distribute in Maoniuping in the western Mianning and Dalu village in the southwest of Dechang county. The representative rare earth distribution is listed in Table I.

Table I. Rare Earth Distribution of Mianning and Dechang Rare Earth Ore (%)

Rare earth oxides	La_2O_3	Ce_2O_3	Pr_2O_3	Nd_2O_3	Sm_2O_3	Eu_2O_3	Gd_2O_3	Tb_2O_3	Dy_2O_3	Ho_2O_3	Er_2O_3	Tm_2O_3	Yb_2O_3	Lu_2O_3	Y_2O_3
Mianning Maoniuping	29.49	47.56	4.42	15.18	1.24	0.23	0.65	0.12	0.21	0.05	0.06	0.04	0.05	0.007	0.7
Dechang Dalu	35.63	43.81	4.73	13.06	1.22	0.225	0.52	0.06	0.09	0.045	0.04	0.01	0.055	0	0.40

*Note: Quoted from CSRE Yearbook 2011 [7]

Maoniuping rare earth ore is the largest one in Sichuan. The main industrial mineral is bastnaesite with 80% REO, only followed by parisite and a small amount of tschewkinite. It is a typical light rare earth ore with a high content of light rare earth (96%). The ore in the rare earth ore usually associated with lead, molybdenum, barite ($BaSO_4$), barian celestine (Sr, $Ba(SO_4)$), fluorite etc which can be recovered, and the radioactive elements are at a low level. Except the Dalu rare earth ores, all other rare earth minerals in Liangshan occur in coarse mineral crystals and with a high weathered dissociation degree, so they are easily beneficiated.

Shandong Weishan Rare Earth Ore: Shandong Weishan rare earth ore is a quartz-barite- carbonate rare earth deposit with a reserve of 0.9 million tonnes. The mineral and gangue components of the deposit are simple, and the main mineral is bastnaesite, associated with a small amount of bunsite, quartz, barite etc. The particle size of Weishan rare earth ore is about 0.5~0.04 mm and can be easily enriched. The single RE element can be easily separated from the rare earth concentrate through beneficiating and 98% of the rare earth can be recovered. The original ore in Weishan contains 3.5~5% REO, and lanthanum, cerium, praseodymium, neodymium occupies more than 95% of the total amount, as shown in Table II.

Table II. Rare Earth Distribution of Weishan Rare Earth Ore (%)

Rare earth oxides	La_2O_3	Ce_2O_3	Pr_2O_3	Nd_2O_3	Sm_2O_3	Eu_2O_3	Gd_2O_3	Tb_2O_3	Dy_2O_3	Ho_2O_3	Er_2O_3	Tm_2O_3	Yb_2O_3	Lu_2O_3	Y_2O_3
Distribution (%)	35.46	47.76	3.95	10.90	0.79	0.13	0.53	0.14	-	-	-	-	0.03	-	0.76

*Note: Quoted from CSRE Yearbook 2011 [7]

The Weathered Crust Elution-deposited Rare Earth Ore

The weathered crust elution-deposited rare earth ore (ion-absorbed type rare earth ore) is a unique ion-absorbed rare earth ore only exploited in China, and it is mainly located in Jiangxi, Guangdong, Fujian, Hunan, Guangxi, Hainan, Yunnan and Sichuan province. The formation of the weathered rare earth ores could be due to physical, chemical and biological weathering processes of the granodiorite and volcanic rocks [8]. Rare earth in the ores mainly exists as the hydration ions and hydroxyl hydration ions adsorbed on the clay minerals. Four major effects of ion phase RE partitioning are Ce loss, rich Eu, fractionation and Gd broken [9].

Weathered crust elution-deposited rare earth minerals are the yellow, light red and white mixture of sand and clay, which can be directly exploited by manual work. The rare earth grade is about 0.05~0.3% of REO, and more than 50% of REO enrich in the minerals with a particles size below -0.78 mm but which only account for 24~32% of the total mineral mass. The separated clay minerals of kaolin and halloysite have a REO grade of 1%.The rare earth grade along the depth of the deposit is low in the upper and bottom level but rich in the middle, but higher than rare earth grade of the bedrock at all depths. As for the transverse direction in a scale of 0~50 m, the rare earth grade has a small fluctuation, and rare earths is rich in the topographic high areas but poor in the valleys. The REO grade of different mines in the deposit greatly differs from each other with a difference of 2~6 times, and showed no apparent rules.

According to the RE partitioning, the weathered ores can be classified into three types: heavy rare earth ores, light rare earth ores and Middle Y and Rich Eu ores.

<u>Heavy Rare Earth Ore:</u> The weathered crust elution-deposited rare earth ore in Longnan Zudong, Jiangxi province is a typical heavy rare earth ore. The original rocks are muscovite-granite and biotite-granite, in which the major independent RE minerals are gadolinite and yttroparisite. The heavy rare earth ores is formed after weathering of the original rocks, and it is end member mineral deposit of heavy rare earth featured with rich yttrium. The reserve of such resource is 37 thousand tonnes, and the average rare earth grade is about 0.09% with 7% of light rare earth, 8% of middle rare earth and 85% of heavy rare earth. As seen in Table III Y_2O_3 occupies more than 60% of the total amount and Dy_2O_3 about 7%.

Table III. Rare Earth Partition of Longnan Rare Earth Ore in Jiangxi（%）

RE oxides	La_2O_3	Ce_2O_3	Pr_2O_3	Nd_2O_3	Sm_2O_3	Eu_2O_3	Gd_2O_3	Tb_2O_3	Dy_2O_3	Ho_2O_3	Er_2O_3	Tm_2O_3	Yb_2O_3	Lu_2O_3	Y_2O_3
Partition	2.18	<1.09	1.08	3.47	2.34	<0.37	5.69	1.13	7.48	1.60	4.26	0.60	3.34	0.47	64.90

*Note: Quoted from CSRE Yearbook 2011 [7]

<u>Light Rare Earth Ore:</u> The weathered crust elution-deposited rare earth ore in Xunwu, Gannan, Jiangxi province is poor in yttrium and rich in cerium [10]. It has a reserve of 22 thousand tonnes, and the rare earth grade is about 0.1%. Light rare earth occupies about 70% of the total REO, middle rare earth is 10% and heavy rare earth is 14%. Lanthanum accounts for 30~40% as listed in Table IV.

Table IV. Rare Earth Partition of Xunwu Ore in Jiangxi（%）

RE oxides	La_2O_3	Ce_2O_3	Pr_2O_3	Nd_2O_3	Sm_2O_3	Eu_2O_3	Gd_2O_3	Tb_2O_3	Dy_2O_3	Ho_2O_3	Er_2O_3	Tm_2O_3	Yb_2O_3	Lu_2O_3	Y_2O_3
Partition	38.00	3.50	7.41	30.18	5.32	0.51	4.21	0.46	1.77	0.27	0.88	0.13	0.62	0.13	10.07

*Note: Quoted from CSRE Yearbook 2011 [7]

Mid-Heavy Rare Earth Ore: The weathered crust elution-deposited rare earth ore in Ganzhou Xinfeng, Jiangxi province is a typical mid-heavy rare earth ore. It has a reserve of 22 thousand tonnes, and the average rare earth grade is about 0.05%. Light rare earth occupies about 50% of the total REO, middle rare earth is 10% and heavy rare earth is 35%. The partitioning of Eu_2O_3 is very high with an average value of 1.0% and the highest value can reach 1.4%, and this kind of minerals also contain 25% of Y_2O_3, as shown in Table Ⅴ. Mid-heavy rare earth ores were also found in Guangdong, Fujian, Hunan, Yunnan and Guangxi, which usually contains 20~30% of Y_2O_3 and 0.5~1% of Eu_2O_3.

Table V. Rare Earth Partition of Xinfeng Ore in Jiangxi（%）

RE oxides	La_2O_3	Ce_2O_3	Pr_2O_3	Nd_2O_3	Sm_2O_3	Eu_2O_3	Gd_2O_3	Tb_2O_3	Dy_2O_3	Ho_2O_3	Er_2O_3	Tm_2O_3	Yb_2O_3	Lu_2O_3	Y_2O_3
Partition	27.56	3.23	5.62	17.55	4.54	0.93	5.96	0.68	3.71	0.74	2.48	0.27	1.13	0.21	24.26

*Note: Quoted from CSRE Yearbook 2011 [7]

Enrichment and Extraction Technology

The Mineral Type Rare Earth Ore

Baiyunebo Rare Earth Ore in Inner Mongolia: It is difficult to separate rare earth from Baiyunebo ore due to the complex minerals. The specific gravity, magnetic ratio susceptibility and floatability of the minerals are relatively close just like the bastnaesite and monazite, and the mineral particles are very fine. Numerous research institutes and universities in China have put forward many new schemes and techniques for better utilization of the rare earth resource. Baogang rare earth dressing plant has improved its enrichment techniques several times during the 40 years of operation. More than ten processes have been used as follows: the mixed flotation-selective flotation and mixed flotation-gravity separation processes, the weak magnetic dressing-mixed flotation-selective flotation process, weak magnetic dressing-selective flotation to remove fluorite-bulk flotation-gravity separation with shaking table, and weak magnetic separation-strong magnetic separation- flotation process [11].

Particularly, the improved weak magnetic separation-strong magnetic separation- flotation process improve the recovery ratio of REO by 4~6 times compared to the weak magnetic separation-half selective half bulk flotation-gravity separation-flotation process. The raw material used in the process is strong magnetic middlings which contains 12% REO with a recovery ratio of 25~30%

from the original ores, and a mixture of H205, sodium silicate and H103 is used as the flotation agents. It can obtain rare earth concentrate containing REO 50~60% with a rare earth recovery ratio of 52.20% and secondary rare earth concentrate containing REO 34.48% with a rare earth recovery ratio of 20.55%, and the total recovery ratio of REO is 72.75% to the middlings and 18.37% to the original ores [12].

In the present beneficiation process in Baogang rare earth dressing plant, the operation conditions are as follows: sodium silicate (baume degree: 20, usage: 4.5~5.0 kg/t) is used as the inhibitor, LF-8 which has double activating group is used as the collector, the pH is about 7.0~8.5, the pulp density is 60~65%, mineral particles with the size of 85~90% -0.074 mm, and the flotation temperature is about 70^0C. After one roughing and two cleaning, the REO grade can be up to 50% from the original 7%, and the recovery of REO is about 55% [13].

Zeng Yongjie et al. [14] carried on an industrial experiment of getting the rare earth from the magnetic ore tailings which contains 7.0% of REO, and obtained a flotation concentrate containing 45.69% of REO. The recovery ratio of REO is 28.87% to the original ores and 32.24% to the ore tailings.

The beneficiation work of Baotou Damao Rare Earth Co., Ltd and Boyu company of Baiyunebo iron mine concerns ores which have a great amount of magnetite using the weak magnetic separation-flotation technique. The original ores are ground to 90% -0.074 mm. After the weak magnetic separation of the magnetite, the tailings are concentrated in rare earths which are floated with a combined reagent of sodium silicate, J102 and H205. The REO grade of the concentrate can be 50~60% and the secondary concentrate is 34~40% [15].

Zhang Xinmin et al. [16] has carried on experiments about the pH, collector, inhibitor and frother used in the flotation of Baotou rare earth ore. When pH is 5~6, alums is used as the inhibitor of monazite and phthalandione or 802 as the collector, bastnaesite can be separated from monazite.

Ren Jun and Lu Shouci [17] use H894 (a kind of methanoic acid) as the collector, H103 (a kind of alcohol) as the frother, and aluminum potassium sulfate as the modifier in the separation of bastnaesite and monazite. When pH of the mineral pulp is 4.5~5.5, bastnaesite can be effectively separated from monazite.

Wang Guoqiang and Xu Gencan [18] have found a new collector L247. After adjusting the pH to 4.5~5, mineral pulp density 24%, flotation temperature 24^0C, one roughing and two cleaning were carried out. The final bastnaesite concentrate has a REO grade of 66.43% with rare earth recovery ratio of 27.82%, and the content of bastnaesite is about 97.36%.

Li Mei et al. [19] have put forward a new theory of fractional mineral processing. Under the guidance of this theory, the tailing with 7.02% of rare earth (REO) was chosen as the raw material. The crude concentrate with 18.80% REO was obtained after the bulk flotation and foam separation. Then, from the crude concentrate of rare earth, the flotation process was used to separate high-grade rare earth concentrate whose REO content is greater than or equal to 65%, and the recovery ratio of this method is not smaller than 85%.

<u>Sichuang Liangshan Rare Earth Ore:</u> The conventional beneficiation processes for the

bastnaesite-featured rare earth ore are mainly gravity separation, magnetic separation, flotation, and the combination of the three methods. Bastnaesite usually co-exists with the gangue minerals such as calcite and fluorite, and their physical and chemical properties are similar. So the normal flotation agents or beneficiation methods do not provide a satisfactory result, and special enrichment methods are needed to effectively separate bastnaesite from the complex minerals. For example, heat the mineral pulp before flotation, use aromatic acid hydroxyl oxime and its salt as the flotation collector and so forth [20].

Ganzhou non-ferrous metallurgy research institutes [21] has proposed a magnetic separation-gravity separation process, and achieved good results. The original ore with a rare earth grade of 5.72% is chosen as the raw material, and a great amount of tailings were removed in the magnetic separation process. Finally, a rare earth concentrate containing 53.11% of REO with a recovery ratio of 55.36% was obtained.

Xiong Shuqin [22] has adopted a combined technique of primary grinding-classification- tabling and middlings regrinding flotation to the beneficiation of the rare earth ore, and obtained a rare earth concentrate with a REO grade of 61.18%, REO recovery ratio of 75.74%.

Xiong Wenliang and Chen Bingyan [23] use sodium silicate as modifier, derivative of hydroxamic acid as collector, at pH value within 7.15~8, and recovered a rare earth concentrate with REO content of 62.11% and REO recovery ratio of 86.98%.

Shandong Weishan Rare Earth Ore: Weishan rare earth dressing plant is a small one that was built in 1982. From 1991 to 2001, the rare earth concentrate it produced was high grade at 45~50% REO. But when the mining work switched to the underground in 2002, the REO grade of the original ores decreased. The output of the rare earth concentrate declined sharply, and so did the market share [2].

Zeng Xinnan and Li Fangji [24] recently selected reverse flotation-flotation-gravity separation process according to the floatability and the difference of specific gravity of the minerals. Firstly, NaOH, L101 (hydroxy oximino acid floating agent) and Na_2SiO_3 mixture is used for beneficiation of rare earth ore. To guarantee a satisfactory recovery ratio of rare earth, a small amount of carbonate mineral enters the rare earth rougher concentrate. This is upgraded to a high quality rare earth concentrate containing REO 68% and a middle grade concentrate containing REO 30% using a shaking table. The total recovery ratio of rare earth is 77~84%. After 3~4 times cleaning, a barite concentrate containing $BaSO_4$ 92~95% is also obtained and its recovery ratio is 61~68%.

Feng Jie and Lv Dawei [25] adopted a single flotation technique in which Na_2CO_3 was used as modifier of pH value, CH and xp-2 as mixed collectors, Na_2SiO_3 and Na_2SiF_6 as mixed inhibitors, and produced a high grade concentrate containing 68.48% REO and medium grade containing 38.60% REO. The total recovery of rare earth elements is 81.05%.

Weathered Crust Elution-deposited Rare Earth Ore

The generation of the weathered crust elution-deposited rare earth ore could be due to weathering processes of the granite and volcanic rocks which were rich in rare earth. The ore deposit is shallow and the mineral particle is loose and fine. More than 80~90% of the rare earths are adsorbed on the clay minerals of kaolin, halloysite and hydromica as hydration ions and hydroxyl hydration ions. It is not extracted by water and alcohol, but can be extracted in electrolyte solution (NaCl, $(NH_4)_2SO_4$, NH_4Cl, NH_4Ac etc) through ion exchanging and it is a reversible process.

In 1970s, China had begun to exploit and utilize the ion-absorbed type rare earth ore. After over twenty years development and substantial practice of production, in-situ leaching has been partly utilized in which the electrolyte solution is directly permeated into ore body underground, after removing impurities, adjusting pH value, precipitating with oxalic acid (or other precipitating agents) and roasting etc., a rare earth mixture containing REO over 92% is obtained. Separating the solution which has been removed impurities in factory, the necessary rare earth product can also be obtained [26]. Compared with the heap leaching technology, there are many obvious advantages of in-situ leaching technology such as a high recovery ratio of RE resources (75%), a low cost of production, and especially a great decrease in environmental pollution and ecological destruction. Using heap leaching technology to producing one tonne of RE product, 200~800 m^3 of the surface area would be exploited, and 1200~1500 m^3 of ore would be mined and left on the surface, all of which is not needed in in-situ leaching.

The geological structure and subsurface drainage of weathered crust elution- deposited rare earth mines are complicated. Different leaching processes should be appropriately used in accordance with the structure of deposits. It is suggested that the in-situ leaching technology can be applied only in an orebody with solid bedrock without fissures or cracks otherwise, the leaching agents may leak away and pollute the ground water. Therefore, it is appropriate for an orebody without a solid bedrock to select the heap leaching technology combining with land leveling and tailings-reclamation [20, 25].

Conclusions

Rare earth resources in China have the characteristics as follows:

1. The resource distribution features light rare earths mainly in the north and heavy rare earths in the south. Light rare earth ores mainly occur in Baotou, Inner Mongolia, and Sichuan Liangshan. Weathered crust elution-deposited mid-heavy rare earth ores mainly distribute in Jiangxi Ganzhou, Fujian Longyan and some other regions in the south;

2. The industrial categories of rare earth minerals are abundant, including bastnaesite, monazite, ion-adsorbed minerals, xenotime, fergusonite and so on. The RE resource is varietal and covers every RE element. The weathered crust elution-deposited mid-heavy rare earth ore play an important role in the world;

3. There are various enrichment and extraction technologies for the rare earths that should be reasonably applied according to the different characteristics of the RE deposit and form of the RE mineralization.

Acknowledgements

Financial support for this work from National Natural Science Foundation of China (no. 50974098, 51274152) and Changjiang Scholars and Innovative Research Team in University (no. IRT0974) is

greatly appreciated.

References

1. Chi Ruan and Tian Jun, Weathered crust elution-deposited rare earth ore (New York: Nova Science Pub Inc, 2008).

2. Cheng Jianzhong and Che Liping, "Current Mining Situation and Potential Development of Rare Earth in China," *Chinese Rare Earths*, 31 (2) (2010), 65-69+85.

3. Yu Yongfu, "Dressing Technology of REO Ore and It s Development in China," *Journal of Chinese University of Mining & Technology*, 30 (6) (2001), 537-542.

4. Hu Peng, "Exploitation and utilization of rare earth resources abroad," *World Nonferrous Metal*, 9 (2009) 71-74.

5. Wang Guozhen, Liu Yujiu, and Lu Zhongxiao, "The current situation and problems of light rare earth resources in China" (Paper presented at the meeting of proceedings of the 10th Chinese entrepreneurs association, 2004).

6. Cheng Jiangzhong, Hou Yunbing, and Che Liping, "Making Rational Multipurpose Use of Resources of RE in Baiyunebo Deposit," *Chinese Rare Earths*, 28 (1) (2007), 70-74.

7. Editorial Board of CSRE Yearbook, CSRE Yearbook 2011 (Beijing: The Chinese Society of Rare Earths Pub Inc, 2011)

8. Lin Chuanping and Zheng Zuoping, "Experimental studies on metallogenetic mechanism of weathering crust-leaching REE deposits in southern China," *Geochemistry*, 23 (2) (1994), 189.

9. Chi Ruan and Zhu Guocai, "Rare earth partitioning of granitoid weathering crust in southern China," *Transactions of Nonferrous Metals Society of China*, 8 (4) (1998), 69.

10. Chi Ruan et al., "Chemical behavior of cerium element in rock weathering system," *Transactions of Nonferrous Metals Society of China*, 9 (1) (1999), 15.

11. Cao Yongdan et al., "Current study situation and development on flotation of rare earth in Bayan Obo Mine," *Mining Machinery*, 41 (1) (2013), 93-96.

12. Li Yong, Zuo Jicheng, and Liu Yanhui, "Application and Research of Hydroximic Acid as Collectors on Flotation of Rare Earth Ores," *Non-ferrous Mining and Metallurgy*, 23 (3) (2007), 30-33.

13. Zhao Chunhui, Chen Hongchao, and Yue Xuechen, "Application of LF-8 and LF-6 Collectors in Rare Earth Beneficiation," *Chinese Rare Earths*, 21 (3) (2000), 1-8.

14. Zeng Yongjie, Sun Ping, and Zhao Degui, "Experimental study on recycling of the rare earth from the Baiyunebo magnetite," *Science & Technology of Baotou Steel (Group) Corporation*, 31 (4) (2005), 25-27+91.

15. Lin Ludong, Li Chunlong, and Wu Hulin, *Baiyunebo special mining metallurgy technology research and technical progress* (Beijing: Metallurgical Industry Press, 2006), 114-121.

16. Zhang Xinmin et al., “Studies about separation of bastnaesite and monazite in Baotou coarse and concentrated rare earth ore,” *Multipurpose Utilization of Mineral Resources*, (1) (1984), 14-17.

17. Ren Jun and Lu Shouci, “Mechanism of aluminum salt in flotation of bastnaesite and monazite,” *Nonferrous metals*, 49 (2) (1997), 30-35.

18. Wang Guoqiang and Xu Gencan, “Industrial experiment on the concentration of bastnaesite from the mixed rare earth ore,” *Chinese rare earths*, (2) (1985), 49-51.

19. Li Mei et al., “The application of fractional extraction theory in the rare earth mineral processing of Baiyunebo tailing,”*Journal of Inner Mongolia University of Science and Technology*, 31 (1) (2012), 4-8.

20. Yang Genlai, “Possibility of Improving Flow Sheet of Rare Earth Flotation Beneficiation,” *Chinese Rare Earths*, 26 (1) (2005), 74-75.

21. Scientific research office of Ganzhou non-ferrous metallurgy research institute, “A good target gained in the magnetic separation-gravity separation of Sichuan Dechang rare earth ore,” *Jiangxi Nonferrous Metals*, 15 (2) (2001), 29.

22. Xiong Shuqing, “An Experimental Research on Combined Gravity-Flotation flowsheet for a Rare Earth Ore in Sichuan,” *Multipurpose Utilization of Mineral Resources*, (5) (2002), 3-6.

23. Xiong Wenliang and Chen Bingyan, “Beneficiation Study on Rare Earth Ore in Mianning of Sichuan,” *Chinese rare earths*, 30 (3) (2009), 89-92.

24. Zeng Xinnan and Li Fangji, “Processing technology of bastnasite in the maoniuping rare earth deposit” (Paper presented at the academic conference on exploit and utilization of Chinese rare earth resources, Xichang, Sichuan, December 1993), 47-56.

25. Feng Jie and Lv Dawei, “Beneficiation experiment on primary minerals of Weishan rare earth mine,” *Chinese Rare Earths*, 20 (3) (1999), 5-8+15.

26. Chi Ruan, Deng Ruxin and Xu jingming, “On the comprehensive utilization of valuable elements for a rare earth deposit in South-west territory of China,” *Multipurpose Utilization of Mineral Resources*, (1) (1995), 34- 40.

RARE EARTH ELEMENTS IN TRANSPORTATION

Steve Constantinides

Arnold Magnetic Technologies Corporation
770 Linden Avenue
Rochester, NY 14625 USA

Keywords: Rare Earth, Automotive, Magnet, Phosphor, Catalyst

Abstract

Rare earth elements have a unique (atomic) electronic structure that makes them especially useful in numerous alloys and compounds. For example, they can enhance metal alloy physical strength, lend color to optics, catalyze reactions, and amplify the anisotropy field of magnets. As a result, rare earths are increasingly used to satisfy demands in the transportation industry for improved efficiencies and customer convenience. We'll review some of these applications including forecasts for growth.

Introduction

The steam engine promoted the industrial revolution, especially the invention by James Watt in 1781 which provided for continuous rotative motion in both stationary equipment and in mobile machinery such as trains, steam automobiles and steam tractors. The concept of using a compressed gas to drive a piston in a cylinder was revolutionary. The use of steam vis-à-vis water and heating with combustible materials provided a revolutionary mode of transportation. Numerous companies produced steam-powered personal transportation. The first steam car on record is from 1788, but it wasn't until the late 1800s when roads were in better condition and the mechanical workings were more dependable that steam transportation became commonplace. Steam car producers included the Locomobile Company, Stanley Company (Stanley Steamer), the American Bicycle Co., the White Motor Company, and many more. Many enthusiast clubs still maintain and show steam-powered vehicles.

Figure 1. Left picture is a Stanley Steamer manufactured c.1912. Right picture is a Riker electric car from 1897 (as shown on www.curbsideclassic.com/curbside-classics-american/curbside-classic-1897-riker-electric-back-to-the-future/)

By the late 1800s battery and motor technology had progressed to the point that vehicles could be propelled successfully for adequate distances and an acceptable speed. Battery-powered electric vehicles were utilized in Europe about 15 years prior to production and use in North America. Among the first to develop and offer an electric car in North America was William Morrison of Des Moines, Iowa, 1890-91. The six-passenger wagon was capable of 14 miles per hour. Companies that produced and sold electrically driven vehicles included the Electric Carriage and Wagon Company of Philadelphia, Anthony Electric, Baker Electric (1899-1915), and Detroit Electric (1907-1939).

By 1910 large reserves of oil had been discovered paving the way for the gasoline engine to dominate especially for longer trips where battery technology had been inadequate and steam-powered engines less convenient. The biggest drawback to the gasoline engine during the early years of adoption was the hand crank. Numerous hand and arm injuries were attributed to the crank rotating rapidly backward. The invention of the electric starter motor by Charles Kettering in 1912 mitigated this problem.

Both steam and electric cars dropped-off in popularity following the adoption of the electric starter which eliminated the need for risky hand cranking to start gasoline-powered cars. Furthermore, the introduction of assembly-line mass production of the Model T by Henry Ford, which hugely reduced the cost of owning a conventional automobile, was also a strong factor in the electric and steam car's demise as the Model T was both cheap and relatively reliable. During the 'heyday' of steam cars, the internal combustion engine made steady gains in efficiency, matching and then surpassing the efficiency of a steam engine.

Although steam-powered vehicle production essentially stopped, electrically-powered vehicle design, construction and sales have continued sporadically in many countries though at a purchase price considerably higher than that of a comparable gas-powered car. Specialty electric vehicles continue to be produced for such purposes as warehouse fork lifts, golf carts and resort transportation, short-haul urban transportation and “even the lunar rover.”

A combination of pollution and the increasingly high cost of oil renewed interest in electric-powered vehicles with numerous companies pursuing technologies of hybrid drives, full electric and plug-in electric drive trains.

Utilization of Rare Earths

Technologies for automobiles, small and large trucks, off-road and construction vehicles have evolved for decades. Most of the changes either satisfy a need (utility), provide user comfort, or offer appearance and style. Among the changes are incorporation of vehicle air conditioning for comfort or preservation of transported food quality, sound systems for enjoyment of music or warning signals, improved lighting for both on-road and in-vehicle purposes, smoothness of ride, sound-deadening, remotely operated door locks, and more. Many of these devices utilize magnetic materials and permanent or electro-magnets.

It has been estimated that a modern luxury automobile contains over 150 individual magnets. Using the sound system as an example, each speaker will contain a permanent magnet.

Sophisticated sound systems use six or more speakers. If the system has a CD drive, that uses at least one and possibly two magnets. High-end systems may also contain a hard drive which uses two permanent magnets. In other examples, three-way adjustable seats are driven in each axis by permanent magnet motors and each window uses a window-lift motor.

Cars have depended upon hydraulic and mechanical linkages to perform functions (e.g., apply brakes) and monitor performance (e.g., speedometer). Numerous illustrations of devices for cars that use permanent magnets have been published. The first one shown here is an edited version from Hitachi and additionally shows the likely magnet material used in the identified applications, either ferrite (aka ceramic) or neodymium ("Neo"). The second illustration is of the Chevy Volt from GM and indicates rare earth materials that are used to manufacture some of the car's components (e.g., cerium to polish glass) or used as a catalyst to produce the fuel for the internal combustion engine (cerium and lanthanum).

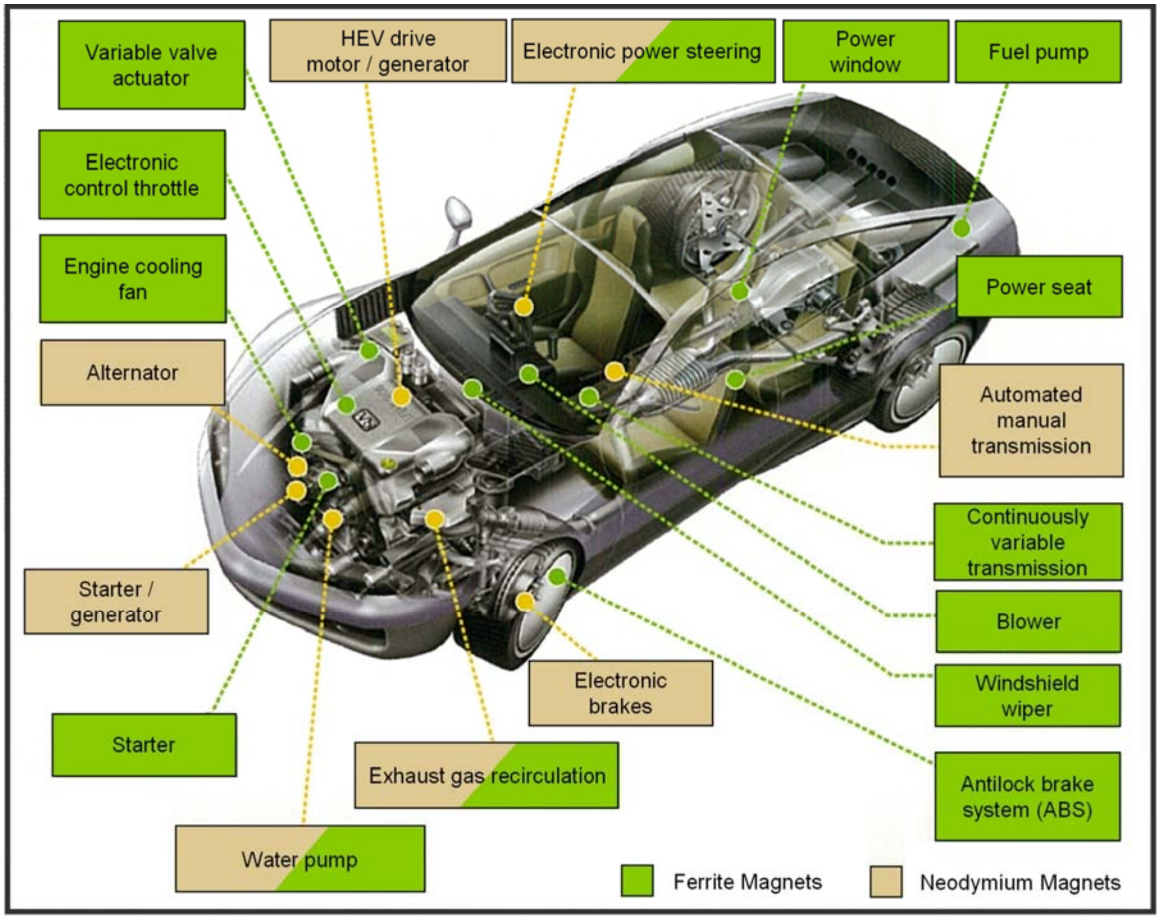

Figure 2a. Examples of uses in automotive applications. Image from Hitachi (edited to improve readability).

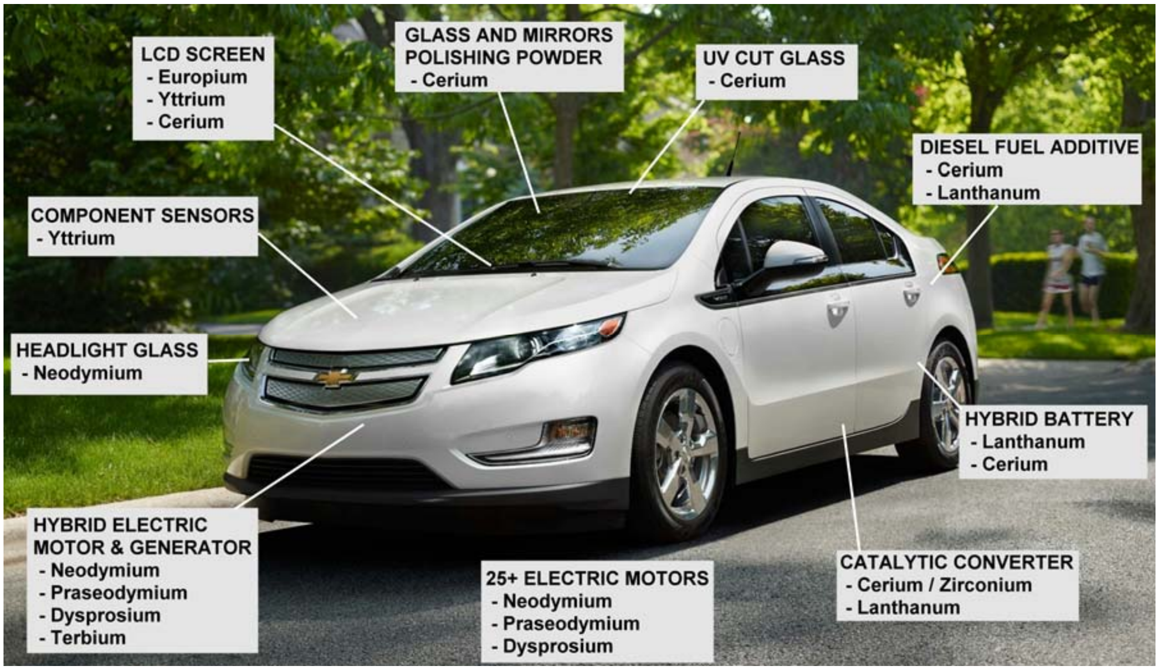

Figure 2b. Examples of uses in automotive applications: Chevy Volt (GM on-line brochure).

The increasing use of electrical rather than mechanical linkages is referred to as “drive-by-wire”. Control of the car’s functions starts with sensor input to the car’s computer and control output to motors and actuators providing desired function. One example is control of the fuel-air mixture to the cylinders via valve positioning. Another example is control of brake application pressure during uneven braking and known as ABS (Anti-lock Brake System). Speedometers (and odometers) used to be driven by a flexible cable running from the transmission to the instrument cluster. For many years now the speed of the transmission, and the speed of the car on the road, is conveyed as an electrical signal to the computer and the output used to drive gauges on the dashboard. Dashboard gauges are mostly stepper motor-driven with upwards of 100 million gauges produced each year.

According to Ali Emadi of McMaster University, “Transportation is at the center of the energy challenge, since current transportation systems are not sustainable. The most practical solution is electrification, and there is a clear shift under way from the dominant ICE and mechanical technologies toward electrical and electromechanical systems… It includes various electrification technologies, from more-electric and lightly hybridized vehicles with low electrification levels to full hybrids with medium electrification levels to plug-in hybrid and all-electric vehicles with high electrification levels.” [1]

Rare earth compounds and metals are used in many technologies associated with this transformation. The United States Geological Survey (USGS) maintains and updates statistics regarding rare earths on an annual basis and periodically publishes extended information on timely subjects. In a report published in 2011 [3], “Rare Earth Elements – End Use and Recyclability”, the global production and usage of rare earths is presented. Specifically, Table II on page 5 of the report presents the “distribution of rare earth oxide consumption by market sector" for 2008. (Refer to the accompanying Table I). Applications directly affecting the transportation marketplace are:

- Catalysts: fluid cracking catalysts (FCC) and catalysts for converters;
- Glass: polishing and dopants for clarity and color;
- Metallurgy: high strength and temperature resistant alloys;
- Magnets: sensors, speakers, motors, actuators;
- Batteries: especially NiMH;
- LCD screens: in-dash displays.

Rare earths are essential to modern transportation.

Table I. Distribution of rare earth oxide consumption by market sector in 2008. [2]

Rare Earth Oxide	**Catalysts FCCs**	**Catalytic Converters (auto)**	**Ceramics**	**Glass industry**	**Metallurgy except batteries**	**Neodymium magnets**	**Battery alloys**	**Phosphors**	**Other**	**Total**
Cerium	1,980	6,840	840	18,620	5,980	-	4,040	990	2,930	42,220
Dysprosium	-	-	-	-	-	1,310	-	-	-	1,310
Europium	-	-	-	-	-	-	-	441	-	441
Gadolinium	-	-	-	-	-	525	-	162	75	762
Lanthanum	17,800	380	1,190	8,050	2,990	-	6,050	765	1,430	38,700
Neodymium	-	228	840	360	1,900	18,200	1,210	-	1,130	23,900
Praseodymium	-	152	420	694	633	6,140	399	-	300	8,740
Samarium	-	-	-	-	-	-	399	-	150	549
Terbium	-	-	-	-	-	53	-	414	-	467
Yttrium	-	-	3,710	240	-	-	-	6,230	1,430	11,600
Other oxides	-	-	-	480	-	-	-	-	75	555
Total	19,800	7,600	7,000	28,400	11,500	26,300	12,100	9,000	7,500	129,000

Values are rounded

It will be time and space prohibitive to attempt communicating about more than a few uses for rare earths in the automotive market. We will limit ourselves here to the following: 1) Catalysts for the conversion of crude oil into fuels for internal combustion engines and for pollution minimization, 2) rare earth use in batteries and 3) electric traction drive motors as used in hybrids (HEV and PHEV) and full electric vehicles (EV and PEV).

Catalysts

The automotive market depends on catalytic reactions in at least two ways: for the production of fuels and for completing combustion in exhaust gases in vehicle catalytic converters. Rare earths are used for catalysts in both these applications. FCCs (fluid cracking catalysts) used in crude oil refining can include lanthanum and cerium which are added to take advantage of their ability to interact with the hydrogen atoms found in long-chain molecules in the starting materials.

In an article by Srikantharajah, Baillie, Zahnbrecher and Wache [3] they state: “Rare earth metals have played an important role in the refining industry since the 1970s, when it was discovered that they could be used to stabilize the zeolite-Y component of FCC catalysts to provide higher activity, as well as being used to influence product selectivity. Rare earths play an additional role in resid [residuum, “bottom of the barrel”] processing applications, as they have proven to be until now the most effective vanadium trap, helping to maintain stability and activity.”

On average from 1997 through 2009, 14% of rare earth imports into the USA were used in petroleum refining and 32% were used for automotive catalytic converters [4]. The two elements most used in catalytic reactions are cerium and lanthanum, but praseodymium and neodymium have also been used or substituted for a portion of cerium and lanthanum. Per Molycorp: “Current catalytic converters contain ≈75 grams per converter of finely divided ceria dispersed within the wash-coat.”[20] Other estimates are 80 to 100 grams of cerium oxide per unit. [21] More may be required for the converters in larger vehicles.

In a January 2012 presentation [5] by Diana Bauer she stated that: 1) lanthanum in fluid catalytic cracking (FCC) increases gasoline yield, 2) with reduced rare earth content, a shift in product yields including lower gasoline yields results in lower revenues, 3) recent [2010-11] lanthanum price increases have likely added less than 1 penny to the price of gasoline as the supply of lanthanum is less tight than some of the other rare earths and FCC manufacturers are developing zero and low rare earth catalysts. Her conclusions were stated as follows: “Rare earths play an important role in petroleum refining, but the sector’s vulnerability to rare earth supply disruptions is limited.”

Prior to about 2002 automotive catalytic converters depended only on platinum, palladium and rhodium as catalyst materials. With precious metals prices rising and consumption of these rare metals increasing, rare earths were increasingly substituted for a portion of the precious metals. According to Wards in a 2002 news story [6] “Ford Motor Co. is set to begin using rare earth oxides as a substitute for precious metals in automotive catalytic converters.” Prices for the precious metals from 1992 through 2011 are shown in Figure 3.

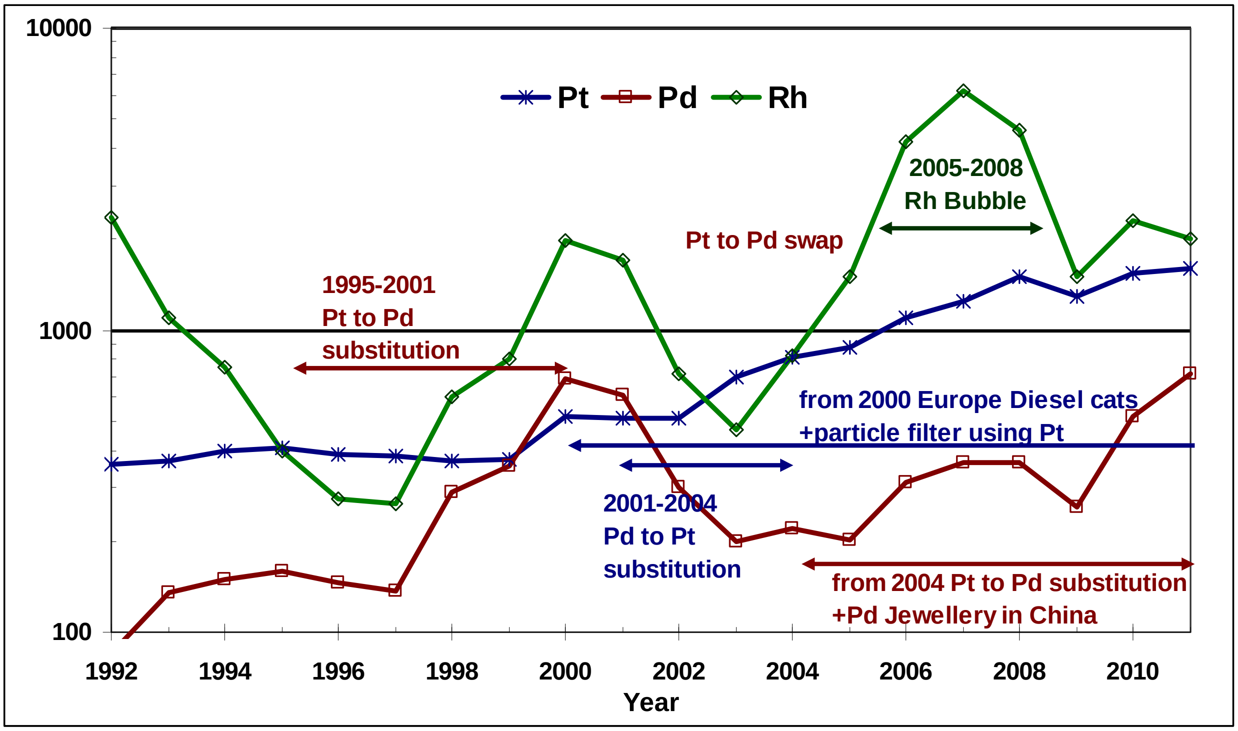

Figure 3. Precious metal pricing from 1992 through 2010. [7]

Recent reduced-content rare earth FCC catalysts are proving equally effective at catalyzing reactions. Grace Davison announced in 2011 successful commercialization of eight FCC catalysts and additives with zero or low rare earth content while maintaining a low precious metals content [8].

Automotive Batteries

Probably the single most important technology affecting growth of EV and hybrid electric vehicles is the battery. The battery provides an energy reservoir which can be filled (charged) when excess energy is available either from the drive engine, braking of the vehicle or during plug-in charging. Sales of electric motor-powered vehicles lag when the driving range of the vehicle is perceived to be inadequate for consumer needs (range anxiety). Full acceptance of EVs is said to be dependent upon expansion of the driving range. Electric vehicles have been sensitive to battery capability for over 100 years.

Current hybrid and range extender technology addresses this “long trip” anxiety. The Prius hybrid has been widely accepted having exceeded 3 1/2 million in vehicle sales since its introduction in 1997. The Chevy Volt, using range extender technology, is only two years out of the gate and has 60,000 or more units on the road. Sales of the Volt might be greater but for its relatively higher selling price of ~$40,000 (versus the Prius’ at ~$25,000).

The key figures of merit for auto batteries are the specific energy in watt•hours/kg (or watt•hours/liter, volume sensitivity) and the specific power in watts/kg. Additional figures of importance are cycles to failure, delivery of electric charge over a wide temperature range, and maintenance of charge over long periods of disuse. The first two figures of merit are often expressed on an X-Y plot called a Ragone chart (named after David Ragone). The vertical axis expresses how much total energy is available. The horizontal axis represents how quickly the electrical energy can be delivered. A plot of energy density for many types of batteries is shown in Figure 4.

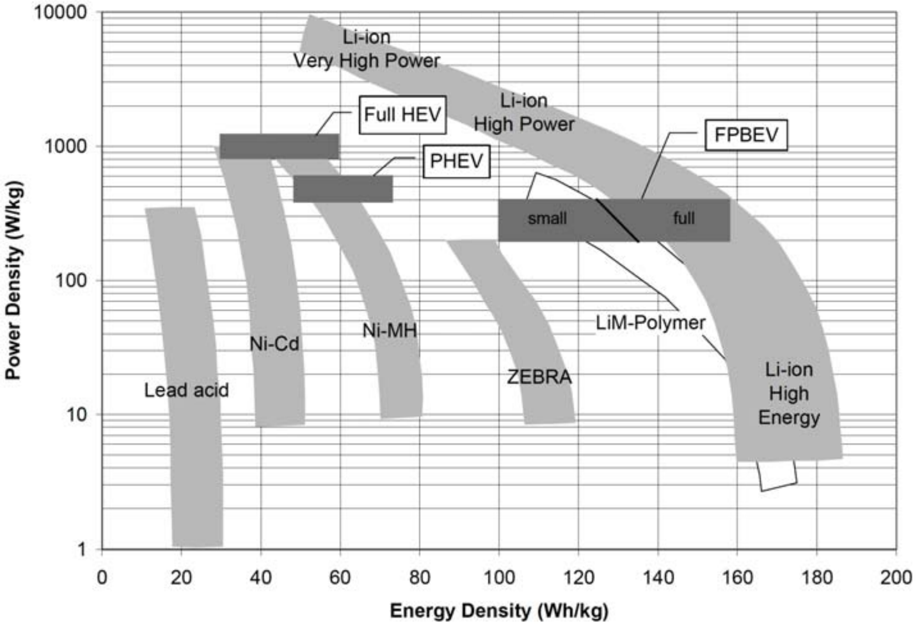

Figure 4. Ragone chart showing potential of battery technologies for HEV, PHEV, and EV applications. [9]

Lead acid batteries have been used for decades to supply current to a motor for starting the engine. They are the oldest rechargeable batteries. They are robust, provide large cranking currents and recharge repeatedly. Auto battery life of 5 to 7 years is the norm. Major shortcomings include high weight for stored charge, use of toxic components (lead, sulfuric acid), and reduction of life when repeatedly discharged (deep discharge). The development of NiMH batteries in 1989 improved battery performance, expanding the range of electric vehicles. The Toyota Prius has used NiMH batteries from its inception in 1997 through 2012. Other hybrid and electric vehicles have also used NiMH batteries though the trend is now to higher energy density, lighter weight Li-ion batteries, including for the next generation Prius.

Table II. Batteries and Related Items in Selected Hybrid Vehicles, 2004 to 2011 [10]

Year	2004	2006	2006	2007	2007	2008	2010	2010	2010	2010	2011	2011
Mfg	Toyota	Lexus	Honda	Toyota	Nissan	Chevrolet	Toyota	Honda	Ford	Mercedes-I	Hyundai	Honda
Attribute Model	Prius	RX 400h	Civic	Camry	Altima	Tahoe	Prius	Insight	Fusion	S400	Sonata	CRZ
Battery Type	NiMH	NiMH	NiMH	NiMH	NiMH	NiMH	NiMH	NiMH	NiMH	Li-Ion	Li-polymer	NiMH
Number of Modules	28	30	22	34	34	240	168	84	204	32	72	84
Battery Weight	29.4	-	-	160	160	145	64.7	65	-	-	96	65
Rare Earth Weight**, kg	8.8	-	-	48.0	48.0	43.5	19.4	19.5	-	-	-	19.5
System Voltage	201.6	288	158.4	244.8	244.8	288	201.6	100.8	275	126	270	100.8
Peak Capacity, Ah	6.5	6.5	5.5	6.5	6.5	5.76	6.5	5.75	5.5	6.5	5.3	5.75
Motor Size, kW	50	123 + 50	15	105	105	120	60	10	60	15	30	10
Fuel tank, gal	11.9	17.2	12.4	17.2	20	24.5	11.9	10.6	17.5	23.8	17.2	10.6
Driving Range*, miles	628	558	690.7	779.2	860	596	774	585	837	643	-	471
Fuel efficiency*, mpg	53	32	56	45	43	24	65	55	48	27	-	44

*Driving range and fuel efficiency w/o using accessories
** Estimated rare earth metal weight from approximate battery composition percent of total battery weight

Virtually all NiMH batteries are of the AB$_5$ type and use a mixture of four rare earth elements: lanthanum, cerium, praseodymium and neodymium. Compositions range from high cerium content to high lanthanum with praseodymium and neodymium being minor constituents of about 1 and 5 weight percent respectively. According to Linden and Reddy [11], “Two types of metallic alloys are generally used. These are the rare-earth (Misch metal) alloys based on lanthanum nickel (LaNi$_5$), known as the AB$_5$ class of alloys and alloys consisting of titanium and zirconium, known as the AB$_2$ class of alloys. In both cases, some of the base metals are replaced by other metals to improve performance characteristics. In the case of the AB$_5$ class of alloys, substitutions have improved the alloy as follows:

1. Ce, Nd, Pr, Gd and Y as a mixed or Misch metal (a naturally occurring mixture of rare earth metals) are low cost substitutes for La;
2. Ni and Co are major constituents and suppress corrosion resulting in longer cycle life;
3. Al, Ti, Zr and Si are minor constituents and increase corrosion resistance resulting in longer cycle life.”

Toyota vehicles have used NiMH battery packs made up of modules. Each module consists of 6 cells in series producing a total of 7.2 volts. Weight per module varies considerably. Depending on the vehicle and year, 28 or more modules are connected to form the battery pack. For example, in 2004 a pack of 28 modules, at an estimated 92% of pack weight being NiMH alloy contains approximately 8.8 kg of rare earth metal, the majority being lanthanum and cerium.

Figure 5. Toyota 3rd generation Prius Ni-MH battery, 28 modules, ©Toyota [17].

NiMH batteries are performing satisfactorily for longer than ten years. However, the higher performance (and lighter weight) of Li-ion batteries has proven irresistible. Toyota announced (May 2013) they are increasing production and use of Li-ion batteries six-fold in 2013 to 200,000 packs per year [17]. The intent is to upgrade the Prius family which currently uses NiMH batteries to Li-ion for all but one model.

Lithium-ion batteries offer both higher energy density and faster delivery of power. However, since their introduction in 1991 they have been plagued with problems associated with structural soundness and chemical reactivity. A few of the famous incidents are the Dell computer that caught on fire on an airplane, the battery system failure on the Boeing 787 Dreamliner and recent test failures on the Chevy Volt. The last two incidents were not problems with the battery but with the power control and structural systems. The Li-ion battery sits poised for large scale utilization in the automotive arena.

Traction Drive Motors

By definition, hybrid electric vehicles (HEV), plug-in hybrids (PHEV), full electric (EV) and battery electric (BEV) driven vehicles all use motors. Demand for the motors depends on size of the market for these vehicles and market size is a function of many factors among which are:

- Public acceptance of the change in technology;
- Perceived dependability;
- Performance: acceleration, handling, stopping, safety;
- Warranties and forecast life of vehicle and subsystems;
- How closely the new technology satisfies consumer expectations for driving range, comfort and economy;
- Vehicle cost (as compared with conventional technology);
- Expectations regarding efficiency and cost of improvements in conventional technology;

- Confidence (or lack of confidence) in pricing and availability of gasoline;
- Style and acceptability.

Furthermore, there are many kinds of motors. Those used for propelling vehicles, traction drives, fall into two general categories: 1) embedded magnet synchronous reluctance motors and 2) induction motors. There are advantages and shortcomings to each type. Induction motors do not use permanent magnets – they depend upon interaction between the stator field and an induced field in the rotor. Since there are no magnets, the magnetic fields are only slightly impacted with increasing (or decreasing) temperature of operation. Permanent magnets experience a drop in magnetic field strength as temperature increases. Maximum temperature of operation for induction motors is determined by wire insulation and rotor shaft bearings. These two components are also the primary source of motor failure. Operating efficiency is less than that for permanent magnet motors and a comparison will be shown below.

Table III. Comparison of Traction Drive Motor Technologies [14]

	Permanent Magnet Motor	**Induction Motor**	**Reluctance Motor**
Cost ($/kW)	$$$	$$	$
Power density (kW/L)	Highest	Moderate	Moderate
Specific power (kW/kg)	Highest	Moderate	Moderate
Efficiency (%)	Best	Good	Better
Noise and vibration	Good	Good	Unacceptable
Manufacturability	Difficult	Mature	Easy
Potential for technical improvement for automotive applications	Significant	Minimal	Significant

In a permanent magnet motor, size is largely determined by magnetic strength of the magnets coupled with motor rpm. For magnets, the key figure of merit is maximum energy product expressed in units MGOe (megagauss-oersted) or kA/m (kiloamps per meter). Automotive applications are volume and weight-sensitive, so the most powerful magnets are preferred – neodymium iron boron ("Neo"). Embedded permanent magnet motors require operation within a temperature range acceptable for the permanent magnet in the presence of demagnetizing stress. Neo magnets are not good high temperature magnets – they require the substitution of the heavy rare elements dysprosium or terbium to perform acceptably above about 100 °C. Dysprosium is preferred over terbium as it is more abundant and lower in price. For a magnet to perform to 180 °C requires use of 8 to 10 weight percent dysprosium. Over the last several years (2008-2012) the supply chain for rare earths into the magnet industry has been disrupted causing price increases and spot shortages. This has been largely mitigated for the light rare earths neodymium and praseodymium, but heavy rare earths are still in short supply and expected to remain so for the foreseeable future.

High raw material prices and shortages have caused consternation among motor manufacturers and the user community, most notably the automotive community as their product development cycle is 3 to 5 years long. Therefore several EV manufacturers have chosen to use induction motors, for example, Tesla Motors.

To increase power density, motor speed has been raised. Prius motor speed has been increased from 5600 rpm on the Prius THS-I to 14500 on a recent model Camry. Higher rotational speed has also permitted a reduction in total magnet weight from about 1.3 to 0.8 kg per motor.

The largest selling hybrid vehicle is the Prius. Since their introduction in 1997 and to mid-2013 sale of Prius-family vehicles have exceeded 3 ½ million vehicles. In 2012, the Prius represented 63% of hybrid and EV sales in the USA. The technology of the Prius has utilized NiMH batteries and an embedded Neo magnet drive motor. The motor allows downsizing of the internal combustion engine (ICE) without sacrificing performance. At stoplights, the ICE is turned off, saving fuel. When the accelerator is depressed, the electric motor starts the car moving while the engine re-starts.

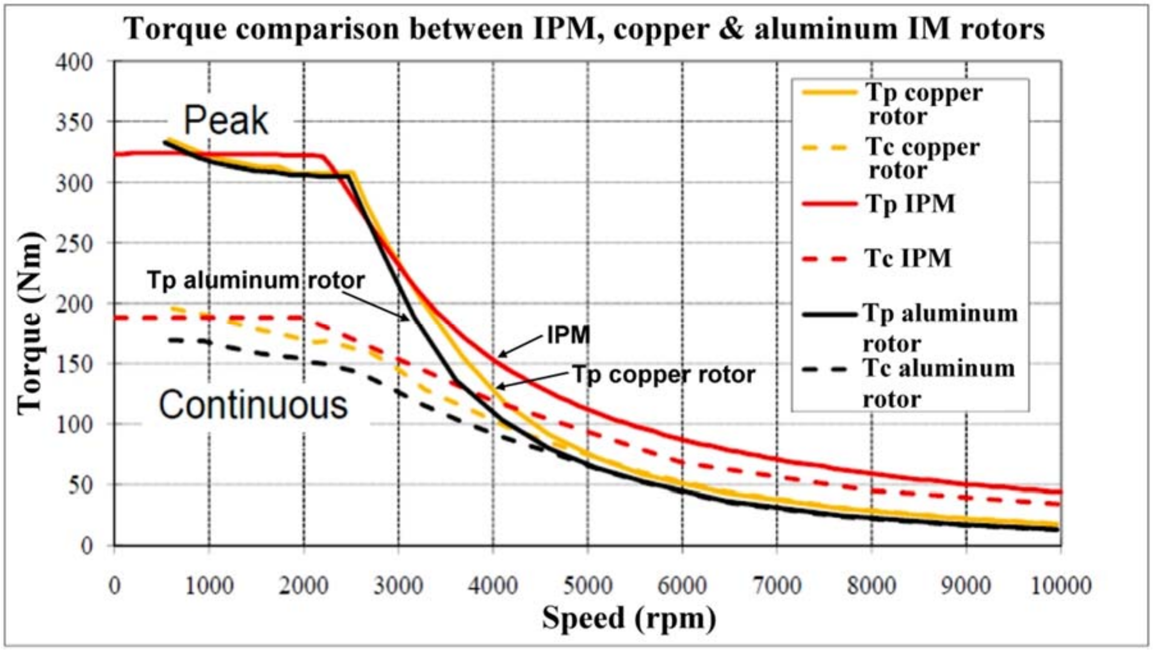

Figure 6. Torque versus Speed plot showing superior torque over a wide range of speeds for permanent magnet drives. Machine comparisons made by Remy. [12]

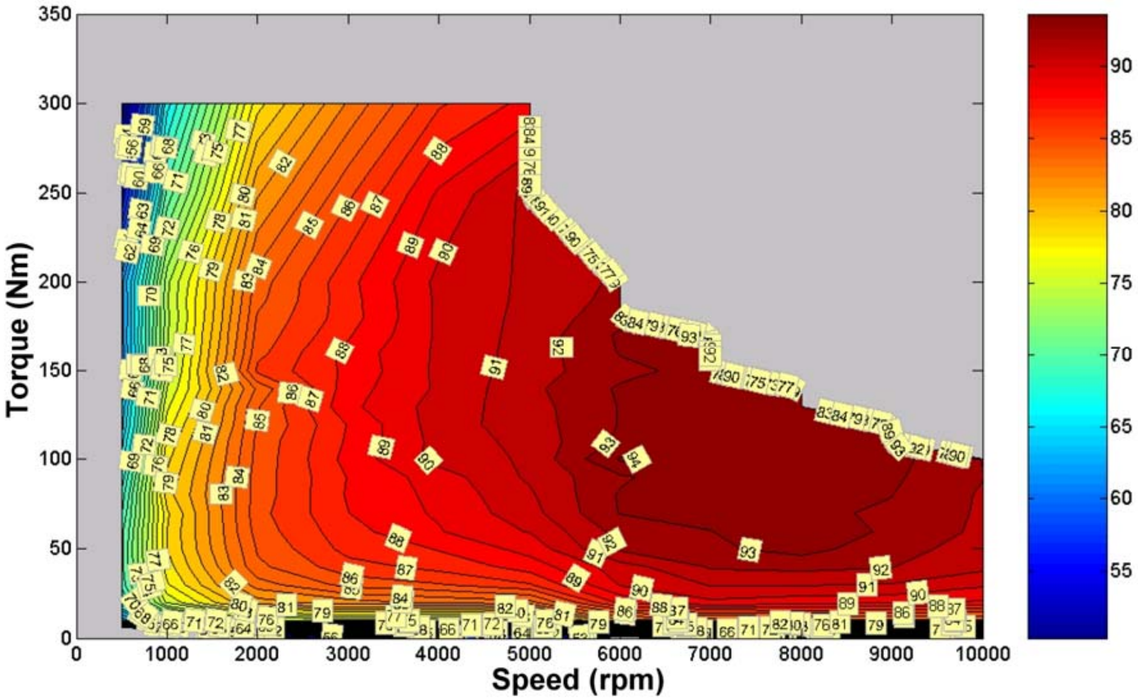

Figure 7. Efficiency plot for 2008 Lexus LS600h combined inverter-motor efficiency contours [13].

Efficient, high power density traction drive motors require sophisticated power electronics to provide drive power and control battery recharging. A simplified electronics schematic is shown in Figure 7. Hybrid vehicles have two batteries one of which is high voltage for supplying the traction drive motor and a standard "12-volt" battery to supply dashboard instruments, headlights and conventional motors.

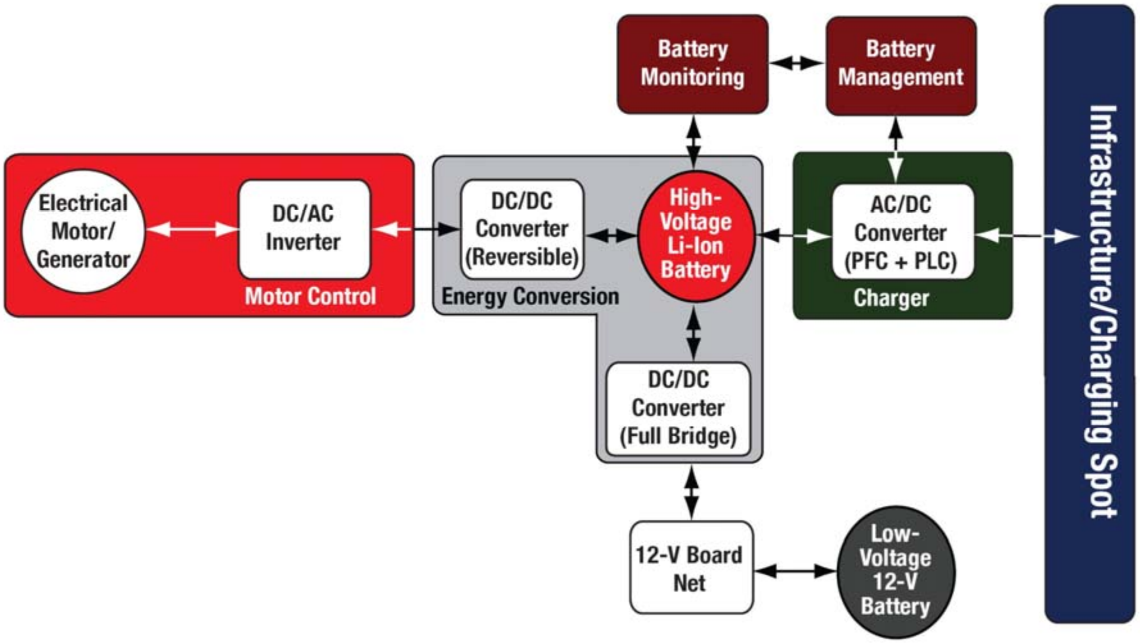

Figure 8. Electrical system architecture of HEV / EV. From Texas Instruments [19].

Several forecasts have been produced which predict the rate of market penetration for hybrid and full electric vehicles. They have been generally too optimistic. In one example, a forecast by J.D. Powers[19] is about 40% higher than actual sales by units sold in years 2011-2012. Another forecast by Frost and Sullivan compares several fuel types with hybrid adoption and by country. Adoption of hybrid drives in the Frost & Sullivan report is predicted to reach 11 to 12% of vehicle production in year 2015 with gasoline remaining high at 58-59%. In the USA, the year 2012 ended with 3.1% hybrid and EV sales. That indicates a roughly four-fold HEV and EV sales increase is required to match the forecast in Figure 7 between years 2012 and 2015.

As electric vehicle production rises, consumption of rare earths becomes of increasing interest. Production of 1 million (Toyota) hybrids at an average 0.85 kilograms Neo magnets per traction drive totals 850 tons of Neo magnets. That quantity is about 1.3% of the estimated 2010 global production of Neo magnets. Including magnet production yield loss, these magnets would require about 440 tons of rare earth oxides – approximately 0.34% of global production of all rare earth oxides in 2010. To operate at high temperature, dysprosium must be substituted for a portion of the neodymium. Traction drive motors have used 8 to 10% weight percent dysprosium. Newer magnet technologies may permit reducing the dysprosium to 6 percent. At 6% dysprosium, 19.5 tons of dysprosium oxide would be required, about 1.2% of reported 2010 production.

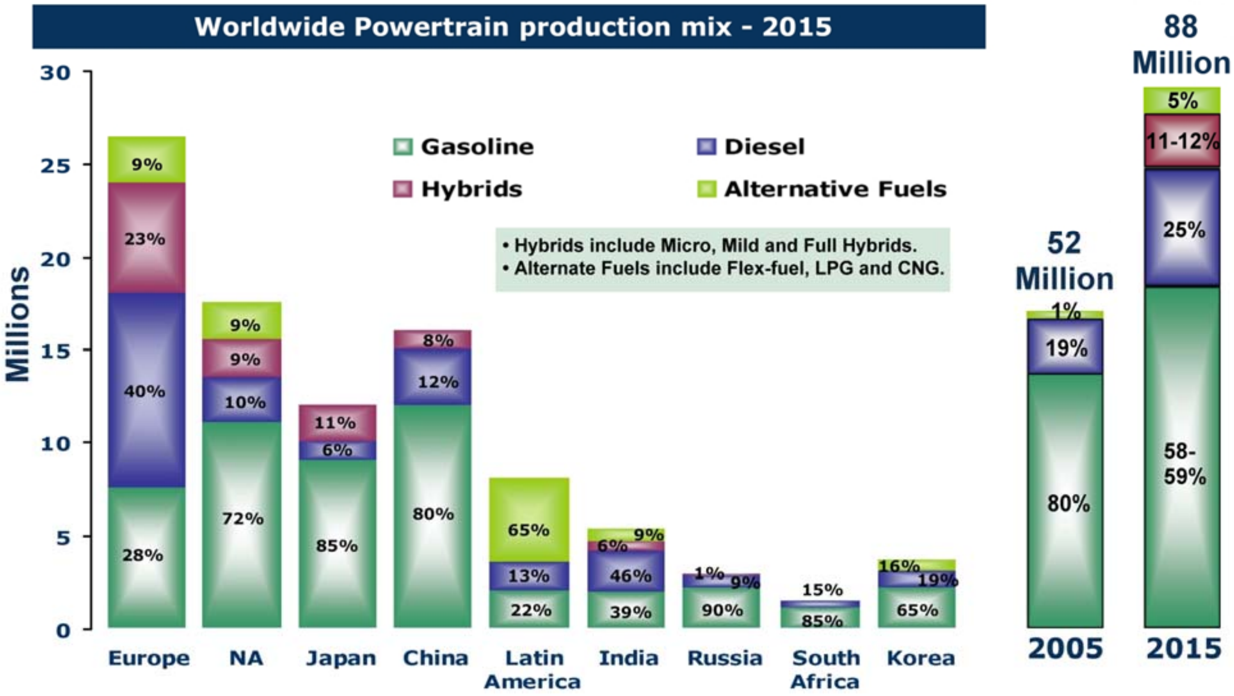

Figure 9. Worldwide Powertrain production mix for the year 2015 [15].

Summary

Automotive technologies are very dependent upon rare earth oxides, compounds, alloys and products made from them. The growing global automotive market will increase pressure on the supply chain for these products.

Adoption of more electric strategies will be influenced by cost of competitive technologies including cost of gasoline and diesel fuels. Ultimately, as communicated by Dr. Emadi [1], "Transportation 1" (internal combustion engine-driven vehicles) is not sustainable. As he states: "Power electrification results in more efficient higher performance, higher tech, cleaner, and safer vehicles."

More electric vehicles will require higher magnetic materials content: soft magnetic steels, magnets for sensors, and motor drive magnets. Many of these will be high performance rare earth-based magnets. On the other hand, transition to electric drive systems to the elimination of the internal combustion engine will reduce the demand for catalytic converters and rare earths used in them. Other magnets used in the control of combustion engine functions will also be reduced or eliminated, one example being the gas pump motor.

Mapping the transition from one set of technologies to the next will be critical in avoiding material shortages and supply chain disruption.

References

1. Ali Emadi, Transportation 2.0, IEEE power & energy magazine, 23 June 2011.
2. Thomas G. Goonan, *Rare Earth Elements – End Use and Recyclability*, USGS Scientific Investigations Report 2011-5094, Table 2, p.5.
3. Srikantharajah, Baillie, Zahnbrecher and Wache, *Evaluation of a low rare earth resid FCC catalyst*, www.digitalrefining.com/article/1000266, downloaded 5/29/2013.
4. USGS annual Mineral Commodity Summaries for the years 1997 through 2011, downloaded from www.usgs.gov
5. Diana Bauer, Office of Policy & International Affairs, Critical Materials Workshop, 3 April 2012, p.53.
6. Wards Auto Staff report, *Rare Earth Oxides for Catalysts*, http://wardsauto.com/news-amp-analysis/rare-earth-oxides-catalysts, 21 May 2002 .
7. *Determination of Platinum, Palladium, and Rhodium in Spent Automotive Catalytic Converters with Thermo Scientific Niton XL3t Series Analyzers*, Thermo Fisher Scientific, 2012.
8. Shawn A. Abrams, *Zero/Low Rare Earth FCC Catalyst Technology Ready for Commercialization*, Refinery Operations, Vol.2 ISS.14, 20 July 2011.
9. Kalhammer et al, *Status and Prospects for Zero Emissions Vehicle Technology*, Report of the ARB Independent Expert Panel 2007, April 3, 2007, p.25.

10. Advanced Electric Vehicle Testing Reports, http://www1.eere.energy.gov/vehiclesandfuels/avta/light_duty/hev/hev_reports.html, downloaded during May 2013.

11. David Linden, Thomas B. Reddy editors, *Handbook of Batteries, Third Edition*, McGraw-Hill, 2002, p.29.3.

12. John M. Miller, *APEEM Electric Motors Overview*, DOE Vehicle Technologies Program, FY13 Kickoff Meeting, Oak Ridge National Laboratory, November 13, 2012.

13. Tim Burress, *Benchmarking of Competitive Technologies*, DOE Vehicle Technologies Program, FY13 Kickoff Meeting, Oak Ridge National Laboratory, November 3, 2011.

14. Laura D. Marlino, *Electric Motors Overview*, DOE Vehicle Technologies Program, FY13 Kickoff Meeting, Oak Ridge National Laboratory, November 4, 2011.

15. *The Global Oil paradox - Transforming the Automotive Industry: Strategic Assessment of the Global Alternative Powertrain Market*, Frost & Sullivan, 2008.

16. Published in Nikkei business daily, as reported by Reuters, *Toyota plans to increase lithium-ion car battery output*, 19 May 2013, downloaded 2013-05-21 from: www.reuters.com/article/2013/05/19/toyota-battery-idUSL3N0E002O20130519

17. Picture of 3rd generation Prius Ni-MH battery, downloaded 27 May 2013 from www.toyota.com/esq/vehicles/batteries/nickel-metal-hydride.html

18. *Hybrid and Electric Vehicle Solutions Guide, System Solutions for Hybrid and Electric Vehicles 2013*, Texas Instruments, downloaded from www.ti.com/hev

19. *2011 US Green Automotive Study*, J.D. Powers and Associates, 2011, downloaded from https://pictures.dealer.com/jdpower/f0391cbb0a0d02b7004dd014ba12057d.pdf

20. Quote downloaded from Molycorp website on Jun 6, 2013.

21. *Potential for Recovery of Cerium Contained in Automotive Catalytic Converters*, Donald I. Bleiwas, U.S. Geological Survey, January 1, 2013, p.2.

MITIGATION OF RARE EARTH SUPPLY RISK POSED BY PERMANENT MAGNETS USED IN ELECTRIC MACHINES

Francis Johnson

GE Global Research
One Research Circle, MB-241
Niskayuna, NY 12309 -518-387-5087
johnsonf@ge.com

Keywords: Rare Earths, Critical Materials, Permanent Magnets, Electric Machines

Extended Abstract

Electric machines utilizing rare earth-based permanent magnets have permeated the economy. These include electric vehicles and wind generators. In 2010, 274,600 hybrid electric vehicles were sold in the United States [1]. Each hybrid vehicle utilizes a permanent magnet electric motor that requires approximately 2 kilograms of high performance neodymium iron boron (NdFeB) permanent magnets [2] per motor. In 2012, 13,131 MW of wind power installations were completed in the United States [3]. Both on-shore and off-shore wind turbines can utilize permanent magnet based generators. Direct-drive off-shore wind turbines can require over 500 kilograms of NdFeB permanent magnets per MW of rated generation capacity. These clean energy technologies have driven substantial increases in the demand for the rare earth elements used to manufacture NdFeB and other permanent magnet compositions.

NdFeB magnets are based on the $Nd_2Fe_{14}B$ compound. First reported in 1983 [4,5] these materials systems have the highest energy product of any commercially available permanent magnet. Commercially produced grades typically contain up to 30 weight % of Neodymium (Nd). NdFeB compositions used in electric machines must be modified to overcome the steeply negative temperature coefficient of intrinsic coercivity displayed by $Nd_2Fe_{14}B$-based magnets. The intrinsic coercivity is a material property that sets the temperature capability of a permanent magnet. One effective strategy to increase the intrinsic coercivity of NdFeB is to substitute Dysprosium (Dy) for Nd [6]. High temperature NdFeB grades may contain up to 10 weight % Dy.

Figure 1 indicates the limitation of this approach. Dy is less abundant than Nd and its price is correspondingly higher. Both Nd and Dy have been identified as critical elements and are subject to supply constraint in the short and medium term [7]. Volatility of the price of rare earth elements highlights the importance of a co-ordinated strategy to mitigate their supply risk. The situation is complicated by the disparate functionality of the rare earth elements used in magnets coupled with the need for other critical elements like Cobalt.

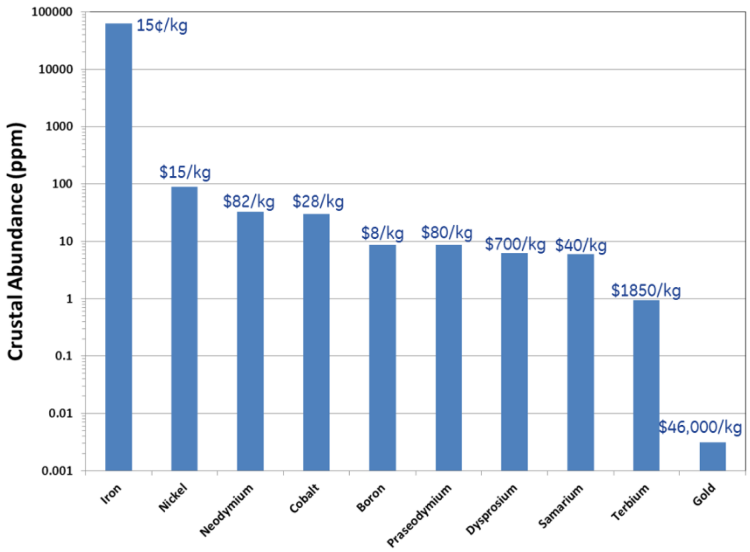

Figure 1. Relative abundance of elements in the earths crust, including those used in rare earth magnets, and their prices as of May, 2013 [8].

Several technology development paths are being pursued to develop alternatives to rare earth permanent magnets such as NdFeB. Material developments include advanced rare-earth permanent magnets that minimize the need of critical heavy rare earths such as Dy, nanocomposite permanent magnets that partly substitute non-critical elements, as well the search for new permanent magnets based compounds with no rare earths.

Nanocomposite permanent magnets have the potential to exceed the energy product of bulk NdFeB while simultaneously achieving reduced rare earth content [9,10]. In these materials a high magnetization, soft magnetic phase such as Iron-Cobalt is substituted for some fraction of a high coercivity permanent magnet phase. The remanence is increased due to the increase in average magnetization of the two phases. An increase in energy product requires both exchange coupling between the constituent phases as well as crystallographic alignment of the hard phase grains. Satisfying these conditions requires achieving nanoscale control of the composite microstructure. This necessitates the development of novel processing methods to manufacture kilogram-scale magnets needed for electric machine applications. Figure 2 shows a schematic of a nanocomposite structure that could show an enhancement in energy product.

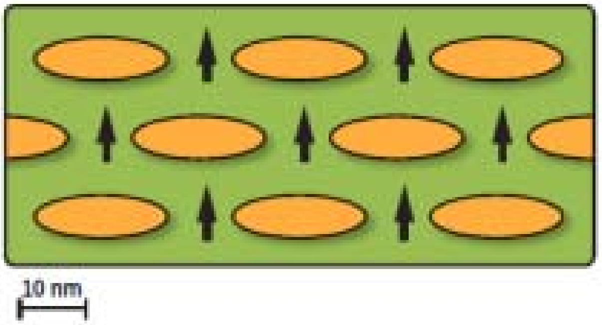

Figure 2. Schematic nanocomposite permanent magnet structures. Hard permanent magnet grains are crystallographically aligned and dispersed in soft magnet matrix. Length scales are on the order of 10 nm in order to promote exchange coupling of the two phases.

Permanent magnet machines operate by combining torque produced by permanent magnets with reluctance torque from the electrical steel laminations of the rotor. The left side of Figure 3 shows a permanent magnet machine in which the magnets are internal to the rotor. The magnetic flux produced by the magnets reacts across the airgap with an AC field generated by the windings on the teeth of the stator. The right side of the figure shows an alternate synchronous design powered completely by reluctance torque. Such switched reluctance machines use no permanent magnets but face challenges in noise, power density, efficiency, and manufacturability. Alternative machine technologies under development also include advanced permanent magnet machine designs as well as other non-permanent magnet based designs such as induction and superconductor machines.

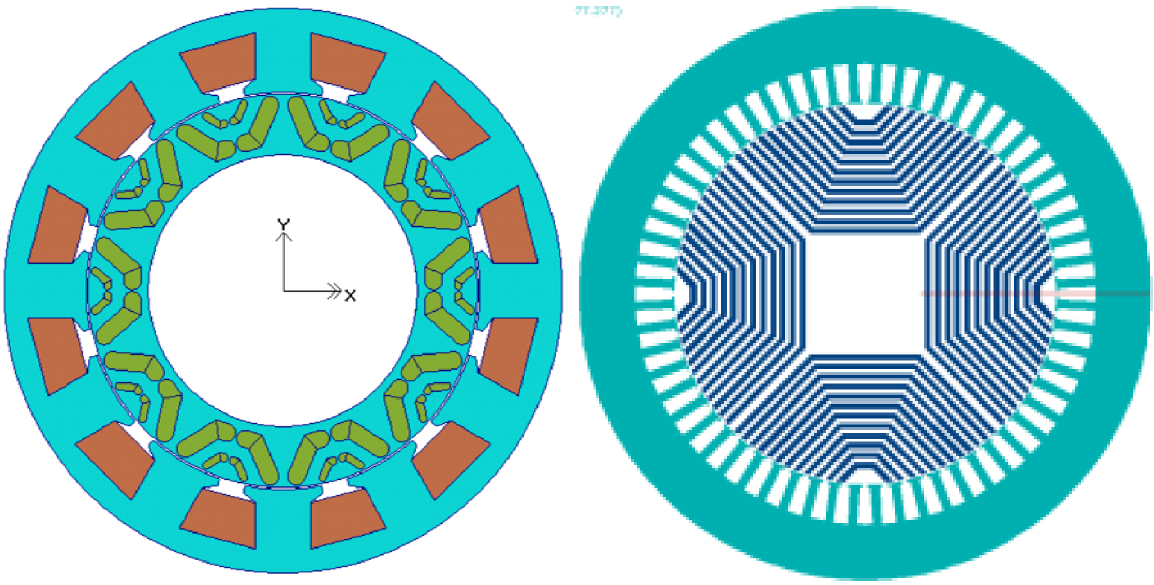

Figure 3. Left image is a schematic of an internal permanent magnet machine in which the permanent magnets are embedded in the rotor. Right image is a schematic of a synchronous reluctance machine [11].

Mitigation of the supply risk posed by rare earths to electric machines requires a co-ordinated approach including the development of new materials, new manufacturing methods, and new machine topologies. New materials will inherently have new trade-offs in properties. Parallel development of materials and machines enables designers to leverage these trade-offs to optimize total system performance.

References

1. Transportation Energy Data Book, U.S. Department of Energy, 31st, edition, 2012.

2. FreedomCar Advanced Traction Motor Development Phase I report, ORNL/TM-2006/UQM, 08-04-2006.

3. 2012 U.S. Wind Industry Market Update, American Wind Energy Association.

4. J.J. Croat., J.F. Herbst, R.W. Lee., and F.E. Pinkerton, "High-energy product Nd-Fe-B permanent magnets," *Appl. Phys. Lett.,* 44, (1984), 148-149.

5. M.S. Sagawa,, S. Fujimora, N. Togawa, H. Yamamoto, and Y. Matsuura, "New material for permanent magnets on a base of Nd and Fe," *J. Appl. Phys.,* 55, (1984), 2083-2087.

6. M. Sagawa, S. Hirosawa, K. Tokuhara, H. Yamamoto, S. Fujimura, Y. Tsubokawa, and R. Shimizu, "Dependence of coercivity on the anisotropy field in the $Nd_2Fe_{14}B$-type sintered magnets," *J. Appl. Phys.,* 61, (1987), 3559-3591.

7. Critical Materials Strategy, U.S. Department of Energy, December 2011.

8. Pricing data from www.metal-pages.com and www.lme.com.

9. E.F. Kneller and R. Hawig, "The exchange-spring magnet: A new material principle for permanent magnets," *IEEE Trans. Mag.,* 27 (1991), 3588-3600.

10. R. Skomski and J.M.D. Coey, "Giant energy product in nanostructured two-phase magnets, " *Phys. Rev. B*, 48 (1993), 15812-816.

11. Manoj Shah et al., US Patent # 7,489,062.

ASSESSMENT AND MANAGEMENT OF RADIOACTIVITY IN RARE EARTH ELEMENT PRODUCTION

D. Grant Feasby[1], Douglas B. Chambers[2] and Leo M. Lowe[3]

[1]Senior Specialist, Metallurgy and Mine Environment
[2]Director of Risk and Radioactivity Studies
[3]Principal, Senior Health and Environmental Physicist

ARCADIS SENES Canada Inc, 121 Granton Drive, Unit 12
Richmond Hill, ON L4B 3N4

Keywords: Rare Earth Elements, NORM, Radioactivity, Radiation Dose

Abstract

All rare earth element (REE) ore deposits contain minor levels of thorium- and uranium-based radioactivity. Usually, the radioactivity levels are so low that they are of minimal concern for workers' health and safety and environmental management. Potentially economic deposits of REE normally contain slightly elevated levels of thorium and uranium (compared to background) – these are classified as naturally occurring radioactive materials (NORM). In this paper, example concentrations of NORM in REE resources are given for Canadian and other deposits around the world. The significance of these concentrations in terms of potential occupational radiation exposures, regulations and measures to be considered in developing a REE mine, metallurgical extraction and waste management facilities are outlined.

The presence of mineral-based radioactivity is frequently a concern to the general public as well as workers. This concern can affect decisions of regulatory institutions. Transparent information sharing is essential to avoid uninformed resistance to REE resource development. A suggested approach in addressing public concern is outlined.

Introduction

Rare Earth Elements (REE) are a group of 15 metallic elements known as lanthanides, plus 2 other elements – scandium, and yttrium. Commonly, these elements are termed light (LREE) or heavy (HREE) as highlighted in the familiar version of the periodic table shown in Figure 1.

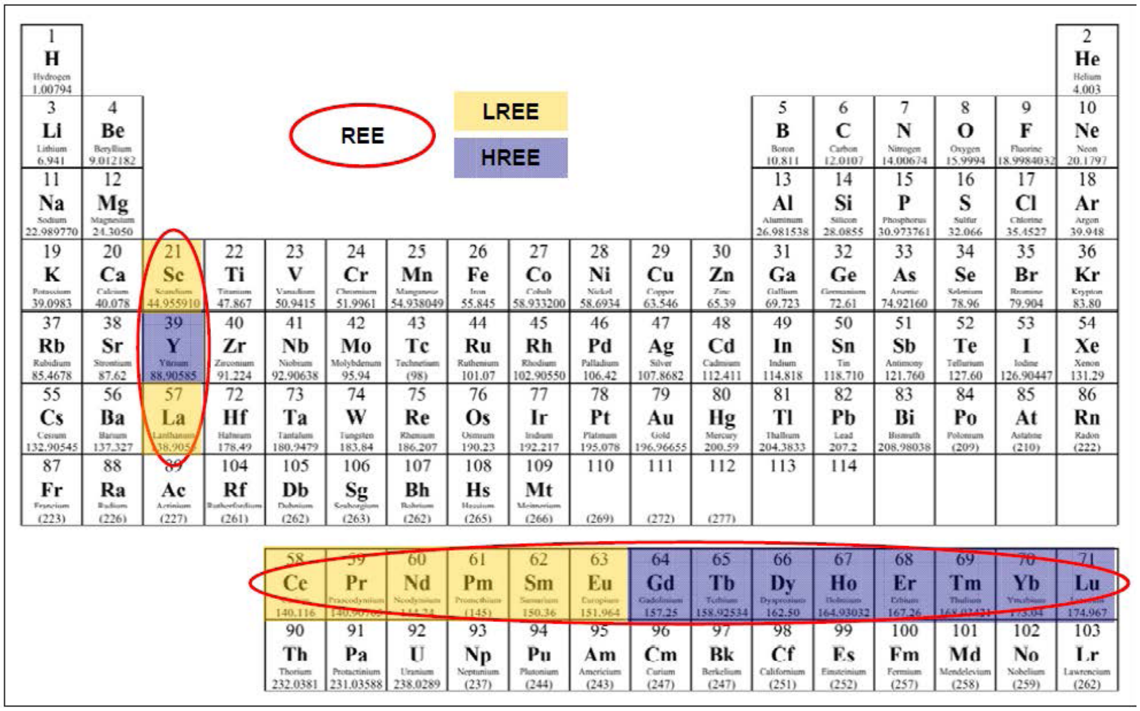

Figure 1. Period table of the elements (REE highlighted).

Paradoxically, these elements are not so rare in the rocks and soils around us. For example, the element crustal abundance of lead, tin is similar to the abundance of REE, but the abundance of precious metals – gold, silver, platinum - is much lower. Example concentrations of REE and other metals are shown in Table I. [1]

Table I. Earth's Crustal Abundance of REE and Common Metals

Element	Concentration (ppm)	Comments
Copper	68	
Cerium (Ce)	60	LREE
Lanthanam (La)	30	LREE
Neodymium (Nd)	27	LREE
Yttrium (Y)	24	HREE
Scandium (Sc)	16	LREE
Lead	10	
Praseodymium (Pr)	7	LREE
Thorium	11	Radioactive
Samarium (Sm)	5	LREE
Gadolinium (Gd)	4	HREE
Dysprosium (Dy)	4	HREE
Uranium	2.5	Radioactive
Tin	2	
Erbium (Er), Ytterbium (Yb), Europium (Eu), Holmium (Ho), Terbium (Tb), Lutetium (Lu)	0.5 – 2	
Silver	0.1	
Gold	0.003	

While the main source of REE production from ore resources to meet modern industrial needs has been and is currently China, there are a large number of emerging and potential REE developments in Canada and around the world. With minor exceptions, all RE deposits contain some amounts of thorium and uranium-based radioactivity. Although the thorium and uranium contents may be low, public and institutional interest in RE resource development has increasingly focused on the radioactivity aspects related to these developments.

Concern about radioactivity associated with REE developments can be due to exaggerated legacy issues that arose because of historically careless practices combined with poor regulatory oversight and the absence of precise documentation and measurements. Such concerns are also often inflamed by unfounded claims of individuals and non-governmental organizations (NGO's).

This paper provides a review of the thorium and uranium content of a number of REE resources, an assessment of radioactivity and radiation exposure levels and a discussion of established and reliable methods of managing exposure to radiation and radioactivity.

Uranium and Thorium Based Radioactivity in REE Ores and Resources

The radioactivity in REE resources is principally due to the presence of thorium (Th-232 "decay series" radionuclides) and to a lesser extent uranium (both the U-238 and U-235 decay series radionuclides). Thorium and uranium are only two of the many (about 85) naturally-occurring radioactive elements found on earth. From an ambient radiation perspective, other important elements include potassium (K-40) which is a small fraction (0.01%) of total potassium, carbon

Table II. Principle Radioactive Elements Associated with REE Radioactivity

Source Element	Decay Half Life, Years	% of total element	#Number of Elements in Decay Series	Comments
U-238	$4.4 (10)^9$	99.7	14	Ra-226, Rn-222, Pb-210, Po-210 key daughters, from risk top people perspective
U-235	$7.0 (10)^8$	0.3	12	
Th-232	$1.4 (10)^{10}$	99.999	10	Ra-228, Rn-220 key daughters from risk perspective
La-138	$2 (10)^{11}$	0.09	2	Very low specific activity
Nd-144	$5 (10)^{15}$	23	2	Extremely low specific activity as a result of very long half life
Sm-147	$1.3 (10)^{11}$	2.6	2	Very low specific activity
Ac -227	22	-	-	Decay product of U-235. Ac behaves chemically like REE and can be concentrated in REE products[1]

---

[1] Technologies for removal of Ac-227 are discussed in [2].

(C-14) and tritium (H-3). C-14 and H-3 are produced by the interaction of cosmic and solar radiation on the earth's atmosphere. Of some interest is the fact that some of the REE has radioactive isotopes. These, plus other elements in the radiation pedigree of REE production, are the elements shown in Table II.

The radioactive elements decay to other radioactive elements and eventually to stable elements by emitting combinations of alpha particles (a helium nucleus), beta particles (an electron) and gamma radiation (penetrating electromagnetic radiation, identical to X-rays but of higher energy). Radioactivity, whether natural or technologically-enhanced, is typically a banner public concern.

Naturally occurring radioactive materials (NORM) are present in resource-based industries throughout the world. These include, to name a few, the oil and gas industry, phosphate fertilizer facilities, aluminum wastes, gold and silver mining, and titanium production wastes, as well as REE developments. Comparisons of the NORM radioactivity (in Becquerel's/gm, Bq/g) are shown in Figure 2. The becquerel (Bq) is the unit used in the International System of Units (SI) (the "metric" system) to represent the activity of a radionuclide. One becquerel equals one nuclear disintegration per second. There is a direct relationship between the mass and the radioactivity of a radionuclide, which is called its "specific activity". The specific activity is inversely proportional to the half-life of the radionuclide and is expressed in becquerels per gram (Bq/g). The longer the half-life, the smaller the specific activity. In particular, a concentration of 1 ppm of natural uranium (U-nat) corresponds to 0.01235 Bq of U-238 per gram. At equilibrium (i.e., the uranium has not been chemically or physically altered), natural uranium contains equal radioactivity concentrations (in Bq/g) of all 14 radionuclides in the U-238 series. A concentration

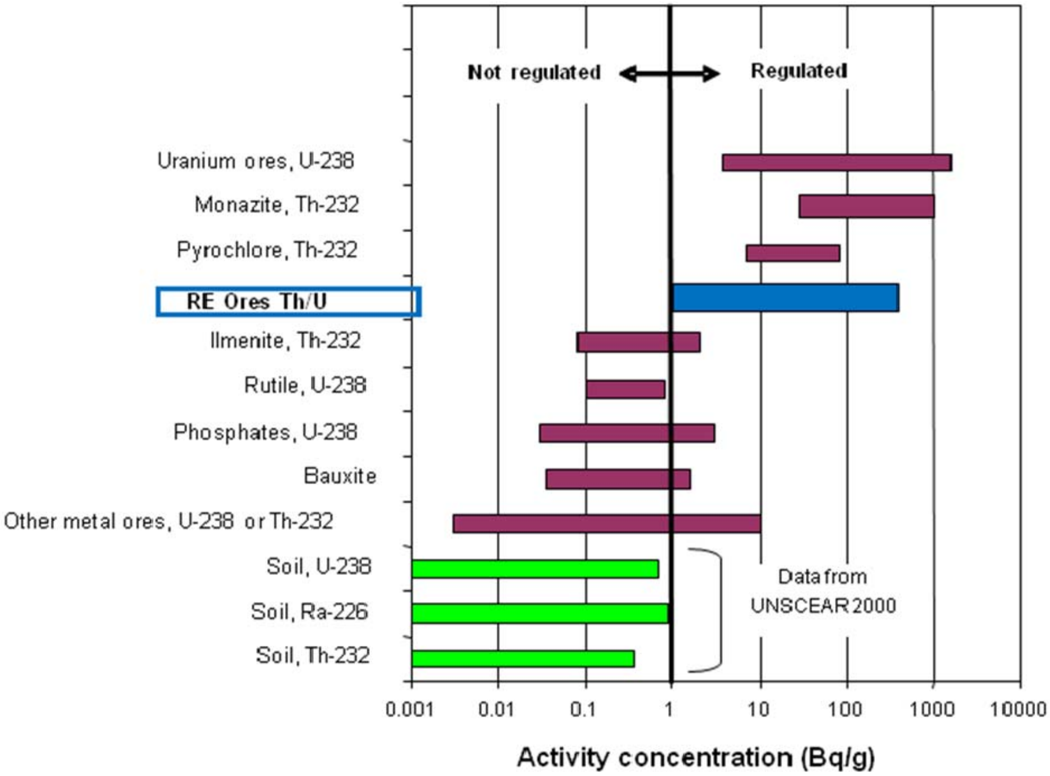

Figure 2. Naturally occurring radioactive material (NORM) in mineral resources and soils.

of 1 ppm of natural thorium (Th-nat), which has a half-life about three times longer than U-238, corresponds to 0.00406 Bq of Th-232 per gram. Natural thorium contains equal concentrations (in Bq/g) of all the radionuclides in the Th-232 decay series. [Natural uranium (or natural thorium) refers to uranium (or thorium) with its natural isotopic abundances.]

A comparison of uranium and thorium concentrations in REE ores, mineralised zones and resources with natural background concentrations and two types of uranium ore (assumed to be in equilibrium) is shown in Table III.

Table III. Example Uranium and Thorium Concentrations

Location	Uranium (ppm)	Thorium (ppm)	Total Activity (Bq/g) Assuming Equilibrium
Fresh water	0.001 - 0.10	0.00003-0.0005	
Hard rock	0.5 - 5	2 - 20	Up to 1.9
Soils	0.5 - 10	10 - 20	Up to 2.5
Historical Ontario U ores (two types)	800-1200	250-1800	150-220
REE Ore Resources			
Bastnasite (US)	20	200	12
Xenotime (Malaysia, mineral alone)	6,800	7,000	1500
Monazite (South Africa)	150	3500	170
Zircon sands (Australia)	100	450	35
REE hard rock ore 1 (Canada)	30	250	14
REE hard rock ore 2 (Canada)	23	110	8.5
REE hard rock ore 3 (Canada)	340	290	71
REE hard rock (Sweden)	7	14	1.8
REE hard rock 1 (Africa)	300	1000	92
REE hard rock 2 (Africa) (monazite vein)	200	25,000	110

Usually, NORM concentrations are not sufficiently elevated to pose a potential hazard to people. In some cases however, where the radionuclide concentrations are much higher than the normal range of background levels, such as in REE minerals, there may be potential for correspondingly elevated radiation doses to people and the environment.

The development of REE resources and the production of REE concentrates involve the handling of rock, tailings, metallurgical concentrates, solutions and residues. The radioactivity in these materials mainly originates from the Th-232 and the U-238 series – chains of 10 and 14 decay products or radionuclides, respectively. The U-235 series is also present in natural uranium but at a low concentration (0.7% of uranium by mass). As previously noted in Table II, actinium-227 (a product of U-235) may concentrate in REE products.

In managing the radioactivity from the thorium and uranium series, several radioactive decay elements have been identified that may need to be followed in REE metallurgical processes. The main ones from a radiological protection perspective are shown in Table IV.

Table IV. Principle Decay Elements (other than Th and U parents) to be Managed in REE Production

Radionuclide	Series	Comment
Th-230	U-238	Behaves chemically the same as Thorium -232.
Radium-226	U-238	Chemically similar to calcium and barium.
Radon-222	U-238	A radioactive noble gas. Naturally present in ambient air, typically in the range of 5-50 Bq/m^3. Responsible for about 50% of background radiation dose.
Lead-210	U-238	A radioactive isotope of lead.
Polonium-210	U-238	An important source of radiation dose if ingested.
Actinium-227	U-235	Chemically similar to REE. Originates from the less abundant U-235 series.
Radium-228	Th-232	
Radon-220	Th-232	A radioactive noble gas.

Distribution of Radioactivity in Extraction Processes and Products

Mining and processing strategies for REE concentrate production are resource and location specific and are generally as follows:

(i) RE mineral concentration – gravity and/or froth flotation, wet magnetic separation. This mineral concentrate can be processed at the mine site or shipped to a dedicated hydro-(or occasionally pyro-) metallurgical facility. Unless disturbed by chemical or metallurgical processing, Th and U are usually in radioactive "equilibrium" with the radionuclides in their respective decay series, i.e., the radioactivity concentration of each radionuclide (Bq/g) is equal to the U-238 or the Th-232 concentration in each series. The radioactivity represented in each chain will be slightly concentrated in the mineral concentrate, but radioactive equilibrium will be maintained;

(ii) REE mineral "breakdown" using aggressive chemical leaching processes such as:
- Acid baking with concentrated sulphuric acid at high temperature (e.g.150°C or much higher). Hydrochloric acid is an alternative,
- Hot fusion with caustic soda (sodium hydroxide), water leaching of soluble silicates, followed by acid dissolution of residue, or
- For certain mineral concentrates (e.g. Eastern Canadian), weak acid sulphuric acid leaching at ambient temperatures.

(iii) The leaching solutions containing the REE, impurities such as Fe, Zr, U, Th and Ra-226 and Ra-228, Pb-210 and Po-210, are purified using a combination of selective precipitation, solvent extraction and ion exchange;

(iv) Thorium removal is completed by precipitation as $Th(OH)_4$ and uranium can be selectively removed from solution by ion exchange and subsequently precipitated with lime and magnesia. Radium removal is assisted by the addition of barium salts to precipitate $Ba(Ra)SO_4$. Lead and polonium also report to the residues;

(v) The REE are precipitated as either oxalates or carbonates, dried and shipped or transferred to the specialised processing facilities for separation into specific elements using solvent extraction;

(vi) Alternative sources of REE include recovery as a by-product from uranium mining or tin mining. A potential REE-U resource is being actively investigated in the historical Elliot Lake, Ontario uranium mining district in Canada. Some tin resources (Brazil) contain REE as well as Th and U which can concentrate in metallurgical slags. These two REE sources require tailored processes, which could involve the isolation and sale of uranium concentrates.

Hydrometallurgical REE concentrate specifications typically stipulate very low levels of radioactivity in the concentrate, e.g. < 0.04 Bq/g for each radionuclide [3]. For example, this translates into a maximum of 3 ppm uranium or 10 ppm thorium in the REE concentrate, levels which are similar to ambient background levels in soil. Typically, radionuclides such as Th, U, Ra are selectively removed in the hydrometallurgical processes and are combined with metallurgical wastes. The reasons for the tight specifications include the avoidance of elevated radiation doses at the concentrate processing (REE separation) facility and elimination of the need for specially-designed and permitted disposal facilities at the location of the REE separation facilities (which produce individual RE's for use by manufacturers).

With the minimal presence of radioactive elements in the RE product, essentially all of the activity will remain in the mineral concentration rejects (tailings) and the metallurgical residues. Depending on the specific resource mineralogy and process selection, the tailings will be somewhat depleted of radioactive elements and the residue somewhat enhanced. The measurement and management of radiation doses to workers and provision of secure long-term waste management are important components to success in permitting and public acceptance of REE resource development.

Radiation Dose Assessment and Implications in REE Developments

All people are exposed to radiation and radioactivity from natural sources outside of the body (principally from external gamma radiation) and from sources of radioactivity taken into the body through inhalation or ingestion. In an occupational setting, inhalation and external radiation

Table V. Typical Radiation Doses

	Per Exposure (mSv)	Annual Exposure (mSv/y)
Average natural background Canada, World		1.8, 2.4
Calgary, Winnipeg [4]		2.3, 4.0
High Background Locations Caused by presence of Th -Brazil, India, Iran		20-50+
Chest x-ray	0.03 – 0.05	
CT Scan	2-11	
International Air Crew		1-5
Miners – high grade Canadian uranium mines (2001-2005)		1-5
Dose limit for radiation worker in Canada		20 averaged over 5 years
Dose limit for member of the public		1
Dose below which no statistically significant health impacts observed in scientific studies	100	

are typically the exposure pathways of focus in radiation protection programs, while for members of the public, ingestion (such as via water pathways) and to a lesser extent, inhalation, are the primary routes of exposure.

Radiation dose is the product of radiation exposure rate and duration of exposure.

The internationally accepted unit for radiation exposure is a Sievert. Typical personal radiation doses are millisieverts (mSv). Depending on where on lives, the background radiation doses in Canada are typically about 2 mSv/y. An illustration of variations in background doses and associated with human activity are shown in Table V.

While NORM is not regulated in Canada as in most other countries, guidelines for the management of NORM have been issued by Health Canada [5]. The classification of NORM radiation protection programs, which depend on the expected level of radiation dose to workers, are summarised in Table VI.

Table VI. NORM Radiation Program Classifications

Annual Dose (mSv/y)	**Radiation Protection Program**
Dose < 0.3	None No requirements for dose management.
0.3<Dose<1.0	NORM Management Introduction of access restrictions to non-NORM workers and public. Introduction of shipping and/or material management.
1.0 < Dose < 5.0	Dose Management Training to control and reduce workers doses. Dose estimates via radiation surveys and worker exposure times. Engineering controls where appropriate. Worker dose to be reported to National Dose Registry. Expert advice recommended.
Dose > 5.0	Radiation Management Formal radiation protection program and the use of TLDs and other monitors for worker dose measurement. Provision of equipment and procedures to reduce worker dose. Expert advice should be obtained.

A question might be: *what do such dose criteria mean for REE mining and production*? The following is an example dose calculation:

Exposure scenario assumptions:
REE ore radioactive element content: 500 ppm Th, 50 ppm U (decay products all in equilibrium).

Worker exposure conditions: inhales ore dust (at 1 mg/m^3), incidentally ingests ore (at 100 mg/day), and stands 1 metre away from a large mass of ore for an entire working year (2000 hours).

Estimated annual worker doses:

Inhalation = 0.28 mSv/y
Ingestion = 0.08 mSv/y
External (gamma) = 2.1 mSv/y
Total = 2.4 mSv/y

While the results above indicate a low worker dose (relative to the worker dose limit of 20 mSv/y), simple measures could be put in place to reduce exposure – reduce dust inhalation and ingestion and most importantly be distant from external radiation sources. It is a principal of radiation protection that radiation dose be kept as low as reasonably achievable (known as ALARA) even if the maximally exposed workers are below regulatory limits. For REE facilities that would be built for Canadian REE resources, doses less than a few mSv/y could be reasonably expected with the implementation of a sensible radiation management plan.

Acceptance by People Who Live Near or Frequent Locations Near REE Mining and Processing Facilities

In addition to concern about workers' health, safety and potential radiation exposure, the presence or radioactive substances in the REE resource and subsequently in wastes, if not managed and communicated effectively, can become a public concern [6], [7], [8]. This concern may be amplified by the following factors:

- Unfamiliarity with REE mining and processing by public and institutional stakeholders;
- Reported (and possibly unsubstantiated) claims of harm at historical REE operations in other countries;
- Technical complexity of managing NORM radioactivity; and
- Generation of three or four distinct waste types, and depositing these materials with diverse characteristics and levels of radioactivity in locations other than waste rock at the mine site - process tailings, metallurgical residues and RE separation wastes.

Social acceptability has become an increasingly important component of any type of mine development anywhere in the world. The presence of NORM can render acceptability much more challenging. Recent experience in Canada and other countries has shown that the following steps would need to be considered in a REE development:

- Detailed understanding of the distribution of radiological materials in all phases of the process. Complete radiological exposure pathways assessments of all phases of the project by qualified independent third parties;
- A full discussion of the NORM content of the REE resource <u>and</u> natural background radioactivity with the public and institutional regulators;

- Discussion of radiation dose to workers and the interested public from natural sources and from the proposed REE development; and
- A review, with public and regulators, of waste management options and the potential radiation dose and environment impact from the REE development during operations and following closure;
- Selection of best options for development and waste disposal based on cost, environment, regulatory and social considerations.

While the levels of radioactivity in most REE developments are low, and while technical expertise can ensure the design of safe operations and robust waste management strategies, the intuitive public response to the presence of NORM can derail any REE development.

Some aspects that can provide assurance of safety and environmental stewardship in REE developments are:

(i) Radiation doses to the general public can be engineered to be below the “unrestricted” levels of 0.3 mSv/y (Table VI);

(ii) The radioactivity associated with REE developments is principally thorium-based. Thorium is naturally a very insoluble and immobile element in the environment. Ample supporting evidence to thorium’s immobility is found in the historical uranium mine wastes at 14 uranium mines in Ontario, Canada where Th-232 concentrations exceeded most that in most REE resources around the world;

(iii) No concentrating of radioactivity to levels of concern occurs in the processing of RE resources;

(iv) International exemption limits [9] for the transport of NORM are higher than Th and U contents in REE resources, e.g. if Th(ppm)/2460 + U(ppm)/810 = <1; and

(v) Independently-reported records of radiation exposure to Canadian workers working in mines extracting ores containing 20% (200,000 ppm) uranium indicate that: (a) workers can and are being protected from excess radiation exposure; and (b) acceptable waste management strategies have been developed.

Conclusions

REE resources contain naturally occurring thorium and uranium radioactivity and their radioactive decay products (NORM) at concentrations above general background levels. Radiological management involved in REE ore processing, concentrate production and element separation involves the minimisation of radiation exposure to workers and to the public. Credible expertise and experience exists to ensure that radiation exposure is below very conservative limits.

Public concerns about REE developments, whether based on intuition, facts, or fears fed by third party exaggeration can in large part be addressed by development of an understanding of ambient radiation and by radiation dose assessments coupled with the application of proven and robust waste management strategies.

References

1. United States Environmental Protection Agency (US EPA), 2012. Rare Earth Elements: A Review of Production, Processing, Recycling and Associated Environmental Issues, EPA 600/R-12-572 December 2012.

2. Kosynkin, V.D., S.D. Moisev and V.S.Vdocichev 1995. Cleaning Rare Earth Elements from Actinium. Jof Alloys and Compounds 225:320-323.

3. Feasby, D.G., 2012. Personal communication with Rhodia Rare Earth Systems.

4. Grasty, R.L. and J.R. LaMarre, 2004. The Annual Effective Dose from Natural Sources of Ionising Radiation in Canada. Radiation Protection Dosimetry, Vol. 108, No. 3, 215-226.

5. Health Canada (HC), 2000. Canadian Guidelines for the Management of Naturally Occurring Radioactive Material (NORM). Prepared by the Canadian NORM Working Group of the Federal Provincial Territorial Radiation Protection Committee, First Edition, October.

6. International Atomic Energy Agency (IAEA), 2011a. Radiation Protection and NORM Residue Management in the Production of Rare Earths from Thorium Containing Minerals. IAEA Safety Reports Series No. 68.

7. International Atomic Energy Agency (IAEA), 2011b. Report of the International Review Mission on the Radiation Safety Aspects of a Proposed Rare Earths Processing Facility (the Lynas Project). 29-May – 3 June 2011, Malaysia. Available at: http://www.iaea.org/newscenter/news/pdf/lynas-report2011.pdf.

8. SENES Consultants Limited (SENES), 2011. Radiation Protection Program in Support of the Thor Lake Project. Prepared for Avalon Rare Earth Metals Inc. Appendix G of Thor Lake Project DAR, available on Mackenzie Valley Review Board web site http://www.reviewboard.ca.

9. International Atomic Energy Agency (IAEA), 2009. Regulations for the Safe Transport of Radioactive Material – 2009 Edition. IAEA Safety Standards Series No. TS-R-1.

Mineralogy and Beneficiation of Rare Earth Resources

CHARACTERIZATION OF RARE EARTH MINERALS WITH FIELD EMISSION SCANNING ELECTRON MICROSCOPY

*Raynald Gauvin, Hendrix Demers, Kristian Waters and Nicolas Brodusch

Department of Mining and Materials Engineering
McGill University
Montreal, Quebec, Canada, H3A 0C5
*raynald.gauvin@mcgill.ca

Keywords: Backscattered Electron Imaging, Field Emission Electron Probe Microanalysis (FE-EPMA), Field Emission Scanning Electron Microscopy (FE-SEM) , Quantitative X-Ray Microanalysis, Rare Earth Elements (Rees), Silicon Drift Detector (SDD-EDS), Silicon Lithium-Drifted Energy-Dispersive Spectrometer (Si(Li) EDS), Wavelength-Dispersive Spectrometers (WDS)

Abstract

Rare earth elements are becoming increasingly in demand, due to their prevalence in both renewable energy devices and high-end electronics. The characterization of the composition, morphology and volume fraction of the various phases that have valuable rare earth elements in the ores are needed to find the optimal industrial process to extract the ores containing the rare earth elements. Rare earth-bearing minerals contain many elements with the M-and L-lines overlap, requiring a high degree of resolution, pushing the boundaries of scanning electron microscopy quantitative analysis. Enhanced microscopy at a high spatial resolution with improved x-ray quantitative analysis enables the accurate determination of the distribution of the desired rare earth elements in various mineral phases.

Introduction

Rare earth elements (REEs) are becoming increasingly in demand, due to their prevalence in both renewable energy devices and high-end electronics. From batteries (lanthanum and cerium), to magnets (dysprosium and neodymium) and lighting (yttrium), the REEs are crucial to the advancement of technology, and to energy saving devices [1]. The goal of this project is to characterize the composition of various small phases (less than 10 μm) that may have valuable REEs in the ores. In order to study small phases, high spatial resolution imaging and x-ray microanalysis are needed and they can only be obtained simultaneously by working at low accelerating voltage. In this work, the results obtained, at medium and high accelerating voltage, with a cold field emission scanning electron microscope (FE-SEM) and a silicon drift detector energy dispersive spectrometry (SDD-EDS) detector are compared to the results obtained with a field emission electron probe microanalysis (FE-EPMA) instrument with both silicon lithium-drifted energy-dispersive spectrometer (Si(Li) EDS) and wavelength dispersive spectrometry (WDS). The performance of FE-SEM/ SDD-EDS was studied elsewhere [2].

Materials and Methods

A bulk sample from the Nechalacho deposit ore in the North West Territories was prepared for scanning electron microscopy imaging and x-ray microanalysis. The sample was mechanically fractured and a 1 cm^3 block was mounted in a conductive resin. Then it was polished with silicon carbide papers until the 1200 grit unit followed by polishing with diamond suspensions of 3 and 1 µm grain size. Final polishing was performed using an alumina suspension of 50 nm grain size. To prevent surface charging, the sample was coated with a nominal 10-20 nm-thick amorphous carbon layer using an Edwards vacuum carbon coater E306.

FE-EPMA measurements have been performed with a JEOL JXA-8530F field emission electron probe microanalysis located at RWTH Aachen, Germany. The FE-EPMA, with a high brightness Schottky field emission electron gun, provides a high probe current with a small electron probe diameter. This FE-EPMA have a JEOL Si(Li) EDS, a Bruker SDD-EDS and five WDSs with multiple analysing crystals with a takeoff angle of 40 °. The results were obtained with an accelerating voltage of 15 kV and probe current of 198 nA. The point analysis acquisition time and the pixel dwell time for the x-ray map were 125 s (30 s for each element). The quantification was performed with the Probe Software with a SPI 02759-AB rare earth pentaphosphates and Charles M. Taylor standards. Elements were acquired using analyzing crystals: LiF for La Lα, Ce Lα, Nd Lα, and Gd Lα; LiFH for Fe Kα, Mn Kα, and Dy Lα; PETJ for Y Lα, Nb Lα, Zr Lα, and Ca Kα; TAP for Ta Mα, Mg Kα, and Si Kα; LDE1 for F Kα. The standards were MgO for Mg Kα, quartz for Si Kα, calcite for Ca Kα, MnF2 for F Kα and Mn Kα, hematite for Fe Kα, LiNbO3 for Nb Lα, LiTaO3 for Ta Mα, Zr for Zr Lα, yttrium pentaphosphate for Y Lα, lanthanum pentaphosphate for La Lα, cerium pentaphosphate for Ce Lα, neodynium pentaphosphate for Nd Lα, gadolinnium pentaphosphate for Gd Lα, and dysprosium pentaphosphate for Dy Lα. The Pouchou and Pichoir correction method [3] was used with a linear off peak correction (20 s counting time). Interference corrections [4] were applied to Si for interference by Ta, to F for interference by Fe and Ce, to Gd for interference by Ce, to Ca for interference by Dy, to Y for interference by Nb, and to Dy for interference by Fe and Mn.

FE-SEM observations have been performed with a Hitachi SU8000 cold field emission scanning electron microscope located at McGill University. The FE-SEM provides accelerating voltages ranging from 0.1 to 30 kV with a maximum available current near 20 nA. The microscope column is equipped with a snorkel lens generating a magnetic field allowing high electron collection rates by the detectors located inside the column. This FE-SEM has 1 secondary (SE) lower detector, 2 SE upper detectors with various modes of energy filtration, a semi-conductor type five quadrant backscattered electron (BSE) detector, a scanning transmission electron microscopy (STEM) detector that works in bright field, an electron convertor that allows to use the SE lower detector for dark field STEM imaging. The FE-SEM is also equipped with an X-MAX silicon drift detector energy dispersive spectrometry detector from Oxford Instruments presenting an 80 mm^2 collecting area allowing acquiring x-ray spectra with 500,000 counts per second. The x-ray map was acquired with a probe current of 140 pA, an accelerating voltage of 30 kV, and a working distance was 15 mm. The total acquisition time was 403 s and the INCAEnergy drift correction was used. Peaks were identified using INCAEnergy software from Oxford Instruments and x-ray lines database from the DTSA software [5]. More information about these instruments and the related techniques is given elsewhere.[6, 7].

Results and Discussion

The Nechalacho deposit ore is very complex with over 75 minerals found in it [8]. Also many of the elements are of similar atomic number, the M- and L-lines overlap, requiring a high degree of spectral resolution, pushing the boundaries of SEM/EDS application. Enhanced microscopy at a high spatial resolution enables the researchers to determine accurately the distribution of the desired rare earths in various mineral phases, which can then be utilised in the processing section, where certain minerals will be selectively recovered.

One advantage of FE-SEM and FE-EPMA instruments are the excellent spatial resolution at low accelerating voltage. The resolution is mainly determined by the probe diameter, a few nanometer for a FE-SEM/EPMA. The resolution of a BSE image or x-ray map also depends of the size of the electron interaction volume. The different phases of rare earth samples are imaged with a BSE detector, which allows the observation of composition variation. The brighter area is region of higher mean atomic number. The composition of different phases can be determined qualitatively or quantitatively using the emitted x-ray which is detected by either an EDS or a WDS.

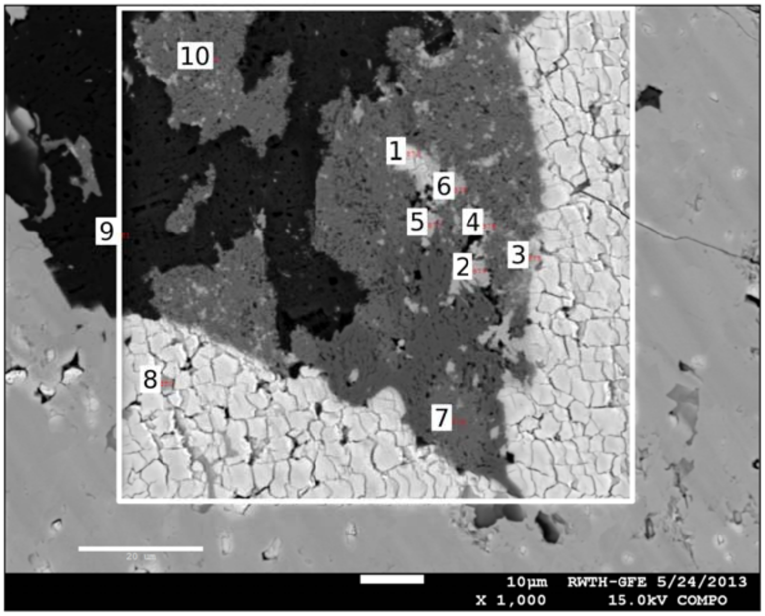

Figure 1. Quantitative x-ray microanalysis of the Nechalacho ore with an accelerating voltage of 15 kV at ten different locations.

Figure 1 shows BSE images obtained for a polished (flat) Nechalacho deposit ore sample at 15 kV. The phase compositions were determined using the quantitative microanalysis with the EPMA WDS for ten locations. Tables I and II reports the composition obtained for the 10 locations. The analysis was performed using the intensity k-ratio and the ZAF correction method [6, 7]. In Table II, the oxygen concentration was obtained by difference, the weight percentages were normalized to obtain a total composition of 100 % for each location.

This analysis allows the identification of the different phases and also the concentration of rare earth element inside them. For example, locations 7 and 10 were identified as zircon with less than 1% of REE. The locations 2 to 6 were identified as fergusonite-Y phases from the relative concentration of Nb, Y, and O. The other phases were not clearly identified. However, the concentration of REEs was different for each location. The location 1 shows a strong concentration of lanthanum, cerium and neodymium inside a fergusonite phase. This phase could contain C, but the C Kα line was not analyzed for this sample. Also the EDS spectrum obtained at location 1 shown a F Kα peak, but the EPMA analysis give a zero concentration of F. An acquisition problem could explain this difference.

Table I. Weight Percentage Obtained by Quantitative X-ray Microanalysis of the Nechalacho Ore With an Accelerating Voltage of 15 Kv at Ten Different Locations (Shown in Figure 1) Without Normalization

Point	Mg	Si	F	Ta	La	Ce	Nd	Gd	Nb	Zr	Ca	Y	Fe	Mn	Dy	O	Total
1	0.00	1.83	0.00	0.03	15.27	48.50	16.67	0.00	0.13	4.21	0.08	1.01	0.77	0.03	0.00	0.00	88.53
2	0.00	0.20	0.00	0.88	0.16	0.69	1.49	9.15	30.31	0.00	0.13	16.09	0.55	0.01	6.53	0.00	66.19
3	0.09	1.64	0.00	1.44	0.30	1.30	1.91	6.77	27.36	1.99	0.40	15.09	0.48	0.23	5.97	0.00	64.97
4	0.05	0.51	0.00	2.36	0.20	1.25	2.37	6.40	29.14	0.14	0.34	16.03	0.95	0.24	5.69	0.00	65.67
5	0.48	1.96	0.00	1.46	0.08	0.91	1.83	6.72	28.06	1.10	0.25	16.04	0.85	0.09	5.77	0.00	65.60
6	0.06	0.57	0.00	2.50	0.14	1.39	2.62	5.13	29.20	0.02	0.36	16.78	1.17	0.18	5.49	0.00	65.61
7	0.00	14.35	0.00	0.33	0.12	0.75	0.25	0.10	0.35	43.33	0.05	1.91	0.45	0.01	0.20	0.00	62.20
8	0.00	0.00	0.00	0.12	3.75	11.67	7.41	8.96	0.00	0.00	11.94	20.97	0.00	0.02	4.10	0.00	68.94
9	8.46	0.00	0.00	0.00	0.02	0.15	0.04	0.00	0.00	0.06	19.64	0.00	2.66	16.15	0.00	0.00	47.18
10	0.28	14.17	0.00	0.33	0.05	0.39	0.04	0.05	0.24	40.69	0.09	1.67	1.83	0.14	0.18	0.00	60.15

Table II. Weight Percentage Obtained by Quantitative X-ray Microanalysis of the Nechalacho Ore With an Accelerating Voltage of 15 kV at Ten Different Locations (Shown in Figure 1) With Normalization to Obtain O Concentration by Difference

Point	Mg	Si	F	Ta	La	Ce	Nd	Gd	Nb	Zr	Ca	Y	Fe	Mn	Dy	O	Total
1	0.00	1.81	0.16	0.03	15.99	48.74	17.50	0.00	0.13	4.23	0.08	1.01	0.80	0.03	0.00	9.47	100.00
2	0.00	0.21	0.00	0.93	0.18	0.77	1.66	10.35	31.15	0.00	0.14	17.11	0.63	0.01	7.42	29.44	100.00
3	0.10	1.74	0.00	1.53	0.33	1.44	2.13	7.67	28.09	2.12	0.42	16.00	0.55	0.26	6.79	30.82	100.00
4	0.06	0.54	0.00	2.50	0.22	1.39	2.65	7.25	29.91	0.15	0.36	17.02	1.07	0.27	6.48	30.15	100.00
5	0.51	2.08	0.00	1.55	0.09	1.00	2.04	7.58	28.74	1.17	0.26	16.99	0.96	0.10	6.54	30.40	100.00
6	0.06	0.61	0.00	2.65	0.16	1.54	2.93	5.80	29.95	0.03	0.38	17.85	1.32	0.20	6.24	30.27	100.00
7	0.00	15.99	0.00	0.37	0.13	0.81	0.28	0.11	0.37	45.82	0.05	2.01	0.50	0.01	0.23	33.33	100.00
8	0.00	0.00	0.00	0.12	4.08	12.75	8.15	9.92	0.00	0.00	12.82	21.50	0.00	0.02	4.54	26.10	100.00
9	8.90	0.00	0.00	0.00	0.02	0.16	0.05	0.00	0.00	0.06	21.24	0.00	2.88	17.39	0.00	49.30	100.00
10	0.32	15.85	0.00	0.37	0.05	0.42	0.04	0.06	0.25	43.02	0.10	1.76	2.04	0.15	0.20	35.36	100.00

X-ray intensity maps were used to understand the relationship between the fergusonite phase and high concentration of some rare earth elements. Figure 2 and 3 show the x-ray map obtained simultaneously with the FE-EPMA: Figure 2 with a Si(Li) EDS and Figure 3 with WDSs. In that case, the WDSs give better x-ray maps where the region of high concentration is clearly separated from the region of low concentration. However, the WDSs are limited to analyze a small number of elements at the same time. The Si(Li) EDS does not have this limitation. However, the background removal is important for EDS mapping. In Figure 2, the experimental parameters were not optimal for EDS mapping because the parameters were optimized for WDS analysis and no background removal was available for this EDS.

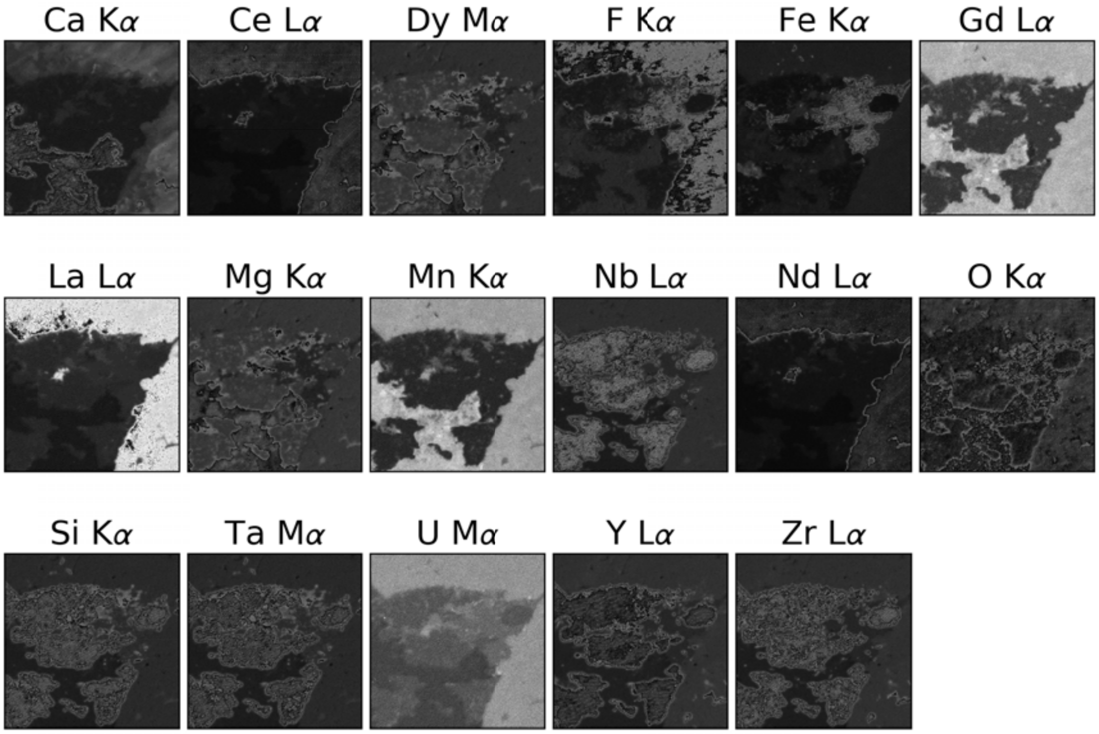

Figure 2. X-ray Si(Li) EDS map of the Nechalacho ore sample at 15 kV obtained with a FE-EPMA. The x-ray line used are indicated in the top right of each micrograph.

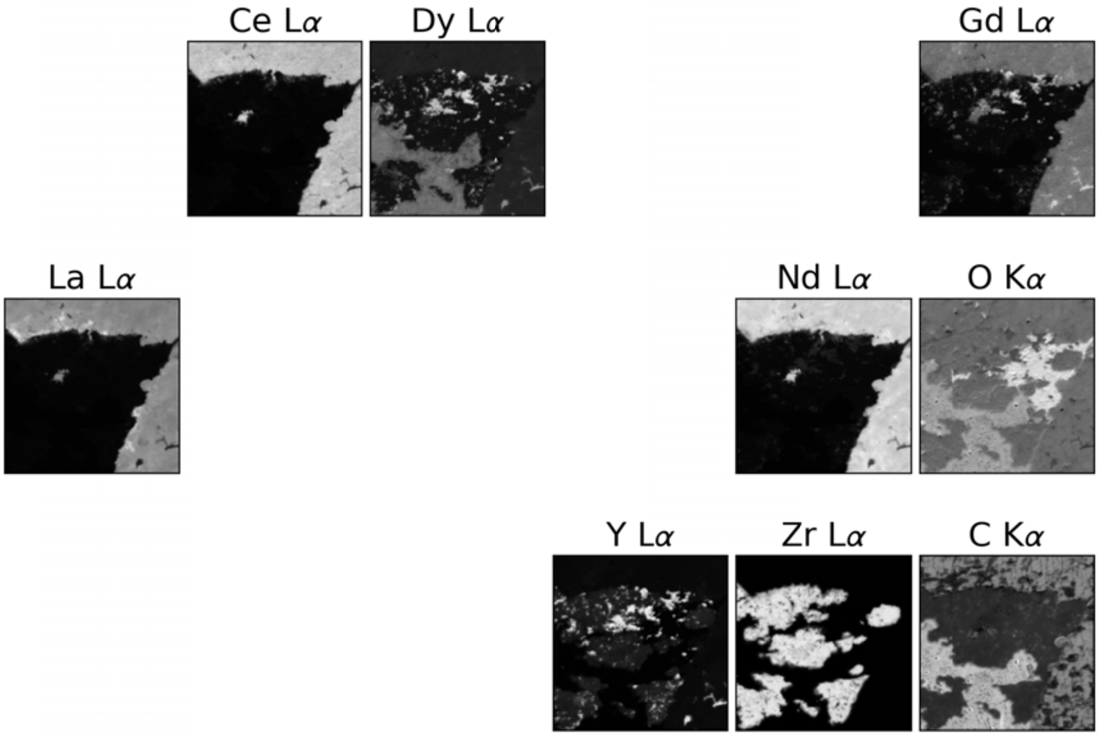

Figure 3. X-ray WDS map of the Nechalacho ore sample at 15 kV obtained with a FE-EPMA. The x-ray line used are indicated in the top right of each micrograph.

The total acquisition time for the x-ray maps shown in Figure 2 and 3 was 8 h. Figure 4 shows x-ray maps of the same sample, but at a different location, obtained with a FE-SEM and SDD-EDS. The acquisition parameters were optimized for EDS mapping and the acquisition time was only ~400 s. The background removal was used and the map quality (each element distribution show the phase boundary, i.e., no background pixel observed) is similar that the one obtained with FE-EPMA and WDSs. Also, the current used with the FE-SEM maps was lower than the one used for FE-EPMA, which decrease the contamination and specimen damage. This effect was observed on Figure 1, where the BSE image was acquired after the 8 h x-ray map with a 198 nA probe current. The area of the x-ray map is outlined by the white square on Figure 1.

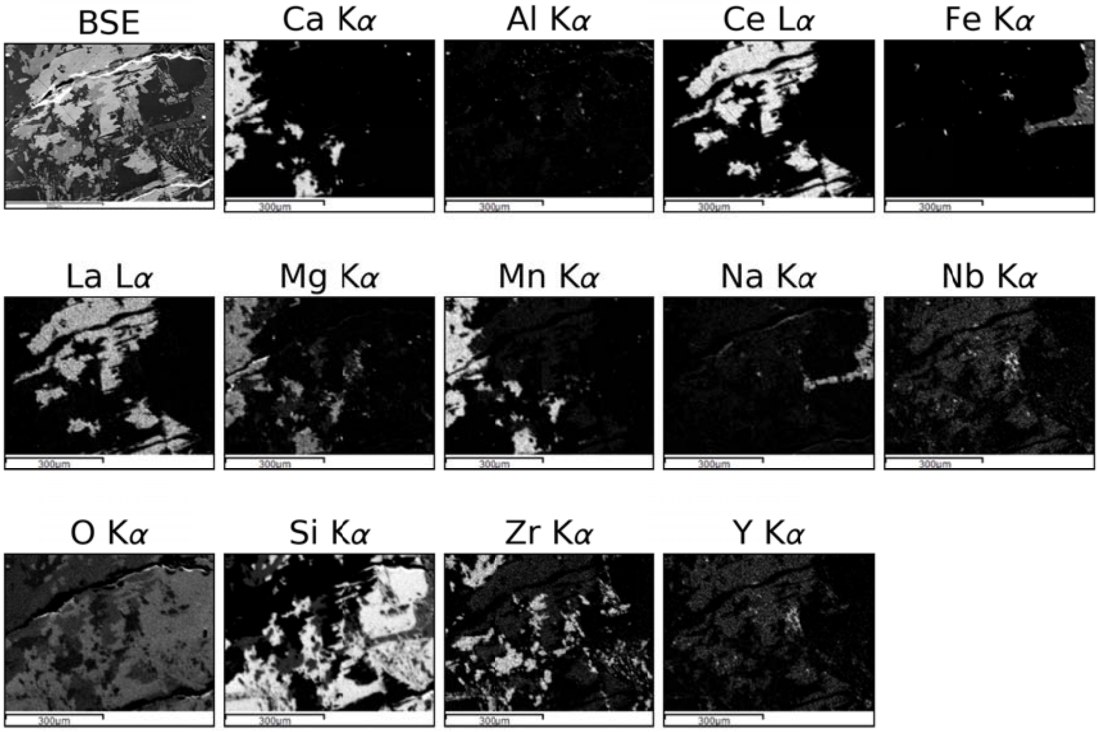

Figure 4. X-ray SDD-EDS map of the Nechalacho ore sample at 30 kV obtained with a FE-SEM. The x-ray line used are indicated in the top right of each micrograph.

Summary

Field emission scanning electron microscope (FE-SEM) and field emission electron probe microanalysis (FE-EPMA) equipped with a photo-diode-backscattered electron detector allows the x-ray map imaging of small phases in the Nechalacho deposit ore. The WDSs was used to quantify phases. The quality of x-ray maps obtained with WDSs, Si(Li) EDS and SDD-EDS were compared. The WDSs and SDD-EDS give detailed x-ray map. However, the SDD-EDS maps were obtained with an acquisition time 72 times smaller than WDSs and with a smaller probe current.

Acknowledgements

Acknowledgement is presented to Avalon Rare Metals Inc. for providing a bulk sample and Philippe T.-Pinard and Silvia Richter at RWTH Aachen for EPMA microanalysis. Finally, we are thankful to the reviewers for their comments, which have improved the quality of the manuscript.

References

1. Crow, J.M., *13 exotic elements we can't live without.* New Scientist, 2011. 2817: p. 36-41.

2. Demers, H., et al., *Characterization of Rare Earth Minerals with Field Emission Scanning Electron Microscopy.* Canadian Metallurgical Quarterly, 2013.

3. Pouchou, J.-L. and F.c. Pichoir, oise, *Electron Probe Quantitation*, K.F.J. Heinrich and D.E. Newbury, Editors. 1991, Plenum Press. p. 31-75.

4. Donovan, J.J., D.A. Snyder, and M.L. Rivers, *An Improved Interference Correction for Trace Element Analysis.* Microbeam Analyis, 1993. 2: p. 23-28.

5. Fiori, C., C. Swyt-Thomas, and R.L. Myklebust, *Desk Top Spectrum Analyzer*, 2007, National Institute of Standards and Technology: Gaithersburg, MD.

6. Goldstein, J.I., et al., *Scanning Electron Microscopy and X-Ray Microanalysis: A Text for Biologists, Materials Scientists, and Geologists*2003: Kluwer Academic/Plenum Publishers. xix, 689 p.

7. Reimer, L., *Scanning Electron Microscopy: Physics of Image Formation and Microanalysis*. Second ed. Springer Series in Optical Sciences. Vol. 45. 1998: Springer.

8. Sheard, E.R., et al., *Controls on the Concentration of Zirconium, Niobium, and the Rare Earth Elements in the Thor Lake Rare Metal Deposit, Northwest Territories, Canada.* Economic Geology, 2012. 107(1): p. 81-104.

GEOMETALLURGICAL APPROACH TO REE DEPOSITS USING QUANTITATIVE MINERALOGY

T. Grammatikopoulos* and C. Gunning

SGS Canada Inc., Advanced Mineralogy Facility,
185 Concession St., Lakefield, Canada, K0L 2H0
*tassos.grammatikopoulos@sgs.com

Keywords: REE, QEMSCAN, Process Mineralogy, Geometallurgy

Abstract

Conventional mineralogical and analytical techniques e.g., XRD, optical and electron microscopy, mineral chemistry, and geochemistry, are conducted to understand the petrogenesis of the REE deposits. However, the critical factor to understand the distribution of REE minerals (REM) is quantification of mineral mass, liberation and association with the host minerals. This can only be achieved by means of quantitative mineralogical techniques such as the QEMSCAN (QS). QS is used in a variety of REE projects (i.e., alkaline complexes, carbonatites). QS data have been utilized to define quantitatively the variability and distribution of the REM; differentiate between LREE and HREE zones to delineate the ore; provide mineralogical parameters to aid the physical and hydrometallurgical separation; and predict minerals/REE behaviour during processing. Therefore, the QS data, coupled with mineral chemistry and gecohemistry, can assist to geometallurgically model complex REE deposits.

Introduction

The term rare earth elements (REE) is used to describe the 15 metallic lanthanide elements, lanthanum through lutetium, plus the elements yttrium and scandium, which display similar physical and chemical properties (see IUPAC Nomenclature of Inorganic Chemistry, IR 3-6-2, 2004)[1].

Economic and potentially economic REE deposits form two main groups. The first is a commonly occurring “light rare earth element” (LREE) rich group of deposits containing mainly lanthanum (La), cerium (Ce), praseodymium (Pr), neodymium (Nd), and samarium (Sm). The second is a less commonly occurring “heavy rare earth element” (HREE) rich group which, in addition to the LREE, contains elevated concentrations of the more valuable lanthanides such as europium (Eu), gadolinium (Gd), terbium (Tb), dysprosium (Dy), holmium (Ho), erbium (Er), thulium (Tm), ytterbium (Yb) and lutetium (Lu) as well as yttrium (Y). The LREE are hosted primarily by carbonatites and the HREE by highly alkaline to peralkaline (Na + K > Al) silicate igneous rocks. The LREE are produced mainly from bastnaesite, monazite, etc., while HREE are produced almost exclusively from low-grade secondary ion adsorption clay deposits in which the REE are adsorbed onto surfaces of kaolinite and halloysite, the products of weathering of granites and sediments [2,3]. HREE are also found in fergusonite, zircon, xenotime, but are not produced presently from these minerals though a number of deposits are advancing towards production. China is responsible for 97% of the World’s production of the REE [4], mainly from the giant Bayan Obo deposit, an enigmatic carbonate-hosted, possibly carbonatite-related deposit [5] and from the above mentioned clay deposits.

Quantitative automated mineralogy is increasingly being applied to the study of ore deposits. The quantification and improved understanding of mineralogical parameters is a great contribution to geometallurgy [6]. This paper summarizes mineralogical studies on a number of REE deposits using QS technology and subordinate techniques. Related data include textural characterization, quantification and distribution of ore and gangue minerals, liberation attributes, and spatial and textural association of the REM. These data are used to define mineralogical domains and predict the ore's metallurgical response.

Methodology and Analytical Techniques

QS Analysis

QS work is carried out at the Advanced Mineralogy Facility at SGS Canada, Lakefield site. The QS there is an EVO 430 automated scanning electron microscope which is equipped with four light-element energy-dispersive X-ray spectrometers and iDiscover software capable of processing the data and images. QS operates with a 25 kV accelerating voltage and a 5nA beam current. The QS measures, and the iDiscover software processes data from every pixel across a sample with a pixel size defined based on the scope of the analysis. The data can be processed off line. The software assigns each pixel a mineral name based on 1,000 counts of energy dispersive X-ray spectral data and backscatter electron intensities.

Intact drill core samples are analysed by the, conventionally termed, Field Image method, to determine rock-types and provide a textural characterization of selected samples. This analysis is conducted on a core sample mounted as a thin or polished section. Chemical spectra are collected at a set interval within the field of view. Each field of view is then processed offline and a pseudo image of the core sample is produced from which the modal mineralogy and texture of the sample are defined. Data are acquired over the polished thin sections at a 5-25 µm pixel size.

Coarse reject samples from 2-3-meter intervals, used for geochemical analyses, are analyzed to determine the mineral variability. Individual samples are stage crushed to K_{80} (80% passing) 150-212 µm, and analyzed as a single fraction by the Particle Mineral Analysis (PMA) method. PMA is a two-dimensional mapping analysis aimed at resolving liberation and locking characteristics of a generic set of particles. A pre-defined number of particles are mapped at a point of 3-5 µm pixel size.

Composite samples are made from multiple drill core or channel samples. They are analyzed to determine the variability of the minerals but also the liberation of the REM in order to predict the metallurgical beneficiation performance. The composites are analyzed using two separate measurement routines by QS including PMA and Specific Mineral Search (SMS), which is a modified PMA. The SMS method differs from conventional PMA in that the location of a phase that is present in low concentrations is improved by applying a threshold to the back-scattered electron intensity [7].

X-ray Diffraction, ICP, XRF and EPMA

XRD analyses are conducted for QS set up purposes, whole rock analyses by X-ray fluorescence (XRF) and ICP for reconciliation purposes. The composition of the REM is determined with electron probe micro analysis (EMPA) [7].

Results

XRD, SEM, EPMA and QS analysis have been performed on a number of deposits including carbonates, alkaline complexes, metamorphic, and weathered and clay deposits. The mass % and the chemistry of the REM in the deposits vary widely. Table I shows some common REE minerals and their formulas to illustrate the complexity. Zircon, titanite and apatite, and others are not primary REE-bearing minerals but are important REE-Y-Nb carriers in some deposits.

Textural Analysis

This study aims to characterize the different rock types from the drill cores, distribution of REM, alteration, and overall textural features of the rocks associated with the mineralization. The digital images, generated from the QS analysis, provide unperturbed textural features of the samples on a mesoscopic level (mm-cm in scale) that cannot be quantitatively captured in the field during drill core logging. REM are typically very fine-grained in the rocks examined (<10 µm to rarely 1 mm in size).

Table I. Common REE Minerals and Formulas

Mineral	Formula
Y-allanite	$(Ca,Y)_2(Al,Fe,REE)_3Si_3O_{12}(OH)$
Monazite	$(LREE,Y,Th)PO_4$
Bastnaesite	$REE(CO_3)F$
Synchysite	$Ca(Ce,REE)(CO_3)_2F$
Fergusonite	$(REE,Y)NbO_4$
Eudialyte	$Na_4Ca_{1.5}Ce_{0.5}Fe^{2+}{}_{0.6}Mn^{2+}{}_{0.3}Y_{0.1}ZrSi_8O_{22}(OH)_{1.5}Cl_{0.5}$
Xenotime	$(Y,Yb,HREE)(PO_4)$
Mosandrite	$Na_2Ca_3Ce_{1.5}Y_{0.5}Ti_{0.6}Nb_{0.3}Zr_{0.1}(Si_2O_7)_2O_{1.5}F_{3.5}$
Chevkinite	$Ce_{1.7}La_{1.4}Ca_{0.8}Th_{0.1}Fe^{2+}{}_{1.8}Mg_{0.2}Ti_{2.5}Fe^{3+}{}_{0.5}Si_4O_{22}$
Zircon	$Zr_{0.9}Hf_{0.05}REE_{0.05}SiO_4$
Columbite	$(Fe,Mn,Mg)(Nb,Ta)_2O_6$
Apatite	$(Ca, REE,Sr)_5(PO_4)_3(OH,F,Cl)$
Titanite	$Ca_{0.95}REE_{0.05}Ti_{0.75}Al_{0.2}Fe^{3+}{}_{0.05}SiO_{4.9}F_{0.1}$

The complexity of the REE deposits varies widely. Figure 1 shows back scattered images to illustrate accumulations of zircon from the Nechalacho deposit in Canada's Northwest Territories (a-b). They show columbite complexly intergrown with strongly zoned zircon grains. Images (c-d) are from undisclosed deposits and display aggregates of fine-grained monazite and bastnaesite/synchysite hosted by various gangue minerals. Rugged outlines and irregularly developed masses indicate a secondary (hydrothermal) origin.

Figure 2 illustrates representative pseudo color images from the Field Image analysis of drill core samples. The samples are chosen to illustrate the contrasting mineral assemblages of the gangue minerals and REE styles of mineralization *in situ*. Figure 2a is from a lithologically distinct horizon of banded carbonates within an amphibolite unit. Figure 2b is from an alkaline and Figure 3c from a carbonatite complex. The REM are associated with a variety of minerals. They exhibit patchy to brecciated and structurally controlled alteration, while other features such as mineral and grain size layering are very often apparent.

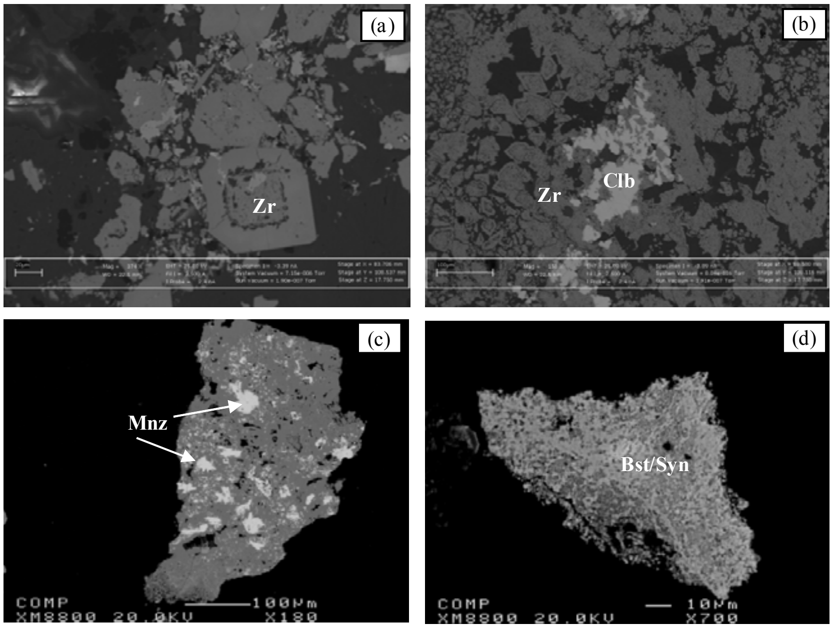

Figure 1. Back scattered electron image (BSE) showing (a) two generations and strongly zoned zircon (Zr); (b) columbite (Clb) intergrown with zircon; (c) monazite (Mnz) in Fe-oxyhydroxides, and bastnaesite/synchysite (Bst/Syn) in carbonates.

Ore Variability

Ore variability is defined across drill holes and along depth. The samples typically represent 2-meter intervals. Therefore, the mineralogical results do not reflect an isolated single sample, but a continuum of larger samples analogous to and coupled with, the geochemical analyses.

Variability analyses aim to quantify the mineralogy of intervals in order to define potential HREE and LREE zones. By comparing the geochemical analysis and mineral distributions of the zones of enriched LREE and HREE, a mineralogical differentiation is demonstrated (e.g., Nechalacho, Figure 3).

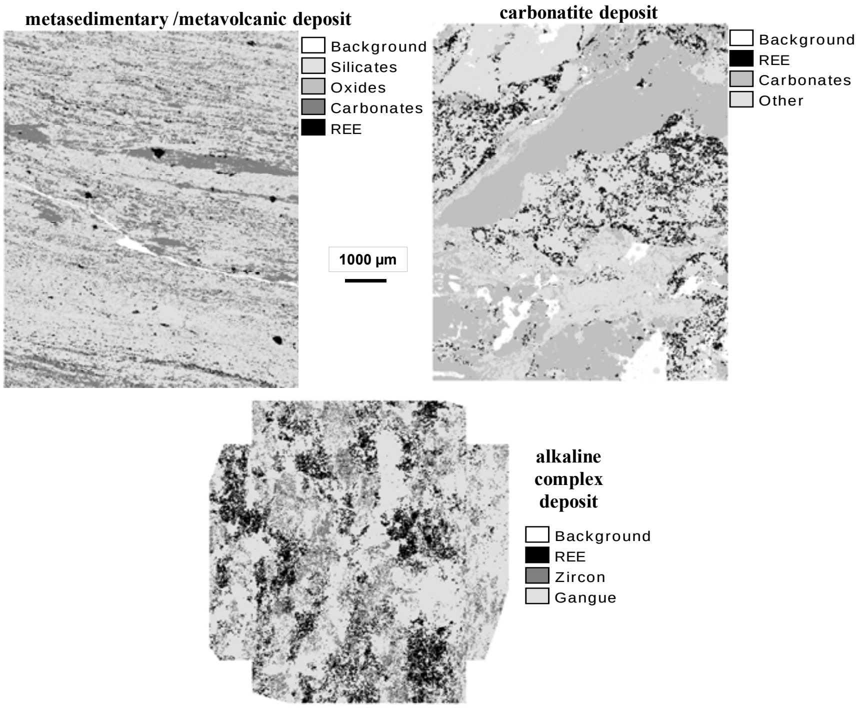

Figure 2. Representative images from the Field Image analysis of drill core samples.

For example, Ore C, D and F are enriched in LREM but show wide internal variations. Fergusonite, which is a HREE carrier, is enriched mainly in Ores C and D. It is interesting to note that zircon and REM show a positive correlation (R^2=0.8) and higher REE mineralization is marked by higher zircon grades.

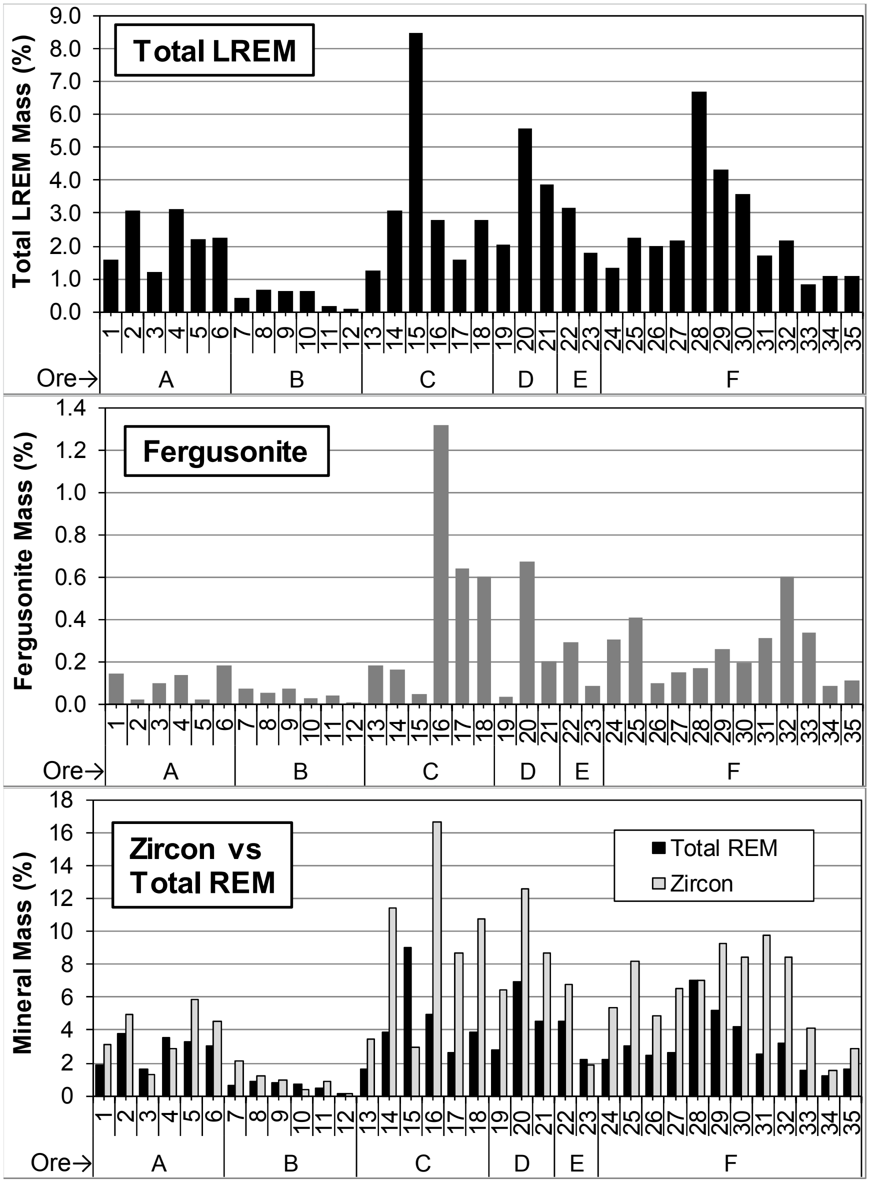

Figure 3. Variation of LREM, fergusonite, zircon and total REM from selected zones of Nechalacho HREE deposit.

Composite Samples

Composite samples, prepared from a number of drill cores, represent domains within the deposits. They are analysed to provide the liberation and association attributes of the REM and define the initial target grind sizes. For liberation and association analysis, particle liberation is defined based on 2D particle area percent. Particles are classified as free (≥95% surface area) and liberated (≥80%).

Non-liberated grains are classified according to association characteristics, where binary association groups refer to particle area percent ≥95% of the two minerals or mineral groups. Complex groups refer to particles with ternary, quaternary and greater mineral associations including the mineral of interest.

Figure 4 shows an example of liberation of monazite from a carbonatite deposit. Liberation calculated for the head sample is ~55% (free and liberated combined). Liberation values generally increase with decreasing size. REM, from a number of carbonates around the globe, yield similar liberation values of 60% (±10%) at grind K_{80}'s of 150 μm (80% of weight passing 150 μm).

Monazite can be re-classified based on its surface exposure (Figure 5). Thus, well exposed particles (>30% exposed surface) account for 72% in the sample. This indicates that the potential to physically recover monazite is higher than that indicated by the liberation values.

REM Distribution

REM display wide-ranging solid solution compositions that vary among and across deposits. In addition, commonly occurring silicate minerals e.g., apatite, zircon and titanite can carry significant REE in their matrices. The available EMPA have shown ΣREE concentrations of up to 7% in titanite and up to 12% (heavy REE are <3%) in apatite, though generally <3% in zircon.

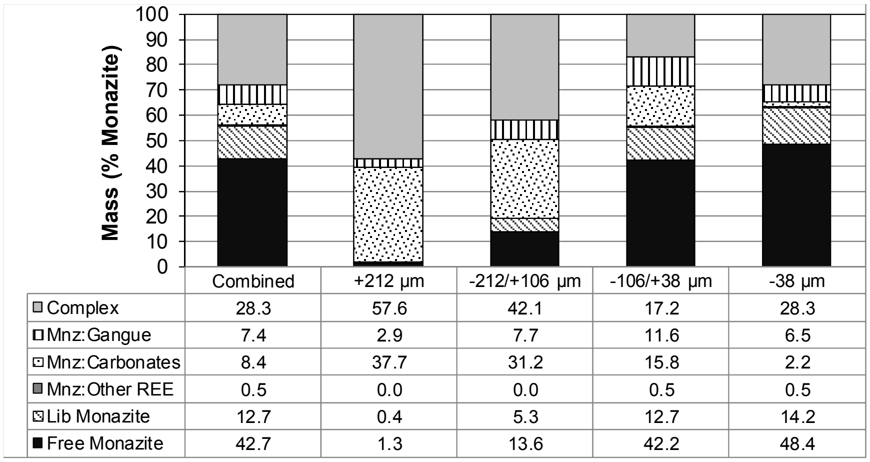

	Combined	+212 μm	-212/+106 μm	-106/+38 μm	-38 μm
□ Complex	28.3	57.6	42.1	17.2	28.3
□ Mnz:Gangue	7.4	2.9	7.7	11.6	6.5
□ Mnz:Carbonates	8.4	37.7	31.2	15.8	2.2
■ Mnz:Other REE	0.5	0.0	0.0	0.5	0.5
▨ Lib Monazite	12.7	0.4	5.3	12.7	14.2
■ Free Monazite	42.7	1.3	13.6	42.2	48.4

Figure 4. Liberation and association of monazite from a carbonatite complex.

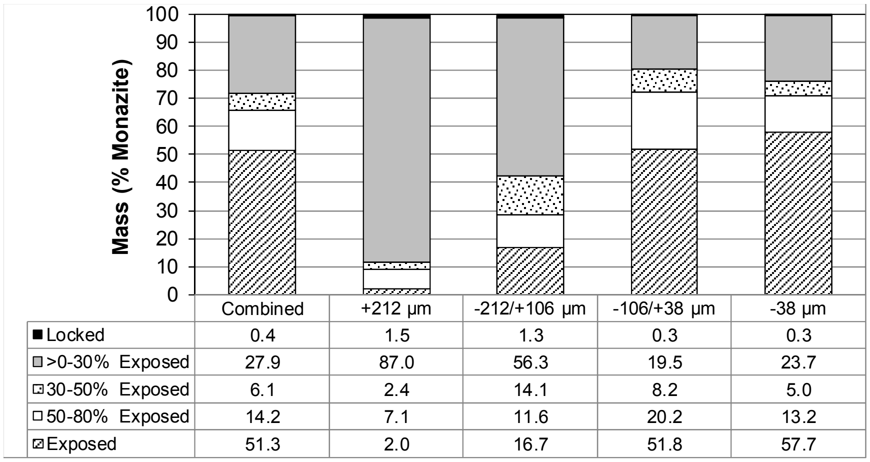

	Combined	+212 μm	-212/+106 μm	-106/+38 μm	-38 μm
■ Locked	0.4	1.5	1.3	0.3	0.3
□ >0-30% Exposed	27.9	87.0	56.3	19.5	23.7
□ 30-50% Exposed	6.1	2.4	14.1	8.2	5.0
□ 50-80% Exposed	14.2	7.1	11.6	20.2	13.2
▨ Exposed	51.3	2.0	16.7	51.8	57.7

Figure 5. Exposure of monazite from a carbonatite complex.

The distribution of the REE is critical because it provides insights to the main LREE and HREE carriers. It enables mass balance calculations to predict potential concentrates and tailings losses. Figure 6 illustrates an example of the elemental deportment calculated for a composite sample. Titanite and apatite carry significant amounts of Ce (32% and 17%) and Y (45% and 21%).

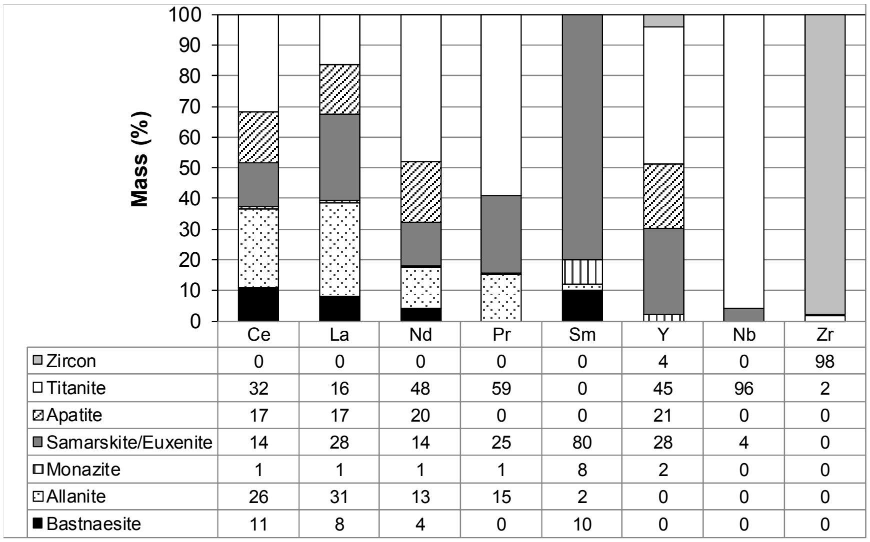

	Ce	La	Nd	Pr	Sm	Y	Nb	Zr
□ Zircon	0	0	0	0	0	4	0	98
□ Titanite	32	16	48	59	0	45	96	2
▨ Apatite	17	17	20	0	0	21	0	0
■ Samarskite/Euxenite	14	28	14	25	80	28	4	0
□ Monazite	1	1	1	1	8	2	0	0
⊡ Allanite	26	31	13	15	2	0	0	0
■ Bastnaesite	11	8	4	0	10	0	0	0

Figure 6. REE, Y, Nb and Zr distribution.

<u>Grade-recovery Calculations</u>

Mineralogically limited grade-recovery analyses provide an indication of the theoretical maximum achievable elemental (or mineral) grade and recovery and are based on individual particle liberation and grade. Thus, deviations from the actual metallurgical values are expected but indicate the potential for beneficiation. It is noted that these values refer only to physical separation. Figure 7 shows the REE recovery from an alkaline (A) and two different carbonatite (C-1 and C-2) complexes. The predicted mineralogical (MIN-A-1) values are similar to those of the metallurgical values (MET-A-1) for the alkaline deposit, but the values deviate for one of carbonatite sample (MIN-C-1). The reason is that the fine-grained liberated REM are not well recovered, but are lost to the slimes. Therefore, metallurgical performance might not necessarily reflect the mineral liberation values. The intention of calculating mineralogical grade and recovery curves is not only to predict the mineral recovery but also to explain and understand the metallurgical performance.

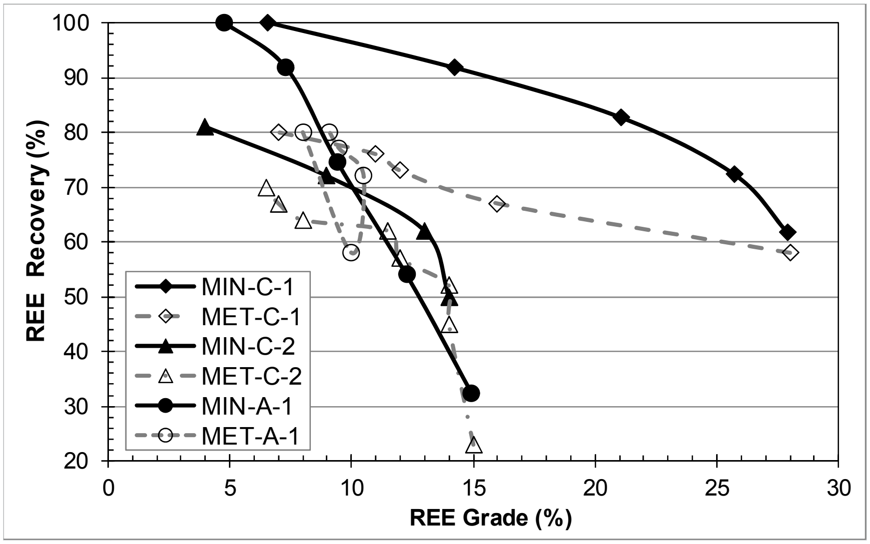

Figure 7. Grade-recovery analysis based on monazite liberation.

Discussion

REE deposits typically display both magmatic and hydrothermal features and the distribution of the REM is complex. Thus, the textural analysis indicates contrasting rock types and styles of mineralization and unlocks the in situ texture of the REM. Quantification of the REM, coupled with geological and geochemical data, can help delineate HREE and LREE zones, map the orebody, and assist in selection of samples for metallurgical test work etc. The REE distribution among the main carriers and common gangue minerals (e.g., apatite, titanite), is critical for metallurgical test work. The liberation and association of the REM is also critical for selecting the proper beneficiation method (i.e., flotation, gravity).

These analyses belong to the emerging discipline of geometallurgy that is becoming increasingly recognized as a discrete and high value activity aimed at a more effective integration of exploration, mine development and process optimization. Automated and quantitative mineralogy constitutes an integral part of the geometallurgical framework.

Acknowledgements

We are grateful to Drs. R. Molnar and Gerhard Heinrich for their comments that helped to improve the content of the manuscript.

References

1. Cornell, David H., "Rare earths from supernova to superconductor", *Pure Applied Chemistry,* 85 (1993), 2453-2464.

2. Chi, Ruan, and Jun Tian, 'Weathered **Crust** Elution- Deposited Rare Earth Ores', Nova Science Pub Inc, 2009, 288 pp.

3. Bao, Z., and Z. Zhao, “Geochemistry of mineralization with exchangeable REY in the weathering crusts of granitic rocks in South China”, *Ore Geology Reviews*, 33 (2008), 519-535.

4. Chakhmouradian, A.R., and F. Wall, “Rare Earth Elements: Minerals, Mines, Magnets (and More)” *Elements*, 8 (2012), 333-340.

5. Kynicky, J., M. Smith and C. Xu, “Diversity of Rare Earth Deposits: A Key Example of China”, *Elements*, 8 (2012), 361-367.

6. Lotter, N.O., “Modern Process Mineralogy: An integrated multi-disciplined approach to flowsheeting”, *Minerals Engineering* 24 (2011), 1229-1237.

7. Grammatikopoulos, T., W. Mercer and C. Gunning, “Mineralogical characterization using the QEMSCAN of the Nechalacho heavy rare earth metal deposit, Northwest Territories, Canada”, Canadian Metallurgical Quarterly (in press).

CHARACTERIZATION OF INDONESIA RARE EARTH MINERALS AND THEIR POTENTIAL PROCESSING TECHNIQUES

Sri Harjanto[1], Shinta Virdhian[2] and Eva Afrilinda[2]

[1]Department of Metallurgy and Materials Engineering, University of Indonesia,
Depok, Indonesia 16424
[2] Department of Foundry and Heat Treatment, Metal Industries Development Center, Bandung,
Indonesia 40135

Keywords: REEs Elements, Monazite, Xenotime, Tin Ore Processing By-product

Abstract

Indonesia has many potential mineral resources including some rare earth elements (REE) minerals, such as monazite and xenotime.Their occurence is in association with tin ores (cassiterite). This paper reports some basic characteristics of mineralogy and chemical composition of the REE minerals associated with tin ores. The main REE minerals in such ores include monazite and xenotime, which contain small amounts of radioactive elements such as thorium (Th) and uranium (U). Potential methods of REE mineral beneficiation and extraction are discussed.

Introduction

Monazite and xenotime are phospate rare earth elements (REE) minerals, which can be found in alluvial deposits. Based on their coordination numbers, Monazite can occur in a number of light and heavy REE deposits, xenotime mainly in heavy REE deposits. They are important minerals for REE production. Monazite (REE,Th)PO_4 can be either Ce, La or Nd rich as it exhibits solid solution chemistry [1]. The density of the monazite ranges from 4.98-5.43 g/cm^3. Xenotime is an yttrium phosphate mineral (YPO_4) with the density of 4.40-5.10 g/cm^3.

In Indonesia, the REE minerals, monazite, xenotime, and zircon are associated with tin, uranium and gold in alluvial deposits. REE minerals are found as by-product of tin ore mining and extraction process activities. The Bangka and Belitung Islands, located in the region between the Peninsular Malaysia and Eastern Sumatra, are known as major alluvial tin deposits in Indonesia. Ikuno *et al.* [2] report that REE range from 30 to 400 ppm in raw sands on Bangka and Belitung islands. Lower grade Monazite and xenotime are found also as alluvial in Kampar and Riau Islands. Rifandriyah *et al.* [3] report the occurrence of REE minerals from the uranium alluvial in West Kalimantan. The ore contains REE minerals (60.85%), PO_4 (32.84 %), U (8528 ppm), Th (816.5 ppm). Indonesia's Center of Geological Resources estimates that the potential deposits of monazite, xenotime and zircon from tin ore mining area in Indonesia is about 951.000 ton [4]. It is expected that this amount would be increased with more extensive exploration activities.

Though the occurrence of REE minerals in Indonesia is already known, intensive mining and extraction of REE minerals as main products has not been developed. This is because of the relatively low production quantity and relatively high processing cost as well. In addition, some REE minerals contain radioactive elements such as uranium and thorium, which hinder the effort to extract the REE from the minerals. According to the Indonesian Government act on minerals and coal at 2010, monazite is classified as a radioactive mineral. This regulation makes the National Agency for Atomic Energy the only authorized institution to conduct the research, exploration and exploitation of radioactive materials in Indonesia. Since then, The National Agency for Atomic Energy has established joint cooperation with a major tin mining and processing company (PT. Timah, Tbk.) in Bangka and Belitung Islands to develop beneficiation and extraction method of the REE from the monazite.

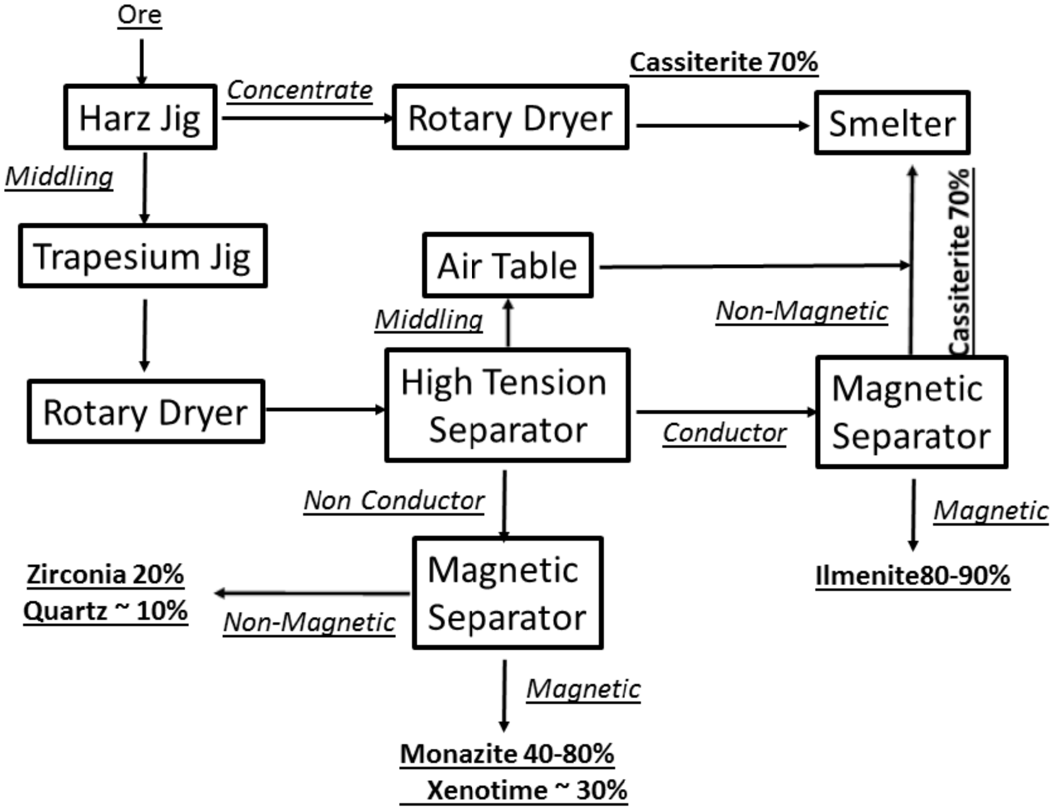

Figure 1. Flow diagram of tin ore processing plant in Indonesia which produces REE minerals as by-product.

Figure 1 reveals a typical tin ore processing flow sheet in Indonesia which could also produce REE minerals by-product. The smelters require high grade cassiterite 70%. REE minerals are separated using high tension electrostatic separation of tin ore middling, as non- conductor fraction. Then, magnetic separation of the non-conductor fraction produces separately monazite (40-80%) and xenotime as magnetic fractions and zircon (20%) and quartz (~10%) as non-magnetic fractions. On the other hand, magnetic separator separates conductor fraction to produce magnetic fraction of ilmenite 80-90% and non-magnetic fraction of cassiterite 70%. However, practically REE minerals by-products end in stock-pile without further extraction process is undertaken.

To increase added value of REE minerals which are produced as by-product of tin ore processing, research and development on the REE beneficiation and extraction have been intensified in both academic and the industries in Indonesia. Therefore, the basic characterictics, in terms of particle size distribution, chemical composition and liberation, of REE minerals should be understood properly for beneficiation and extraction process selection. The present study aims to discuss the basic characteristics of Indonesian REE minerals in terms of their morphology and composition that can affect the potential extraction processes.

Materials and Method

Typical composition of REE minerals associated with tin ore samples from Bangka and Belitung islands are listed in Table I [4, 5]. In general, the content of monazite and xenotime in the tin ores ranges from about 0.67-1.31 % and 0.23- 0.56%, respectively of the total mineral content.

Table I. Typical content of Monazite and Xenotime in unprocessed tin ore (raw sand) in Bangka and Belitung Islands

Minerals	Bangka (%)	Belitung (%)
Cassiterite	40.2	41.0
Monazite	1.31	0.67
Xenotime	0.23	0.56

Figure 2 shows particle size distribution of washed and dried raw sand of tin ore. Median diameter (d_{50}) of the samples is 165 μm. For further characterization, the samples were sieved to the size of less than 100 mesh (149 μm).

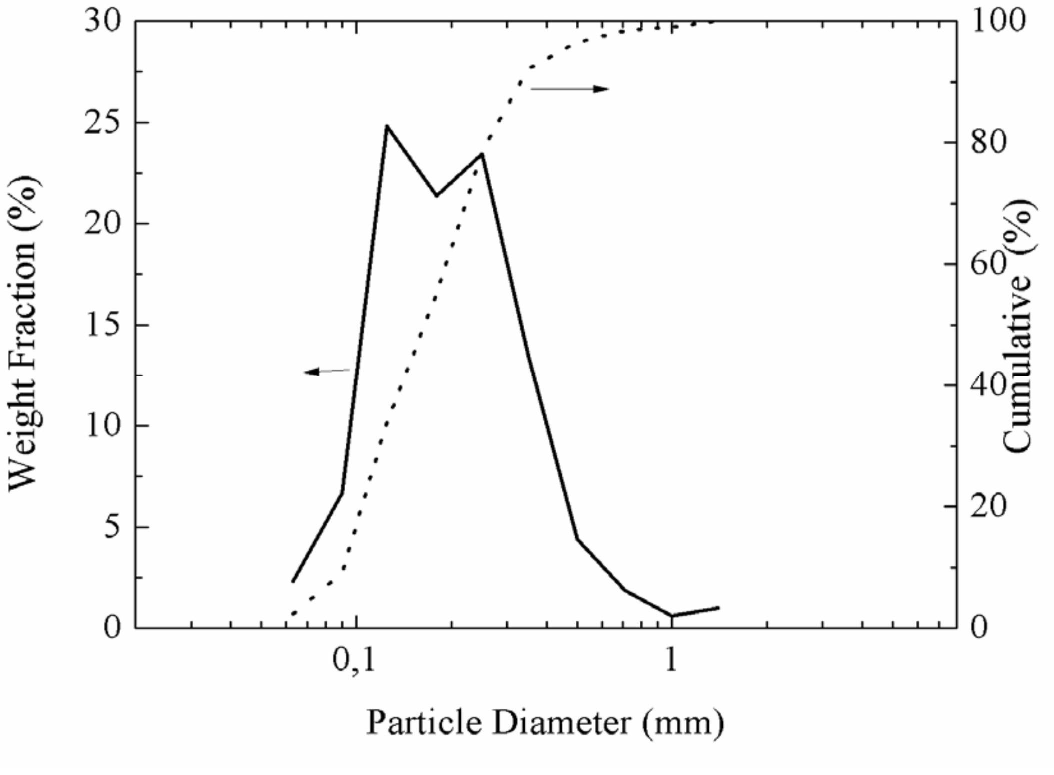

Figure 2. Particle size distribution of washed and dried raw sand of tin ores.

X-ray diffraction (XRD, Phillips Instrument, Inc.) analysis was carried out to determine the bulk chemical composition of the raw sand sample. A scanning electron microscope with energy dispersive spectrometer (SEM/EDX; FEI INSPECT F50, Apolox EDS Analyzer) was employed to evaluate the distribution of REE in particles cross section and the elemental composition of the samples. For SEM/EDX analysis, the samples were taken from the feed of high tension separator (see Fig. 1)

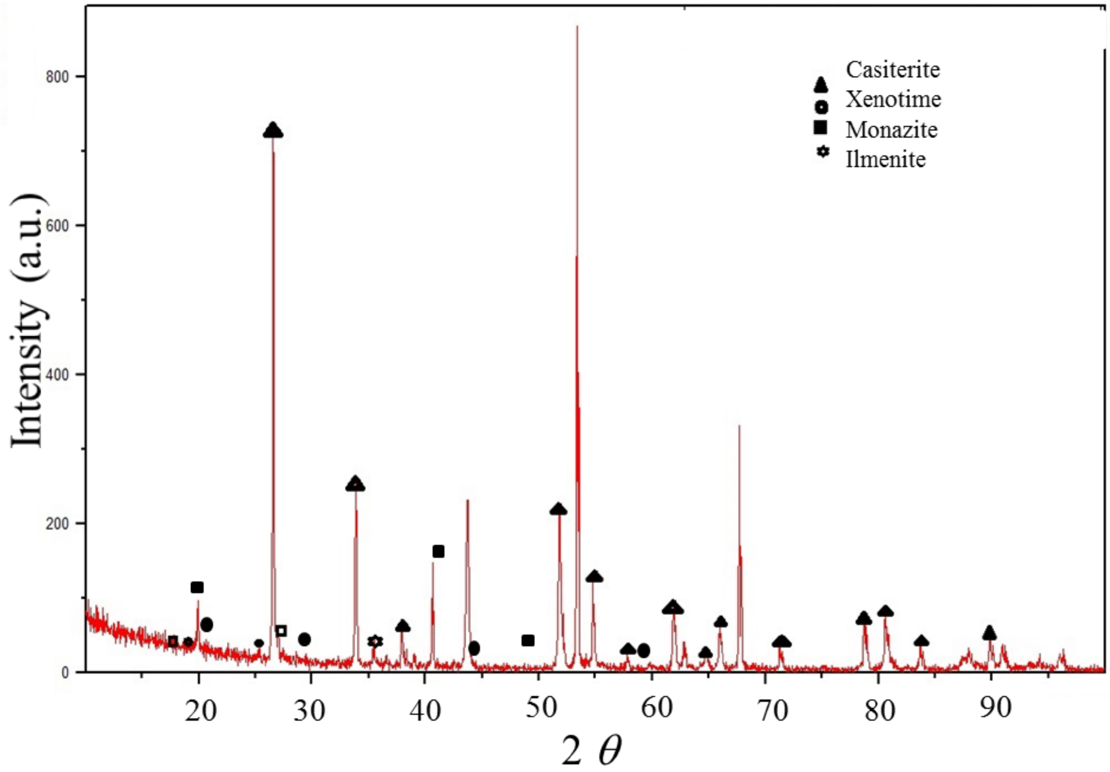

Figure 3. XRD pattern of a tin ore samples containing REE compounds.

Results and Discussion

<u>XRD Pattern of Tin Ore Containing REE</u>

Figure 3 illustrates an XRD pattern that identifies the qualitative mineralogy of the analyzed sample. The sample consists of cassiterite, with minor monazite and xenotime, and ilmenite. Other minerals might be present in low quantities and cannot be determined with the XRD analysis.

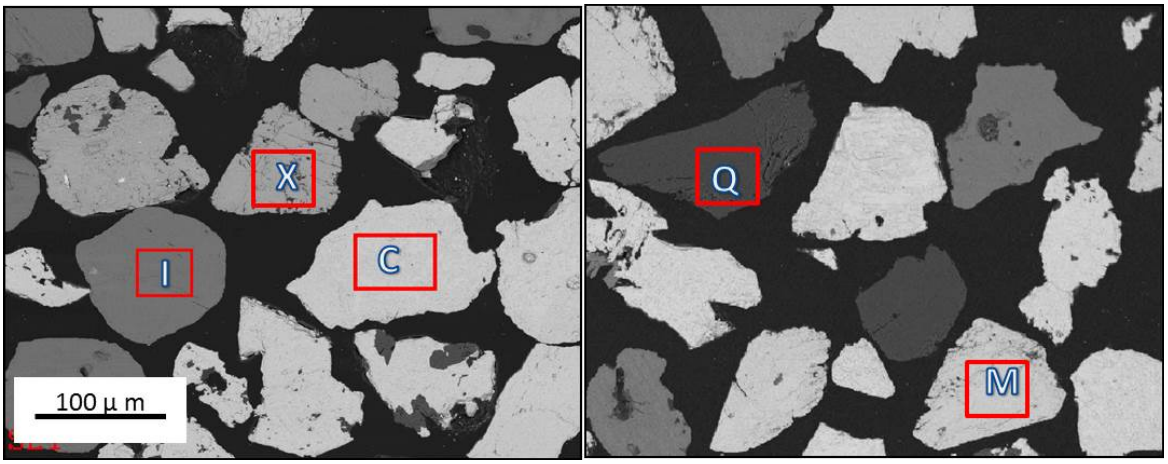

Figure 4. Back scattered SEM images illustrating M = Monazite, C = Cassiterite, X = Xenotime, I = ilmenite, and Q = Quartz. The samples were taken from feed of high tension separator process (see Fig. 1).

Elemental Composisition and Mapping

The main mineral components of the samples as shown in Figure 4 are cassiterite (SnO_2), quartz (SiO_2), ilmenite ($FeTiO_3$), monazite ((Ce, La, Nd, Th)PO_4), xenotime (Y(PO_4)), and zircon ((Zr, REE)SiO_4). The SEM/EDX observations indicate that monazite and xenotime occur as liberated particles [6]. Semi quantitative analysis of monazite indicates that it is rich in Ce, La and Sm, but also contains U and Th, whereas xenotime contains mainly Y and minor Gd and Dy (Fig. 4 (a) and (b)).

The EDX analysis of the selected particles composition is given in Table II. The results indicate that xenotime and monazite exhibit chemical variation. The range of compositions are observed and analysed from several particles of the samples. Monazite and zircon contain the highest content of Th (5-7 wt%) while xenotime hosts less than 2%.

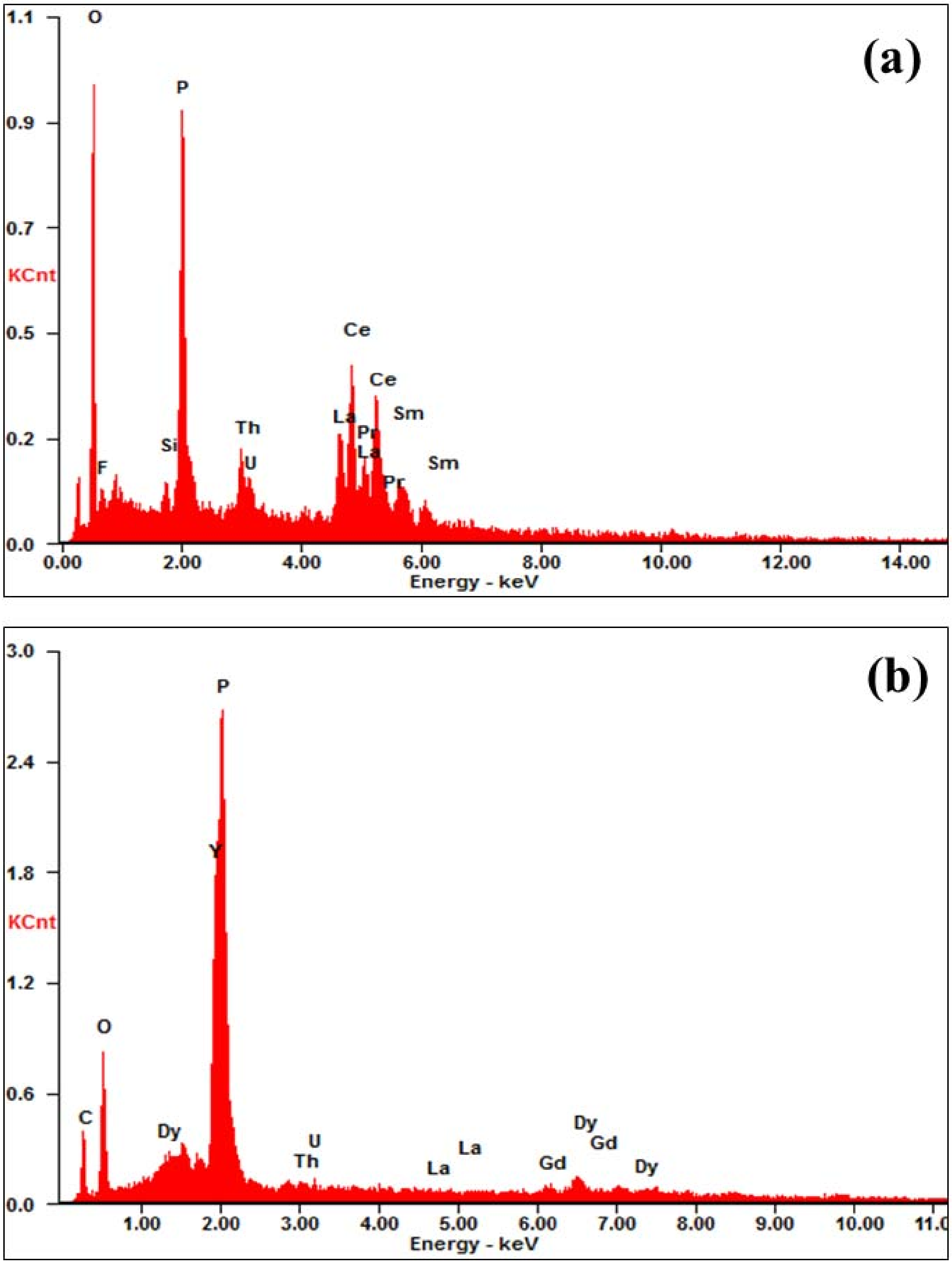

Figure 4. Elements analysis from EDX spectrum; a) monazite, and b) xenotime.

Figure 5 and Table III depict the cross section morphology and elemental composition of a single monazite particle. Spots analysis of EDX expresses that major monazite is intergrown with other minerals. Point (1) and (2) analyses indicate monazite, and point (3) an silicate gangue mineral.

Table II. Semi-quantitative EDX Analysis of Selected RE Minerals Particles

Elements	Wt%	
	Monazite	Xenotime
O	15.2 - 30.8	30.4 - 31.8
P	9.7 - 16.3	17.4 - 21.3
La	9.7 - 12.7	0.3 - 0.9
Ce	23.3 - 28.2	-
Pr	2.2 - 9.8	-
Sm	0.8 - 2.2	-
Dy	-	5.5 - 8.7
Gd	1.8 - 5.6	2.2 - 8.5
Nd	~9.4	0.6
Y	-	30.2 - 34.5
Zr	~19.3	-
Th	5.4 - 7	1.5
U	0.8 - 1.8	0.7

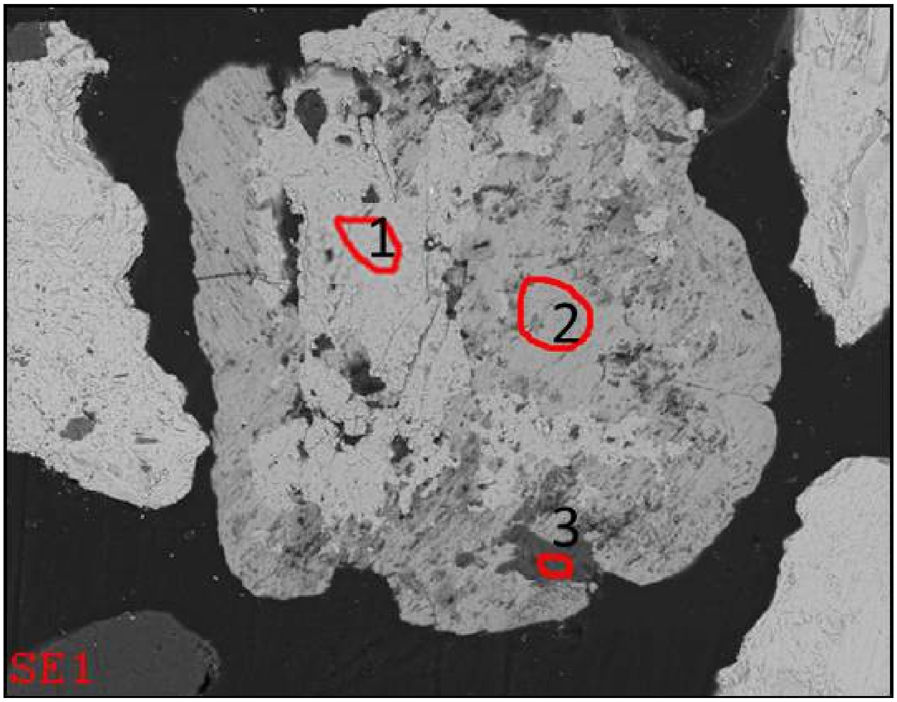

Figure 5. Cross section of a monazite particle analysed by using EDX at spot 1, 2 and 3.

The elemental distribution maps of monazite and xenotime are shown in Figure 6(a) and 6(b), respectively. Brighter figure of particle indicates relatively higher intensity of element analysed in the cross section of particle. Figure 6(a) shows that La, Ce, Pr, Sm, U and Th are distributed homogenously in the grains. Xenotime exhibits almost the same characteristic (Figure 6 (b)). Y, La, Gd, Th and U do not show zoning but Dy appears to be sporadically distributed.

Table III. EDX Analysis of One Monazite Particle as Shown in Figure 5

Element	Wt %		
	Point 1	Point 2	Point 3
O	27.7	33.8	40.9
P	18.2	18.6	-
U	1.4	-	-
La	14.4	12.0	-
Pr	4.9	-	-
Ce	33.4	28.8	-
Fe	-	04.9	9.3
Mg	-	-	1.0
Al	-	-	17.1
Si	-	-	23.6
Ca	-	1.9	-
Nb	-	-	3.3
K	-	-	4.6

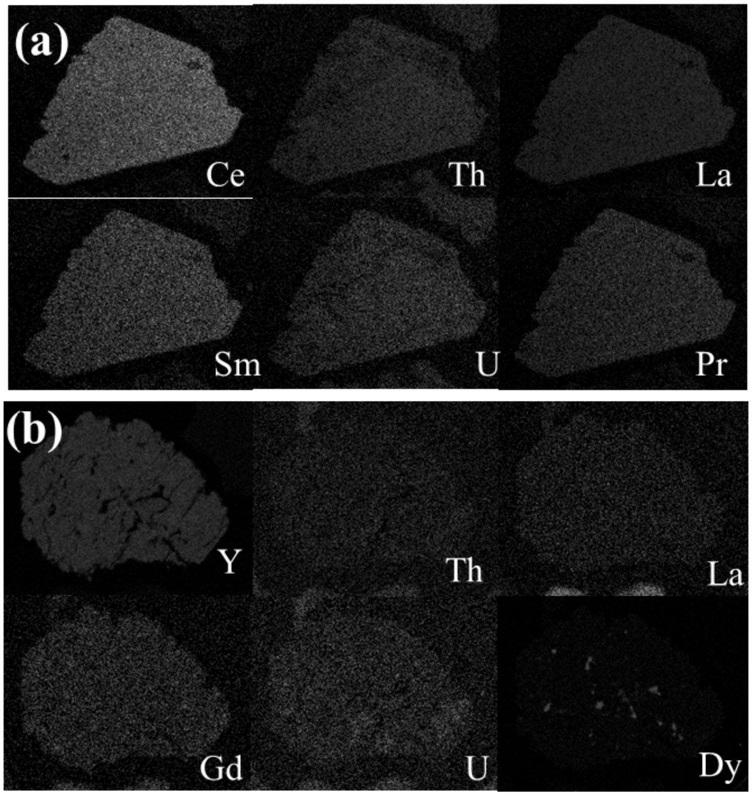

Figure 6. Elementals mapping of (a) monazite and (b) xenotime particles. The composition of monazite and xenotime refers to Table II. Brighter figure of particle indicates higher intensity.

Potential Processing Techniques

Processing techniques of REE minerals associated with tin ore includes concentration and extraction process. Since, monazite and xenotime are categorized as paramagnetic materials, separation processes based on the difference of their magnetic properties is possible to be undertaken. Concentration process of monazite by using combination of magnetic separator and high tension separator of ore is often utilized and gives adequate separation product. In the case of Egyptian beach sand, this concentration process produce high grade monazite concentrate of 97% [7]. In the case of REE minerals associated with tin ores in Indonesia, beneficiation process of tin ores produces monazite, xenotime and ilmenite as by-products. To produce REE minerals as main product from REE minerals associated with tin ores with higher grade, the concentration process should be modified and optimized.

Figure 7 shows simplification of REE selective extraction from their radioactive elements, such as Th and U [8]. The process is based on two stages sulfuric acid leaching at relatively high temperature. It succesfully reduces the radioactive elements content from typically U=0.3%, Th= 3.0% to U= 2ppm and Th=16 ppm, respectively [9]. The REE grade increases from 60% in the feed to about 85% in the product.

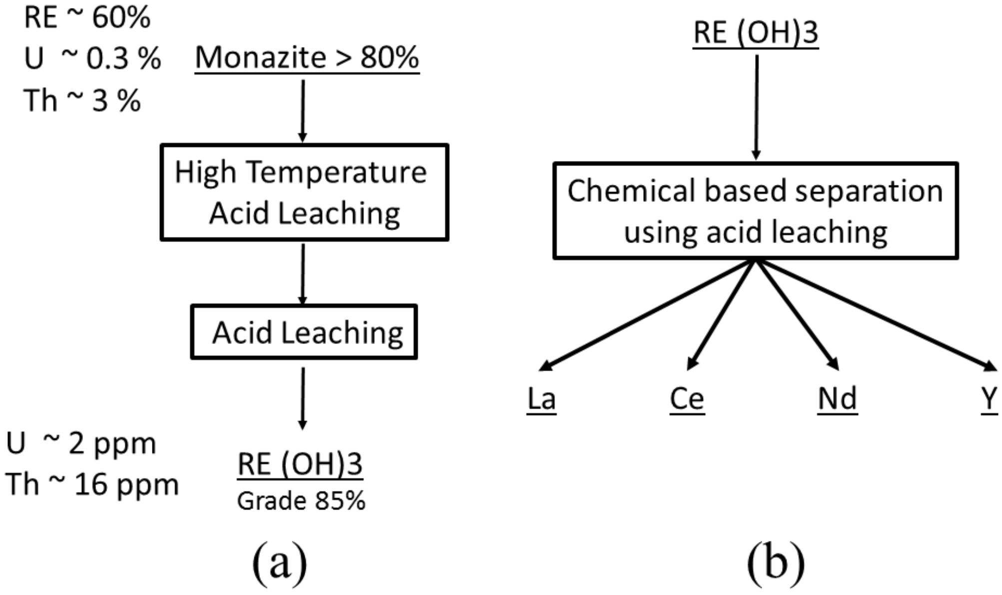

Figure 7. (a) Extraction process of REE minerals to RE(OH)3 by acid leaching, and (b) separation process of $RE(OH)_3$ to individual REE.

Further selective extraction of REE concentrates and/or crude oxide or phosphate to individual rare earth elements compounds had been reported [9, 10] previously. By using KCl and $AlCl_3$ as transporting agents, REE mineral concentrates were extracted as vapor complexes, and selectively deposited in the furnace wall at the temperature range of 600-700^{o}C for heavier fractions and 800-900^{o}C for lighter fractions. Radioactive elements, such as Th and U were deposited at lower temperature range. Uda et al. (2000) also utilized separation process based on combination of selective reduction and vacuum distillation of REE halides [11]. It was reported that the process enhances separation of samarium and neodymium from the REE mixtures. Figure

7 shows simplification separation process of RE(OH)3 to individual elements, i.e. La, Ce, Nd and Y, based on sulfuric acid leaching [12].

Conclusions

Preliminary mineralogical results of REE minerals associated with tin ores from Bangka Island reveals that the main REE minerals are monazite and xenotime. Analysis of particles samples with the size of less than 149 µm showed that Monazite consists mainly of Ce, La, Nd and Xenotime of Y, Dy, Gd elements. Radioactive elements such as Th (6-7%) was detected in monazite and it is lower in xenotime (< 2%). Uranium was also detected within lower range. Concentration of REE minerals associated with tin ore may utilize the combination of magnetic and high tension separator process. Modification and optimization of the concentration process in tin ore processing plant should be undertaken to produce higher grade REE minerals products. Further evaluation to select the extraction process of minerals concentrate to individual REE compounds should be undertaken based on their mineralogy, physical and chemical characteristics.

References

1. A. Jordens et al.,"A Review of the Beneficiation of Rare Earth Element Bearing Minerals", *Min. Eng*, 41(2013) 97-114.
2. T. Ikuno et al. "Concentration and Geochemical behavior of REE in Hydrothermally Altered and Weathered Granitic Rocks in Southern Thailand and Bangka Island, Indonesia", *Int. Symposium on Earth Science and Technology*, (2010) 269-273.
3. E. Rifandriyah et al., " Determination of Optimal Decomposition of Rirang Kalan Uranium Ore", (Reports of Nuclear Geology Development Center – National Nuclear Agency of Indonesia).
4. R. Sukhyar, "Potential and Distribution of Indonesia Mineral Resources and Deposits", (Seminar on Acceleration Attempts to Increase Domestic Minerals Added Value, Jakarta 10 April 2013)
5. S. Irawan, "Rare Earth Element Minerals Processing in PT. Timah Tbk", (Workshop on Rare Earth Element Minerals Processing and Refining in Indonesia, 2013)
6. J.S. Suprapto., "Study of Rare Earth Elements", *Journal of Geology Resources* vol. 4, no 1 (2009).
7. M.I. Moustafa and N.A. Abdelfattah, "Physical and chemical beneficiation of the Egyptian Beach Monazite", Resource Geology 60 (3) (2010), 288-299
8. T. Wahyudi et.al., *Rare Earth Mineral, Crude Oil 21st Century*, (Minerals and Coal Research and Development Center, 2012) 95.
9. E. Rifandriyah, et al. (Indonesia Patent.00201000727), Monazite ore processing to produce free radioactive element of $RE(OH)_3$, 2010.
10. K. Murase et al., " Extraction and mutual separation of rare earths from concentrates and crude oxides using chemical vapor transport", *J. Alloys and Comp.* , 233 (1996) 96-106.
11. T. Uda, K. T. Jacob and M. Hirasawa, "Technique for Enhanced Rare earth Separation", *Science*, Vol. 289(5488), (2000) pp. 2326-2329.
12. PTAPB, Indonesia Paten P.002.003.004.95, 2003.

APPLICATION OF REACTIVE OILY BUBBLE FLOTATION TECHNOLOGY TO RARE EARTH MINERAL FLOTATION

Zhenghe Xu[1,2], Fang Zhou[3], Louxiang Wang[1], Qingxia Liu[1], Jacob Masliyah[1], Ni Xiao[1]
Qi Liu[1], Ruan Chi[3], Shengming Xu[2]

[1]Department of Chemical and Materials Engineering, University of Alberta
Edmonton, Alberta, Canada T6G 2V4

[2]Institute of Nuclear and New Energy Technology, Tsinghua University
Beijing, P.R. China 100084

[3]School of Minerals Processing & Bioengineering, Central South University
Changsha, Hunan, P.R. China 410083

Keywords: Flotation, Reactive Oily Bubble, Bastnaesite, Induction Time, Zeta Potential

Extended Abstract

A novel concept of reactive oily bubbles (i.e., bubbles covered by a thin layer of oil containing oil-soluble collectors) as a carrier in flotation as shown in Figure 1 is proposed. In contrast to oil flotation or oil bubble flotation where collector is added in the pulp, in reactive oily bubble flotation [1], sparingly water soluble collector (oleic acid or hydroxamic acid) is added in the oil which covers air bubbles in the form of thin oily film. In the reactive oily bubble flotation, there is no need for collector to fully cover the mineral surfaces. In contrast to conventional flotation where collector is added in aqueous phase, since the collector is added in the oil phase with limited solubility in water, the reactive oily bubble flotation could avoid undesired synergetic interactions among collectors, activators, depressants and dispersants present in slurry, minimize undesired activation of gangue particles and significantly reduce the amount of collectors needed.

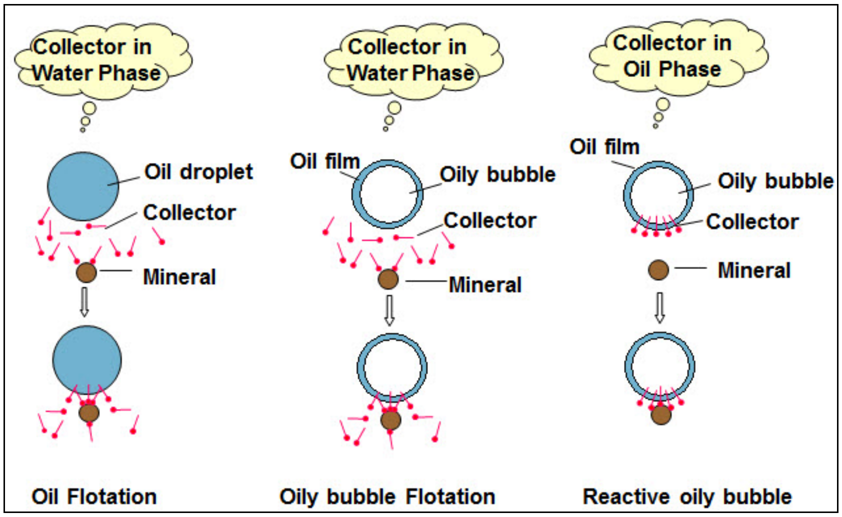

Figure 1. Concept of reactive oil bubble flotation [1].

In this study, the reactive oily bubble flotation technology is tested for rare earth (bastnaesite) mineral flotation. The XRF microprobe analysis on several mineral particles showed that the mineral samples used in the current study contain 24-29 wt% La and 34-39% Ce, with 2-3% Si, 4-5% S, ~7% P, 1-2% Ca, 13-19% Ba and ~3% Fe. The qualitative RXD analysis confirmed the sample being mainly bastnaesite. The zeta potential measurement showed an isoelectric point of pH 6.5 for the bastnaesite samples, as shown in Figure 2.

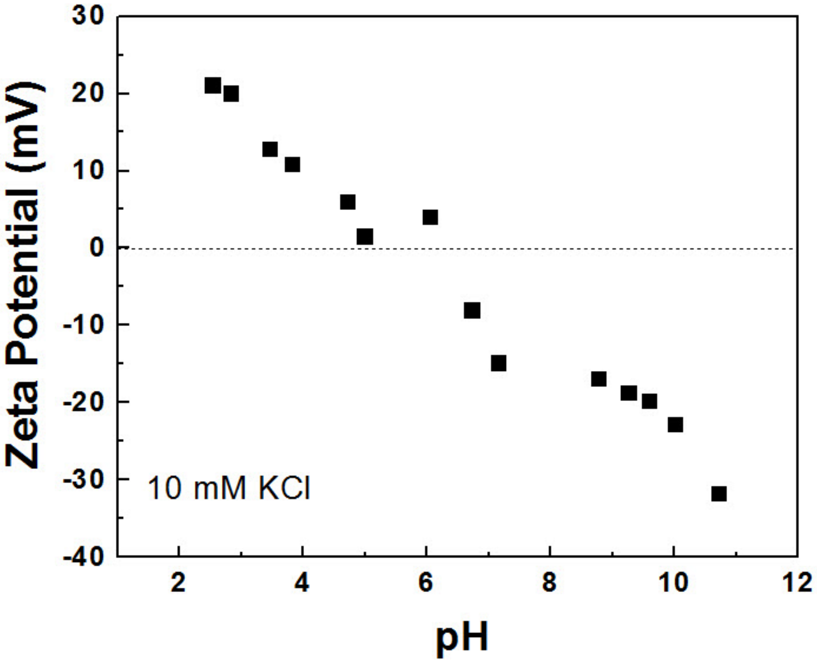

Figure 2. Zeta potential of bastnaesite as a function of pH in 10 mM KCl solutions.

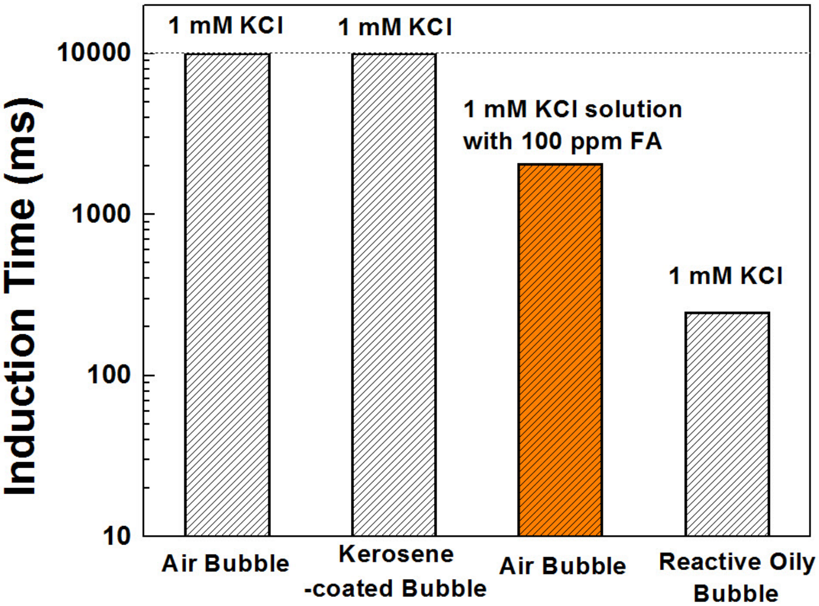

Figure 3. Induction time of various types of bubbles attaching to bastnaesite.

The floatability of bastnaesite by reactive oily bubble flotation is evaluated by the induction time measurement of bubble-particle attachment. As shown by the results in Figure 3, air bubbles do not attach to bastnaesite in 1 mM KCl solutions at pH 6 (induction time > 10,000 ms) without collector addition, as anticipated. Similarly, oily bubbles, i.e., air bubbles covered with a thin layer of kerosene, do not attached to bastnaesite either in 1 mM KCl solutions at pH 6. Conditioning the bastnaesite in 1 mM KCl solutions containing 100 ppm fatty acids at pH 6, air bubbles are able to attached to the conditioned bastnaesite, with an induction time close to 2000 ms. A significant reduction in induction time of reactive oil bubble attaching to bastnaesite was observed with induction time to be around 200 ms, indicating a much stronger collecting power of reactive oily bubbles than air bubbles. Similar observation has been reported for sulfide mineral flotation systems [2].

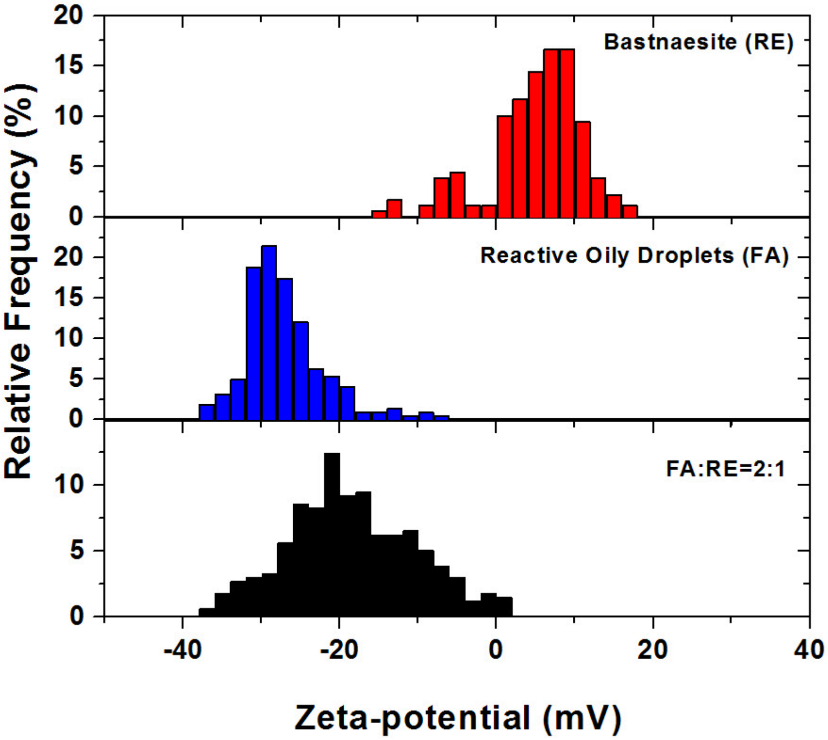

Figure 4. Zeta potential distribution of bastnaesite and reactively oily bubbles, either alone or in a mixture of the two in 10 mM KCl solutions of pH 6.

The attachment of fatty acid reactive oily bubble to bastnaesite is confirmed by the results of zeta potential measurement [2], as shown in Figure 4. When measured individually in 10 mM KCl solutions at pH 6, bastnaesite is positively charged with a zeta potential distribution centered at around 10 mV while the fatty acid reactively oily bubbles are negatively charged with a zeta potential distribution being centered at around -28 mV. Considering a pKa value of around pH 4.5 for carbolic acid group, the observed negative surface charge of fatty acid reactive oily bubble is not unexpected. It is interesting to note that when the fatty acid reactive oily bubble suspension is mixed with the bastnaesite suspension at 2:1 volume ratio, only a single model zeta potential distribution is observed with the distribution centered at the location close to the distribution of fatty acid reactive oily bubbles, suggesting that the reactive oily bubble almost fully covered bastnaesite by either simple attachment to or spreading of reactive oily bubbles on bastnaesite. This finding again suggests that the fatty acid reactive oily bubble could effectively float bastnaesite at pH 6.

The flotation results of bastnaesite using conventional air bubbles and reactive oily bubbles are shown in Figure 5. It is not surprising that a much higher flotation recovery is obtained using fatty acid reactive oily bubbles than using conventional flotation, as predicted by the results of the induction time measurement.

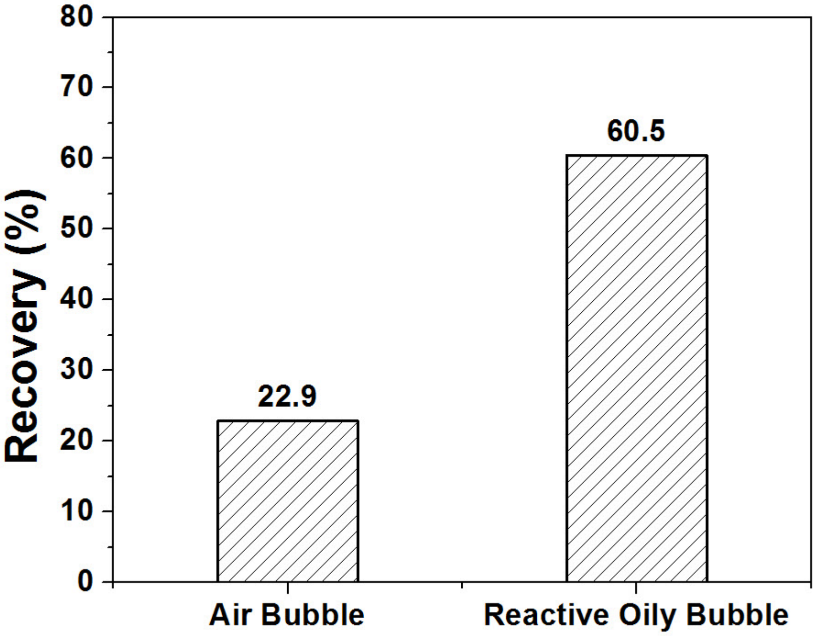

Figure 5. Flotation of bastnaesite using conventional and reactive oily bubble flotation at pH 6.

Although a significant improvement in bastnaesite recovery was obtained with fatty acid reactive oily bubbles, hydroxamic acid reactive oily bubble showed an opposite effect as shown in Figure 6 by the measured induction time. Although a very short induction time was observed with air bubbles for the conditioned bastnaesite with hydroxamic acid, no attachment of hydroxamic acid reactive oily bubble to bastnaesite was observed. This finding suggests that careful engineering of collector is of critical importance to realize the advantage of reactive oily bubble flotation.

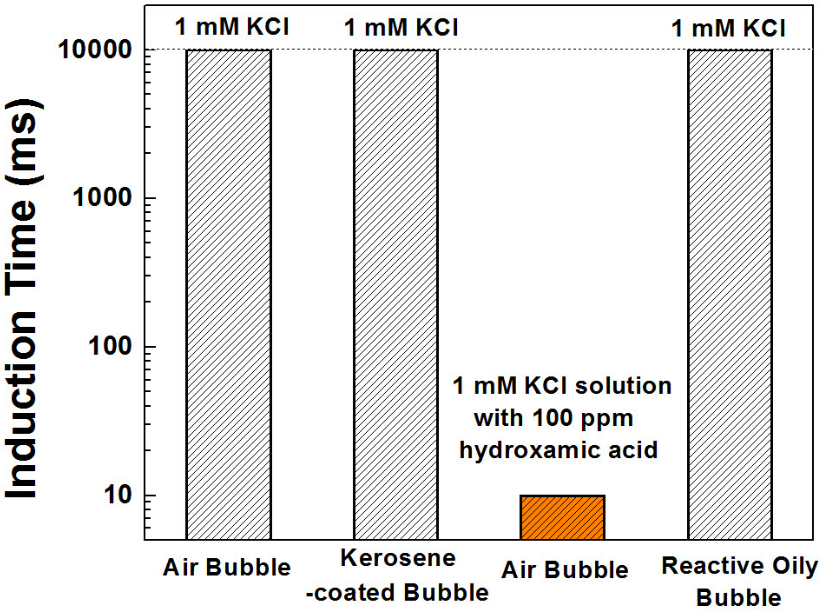

Figure 6. Induction time of various types of bubbles in bastnaesite and hydroxamic acid systems at pH 6.5.

References

1. Liu, J., Mak, T., Zhou, Z. and Z. Xu, Fundamental Study of Reactive Oily-bubble flotation, *Minerals Engineering*, 15 (2002), 667-676.

2. Xu, Z., Liu, J., Choung, J. and Z. Zhou, Electrokinetic Study of Clay Interactions with Coal in Flotation, *Int. J. Miner. Process.*, 68 (2003), 183-196.

FLOTATION FLOWSHEET DEVELOPMENT FOR AVALON RARE METAL'S NECHALACHO DEPOSIT

J. Guan[1], *B. Yu[2], D. Qi[3]

[1,3]Avalon Rare Metals Inc.
1901 - 130 Adelaide Street West
Toronto, ON M5H 3P5, Canada
jguan@avalonraremetals.com
dqi@avalonraremetals.com

[2]SGS Minerals Services – Lakefield site
PO Box 4300
185 Concession Street
Lakefield, ON K0L 2H0, Canada
*ben.yu@sgs.com

Keywords: Rare Earth Elements, Mineralogy, Flotation

Abstract

A feasibility study on Avalon Rare Metal's Nechalacho deposit located in the Northwest Territories has been completed recently. The deposit contains rare earth element minerals such as allanite, monazite, synchysite, columbite, fergusonite, zircon and bastnaesite contained in two ore zones- the Upper and Basal Zones. Various bench scale tests in grinding, magnetic separation, desliming, flotation, gravity concentration and dewatering were performed on four different ore composites made from the two zones to develop the flotation flowsheet. Three continuous pilot plants were set up to test the results from the various tests. Results from the bench scale tests and pilot plants at SGS will be reviewed to explain the development of the final flotation plant flowsheet incorporated in the feasibility study.

Introduction

Rare earths are becoming a necessity to life in the 21st century. Rare Earth Elements (REE) are the 15 elements that make up the Lanthanide series in the periodic table. Light rare earth elements (LREE) such as lanthanum can be used in fuel cells, while heavy rare earth elements (HREE) such as yttrium are used as phosphors for LEDs. In recent years, they have been sourced almost exclusively from China and rare earths are becoming a strategic resource for the developed world. Avalon Rare Metals Inc. is a mineral development company focused on the rare metal deposits in Canada. Its flagship project, the 100%-owned Nechalacho Deposit, Thor Lake, Northwest Territories, is emerging as one of the largest undeveloped rare earth elements resources in the world. Its exceptional enrichment in the more valuable 'heavy' rare earth elements, key to enabling advances in green energy technology and other growing high-tech applications, is one of the few potential sources of these critical elements outside of China, currently the source of over 95% of the world supply.

Two separate pilot plants were held at SGS Minerals in Lakefield, Ontario to demonstrate the Nechalacho flowsheet and reagent scheme. The first was a small scale plant, putting through approximately 4 tonnes of material, while the latter was a 40 tonne pilot plant. The two pilot plants generated valuable information for the development of the Nechalacho flowsheet and will be discussed throughout this paper.

A Feasibility Study for the Thor Lake project was published in April 2013. This paper will discuss the flowsheet development for the Nechalacho site as included in the feasibility study.

Figure 1 below shows a simplified block diagram of the Nechalacho flowsheet. Ore is milled, deslimed, and magnetically separated before entering flotation. The final cleaner concentrate is sent to a gravity concentrator for upgrading, before being dewatered as the final product.

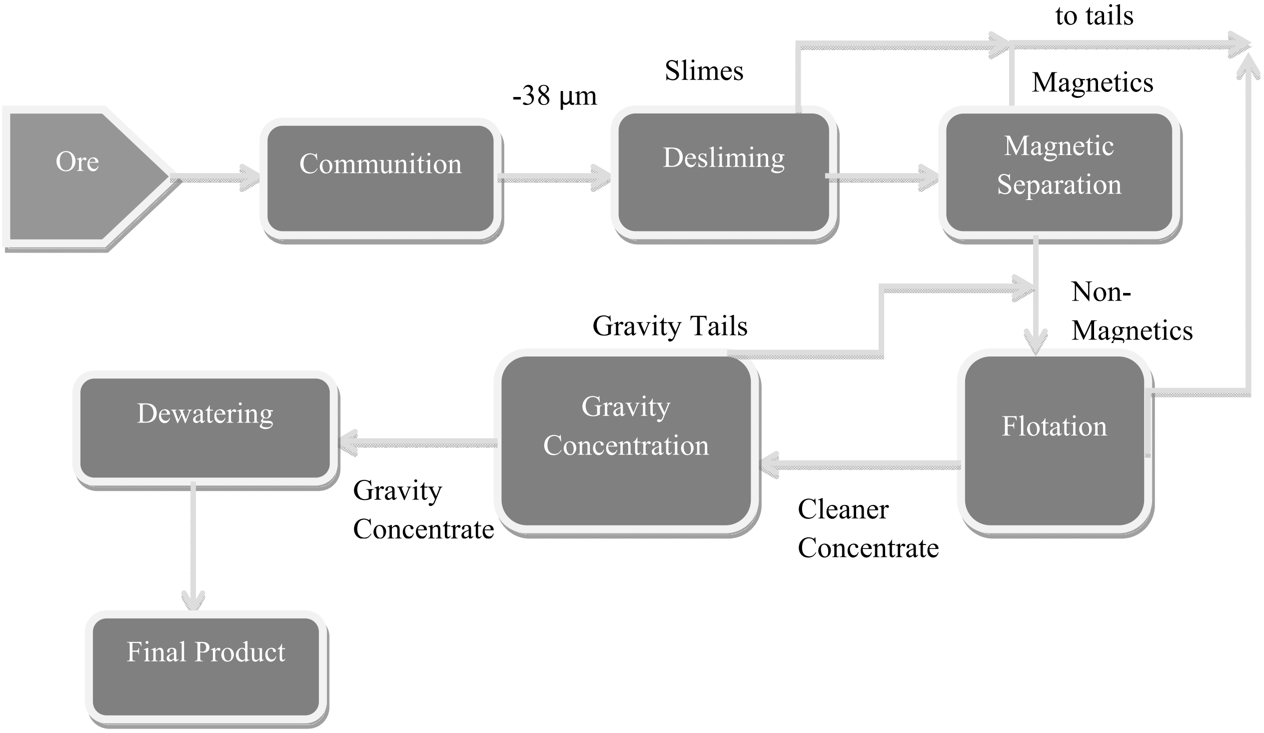

Figure 1. Overview of Necholacho flowsheet.

Design Criteria

The following flowsheet is designed for a facility treating 2,000 tpd of ore, with the option to double the capacity to 4,000 tpd. A bulk rare earth concentrate rich in Nb, Zr, Y and other REE will be produced with approximately 10% moisture content and the final concentrate mass pull will be approximately 18% of the mill feed.

Mineralization

Deposit and Bulk Samples

The Nechalacho deposit is a tabular hydrothermal alteration zone extending typically from surface to depths of 200- 250 metres, characterized by alternating sub-horizontal layers of relatively high and lower grade REE mineralization. There is a gradual increase in HREE from surface to depth with the lowermost sub-horizontal layer, which is also the most laterally continuous, being referred to as the Basal Zone (BZ). The Basal Zone part of the orebody is the part that is planned to be mined due to the higher grade of rare earths, niobium and zircon with high higher percentage of HREO relative to TREO compared to the upper parts of the mineralization.

Four bulk samples were prepared for the 40 tonne pilot plant, with one referred to as BZ-MP being the Basal Zone portion most closely representing the material to be extracted through the present mine plan.

Mineral Abundance

Table I lists the mineral abundance of BZ-MP ore. BZ-MP ore head is dominated by plagioclase (15.7%), biotite (23.0%), quartz (21.3%), K-feldspar (15.6%), minor Fe oxides (6.3%), zircon (5.6%), ankerite (2.8%), calcite (1.3%), allanite (1.0%) and trace amounts (<1%) of dolomite, fluorite, bastnaesite, fergusonite, monazite, columbite (Fe), synchysite, chlorite, amphibole, other silicates, apatite and other minerals.

The payable elements of the Nechalacho deposit are hosted in a number of ore minerals, summarized as follows:

- Light rare earths (LREE) dominantly occur in bastnaesite, synchysite, monazite and allanite;
- Heavy rare earths (HREE) dominantly occur in zircon and fergusonite ;
- Zr (along with HREE, Nb and Ta) occurs in zircon;
- Nb and Ta occur in columbite (Fe), fergusonite and zircon.

Table I. Mineral abundance for BZ-MP Bulk Sample

Fraction		Combined	+25um		-25um	
Mass Size Distribution (%)			52.7		47.3	
Calculated ESD Particle Size		13	32		8	
		Sample	Sample	Fraction	Sample	Fraction
Mineral Mass (%)	Columbite(Fe)	0.3	0.1	0.2	0.2	0.3
	Fergusonite	0.7	0.3	0.6	0.4	0.8

Fraction		Combined	+25um		-25um	
Mass Size Distribution (%)			52.7		47.3	
Calculated ESD Particle Size		13	32		8	
		Sample	Sample	Fraction	Sample	Fraction
	Bastnaesite	0.5	0.3	0.6	0.2	0.3
	Synchysite	0.7	0.3	0.6	0.4	0.8
	Allanite	1.0	0.4	0.8	0.6	1.2
	Monazite	0.3	0.1	0.2	0.2	0.3
	Other REE	0.0	0.0	0.0	0.0	0.0
	Zircon	5.6	3.5	6.7	2.1	4.5
	Apatite	0.1	0.0	0.1	0.0	0.1
	Quartz	21.3	11.6	22.1	9.7	20.5
	Plagioclase	15.7	11.8	22.5	3.8	8.1
	K-Feldspar	15.6	11.3	21.5	4.3	9.0
	Microcline	2.5	0.2	0.3	2.4	5.0
	Biotite	23.0	6.9	13.1	16.2	34.1
	Muscovite/Clays	0.1	0.1	0.1	0.0	0.0
	Chlorite	0.2	0.2	0.3	0.1	0.2
	Other Silicates	0.5	0.1	0.3	0.3	0.7
	Calcite	1.3	0.5	1.0	0.7	1.5
	Dolomite	0.9	0.5	1.0	0.3	0.7
	Ankerite	2.8	0.9	1.7	1.9	4.0
	Other Carbonates	0.0	0.0	0.0	0.0	0.0
	Fluorite	0.6	0.3	0.6	0.3	0.6
	Fe-Oxides	6.3	3.0	5.7	3.3	6.9
	Other	0.1	0.0	0.0	0.1	0.1
	Total	100.0	52.7	100.0	47.3	100.0
Mean Grain Size by Frequency (µm)	Columbite(Fe)	6	10		5	
	Fergusonite	9	16		7	
	Bastnaesite	12	17		7	
	Synchysite	9	16		7	
	Allanite	10	17		7	
	Monazite	7	12		6	
	Other REE	4	6		3	
	Zircon	11	22		8	
	Apatite	9	13		7	
	Quartz	11	25		7	
	Plagioclase	19	31		9	

Fraction		Combined	+25um		-25um	
Mass Size Distribution (%)			52.7		47.3	
Calculated ESD Particle Size		13	32		8	
		Sample	Sample	Fraction	Sample	Fraction
	K-Feldspar	22	30		12	
	Microcline	6	8		5	
	Biotite	9	20		7	
	Muscovite/Clays	5	8		4	
	Chlorite	13	18		9	
	Other Silicates	5	9		4	
	Calcite	10	19		7	
	Dolomite	11	23		6	
	Ankerite	8	16		7	
	Other Carbonates	11	11		0	
	Fluorite	16	25		11	
	Fe-Oxides	11	24		7	
	Other	5	7		4	

Head Assay

Table II lists the head assay for BZ-MP sample. The total rare earth content was 1.847% and proportion of HREO of TREO was 22.1%; with Nb_2O_5 at 0.43% and ZrO_2 at 3.83%.

Table II. Head Assay for BZ-MP

La_2O_3	Ce_2O_3	Pr_6O_{11}	Nd_2O_3	Sm_2O_3	Eu_2O_3	Gd_2O_3	Tb_4O_7	Dy_2O_3	Ho_2O_3	Er_2O_3	Tm_2O_3	Yb_2O_3	Lu_2O_3	Y_2O_3	**TREO**	Ta_2O_5	Nb_2O_5	ZrO_2
0.300	0.660	0.047	0.362	0.070	0.009	0.068	0.011	0.062	0.011	0.028	0.004	0.022	0.003	0.190	**1.847**	0.04	0.43	3.83
Whole Rock Assay %														Other ppm				
SiO_2	Al_2O_3	Fe_2O_3	MgO	CaO	Na_2O	K_2O	TiO_2	P_2O_5	MnO	Cr_2O_3	V_2O_5	LOI	Sum		Th	U		
53.2	10.1	12.5	3.03	3.19	2.73	4.65	0.04	0.10	0.28	< 0.01	< 0.01	3.48	93.3		105	23.1		

Comminution: Ore will be first crushed to -13.5 mm in a three-stage crushing process before entering the grinding circuit, which consists of an open circuit rod mill, classifying cyclones, and a closed circuit ball mill. The rod mill will grind the material to -1.75 mm, which is then sent to be classified by the cyclones, where the underflow is sent to the ball mill while the overflow with a P80 of 36μm is sent to magnetic separation. The ball mill further grinds the cyclone underflow, with discharge being recycled back to the classifying cyclones. Bond Rod mill index and Abrasion Index tests results for the tests can be seen below in Tables III and IV respectively. These tests were conducted on Thor Lake ore during a 40t pilot test and later in October 2012 to confirm results from the 40t pilot. For later confirmatory work in October, 2012, samples representing the Basal Zone represented in the mine plan were split into two composites Q3 and Q4 which together represent similar material to the BZ-MP. The feed size for all the tests were

12.7 mm while the rod mill closing size was 14 mesh, and the ball mill closing size was 200 mesh.

Table III. Bond Rod Mill Data

Parameter	Unit	40t	October 2012	
		BZ-MP	BZ-Q3	BZ-Q4
Bond Rod Mill RWi	kWh/t	14.8	15.8	15.5
Bond Rod Mill Hardness Percentile	%	56	67	64

The ore was found to be medium in the hardness range. The subsequent tests done in October 2012 indicated that the deeper material was harder than results from the 40t pilot plant, with the BZ-Q3 material being in the 67th percentile of hardness compared to historical SGS reference database.

According to the results from the Bond Ball Mill work index, the various composites are similar in terms of hardness, ranging from 14.7 to 17.6 kWh/t, and were found to be in the medium hard (?range) relative to the SGS reference database. [1]

Table IV. Bond Ball Mill Data

Parameter	Units	40 t	Oct 2012	Oct 2012
		BZ-MP	BZ-Q3	BZ-Q4
Bond Ball Mill BWi	kWh/t	15.4	17.6	17.0
Bond Ball Mill Hardness Percentile	%	58.9	81	76

BZ-MP was found to be the most abrasive among the four composites with the highest abrasion index of 0.607. The BZ-Q3 & Q4 results were generated from the work in October 2012 [1].

Table V. Abrasion Index Test Summary

Sample	AI	Percentile
BZ-MP	0.607	86
BZ-Q3	0.588	85
BZ-Q4	0.581	85

All three composites fell in the abrasive range relative to SGS reference database.

Magnetic Separation: Magnetic Separation by low intensity magnets (LIMS) was thought to be necessary due to the magnetite content in the ore. Additional benefits to removing the iron include reducing the reagent dosage for flotation decreasing the throughput downstream and reducing downstream operating costs at the hydrometallurgical plant.

The results of magnetic separation test work for flotation feed from the various test work campaigns are summarised in Table VI reflecting mass pull to magnetics plus associated losses for ZrO_2, Nb_2O_5, Y_2O_3 (representing heavy rare earths) and Ce_2O_3 (representing light rare earths). The values below have been ratioed to PP22, one of the smoothest runs of the pilot plant. Final mass pull to magnetics varies depending on feed material but metal losses stay relatively constant. BZ-Comp was a composite of the basal zone.

Table VI. Magnetic Separation Performance

Parameter			Final Mag Sep Wt %	Losses to Magnetics %			
				ZrO_2	Nb_2O_5	Y_2O_3	Ce_2O_3
3.7 t	PP05	BZ-Comp	2.5	1.9	2.0	0.6	2.0
3.7 t	PP06	BZ-Comp	2.6	2.1	2.1	1.9	2.3
3.7 t	PP07	BZ-Comp	2.6	2.7	2.6	2.1	3.1
40 t	**PP22**	**BZ-MP**	**1.0**	**1.0**	**1.0**	**1.0**	**1.0**
40 t	PP24	BZ-MP	1.8	1.4	1.8	1.5	1.3
40 t	PP25	BZ-MP	2.4	1.4	1.7	1.0	1.1
40 t	PP26A	BZ-MP	1.8	1.4	1.5	1.2	0.9

Desliming: The Nechalacho ore must be milled fine (-38µm) to achieve target liberation in flotation, and as a result of this, slimes will be generated and it should be removed before flotation. Slime removal has a number of advantages including potentially reducing the reagents consumption and improving the grade-recovery performance. Reagents often perform better in the absence of slimes as well. A target cut point (K_{80}) in the range of 7 to 10 µm was selected for slimes removal after trade off studies on recovery and slimes removal mass pull.

Various test programs generated data which indicates typical mass of slimes removed is generally between 8-15% with losses of REOs ranging from 4% right up to 15%. Values in Table VII have been amended to show PP 22 as the baseline performance.

Desliming cyclone simulations including material balances were conducted by FLS-Krebbs. It was determined that either two or three stages of desliming cyclones would be suitable for the system, conditional to acceptable REE losses. The Krebs simulation shows that a 2-stage system would have approximately 21.5% of RE loss in the slimes while a 3-stage system will lose 13.6% REE. [1]

Table VII. Desliming Performance

Parameter			Losses				
			Wt	ZrO_2	Nb_2O_5	Y_2O_3	Ce_2O_3
Unit			%	%	%	%	%
3.7 t	PP05	BZ-Comp	1.1	1.0	1.3	1.0	1.2
3.7 t	PP06	BZ-Comp	1.2	1.1	1.6	1.2	1.4
3.7 t	PP07	BZ-Comp	1.2	1.6	1.6	1.4	1.6
40 t	PP22	BZ-MP-HG	1.0	1.0	1.0	1.0	1.0
40 t	PP24	BZ-MP-HG	0.9	1.1	1.1	0.9	1.1
40 t	PP25	BZ-MP-HG	1.3	0.2	0.3	0.3	0.1
40 t	PP26A	BZ-MP-HG	1.2	1.4	1.2	1.2	1.1

Due to the higher indicated losses to slimes with the 2 stage circuit, a 3 stage desliming circuit was selected for the flowsheet. Based on the simulations by Krebbs, the number of cyclones required per stage is indicated in Table VIII for the 2,000 tpd scenario.

Table VIII. Cyclones Requirements for Three Stage Desliming

Desliming Stage	Cyclones operating	Cyclones Spare	Cyclone Dia. (mm)
First	40	2	102
Second	58	2	51
Third	220	20	25

It is acknowledged that potentially only a 2 stage system could be utilised as the size of the material saved by the third stage of desliming is primarily finer than 5 µm and flotation is probably ineffective at recovering particles this fine. Further, the equipment required for the third stage of desliming could present an operational and maintenance challenge.

Flotation

A 40 t pilot plant was completed at SGS Lakefield for Avalon Rare Metals Inc. to produce a bulk concentrate for use in the development of the down-stream hydrometallurgical process as well as to confirm laboratory results in a large-scale, continuous operating environment. The 40t flotation flowsheet was a closed-circuit design with three stages of rougher/scavenger flotation and five stages of cleaner flotation and can be seen in Figure 2. This section describes the flotation and gravity performance of the laboratory cleaner test (open circuit) and locked cycle test (LCT), which simulate a close circuit environment. The 40 t pilot plant results are compared against the LCT results.

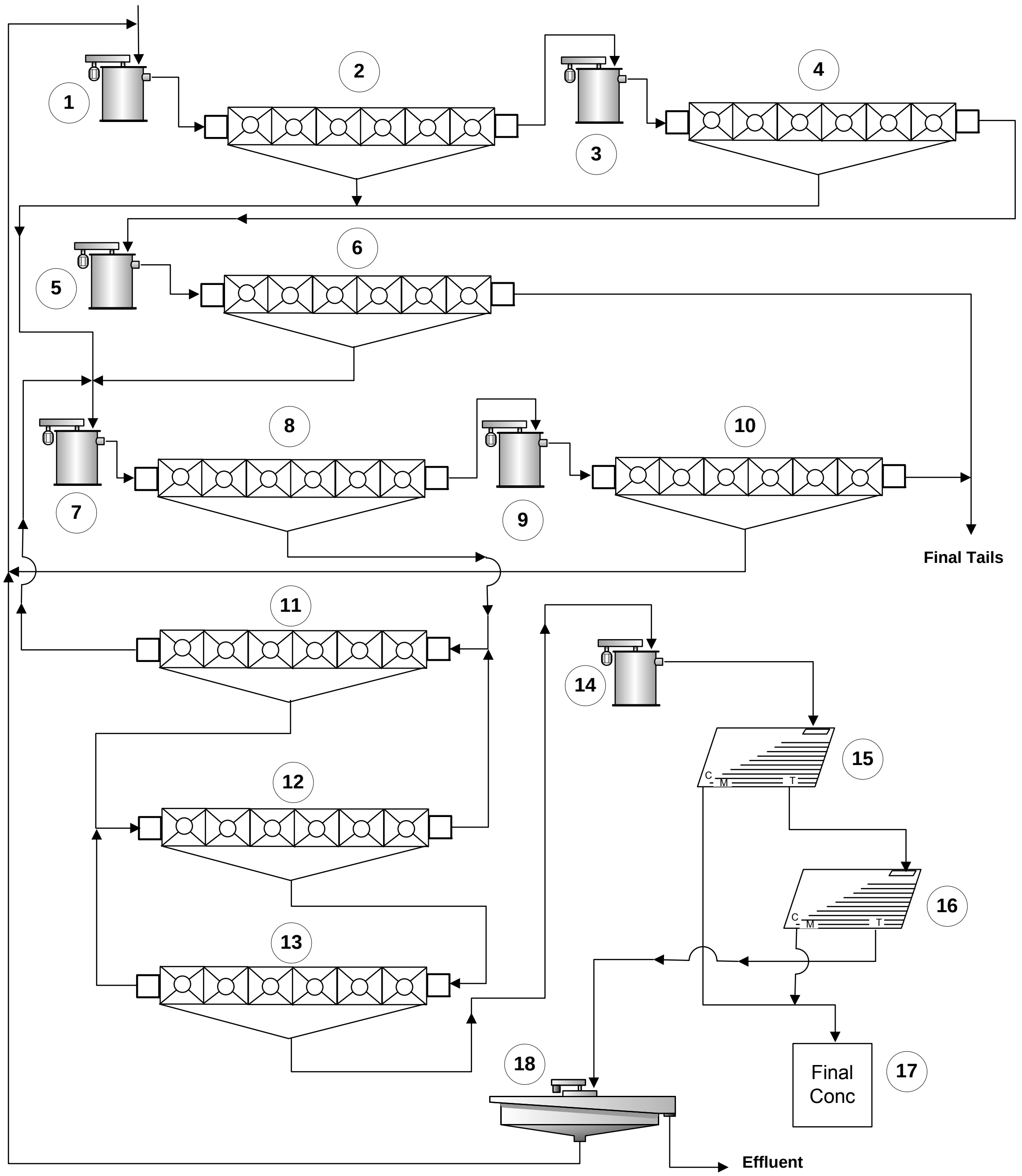

Figure 2. Flotation-gravity flowsheet.

Composite Head Chemical Analysis

As mentioned above, several composites (UZ-AG, BZ-AG, and BZ-MP), representing samples that are gradually deeper in the deposit in terms of elevation, were evaluated in the 40 tonne pilot plant test. An overview of the chemical head compositions is included in Table IX and Figure 3. The overall TREO, Nb_2O_5, and ZrO_2 grades of the UZ-AG and BZ-AG were similar. The ZrO_2 grade in BZ-MP was higher than both UZ-AG and BZ-AG. An increase in HREO distribution in the order of UZ-AG, BZ-AG, and BZ-MP were found. This agrees with the mineralogical results where the BZ composites contained greater amounts of HREO bearing minerals relative to LREO minerals with depth in the ore zones. In the whole rock analysis, SiO_2, K_2O, and Al_2O_3 decreased with depth while CaO and MgO increased which also relates to an increase in Ca, Mg and Fe bearing carbonate minerals with depth in the deposit.

Table IX. Composite Head Chemical Analysis

Composite	**UZAG**	**BZAG**	**BZMP**
Ta_2O_5	0.020	0.030	0.040
Nb_2O_5	0.330	0.360	0.430
ZrO_2	2.62	2.84	3.83
Ce_2O_3	0.670	0.570	0.660
La_2O_3	0.310	0.260	0.300
Pr_2O_3	0.070	0.059	0.047
Nd_2O_3	0.327	0.303	0.362
Sm_2O_3	0.063	0.059	0.070
Eu_2O_3	0.007	0.007	0.009
Gd_2O_3	0.045	0.053	0.068
Tb_2O_3	0.005	0.008	0.011
Dy_2O_3	0.020	0.037	0.062
Ho_2O_3	0.003	0.006	0.011
Er_2O_3	0.006	0.015	0.028
Tm_2O_3	0.001	0.002	0.004
Yb_2O_3	0.005	0.012	0.022
Lu_2O_3	0.001	0.002	0.003
Y_2O_3	0.100	0.130	0.190
TREO	1.63	1.52	1.85
SiO_2	56.7	55.6	53.2
Al_2O_3	11.7	11.4	10.1
Fe_2O_3	11.2	11.8	12.5
MgO	2.56	2.73	3.03
CaO	1.68	2.11	3.19
Na_2O	2.88	2.76	2.73
K_2O	5.46	5.58	4.65
TiO_2	0.080	0.050	0.040
P_2O_5	0.230	0.140	0.100
MnO	0.160	0.200	0.280

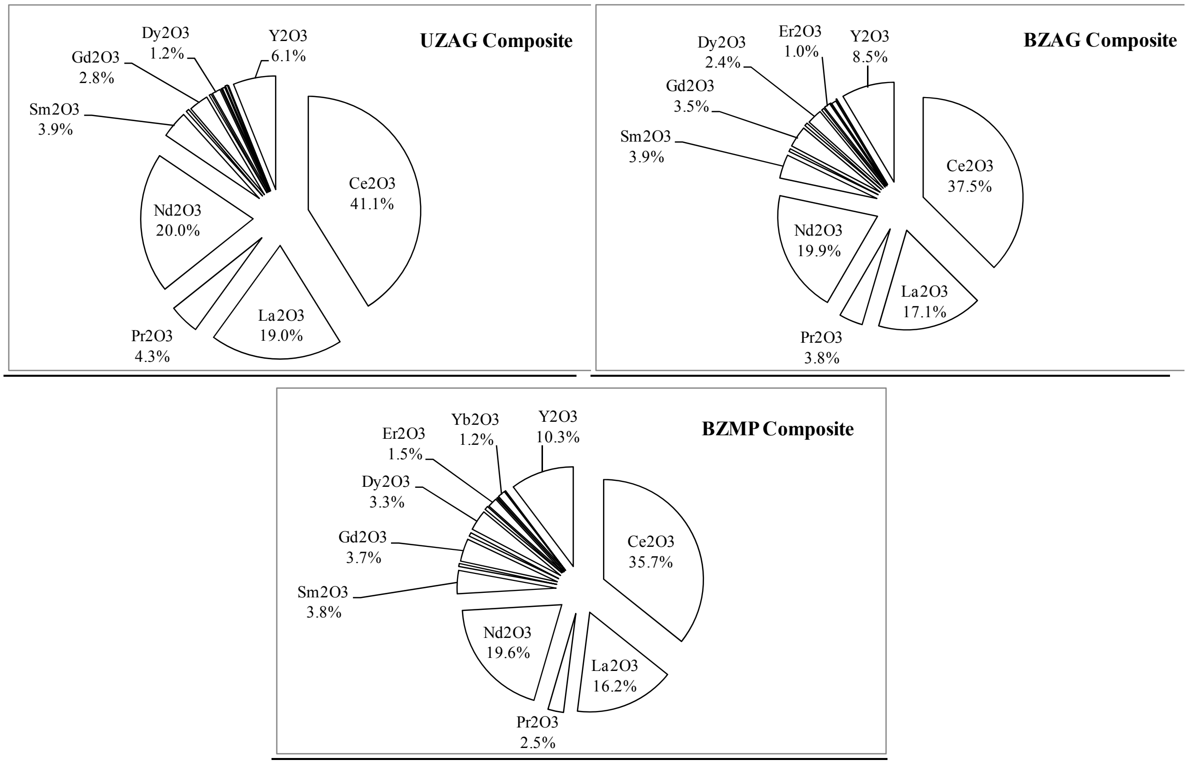

Figure 3. Composite head REO distribution.

Laboratory Testwork

Figure 4 compares the lab open circuit cleaner results to the LCT close circuit results. The calculated mass and relative recoveries for each of the rougher, cleaner, and gravity concentrates in the open circuit cleaner test are presented and compared to the LCT gravity concentrate. For both the UZ-AG and BZ-MP, the LCT gravity concentrates mass and recoveries for all elements of interest were similar to the open circuit cleaner gravity concentrates. For the BZ-AG, the LCT gravity concentrate achieved the same recoveries for all elements of interest in the open circuit cleaner gravity concentrate in a significantly reduced amount of mass.

Figure 5 shows the losses of all elements of interest as well as mass rejection by each flotation and gravity stage. For both UZ-AG and BZ-AG, the rougher flotation stage rejects in excess of 40% mass but the losses for all elements of interest were greater for BZ-AG. A similar trend was observed for all cleaner flotation stages. For BZ-MP, the rougher flotation stage rejected less mass by ~10% than both UZ-AG and BZ-AG while the final gravity stage rejected significant amount of mass but at the expense of significant losses for all elements of interest.

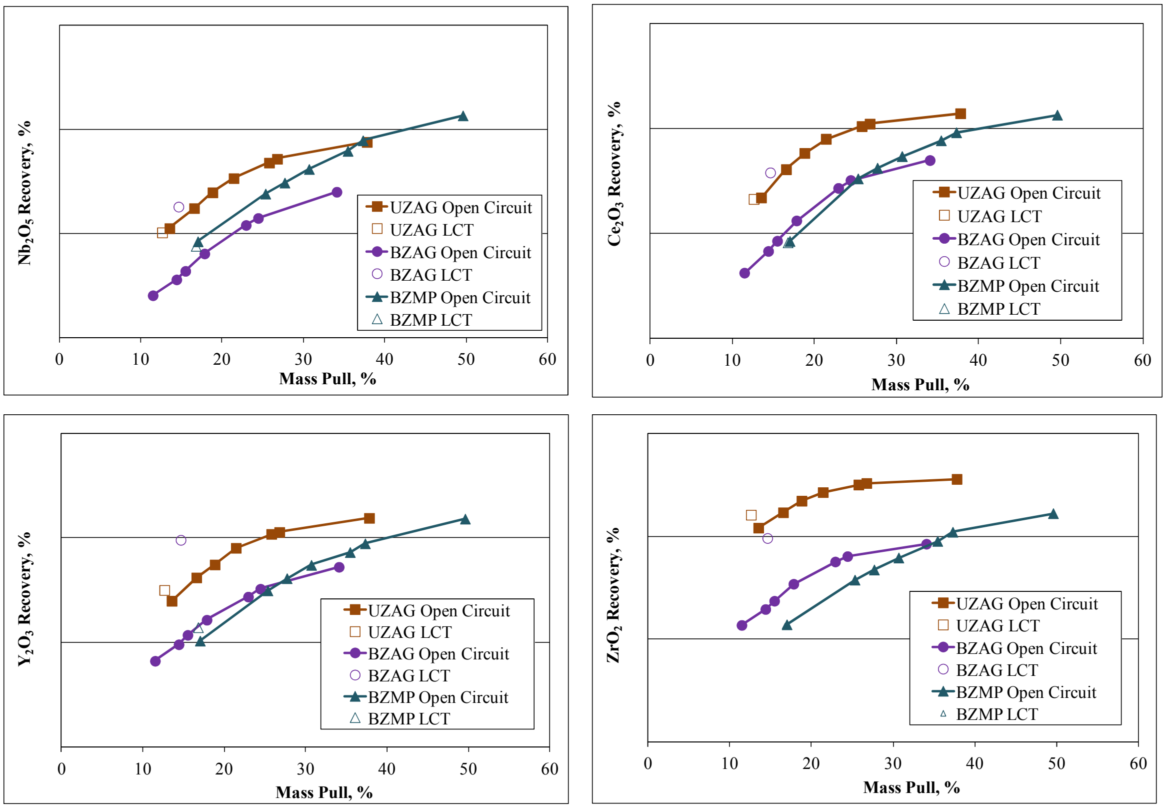

Figure 4. Laboratory open circuit cleaner to LCT close circuit comparison.

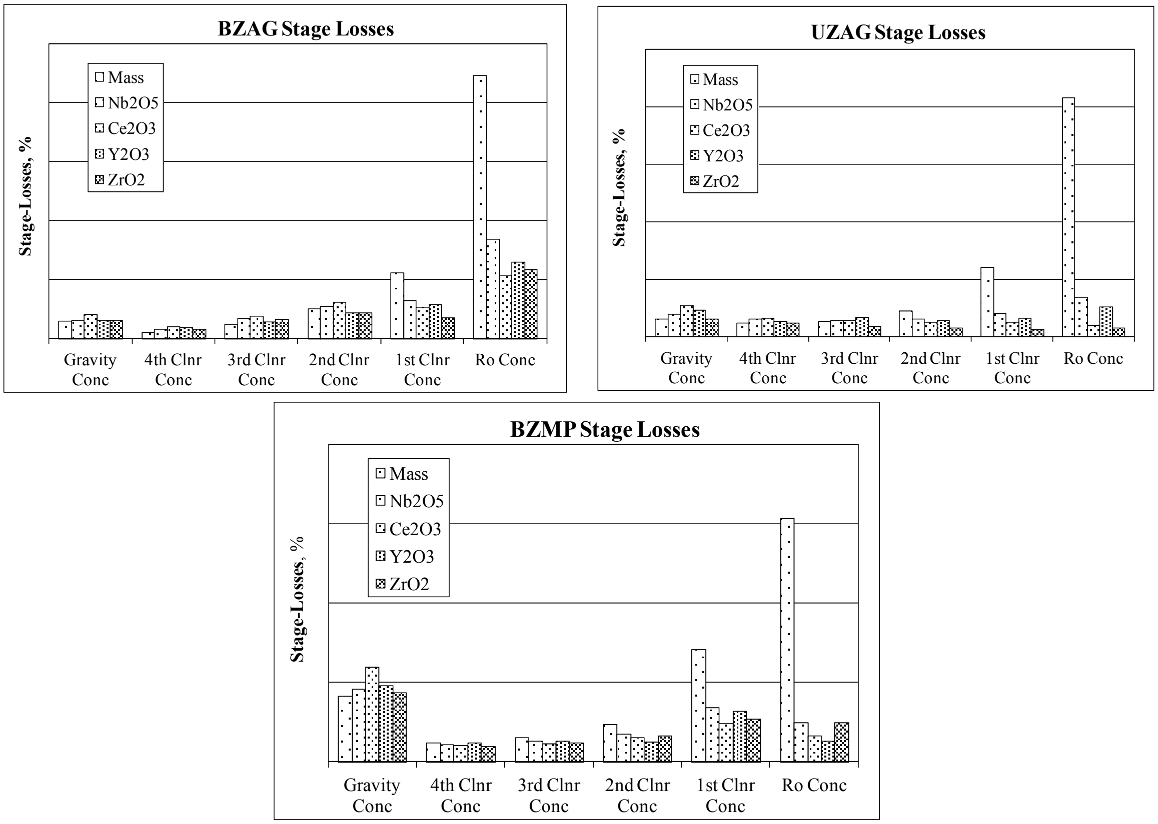

Figure 5. Stage losses in open circuit cleaner test.

Figure 6 presents the upgrading factor (vs. head grade) for all elements of interest at each of the calculated concentrates in the open circuit cleaner test. The upgrading factor at each flotation and gravity stage is marginally better for UZ-AG when compared to BZ-AG. The final gravity stage provided the greatest upgrade for ZrO_2 for both UZ-AG and BZ-AG. Poor upgrading was found in all flotation stages for BZ-MP. The gravity stage provided the greatest upgrading in comparison to flotation. QEMSCAN mineralogical examination of the head composite identified poor liberation for BZ-MP which may impact on selectivity or recovery. A finer primary grind may be required for BZ-MP to liberate the locked minerals in order to achieve similar recoveries and mass pull as BZ-AG.

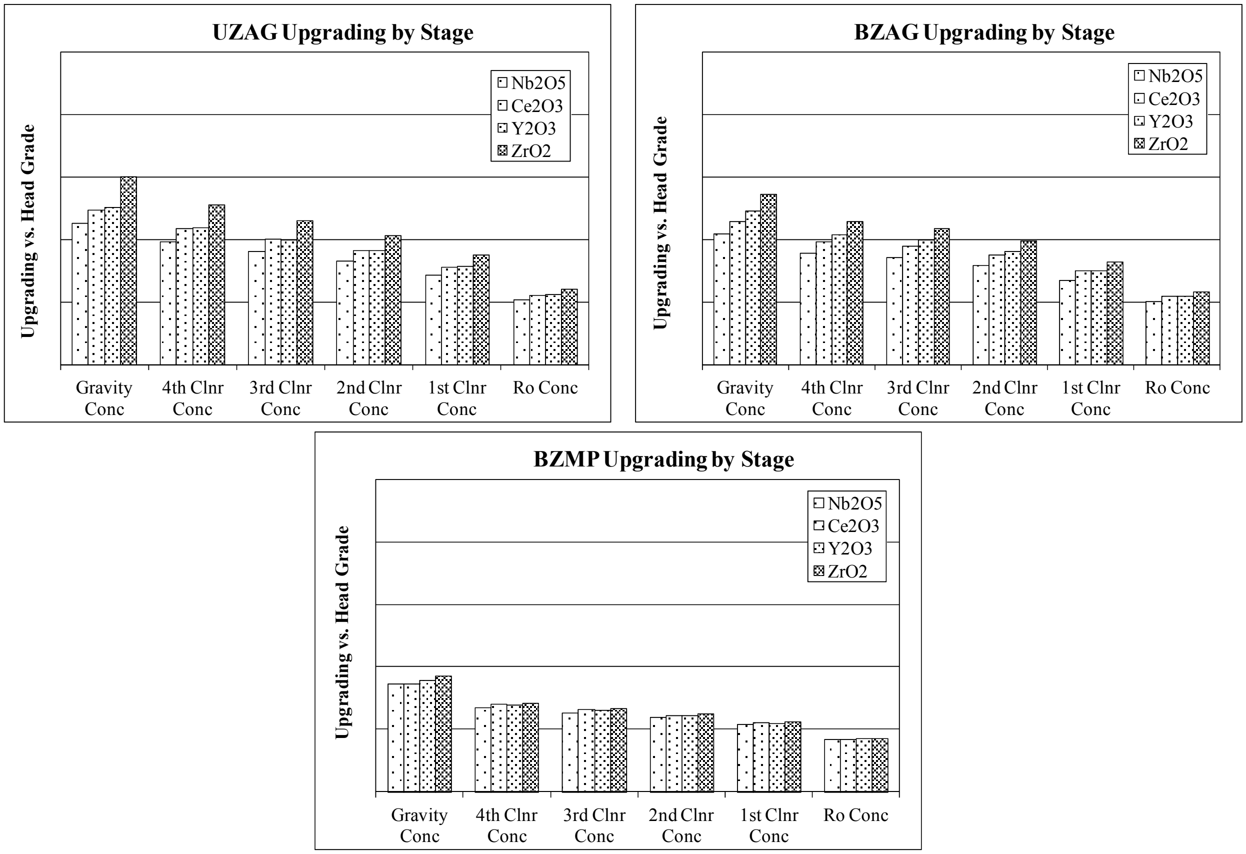

Figure 6. Upgrading factor by stage.

Figure 7 presents the mass pull versus relative recoveries of the final gravity concentrates from various pilot plant test runs. In comparing to the laboratory LCT results, similar mass and recoveries for the respective composites were achieved. Similar trends observed from the laboratory testwork were also found in the pilot. The flotation response of the BZ composites was much different to that of the UZ-AG. In particular, BZ-MP, a significant increase in mass pull is required to achieve similar recoveries as that of UZ-AG and BZ-AG.

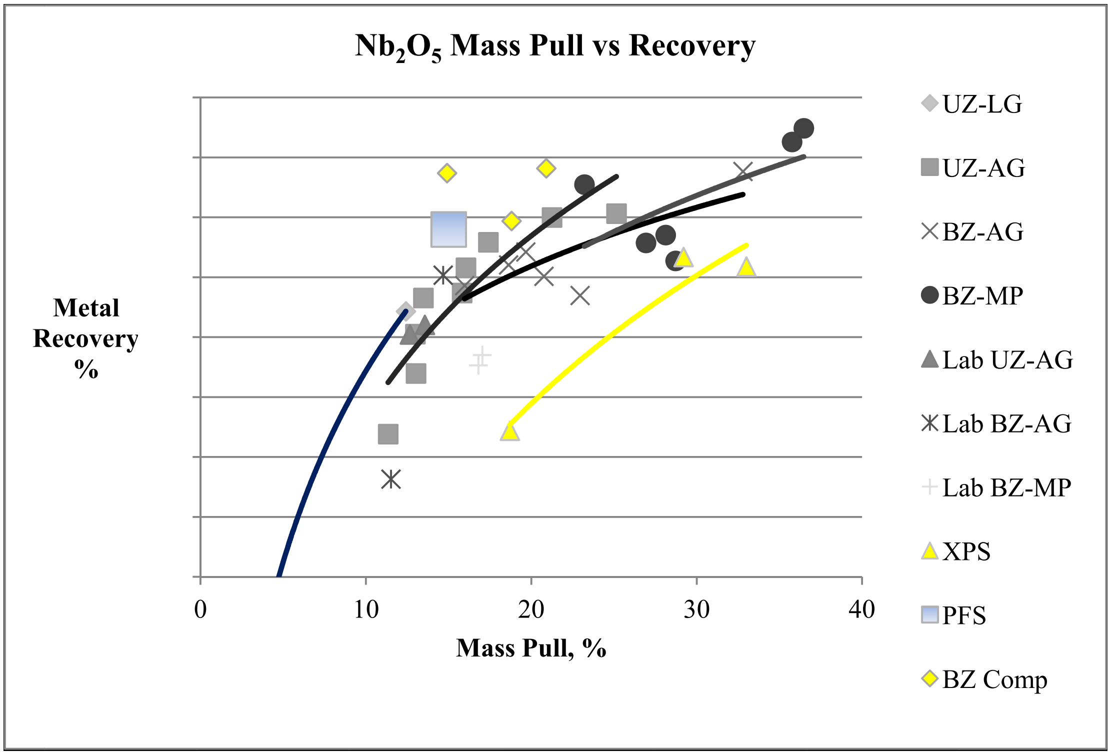
Nb_2O_5 Mass Pull vs Recovery
Metal Recovery %
Mass Pull, %
0
10
20
30
40
UZ-LG
UZ-AG
BZ-AG
BZ-MP
Lab UZ-AG
Lab BZ-AG
Lab BZ-MP
XPS
PFS
BZ Comp

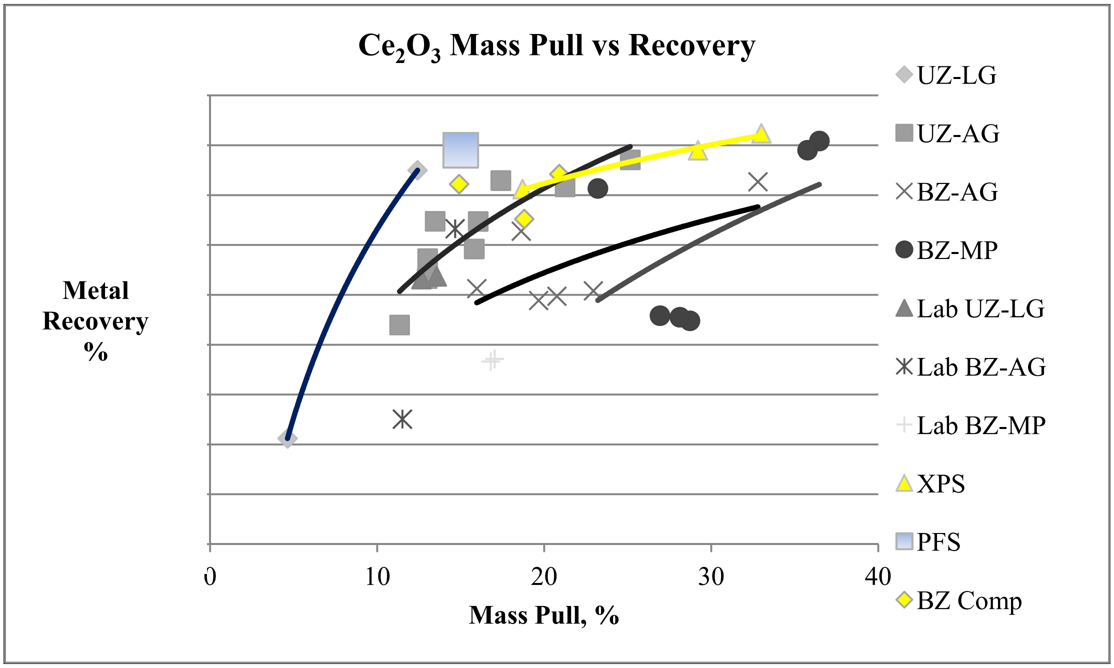
Ce_2O_3 Mass Pull vs Recovery
Metal Recovery %
Mass Pull, %
0
10
20
30
40
UZ-LG
UZ-AG
BZ-AG
BZ-MP
Lab UZ-LG
Lab BZ-AG
Lab BZ-MP
XPS
PFS
BZ Comp

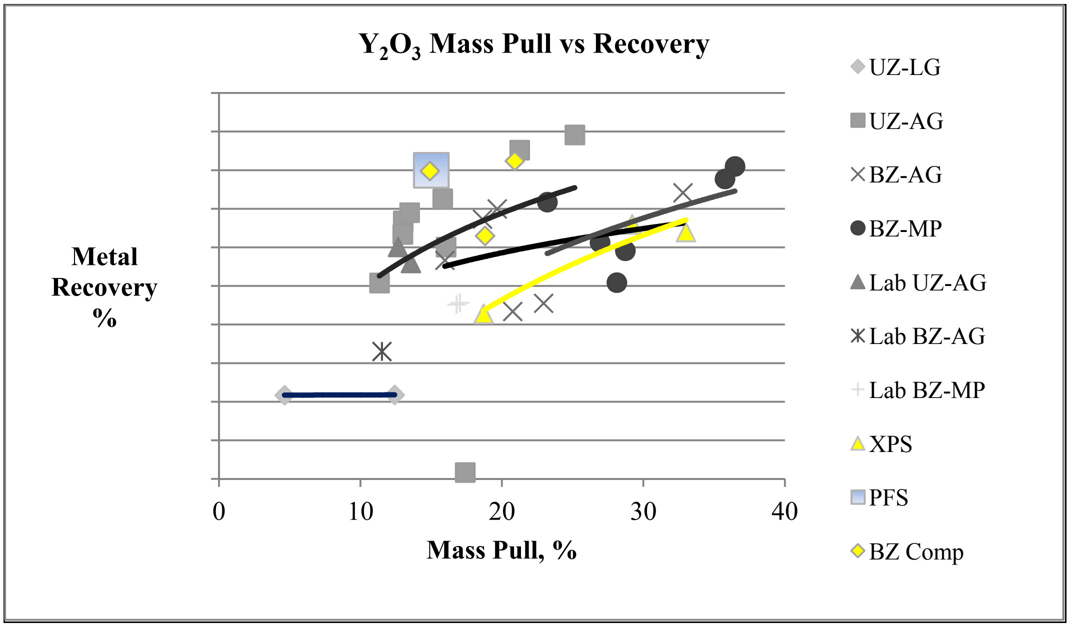

Figure 7. 40 t Pilot plant mass-recoveries.

Gravity Separation

Gravity separation test work was proposed for cleaner concentrate from the 40t pilot plant- the objective being to up-grade the concentrate by removal of lighter, gangue material.

Various gravity concentrators were tested, and the Mozley Multi Gravity Separator (MGS), showed the best performance for upgrading the concentrate. The MGS had the best recovery versus mass pulled in all the trials using 4th cleaner flotation concentrate; results can be seen in

Figure 8.

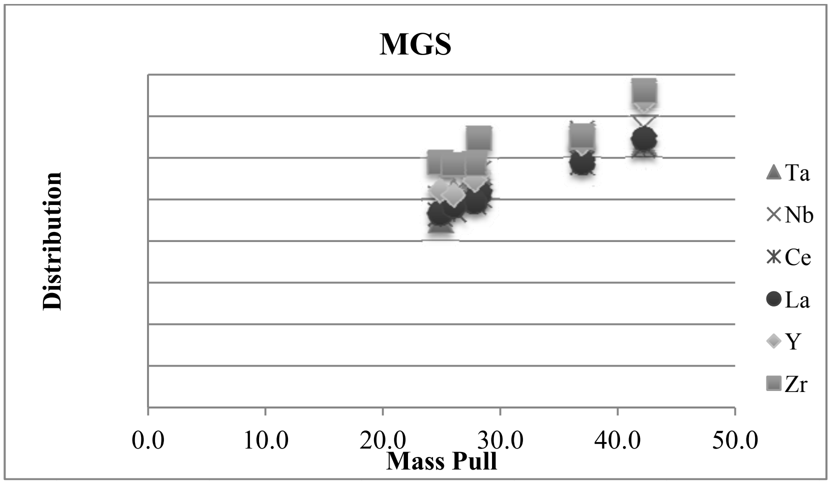

Figure 8. Comparison of Recovery vs. Mass Pull for the Falcon Concentrator.

Tests were conducted at various rotational drum speeds, wash water flow rates and tilt angle of the drum.

Table X**.** shows the best results achieved [2].

Table X. MGS Performance on Concentrate, and MGS Products

MGS Run 7	Mass %	Assays %					
		Ta_2O_5	Nb_2O_5	Ce_2O_3	La_2O_3	Y_2O_3	ZrO_2
Conc.	19.8	0.16	1.95	3.57	1.55	1.10	20.2
Tailing	80.2	0.04	0.36	0.89	0.42	0.19	2.81
Calc. Head	100.0	0.06	0.68	1.42	0.64	0.37	6.26
Direct Head	-	0.08	0.78	1.57	0.75	0.36	7.44
		Upgrade Factors					
		Ta_2O_5	Nb_2O_5	Ce_2O_3	La_2O_3	Y_2O_3	ZrO_2
Conc.		2.00	2.50	2.27	2.07	3.06	2.72
Tailing		0.50	0.46	0.57	0.56	0.53	0.38
Calc. Head		0.80	0.87	0.91	0.86	1.03	0.84
Direct Head		1	1	1	1	1	1

Table XI. 1st Cleaner Scavenger Concentrate Thickener Data

Streams	pH	Feed %WW Solids	Solids Loading Rate (t/m^2h)	Floc Dosage (g/t)	Underflow Density (%w/w solids)	Overflow Turbidity (NTU)	Un-sheared Underflow Vane Yield Stress (Pa)
Final Combined Tailings	9.5	~16	0.21-0.37	21-46	56-61	Over Reg	63
Gravity Tailings	11	~11	0.52-0.68	21-40	52-54	78-1042	41
Gravity Concentrate	9.1	~21	0.28-0.45	9-22	70-72	19-272	134
1st Cleaner Scavenger Concentrate	8.1	~19	0.29-0.45	13-31	66-69	90-200	80

Dewatering: Gravity concentrate will be thickened and filtered before sent to the hydrometallurgical plant for further processing. Tailings will also be thickened to approximately 65% before being disposed of in the Tailings Management Facility. Thickening and filtration tests were conducted at Outotec. The data summarized in Table XI., of tests conducted by Outotec, were completed using dynamic thickening tests and are therefore considered sufficiently representative of the eventual thickening parameters.

Conclusion

From the various laboratory tests, a flotation flowsheet was developed to process the Nechalacho ore. This flowsheet has been successfully demonstrated in three different pilot plant campaigns that produced a bulk rare earth concentrate containing monazite, bastnaesite, zircon, fergusonite and other rare-earth bearing minerals. This flowsheet comprises of a three-stage crushing and milling circuit, a desliming and magnetic separation circuit to remove slimes and naturally occurring magnetite in the ore. The material then goes through flotation where a bulk flotation concentrate is then gravity separated and dewatered before moving to the Hydrometallurgical facility.

Future Areas of Improvement

During the course of developing the flowsheet adopted for the feasibility study a number of areas of potential optimisation were identified which are currently still under investigation. These items include the following:

- Crushing & milling circuit- optimize crushing and mill selection to reduce costs and minimize generation of fines;
- Flotation reagent suite -alternative reagents after the potential for improved performance and a simpler circuit;
- Potential to remove desliming & gravity circuits to reduce costs and simplify overall circuit flowsheet.

Acknowledgements

The authors of this paper would like to express their gratitude to Avalon management for allowing us to publish this paper. We are particularly grateful for the assistance and guidance given by Dave Marsh and Dr. William Mercer. Finally, we would like to thank SGS Minerals and Xstrata Process Support for their work in the three pilot plant campaigns.

References

1. SGS Mineral Services, "13185-006 the Grindability Characteristcs of 2 Samples from the Thor Lake Project," Lakefield, Ontario, 2012.

2. FLSmidth , "RFI-013 Attachment--2 or 3 Stages of Desliming-Cyclones," Salt Lake City, 2011.

3. SGS Minerals Services, " Project 13023-001 Gravity characterisation of pilot plant products," Lakefield, Ontario, 2011.

REO MINERAL SEPARATION FROM SILICATES AND CARBONATE GANGUE MINERALS

*B. Yu, M. Aghamirian

SGS Mineral Services – Lakefield Site
185 Concession Street
PO Box 4300
Lakefield, Ontario K02 2H0
*Ben.Yu@sgs.com

Keywords: Rare Earth Deposit, Flotation, Beneficiation, Roasting, Magnetic Separation, Gravity Separation

Abstract

The increasing development of new technologies requiring rare earth elements has resulted in greater demand for rare earth element (REE) extraction and processing. However, REE concentration is a complex process and usually deposit specific. The mineralogy of each deposit can vary widely but is essentially characterized by the type of REE and host gangue, chemistry, and degree of liberation of the minerals that dictate the processing route. This paper presents REE mineral processing routes for the recovery of commercially valuable REE-bearing minerals, such as REE-fluorocarbonates and monazite, from silicates and carbonate gangue minerals.

Introduction

Rare earth elements are comprised of the fifteen elements in the lanthanide series as well as yttrium and scandium. Over 250 REE bearing minerals exist in forms of carbonates, phosphates, and silicates. Often times, REE are also found in minerals such as zircon and apatite by substitution. The diversity and complexity of REE minerals along with the gangue present in the ore system means that each deposit is unique and requiring different beneficiation processes. Similar ore bodies have also shown to produce different results when using similar beneficiation processes due to mineral liberation and association. The existing literature has revolved around the operation at Mountain Pass over twenty years ago and the significant amount of research conducted in China. The increasing demand of REE from novel technologies have created a surge in research and testing for REE extraction which includes mineralogy, physical separation, leaching, and separation over the past few years.

Beneficiation findings on currently developing REE projects are scarce in literature. This paper presents several REE beneficiation projects completed at SGS Lakefield over the past few years. Physical separation investigations of various valuable REE and targeted minerals from different gangue systems are presented. Successes and failures from the different beneficiation technologies investigated are summarized. An emphasis on the linkage between mineralogy and beneficiation as well as the impact of beneficiation to downstream hydrometallurgical processes is illustrated.

Literature Review

The dominant literature pertains to the operation at Mountain Pass which stopped production in 2002 but has since been re-started. Prior to 2002, the flotation plant processed 1,700 t/day of ore at ~7% REO. The run of mine ore was crushed and ground to 80% passing 150 μm prior to desliming. The deslimed sand was subjected to a roughing stage followed by four cleaner stages. The REO collector used was tall oil with sodium fluorsilicate and ammonium lignin sulfonate as depressants. Soda ash was used as a pH modifier. Pulp temperature and pH were critical for selectivity between the predominant REO bearing minerals, bastnaesite, and the gangue minerals of calcite, dolomite, and barite. A final flotation concentrate grade of 63% REO with 65-70% overall recovery was achieved [1-3]. An alternate reagent scheme was developed by Pradip and Fuerstenau [4] following a critical review of the plant results that indicate poor selectivity by fatty acid collectors and poor calcite separation from bastnaesite. High temperature is required due to poor separation at room temperature when using fatty acids. The most promising collector developed, potassium octyl hydroxamate, demonstrated improve separation of bastnaesite from calcite and barite at room temperature. Above 40% REO grade and 80% recovery was achieved with the developed collector.

Recent reviews on rare earth beneficiation processing technologies [5-6] demonstrated the diversity in REE physical separation processes. A number of beneficiation flowsheet configurations exist to recover the three most commonly commercialized REE minerals: bastnaesite, monazite, and xenotime. Depending on the REE and gangue minerals, gravity, magnetic separation, and flotation are used in combination. Aside from Mountain Pass and Mount Weld, the major rare earth mines, excluding ion clay, are Baiyuan Obo, Weishan, and Maoniuping in China. Zhang and Edwards [6] summarized the evolution of the Baiyuan Obo flowsheet that started with calcination, magnetic separation, and flotation. Calcination was eventually eliminated. The primary REO concentrate at Baiyuan Obo achieved 55.6% REO at ~13% recovery while the secondary REO concentrate graded 34.1% REO at ~6% recovery.

The Weishan rare earth deposit, located in Shandong province composed of mainly LREE with barite, carbonatite, quartz, feldspar, mica, amphibole, and iron minerals. Bastnaesite is the main REE mineral of interest. A flotation only flowsheet with one roughing and four cleaning stages is employed. A final reverse flotation stage separates the 4th cleaner concentrate into a high grade primary REO concentrate and a low grade secondary REO concentrate. A hydroxamate identified as H205 was used as the REO collector with sodium silicate and alums as depressants. The primary REO concentrate graded 61.2% REO at ~60% recovery while the secondary REO concentrate graded 33.5% REO at ~24% recovery.

The Maoniuping rare earth deposit, located in Sichuan contains bastnaesite, barite, celestine fluorite, aegirine, quartz, feldspar, arfvedsonite, biotite, pyrite, galena, magnetite, hematite, limonite, and calcite. A combination of gravity, magnetic separation, and flotation is used. The gravity concentrate, magnetics, and flotation concentrate are graded 57.7%, 73.2%, and 64.3% REO, respectively, with an overall REO recovery of 83.1%.

The development of hydroxamates [7-12] in rare earth flotation by China has improved selectivity and recovery immensely. Li et al. [13] compared various hydroxamates labelled as

L102 against H316, H205, and JD-2 in plant trials at the Maoniuping rare earth deposit. Flotation was conducted at 35-55% solids, 33-42ºC, 7-9 pH, and 75-85% passing 200 mesh. The collector L102 achieved the best results with average concentrate grade of 63.6% REO at ~88% recovery. In a more recent study [14], several collectors including the Maoniuping collector (principal components are hydroxyl naphthalene-containing hydroximic acid) for bastnaesite flotation was evaluated. A pH range of 8-10.5 for the Maoniuping collector was established for optimum REO recovery (~80%). Sodium silicate dosage (10-16x10^{-5}g/mL) and Maoniuping collector dosage (4-10x10^{-5} g/mL) was also established for the greatest REO recovery (~80%).

An increase in REE publication has provided greater flow of information. REE data and flowsheet/reagent scheme publication on current REE developing projects remains scarce in the public domain. More so, the understanding of how reagents interact with REE and gangue minerals is still lacking. The mechanism for REE separation from gangue mineral by flotation is only beginning to be explored [15]. Further opportunities for future research exist to connect industrial flowsheet development to understanding the mechanism.

Uranium and Ree With Quartzile Gangue

The Elliot Lake site has been a uranium producer between 1955 and 1996. Operations were terminated with the Athabaska Basin discovery and development. A number of studies were conducted in the past investigating the various beneficiation technologies for uranium upgrading [16-18]. Limited focus was placed on REE recovery either along with the U pre-concentrate or in a separate REE pre-concentrate. Two separate studies, identified in this paper as U-REE A and U-REE B, were carried out at SGS Lakefield on samples from the Elliot Lake region. Pre-concentration of both U and REE in a single bulk pre-concentrate or separate U and REE pre-concentrate was investigated.

Head Chemical Analysis

Table I presents the head chemical analysis on the two different samples from Elliot Lake. The U and REE composition were similar between the two samples indicating the potential of similar physical separation behaviour. The REE content at <0.2% is considered low as the currently developing REE projects are typically graded 1-2% REE. The two largest producers, Baiyuan Obo and Mountain Pass, have a cut-off grade of ~7% REO. High recoveries of both U and REE in a pre-concentrate may be critical to ensure positive economics. The containing REEs are light rare earth (LRE) at ~70% La+Ce. The Nd and Dy would likely contribute a significant portion of economical value.

Table I. U-REE Head Chemical Analysis

Composite	LREE, g/t	HREE, g/t	TREE, g/t	U, g/t	SiO_2, %	Al_2O_3, %	Fe_2O_3, %	K_2O, %
U-REE A	1554	149	1702	270	83.4	6.43	2.75	3.30
U-REE B	1285	118	1403	339	83.3	7.00	3.61	3.48

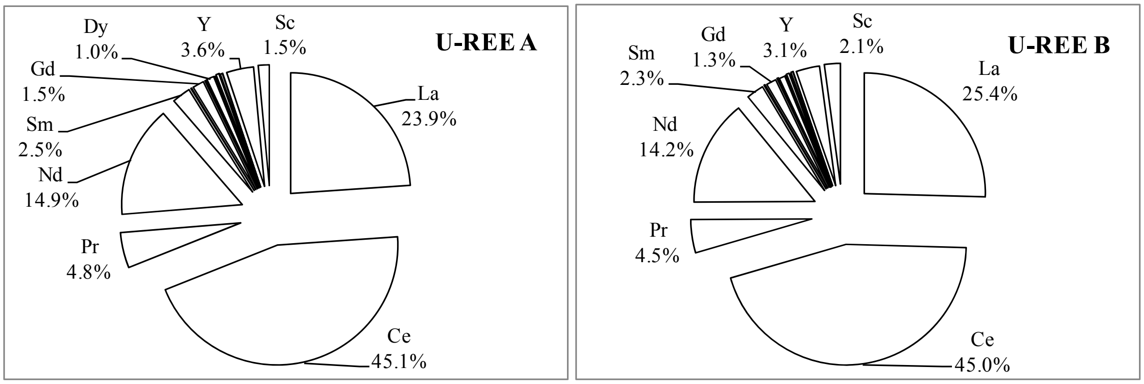

Figure 1. U-REE distribution.

Head Mineralogical Analysis

Mineralogical examination on the U-REE A sample was completed at SGS Lakefield. Figure 2 summarizes the mineral distribution. The U and REE are found in only several minerals having similar physical characteristics. Likewise, the gangue minerals are mainly quartz and silicate-based as well as pyrite. The valuable and gangue minerals have different physical characteristics in terms of specific gravity, magnetic properties, and flotation behaviour. This may potentially result in effective separation by various beneficiation options.

The monazite and U-Th minerals liberation and association, for the U-REE A sample ground to 80% passing 150 µm, are shown in Figure 3 and Figure 4, respectively. Monazite was not well liberated with a significant amount of the free and liberated monazite (defined as ≥80% mineral-of-interest area percent exposed) being less than 30 µm. The U-Th minerals were similarly not well liberated but the free and liberated particles are much coarser in the 60-70 µm range, which may allowed for more effective physical separation. Liberation may hinder effective physical separation, resulting in either significant losses or poor upgrading, despite the simple mineral distribution.

Mineralogy for U-REE B was not completed by SGS. A mineralogy report provided by company management revealed that the principal minerals carrying U and REE are: Th-uraninite, monazite, Th-rich monazite, thorite, allanite, coffinite, brannerite, florencite, xenotime, UO_2-rutile, monazite-silicate, and UO_2-pyrite.

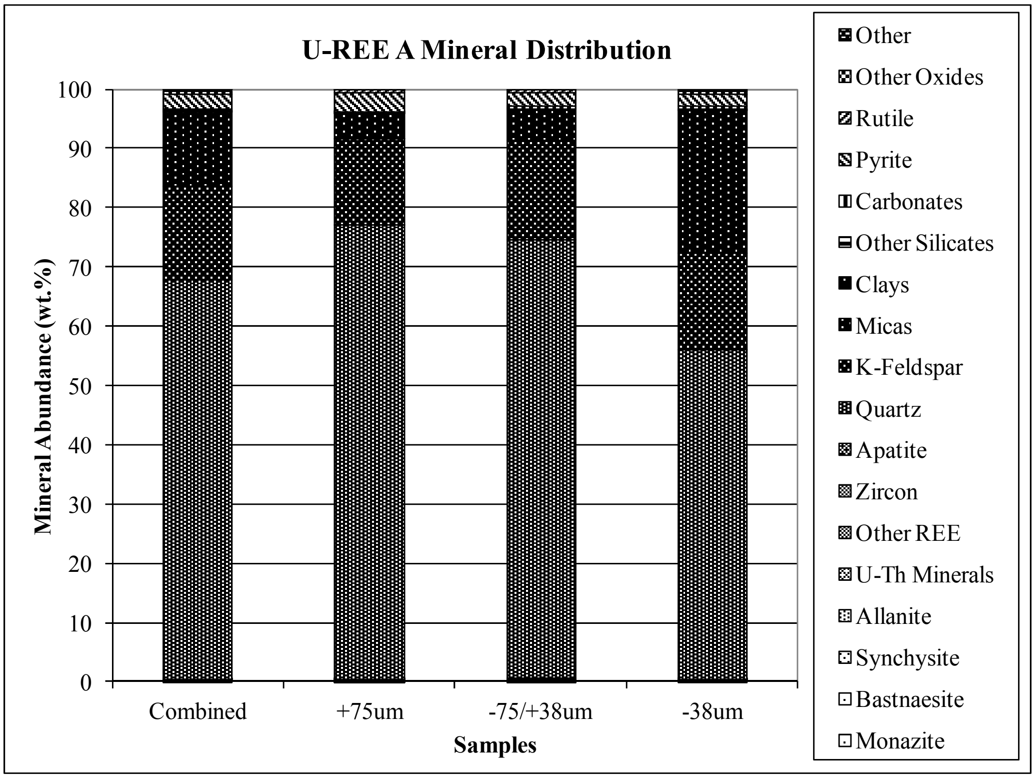

Figure 2. U-REE a mineral distribution.

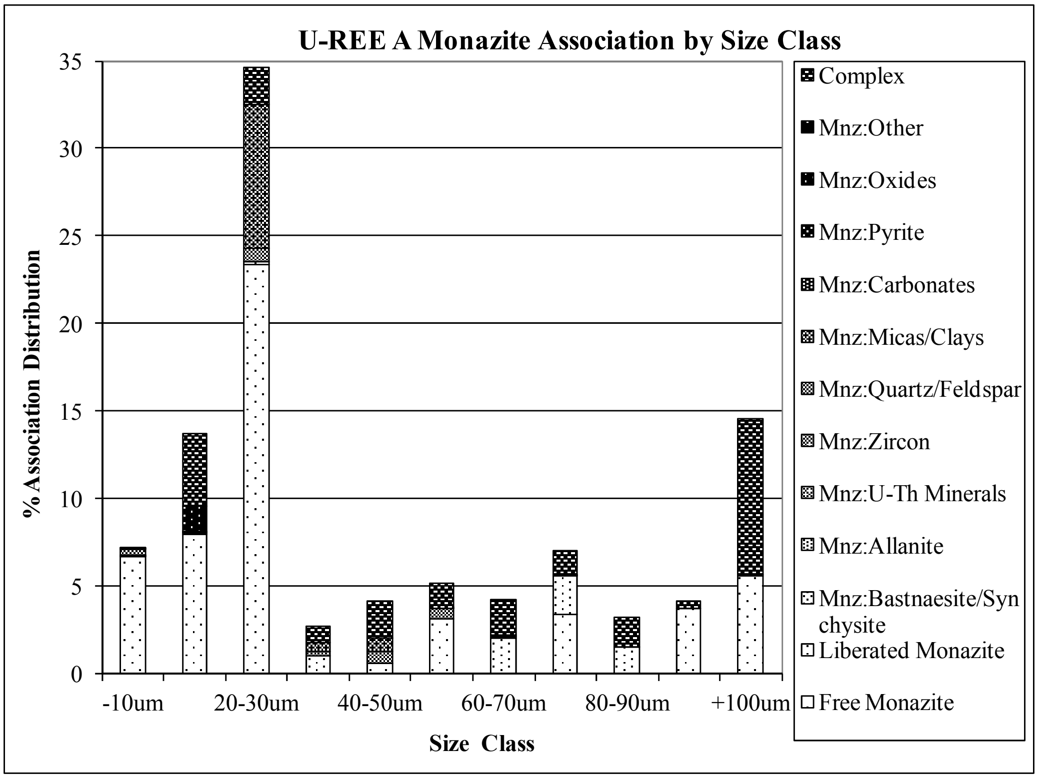

Figure 3. U-REE a monazite liberation and association.

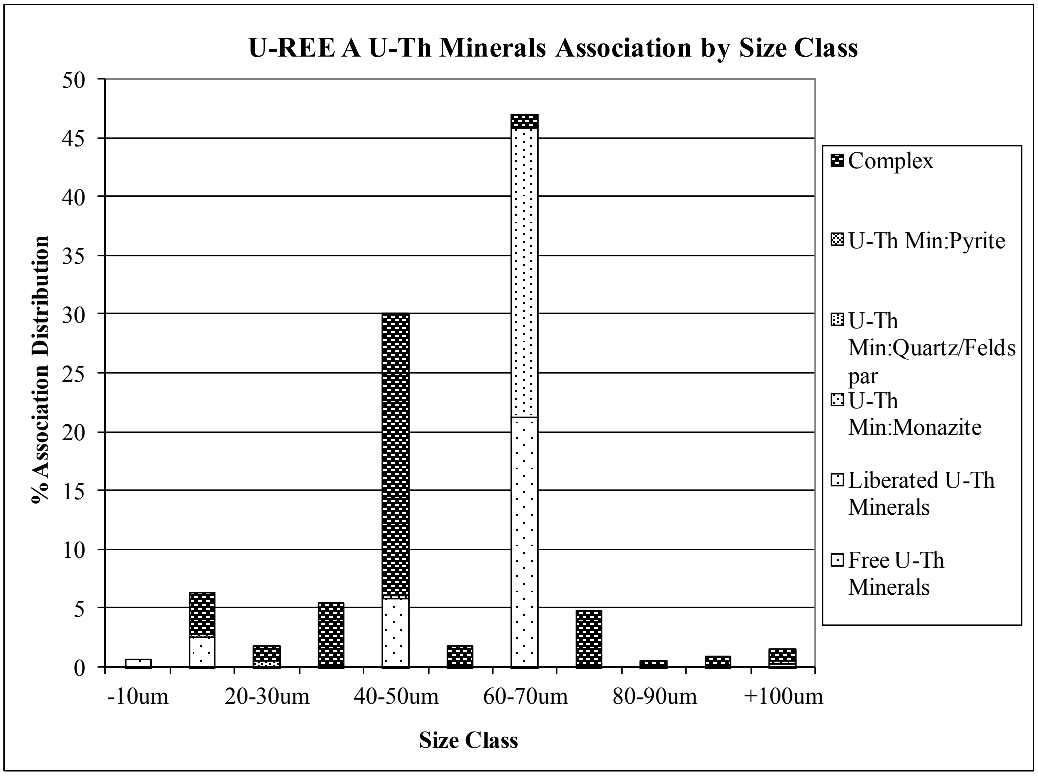

Figure 4. U-REE A U-Th minerals liberation and association.

Beneficiation

Figure 5 presents the beneficiation results. The best recovery/selectivity achieved for U-REE A was by flotation>gravity>magnetic separation. The flotation pre-concentrate for U-REE A recovered ~90% REE and U in 24% mass. The U-REE B pre-concentrate, subjected to flotation, achieved 90+% REE and U recoveries but at a greater mass recovery of 39%. Magnetic separation conducted on the U-REE B pre-concentrate resulted in mass reduction in the magnetic of ~17% along with 36% U and ~19% REE lost. The magnetic concentrate was subjected to REE extraction via acid bake. The acid bake residue was then combined with the non-magnetic for U extraction. The magnetic separation would in effect reduce the acid bake throughput and acid consumption.

Various beneficiation technologies, standalone or in combination, could be used to achieve physical separation on the U-REE samples from Elliot Lake. The preferred method or the combination of technologies could only be determined by capital and operating cost in relation to REE and U recoveries by each method. The reduction in downstream leach throughput and acid consumption would be major determining factor.

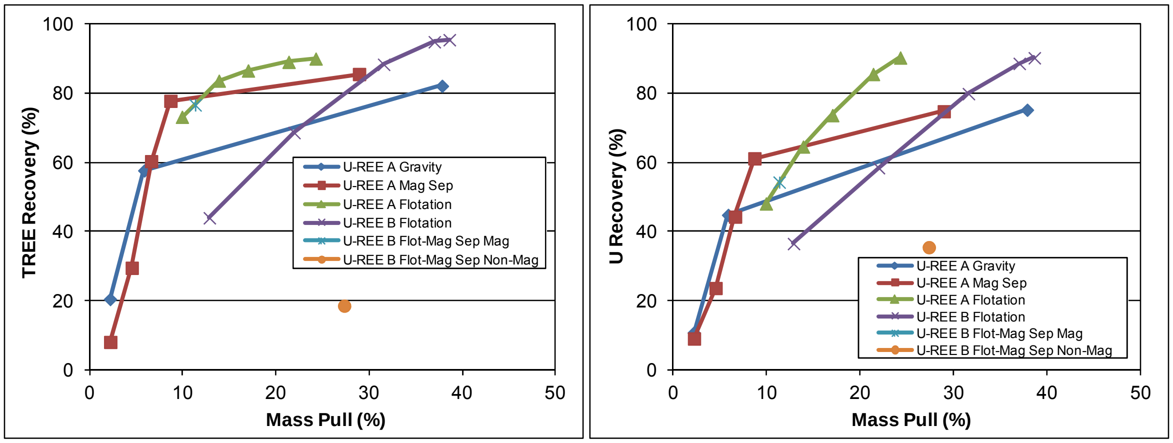

Figure 5. U-REE beneficiation results.

Leach Liquor Impurities

Whole ore and pre-concentrate leaching from the U-REE A sample was conducted. The whole ore consumed ~60 kg/t (kg of acid per tonne of mill feed) while the pre-concentrate was around ~33 kg/t. Table II presents the leach liquor impurities from the whole ore and pre-concentrate leaching. The gangue to REE in the liquor decreased significantly with the pre-concentrate which would likely reduced the reagent consumption for impurity removal.

Table II. U-REE A Leach Liquor Impurities

Leach Feed	Leach Liquor Composition, mg/L											Gangue:REE
	Al	Ca	Cr	Cu	Fe	K	Mg	Mn	Na	P	Ti	
U-REE A Whole Ore	6130	1010	72.2	45.5	8650	4800	420	121	300	441	181	47
U-REE A Pre-Conc	5220	1300	59.9	83.7	21300	1990	515	302	265	1220	386	13

REE Carbonatitte Complex with Carbonate Gangue

Niobium carrying minerals such as pyrochlore and columbite in association with carbonates are commercially recovered in Brazil and Canada. The beneficiation process is typically complex and unselective due to surface similarities between Nb and gangue minerals [19]. Similar carbonatite deposits exist where REE bearing minerals are found in association with carbonate gangue. Two separate studies on carbonatite complex from different locations, identified as CC A and CC B, were conducted at SGS Lakefield. The REE carrying minerals are typically bastnaesite (or REE-F-carbonates) and monazites with carbonate gangue (ankerite, siderite, dolomite, and calcite). Gravity, magnetic separation, and flotation (using fatty acids) showed insignificant upgrading as the REE and gangue minerals share many similar physical properties. REE pre-concentration into a single bulk pre-concentrate was investigated.

Head Chemical Analysis

Table II presents the head chemical analysis on the carbonatite complex samples. Both samples had similar REE head grades at ~1.5-2% REE. The majority of the REEs are LRE at ~70-75% La+Ce. The gangue in both samples mainly contained Si, Fe, Mg, Ca, and P with minor variation.

Table III. CC Head Chemical Analysis

Composite	LREE, g/t	HREE, g/t	TREE, g/t	SiO_2, %	Fe_2O_3, %	MgO, %	CaO, %	P_2O_5, %
CC A	19765	320	20086	1.80	17.0	8.76	24.4	3.45
CC B	17298	333	17630	4.56	21.3	7.51	20.1	0.71

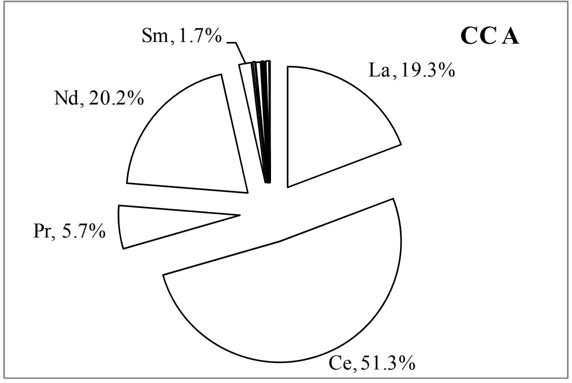

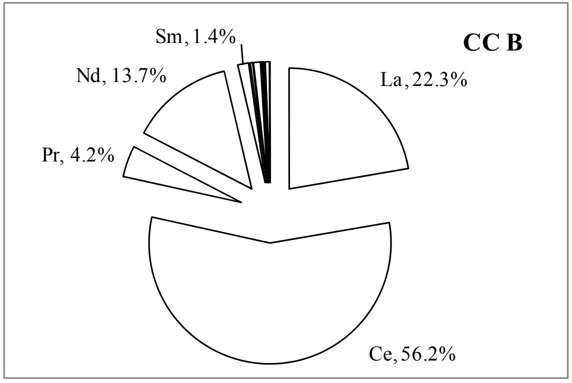

Head Mineralogical Analysis

Mineralogical examination on both the CC A and CC B samples were completed at SGS Lakefield. The mineral distribution, presented in Figure 6, revealed that the major REE bearing minerals for CC A is monazite and Ba-Ce carbonates for CC B. The gangue composition is similar, mainly consisting of ankerite, siderite, dolomite, and calcite. The gangue carbonates are acid consumers for leaching which would render whole ore leaching uneconomical. The REE and gangue minerals share many physical characteristics such as specific gravity and magnetic property. Selectivity for monazite and Ba-Ce carbonates from carbonate gangue by flotation may be limited when using fatty acids.

Liberation and association for monazite in CC A and Ba-Ce carbonates in CC B are shown in Figure 7 and Figure 8, respectively. The samples for CC A and CC B submitted for mineralogical examination were 100% passing 38 µm and 75 µm, respectively. The major REE bearing minerals for both CC A and CC B were not well liberated. A significant portion of the free and liberated REE minerals were found below 30 µm. The finely liberated REE particles would be outside the operating ranges of many beneficiation technologies. The poorly liberated REE minerals would likely result in either poor upgrading or significant losses.

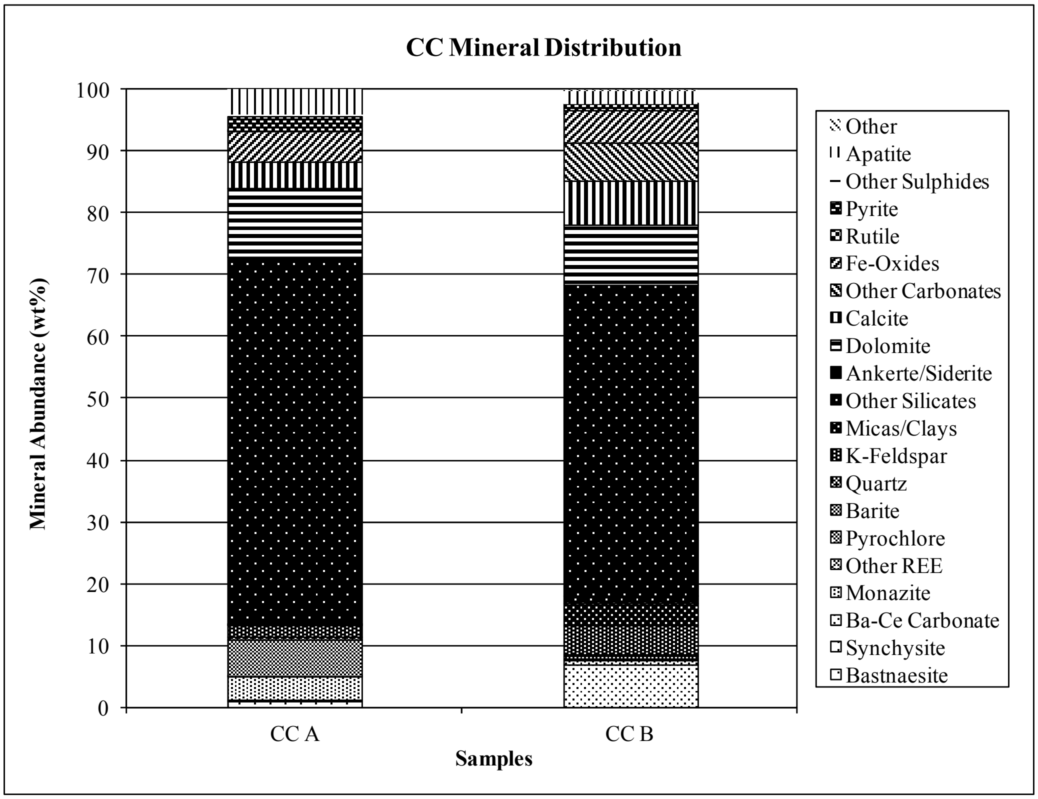

Figure 6. CC Mineral distribution.

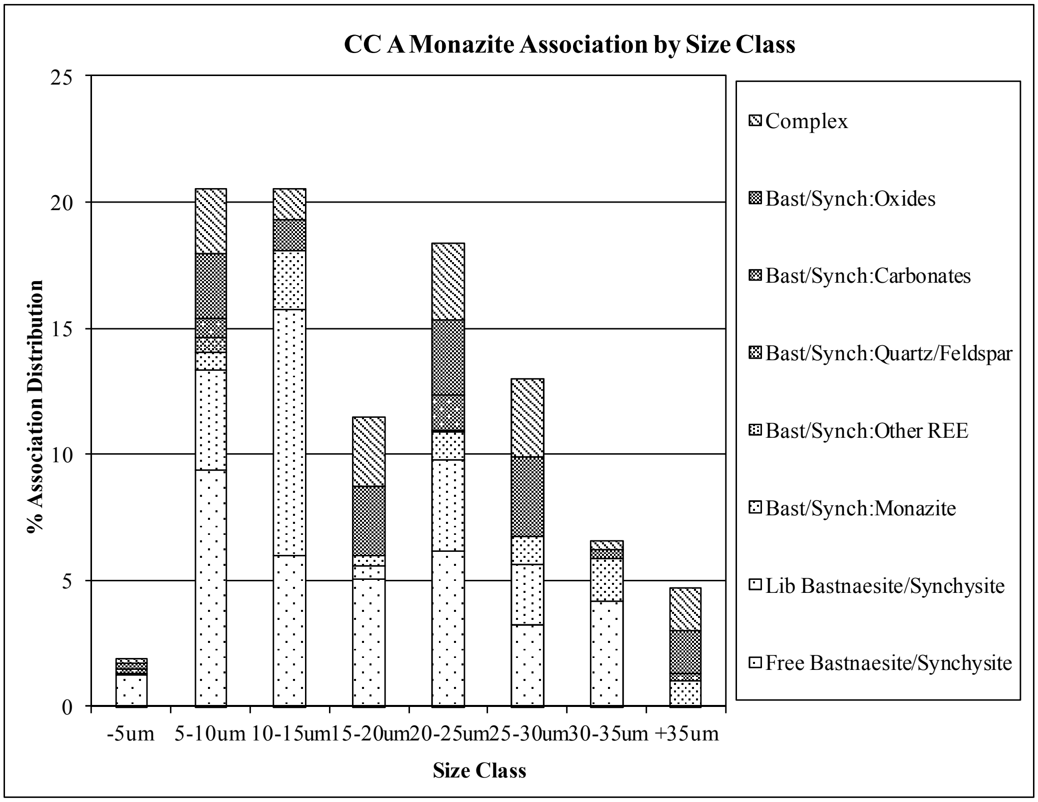

Figure 7. CC A monazite liberation and association.

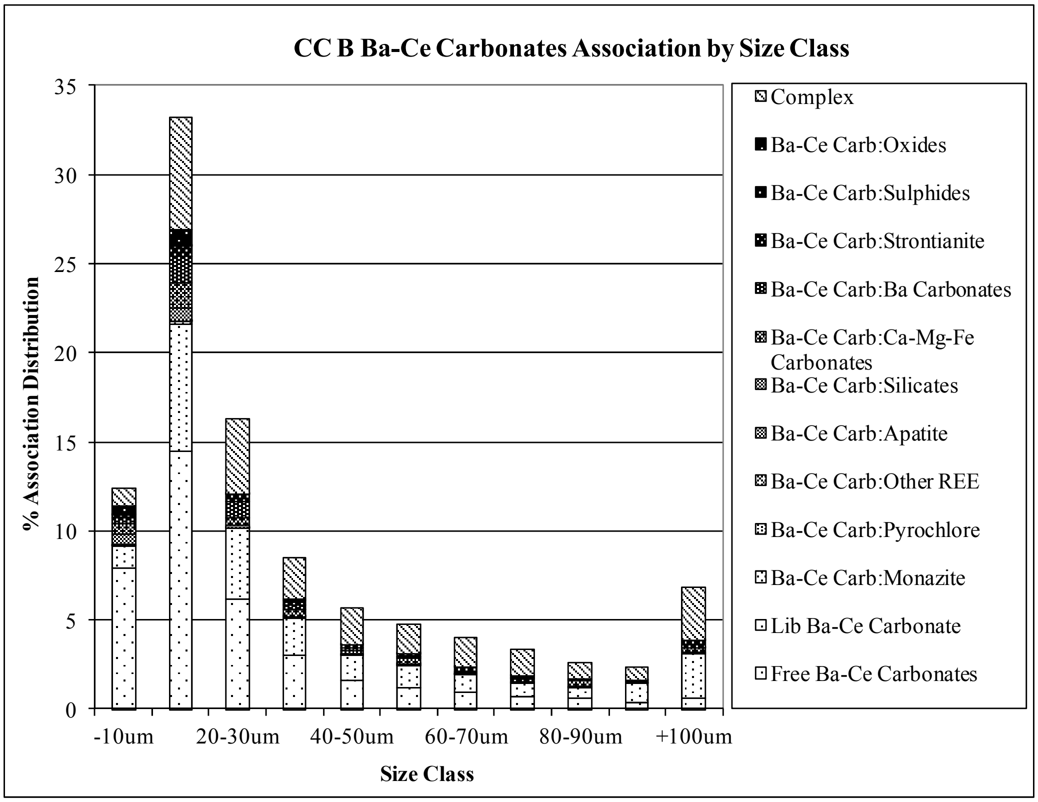

Figure 8. CC B Ba-Ce carbonates liberation and association.

Beneficiation

Figure 9 presents the best beneficiation results achieved for the CC samples. Flotation provided the best upgrading option, achieving ~75% REE recovery in ~20% mass in both CC samples. A combination of gravity and flotation as well as roasting and magnetic separation, achieved similar recoveries to flotation in CC B but with reduce selectivity. Unlike the U-REE samples which may have different processing routes, flotation clearly provide the best option for the CC samples.

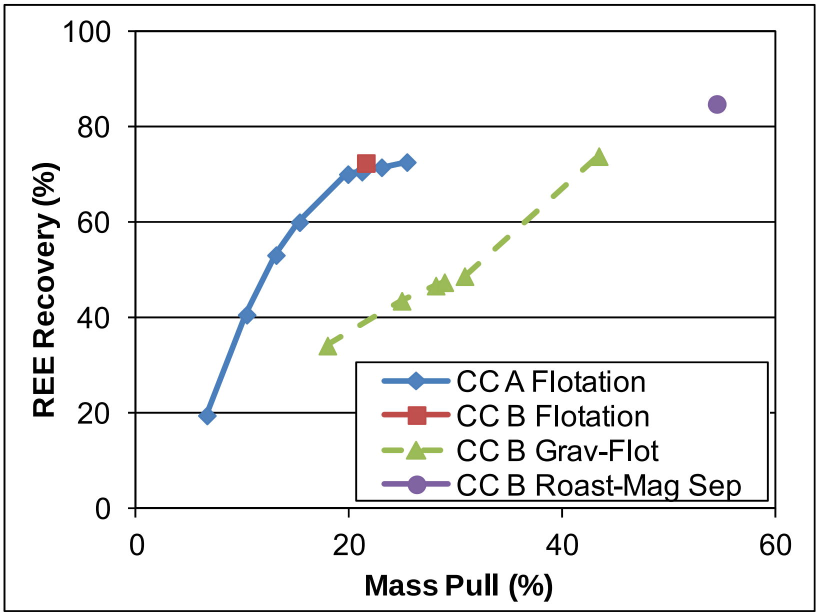

Figure 9. CC REE beneficiation results.

<u>Leach Liquor Impurities</u>

Whole ore and pre-concentrate leaching from the CC B sample was conducted. The whole ore consumed ~660 kg/t (kg of acid per tonne of mill feed). Table IV presents the leach liquor impurities between the whole ore and pre-concentrate leaching. The gangue to REE in the liquor decreased from 26 to 6.5 which would likely reduced the reagent consumption for impurity removal.

Table IV. CC B Leach Liquor Impurities

Leach Feed	**Leach Liquor Composition, mg/L**									**Gangue:REE**
	Fe	**Mg**	**Ca**	**Al**	**P**	**Mn**	**Si**	**Ba**	**Sr**	
CC B Whole Ore	20000	6000	20000	-	-	2400	-	3000	3000	26
CC B Pre-Conc	21000	6420	20600	722	302	2460	29.5	15600	13600	6.5

Multi-REE Minerals with Silicates Gangue

The U-REE and CC samples typically contained only a few REE bearing minerals against a major gangue mineral where recovering the major REE minerals against the major gangue mineral is required. In some REE deposit, REEs are found in multiple minerals. Light rare elements (LRE) and heavy rare elements (HRE) bearing minerals may be different. In addition, recovering other minerals of interest such as Nb and Zr carrying minerals would also be required. REE deportment would be critical for beneficiation flowsheet development. A single study, identified as M REE-S, on recovering multiple REE minerals from silicate gangue into a single pre-concentrate was conducted.

Head Chemical Analysis

Table V summarizes the head chemical analysis and REE distribution of the M REE-S sample. The head REE grade of ~1% REE is typical of currently developing projects but the ~0.1% Nb_2O_5 would be considered low when compared against commercially operating facilities. The combined La+Ce are ~55% which is considerably lower than the U-REE and CC samples. A higher proportion of HRE is found, such as ~13% Dy.

Table V. M REE-S Head Chemical Analysis

Composite	M REE-S
LREE, g/t	7703
HREE, g/t	2153
TREE, g/t	9856
Nb_2O_5, %	0.13
SiO_2, %	65.7
Al_2O_3, %	7.00
Fe_2O_3, %	11.1
CaO, %	2.02
Na_2O, %	2.80
K_2O, %	3.69

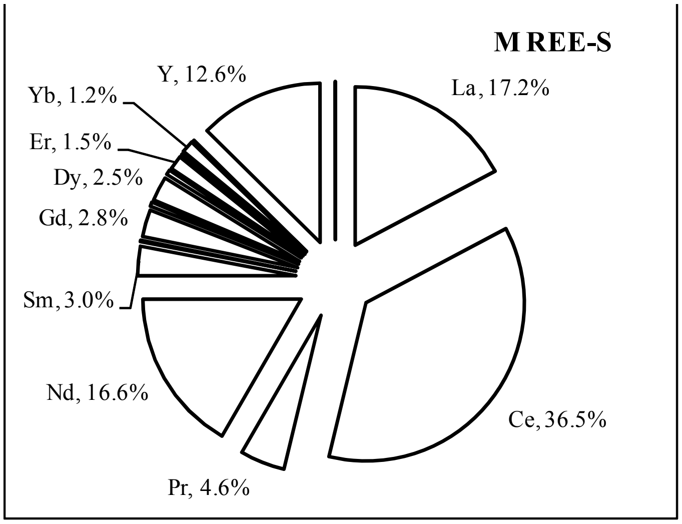

Head Mineralogical Analysis

Mineralogical examination was completed on the M REE-S sample ground to 80% passing 150 µm. The REE carrying minerals, as shown in Figure 10, include bastnaesite, allanite, monazite, chevkinite, and fergusonite. Other minerals of interest include zircon. The major gangue minerals include quartz/feldspar, muscovite, clays, and other silicates.

Elemental deportment for Nd and Dy is presented in Figure 11. Nd and Dy are found in multiple minerals. Successful physical separation would require recovering multiple REE minerals.

Liberation and association for allanite, fergusonite, other REE, and zircon is shown in Figure 12. Allanite is well liberated while fergusonite, other REE, and zircon are poorly liberated. The majority of the free and liberated particles for fergusonite, other REE, and zircon are found below 30 µm. Liberation could be an issue during separation.

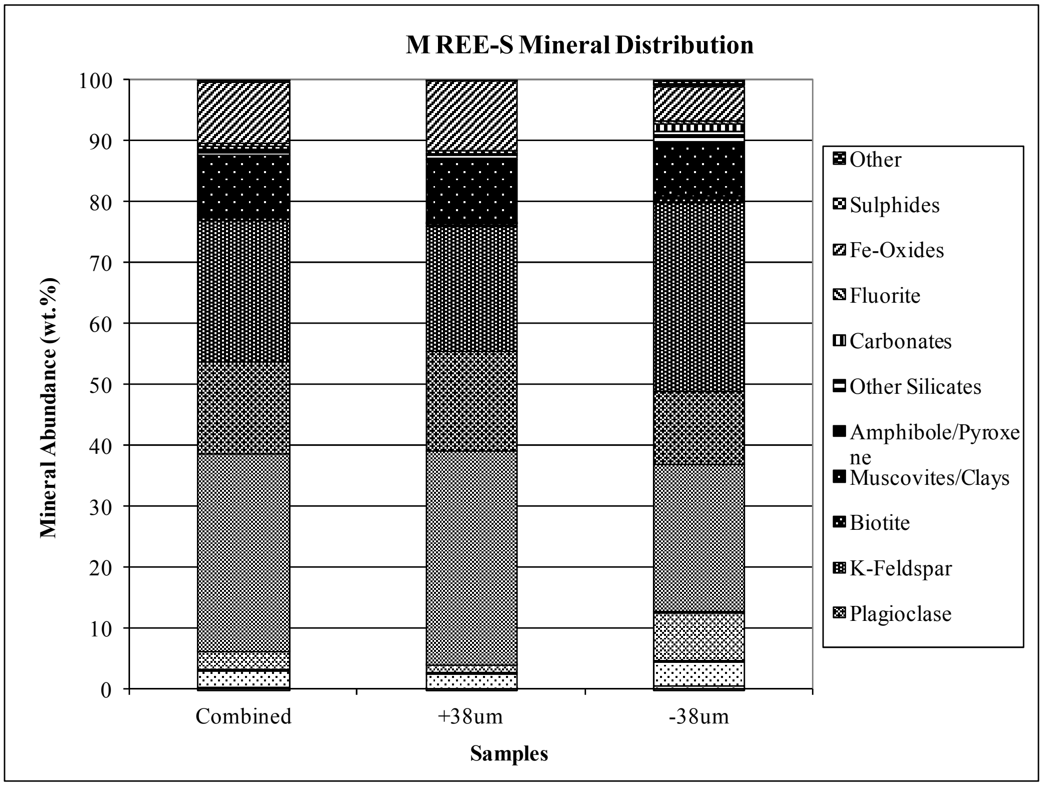

Figure 10. M REE-S mineral distribution.

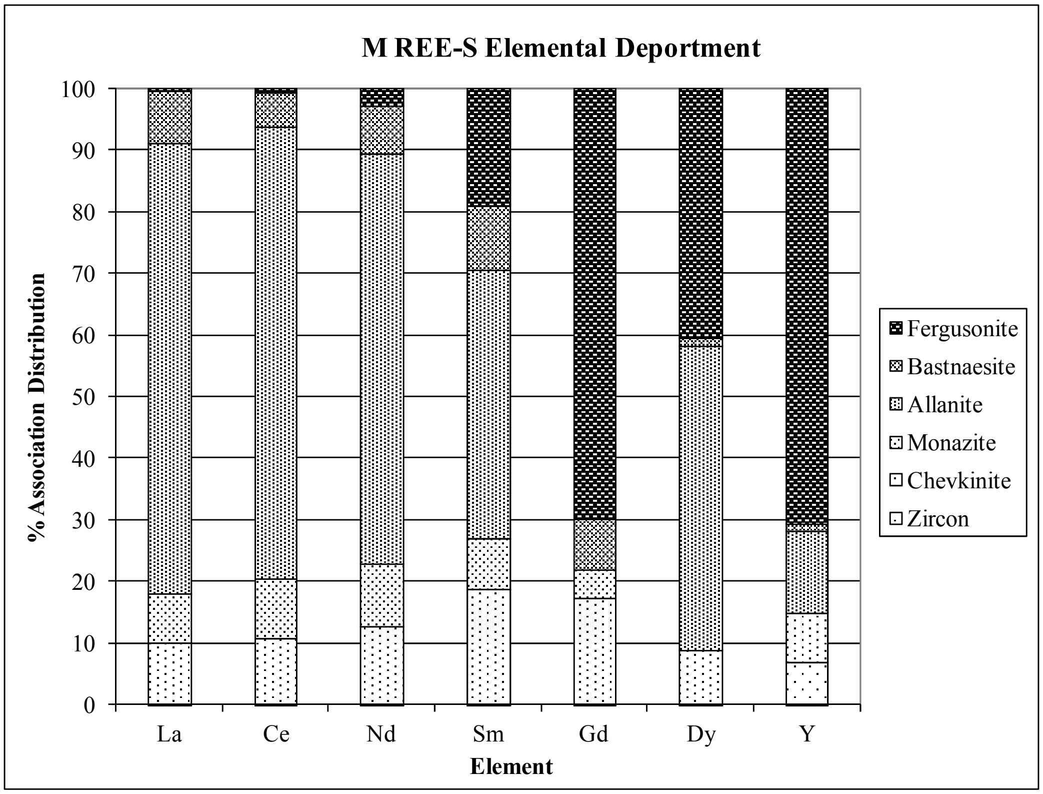

Figure 11. M REE-S elemental deportment.

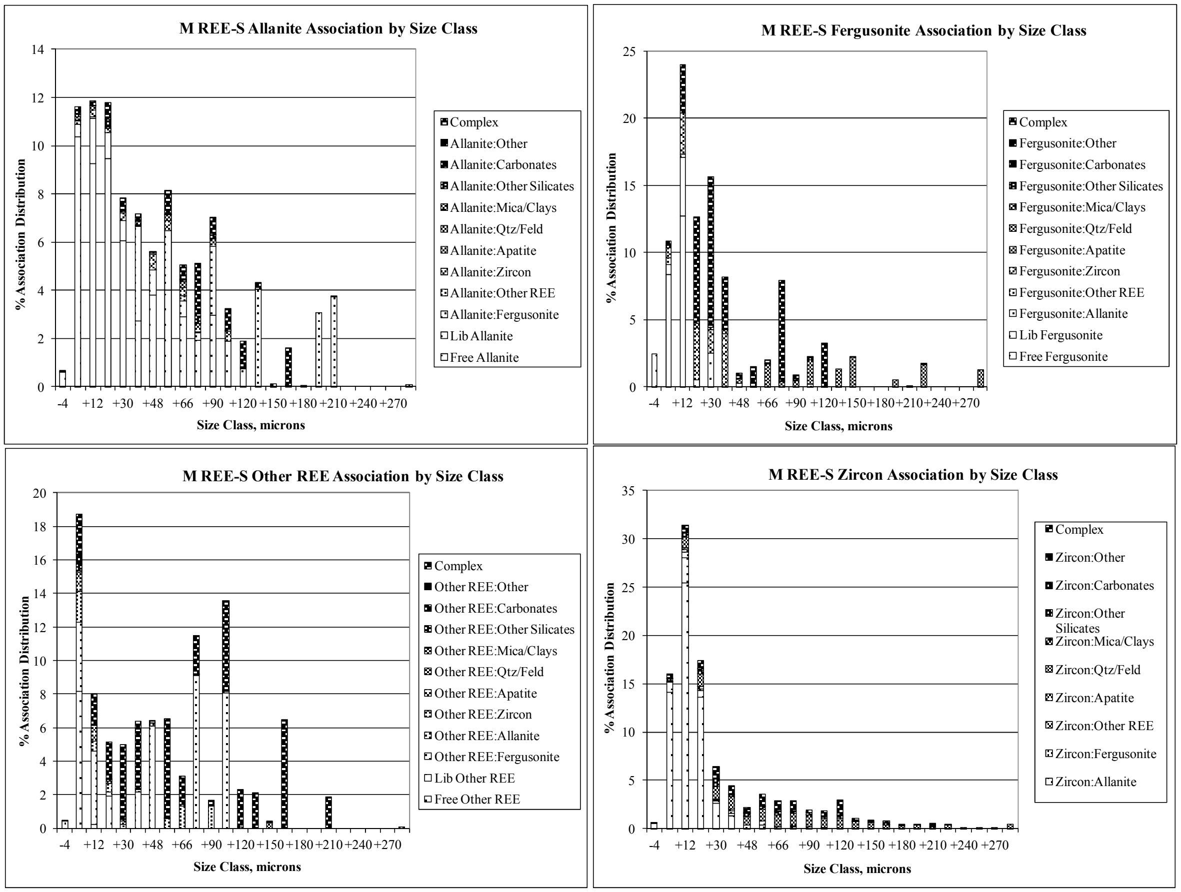

Figure 12. M REE-S REE and zircon liberation and association.

Beneficiation

Three processing routes developed for the M REE-S sample included: i) flotation, ii) gravity-magnetic separation (G-MS), and iii) gravity-magnetic separation-flotation (G-MS-F), where flotation was used to scavenge from the gravity tailings. Different assaying elements were used to track the various minerals. Ce and Nd were used as indicators for recovering LRE minerals such as monazite while Y was used for HRE minerals such as fergusonite. Nb and Zr were used to track pyrochlore and zircon, respectively.

The flotation route resulted in similar recoveries for Nb, Ce, and Nd but with increased recoveries for Y and Zr when comparing to the gravity-magnetic separation process. The improvements magnified when the individual REE value is considered. LRE such as La and Ce typically have the least value while HRE such as Y have greater value. As such, significant LRE recovery gains may not have a significant impact on economics as perhaps smaller HRE recovery gains. The combination of gravity-magnetic separation-flotation resulted in the greatest recoveries, exceeding 80% for Nb, Ce, Nd, and Y but with an increase in mass pull by ~10-15%. The increased mass may result in greater acid consumption in the downstream hydrometallurgical process.

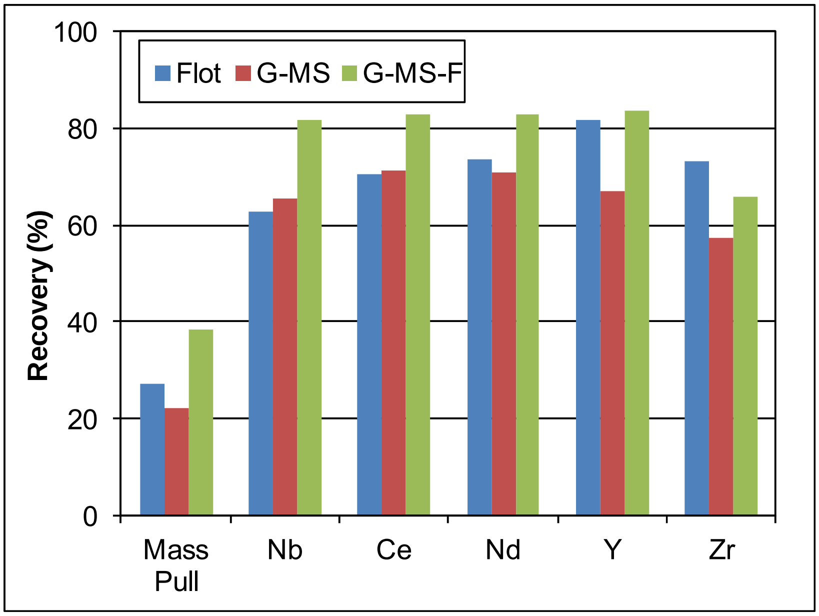

Figure 13. M REE-S beneficiation results.

Conclusions

A number of mineral processing options for various REE deposits are presented. Complex flowsheets requiring a combination of beneficiation technologies or reagent scheme that are not common for industrial minerals flotation outside of China are often required. In some REE deposit, such as the U-REE deposits from the Elliot Lake region, various processing routes are available that recovered ~90% U and REE in ~25% mass. For REE-carbonatite complex, flotation was demonstrated as the best option for REO selectivity against carbonate gangue. REO recovery of ~75% in 20% mass was obtained. A complex gravity-magnetic separation-flotation process was developed for a multiple REE minerals-silicate deposit. The final pre-concentrate recovered ~80% REO along with ~65% ZrO2 in ~40% mass.

Acknowledgements

The authors of the paper express their gratitude and appreciation to Company management for allowing us to publish this data. The efforts of Tassos Grammatikopoulos of SGS, who undertook the mineralogical work, are appreciated and acknowledged.

References

1. Morrice, E., M.M. Wong, “Flotation of Rare Earths rom Bastnasite Ore” (Bureau of Mines Report of Investigation 8689, 1982).

2. Pradip, D.W. Fuerstenau, “Design and development of novel flotation reagents for the beneficiation of Mountain Pass rare-earth ore”, *Minerals & Metallurgical Processing*, 30 (2013), 1-9.

3. Fuerstenau, D.W., Pradip, R. Herrera-Urbina, "The surface chemistry of bastnaesite, barite and calcite in aqueous carbonate solutions", *Colloids and Surfaces*, 68 (1992), 95-102.

4. Pradip, D.W. Fuerstenau, "Alkyl hydroxamates as collectors for the flotation of bastnaesite rare-earth ores", *The Minerals, Metals & Materials Society*, (1988), 57-70.

5. Jordens, A., Y.P. Cheng, K.E. Waters, "A review of the beneficiation of rare earth element bearing minerals", *Minerals Engineering*, 41 (2013), 97-114.

6. Zhang, J., C. Edwards, "Review of rare earth mineral processing technology", *CIM Journal*, 4 (2013), 38-52.

7. Cheng, J., Y. Hou, L. Che, "Flotation separation on rare earth minerals and gangues", *Journal of Rare Earths*, 25 (2007) 62.-68.

8. Ren, J., W. Wang, J. Luo, G. Zhou, F. Tang, "Progress of flotation reagents of rare earth minerals in China", *Journal of Rare Earths*, 21 (2003), 1-8.

9. Ren, J., S. Lu, S. Song, J. Niu, "A new collector for rare earth mineral flotation", *Minerals Engineering*, 10 (1997) 1395-1404.

10. Ren, J., S. Song, A. Lopez-Valdivieso, S. Lu, "Selective flotation of bastnaesite from monazite in rare earth concentrates using potassium alum as depressant", *Int. J. Miner. Process.*, 59 (2000), 237-245.

11. Luo, J., J. Ren, F. Tang, G. Zhou, "Development on flotation reagents of rare earth minerals in China", *Journal of the Chinese Rare Earth Society*, 20 (2002) 385-391.

12. Che, L., Y.F. Yu, J. Yuan, F.G. Zhang, "Application and trend of hydroximic acid as collectors on flotation of RE minerals", *Chinese Rare Earths*, 25 (2004), 49-54.

13. Li, F.J., X.L. Zeng, Y.J. Zhu, "Application of collector L102 in Changlan Rare Earth Dressing Plant", *Chinese Rare Earths*, 23 (2002) 1-5.

14. Jia, L., X. Che, Z. Qi, L. Zhang, "Flotation study of three kidns of collectors towards bastnaesite", *Metal Mine*, 421 (2011), 106-109.

15. Zhang, X., H. Du, X. Wang, J.D. Miller, "Surface chemistry considerations in the flotation of rare-earth and other semisoluble salt minerals", *Minerals & Metallurgical Processing*, 30 (2013), 24-37.

16. Grimes, M.E., "Rio Algom investigations into preconcentration of uranium ore", *Society of Mining Engineers*, 254 (1973), 312-318.

17. Raicevic, D., D.R. McCarthy, "Preconcentration of low-grade uranium ores with environmentally acceptable tailings", *Canmet project MRP-4.3.6.0.04*, (1979).

18. Muthuswami, S.V., S. Vijayan, D.R. Woods, S. Banerjee, “Flotation of uranium from uranium ores in Canada”, *The Canadian Journal of Chemical Engineering*, 61 (1983), 728-744.

19. Ni, X., M. Parrent, M. Cao, L. Huang, A. Bouajila, Q. Liu, “Developing flotation reagents for niobium oxide recovery from carbonatite Nb ores”, *Minerals Engineering*, 36-38 (2012), 111-118.

Hydrometallurgy of Rare Earth Mineral Concentrates

ALTERNATIVE PROCESS FOR RARE EARTHS RECOVERY FROM BASTNASITE CONTAINING ORE

Mellodee Anvia[1], Elizabeth Ho and Karin Soldenhoff*

ANSTO Minerals, Locked Bag 2001, Kirrawee DC, NSW 2232, Australia
[1]School of Chemistry, The University of Sydney, NSW 2006, Australia

*khs@ansto.gov.au

Keywords: Bastnasite, Hydrochloric Acid, Rare Earths, Rare Earth Oxalate

Abstract

Bastnasite is a rare earth fluorocarbonate mineral of major economic significance. The mineral is enriched in the light rare earths and is readily soluble in acid under atmospheric leach conditions. Bastnasite concentrate is commercially processed *via* a calcination/HCl leach route, with a crucial part of the process being the beneficiation which provides a significant upgrade in the rare earth concentrations. Recently, there is increased interest in processing ores of much lower grade that are not readily amenable to beneficiation.

This paper briefly reviews processing options for bastnasite and presents results of a laboratory investigation of an alternative process route. The proposed process is based on hydrochloric acid leaching, with an intermediate chemical rare earth concentrate produced *via* oxalate precipitation. The final product is a concentrated rare earth chloride solution, which is amenable as a feedstock for solvent extraction, to separate the rare earths into individual products.

Introduction

Over the last 50 years, bastnasite has replaced monazite as the main source of rare earth elements (REEs) due to the development of bastnasite deposits such as the Mountain Pass mine in California, and the Bayan Obo mine in China [1]. Bastnasite ores from Mountain Pass and Bayan Obo are able to be beneficiated by froth flotation and other unit operations to produce high grade concentrates containing up to 60% REO [2,3]. Molycorp also produced a 70% concentrate at Mountain Pass by leaching the 60% concentrate in 10% HCl to dissolve calcite [4].

Bastnasite processing options include an air roast/acid leach [3,5,16], sulfuric acid roast/ leach [6–12], alkaline or ammonium chloride roast [13–15], direct acid leach [17–18] and chlorination [5].

In the Molycorp process operated in the 1960's at Mountain Pass, the bastnasite concentrate was roasted in air at 620 °C to eliminate carbon dioxide and oxidise the cerium(III) to cerium(IV) [3,5]. The calcine was leached with hydrochloric acid, leaving cerium(IV) in the residue, producing a leach solution containing approximately 100 g/L REO. The Mountain Pass mine operated from 1952 to 2002 and mine production resumed in 2012. The current Molycorp process reportedly contains process improvements to recover and recycle reagents and water, but details are not in the public domain.

At Baotou, the bastnasite concentrate is roasted with 98% sulfuric acid, which eliminates carbon dioxide [6]. The rare earths are converted to rare earth sulfates and solubilised in a water leach. Rare earths can be recovered by precipitation as sodium double sulfates and converted to rare earth hydroxide by digestion in caustic soda. The rare earth hydroxide is dissolved in hydrochloric acid to produce a chloride liquor suitable for rare earth separation by solvent extraction. More recently, direct solvent extraction of rare earths from sulfate liquor and stripping with hydrochloric acid to transfer them to a chloride solution at a plant in Baotou has also been reported [7]. Sulfuric acid bake/leach of a bastnasite concentrate and recovery of rare earths from the leach liquor as a double sulfate salt has also been investigated by Topkaya and Akkurt [8] and Kul *et al.* [9].

In a sulfuric acid roast at 500 °C, the cerium(III) is converted to cerium(IV) which dissolves in sulfuric acid. Various solvent extraction processes for recovering a pure cerium(IV) product from the sulfate liquor have been reported [10–12].

Alkaline roasting with sodium carbonate at 390-530 °C has also been reported [13, 14]. The calcine was washed with water to remove unreacted sodium carbonate and sodium fluoride [14]. The rare earths were then leached with hydrochloric acid.

Chi *et al.* [15] report roasting of bastnasite concentrate with MgO as a defluorinating agent at 500 °C to convert the fluoride to magnesium fluoride, which is insoluble in water. The rare earth oxides in the calcine were then converted to rare earth chlorides by roasting with ammonium chloride at 325 °C. The rare earth chlorides were dissolved in water and the rare earths precipitated as oxalate which was calcined to produce a 94% rare earth oxide.

Kruesi *et al.* investigated the direct leaching of bastnasite concentrate with concentrated hydrochloric acid, at 93 °C for 4 h [17]. Some of the rare earths reacted to form rare earth fluoride which was not leached by the hydrochloric acid. The leach residue was reacted with sodium hydroxide to convert the rare earth fluoride to rare earth hydroxide and this was leached again with concentrated hydrochloric acid to recover the remaining rare earths. Thorium, iron, lead and sulfate were removed by neutralising the rare earth chloride liquor to pH 3.0 and adding peroxide, sulfuric acid and barium chloride to the solution.

Recently, there has been increased interest in processing lower grade ores that are not readily amenable to beneficiation. Impurity separation from rare earths during processing of lower grade ores becomes a greater challenge.

In this study we investigate direct hydrochloric acid leaching of a bastnasite containing ore followed by rare earth oxalate precipitation to affect the separation of rare earths from impurities. Rather than using calcination of the oxalate to produce a mixed rare earth oxide which requires relatively aggressive acid condition for further dissolution, we investigate the option of conversion of the rare earth oxalate to rare earth hydroxides and the subsequent dissolution in HCl to produce a concentrated purified rare earth chloride solution.

Experimental

The following AR grade reagents were all used as received: ammonia (28 wt%), hydrochloric acid (37 wt%), sodium hydroxide and sodium oxalate (Merck). Liquors were assayed using a combination of inductively-coupled plasma atomic emission spectrometry (ICP-AES) and inductively-coupled plasma mass spectrometry (ICP-MS). Solids were assayed by x-ray fluorescence spectrometry. Mineralogy by SEM and x-ray microanalysis was carried out on epoxy resin impregnated portions of the sample using a Quanta 650F electron microscope with dual Bruker XFlash 5030 energy dispersive detectors. The SEM was operated at an accelerating voltage of 15 kV. Images were acquired in backscattered electron (BSE) imaging mode.

Acid Leach Test procedure: Ore ($P_{80} \approx 100$ μm), was slurried up in water in a baffled titanium tank with concentrated hydrochloric acid (250–850 g 100% HCl/kg ore) added to target an initial acid concentration. The leach was agitated by means of an overhead stirrer. The initial HCl concentration in the slurry was kept constant at 24%, unless otherwise stated. Other leach parameters were as follows: initial solids density of the acidic slurry varied from 22 to 40 wt%, temperature ranged between 40–80 °C and the leach was conducted for 3 hours.

Results and Discussion

Ore Characterisation

The bastnasite ore sample contained 5.2% TREE+Y (total rare earth elements plus yttrium). The ore composition is given in Table I and the distribution of light rare earth elements (LREE, defined in this paper as La, Ce, Pr and Nd) is given in Table II. Major impurity elements in the sample included barium, iron and silicon.

Table I. Composition of the Bastnasite Ore

Element	TREE + Y	Al	Ba	Fe	Mn	Si	Ti	Zn
Content (%)	5.2	0.32	21.3	23.1	1.2	7.9	0.48	0.08

Table II. Distribution of Light Rare Earth Elements

Element	La	Ce	Pr	Nd	Total LREE
Content relative to TREE (%)	29.8	46.9	4.7	15.8	97.2

Energy dispersive (EDS) microanalysis conducted on the sample indicated that iron oxide/hydroxide (Fe_xO_y/FeO(OH)) was the dominant phase, with an estimated abundance of greater than 50 wt%. Barite ($BaSO_4$) and quartz (SiO_2) were the other major gangue phases with estimated abundances of 25 and 10 wt%, respectively. Bastnasite was the main rare earth mineral in the ore sample. Scanning electron microscopy (SEM) analysis indicated that the majority of this mineral occurred as liberated particles, though a small proportion of bastnasite was also contained in binary or ternary phase particles or in multi-phase clusters of the gangue minerals. Backscattered electron (BSE) images of the as-received bastnasite ore are shown in Figure 1.

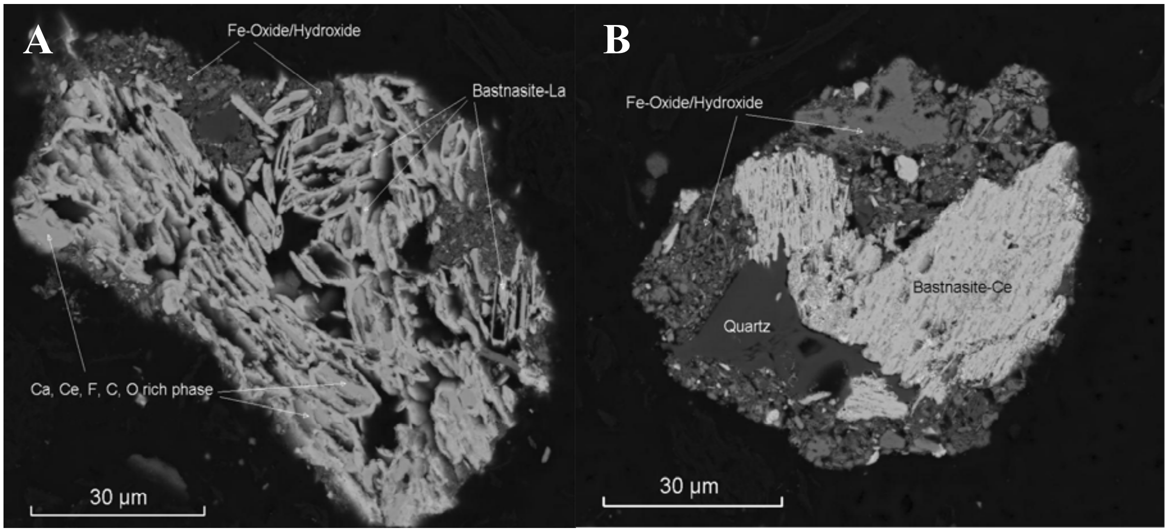

Figure 1. BSE images showing (a) a particle containing bastnasite-La and a Ca, Ce, F, C, O-rich phase; (b) a multi-phase particle comprised of bastnasite, quartz and iron oxide/hydroxide.

Hydrochloric Acid Leach

Initial optimisation of HCl leaching of the ore sample examined the effect of hydrochloric acid addition on rare earth extraction. A series of tests were carried out varying the acid addition from 250 to 850 g 100% HCl/kg ore. The initial HCl concentration was kept at 24 wt% for all leaches except for the leach at 250 g HCl/kg ore where it was 16 wt%. The leach time and leach temperature were kept constant at 3 h and 80 °C. The results are presented in Figure 2.

As can be seen in Figure 2 , leaching of the LREEs was heavily dependent on the hydrochloric acid addition, with 64% of LREEs extracted at 250 g HCl/kg ore, increasing to a maximum extraction of 97% at 850 g HCl/kg ore. Decreasing the acid addition to 750 g HCl/kg ore only resulted in a 2% decrease in LREE recovery, and was therefore considered to be the optimum acid addition at an initial acid concentration of 24 wt% HCl.

Acid addition had an analogous impact on extraction of iron, titanium and manganese from the ore. Barium extraction was low and independent of acid addition. High Mn extraction (95%) was achieved at a relatively low acid addition of 350 g HCl/kg ore. The extraction of iron with respect to acid addition resembled that of the LREEs more closely, and increased continuously with increasing acid addition from 250 to 850 g HCl/kg ore. The iron extraction was 36% at 250 g HCl/kg ore, but this increased to 82% extraction at the optimum acid addition of 750 g HCl/kg ore. Only 1% of titanium leached at 250 g HCl/kg ore, with a significant increase measured once acid addition increased above 650 g HCl/kg ore. Maximum titanium extraction was 49% at 850 g HCl/kg ore and 34% was leached at the optimum acid addition of 750 g HCl/kg ore.

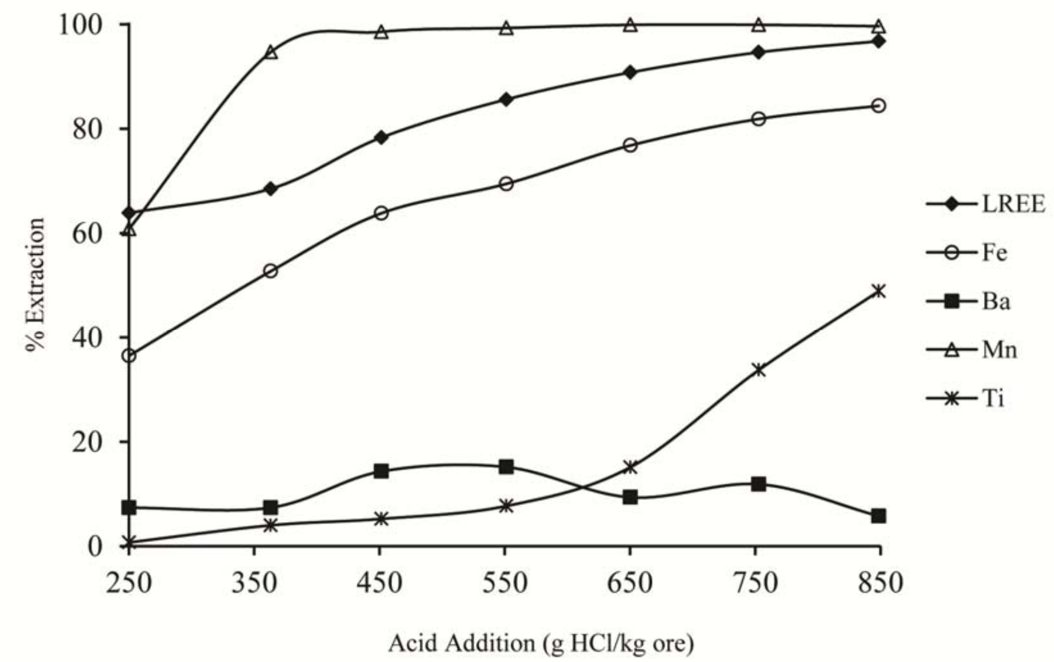

Figure 2. Effect of hydrochloric acid addition on leach extractions.
Leaches conducted at 80 °C for 3 h.

As the acid addition increased, the hydrochloric acid concentration in the final leach liquor also increased (Figure 3). For the leach at 250 g HCl/kg ore, the HCl concentration in the final leach liquor was 0.22 M and this increased to 2.3 M at an acid addition of 750 g HCl/kg ore. Figure 3 also demonstrates that the extraction of the LREEs correlated strongly with the increase in free acidity, and as the free acidity of the leach liquor increased, the extraction of LREEs is also increased.

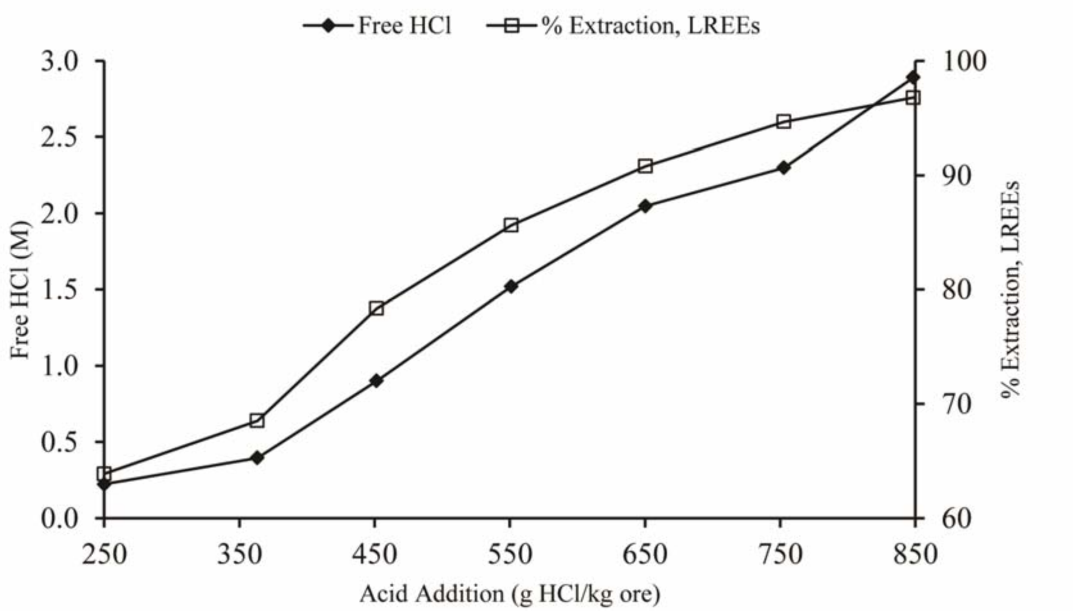

Figure 3. HCl concentration in the leach liquor versus HCl addition to the leach.
Leaches conducted at 80 °C for 3 h.

The mass loss during leaching increased as the hydrochloric acid addition increased, particularly between 250 and 450 g HCl/kg ore (Figure 4). As can be seen from Figure 4, LREE extraction was also related to the mass loss during the leach, and increased with increasing dissolution of the ore.

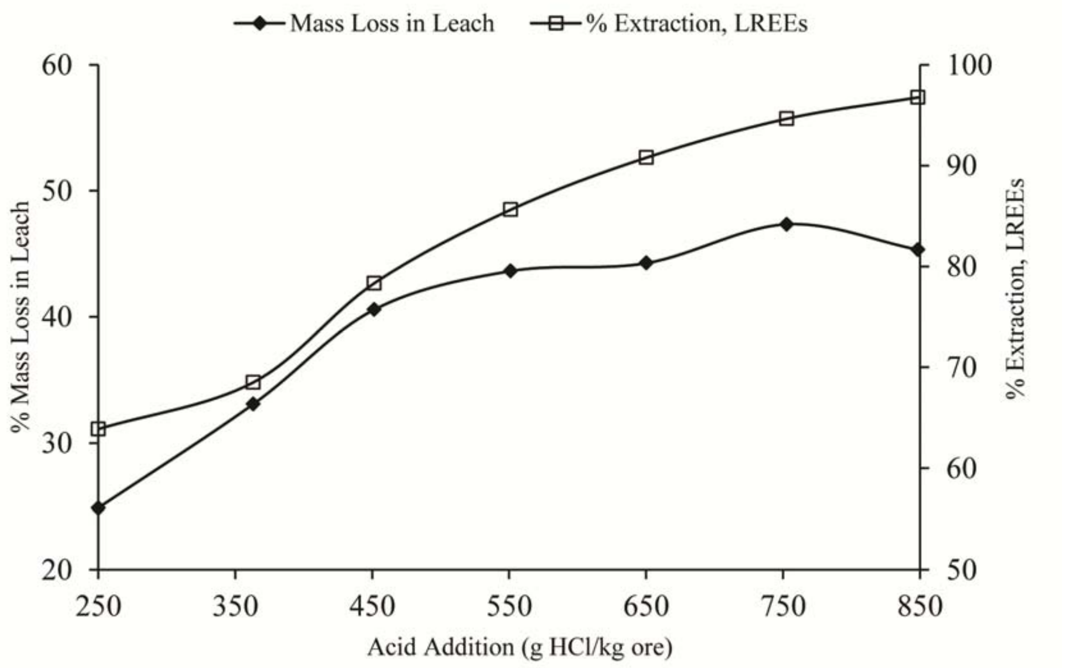

Figure 4. Mass loss of ore during the HCl leach at 80 °C for 3 h versus acid addition.

Leach temperature was found to have a significant impact on LREE and iron extraction. The impact of temperature on extraction for an acid addition of 750 g HCl/kg ore is presented in Figure 5. Decreasing the leaching temperature resulted in a significant decrease in extraction of LREEs. At 80 °C, 95% of LREEs was extracted, decreasing to 68% at 40 °C.

The effect of temperature on leaching of iron was analogous to that of the effect on the LREEs. In contrast, temperature did not play a significant role in either barium or manganese extraction. The temperature did have an impact on titanium extraction however, increasing from 6% extraction at 40 °C to 34% at 80 °C.

The effect of leach time on extractions is presented in Figure 6. Leaching was conducted at 750 g HCl/kg ore and 80 °C and slurry samples were taken during the leach. Increasing the leach time from 1 to 3 h resulted in a slight increase in extraction of the LREEs. This effect was most pronounced in the first two hours of the leach; after 2 h, 94% of LREEs was recovered compared to 91% LREE recovery after 1 h. The LREE extraction at 3 h was 95%. As can be seen from Figure 6, manganese was readily extracted from the ore whilst barium extraction was low. On the other hand iron extraction increased by 13% after 2 h of leaching, increasing from 69% extraction at 2 h to 82% extraction at the end of 3 h. After one hour, 15% of the titanium had leached, and this increased to 24% after 2 h.

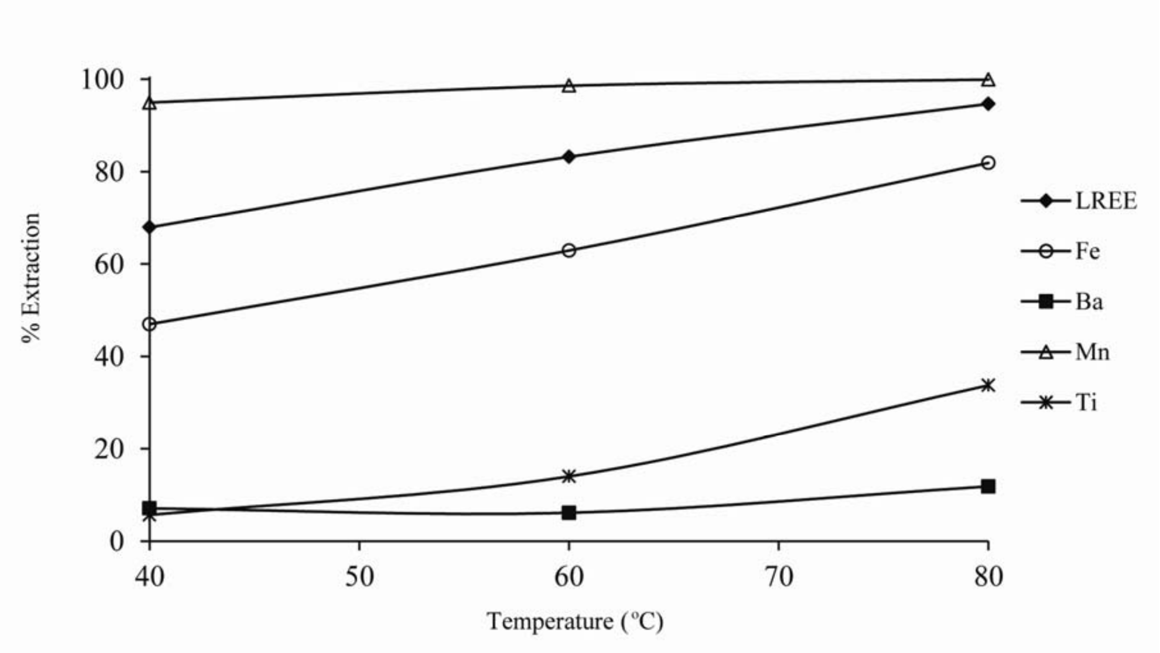

Figure 5. Effect of temperature on leach extractions
750 g HCl/kg ore, 3 h, 24 wt% HCl initially, 24% solids.

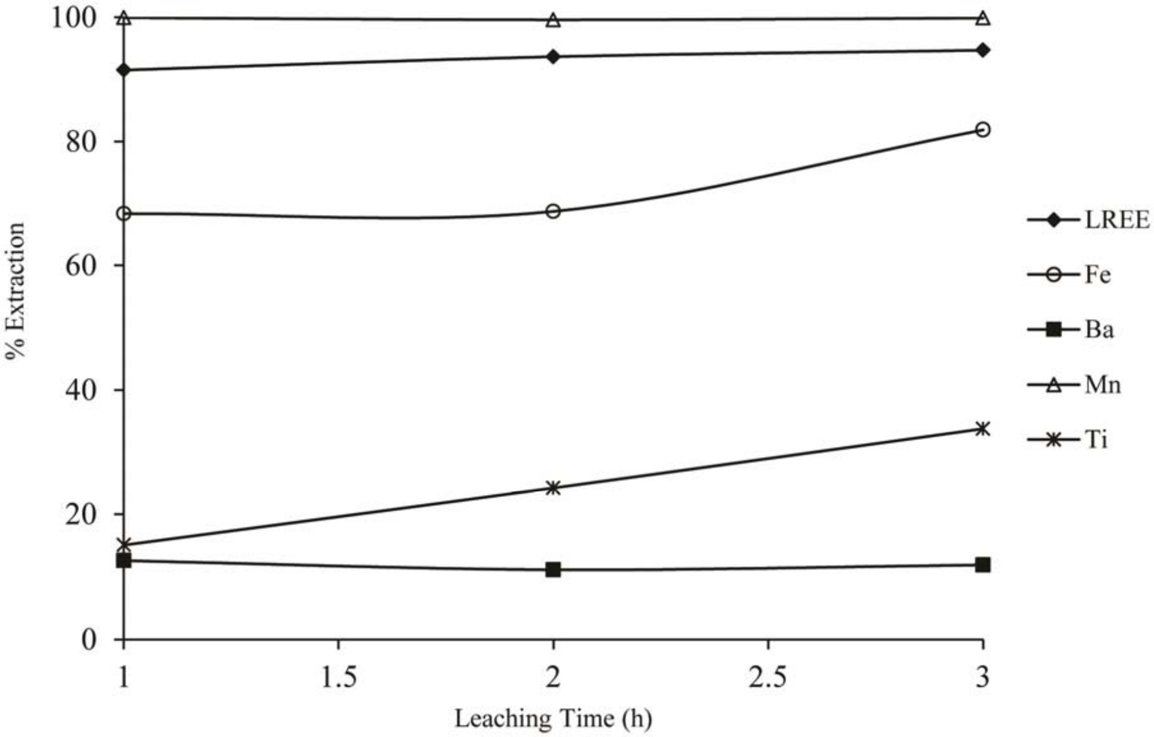

Figure 6. Leaching kinetics of the 750 g HCl/kg ore leach at 80 °C.

Using the results of the above tests, the optimum conditions for leaching the bastnasite ore were determined to be 750 g HCl/kg ore at 80 °C for 2–3 h, with 24% solids.

The consumption of hydrochloric acid by the individual elements for the test at 750 g HCl/kg ore was calculated based on the composition of the leach liquor, the measured free acid concentration and the chloride required to complex each element. Figure 7 demonstrates that of the total acid which was added to the reaction, 59% of the acid was actually consumed by the REEs and impurities in the rare earth chloride liquor and 41% was present as free HCl in the leach liquor. Acid consumption by Fe was significant at 53%, whilst 5% of the acid was consumed by the rare earths and approximately 1% by the remaining impurities. These results indicate that whilst further optimisation of the leach conditions can decrease acid consumption, significant benefits can be obtained with respect to reduction in acid consumption by any rejection of Fe containing gangue minerals prior to leaching.

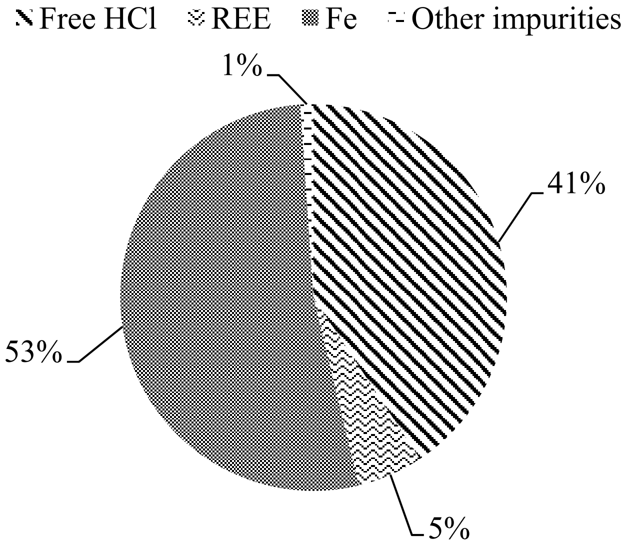

Figure 7. Calculated HCl consumption for the leach at 750 g HCl/kg ore and 80 °C.

Rare Earth Oxalate Precipitation

The liquors from the HCl leach tests were combined to produce a bulk liquor for the rare earth oxalate precipitation tests. The assay of the combined liquor is presented in Table III. The liquor had a total rare earth concentration of 19.5 g/L. Major impurities in the liquor included barium, iron and manganese.

Rare earths were precipitated from the chloride leach liquor after it was neutralised to a free acidity of ~ 0.4 M using ammonia. Solid sodium oxalate was added and the rare earths were precipitated at 50 °C over 2 hours. The oxalate precipitation step was not optimised. It is known that rare earth oxalate solubility is acid dependent [19]. For these tests the liquor was neutralised and sodium oxalate added. With further optimisation, it is expected that the free acidity of the leach liquor will be reduced and therefore no acidity adjustment will be required for oxalate precipitation. With the decrease in free acidity in the leach liquor, addition of oxalic acid can also be considered.

Table III: Assay of the Combined Leach Liquors From the HCl Leach Tests

TREE+Y	Concentration (mg/L)	Major Impurity Elements	Concentration (mg/L)
La	4940	Al	1120
Ce	9894	Ba	1190
Pr	824	Ca	340
Nd	3359	Fe	65600
LREE	19000	Mn	5550
MREE	410	Ti	142
HREE	54	Zn	368
TREE+Y	19500	Fluoride	1200

The stoichiometric requirement of sodium oxalate was calculated based on the amount of oxalate required to complex all of the rare earths and impurities in the feed liquor. Figure 8 shows the theoretical consumption of oxalate by TREE+Y, Fe and the remaining impurities present in the neutralised rare earth chloride liquor. The calculations demonstrate that 90% of the oxalate requirement is theoretically complexed by iron and other impurities. Iron is the largest consumer of oxalate, requiring approximately 80% of the total oxalate added. In contrast, 10% of the oxalate is consumed by the rare earth elements and yttrium.

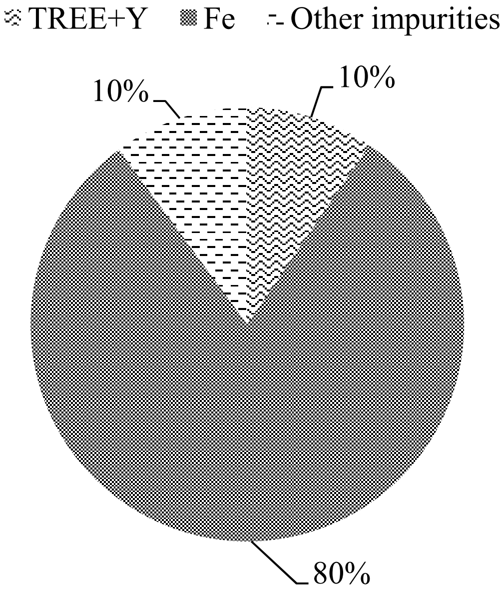

Figure 8. Consumption of sodium oxalate by REEs, iron and other impurities.

Three oxalate precipitation tests were carried out with sodium oxalate addition at 80, 100 and 120% of the calculated stoichiometric requirement. The effect of sodium oxalate addition on LREE precipitation is shown in Figure 9. The maximum precipitation of LREE was ~90% when

120% of the stoichiometric oxalate requirement was added to the neutralised liquor. At 80% of the stoichiometric requirement, only 32% of LREEs was recovered since most of the oxalate was consumed in complexing other elements.

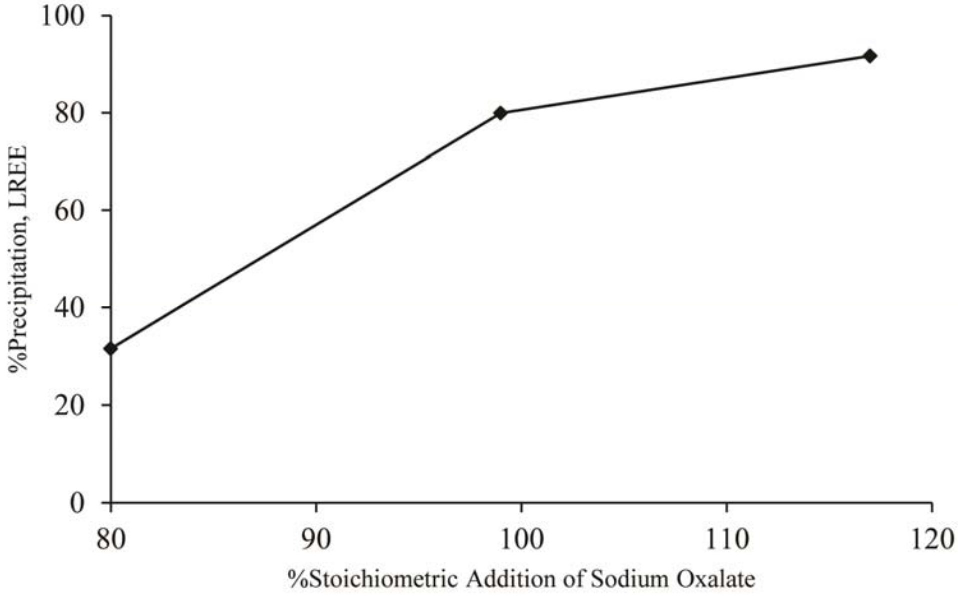

Figure 9. Effect of sodium oxalate addition on precipitation of rare earth elements. Precipitation conditions: 50°C for 2 h.

A 4 L scale oxalate precipitation was conducted at an oxalate addition of 120% stoichiometric to generate precipitate for downstream test work. Table IV shows the precipitation of LREEs and major impurities for the bulk precipitation test. As can be seen, precipitation was very selective, with 90% of LREEs recovered but <0.3% aluminium, iron, manganese and zinc co-precipitated. Approximately 1% titanium and 5% barium co-precipitated with the rare earths. The composition of the bulk precipitate is shown in Table V.

Table IV. Precipitation of LREEs and Impurity Elements by Sodium Oxalate Addition at 120% of Stoichiometric Requirement for 2 h at 50 °C

Element	LREE	MRE	Al	Ba	Ca	Fe	Mn	Ti	Zn
Precipitation, %	90	61	0.2	5	<2	0.004	0.1	1	0.1

Table V. Composition of the Oxalate Precipitate Produced by Sodium Oxalate Addition at 120% of Stoichiometric Requirement for 2 h at 50 °C

Element	LREE	MRE	Al	Ba	Ca	Fe	Mn	Ti	Zn
wt%	37.6	0.65	0.005	0.14	0.016	0.006	0.012	0.004	0.001

Caustic Conversion of Rare Earth Oxalate Precipitate and HCl Leaching

Caustic conversion of the rare earth oxalate was conducted at 95 °C using 2.5 M NaOH [20] at 150% of the calculated stoichiometric requirement for rare earths and impurities. After conversion, the residue was washed well with hot water and then leached at pH 1 by the addition of concentrated hydrochloric acid at ambient temperature.

Leaching of the rare earth hydroxide residue with hydrochloric acid produced a rare earth chloride liquor containing 100 g/L TREE+Y. The assay of the rare earth chloride liquor is given in Table VI. Relatively low concentrations of impurities including Mn, Ti, Fe and Si were also present in the liquor, but these can be reduced with further optimisation of leaching pH.

Leach extractions for the individual LREEs are given in Table VII. Greater than 99% of Pr and Nd and over 90% of the Ce and La were extracted.

Table VI. Assay of the Rare Earth Chloride liquor From the Rare Earth Hydroxide Leach at pH 1

TREE+Y	Concentration (mg/L)	Major impurity elements	Concentration (mg/L)
La	29815	Al	2
Ce	48600	Ba	86
Pr	4677	Ca	153
Nd	15424	Fe	49
MRE+HRE	1925	Mn	32
TREE+Y	100438	Ti	281
		Zn	6

Table VII. Extraction of LREEs for HCl Leach at pH 1.0 of the Conversion Residue

Element	% Extraction
La	93
Ce	95
Pr	>99
Nd	>99

Process Flowsheet

The overall approach to processing of bastnasite rich ore investigated in this study is outlined in Figure 10. Oxalate precipitation was used as a means to concentrate and separate the rare earths from major impurities resulting from the leaching of gangue minerals. Conversion of the oxalate precipitate to a rare earth hydroxide provides a means of producing a high concentration rare earth liquor suitable for feeding a solvent extraction purification circuit.

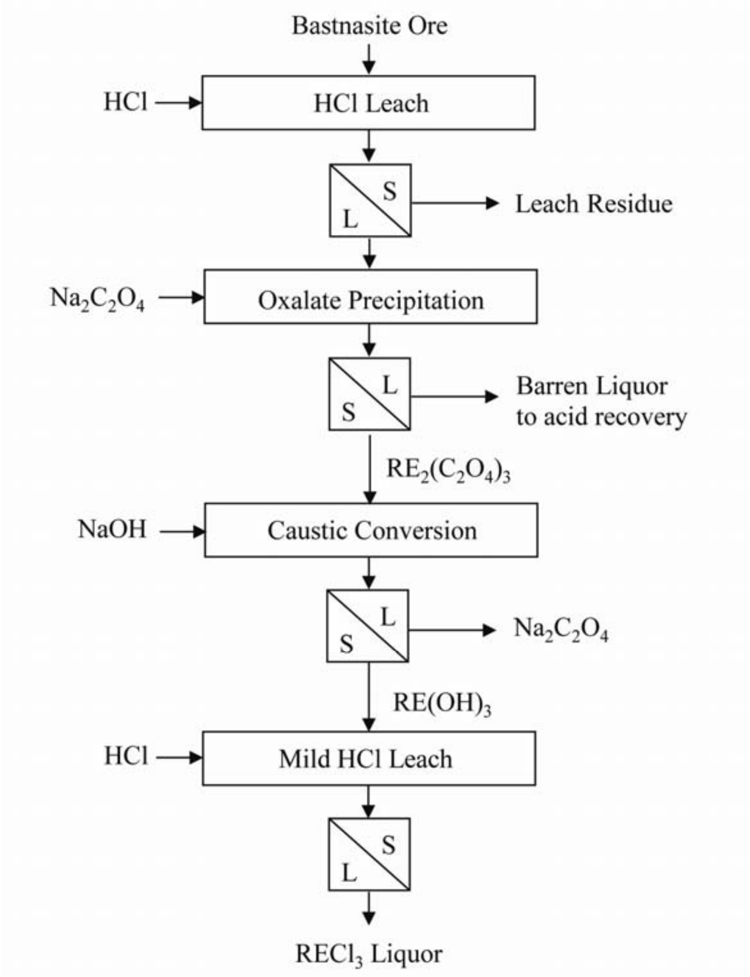

Figure 10. Outline of process investigated in this study.

Conclusions

An alternative process for extracting rare earth elements from a bastnasite ore was investigated comprising of hydrochloric acid leaching, precipitation of rare earth oxalates, conversion of rare earth oxalate to rare earth hydroxide and leaching of the rare earth hydroxide with hydrochloric acid. High recovery of rare earths was achieved with hydrochloric acid leaching using 750 g HCl/kg ore for 3 hours at 80 °C. Oxalate precipitation separated rare earths from impurities such as iron, aluminium, manganese and zinc. Impurities and in particular iron were significant consumers of hydrochloric acid and oxalate. Caustic conversion of the rare earth oxalates was performed at 95 °C for 1 h using 150% of the stoichiometric NaOH requirement. Leaching with hydrochloric acid resulted in a 100 g/L TREE+Y solution.

Acknowledgements

The authors would like to thank the following people for their assistance with this work: Kathryn Prince and Brian Young for undertaking the mineralogical analysis, Chris Chipeta, Damian Conroy, Patrick Yee, Avalin Edisho and Khursheed Anwar for ICP analysis, and Ariunaa Altantsetseg and Anny Toch for providing XRF analysis.

References

1. Jordens, A., Cheng, Y.P. and Waters, K.E. “A Review of the Beneficiation of Rare Earth Element Bearing Minerals,” *Minerals Engineering*, 41 (2013), 97–114.

2. Zang, Z.B, Yi, L.K., Chu, K.K., Cheng, W.W. and Cheng, W.W. “Rare Earth Industry in China,” *Hydrometallurgy*, 9 (1985), 205–210.

3. Harrah, H.W. “Rare Earth Concentration at Molybdenum Corporation of America Part 2. Solvent Extraction Plant,” *Deco Trefoil*, 31(5) (1967), 9–16.

4. Vijayan, S., Melnyk, A.J., Singh, R.D. and Nuttall, K. “Rare Earths: their Mining, Processing, and Growing Industrial Usage,” *Mining Engineering*, January (1989), 13–18.

5. Gupta, C.K. and Krishnamurthy, N. *Extractive Metallurgy of the Rare Earths* (New York: CRC Press, 2005).

6. Hart, K.P. and Levins, D.M. “Management of Wastes from the Processing of Rare Earth Minerals,” (Paper presented at Chemeca 1988, Sydney August 28–31, 1988).

7. Doyle, F.M., Benz, M.G., Shei, J.C., Bao, D.S., Ku, H.S. and Zhen, N.D. “Direct Production of Mixed, Rare Earth Oxide Feed for High Energy-Product Magnets,” *Rare earths and Actinides: Science, Technology and Applications IV*, eds Bautista, R.G. and Mishra, B. (Warrendale, PA: TMS, 2000), 31–44.

8. Topkaya, Y. and Akkurt, S. “Acid Curing and Baking of Bastnaesite Ore and Concentrate,” *Materials Science Forum*, 315–317 (1999), 530–536.

9. Kul, M., Topkaya, Y. and Karakaya, I. “Rare Earth Double Sulfates from Pre-Concentrated Bastnasite” *Hydrometallurgy*, 93 (2008), 129–135.

10. Zhang, Z.F., Li, H.F., Guo, F.Q., Zhang, H., Li, D.Q. and Meng, S.L. “Thermodynamic Behavior and Applications of $KMnO_4$ in Cerium Separation Process using Cyanex 923”, *Industrial and Engineering Chemistry Research*, 46 (2007), 901–906.

11. Zhang, Z., Guo, F., Meng, S., Jia, Q. Li, H. and Li, D. “Simultaneous Recovery of Cerium and Fluorine from Bastnaesite Leach Liquor by Mixtures of Cyanex 923 and HEH(EHP).” *Industrial and Engineering Chemistry Research*, 49 (2010), 6184–6188.

12. Wang, L., Yu, Y., Huang, X., Long, Z. and Cui, D. “Toward Greener Comprehensive Utilisation of Bastnaesite: Simultaneous recovery of Cerium, Fluorine, and Thorium from

Bastnaesite Leach Liquor using HEH(EHP),” *Chemical Engineering Journal*, 215–216 (2013), 162–167.

13. Liu, Z.G., Wei, X.J., Zhang, J.R., Cheng, Y.G. and Liu, X.W. “Roast Reaction of Bastnasite Concentrate Mixed with Sodium Carbonate,” *Journal of Rare Earths*, 16 (1998), 211–214.

14. Chi, R., Li, Z., Peng, C., Gao, H. and Xu, Z. “Preparation of Enriched Cerium Oxide from Bastnasite with Hydrochloric Acid by Two-Step Leaching,” *Metallurgical and Material Transactions B*, 37B (2006), 155–160.

15. Chi, R., Zhang, X., Zhu, G., Zhou, Z.A., Wu, Y., Wang, C. and Yu, F. “Recovery of Rare Earth from Bastnasite by Ammonium Chloride Roasting with Fluorine Deactivation,” *Minerals Engineering*, 17 (2004), 1037–1043.

16. Baroch, C.J., Smutz, M. and Olson, E.H. “Processing California Bastnasite Ore,” *Mining Engineering*, 11 (1959), 315–319.

17. Kruesi, P.R. and Duker, G. “Production of Rare Earth Chloride from Bastnasite,” *Journal of Metals*, 17 (1965), 847–849.

18. Bian, X., Yin, S. and Wu, W. “Leaching Kinetics of Bastnaesite Concentrate in HCl Solution,” *Transactions of Nonferrous Metals Society of China*, 21 (2011), 2306–2310.

19. Chi, R. and Xu, Z. “A Solution Chemistry Approach to the Study of Rare Earth Element Precipitation by Oxalic Acid,” *Metallurgical and Materials Transactions B*, 30B (1999), 189–195.

20. Barghusen Jr., J. and Smutz, M. “Processing of Monazite Sands”, *Industrial and Engineering Chemistry*, 50 (12) (1958), 1754-1755.

RARE EARTHS FROM MONAZITE – INDIAN EXPERIENCE

*C.K. Asnani[1], R.N. Patra[1]

[1]Indian Rare Earths Ltd., Dept. of Atomic Energy, India
*asnani@irel.gov.in

Keywords: Monazite, Rare Earths, Beneficiation, Caustic Crack, Separation

Extended Abstract

Rare Earth Elements (REEs) are a unique group of elements that exhibit special electronic, magnetic, optical and catalytic properties. By volume, the REEs application can be categorized as 30% for permanent magnets, 20% for metallurgical uses, 20% for fluid cracking and auto catalysts, 10% for glass additives, 10% for phosphors and the balance for other applications including pigments and ceramics [1]. A majority of these applications require the use of REEs with a high order of purity.

REEs are relatively plenty in earth's crust. However, because of their geochemistry, REEs are dispersed and not found in concentrated and economically exploitable forms. The few economically exploitable deposits are the minerals bastnasite, ion absorption clays, monazite and xenotime. Monazite has been the principal rare earth containing mineral in India. In fact, India possesses the largest deposits of monazite in the world. Monazite is found in the coastal tracts of the Indian states of Orissa, Andhra Pradesh, Tamil Nadu and Kerala [2].

The beach sands in Kerala and Tamil Nadu are very rich in monazite. Indian Rare Earths Limited (IREL) has been the sole producer of rare earth compounds in India. Monazite is composed primarily of rare earth phosphates and is derived from the weathering of granites, gneisses and pegmatite. In addition to rare earth phosphates, the beach sands normally contain thoria, a minor amount of uranium, iron oxide, titania and silica. The front end processes for production of REEs involve physical separation of other heavy minerals such as ilmenite, rutile, zircon, garnet, sillimanite etc. from monazite, beneficiation of monazite concentrate to above 96% grade, cracking of monazite to solubilize the phosphate and generation of water insoluble thorium, uranium and rare earth hydroxides

Further separation of mixed rare earths and production of high purity individual separated rare earths involves elaborate chemical processing steps. Due to display of similar chemical properties as a result of lanthanide contraction, separation of individual REEs is much more difficult. The solvent extraction process is the heart of the separation plant. Each of the elements of the rare earth group requires multiple extractions, scrubbing and stripping operations.

The Table Igives a typical monazite compositional analysis. Table II shows a typical distribution of REEs in $RECl_3$ produced from monazite.

Physical separation takes advantage of the high density, non-conductor and feebly magnetic properties of monazite. Preliminary concentration, also known as wet up-gradation, often takes place on the dredger using Humphrey spirals to concentrate heavy minerals. The monazite content of most heavy mineral concentrates is 1 – 5%. Table III gives a typical spiral feed and output grade analysis.

Table I. Monazite Composition

Composition	%
REEs as Re_2O_3	59.37
P_2O_5	27.03
ThO_2	8.88
U_3O_8	0.35
CaO	1.24
SiO_2	1.0
MgO	0.63
Fe_2O_3	0.32
Al_2O_3	0.12
PbO	0.18
TiO_2	0.36
ZrO_2	0.49

Table II. Rees Distribution in Monazite

REEs	%
La_2O_3	21.6
CeO_2	48.3
Pr_6O_{11}	5.9
Nd_2O_3	18.9
Sm_2O_3	2.87
Eu_2O_3	0.027
Gd_2O_3	1.4
Tb_4O_7	0.079
Dy_2O_3	0.22
Ho_2O_3	0.021
Er_2O_3	0.033
Tm_2O_3	0.001
Yb_2O_3	0.003
Lu_2O_3	0.0002
Y_2O_3	0.48

Table III. Wet Up-grading Plant - Typical Feed and Output Analysis

Mineral	Feed Grade %	Output Grade %
Ilmenite	6.16	46.16
Garnet	4.55	26.66
Monazite	0.11	1.02
Rutile	0.30	2.39
Zircon	0.25	2.30
Sillimanite	3.59	10.74
Quartz	84.88	9.98
Others	0.16	0.75

The flow sheet for heavy mineral concentrate separation is dependent on the composition. Some typical flow-sheets adopted at various IREL sites are illustrated in Figures 1, 2 & 3

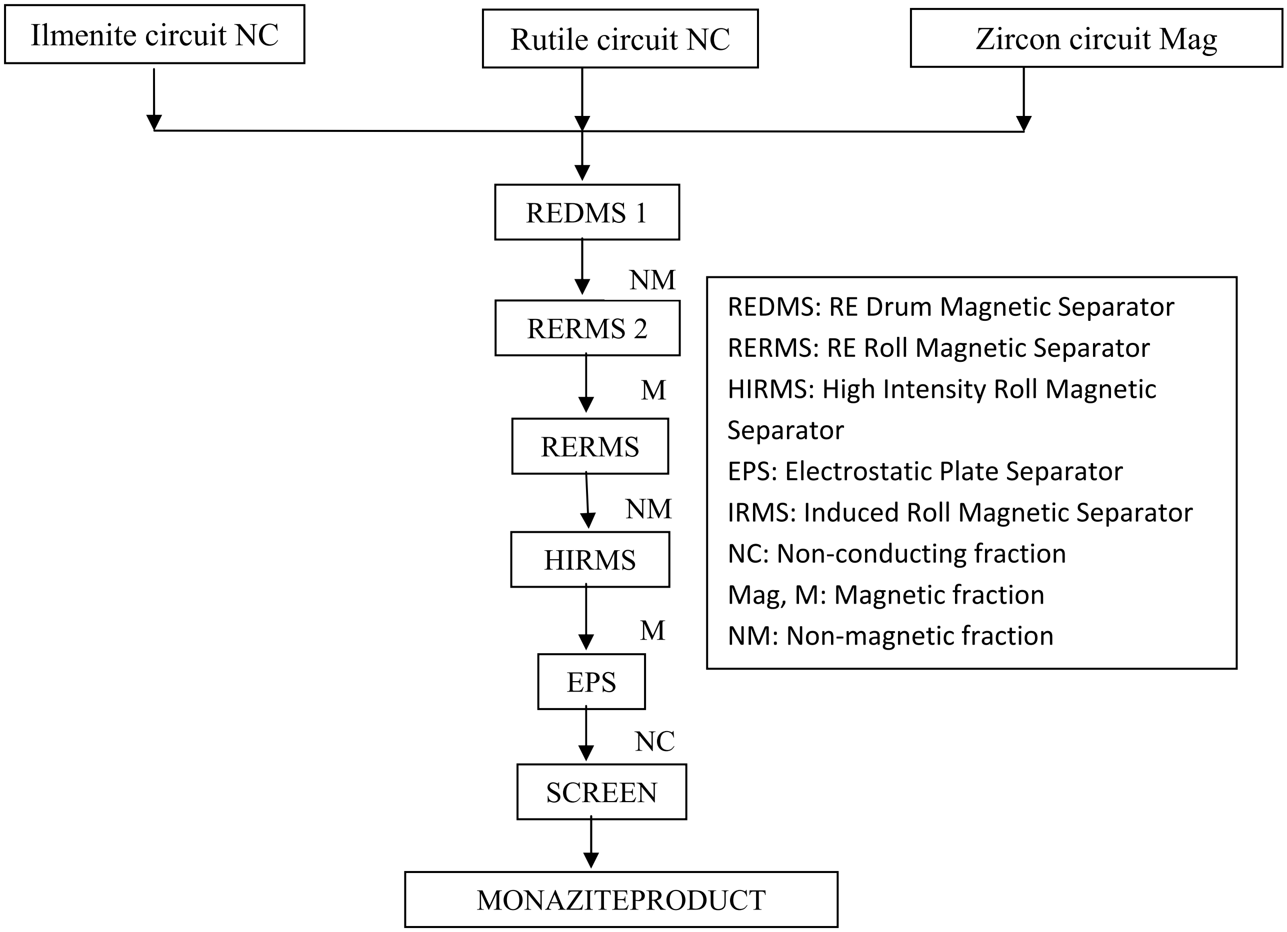

Figure 1. Monazite flow sheet using magnetic separators.

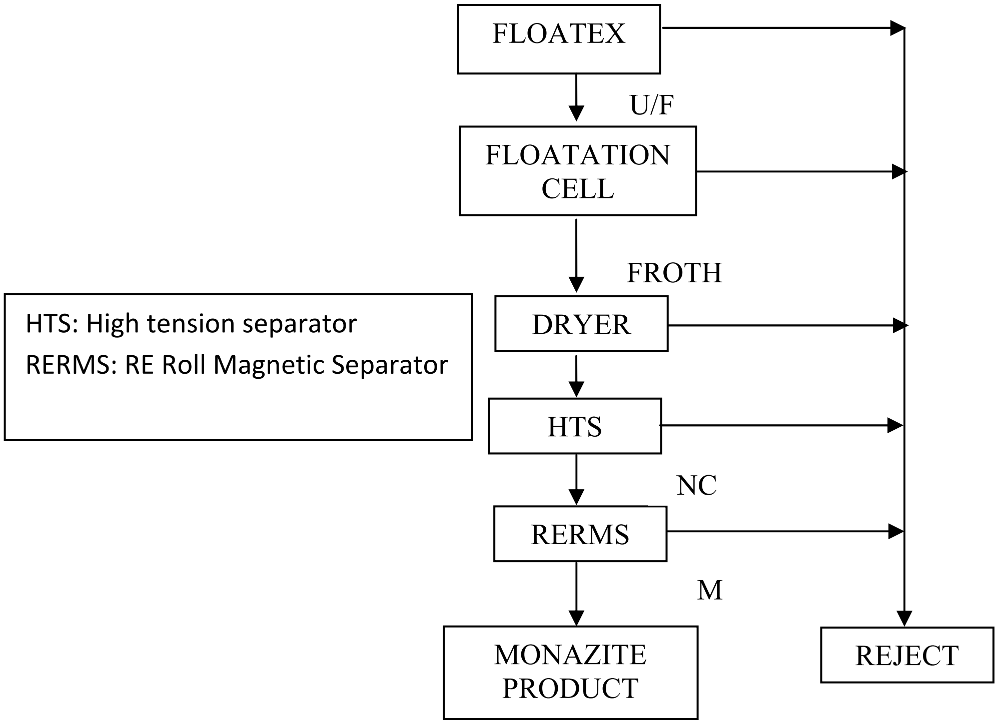

Figure 2. Monazite Flowsheet using gravity separation and froth flotation.

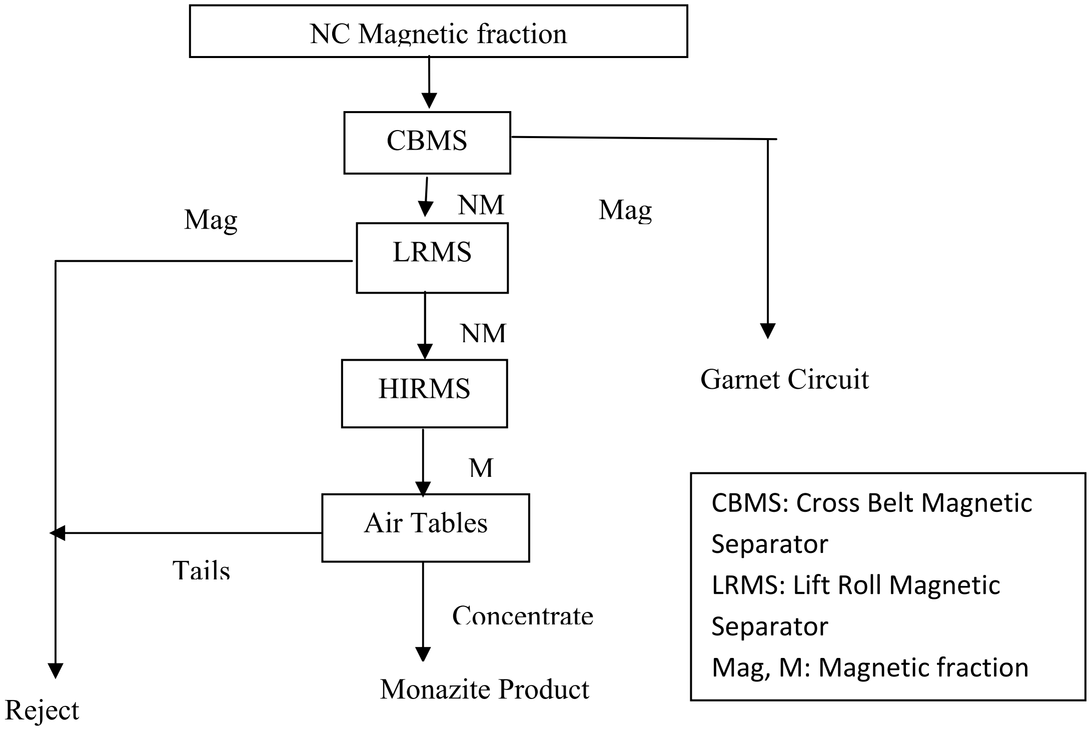

Figure 3. Monazite flowsheet using air tables.

Figure 4 gives the flowsheet for alkali cracking of monazite.

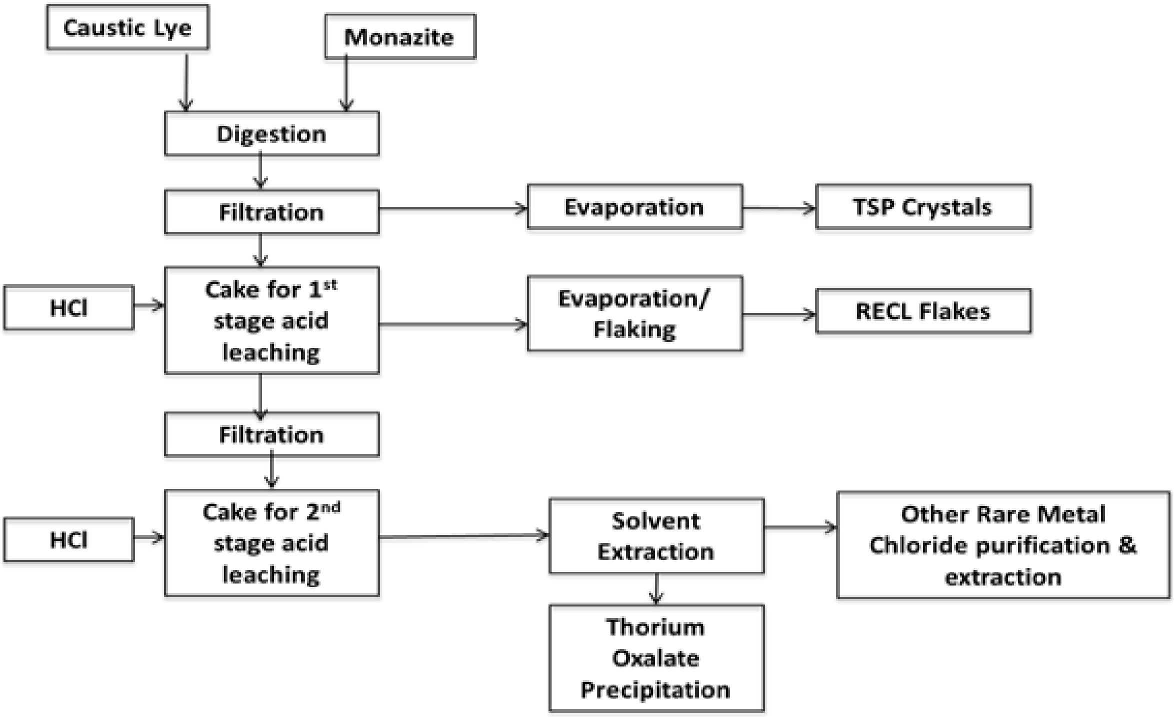

Figure 4. Alkali cracking of monazite.

The Figure 5 shows the flowsheet for separation of individual REEs.

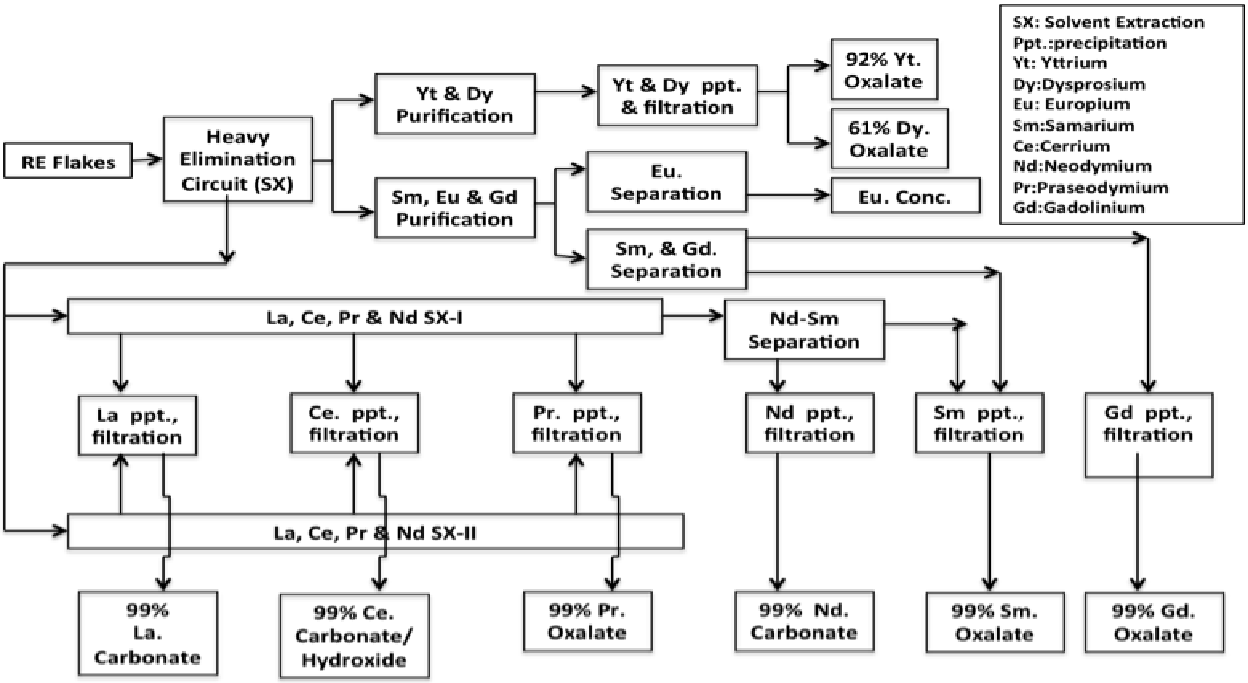

Figure 5. Solvent extraction of individual REEs.

References

1. Roskill Information Services Ltd., “Rare Earths and Yttrium: Market Outlook to 2015”, 4th edition, 2011.

2. Center for study of Science, Technology & Policy, Bangalore & Center for Techno Economic Mineral Policy options, New Delhi, “Rare Earths & Energy Critical Elements: A Roadmap & Strategy for India”, Government of India, Ministry of Mines, 2012.

A PROCESS ROUTE FOR THE SARFARTOQ RARE EARTH PROJECT, GREENLAND

*John R. Goode[1], Ben Yu[2], Niels Verbaan[2], Jim Cambon[3], Jamie Tuer[3]

[1]J.R. Goode and Associates
Suite 1010, 65 Spring Garden Avenue, Toronto, Ontario, Canada M2N 6H9
*jrgoode@sympatico.ca

[2]SGS Canada Inc.
185 Concession Street, Lakefield, Ontario, Canada K0L 2H0

[3]Hudson Resources Inc.
Suite 1460 - 1066 West Hastings St., Vancouver, British Columbia, Canada V6E 3X1

Keywords: Carbonatite Rare Earth Deposit, Flotation, Beneficiation, Hydroximic Flotation Reagent, Hydroximic Flotation Reagent, Roasting, HCl and H_2SO_4 Leaching, Acid Baking, Fluoride Metathesis

Abstract

The Sarfartoq carbonatite deposit contains indicated resources of 5.9 Mt averaging 1.8% rare earth oxides (REO) and inferred resources of 2.5 Mt averaging 1.6% REO. The Nd_2O_3 distribution in the REO is high at 19%.

The rare earth elements (REE) are contained in fine-grained monazite and bastnaesite with ankerite and siderite as gangue. Beneficiation tests included electrostatic, gravity, magnetic, roast-magnetic, and flotation separation methods. The best concentration effect was obtained by flotation with a hydroximic collector giving 73% recovery in 25% mass.
Sulphuric acid pre-leach and baking of whole ore or concentrate gave ~80% extraction of light REE (LREE) but only ~50% of medium REE. Caustic metathesis and re-leaching of concentrate residue increased extraction to +90%. HCl leaching with a pre-roast also gave +90% REE extraction. Without a pre-roast, HCl leaching gave ~40% LREE extraction but there are indications that caustic metathesis can be an alternative to pre-roasting. Fluorine appears to play a significant role in extraction.

Introduction

Hudson Resources Inc. has been active on the west coast of Greenland since 2003, first exploring for diamonds, and then defining the Sarfartoq REE carbonatite deposit. Exploration and evaluation of the White Mountain anorthosite deposit located about 50 km from Sarfartoq has recently begun.

Hudson last announced a resource for the Sarfartoq deposit in 2012 [1] and summary data are provided in Table I. Recent drilling may lead to an update to the resource figures. To assist the reader in evaluating process options, the resource data of Table I, combined with the CIBC forecast of 2015 prices for refined oxides [2], gives an in-situ metal value of $660/t with 92% of the value in the REE from La through to Eu and 38% contained in Nd alone. High recovery of the heavy REE (HREE), though welcome, is not essential to project economics.

This paper discusses the mineralogical and metallurgical testwork performed on Sarfartoq samples in the search for a viable flowsheet for the production of a marketable rare earth concentrate. Work has been done by a number of agencies including: mineralogy by Peter Le Couteur of Micron Geological Ltd (Micron), Hazen Research, Inc. (Hazen), Xstrata Process Support (XPS), and SGS Mineral Services, Lakefield Site (SGS); beneficiation testwork by Hazen, CommodasUltrasort, Saskatchewan Research Council (SRC), Eriez Magnetics (Eriez), and Met-Solve Laboratories Inc. (Met-solve); and hydrometallurgy by SRC and SGS.

Table I. Sarfartoq ST1 Zone Mineral Resource at a Cut-off Grade of 1% TREO

Category	Tonnes 000's	TREO %	La_2O_3 ppm	Ce_2O_3 ppm	Pr_2O_3 ppm	Nd_2O_3 ppm	Sm_2O_3 ppm	Eu_2O_3 ppm	Gd_2O_3 ppm	Tb_2O_3 ppm	Dy_2O_3 ppm	Y_2O_3 ppm
Indicated	5,884	1.77	3,855	8,844	1,012	3,296	321	71	181	14	34	68
Inferred	2,459	1.59	3,343	7,930	932	3,073	310	69	162	13	33	67

Notes to Table I: The resource estimate is classified as Indicated and Inferred Mineral Resources as defined by CIM and referenced in NI 43-101. Total Rare Earth Oxides (TREO) refers to the elements lanthanum through lutetium plus yttrium expressed as oxides in the form REE_2O_3.

Geology and Mineralogy

Druecker [3] reported "Hudson's properties, located in Western Greenland, consist of exposed glacially scoured crystalline basement rocks, which are predominantly granulite-facies orthogneisses intruded by diorite dykes. Cutting approximately NE/SW across the Hudson properties, lies the boundary between the approximately 3 Ga Meso-Archaean North Atlantic Craton to the south and Archaean rocks affected by the 1.9 – 1.8 Ga Palaeoproterozoic Nagssugtoqidian Orogen.

The Sarfartoq Carbonatite Complex (SCC), measuring approximately 13 km in diameter, is situated on this boundary presumably having exploited an area of structural weakness. Similarly, kimberlite bodies and associated ultramafic lamprophyres metasomatised lithospheric mantle-derived rocks occur throughout the area. These are typically Cambrian in age and range from approximately 515 to 600 Ma in age with the SCC dated at approximately 580 Ma.

The target commodities for the Sarfartoq Project are REE (primarily cerium, lanthanum, neodymium, praseodymium, and europium), specialty metals (niobium and tantalum) and diamonds. REE and specialty metals are associated with the SCC and diamonds are found within kimberlite host rock and associated diamondiferous, mafic, igneous rocks."

XPS studied [4] mineralogy using QEMSCAN and electron microprobe analysis (EMPA) and produced the data illustrated in Figures 1. QEMSCAN and various other mineralogical studies showed that the minerals are fine with average grain sizes less than 20 μm. EMPA of the individual minerals, combined with the distribution of the minerals, yielded the data in Table II.

Table II. Contribution of Different Minerals to Total REE Content, %

Monazite	Bastnaesite	Synchysite	Fe Ce Carbonate/Oxide	Mg Fe ankerite (Red)	Fe Mg ankerite (White)
68.2	22.5	6.8	0.7	1.3	0.4

The gangue minerals are dominantly acid-soluble carbonates. Using either QEMSCAN data or whole rock analysis, the expected sulphuric acid demand of the whole ore is about 0.8 t 100% H_2SO_4 per tonne of ore – with 70% due to ankerite. Clearly, a beneficiation process to separate the fine-grained monazite (especially) and bastnaesite from ankerite and siderite would greatly assist in the development of an economical acid leach process. Apatite and bastnaesite in the ore contribute to the F content of about 0.2%.

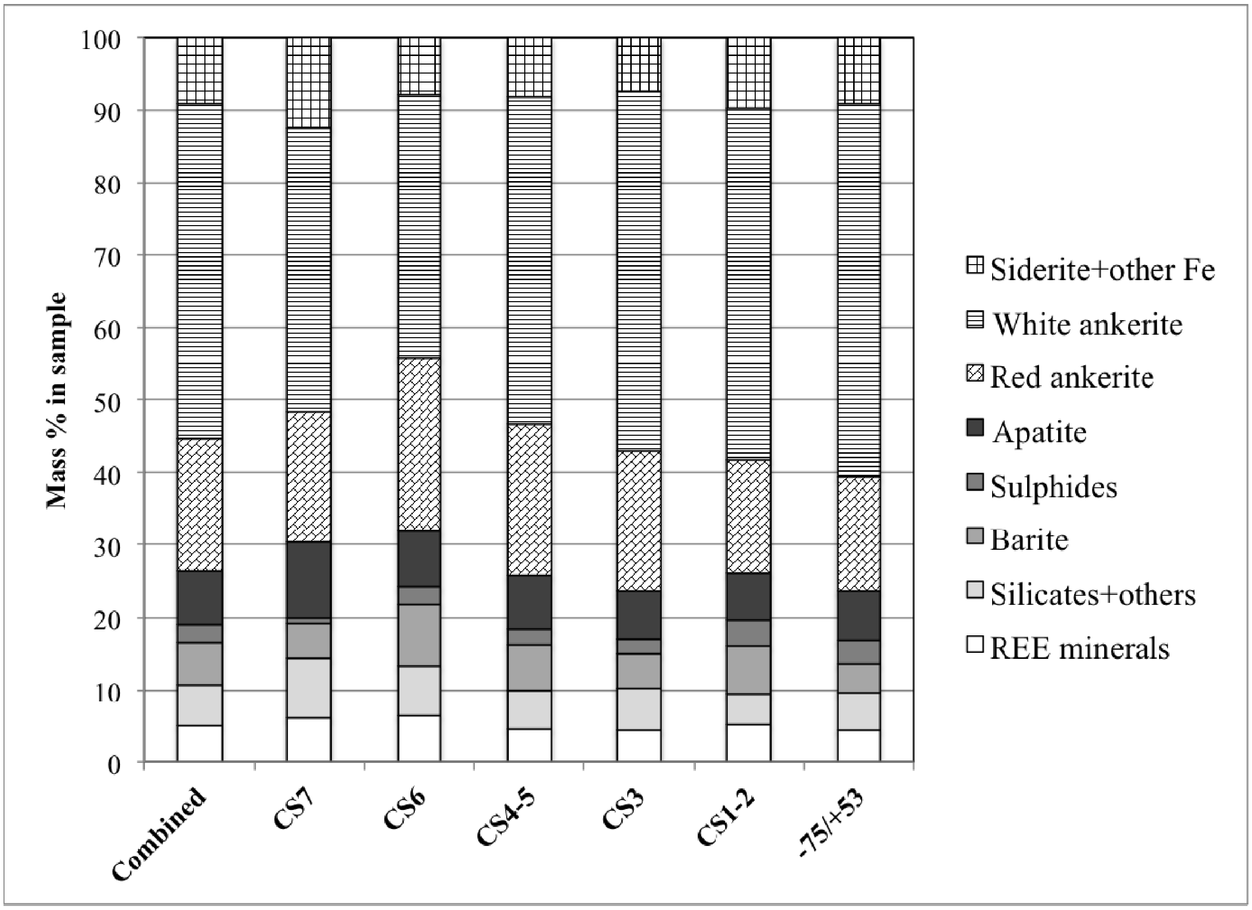

Figure 1. Distribution of minerals in sarfartoq ore.

Beneficiation

Sorting

Hazen [5] sent 50 rocks, crushed and screened to -25+6 mm and prepared from crushed drill core, to CommodasUltrasort for radiometric, photometric, and dual energy x-ray transmission sorting tests. The CommodasUltrasort report showed that the sample set was not very amenable to sorting with about 65% mass pull required to give 90% recovery of REE to the concentrate by all methods. Photometric sorting was shown to be marginally the best of the methods examined. The writer, Evelyn King and Peter Le Couteur of Micron, all very experienced ore sorters, manually sorted 17 kg of -30+12 mm rocks from a bulk sample using radiometric and photometric (visual) techniques and the numerous fractions were assayed. Analysis of the data clearly confirmed that sorting was not a practical option [6].

Electrostatic Separation

Eriez was engaged to undertake electrostatic separation tests using its High Tension Electrostatic Separator (HTES) on a sample of Sarfartoq ore ground to 80% -60 mesh [7]. Conductors amounting to about 1.3% mass were collected and visually observed to be mostly pyrite. Analysis of the several electrostatic bin products showed insignificant upgrading of the REE, U, Th, and Nb.

Magnetic Separation

Eriez also completed magnetic separation work [7]. A 6" diameter Rare Earth Roll (Lab Model 65-1) was used on the non-conductors from the electrostatic separation test. The non-magnetic fraction amounted to 8.5% of the test feed and contained just 3,800 ppm TREE while the magnetic fraction assayed 26,200 ppm TREE – but obviously not a very useful level of upgrading. Eriez applied Wet High Intensity Magnetic Separator (WHIMS – using a model L-4-20 unit) across the range of 2000 to 10000 Gauss to samples of Sarfartoq ore ground to 80% -60 mesh and one ground to 80% -200 mesh. None of the elements of interest were upgraded. Hazen and SRC also undertook magnetic separation tests with similar results.

SGS had experienced some success with other REE carbonatite projects using roasting ahead of magnetic separation. A sample of -6 mesh Sarfartoq ore was roasted for 4 h at 600 ^{0}C then ground to -150 mesh and subjected to magnetic separation. There was no exploitable upgrading of REE minerals [8].

Gravity Concentration

SRC undertook heavy liquid and shaking table separation work at 60% passing 106 µm and observed no exploitable separation [9, 10, 11]. Table separation tests by Hazen [5], SGS [8], and Met-Solve [12], as well as a high gravity test by Met-Solve at various screen sizes all yielded similarly negative results.

Froth Flotation

Hazen [5] completed a total of 45 froth flotation tests investigating ten different collector regimes, five depressant-dispersants, and four modifiers. A range of grinds, conditioning times, and pulp temperatures were investigated as was de-sliming and high-intensity conditioning (HIC). The flotation practices at MolyCorp's Mountain Pass and Lynas's Mt. Weld mine were followed in certain tests.

Six of the Hazen tests achieved a level of REE recovery exceeding 1.5 times the mass pull. Two of these tests used Sylfat FA-1 fatty acid as a collector and four tests used Cytec Aero 6493 alkyl hydroxamate. Sodium lignin sulphonate and NaF or Na_2SiF_6 were used as carbonate depressants.

SRC [9, 10, 11] also completed several flotation tests using various reagents including Chinese hydroximates. The results showed that salicyl hydroximic acid, with a tall oil in one test, was reasonably effective. SRC also performed one flotation test with a modified hydroximate (T-610) after roasting the ore at 650 ^{0}C for 3 h that gave 53% recovery into 24% mass.

SGS [8] completed a total of 54 flotation tests exploring the effects of collector type and dosage, grind fineness, secondary collector type and dosage, activator type and dosage, depressant type and dosage, pulp pH and temperature, and cleaning. The best rougher flotation results achieved 73% REE recovery in 25% mass. Cleaning resulted in further upgrading but at the cost of REE recovery.

Flotation testwork were performed using several batches of crushed material representative of the Sarfartoq deposit. Head assays are shown in Table III.

Table III. Flotation Feed Chemical Head Analyses

Analyte	Master Comp	Master Comp 2	Master Comp 3	Master Comp 4	Analyte	Master Comp	Master Comp 2	Master Comp 3	Master Comp 4
	Multi-Element ICP Scan, g/t					WRA, %			
La	3,670	4,120	3,530	3,870	SiO2	1.8	2.57	1.91	1.8
Ce	9,570	10,300	9,410	10,300	Al2O3	0.4	0.62	0.44	0.43
Pr	1,330	1,180	976	1,150	Fe2O3	17.1	15.4	17.9	17
Nd	3,510	3,830	3,690	4,060	MgO	8.68	8.58	8.71	8.76
Sm	355	341	292	334	CaO	24.4	26	23.4	24.4
Eu	72.8	68.7	57.3	51.4	Na2O	0.19	0.16	0.18	0.2
Gd	137	133	112	132	K2O	0.2	0.4	0.13	0.17
Tb	13.5	11.1	9.5	12.3	TiO2	< 0.01	< 0.01	< 0.01	< 0.01
Dy	38	34.2	30	40.9	P2O5	3.11	2.08	3.23	3.45
Ho	3.9	3.4	2.4	4.9	MnO	1.48	1.39	1.58	1.55
Y	43	42	40	89	Cr2O3	< 0.01	0.09	0.02	< 0.01
Er	5.5	5	3.3	9.6	V2O5	< 0.01	< 0.01	< 0.01	< 0.01
Tm	0.5	0.4	< 0.3	1	LOI	29.6	31.9	30.8	30.6
Yb	1.4	2.3	1.1	4.9	Analyte	Leco, %			
Lu	0.6	0.5	< 0.5	0.7	S	2.38	2.13	-	-
Th	693	604	553	597	S^{2-}	2.06	1.72	-	-
U	15.6	11.6	13.5	13.7					

<u>Effect of Collector Type and Dosage:</u> Several collector types, including alkyl hydroxamates produced by Cytec Industries Inc. and Axis House and a sodium alkyl hydroximic acid from

China were evaluated and compared against ring type hydroximic acids, as shown in Figure 2. The ring type hydroximic acids included salicycl hydroximic acid (SHD), T610 (a derivative of SHD), benzoyl hydroximic acid, and LF-P81. These were obtained from China where they are used for the flotation of REE, W, Sn and other minerals. The most selective collectors were T610 and SHD acid while the majority of the alkyl hydroxamates and alkyl hydroximic acids were not selective.

Effect of Grind Fineness: Grind fineness from 80% passing 80 µm to 32 µm were evaluated using SHD as the collector. As shown in Figure 3, decreasing grind size resulted in reduced selectivity but increased the overall mass and REE recoveries. The finer grind size is required to achieve greater than 60% REE recoveries.

Effect of Secondary Collectors, Activators and Depressants: The addition of a secondary collector, such as oleic acid or LF-P81, was evaluated. The addition of oleic acid to SHD reduced selectivity and increased both mass and REE recoveries. At excessive dosage, the secondary collector, can reduce the selectivity provided by the primary collector.

Activators, including tri-n-butyl phosphate (TBP) and 2-ethylhexyl 2-ethylhexyl phosphate (P507), both solvent extraction reagents, were tested with SHD as the collector. Both activators reduced selectivity.

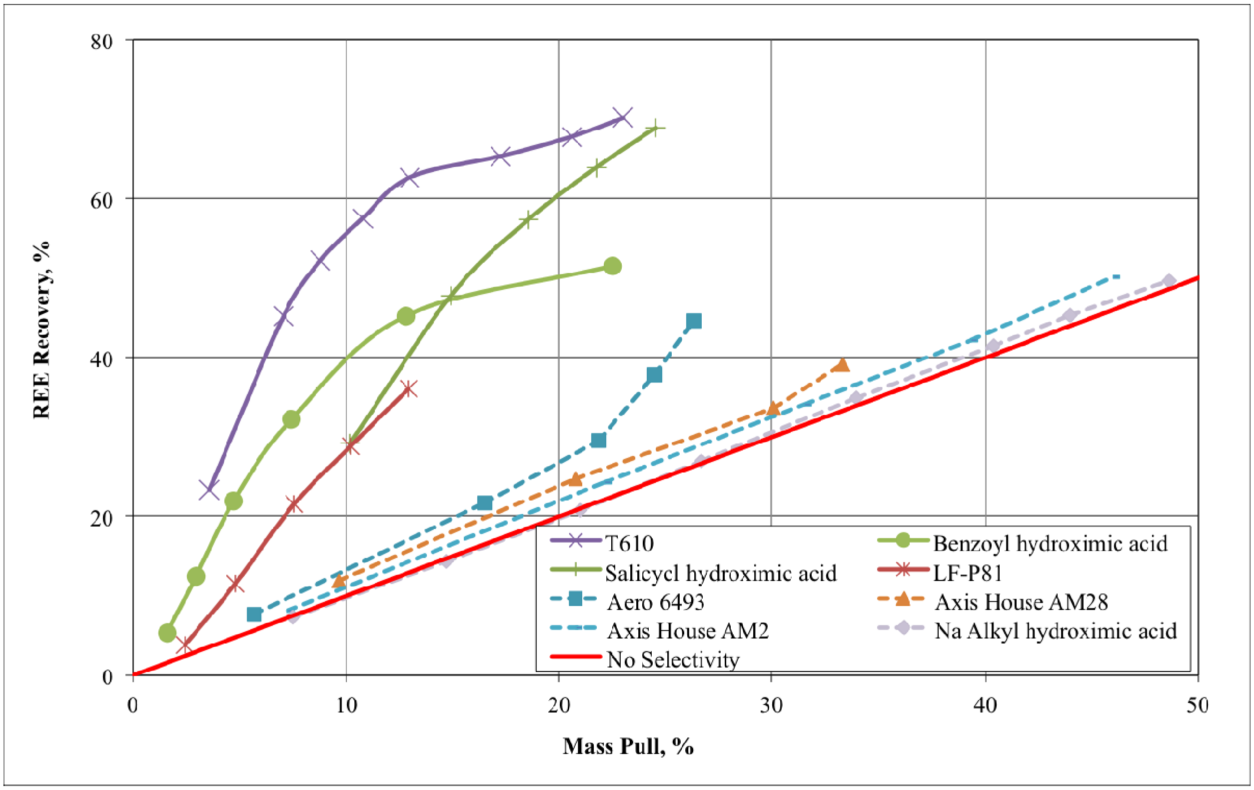

Figure 2. Effect of collector type on flotation recovery.

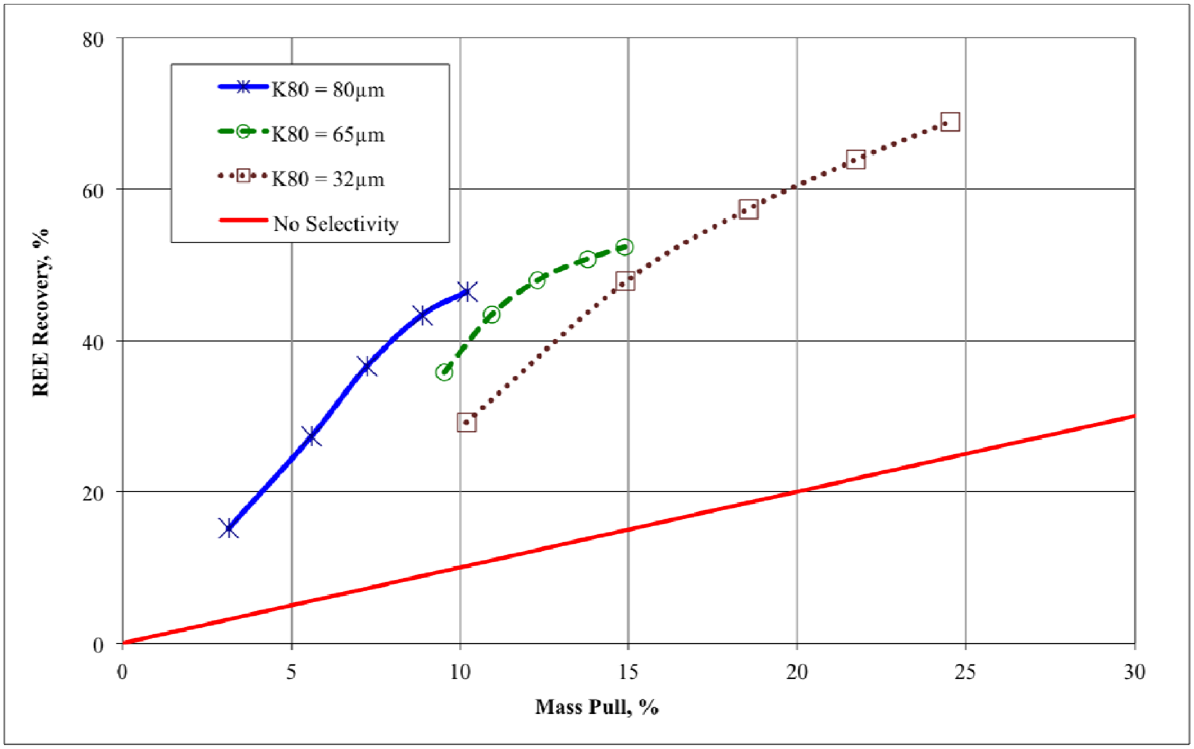

Figure 3. Effect of grind fineness on flotation recovery.

Causticized cornstarch and guar gum were evaluated as depressants. Both were detrimental to REE flotation since both REE and gangue minerals were depressed.

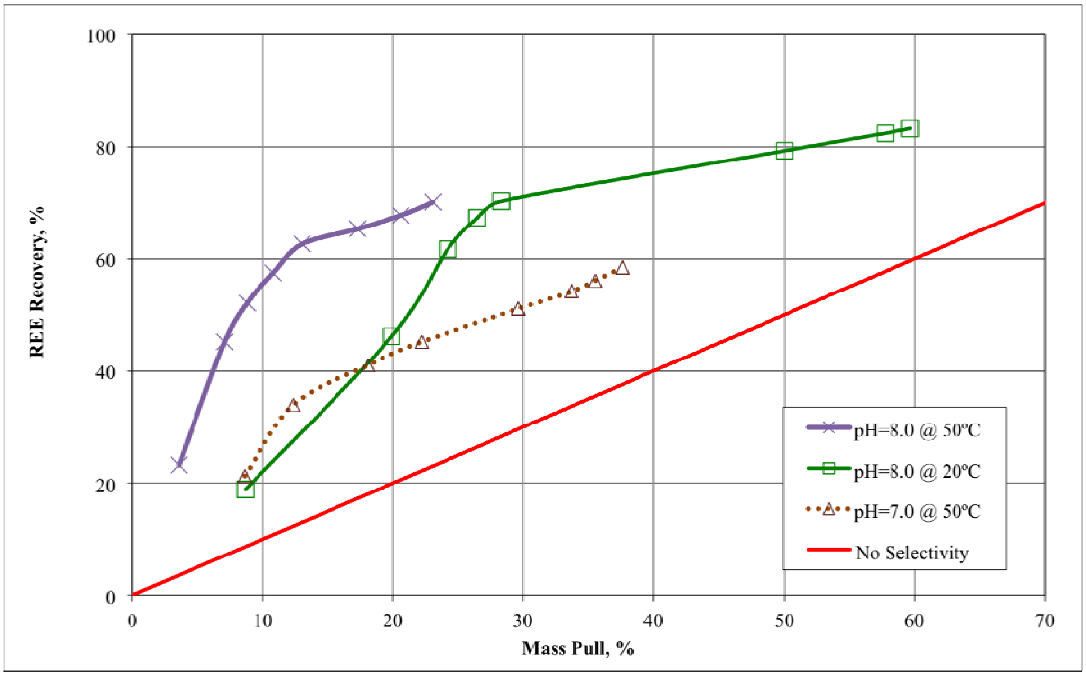

Figure 4. Effect of pulp pH and temperature on flotation recovery.

Effect of Pulp pH and Temperature: As indicated in Figure 4, preferred REE flotation and selectivity is found at a pH of 8 and elevated temperature when using SHD as the collector.

Other Parameters Investigated: Several other factors were tested including the effect of high intensity conditioning, separate treatment of sands and slimes, oil agglomeration, and saponification of the acidic collectors. None of these procedures offered an advantage. However, emulsification of SHD with diesel (95:5) was found to be beneficial.

Rougher Concentrate Cleaning: Limited cleaning work gave disappointing results. Further work is required.

Interim Conclusions on Beneficiation

Beneficiation work will likely continue. In the interim, it is concluded that flotation using hydroximic collectors is the preferred method of upgrading the Sarfartoq ore. The optimum conditions include a grind of 80% passing 32 µm, the use of Silicate N as a depressant, and T610 or emulsified SHD as a collector at doses of about 4 kg/t with elevated conditioning and flotation temperatures. Under these conditions 73% REE recovery into 25% mass of concentrate can be achieved. It is expected that improved grade-recovery parameters can be achieved through further testwork.

Hydrometallurgy

Whole Ore Sulphuric Acid Pre-leach and Bake

Whole ore sulphuric leach tests were done by SRC [9, 11] and SGS [13]. Earlier tests showed that a simple sulphuric acid leach gave low extraction of the REE but whole ore sulphuric acid pre-leaching was a useful procedure ahead of acid baking.

In test PL-6, SGS pre-leached an ore ground to -400 mesh at pH 1.8 with the consumption of 716 kg/t of sulphuric acid and low REE dissolution (2-5% LREE, 5-20% HREE). The pre-leach residue was divided into two parts and acid baked at 200^0 C for 2h with sulphuric acid additions of 900 and 1200 kg/t (AB-13 and 14) followed by water leaching for 4 h at 90^0 C.

Acid bake water leach test results, plotted in Figure 5, show that the higher acid addition led to higher HREE extraction, but lower LREE extraction. Excess acid in the water leach solutions amounted to 628 and 959 kg/t respectively suggesting that a balance between pre-leach acid demand and excess acid from the acid bake would be reached with an acid addition of about 1000 kg/t as part of the bake process.

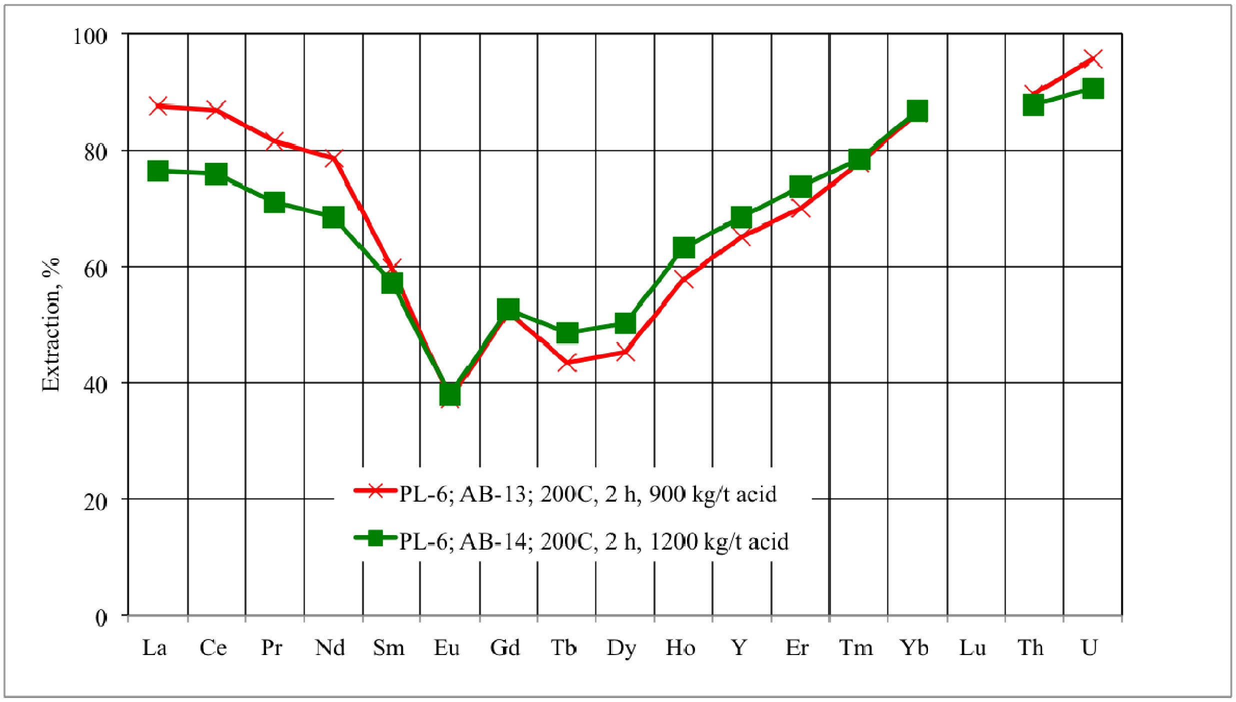

Figure 5. Results of whole ore pre-leach and acid bake.

The very high extraction of the REE at both ends of the series, but depressed extraction of the medium mass REE, coupled with the observation that most of the REE are in a single mineral, monazite, suggests that the minerals are adequately "cracked" but precipitation of certain REE is occurring. This is further discussed below.

Leaching of Flotation Concentrate

SGS performed a series of about 22 agitated leach tests and 15 acid bake tests on various samples of flotation concentrate produced at SGS. Composite rougher concentrate compositions are included in Table IV, showing a TREE grade ranging from 6.2 to 8.2% predominantly LREE, with just 1.3% as HREE – mainly Gd, Dy and Y. The agitated leach work consisted of sulphuric acid and hydrochloric acid leaching and was preceded in several tests by roasting to decompose the fluorides and carbonate minerals. Acid bake tests were also investigated.

HCl Leaching of Concentrate: The data, presented in Figure 5, shows the effect of roasting and roasting temperature on the extraction of REE from concentrate during HCl leaching at 10% solids at 50ºC for 6h. It is evident that roasting significantly increases the extraction of REE and especially LREE. The effect of roasting temperature is also clear with LREE extraction increasing from ~75% at 750^0 C to ~95% at 850^0 C. The effect of roasting and roasting temperature is not as great on HREE extraction as it is on LREE extraction.

The beneficial effect of roasting could be due to the removal of fluorine, present in bastnaesite, which otherwise could combine with REE to form insoluble fluorides. Molycorp encountered this issue when it leached bastnaesite concentrate with HCl at its plant in York, Pennsylvania

[14]. Molycorp solved the problem by doing a caustic metathesis on the HCl leach residue. This converted REE fluorides in the residue to hydroxides that were then dissolved by contacting the treated residue with part of the original acidic leach solution.

Table IV. Flotation Concentrate Used in Leach Tests

Head assays, g/t				Head assays, %			
Analyte	Conc 1	Conc 2	Conc 3	Analyte	Conc 1	Conc 2	Conc 3
La	16,000	9,770	11,900	Si	0.65	0.75	0.72
Ce	43,000	25,200	32,000	Fe	10.5	12.2	14.8
Pr	4,730	3,100	3,900	Mg	4.0	4.4	4.28
Nd	16,100	9,840	12,800	Ca	17.2	16.9	14.7
Sm	1,280	847	1,000	P	3.03	2.63	2.69
Eu	245	154	190	Ba	1.97	2.35	1.88
Gd	529	294	343	CO3	38.2	39.4	37.6
Tb	43	24	31	F	0.3 to 0.6%		
Dy	117	75	85				
Ho	9	6	8				
Y	132	83	94				
Er	11	8	10				
Tm	0.7	0.5	0.7				
Yb	2.7	1.9	2.9				
Lu	0.7	0.5	1.3				
TREE	82,200	49,404	62,366				
Th	1,940	1,320	1,550				
U	24	20	24				

Initial tests of this approach on HCl leach residue indicate increased overall extraction and further tests are planned. As described below, caustic metathesis was effective on Sarfartoq sulphuric acid bake residues. Metathesis of the HCl residue could be more economical than the pre-roast approach. Another approach under study is a direct HCl leach followed by roasting the leach residue which has relatively small mass and could be a less costly and complex process than roasting the entire concentrate (or ore) mass.

The scoping level HCl leach tests were generally carried out at low pulp densities (10% solids) to avoid solubility limitations. However test AL14 was carried out at 40% solids to see if there was any negative impact on extraction. None was observed and the pregnant solution assayed 16 g/L TREE (3.2 g/L Nd) with main impurities being 33 g/L Fe, 12 g/L Mg and 45 g/L Ca.

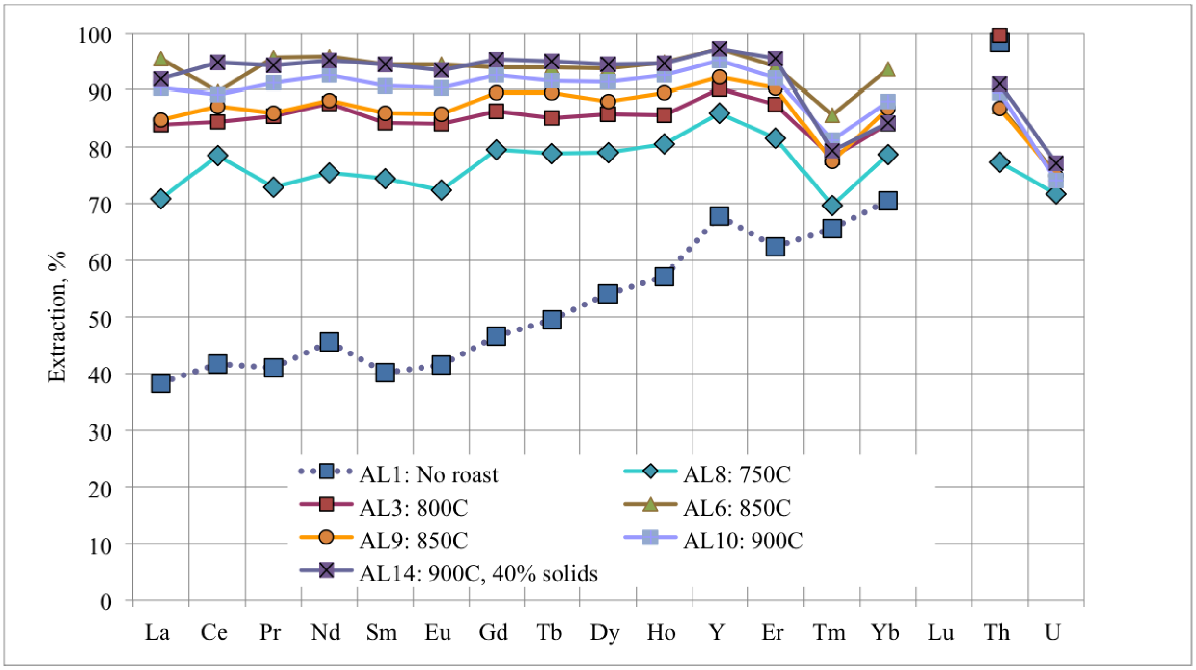

Figure 6. Effect of roast and roasting temperature with 100 g/L HCl leach.

The effect of leach liquor acidity is shown in Figure 7 that shows increasing extraction with higher HCl strengths. At lower acidities (50, 75 g/L HCl) the extraction of Ce is reduced which might be due to the formation of low-solubility CeO_2 during the roast process.

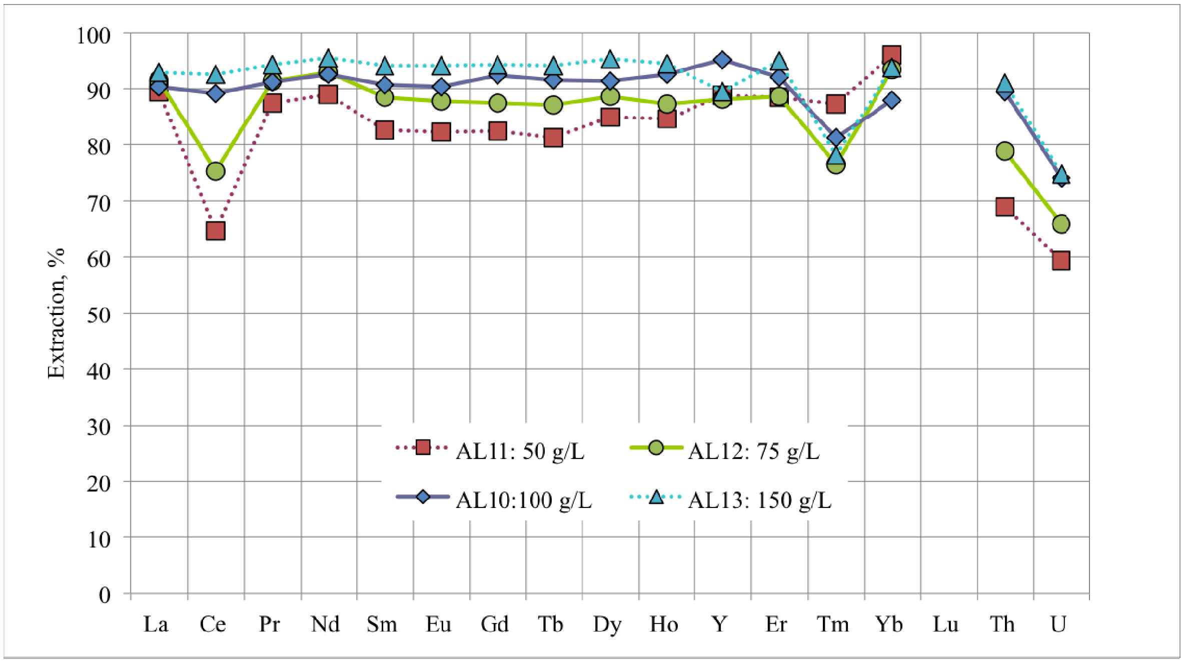

Figure 7. Effect of HCl acidity after 900^0 C roast.

Acid consumption under optimum roast–HCl leach conditions (900^0 C roast, 100 g/L HCl, 40% solids) was 920 kg/t of 100% HCl of which about 6% is related to REE dissolution. The main acid consumers (89%) were the ankerite and siderite in the concentrate, which were completely destroyed. Better rejection of these minerals during flotation would reduce acid demand but HCl regeneration would obviously be needed to make the project economic.

H_2SO_4 Leaching of Concentrate: SGS investigated agitated sulphuric acid leaching of concentrate in 48 h long tests using 50 and 75 g/L free acid and temperatures of 75 and 95^0 C. REE dissolution was poor at less than 30% for the LREE rising to 60% for the HREE. These data are similar to those observed for whole ore leaching. Agitated sulphuric acid leaching is only of interest as a pre-leach ahead of acid baking.

H_2SO_4 Acid Bake of Concentrate: Sulphuric acid bake tests were carried out at various bake temperatures and acid dosages as shown in Figure 8. Whereas all tests gave high extraction of La, Ce, Pr and to a lesser extent Nd, the extraction of Sm-Lu was somewhat depressed for tests AB2 and AB6 but markedly reduced for the other four tests. In test AB2 the ore was roasted at 800^0 C before acid baking. In test AB6, the concentrate was pre-leached before baking.

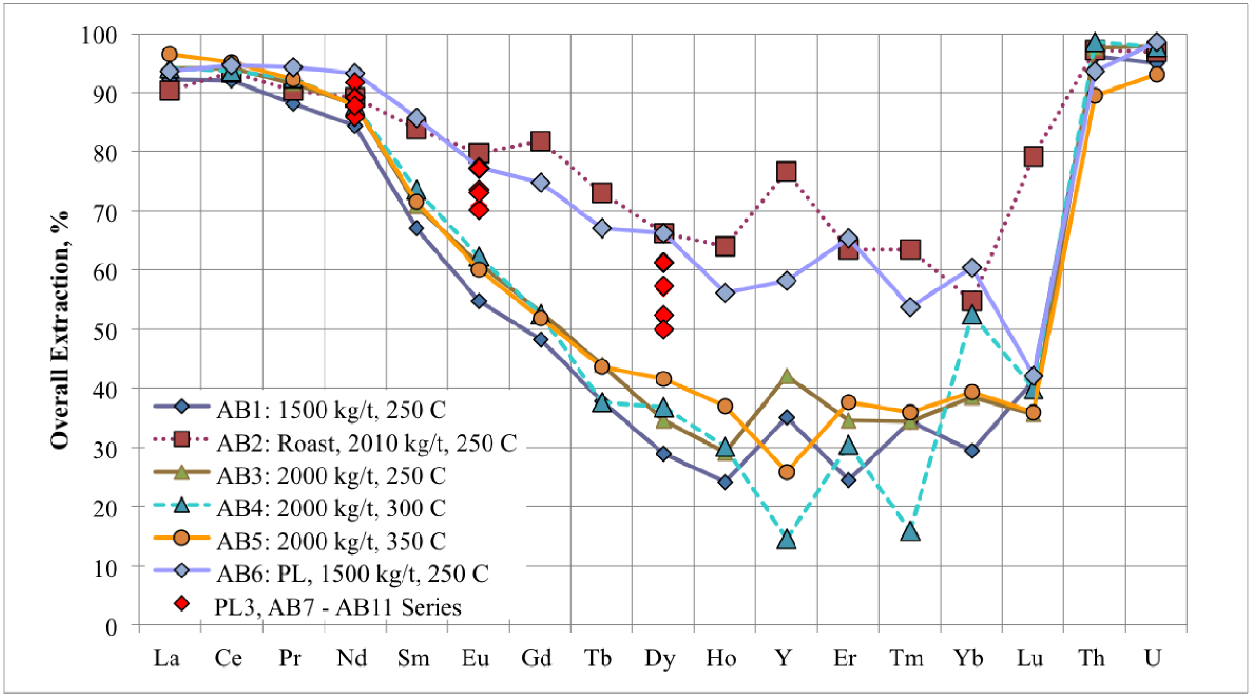

Figure 8. Sulphuric acid baking of flotation concentrate.

The results for the pre-leach and bake procedure of test AB6 were encouraging since extractions were reasonably high, the pre-leach would reduce overall demand for acid and neutralizing reagent, and pre-leaching would be more economical than an 800^0 C pre-roast. SGS performed a series of acid bake tests on a bulk pre-leached concentrate in an attempt to optimize the system. Pre-leach test PL3 was done to a pH of 1.8 and consumed 600 kg/t of sulphuric acid. The pre-leach residue was divided into five charges that were variously baked at 220, 250, and 300^0 C, 2 and 4 h, and with acid additions of 1200 and 1500 kg/t (AB7 to 11 series). The water leach solutions were only assayed for Nd, Eu, and Dy.

A statistical analysis of the results of the five acid bake tests performed on PL3 residue showed poor correlations between REE extraction and the temperature, time and acid dose used in the acid bake. A weak trend in the data indicated improved REE extraction with lower acid bake temperatures – possibly due to reduced acid losses through volatilization.

The high LREE extractions in all acid bake tests suggest that the monazite and bastnaesite were totally decomposed. Therefore high extraction of all REE would be expected. The modest extraction of the HREE in the pre-roast and pre-leach tests, and the very low extraction in the other tests is likely explained by the formation of insoluble REE fluorides during the roast or in the subsequent water leach – somewhat akin to what we believe to take place in the HCl leach system.

The fluoride formation hypothesis was tested by contacting a blended sulphuric acid bake residue with 25% NaOH solution for 4 h at 50^0 C followed by a 1 h long 5% HCl leach. Cumulative extraction values for all REE following this procedure, and procedures using 10% NaOH and 10% sodium carbonate solution were also effective. Less aggressive metathesis conditions, using lime slurry, were not as successful. Results are presented in Figure 9.

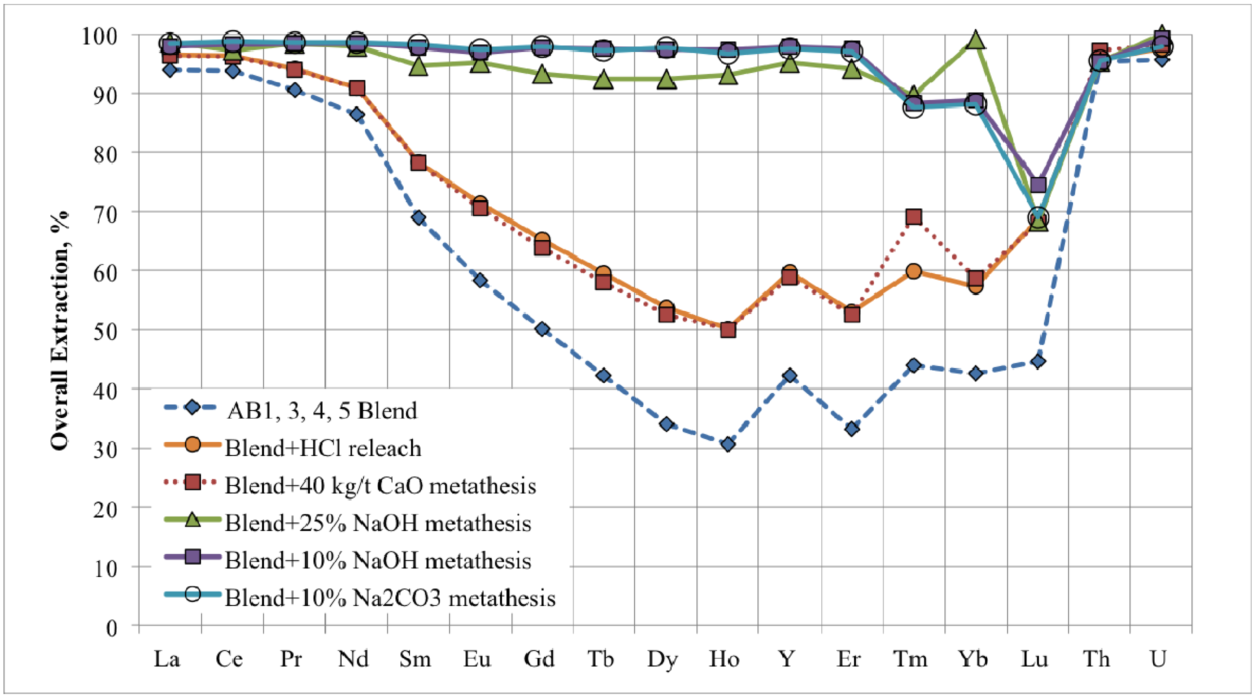

Figure 9. Results of metathesis and re-leach of sulphuric acid bake residue.

Conclusions

Sarfartoq ore is fine-grained and complex and beneficiation has proven to be difficult with 73% REE recovery into 25% mass being the best upgrading effect obtained to date. This was achieved using Chinese hydroximic collectors at elevated temperature. It is believed that further testwork could improve upon these results.

As expected, simple sulphuric acid leaching of whole ore or concentrate is ineffective at cracking the monazite and bastnaesite minerals but is useful as a pre-leach ahead of acid baking since it reduces overall acid and base consumption. Sulphuric acid baking of pre-leached whole ore gives better than 70% extraction of all REE except those between Sm and Y inclusively. A sulphuric acid bake of pre-leached or roasted concentrate gave a somewhat similar response with very high extraction of the LREE but poor extraction for the REE between Sm and Lu. Caustic metathesis of acid bake residue was effective at giving very high REE extraction strongly suggesting that fluoride formation during the bake or subsequent water wash is responsible for the poor extraction.

A simple HCl leach of concentrate gives poor LREE extraction (~40%) and modest extraction of the HREE (70% for Yb). Roasting the concentrate at progressively higher temperatures (between 800^0 C and 900^0 C) increases the extraction to about 95% for all REE. It is surmised that the positive effect of roasting is largely because it negates the adverse effect of fluoride. Initial tests of a metathesis step applied to an HCl residue, similar to that tested on acid bake residue, suggests that this could be a viable alternative to a high temperature pre-roast. A roast of the HCl leach residue could also offer an effective process route.

Acknowledgements

Many dedicated people contributed to this project. Lori Kormos of XPS, and Nicole Morton and Tassos Grammatikopoulos of SGS undertook the mineralogical work; staff at SRC, Hazen, Met-Solve and Eriez, and Hector Sarne and Dan Lang at SGS completed beneficiation work; staff at SRC, and Mike Johnson, Adam Lamey, and Victoria VanderByl of SGS undertook the hydrometallurgical testwork. Their efforts are appreciated and acknowledged.

We thank company management for their agreement to the release of data.

References

1. Hudson Resources Inc. (2012). “Press Release NR2012-02, Hudson Resources reports updated mineral resource: Significant grade increases and indicated resources confirmed”, April 26, 2012. Retrieved from http://www.hudsonresources.ca/files/NR2012-02.pdf

2. CIBC World Markets Inc., “Once ignored on the periodic table, don’t ignore them now. A rare earth industry overview” March 06, 2011.

3. Druecker, M., “Technical report on the Sarfartoq project, West Greenland” April 26, 2012. Retrieved from http://www.hudsonresources.ca/files/Hudson_43-101_30May12.pdf

4. Xstrata Process Support, “Mineralogical Analysis of Three Polished Thin Sections and One Sized Sample Sarfartoq Carbonatite Complex” 13 June, 2012.

5. Hazen Research, Inc., “Laboratory investigation to recover rare earth minerals from Sarfartoq carbonatite, Kangerlussuaq, Greenland” May 17, 2012.

6. J.R. Goode and Associates, “Sarfartoq Rare Earth Project; Radiometric and photometric sorting tests at SRC”, 2011-08-01

7. Eriez Magnetics, “Uranium, thorium & rare earth ore from Hudson Resources MTR #12-044” February 20, 2012.

8. Yu, B., and Dan Imeson, “An Investigation into Scoping Level Beneficiation Testwork on REE Carbonatite Samples from the Sarfartoq Deposit, prepared for Hudson Resources Inc., Project 13594-001 Final Report”, June 18, 2013.

9. SRC, “Draft Metallurgical Test Report. Sarfartoq REE Project – ST1 Zone rare earth processing”, SRC Publication No. 13019-22C11, September 2011.

10. SRC, “Collector screening summary”, SRC Project 13181, 6-Feb-2012.

11. SRC, “HL Separation, Acid-baking + Leaching, Roasting + Flotation”, SRC Project 13181, 15-May-2012.

12. Met-solve Laboratories, Inc., “Gravity recovery of REE on Hudson Sarfartoq deposit. Project MS1395”, May 24, 2012.

13. SGS hydrometallurgical report in preparation.

14. Higbie, Kenneth B. and Ralph C. Kirby, “Review of Metallurgical Technology”, *Bureau of Mines Minerals Yearbook, Metals and Minerals (except fuels) 1965, Volume I (1966)*, 35-46

BASIC RESEARCH ON THE WEATHERED CRUST ELUTION-DEPOSITED RARE EARTH ORES

Ruan Chi [1], Jun Tian [2, 3], Xianping Luo [2], Zhigao Xu [1], Zhengyan He [4]

[1] School of Chemical Engineering & Pharmacy,
Wuhan Institute of Technology, Wuhan 430073, China;

[2] School of Resources and Environmental Engineering,
Jiangxi University of Science and Technology, Ganzhou 341000, China;

[3] Institute of Applied Chemistry,
Jiangxi Academy of Sciences, Nanchang 330029, China;

[4] School of Minerals Processing and Bioengineering,
Central South University, Changsha, 410083, China

Keywords: Weathered Crust, Mineral Deposit Geology, Rare Earth Partitioning, Leaching Technology

Abstract

The basic research was reviewed about the weathered crust elution-deposited rare earth ore for over forty years, including the metallogeny of the deposit, the chemical properties of rare earth ore and the existing states of rare earth elements. Great attentions were also paid to the characteristics of the rare earth element partitioning and the four major effects in the weathered crust elution-deposited rare earth ore. The leaching mechanisms were investigated and the three generation leaching technologies of the weathered crust rare earth ore were also reviewed. The fundamental research, the development of the leaching technology and the problems which should be resolved urgently in the weathered crust elution-deposited rare earth ore were pointed out.

Introduction

Australian scientist H.W. Nesbitt demonstrated in 1979 that fractionation, migration and enrichment would happen on RE elements of granite when it weathering into clay minerals, and he also implied the possibility of mineral formation [1]. However, it was in 1969 that the weathered rare earth in the clay minerals of Jiangxi province of China were found to be industrially exploitable, which laid the foundation of the theory of weathering enrichment into rare earth minerals. This mineral is a novel exogenous ore, and has been called “weathered crust elution-deposited rare earth ore”. There are many advantages for the ore which has a widespread distribution, rich reserves, low radioactivity, complete RE partitioning and is rich in middle and heavy rare earth [2]. Importantly, the unique middle and heavy rare earth resource in southern China, including Jiangxi, Fujian, Hunan, Guangdong, Guangxi, Yunnan and Zhejiang, contributes over 80% to the world’s known resources. The discovery of the weathered crust elution-deposited rare earth ore not only enriched the theories of geochemistry, inorganic chemistry and hydrometallurgy on rare earth, but also created advantaged resource condition for the rare earth industry.

Since weathered crust elution-deposited rare earth ore deposits were discovered more than forty years ago, basic research on the metallogeny mechanism, RE partitioning, extracting theories and leaching technologies have been studied continuously. This paper summarizes fundamental research on weathered crust elution-deposited rare earth ore.

Characteristics of Weathered Crust Elution-deposited Rare Earth Ores

Metallogeny

The formation conditions of weathered crust elution-deposited rare earth ore is very complex, with the main conditions including: (1) Original rocks must contain RE minerals; (2) The rare earth must be occurred in RE minerals and RE accessory minerals which can be easily weathered, and satisfies the internal condition of forming RE ions after the RE minerals have been weathered; (3) Original rocks must be in a warm and humid climate that satisfies the external condition of the original rocks being weathered. Additionally, geological conditions of metallogeny on the weathered crust elution-deposited rare earth ore are also controlled by original rock condition, rock configuration and supergene effects [3, 4].

Chemical Properties

Physicochemical characteristics of weathered crust elution-deposited rare earth ore can be classified in four ways [5]: (1) Water content of ores. Weathered crust elution-deposited rare earth ores are loose and random solids, containing various water forms including planar, interlayered and structural; (2) Stability of absorbing rare earth ions. Rare earth ions absorbed on the clay minerals can be chemically stable and cannot be hydrolysed or dissolved; (3) Buffering of raw ore. Due to the special structures of broken bond existed on the raw ore, raw ores could accept hydrogen ion when met with acid, and liberate hydrogen ion when met with alkali. Therefore, the ore has certain buffer ability in a certain pH range, making pH of rare earth mother liquid stabilized in a certain range; (4) Exchangeability of ions adsorbed. When electrolyte solution is added into the raw ore, rare earth ions and some impurity ions adsorbed on active centers of clay minerals will be exchanged by the cations in electrolyte solution and enter into the solution. It is the theory foundation of rare earth extraction from the weathered crust-elution rare earth ores.

Existing States of RE Elements

RE elements in weathered crust elution-deposited rare earth ores mainly exist in the following four states [6]: (1) Water soluble state. In this state, hydroxyl or hydroxyl aqueous rare earth ions have been leached by water but have not yet been adsorbed; (2) Ion-exchangeable state. In this form, the rare earth is adsorbed on clay minerals as aqueous or hydroxyl ions; (3) Colloid sediment state. This refers to compounds that have been deposited on the mineral as an insoluble oxide or hydroxide colloid, or a new compound combined with some kind of oxide compound; (4) Mineral state. This refers to the rare earth form where the rare earth ion becomes part of a mineral crystal lattice.

Four Major Effects of Ion Phase RE Partitioning

Ce Loss Effect

As known from the full phase RE partitioning, the partitioning value of No. 58 element cerium is lower than No.57 element lanthanum and No.59 element praseodymium. This phenomenon violates the Oddo-Harkins rules of element geochemistry. This is called the Ce loss effect [7]. Due to the special electronic structure ($4f^1 5d^1 s^2$), Ce (Ⅲ) is easily oxidized to Ce (IV) and then forms cerianite which could relatively decrease the content of Ce. Additionally, Ce(IV) can form a stable soluble complex with HCO_3^- which would be taken away by groundwater. The two aspects lead to the Ce loss effect and the second one may be the main reason.

Rich Eu Effect

In comparing the RE elements in the leach products of the weathered crust ore and the weathered crust RE ore with the RE elements in chondrites, the geological partitioning value of europium can be obviously increased. It shows that the europium can be enriched in the weathering process of the original rock. This is called the rich europium effect [8].

Fractionation Effect

The clay minerals in the orebody are adsorbed and desorbed, and exchange continuously, leading to the different RE partitioning at different depths. Eventually, the light RE are enriched in the upper layers and the heavy RE are enriched in the lower layers. This is called the Fractionation effect [9].

Gd Broken Effect

As seen from Table I both positive and negative values of the correlation coefficient appear at the Gd element, showing the existence of an obvious Gd break effect. This is extremely similar to the electronic structure, the spectrum phase and the color change of the RE ions, which illustrates that Gd is the boundary where RE elements are divided into light and heavy groups. The elements La-Eu before Gd belong to the light RE group, while the elements Gd-Lu, Y after Gd, including Gd belong to the heavy RE group. This phenomenon is called the Gd broken effect [10].

Table I. Pearson Correlated Coefficients Matrix Among 15 Kinds Rare Earth Partitioning

	La	Ce	Pr	Nd	Sm	Eu	Gd	Tb	Dy	Ho	Er	Tm	Yb	Lu	Y
La	1.000	-0.060	0.731	0.541	-0.064	0.262	-0.728	-0.624	-0.749	-0.673	-0.707	-0.506	-0.695	-0.470	-0.825
Ce		1.000	0.098	0.157	0.050	-0.033	-0.053	-0.072	-0.068	-0.059	-0.040	-0.101	-0.102	-0.069	-0.150
Pr			1.000	0.834	0.309	0.197	-0.649	-0.661	-0.823	-0.670	-0.721	-0.580	-0.692	-0.541	-0.873
Nd				1.000	0.420	0.268	-0.547	-0.646	-0.761	-0.577	-0.671	-0.586	-0.641	-0.529	-0.846
Sm					1.000	-0.047	0.189	0.031	-0.130	-0.056	-0.160	-0.044	-0.134	-0.066	-0.314
Eu						1.000	-0.194	-0.307	-0.280	-0.172	-0.303	-0.225	-0.343	-0.168	-0.265
Gd							1.000	0.714	0.779	0.605	0.566	0.556	0.553	0.479	0.607
Tb								1.000	0.820	0.711	0.673	0.638	0.656	0.508	0.593
Dy									1.000	0.773	0.802	0.694	0.785	0.591	0.739
Ho										1.000	0.686	0.671	0.674	0.449	0.600
Er											1.000	0.614	0.856	0.561	0.661
Tm												1.000	0.651	0.672	0.502
Yb													1.000	0.569	0.645
Lu														1.000	0.493
Y															1.000

Extracting Theory of RE from the Weathered Crust Elution-deposited Rare Earth Ore

According to the property that RE in this type of ore mainly exists as ion-exchange phase, chemical leaching technology is the only method for RE extraction since the usual physical processing methods cannot enrich the rare earths.

Chemical Reaction

RE in the weathered crust elution-deposited rare earth ore mainly exists as the ion-exchangeable phase adsorbed on clay minerals. Because of this property, ion-exchange leaching is the only method to extract RE from this type of ore [11]. The weathered crust elution-deposited rare earth ore mainly contains quartz, potash feldspar, plagioclase, kaolin, white mica, whose chemical composition is typically SiO_2 70%, Al_2O_3 15%, K_2O 3~5%, Fe_2O_3 2~3%, CaO 0.2~0.5%, MgO 0.1~0.3% and other impurities. The RE grade is very low being only 0.05~0.3%. The clay minerals can be regarded as natural inorganic ion-exchanger. RE was adsorbed by aluminosilicate mineral which can be described as $[Al_2Si_2O_5(OH)_4]_m\cdot nRE^{3+}$ for kaolinite, $[Al(OH)_6Si_2O_5(OH)_3]m\cdot nRE^{3+}$ for halloysite, and $[KAl_2(AlSi_3O_{10})(OH)_2]_m\cdot nRE^{3+}$ for muscovite.

RE ions would be exchanged when this ore is leached with electrolyte solution, similar to the ion-exchange procedure. When meeting cation, ion-exchange reaction will occur. Therefore, the RE adsorbed can be released from the clays into the slurry in the presence of electrolyte solution. The leaching chemical reaction can be described as [12]:

$$[Al_2Si_2(OH)_4]_m \cdot nRE^{3+}_{(s)} + 3nNH^+_{4(aq)} \rightarrow [Al_2Si_2(OH)_4]_m \cdot nRE^{3+}_{(aq)}$$

$$[Al(OH)_6Si_2O_5(OH)_3]_m \cdot nRE^{3+}_{(s)} + 3nNH^+_{4(aq)} \rightarrow [Al(OH)_6Si_2O_5(OH)_3]_m \cdot (NH_4^+)_{3n(s)} + nRE^{3+}_{(aq)}$$

$$[KAl_2(AlSi_3O_{10})(OH)_2]_m \cdot nRE^{3+}_{s} + 3nNH^+_{4(aq)} \rightarrow [KAl_2(AlSi_3O_{10}(OH)_2]_m \cdot (NH_4^+)_{3n(s)} + nRE^{3+}_{(aq)}$$

The In-situ or Heap Leaching Mechanism

(1) Leach hydrodynamics [13]: the relationship between leachate flowing velocity (Q) and pressure-difference (ΔP) follows the Darcy law. Different leaching concentration results in different viscosity so as to affect the permeability. The higher the concentration of leaching reagent is, the lower the permeability is.

(2) Leach kinetics [14]: the leaching process can be described by the shrinking core model with the leaching kinetics controlled by diffusion through a porous solid layer. The apparent activation energy is about 4-12 kJ/mol, and an empirical equation of the leaching kinetics is established as $K = 0.53 \cdot r_0^{-0.52} \cdot e^{RT}$, in which K is the RE leaching rates constant, r_0 is the particle radius of RE ore, R is the gas constant and T is the leaching temperature.

(3) Mass transfer [15]: the mass transfer process could be described with chromatographic plate theory. The effects of the flow rate on the height can be equivalent to a theoretical plate according to the analysis of Van Deemter equation.

The leaching mechanism provides a theoretical basis and a scientific approach with high efficiency and low consumption for the weathered crust elution-deposited rare earth ores. It can be applied to optimize the RE extraction conditions, improve the RE recovery and inhibit impurity leaching in the extraction process [16].

Leaching Technology of the Weathered Crust Elution-deposited Rare Earth Ore

Because the RE mainly exist as ion-exchange phase in the weathered crust elution-deposited rare earth ore, this kind of unique ore has been studied by Chinese researchers for many years. The method of RE leaching with electrolyte solution by ion-exchange was proposed and, to the present time, three generations of technology have been used [17].

The First-generation Leaching Technology

RE is leached with sodium chloride in the first-generation leaching technology, firstly by barrel leaching and then developed into bath leaching (shown in Figure 1). There are many advantages in the first-generation NaCl leaching technology, such as the low price, abundant resources of the leaching reagent, shortened process flow. In addition, using oxalic acid as the precipitant can not only precipitate RE but also separate RE from the associated impurities (Al, Fe, Mn, et al.).

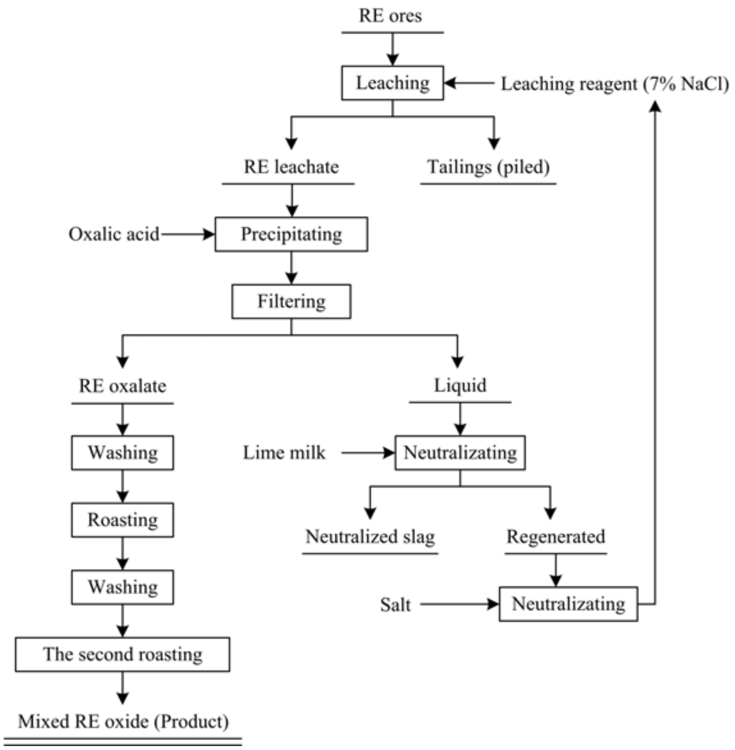

Figure 1. Flow process diagram of the first-generation NaCl leaching technology.

Two vital disadvantages, however, were found after a period of production and application of this technology. One is that the high concentration of leaching reagent which needs 6%～8% is too high. The high content of NaCl in the tailing water results in the salinification of the land and damage to the environment, which had an adverse impact on the growth of the crops. Another one is that large quantities of Na^+ will be co-precipitated with the oxalic acid, which leads to a low total amount of RE (<70%) in the product after the first roasting. So the first roasted product needs to be roasted again after washing with lots of water to obtain a product with higher purity (<92%), which make RE yield lower accompanied by complex operation and procedures.

The Second-generation Leaching Technology

The leaching agent sodium chloride was replaced by ammonium sulfate in the second-generation technology (Figure 2). The leaching process included bath leaching and heap leaching.

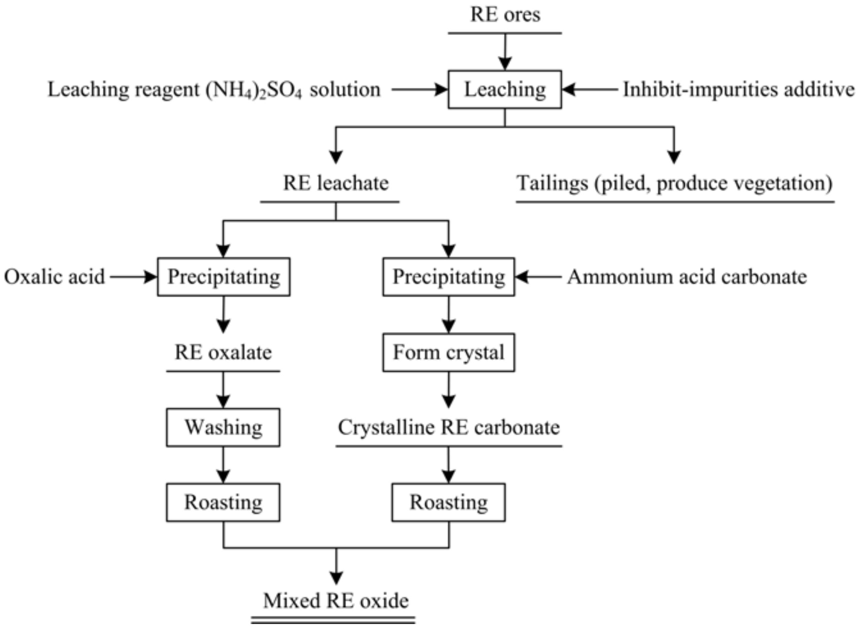

Figure 2. Flow process diagram of the second-generation $(NH_4)_2SO_4$ leaching technology.

Compared with NaCl leaching technology, there were several advantages in ammonium sulfate technology, for example, less consumption and low concentration (1~4% $(NH_4)_2SO_4$) of the leaching reagent, which could reduce the pollution of the environment greatly. And the purity of mixed RE oxide could meet the demands of customers (total amount of RE is above 92%) [18]. However, the ecological environment of the mining area is seriously destroyed by the second-generation leaching technology due to the mining operations and the discharge of tailings. For producing one tonne of RE product, 200~800 m^3 of the surface area are exploited, and 1200~1500 m^3 of ores must be mined and left on the surface. The bath leaching technology has been replaced with the heap leaching and in-situ leaching technology. The heap leaching technology may be widely popularized if the land-reclamation can be performed effectively combined with land leveling and grading.

The Third-generation Leaching Technology

In order to overcome the disadvantages of the two earlier generation technologies described above, in-situ leaching technology was developed with high yield, low cost, and neither erosion nor pollution to environment. The leaching agent (ammonium sulfate) is injected into the natural orebody, and the useful components are leached out selectively, then the leachate is pumped to the above-ground factory through the recovery wells (shown in Figure 3).

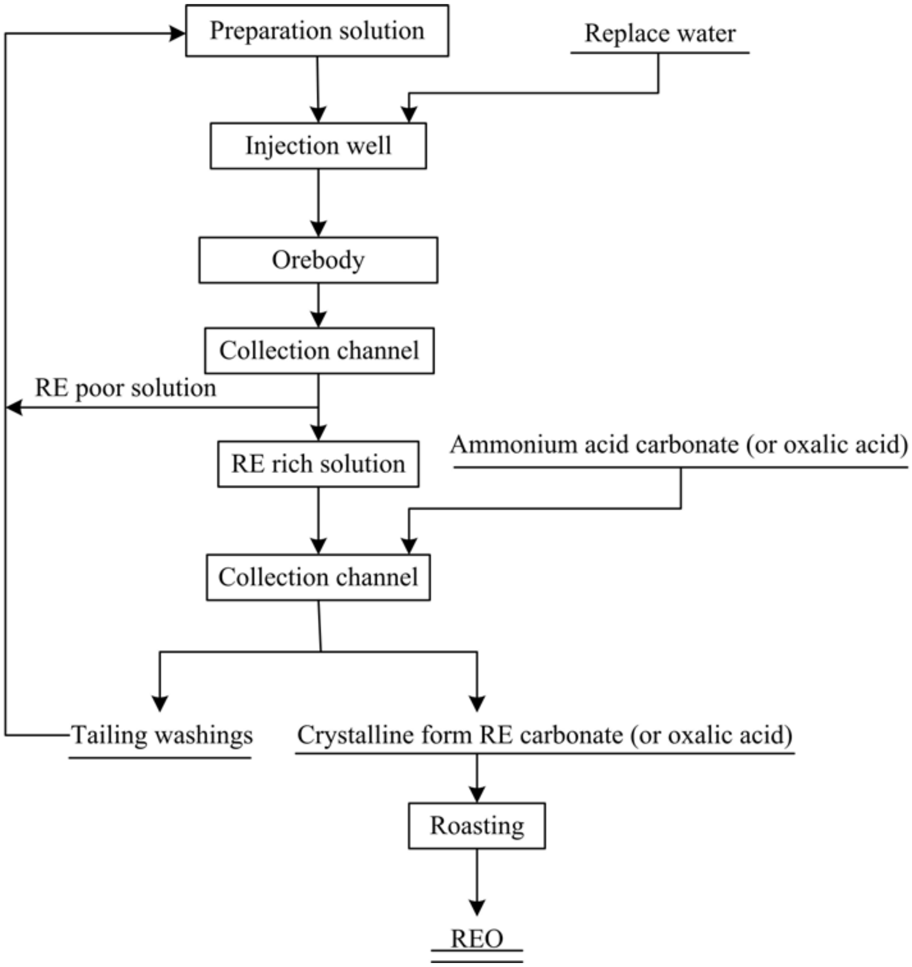

Figure 3. Flow process diagram of in-situ leaching.

Currently, it is suggested that the in-situ leaching technology can be applied only in an orebody with solid bedrock without fissures or cracks otherwise, the leaching agents may leak away and pollute the ground water. Therefore, it is appropriate for an orebody without a solid bedrock to select the heap leaching technology combining with land leveling and tailings-reclamation [19].

Protection and Reconstruction of Vegetation in Exploited Area

It is inevitable that there are some problems, such as destruction of vegetation, and soil and water loss and environment pollution, due to the exploitation of the weathered crust elution-deposited ore. Therefore, methods of strengthening the administration of exploitation for RE ores and revegetation at mine sites are in need of an urgent solution.

The principal task is to restore vegetation in damaged ecosystems, which is the key to preventing soil erosion. The remediation effect on soil and water loss, and the influence of physicochemical properties of soil, are different when using different measures to restore the vegetation. Given the variations in the chemical composition of soils, it is obviously beneficial to restore soil through revegetation [20].

Conclusions

1. The differences in area, climate, rock quality, weathering degree lead to different mineral composition and quality in the same vertical elevation and rare earth grade. However, the relevant data are far from comprehensive and should be further improved.

2. The basic theoretical research into heap leaching and in-situ leaching technology should be improved. For the heap leaching process, the leaching kinetics and hydrodynamics should be investigated to understand the regular pattern of the leaching process and establish a mathematical model. For the in-situ leaching process, the leaching agent with high leaching ratio and good anti-swelling performances should be studied to decrease the occurrences of the landslides.

3. In order to reduce pollution cased by ammonia-nitrogen wastewater, the $MgCl_2$ could be selected as a new leaching agent. The whole leaching process should be investigated to understand the migration and enrichment of Mg^{2+} in the minerals. The effect of $MgCl_2$ on the rare earth quality should be determined.

4. The degradation, migration and enrichment of residual leaching agent in the tailings should be investigated. Additionally, the process and rate of the degradation reaction should be studied.

5. The restoration of ecological environment and vegetation on tailings would be an important research subject in the future. Great attention also should be paid to the control of the migration of rare earths from the tailings which could cause water system to be polluted by RE ions after the exploitation of RE mining. Additionally, high efficiency rare earth recovery technology for low RE concentration in tailings liquid and leaching wastewater is urgently needed. Ammonia-nitrogen wastewater treatment technology is also an important subject for investigation.

Acknowledgements

Financial support for this work from National Natural Science Foundation of China (no. 50974098, 51274152) and Changjiang Scholars and Innovative Research Team in University (no. IRT0974) is greatly appreciated.

References

1. Nesbitt, H.W., “Mobility and Fractionation of Rare Earth Elements During Weathering of a Granodiorite,” *Nature*, 279 (1979), 206-210.

2. Chi Ru-an, and Tian Jun, “Review of Weathered Crust Rare Earth Ore,” *Journal of Chinese Rare Earth Society*, 25 (6) (2007), 641-650.

3. Luo Xiao-ya, “Metallogenic Conditions of Rare Earth Ore in Hunan and Forming Mechanism of Ion Adsorption Type Rare Earth Ore,” *Journal of Minerals*, 1 (2011), 332-333.

4. Yang Da-huan and Xiao Guang-ming, “Regional Metallogenic of the Ion Adsorption Type of Rare Earth Deposits in Guangdong Province,” *Geology and Resources*, 20 (6) (2011), 462-468.

5. Li Hui et al., “Study on Ore Properties of the Weathered Crust Elution-deposited Rare Earth Ore and the Contents in Various Grain-size,” *Chinese Rare Earths*, 33 (2) (2012), 14-18.

6. Chi Ruan et al., “Existing State and Partitioning of Rare Earth on Weathered Ores,” *Journal of Rare Earths*, 23 (6) (2005).

7. Yang Xue-ming and Yang Xiao-yong, “Geochemical Study of REE from Granite Weathering Crust in Dajishan of Jiangxi Province,” *Chinese Rare Earth*, 20 (1) (1999), 1-5.

8. Condie, K.C., J. Dengate, and R.L. Cullers, “Behavior of Rare Earth Elements in a Paleoweathering Profile on Granodiorite in the Front Range, Colorado, USA,” *Geochimica et Cosmochimica Acta*, 59 (2) (1995), 279-294.

9. Aubert, D., Stille P., and Probst A., “REE Fractionation During Granite Weathering and Removal by Waters and Suspended Loads: Sr and Nd Isotopic Evidence,” *Geochemica et Cosmochemica Acta*, 65 (3) (2001), 387.

10. Chi Ru-an et al., “Correlation Analysis on Partition of Rare Earth in Ion-exchangeable Phase From Weathered Crust Ores,” *Transactions of Nonferrous Metals Society of China*, 16 (2006), 1421 .

11. Chi Ru-an et al., “Kinetics of Leaching Flavonoids From Pueraria Lobata with Ethanol,” *Chinese J Chem Eng*, 14 (3) (2006), 402-406.

12. Chi R. and Tian J., *Weathered crust elution-deposited rare earth ores* (New York: Nova Science Pub Inc, 2008).

13. Tian J., “Leaching Hydrodynamics of Weathered Elution-deposited Rare Earth Ore,” *Transactions of Nonferrous Metals Society of China*, 3 (2001), 434-437.

14. Tian Jun et al., “Kinetics on Leaching Rare Earth From the Weathered Crust Elution-deposited Rare Earth Ores with Ammonium Sulfate Solution,” *Hydrometallurgy*, 101 (3-4) (2010), 166-170.

15. Tian Jun et al., “Optimisation of Mass Transfer in Column Elution of Rare Earths from Low Grade Weathered Crust Elution-deposited Rare Earth Ore,” *Hydrometallurgy*, 103 (1) (2010), 211-214.

16. Tian Jun, Chi Ru-an, and Yin Jing-qun, “Leaching Process of Rare Earths from Weathered Crust Elution-deposited Rare Earth Ore,” *Transactions of Nonferrous Metals Society of China*, (20) (2010), 892-896.

17. Wu Hong-qiang, Yin Yan-fen, and Fang Xi-hui, “The Present Situation and Development Trends of the Mining and Separation Technologies of Weathering Crust Ion Absorbed Type Rare-earth Ores,” *Nonferrous Metals Science and Engineering*, 1 (2) (2010), 73-76.

18. Hang Xiao-wei, Zhang Yong-qi, and Li Hong-wei, “Development Trend and Research Progress of Rare Earth Extraction in China,” *China Science Foundation*, 3 (2011), 134-137.

19. Li Chun, “The Generalization and Application of New Technology on Lixiviating Mineral at the Original Place for Ionic Rare Earths,” *Nonferrous Metals Science and Engineering*, 2 (1) (2011), 63-67.

20. Li Yong-xiu, Zhang Ling, and Zhou Xin-mu, “Resource and Environment Protected Exploitation Model for Ion-type Rare Earth Deposit in Southern of China,” *Chinese Rare Earths*, 31 (2) (2010), 80-85.

HYDROMETALLURGICAL PLANT DESIGN PARAMETERS FOR THE AVALON RARE EARTH PROCESS

H. Notzl[1], S. Khan[2] and N. Verbaan[3]

[1]Tenova Mining and Minerals (Australia) Pty Ltd.
Suite 2, 93 Francisco Street
Belmont, WA, 6104, Australia
henrie.notzl@bateman.com

[2]Avalon Rare Metals Inc.
1901 - 130 Adelaide Street West
Toronto, ON M5H 3P5, Canada
skhan@avalonraremetals.com

[3]SGS Minerals Services – Lakefield site
PO Box 4300
185 Concession Street
Lakefield, ON K0L 2H0, Canada
niels.verbaan@sgs.com

Keywords: Rare Earth Elements, Mineralogy, Acid Bake, Leaching, Impurity Removal, Pilot Plant, Concentrate, Flotation, Hydrometallurgy

Abstract

Avalon Rare Metals has completed a Feasibility Study for the Nechalacho deposit located in the Northwest Territories. The rare earth (RE) minerals include allanite, monazite, synchysite, columbite, fergusonite and bastnaesite. Zircon is present in considerable amounts and is a carrier of heavy rare earth elements (HREEs). The processes employed for rare earth (RE) extraction from a rare earth flotation concentrate included pre-leaching the concentrate to remove the excess carbonate, decomposition of the pre-leached residue with concentrated sulphuric acid, selective precipitation of the impurities (Fe, Th, etc.) and bulk precipitation of the rare earths. Testwork was essential in the overall plant design and included bench tests, small continuous tests as well as fully integrated pilot plants. This paper discusses the testwork results and its impact on the overall plant design.

Introduction

Rare Earth Elements (REEs) are a group of fifteen lanthanide series elements (including scandium and yttrium), which are widely known for their applications in electronics, magnets, catalysts, medicine and other advanced material products. REEs are further subdivided into Light Rare Earth Elements (LREEs) and Heavy Rare Earth Elements (HREEs). Avalon Rare Metals Inc. has recently completed a feasibility study to recover REEs from the Nechalacho Deposit located near Thor Lake, North West Territories.

A base-case flow-sheet has been developed to process rare earth ores from Nechalacho and produce marketable rare earth oxides. Broadly speaking, there are three main steps in this process:

1. Flotation: to produce concentrates from rare earth ores, thereby eliminating gangue and other stray minerals.

2. Hydrometallurgical Processing: to solubilize rare earth minerals from the concentrates and selectively precipitate rare earth hydroxides as a bulk mixed product while minimizing co-precipitation of impurities such as uranium, thorium and iron. A by-product from this step is an enriched zircon concentrate which has a high economic value.

3. Separation: to separate individual rare earths from the bulk mixed product using solvent extraction.

Figure 1 shows a simplified overview of the steps required to process rare earth ores:

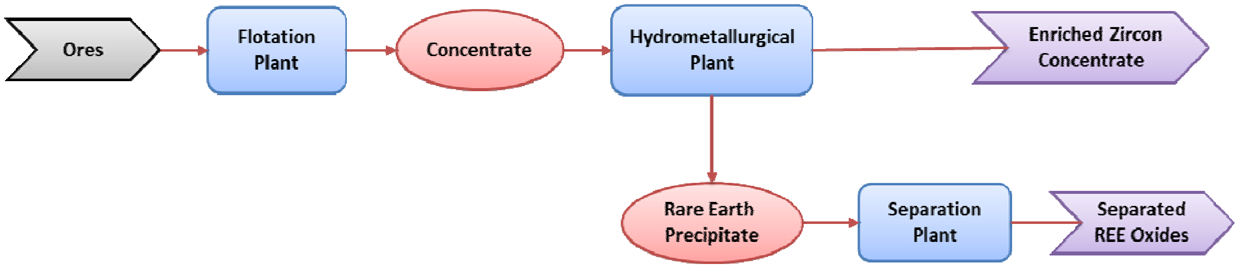

Figure 1. Simplified flow-sheet for processing of rare earth ores to oxides.

An integral step in the hydrometallurgical processing is treatment of rare earth concentrate with concentrated sulphuric acid at an elevated temperature (220 °C) – a process referred to as acid bake. This reaction converts rare earth minerals to water soluble rare earth sulphates which can be subsequently recovered downstream by precipitation. Avalon has conducted hydrometallurgical test-work since late 2008 to demonstrate proof of principle from theory and provide input towards developing the final hydrometallurgical flow-sheet for the feasibility study. Tests have been conducted on both bench and pilot scale on flotation concentrate. Six pilot plant campaigns were conducted at SGS Minerals Services based in Lakefield, Ontario between June and October 2012. The objective of this paper is to present the results from one particular pilot scale campaign (PP6) and derive inferences regarding continuous scale processing of rare earth concentrates.

Mineralogy

The mineralogy of the Nechalacho deposit directly relating to metallurgy was investigated by SGS Minerals using QEMSCAN®, a scanning electron microscope (SEM) and an electron microprobe (EMP). Nechalacho mineralization is hosted in nephelinesyenite that has been extensively hydrothermally altered in areas of mineralization. Thus, the gangue mineralogy of the deposit comprises the nephelinesyenite minerals along with alteration products, many of which are fine grained. The economically significant elements of the Nechalacho deposit are hosted in a number of ore minerals, summarized as follows:

- LREEs which dominantly occur in bastnaesite, synchysite, monazite and allanite;
- HREEs which dominantly occur in zircon, fergusonite and rare xenotime;
- Zr (along with HREE, Nb and Ta) which occurs in zircon and other zirconosilicates (eudialyte), and
- Nb and Ta occur in columbite and ferrocolumbite, fergusonite and zircon.

The mineralogy of the Nechalacho ore is complex. The mineralogy also drives metallurgical performance. Consequently, it is critical to have a comprehensive understanding of the minerals – their textures, compositions – relative to position within the deposit.

Flowsheet and Testwork

The main objectives of the hydrometallurgical pilot plant campaign were to:

- Test a continuous version of the hydrometallurgical flow-sheet and demonstrate steady state operation;
- Optimize REE extraction into the leach solution and upgrade the concentrate (through the pre-leach, acid bake and water leach circuits) into a partially purified rare earth precipitate (RP);
- Remove target contaminants (Fe, Th) in the iron removal (IR) circuit while ensuring minimal REE losses;
- Ensure the final rare earth precipitate (RP) product had an acceptable grade of rare earths higher than that in the input concentrate while minimizing the U and Th content to a target level of 500 ppm or lower, and
- Ensure the concentrations of species in the filtrate from the tailings circuit met target environmental levels determined via hydrological modelling (especially for Mg and SO_4 – 800 mg/L and 4500 mg/L targets respectively).

Typically, the feed rate for each pilot campaign was 2 kg/h of concentrate.

Figure 2 shows the conceptual flow-sheet as piloted.

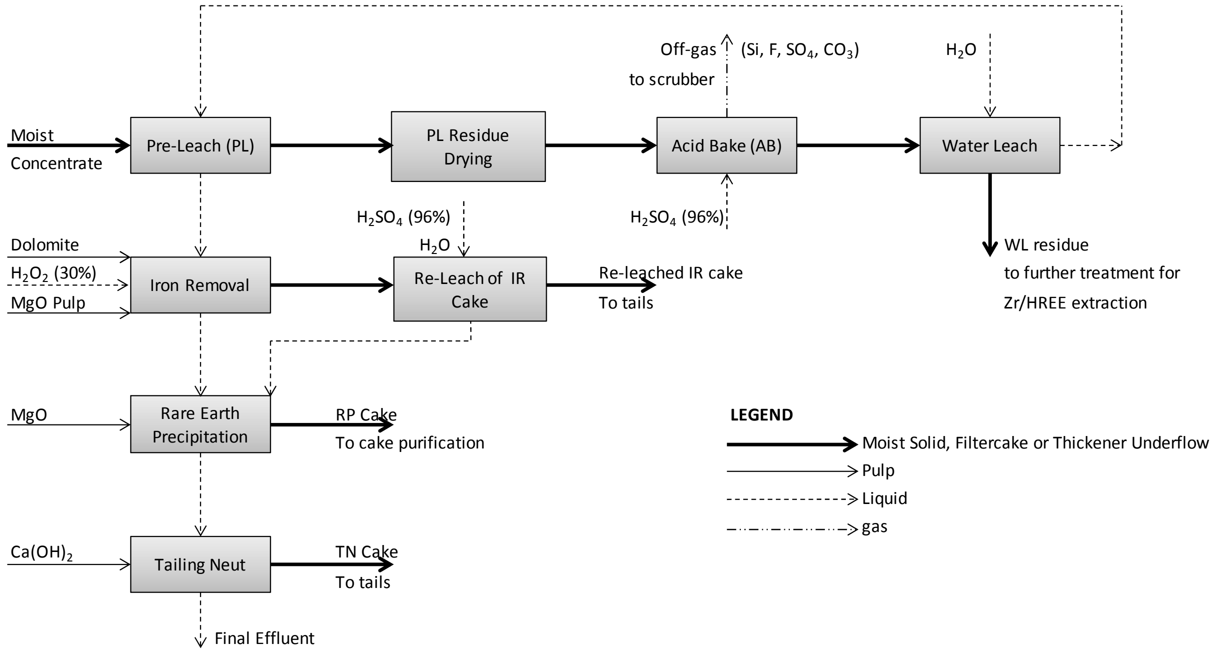

Figure 2. Hydrometallurgical pilot plant flowsheet.

The flowsheet comprised of the following circuits:

- Pre-Leaching (PL): In the PL circuit, acid-consuming minerals from the concentrate (mainly carbonates) reacted with excess free acid of the water leach (WL) circuit and therefore decreased the consumption of neutralization reagent in the iron removal (IR) circuit as well as reduced overall acid consumption. PL solution produced in this circuit advanced to the IR circuit. PL residue in the pilot plant was dried batch-wise and was used as feed to the acid bake (AB) circuit;

- Acid Baking (AB): In the AB circuit, dried PL residue was reacted with concentrated sulphuric acid to convert the rare earth minerals to form rare earth sulphates, commonly known as cracking. The calcined material formed was discharged directly into the WL circuit. Off-gas from the AB circuit contained fluoride and sulphate species which were absorbed in a scrubber using a 10% sodium hydroxide solution;

- Water Leaching (WL): In the WL circuit, sulphated RE minerals were dissolved in water. The resulting pregnant solution with excess acidity was contacted with fresh flotation concentrate in the PL circuit as described above;

- Iron/Thorium Removal (IR): Iron and thorium contained in the PL solution was removed by selective precipitation using a combination of dolomite, hydrogen peroxide and MgO;

- Re-Leach (RL): REEs co-precipitated in the IR circuit were partially recovered in a RL circuit, where IR cakes were re-pulped in dilute sulphuric acid solutions. The RL leach residue cake was disposed as tails. RL solution was then combined with the primary IR solution;

- Rare Earth Precipitation (RP): In the RP circuit, REEs were recovered to produce a mixed REE precipitate by addition of MgO or hydrated lime. RP filtrate was then discharged into the Tailings Neutralization (TN) circuit, and

- Tailing Neutralization (TN): RP filtrates were neutralized to reduce Mn and Mg levels by addition of MgO or hydrated lime.

Results and Discussion

Pilot Plant Performance

The pilot plant parameters were obtained from a variety of bench scale and continuous mini plant test-work on the flotation concentrate. The pre-leach unit operation removed the free carbonates and hydroxides in the flotation concentrate by reacting with the acidic water leach liquor (50 to 130 g/L H_2SO_4).

Figure 3 shows the consumption of the free acidity of the WL liquor over a few select pilot plant shifts, indicating 72% reduction in free acidity on average.

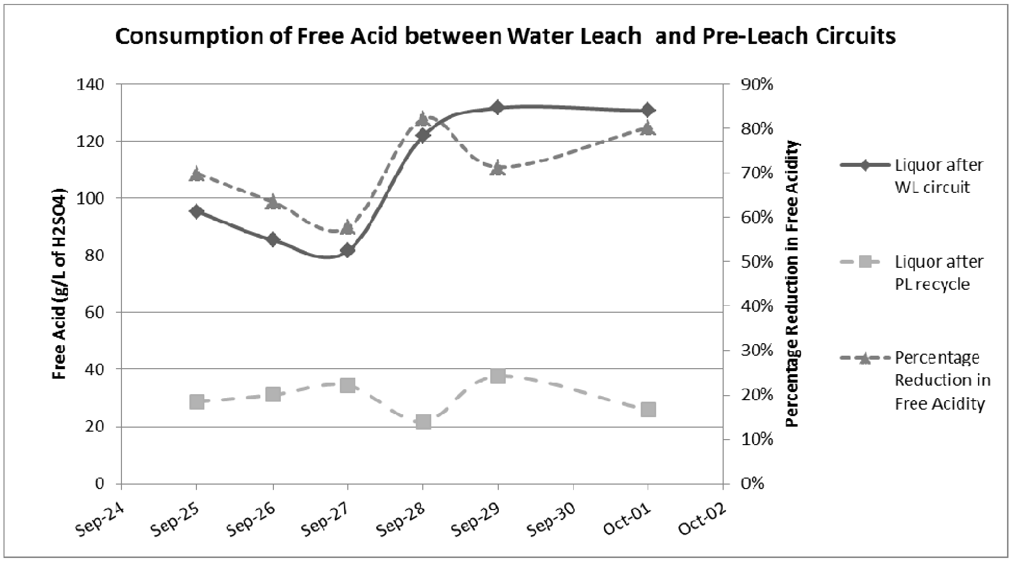

Figure 3. Change in free acidity between water leach liquor and pre-leach recycle filtrate.

This permitted the reduction in downstream use of dolomite for neutralization and minimized the acid requirements in the acid bake circuit. The pre-leach produced two streams:

- Filtrate containing free acidity of 25 to 40 g/L H_2SO_4 together with rare earths and impurities such as Fe, Th and Al, and

- Solids requiring further treatment with sulphuric acid to “crack” the unreacted rare earths minerals.

The solids were dried, and concentrated (96%) sulphuric acid was added (0.6 t H_2SO_4/t of solids) and the mixture was sent to a rotary kiln.

Table I summarizes the key pilot plant parameters and performance for each circuit operated.

Table I. General Pilot Plant Parameters and Performance

Circuit	**Temp °C**	**Retention Time h**	**No. of Units**	**pH**	**Solution Density g/cm^3**	**d_{80}* Size µm**	**FA g/L H_2SO_4**	**Ce Ext %**	**Y Ext %**	**Th Ext %**	**U Ext %**	**Fe Ext %**
PL	33-42	1.8	2		1.2	59	25-36	21	4	13	2	14
Drying	120	6	1									
AB	230	1	1	0.6**								
WL	90	2.2	3		1.1	57	50-95	83	48	59	49	57
IR	75	5.6	6	3	1.1	13	-	8	4	55	5	97
RP	27	7.3	4	7.8	1.1	23	-	100	100	100	100	99
TN	27	4	4	9.7	1.04	9	-	100	100	100	100	100

*Malvern Analyses
** t H_2SO_4/t dry solids

From Table I it can be seen that only small amounts of light and heavy rare earths were pre-leached at 40°C. Similar results at higher pre-leach temperatures and acid concentrations were obtained in bench scale testing indicating the need for a more aggressive solids treatment such as acid bake.

The data in this paper is focused on the pilot plant test-work using H_2SO_4 acid bake treatment at 220 to 240°C. The envisaged hydrometallurgical plant will be located far north in Canada on the south shores of the Great Slave Lake, where transportation of hydrochloric acid, sodium hydroxide or other base chemicals is limited and costly. The cheapest transportation chemical is sulphur for the production of sulphuric acid from an acid plant located on site.

The acid bake reactions in the kiln are complex but believed to occur according to (1) and (2):

Bastnaesite (Ce,La,Y)CO_3F) – Ln stands for a generic REE:

$$2LnCO_3F + 3H_2SO_4 \rightarrow Ln_2(SO_4)_3 + 2CO_2\uparrow + 2HF\uparrow + 2H_2O\uparrow \tag{1}$$

Monazite ($RePO_4$)

$$2LnPO_4 + 3H_2SO_4 \rightarrow Ln_2(SO_4)_3 + 2H_3PO_4 \tag{2}$$

Prior to the pilot plant campaign, extensive method development testwork was conducted by SGS to optimize the performance of the acid bake rotary kiln. Table II summarizes the optimized acid bake parameters:

Table II. Acid Bake Kiln: Optimized Parameters

Parameter	Optimized Value
a. Hot Zone Temperature	220 °C
b. Feed Rate	2 kg/h
c. Acid Dosage	600 kg/t
d. Slope Angle	3.6 degrees
e. Rotational Speed	1 rpm
f. Overall Residence Time	1 h
g. Hot Zone Residence Time	0.48 h

The discharge of the acid baked solids was water leached at 90°C through a series of three reaction tanks. The water leach extracted 75% of the remaining LREEs and 49% of the HREEs. With the combination of the pre-leach and water leach solutions, Table III indicates the extraction of 80% LREEs and 53% HREEs. The water leach solution containing 50 to 95 g/L free acid which, once filtered, was recycled to the preleach circuit. The extraction of the rare earths and the impurities are summarized in Table III.

The pilot plant campaign was operated continuously for 12 days with all units running simultaneously. The variability in the recoveries was produced over two different feeds and two different pulp densities using a silicon tie method to calculate extractions.

Table III. Extraction of Rare Earths and Impurities from the Pre-leach and Water Leach Circuits

Species	Extraction (%)
LREEs	80%
HREEs	53%
TREEs	75%
U	49%
Th	59%
Zr	2%
Fe	57%

The acid bake / water leach circuit also dissolved thorium, uranium and iron. The pre-leach solution containing all the soluble rare earths and impurities was sent to the IR circuit containing 6 neutralization tanks where dolomite, hydrogen peroxide and MgO was added to a solution containing 25-36 g/L FA and the pH was adjusted to 3.0. The adjustment in the six tanks in series included:

- Dolomite addition to pH 1.5;

- H_2O_2 addition to oxidize ferrous to ferric iron (target ORP of 600 mV), and
- MgO to produce a final pH of 3.0.

For the envisaged hydrometallurgical plant at Pine Point, dolomite is readily available from a nearby quarry and will dramatically reduce the chemical costs, which would otherwise need to be transported to this remote part of Canada. Limestone is also available from a nearby location, however mini-plant work showed that significant REE losses were incurred when limestone was used. Therefore, dolomite (15 % Mg, 22 % Ca) was chosen for the pilot plant work.

Table IV. Overall Distribution of Select Rare Earths and Impurities

Solid Products	**Ce Ext %**	**Y Ext %**	**Th Ext %**	**U Ext %**	**Fe Ext %**
WL Residue	13	50	36	50	37
IR Residue	7	2	35	3	61
REE Ppt	80	48	29	48	2
TN Residue	0	0	0	0	0

The IR circuit removed 97% of the iron, 55% of the thorium and only 4% of the uranium in solution. There is a direct relationship (see Figure 4) between the RE loss and Th removal. Hence the IR solids were repulped in a mildly acidic sulphuric acid solution to recover the co-precipitated REEs, while leaving Fe and Th in the residue.

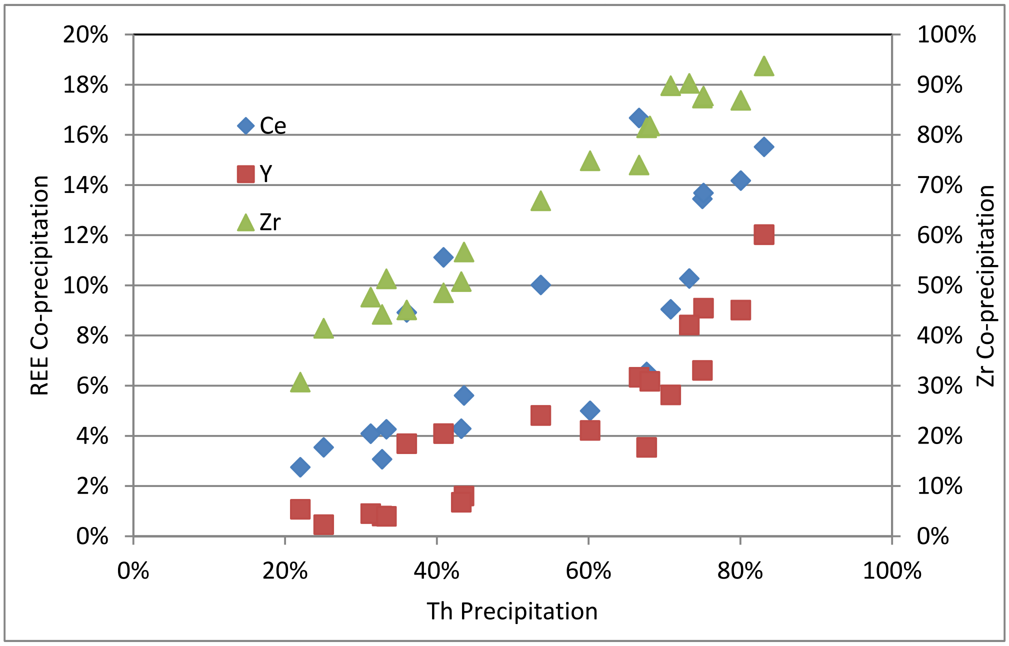

Figure 4. Relationship between Th and rare earth precipitation.

The IR solution at pH 3 was further neutralized in the RP circuit to pH 7.8 to recover all dissolved REE. Further work on the precipitation of rare earths has produced total precipitation at lower pHs such as 6.5. The higher pH during the pilot plant work was chosen to maintain complete precipitation of rare earths even during plant upsets.

During the pilot plant run, MgO slurry as well as slaked lime were used to determine the impact of the neutralizing agent on the overall purity of the rare earths precipitate. The upgraded rare earth product using slaked lime as the precipitating reagent had an overall TREE grade of 14% and the upgrade factors are listed in Table V.

Table V. Upgrade Factors of Rare Earths from the Flotation Concentrate

Species	**Upgrade Factors**
LREEs	2.96
HREEs	2.04
TREEs	2.74
La	2.96
Ce	2.88
Pr	2.75
Nd	2.71
Sm	2.59
Eu	2.52
Gd	2.53
Tb	2.43
Dy	2.25
Ho	2.07
Y	1.97
Er	1.74
Tm	1.40
Yb	1.06
Lu	0.79
Th	0.88
U	2.03

A significant accomplishment of pilot plant campaign PP6 was the reduced Fe, U and Th levels in the final rare earth product from the RP circuit, which was a concern in the previous campaigns. Figure 5, compares the U and Th levels of the RE precipitate produced using MgO and hydrated lime. With MgO, the levels were much higher than the 500 ppm limit governed by transportation regulations in Canada. The reduced U and Th levels were achieved by the formation of gypsum (using hydrated lime instead of magnesium oxide as a precipitating reagent), which acted as a diluent.

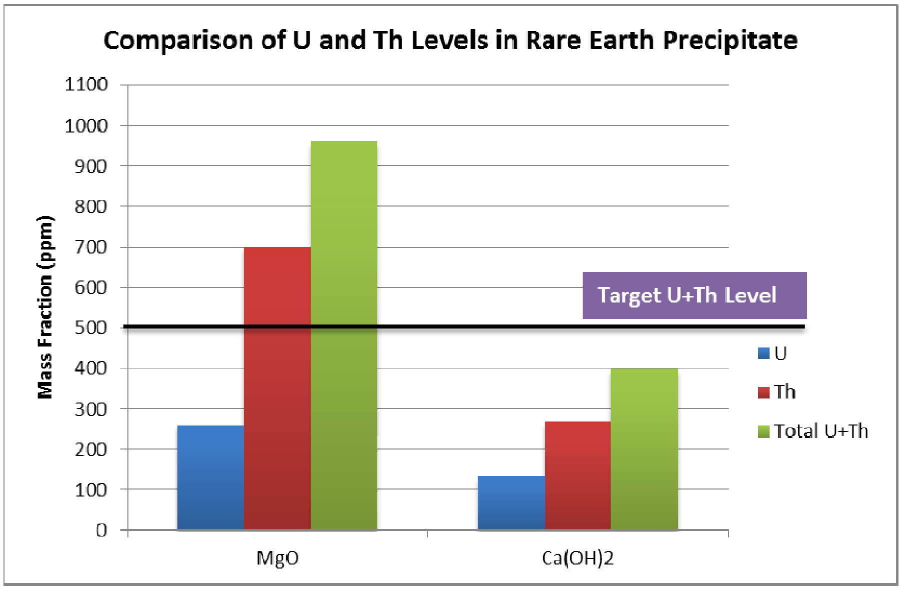

Figure 5. Comparison of U and Th levels in rare earth precipitate.

Fate of Minerals in the Acid Bake Process

The RE minerals in the flotation concentrate were converted from carbonates and hydroxides into soluble sulphates during the acid bake and dissolved in water leach liquor. Of the rare earth minerals (REM) originally present in the flotation feed (12%), only 2.5% remained in the acid bake residue after water leach (verified by QEMSCAN). Table VI indicates that the bastnaesite, synchysite and allanite were broken down while only partial acid attack was observed with columbite, fergusonite and monazite.

Along with the cracking of the rare earth minerals, the gangue material also changed with a complete breakdown of biotite, chlorite, fluorite, calcite, dolomite, ankerite and other sulphides. Only partial breakdown was seen with zircon and some oxides while, as expected, no breakdown was seen with quartz, micas, feldspars, clays and other silicates. The limited conversion of the acid bake for the zircon and fergusonite are an indication of the poor recoveries that were observed with the heavy rare earths while the light rare earth minerals converted to the sulphates very easily.

Table VI. Fate of Minerals in the Acid Bake Process (from Concentrate to WL Residue)

Mineral	Composition	Fate
REM Summary		
Columbite(Fe)	$Fe^{2+}Nb_2O_6$	Partial
Fergusonite	$Y (Nb, Ta)O_4$	Residual
Bastnaesite	$(Ce,La,Y)CO_3F$	Broken Down
Synchysite	$Ca(Ce,La,Nd)(CO_3)_2F$	Broken Down
Allanite	$(Ce,Ca,Y,La)_2(Al,Fe^{+3})_3(SiO_4)_3(OH)$	Broken Down
Monazite	$(Ce,La,Nd,Th,Y)PO_4$	Partial
Other REE	-	Broken Down
Zircon	$ZrSiO_4$	Partial
Apatite	$(F,Cl,OH)Ca_3(PO_4)_2$	Partial
Quartz	SiO_2	Residual
Plagioclase	$(Na,Ca)(Si,Al)_4O_8$	Residual
K-Feldspar	$KAlSi_3O_8$	Residual
Micas	$XY_{2-3}Z_4O_{10}(OH, F)_2$ with X = K, Na, Ba, Ca, Cs, (H_3O), (NH_4); Y = Al, Mg, Fe^{2+}, Li, Cr, Mn, V, Zn; and Z = Si, Al, Fe^{3+}, Be, Ti	Residual
Biotite	$K(Mg,Fe{+}{+})_2(AlSi_3O_{10})(F,OH)_2$	Broken Down
Clays	-	Residual
Chlorites	$Na_{0.5}(Al,Mg)_6(Si,Al)_8O_{18}(OH)_{12}\bullet 5(H_2O)$	Broken Down
Amphibole	e.g., Hornblende $Ca_2(Mg,Fe,Al)_5(Al,Si)_8O_{22}(OH)_2$	Partial
Other Silicates	-	Residual
Fluorite	CaF_2	Broken Down
Fe-Oxides	e.g. Fe_2O_3	Residual
Pyrite	e.g., pyrite FeS_2	Residual
Other Sulphides	e.g., pyrite FeS_2	Broken Down
Other Oxides	-	Partial
Calcite	$CaCO_3$	Broken Down
Dolomite	$CaMg(CO_3)_2$	Broken Down
Ankerite	$Ca(Fe, Mg, Mn)CO_3)_2$	Broken Down
Gypsum	$CaSO_4$	Formed

Thickening

Static and dynamic testing was conducted to evaluate the effect that flocculant dosage, feed density, solids loading rate and rise rate have on the ability to meet target parameters. The best materials for thickening were the preleach and the acid wash solids which met the underflow solids targets of approximately 50% w/w. In previous bench and piloting testwork, the greatest difficulty, as expected, was the iron precipitation solids even with the raised temperature of 70°C and the high dosages of flocculant. The rare earths and neutralization solids did not meet the required underflow solids of 40 % w/w due to the nature of the hydroxides. During the final pilot plant campaign, however, the thickening of the iron precipitation solids, the rare earth solids and the neutralization solids was successful.

Table VII. Thickening Results from Pilot Plant Solids

Circuit	pH	Feed Density % w/w solid	Rise Rate m/h	Solids Loading Rate t/m^2h	Floc Dosage g/t	Achievable Underflow Density % w/w solid	Achievable Overflow Clarity ppm TSS	Maximum Unsheared Underflow Yield Stress Pa	Target Underflow Density % w/w solids
Target							<100 ppm		
PL	1.3	17	1.8-3.4	0.4-0.75	27-43	46-51	<219	60	50-65
WL	<1	16	3.5-5.2	0.73-1.1	21-36	50-57	<90	26	50-65
IR	5	4	0.5-2.5	0.02-0.1	297-449	19-39	<132	120	50
RP	8	4	0.7-1.5	0.03-0.07	30-73	35-40	<370	7	40-60
TN	10.3	6-11	0.5-1.0	0.07-0.13	27-41	30-32	<114	71	40-60

Table VIII. Specific Gravity and Particle Size Data of Pilot Plant Streams

Circuit	Solids SG t/m^3	Calculated Solids SG t/m^3	Particle Size P80, um	Prepared pH	Liquor SG t/m^3	Liquor Solution
PL	2.8	3.23	54	1.3	1.02	TN Liquor – 40 g/l H_2SO_4
WL	2.0	3.00	54	<1	1.0	TN Liquor – 80 g/l H_2SO_4
IR	-	2.68	<50	3.3	1.03	IR Precip Filtrate
RP	-	2.70	<50	8	1.07	RP Filtrate
TN	-	2.98	<50	19	1.0	TN Filtrate

Table IX. Filtration Results from Pilot Plant

	Slurry Density kg/dm^3	Solids Content % w/w solids	pH	Filtration Rate kg/m^{3}h	Cake Moisture % w/w	Cake Thickness mm
Preleach	1.39	41-47	1.3	569-1366	5-14	25-49
Preleach Vacuum	1.39	41-47	1.3	387-1508	12-26	6-24
Acid Wash Labox 25	1.49	45-50	<1	198-293	8-15	24-36
Acid Wash Vacuum	1.49	45-50	<1	101-247	14-19	5-14
Iron Ppt Labox 25	1.26	32-33	5	70-85	-	17-32
Rare Earths Labox 25	1.33-1.36	31-34	8	221-333	36-42	39-51
Neutralization Labox 25	1.15-1.22	26-28	10.3	93-113	29-37	20-38

Conclusions

A successful integrated hydrometallurgical pilot plant campaign was operated for 12 days using flotation concentrate as the feed. The main conclusions include:

- The pilot plant was able to upgrade the total rare earths in the concentrate by an upgrade factor of 2.74;
- Optimum recoveries of 80% LREEs and 53% HREEs were obtained in the upgraded rare earth precipitate;
- By operating the PL-AB-WL in counter current format (ie recycling the acidic WL pregnant solution to PL circuit), dolomite and overall acid consumptions were minimized;
- U and Th levels in RE precipitate were lower than 500 ppm by the use of hydrated lime as a precipitating reagent and thereby meeting transport regulations;
- Bastnaesite, synchysite and allanite were completely broken down in the acid bake step while monazite, zircon, columbite and fergusonite were partially broken down;
- Thickening and filters were successfully used for the solid/liquid separation processes required throughout the pilot plant, and
- The pilot plant was integral in defining the flowsheet and completing the engineering specification requirements towards the feasibility study.

Based on the results from the pilot plant, the following long term predictions for average annual revenues of rare earth products were made [3]:

Table X. REE Prices and Estimated Average Annual Revenues

Metal Oxide	**US$/kg**	**Average Annual Revenue (US$ 000's)**
La_2O_3	8.75	10,278
Ce_2O_3	6.23	15,529
Pr_2O_3	75.20	23,987
Nd_2O_3	76.78	89,561
Sm_2O_3	6.75	1,472
Eu_2O_3	1392.57	43,526
Gd_2O_3	54.99	12,636
Tb_2O_3	1055.70	39,378
Dy_2O_3	688.08	133,740
Ho_2O_3	66.35	2,139
Er_2O_3	48.92	3,480
Tm_2O_3	N/A	N/A
Yb_2O_3	N/A	N/A
Lu_2O_3	1313.60	5,948
Y_2O_3	67.25	48,126

References

1. Avalon Rare Metals Inc., "Nechalacho Project Feasibility Study Report," 2013.
2. J. Zhang and C. Edwards, "Mineral Decomposition and Leaching Processes for Treating Rare Earth Ore Concentrates," in *Proceedings from COM2012*, 2012.
3. Edison Investment Research, "Avalon Rare Metals: Largest ex-China HREE Project," 2013.

BENEFICIATION AND EXTRACTION OF REE FROM GEOMEGA RESOURCES' MONTVIEL PROJECT

*B. Yu[1], N. Verbaan[1], G. Pearse[2], S. Britt[3]

[1]SGS Mineral Services – Lakefield Site
185 Concession Street, PO Box 4300
Lakefield, Ontario K02 2H0
*Ben.Yu@sgs.com

[2]Equapolar Consultants Ltd.
#101-174 Stanley Ave, Ottawa, Ontario K1M 1P1

[3]Geomega Resources Inc.
475 Victoria Avenue, Saint-Lambert, Quebec J4P 2J1

Keywords: Carbonatite Rare Earth Deposit, Flotation, Beneficiation, HCl Leaching, Rare Earth Precipitation

Abstract

Geomega Resources Inc. (GeoMegA) is currently developing the Montviel Rare Earths/Niobium deposit, located at the north end of the Abitibi region in Quebec. The initial NI 43-101 resource estimate totalled 183.9 million tonnes of indicated resources containing 1.45% TREO in addition to 66.7 million tonnes of inferred resources containing 1.46% TREO. The deposit is dominated by gangue carbonates including ankerite, dolomite, siderite, and calcite. The main REE bearing minerals are Ba-REE carbonates and monazite. Magnetization of Fe-bearing carbonates minerals followed by wet low intensity magnetic separation as well as a flotation only route demonstrated potential for separating REE bearing minerals from gangue carbonates. Excellent REE extractions (~ 99%) from beneficiation concentrates were achieved by hydrochloric acid leaching. Through a series of selective precipitation steps, a final mixed REO precipitate (52% TREE, with Th+U below 15 g/t) was produced at an overall (from ore in ground to final precipitate) REE recovery of 80%.

Introduction

The Montviel Rare Earths/Niobium project is 100% owned by Geomega Resources Inc. The initial 43-101 resource estimate is provided in Table I [1].

This paper discusses the mineralogical and metallurgical testwork performed by SGS Minerals (Lakefield Site) on samples from the Montviel deposit in developing a viable beneficiation and hydrometallurgical flowsheet.

Table I. Montviel Mineral Resource

Resources	Tonnage (million T)		Elements					
			Nd_2O_3	Pr_2O_3	Dy_2O_3	Eu_2O_3	Y_2O_3	Nb_2O_5
Indicated	183.9	Kg/Tonne	2.425	0.755	0.023	0.082	0.072	1.257
		Million-Kg in-situ	446.0	139.0	4.2	9.0	13.0	231.0
Inferred	66.7	Kg/Tonne	2.404	0.751	0.025	0.086	0.078	1.403
		Million-Kg in-situ	160.0	50.0	1.7	3.0	5.0	94.0

Geology

The Montviel carbonatite complex (MCC) is located at the junction between the Opatica and Abitibi sub-provinces in Quebec. The MCC is dated 1,894 Ma and is enclosed in the Nomans tonalite, dated 2,708.9 Ma. The MCC Core Zone, measuring 3 square km, is made of a ferrocarbonatite. The target commodities for the Montviel project are REE (cerium, lanthanum, neodymium, praseodymium, dysprosium, europium, and yttrium) and niobium.

Mineralogy

Advanced mineralogical examination using x-ray diffraction, scanning electron microscopy, electron microprobe analysis, and QEMSCAN^{TM} were completed by SGS on a Master Composite [2]. The Master Composite, composed using samples representative of the Montviel deposit, was ground to 100% passing 75 µm and screened into two fractions: -75+25 µm and -25 µm. Both fractions were subjected to QEMSCAN^{TM} using the Particle Mapping Analysis (PMA) mode. The PMA mode provides a statistically robust population of mineral identification based on x-ray chemistry of minerals. PMA is a two-dimensional mapping analysis aimed at resolving liberation and locking characteristics of a generic set of particles.

Mineral Distribution

Figure 1 presents the mineral distribution of the Master Composite. The Nb and REO bearing minerals are Ba-Ce carbonates, monazite, pyrochlore, and other REE minerals, totalling ~8%. The major gangue minerals are ankerite, dolomite, siderite, calcite, barytocalcite, strontianite, amphibole, biotite, apatite, Fe oxides, ilmenite, and other silicates, totalling ~90%. The gangue minerals are dominately acid-soluble carbonates which would be major acid consumers. A beneficiation process that rejects the majority of the gangue carbonates while retaining the majority of the REO and Nb bearing minerals would be beneficial in i) reducing the downstream hydrometallurgical plant size, ii) reducing acid consumption in the acid leach process, and iii) reducing impurities that would otherwise deport to the leach liquor.

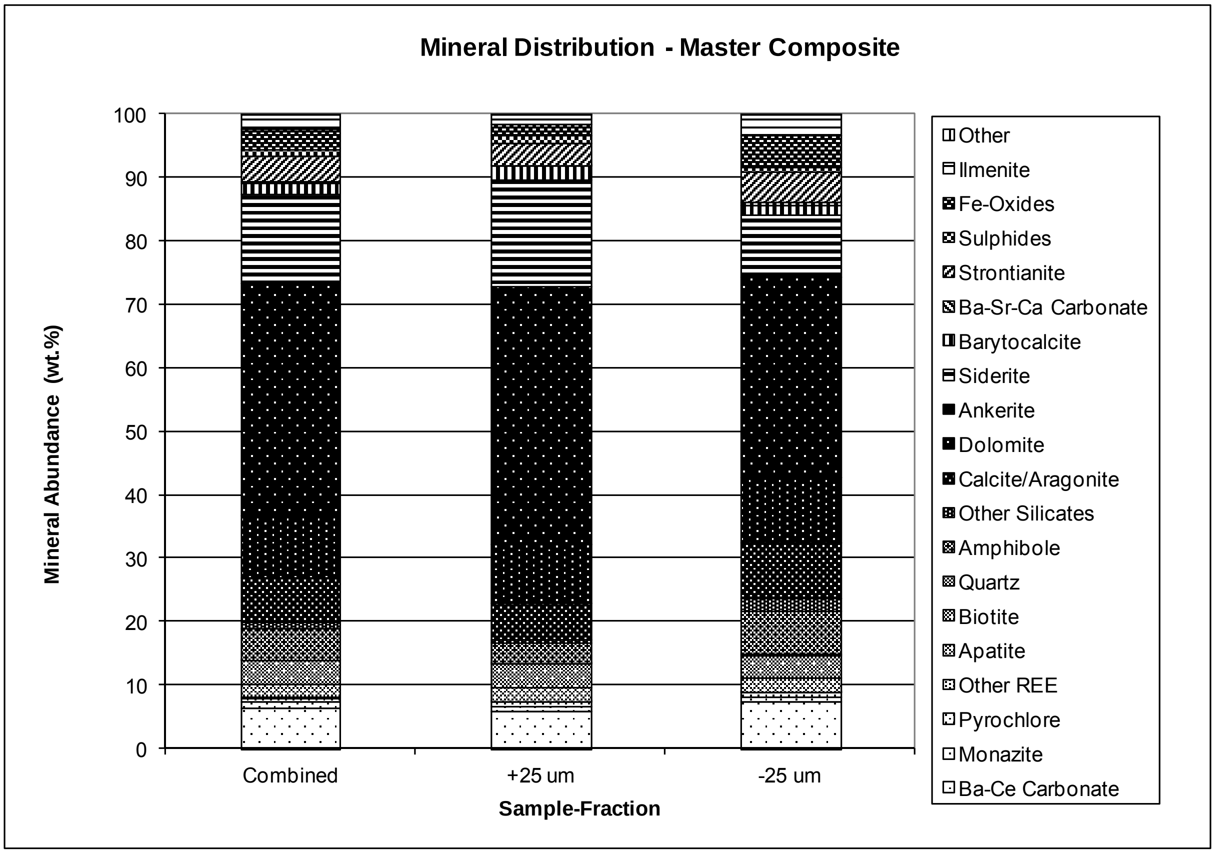

Figure 1. Mineral distribution.

Liberation and Association

Figure 2 presents the major REO minerals liberation and association data. Particles are classified in the following groups (in descending order) based on mineral-of-interest area percent: free (≥95%) and liberated (≥80%). The non-liberated grains have been classified according to association characteristics, where binary association groups refer to particle area percent greater than or equal to 95% of the two minerals or mineral groups. The complex groups refer to particles with ternary, quaternary and greater mineral associations including the mineral of interest.

The REO minerals are very fine and not well liberated at a grind size of 100% passing 75 µm. Monazite is found to be ~10% free (≥95%) and liberated (≥80%) and only improved to ~18% in the -25 µm fraction. The monazite minerals is likely non-recoverable in a selective beneficiation process or if recovered would likely be locked and dilute any pre-concentrate. The Ba-Ce carbonates are much better liberated at ~60% free and liberated. A finer grind would likely improve liberation as the Ba-Ce carbonates are ~67% free and liberated in the -25 µm fraction. Liberation improvement may not be sufficient for effective separation from gangue carbonates.

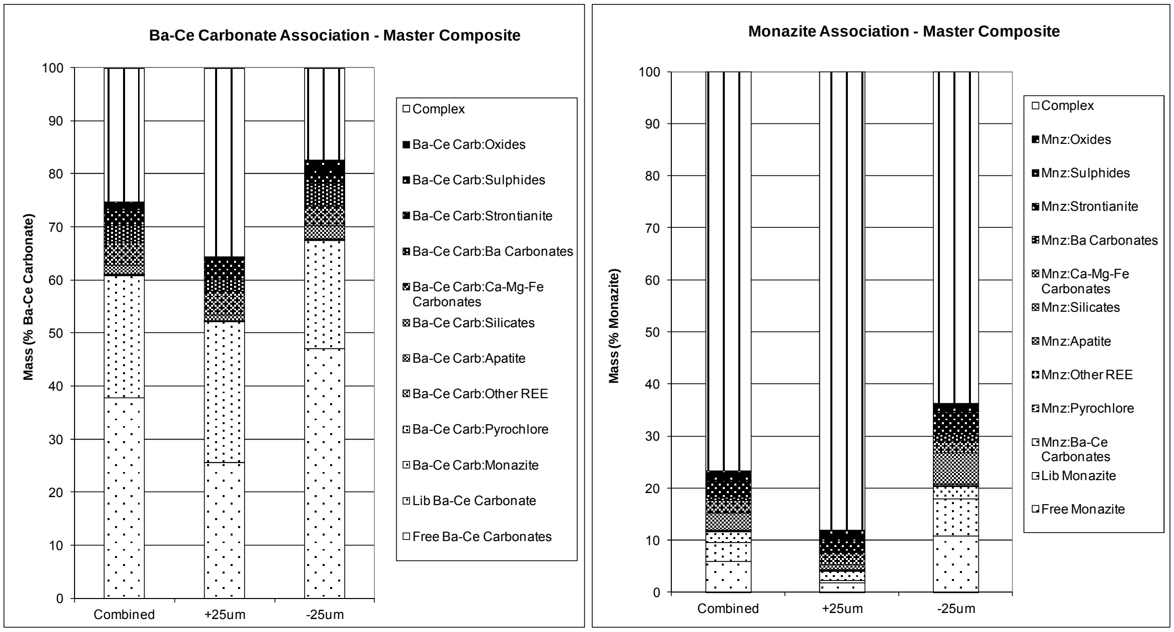

Figure 2. Liberation and Association.

Beneficiation

Beneficiation testwork completed at SGS included a wide range of testing. The three most promising process routes are presented below [3]. It should be noted that results presented in this paper pertain to testwork completed at SGS and do not include testwork completed at other laboratories.

Head Chemical Analysis

Table II. Master Composite Head Chemical Analysis

Composite	Master Comp, %
TREE	1.883
Nb	0.24
SiO_2	4.56
Al_2O_3	0.88
Fe_2O_3	21.3
MgO	7.51
CaO	20.1
Na_2O	0.86
K_2O	0.67
TiO_2	0.59
P_2O_5	0.71
MnO	2.31

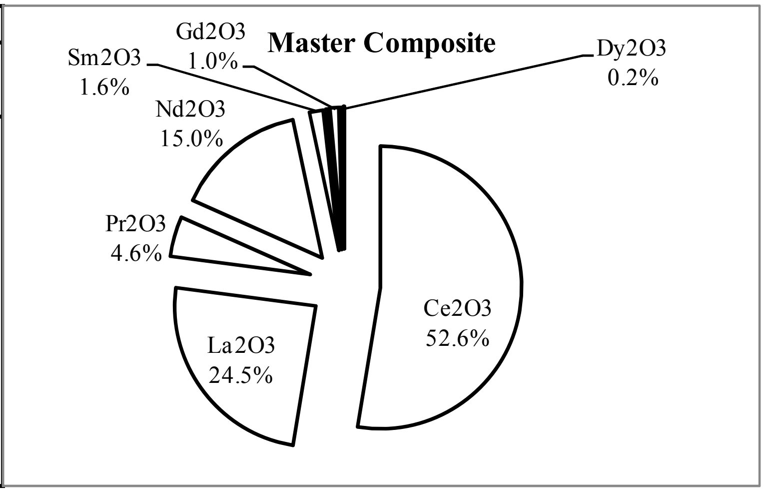

Table II presents the head chemical analysis of the Master Composite. The majority of the REE's present are LRE of which 77% are Ce and La. Neodymium is the most abundant and valuable element. Cerium represents a significant portion of the REE and also is present in the majority of the REO bearing minerals. As such, Ce_2O_3 is used to track REO recovery in all of the beneficiation testwork.

Roasting and Magnetic Separation

Wet low and high intensity magnetic separation from 1-5 kGauss was investigated on the ground Master Composite and on the roasted Master Composite.

Figure 3 presents the amount of Fe_2O_3 rejected in the magnetics under both low and high intensities. Minimum amount of mass and Fe_2O_3 was removed when the ground Master Composite was subjected to low intensity. Under the same low intensities, up to four times the amount of Fe_2O_3 was rejected after roasting. The roasting process appeared to 'magnetize' the ankerite and siderite that would otherwise not be susceptible to magnetic separation at low intensities. At high intensities, both the ground and roasted Master Composite were susceptible to magnetic separation. Upon further optimization to the roasting and wet low intensity magnetic separation process, ~65% Fe_2O_3 was rejected to the magnetics in 46% mass. Up to ~15% each of Nb_2O_5 and Ce_2O_3 was lost.

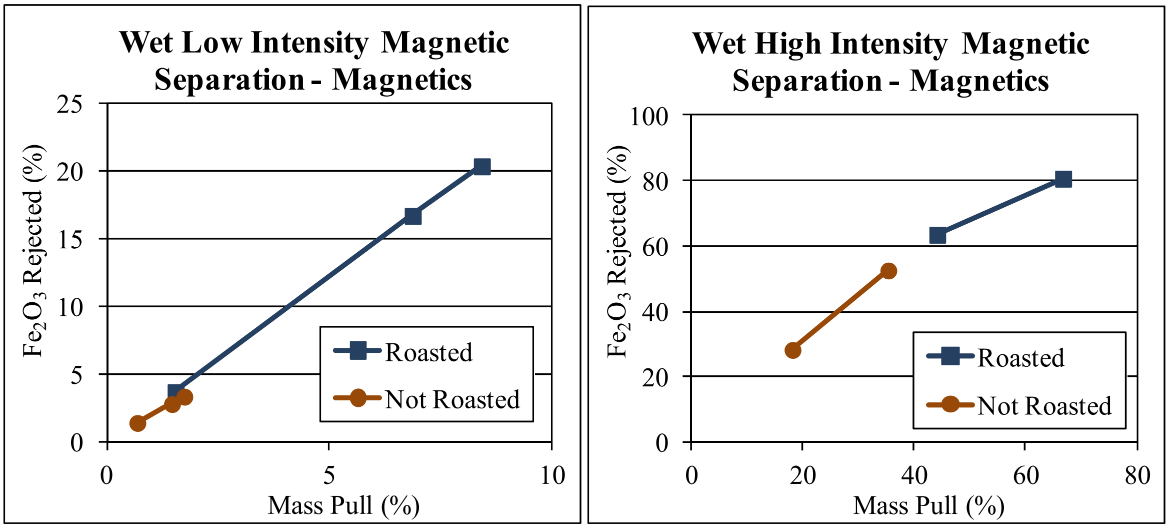

Figure 3. Fe_2O_3 rejection vs. mass pull in magnetics – magnetic separation.

Flotation

SGS completed a total of 15 flotation tests on the ground Master Composite exploring the effects of collector type and dosage, grind fineness, and pulp temperature. Optimum rougher flotation results achieved 73% Ce_2O_3 recovery in 22% mass. Niobium flotation was poor as only 9% Nb_2O_5 was recovered.

Various collector types such as fatty acid (Sylvat FA2), phosphoric acid esther (Clariant 1682), alkylhydroxamate (Aero 6493), salicyl hydroximic acid, and T610 (a derivative of salicyl hydroximic acid) were investigated.

Figure 4 presents the calculated cumulative rougher concentrate recoveries and mass pull relationships. Poor niobium flotation response was observed for all collectors while salicyl hydroximic acid (or T610) demonstrated selective REO flotation.

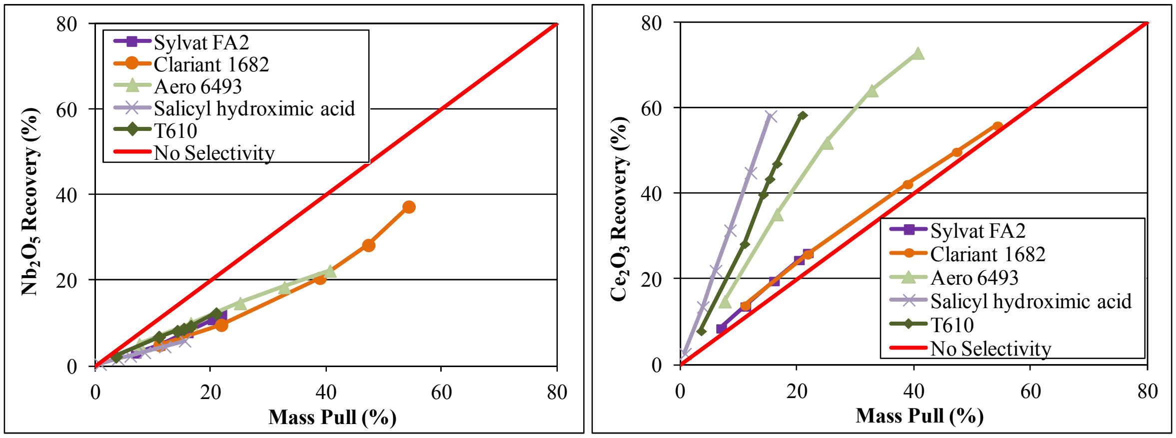

Figure 4. Effect of collector type and dosage.

The effect of grind fineness was evaluated with salicyl hydroximic acid as the collector. As shown in Figure 5, , selectivity did not improve with a finer grind but greater REO recovery was achieved.

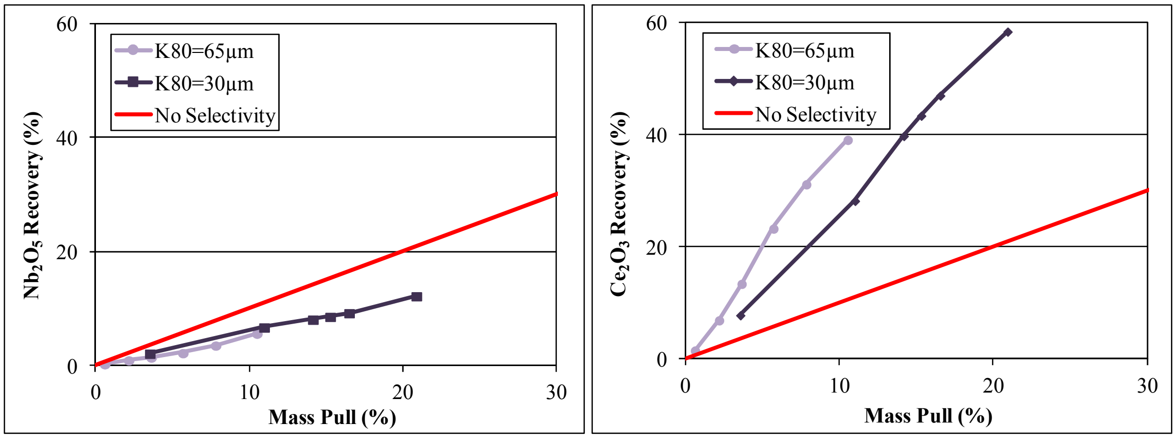

Figure 5. Effect of grind fineness.

Figure 6 presents the effect of pulp temperature. Selectivity did not improve at a higher pulp temperature but a higher REO recovery was achieved.

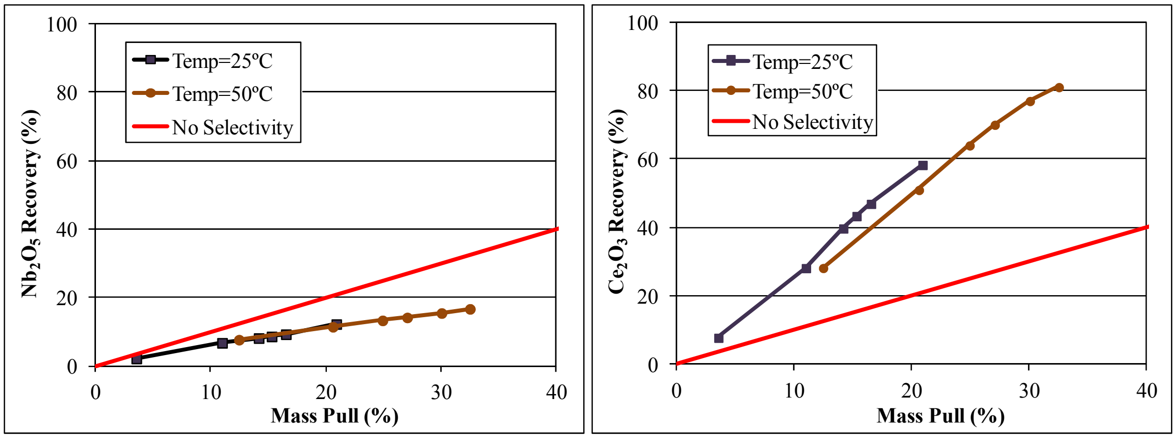

Figure 6. Effect of pulp temperature.

Gravity Separation and Flotation

A combination of gravity separation and flotation was investigated. Limited upgrading was found when using a shaking table on the Master Composite at 80% passing 72 µm. Gravity recovered 32% Nb_2O_5 and 27% Ce_2O_3 in 14% mass. Further cleaning of the gravity concentrate via gravity and magnetic separation as well as flotation observed no exploitable separation. Further niobium and REO scavenging on the gravity tailings by flotation was performed. A combination of alkylhydroxamate (Aero 6493) and fatty acid (Sylvat FA2) was used. Sodium silicate and carboxyl methyl cellulose (CMC) were used as depressants. The combined gravity and flotation concentrate recovered 84% Nb_2O_5 and 74% Ce_2O_3 in 43% mass.

Hydrometallurgy

Hydrometallurgical tests were also conducted at SGS Minerals, Lakefield site. Testing consisted of whole ore leaching, concentrate leaching, leach liquor purification, REE precipitation testing as well as tailing neutralization and acid regeneration testing [4].

Whole Ore Leaching

In parallel to the beneficiation test program, several preliminary tests using the Carbonate Master Comp sample were conducted investigating the possibility of pre-leaching in dilute HCl to selectively dissolve gangue minerals such as calcite and ankerite and producing a high grade leach resdue. However, it became soon apparent that the carbonate composite ore sample was very soluble in dilute hydrochloric acid solution and selective dissolution was not achieved in the pH 1-4 range. In fact at pH 1, around 80% of the REE were already dissolved.

The Carbonate Master Comp sample was subsequently used in a series of whole ore leach / acid bake experiments investigating the use of sulphuric acid leaching (agitated and acid bake) as well as hydrochloric acid leaching to extract REE. Figure 7 shows the REE extraction for 3 whole ore leach experiments. It is apparent that the hydrochloric acid leach system delivered superior extraction (98-99% REE) results at 100 g/L HCl. Typical leach tenors (at low densities of 10% solids) averaged around 2 g/L REE and 55 g/L gangue (20 g/L Fe, 6 g/L Mg, 20 g/L Ca, 2.4 g/L

Mn, 6 g/L Ba/Sr), which led to a gangue/RE ratio of 26. Acid consumption was high 660 kg/t. Nb did not dissolve and concentrated into the leach residue (2.6% Nb). Due to the high acid consumption and high co-extraction of gangue elements, it was evident that pre-concentration of a mineral concentrate was necessary.

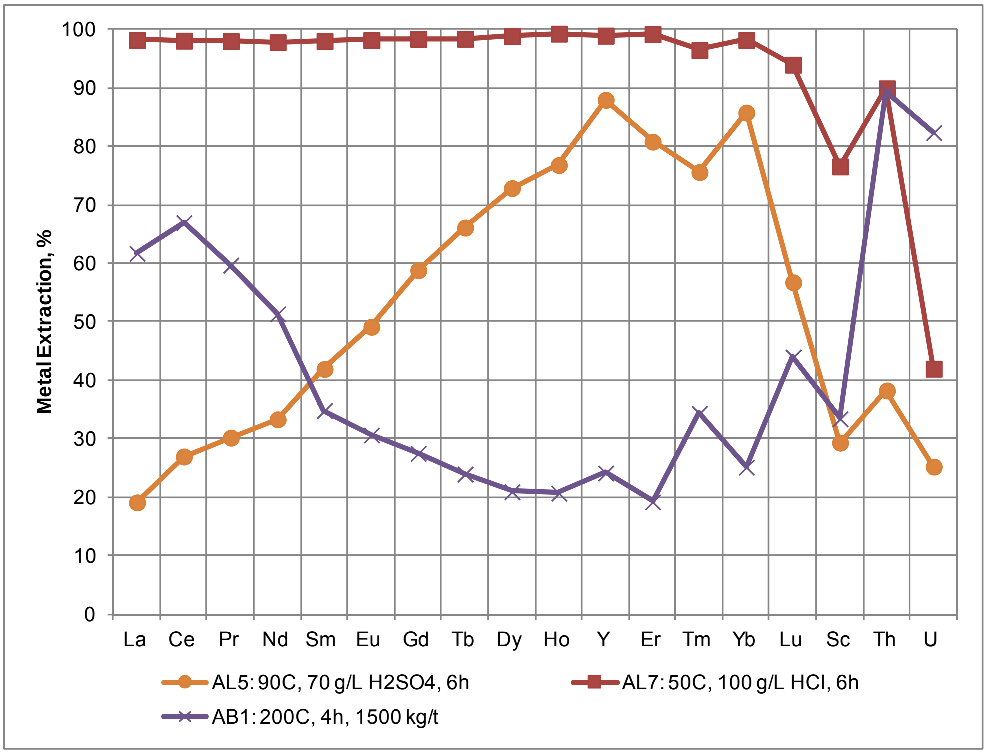

Figure 7. Whole ore leaching / acid baking.

Concentrate Leaching

Several concentrates were used during the concentrate leach work produced at SGS, NRC and Corem. An overview of the concentrates compositions is included in Table III, showing that Nd represents ~ 14% of the total REE.

Table III. Concentrate Composition

%	SGS1	NRC1	Corem1
Fe	16.1	18.5	18.0
Mg	2.40	3.43	2.71
Ca	8.06	9.50	7.79
P	0.13	0.11	0.13
Mn	1.04	1.65	1.60
Si	1.88	2.14	1.88
Ba	7.28	4.24	5.48
Sr	5.35	4.37	4.86
Nb	0.75	0.55	0.61
TREE	5.6	3.9	4.7
rel LREE	98.9	98.7	98.9
rel HREE	1.1	1.3	1.1

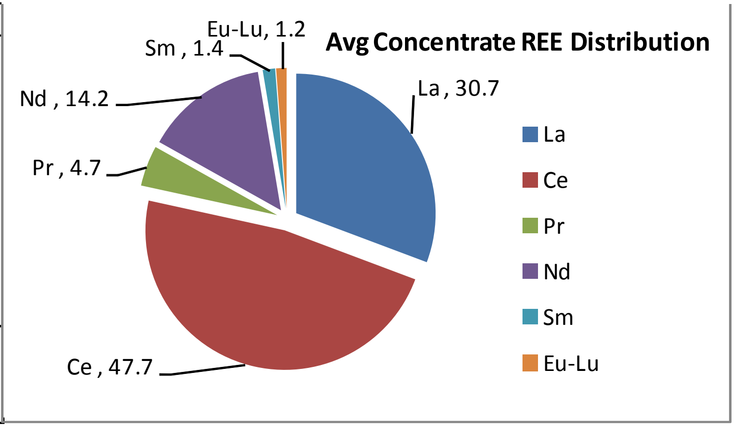

Based on the high extractions observed during the whole ore leaching, concentrate testwork focussed on hydrochloric acid leaching and focussed on optimizing process conditions. Notably several series of tests investigating kinetics, pulp density and acid concentration were conducted.

Figure 8 presents the effect of leach liquor acidity on the extraction of gangue and REE and shows that the concentrate is very reactive even under very mildly acidic conditions. Test AL11 at pH 3.5 was meant as a pre-leach style test with the objective to selectively dissolve gangue elements; however it led to 57% Nd extraction.

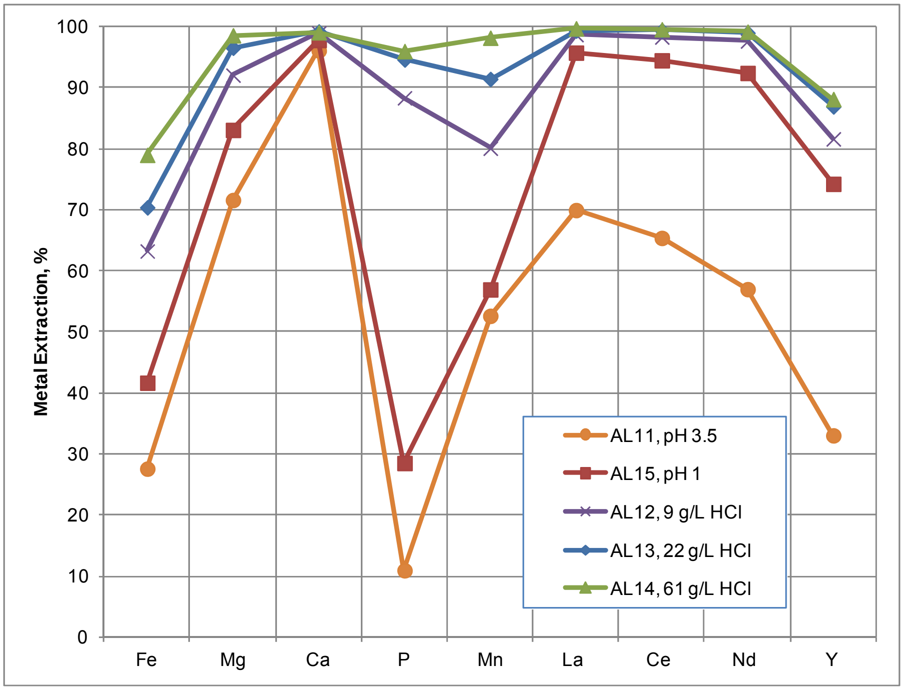

Figure 8. Concentrate leaching – effect of acidity.

Figure 9 shows that leaching at higher densities does not lead to reduced leach extractions, which remained around 97-98% REE. This is a general benefit of hydrochloric acid leaching. At 40% solids (before reagent addition), leach liquor started to crystallize, so further work was conducted at 30% solids and 15 g/L HCl. Under these conditions a PLS was produced with tenors of 12-15 g/L REE and 80-100 g/L gangue cations (~25 g/L Fe(II), ~20 g/L Ca, ~20 g/L Ba, ~15 g/L Sr), equivalent to a gangue/REE ratio of ~6.5 indeed much lower than 26 (whole ore leaching). The leach residue consisted of 28% Fe, 12% Si, 4% Nb, 8% Ti, 0.2% TREE and represented 10-20% of the original concentrate weight. Several bulk tests were conducted under these optimum conditions to produce feed for purification and REE precipitation tests. Acid consumption ranged between 550 and 600 kg of HCl (100%) / t concentrate, which depending on mass pull and extraction translates into a very significant overall net reduction of acid consumption when compared to whole ore leaching (660 kg/t ore).

QEMSCAN mineralogical examination of the leach residue identified the presence of pyrochlore as main carrier of niobium and ilmenite as main carrier of the titanium. It also detected monazite and REE fluoro carbonates as carriers of unleached REEs. Based on the detected degree of liberation, theoretical grade-recovery curves were established for these minerals to investigate if further upgrading of the pyrochlore and ilmenite minerals was feasible. Based on the curves shown in Figure 10, possibilities appear to exist to perform an upgrade of these minerals. The REE minerals were not well liberated and little further upgrading appears feasible.

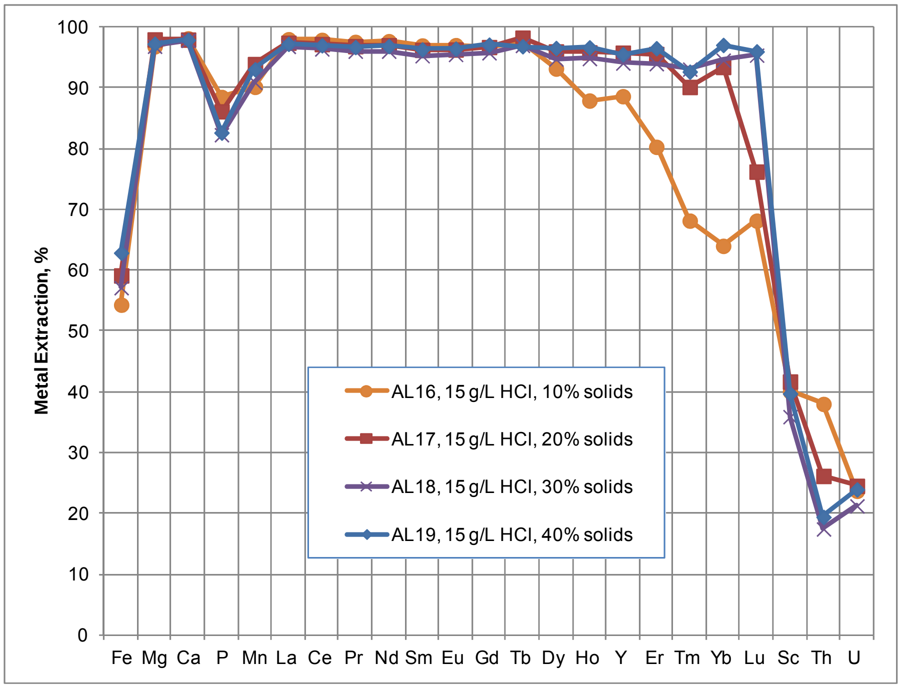

Figure 9. Concentrate leaching – effect of pulp density.

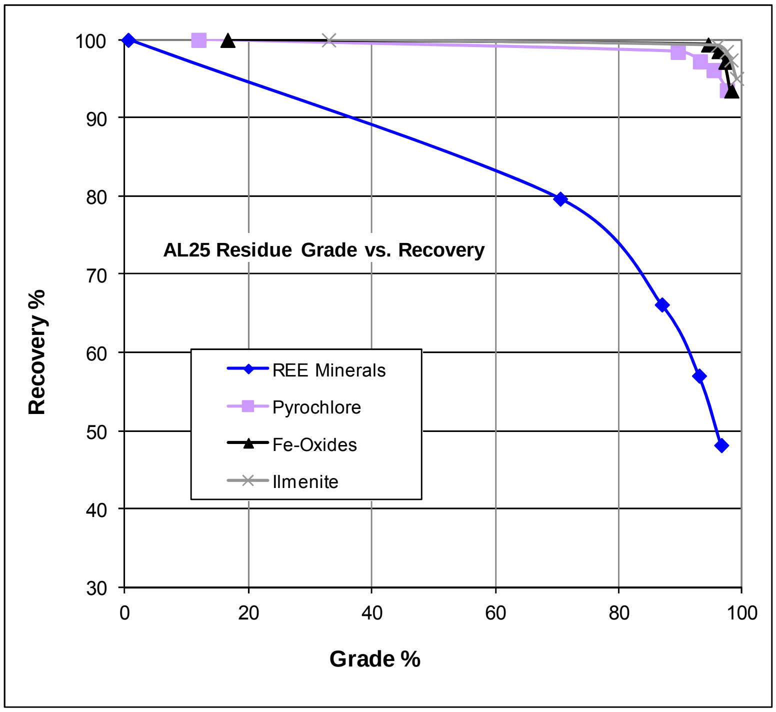

Figure 10. Leach residue - theoretical grade – recovery curve.

Leach Liquor Purification

A typical composition of a bulk leach liquor is shown in Table IV. Leach liquor purification testing focussed on selective removal of Fe, Al and Th, leaving all REE behind in solution. One of the potential routes selected for this consisted of oxidative precipitation of Fe and co-precipitation of Al and Th. While Fe(II) oxidation is relatively easy using NaOCl or H_2O_2, the associated reagents costs prohibit them from being used at large throughputs. Instead testwork focussed Fe(II) oxidation using air or O_2, though bulk tests still used H_2O_2 as a substitute for O_2 to quickly produce feed for downstream tests.

Figure 11 shows the metal precipitation efficiencies of a select few tests. The results show that removal of Fe is successful using either O_2 or H_2O_2 to oxidize Fe(II) to Fe(III) and lime to produce hydroxides of Fe(III), Al, Th and U. It is likely that some of the Fe(III) and Th were precipitated as phosphates as P precipitation was generally high. Purification filtrate compositions are presented in Table V, showing the selective removal of Al, P, Sc, Th and U all in one step. Hydrated lime consumption was calculated to be ~40 kg/m^3 equivalent to ~ 11 kg hydrated lime per ton of concentrate.

Table IV. Leach Liquor Composition

	Leach Liquor Composition, mg/L													
HCl (g/L)	Fe	Mg	Ca	Al	P	Mn	Si	Ba	Sr	La-Sm	Eu-Lu+Y	Sc	Th	U
15	21000	6420	20600	722	302	2460	29.8	15600	13600	14225	178	1.2	49	3.0

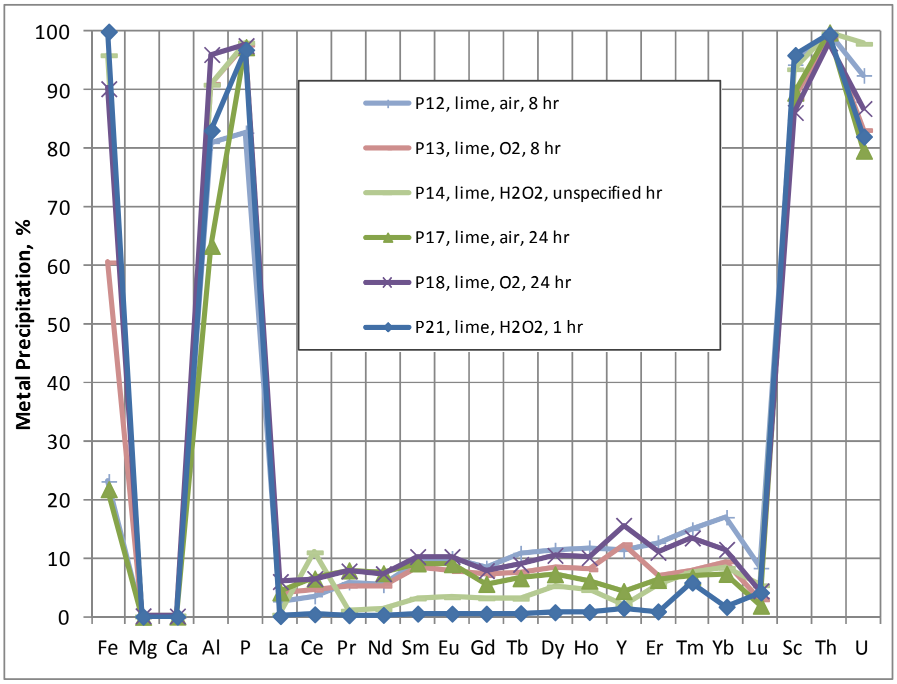

Figure 11. Leach liquor purification.

Iron oxidation using H_2O_2 was fast, but significantly slower using O_2 as is demonstrated in Figure 12, which indicated minimum retention times in excess of 24 hours. It is believed that some of the slow oxidation can be attributed to artefacts of testing in small bench scale apparatus. Larger scale reactors (with higher liquor levels to increase hydrostatic pressure) should lead to improved Fe(II) oxidation kinetics. Nevertheless testing showed that H_2O_2 can be replaced with more economic reagents such as O_2 and perhaps even air.

Table V. Purified Liquor Composition

	Leach Liquor Composition, mg/L													
Stream	HCl (g/L)	Fe	Mg	Ca	Al	P	Mn	Si	Ba	Sr	La-Sm	Eu-Lu+Y	Sc	Th	U
P21 (H_2O_2/$Ca(OH)_2$)	pH 3	<0.7	5650	37600	32.6	<5	2380	22.4	12500	11100	10088	117	<0.07	0.11	0.05
P18 (O_2/$Ca(OH)_2$)	pH 3	936	6420	40500	11.8	<5	2380	17.2	15300	13100	11028	134	<0.07	<0.06	<0.06

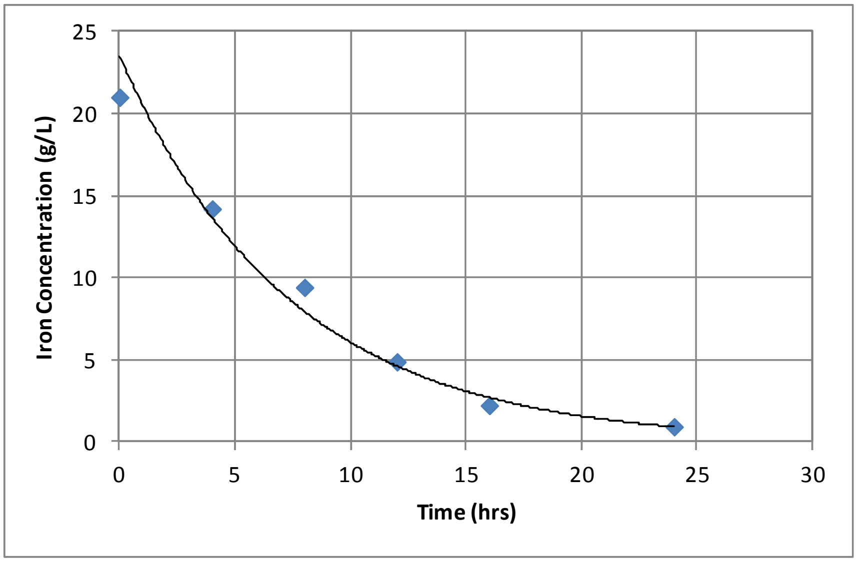

Figure 12. Fe(II) oxidation with O_2 (50ºC, pH 3 HCl).

REE Precipitation

Filtrates from bulk purification tests (similar to test P21 – see Table V) were used in simple bulk REE precipitation tests using amongst others soda ash and hydrated lime. Both reagents worked well (refer to Figure 13) in precipitating REE, but to avoid introducing Na into the flowsheet, final bulk tests were carried out using hydrated lime. A high grade mixed REO product was produced of 52.5% TREE (Table VI) with low key impurity levels (<25 g/t Sc, 9.1 g/t Th, 3.2 g/t U). Other key impurities included 0.35% Fe, 1.7% Ca and 4% Mn. Hydrated lime consumption was determined at ~ 10 kg/m^3 or 2.3 kg/t concentrate. REE filtrate consisted primarily of Mg, Mn, which can be removed by further hydrated lime addition. Ba, Sr and Ca (together 70 g/L) can be reacted with sulphuric acid to produce azeotropic HCl for recycle and a mixture of gypsum and barium / strontium sulphate.

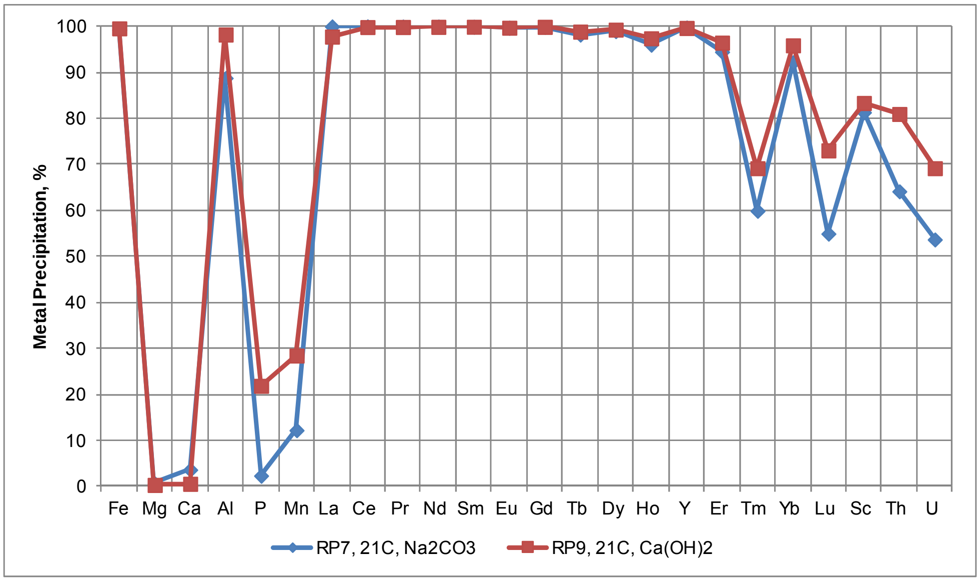

Figure 13. REE precipitation.

Table VI. REE Precipitate Composition

	Fe %	Mg %	Ca %	Al %	P %	Mn %	Si %	Ba %	Sr %	La-Sm %	Eu-Lu+Y %	Sc g/t	Th g/t	U g/t
RP9	0.35	0.14	1.68	0.28	<0.01	3.95	0.89	0.11	0.01	52	0.6	<25	9.1	3.2

Table VII. REE Filtrate Composition

	Fe mg/L	Mg mg/L	Ca mg/L	Al mg/L	P mg/L	Mn mg/L	Si mg/L	Ba mg/L	Sr mg/L	La-Sm mg/L	Eu-Lu+Y mg/L	Sc mg/L	Th mg/L	U mg/L
RP9	<0.2	6150	44700	<0.7	<5	1370	<0.8	13400	11900	39	<0.4	<0.07	<0.03	<0.02

Overall Flowsheet and Recovery

A conceptual flowsheet treating the Montviel ore is shown in Figure 14. Depending on which beneficiation route is selected, an overall recovery from ore to REE precipitate of 83% can be accomplished.

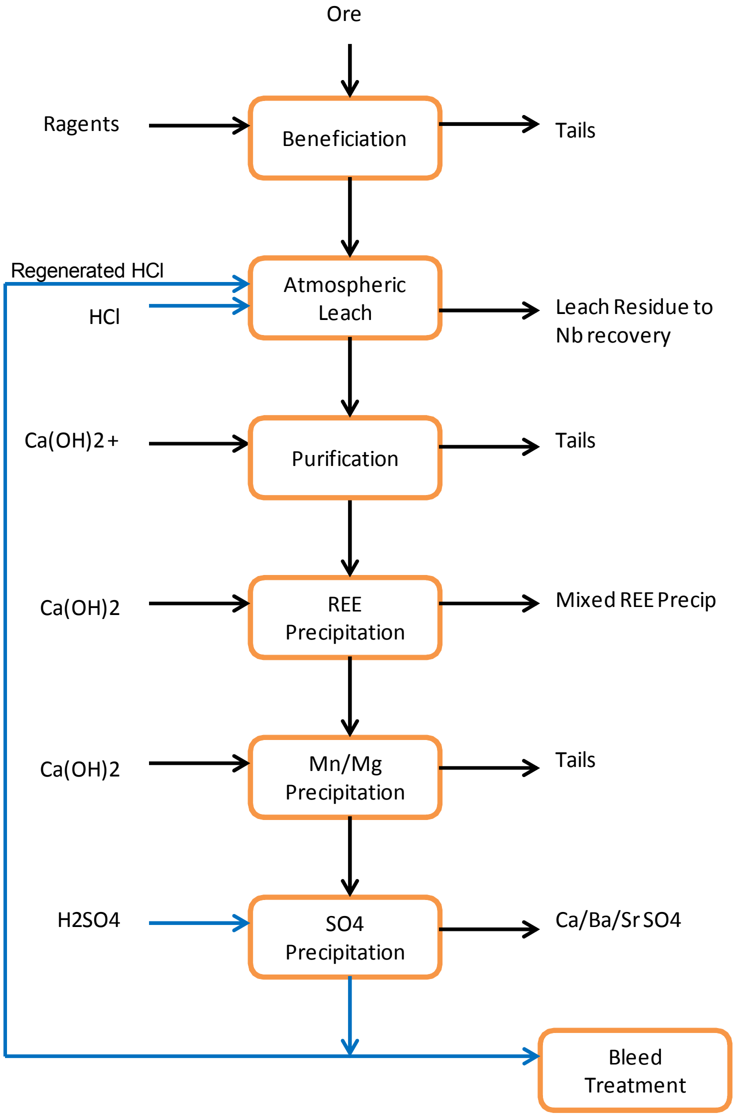

Figure 14. Conceptual flowsheet.

Conclusions

This study demonstrated the potential of processing the Montviel ore from ore to REE precipitate. Advanced mineralogy examination revealed that the valuable REE and Nb bearing minerals are Ba-Ce carbonates, monazite, and pyrochlore. The REE bearing minerals are very fine and poorly liberated. The gangue minerals, although mostly free and liberated, present a challenge for physical separation due to many common properties to the valuable minerals. The gangue minerals are also acid consumers. Several beneficiation processes, roast-magnetic, flotation, and gravity-flotation were developed. The roast-magnetic processes recovered 85% Nb_2O_5 and Ce_2O_3 in 54% mass. The flotation only process recovered 9% Nb_2O_5 and 73 Ce_2O_3 in 22% mass. The final gravity-flotation option recovered 84% Nb_2O_5 and 74 Ce_2O_3 in 43% mass.

The hydrometallurgical testwork showed that the ore and concentrate were very soluble in mildly acidic (15 g/L HCl) hydrochloric acid solutions. Average leach extractions of ~ 98% were routinely accomplished and a partially purified mixed REE precipitate of 52% TREE (with U+Th < 15 g/t, Sc < 25 g/t) was produced through a series of selective precipitation steps.

Acknowledgements

The authors of the paper express their gratitude and appreciation to Geomega management for allowing us to publish this data. Particularly Gary Pearce is acknowledged for his contributions on the roasting and magnetic separation of ankerite from valuable REE minerals.

References

1. Desharnais, G., C. Duplessis, “Montviel Core Zone REE Mineral Resource Estimate Technical Report” (NI 43-101 Report, September 20, 2011, SGS Geostat). Available at www.ressourcesgeomega.ca

2. Grammatikopoulos, T., “An Investigation by High Definition Mineralogy into The Mineralogical Characteristics of a Carbonatite Composite and R9 Roasted and LIMS Mag Samples from the Montviel REE Project” (Report 13378-001, SGS Canada Inc., 2013).

3. Yu, B., “An Investigation into Scoping Level Beneficiation Testwork on Samples from the Montviel Property” (Report 13378-001, SGS Canada Inc., 2013).

4. Verbaan, N., “An Investigation into REE Recovery from Montviel Deposit Sample” (Report 13400-001, SGS Canada Inc., 2013).

DEVELOPMENT OF A HIGH RECOVERY PROCESS FLOWSHEET FOR APPIA'S ELLIOT LAKE URANIUM - RARE EARTH ORE

*John R. Goode[1], Tom Drivas[2], A. Workman[3]

[1]J.R. Goode and Associates
Suite 1010, 65 Spring Garden Avenue, Toronto, Ontario, M2N 6H9
*jrgoode@sympatico.ca

[2]Appia Energy Corp.
25 Adelaide St E., Suite 1010, Toronto, Ontario, M5C 3A1

[3]Watts, Griffis and McOuat Limited
8 King Street East, Suite 400, Toronto, Ontario, M5C 1B5

Keywords: Elliot Lake, Quartz Pebble Conglomerate, Uranium, Rare Earth, Leaching, Flotation, Acid Bake

Abstract

Elliot Lake mines were major producers of uranium between 1957 and 1996 and significant yttrium producers. Appia Energy Corp. is developing its Teasdale Deposit near Elliot Lake and which contains approximately 38.5 Mt of Inferred Resources (237 g/t U3O8, 1,570 g/t TREE) and 13 Mt of Indicated Resources (277 g/t U3O8, 1,650 g/t TREE).

Appia's mineralogical work shows that the U-bearing minerals uraninite, coffinite and uranothorite, cumulatively carry 70% of the yttrium in the ore. The balance of the REE is contained in monazite, a mineral that is not attacked by the agitated leach historically used to recover uranium. Appia has investigated beneficiation and concentrate treatment processes including roasting, acid baking, pug leaching, and pressure oxidation to enhance overall REE recovery. Certain process options offer uranium recovery greater than 90% and REE recoveries between 80% for the LREE to as high as 90% for some HREE.

Introduction

The Elliot Lake camp in Northern Ontario, Canada was a prolific producer of uranium between 1955 and 1996. Thirteen underground mines handled approximately 160 Mt of ore averaging 898 g/t U_3O_8 to produce about 164,000 t of U_3O_8 [1]. The district was also, on an intermittent basis, a significant producer of thorium and rare earths between 1960 and 1990 [2]. Operations in the district were terminated when high-grade open-pittable deposits in the Athabaska Basin were developed.

Appia Energy Corp. (“Appia”), a private company, recognized the potential of the Elliot Lake area for renewed uranium and rare earth recovery operations and acquired property in the district. In 2007 Appia engaged Watts, Griffis and McOuat Limited ("WGM") to undertake a program that eventually included an evaluation of its properties, advise on drilling, preparation of an estimate of the mineral resource, and supervision and interpretation of metallurgical testwork.

As of June 4, 2013, the mineral resources were as summarized in Table I [1].

Table I. Rare Earth Metals and Uranium Mineral Resource Estimate for Teasdale Zone

Category	Tonnes (t)	TREE (%)	U_3O_8 (lb/ton)	Contained TREE (lb)	Contained U_3O_8 (lb)
Indicated	13,095,000	0.165	0.554	47,689,000	7,995,000
Inferred	38,507,000	0.157	0.474	133,175,000	20,115,000

Notes:

1. Mineral Resources, which are not Mineral Reserves, do not have demonstrated economic viability. The estimate of Mineral Resources may be materially affected by environmental, permitting, legal, title, taxation, socio-political, marketing, or other relevant issues.

2. The quantity and grade of reported Inferred Resources in this estimation are uncertain in nature and there has been insufficient exploration to define these Inferred Resources as an Indicated or Measured Mineral Resource and it is uncertain if further exploration will result in upgrading them to an Indicated or Measured Mineral Resource category.

3. The Mineral Resources were estimated using the Canadian Institute of Mining, Metallurgy and Petroleum standards on Mineral Resources and Reserves, Definitions and Guidelines prepared by the CIM Standing Committee on Reserve Definitions and adopted by the CIM Council December 11, 2005.

Following a competition between laboratories, WGM and Appia selected SGS Minerals Services, Lakefield Site (“SGS”) to undertake beneficiation and hydrometallurgical testwork under WGM supervision. Drill core was quarter-cut and dispatched from Elliot Lake, crushed and composited at SGS with testwork commencing early December 2012.

Geology [1]

The Elliot Lake area is underlain by the Huronian Supergroup, a southward-thickening, mainly clastic succession which is well exposed north of Lake Huron. It forms as east-west trending belt overlapping onto the southern portion of the Superior Province of the Canadian Shield. The rock succession is divisible into three megacycles, each composed of coarse-grained fluvial sandstones overlain by glacio-marine/lacustrine mixtites and marine/lacustrine siltstone plus shale with a capping deltaic succession.

In the Elliot Lake district, uranium deposits are found in quartz pebble conglomerates that make up the lowest part of the lowest cycle. The ore-bearing conglomerate beds are found in the Matinenda Formation, the basal unit of the Elliot Lake Group. The uranium-bearing conglomerate is a clean, well-sorted, coarse, quartz-pebble conglomerate which was deposited in a mixed littoral and fluvial-deltaic fan environment. The conglomerate is overlain by and interfingers in a time transgressive relationship with the shallow-marine McKim Formation. Uranium mineralization is stratabound, showing good consistency in grade and thickness over wide areas, both along strike and down dip. The uranium mineralization is readily leachable and high recoveries, typically 95%, were obtained in the operating mines.

Appia's Teasdale deposit is located to the East of the past-producing Denison Mines Limited operations, which together produced about 63 Mt of ore. The Teasdale deposit includes an Upper Reef ("UR") that averages 4.4 m thick, a relatively low-grade Intermediate Quartzite ("IQ") averaging 2.8 m thickness, and a Lower Reef ("LR") averaging 2.7 m thickness.

Samples

Appia and WGM selected drill core to represent the UR, IQ, and LR material. Remaining half core was sawed into quarter core that was shipped to SGS who prepared metallurgical composites of each material type as well as a Master Composite containing appropriate portions of the three individual composites. Analyses for the four composites are presented in Table II.

Table II. Elemental Analysis of Appia Composites

Element	UR Comp	IQ Comp	LR Comp	Master Comp
La	536	259	352	407
Ce	1000	488	681	767
Pr	105	51.7	73.5	81
Nd	328	162	235	254
Sm	54.3	26.2	41.9	42.6
Eu	2.9	1.5	2.7	1.9
Gd	34	15.7	28.5	26.1
Tb	4.7	1.8	4.2	3.3
Dy	20.3	8.6	19.2	16.5
Ho	3.7	1.4	3.4	2.6
Y	76	31	65	62
Er	8.8	3.3	8.2	6.7
Tm	2	0.4	1.3	0.8
Yb	7.1	2.5	5.9	5.2
Lu	2.3	< 0.5	1	0.7
U	218	120	520	270
Th	445	218	350	354
S (%)	1.46	1.04	3.32	1.92

Mineralogy [3]

SGS completed mineralogical examination of the three composites using X-ray diffraction (XRD), QEMSCAN, Electron Microprobe Analysis (EMPA), Scanning Electron Microscopy (SEM) and chemical analysis.

XRD and QEMSCAN showed that all three samples contained about 66% quartz (SiO_2) obviously from the quartz pebbles of the conglomerate. Samples also contained approximately 15% potassium-feldspar ($KAlSi_3O_8$), and pyrite (FeS_2) amounting to 10%, 4.1%, and 2.6% respectively for the LR, UR, and IQ composites respectively. The samples also contained minor graphite and about 10% mica ($K(Mg,Fe)_3Si_3AlO_{10}(OH)_2$) are also present. The distribution of the minerals containing U, Th, and the REE is indicated in Figure 1.

Brannerite is often mentioned as being an important component of Elliot Lake ore. QEMSCAN did not indicate the presence of brannerite but it was tentatively identified during the SEM examination of the samples as either micrometric inclusions in various minerals and local alteration of the U-Th phases.

QEMSCAN demonstrated that the mean grain size of the minerals of interest were below 20 µm in all three composites.

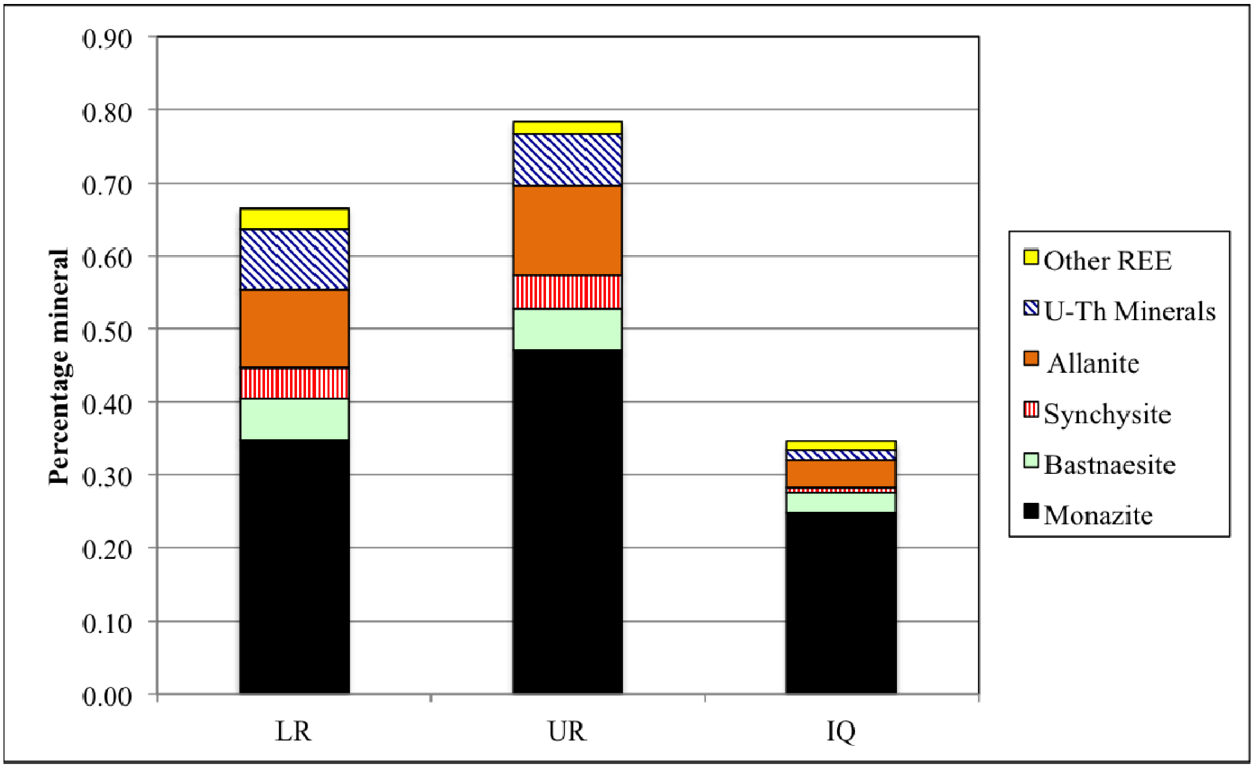

Figure 1. Distribution of U, Th and REE minerals in Appia samples.

EMPA work showed that approximately 70% of the Y was contained in U-Th minerals with the balance in monazite. This distribution agrees well with the historical U and Y leach recovery values for Elliot Lake ore.

Beneficiation [4]

Prior metallurgical data from the Elliot Lake camp, initial hydrometallurgical testwork on Appia samples, and simple economic analyses showed that leaching of whole ore would give good recovery of uranium, reasonable recovery of yttrium but poor recovery of the other REE. In contrast, concentration of the more refractory REE minerals would allow their intensive hydrometallurgical processing and the possibility of high recovery of all elements. Leaching of uranium from flotation tailings was shown to be simple and effective. Hence SGS was directed in a program aimed primarily at concentrating the REE minerals followed by the recovery of pay elements from the concentrate and tailings. Preliminary cost estimates showed that high REE recovery to a concentrate of about 10% mass could be effective.

Earlier literature [5] on the beneficiation of Elliot Lake ore showed that ore sorting and dense media separation could be effective but would not be able to produce the degree of upgrading needed. These methods were therefore not examined in the preliminary work program but could be looked at in the future.

Grinding Work Index

A standard Bond ball mill work index measurement was made using a 150 µm closing screen A metric value of 16.2 was determined.

Gravity Concentration

SGS undertook gravity separation tests on the Master Composite using a Mozley Mineral Separator at grind sizes of 80% passing 208 µm and 80% passing 108 µm. SGS also completed a Wilfley table test starting with material ground to 100% passing 850 µm with the tails ground to -500 µm, re-tabled, tails re-ground to -106 µm and re-tabled. Summary results are provided in Table III.

Table III: Summary Results of Gravity Separation Tests

Test	Conditions	Stream	Distribution, %						
			Mass	U	Th	S	LREE	HREE	TREE
G1	Mozley, 80% past 208	Conc.	6.6	51.5	61.1	84.3	58.7	56.1	58.6
		Conc. + tails -38	25.7	74.7	81.2	94.7	78.6	77.7	78.6
G2	Mozley, 80% past 108	Conc.	5.8	44.8	59.3	81.0	58.0	53.1	57.7
		Conc. + tails -38	37.8	75.2	83.6	94.5	82.3	79.5	82.1
W1	Wilfley, progressive grind	100% past 850 µm	19.9	53.0	59.1	82.9	54.8	48.7	54.3
		+100% past 500 µm	29.0	68.6	75.5	90.6	70.2	62.7	69.6
		+100% past 106 µm	33.0	73.4	80.7	93.3	75.8	67.8	75.2

Notes.

1. LREE are the "light" rare earths including La, Ce, Pr, Nd, Sm, and Eu. HREE are the remaining "heavy" rare earths and Y. TREE is the total REE content, i.e., LREE+HREE.

2. The tails were screened and assayed and enhanced grades found in the -38 mesh fraction hence the combinations shown in Table III.

Magnetic Separation

SGS conducted wet high intensity magnetic separation ("WHIMS") at intensities of approximately 2,000 G (Gauss), 5,000 G, 10,000 G, and 17,000 G on samples of Master Composite ground to 80% passing 208 µm and 108 µm. Results are summarized in Table IV.

Table IV. Summary Results of Magnetic Separation Tests

Test	80% past, µm	Fraction	Distribution, %						
			Mass	U	Th	S	LREE	HREE	TREE
M1	208	0 - 2000 G mag.	2.2	9.1	8.5	7.2	8.1	8.9	8.1
		0 - 5000 G mag.	4.5	23.7	26.3	14.5	29.7	27.0	29.6
		0 - 10,000 G mag.	6.6	44.3	55.4	22.0	60.8	53.9	60.4
		0 - 17,000 G conc.	8.6	61.2	74.2	28.8	78.2	72.2	77.8
		0 - 17,000 G conc.&-38 tail	28.9	74.8	83.8	46.3	85.7	82.4	85.5
M2	108	0 - 2000 G mag.	2.5	8.9	8.8	5.5	8.4	9.2	8.4
		0 - 5000 G mag.	4.9	28.2	35.3	13.8	42.2	35.7	41.7
		0 - 10,000 G mag.	4.9	28.2	35.3	13.8	42.2	35.7	41.7
		0 - 17,000 G conc.	7.6	52.6	64.6	20.9	71.6	62.7	71.0
		0 - 17,000 G conc.&-38 tail	38.5	74.9	81.2	44.5	85.3	80.1	84.9

Froth Flotation

SGS completed twenty batch flotation tests on the Master, UR, IQ, and LR Composites. The collector that was generally used was LR19 which is a blended reagent developed by Lakefield Research (now SGS Minerals Services) for the flotation of Elliot Lake ores in the 1960s [5] and comprising 62% FA2 (a fatty acid), 27% Cytec Aero 855 (a petroleum sulphonate), 9% kerosene, and 2% MIBC. Other collectors that were investigated were cupferron and FS-2 [6] and salicylhydroximate provided by the Tieling Flotation Reagents Factory, Liaoning, China.

Tests with LR19 were shown to be substantially superior to all other reagents when applied to Appia Master Composite. Figure 2 summarizes data for flotation test F6 which comprised rougher flotation and cleaning stages and was done after stage grinding to 80% passing 135 µm. Test F7 done after grinding to 80% passing 80 µm gave identical recovery values. Reagent additions were a nominal 1.5 kg/t of LR19 and 1 kg/t of PQ Metso sodium metasilicate.

Figure 2 shows very high recovery of pyrite and reasonably effective recovery of the LREE at low mass pulls with the HREE and U recovery lagging behind. As discussed later, the lower U and HREE recoveries are not a major concern if the flotation tailings are leached since uranium and HREE dissolution in a tailings leach are reasonably high.

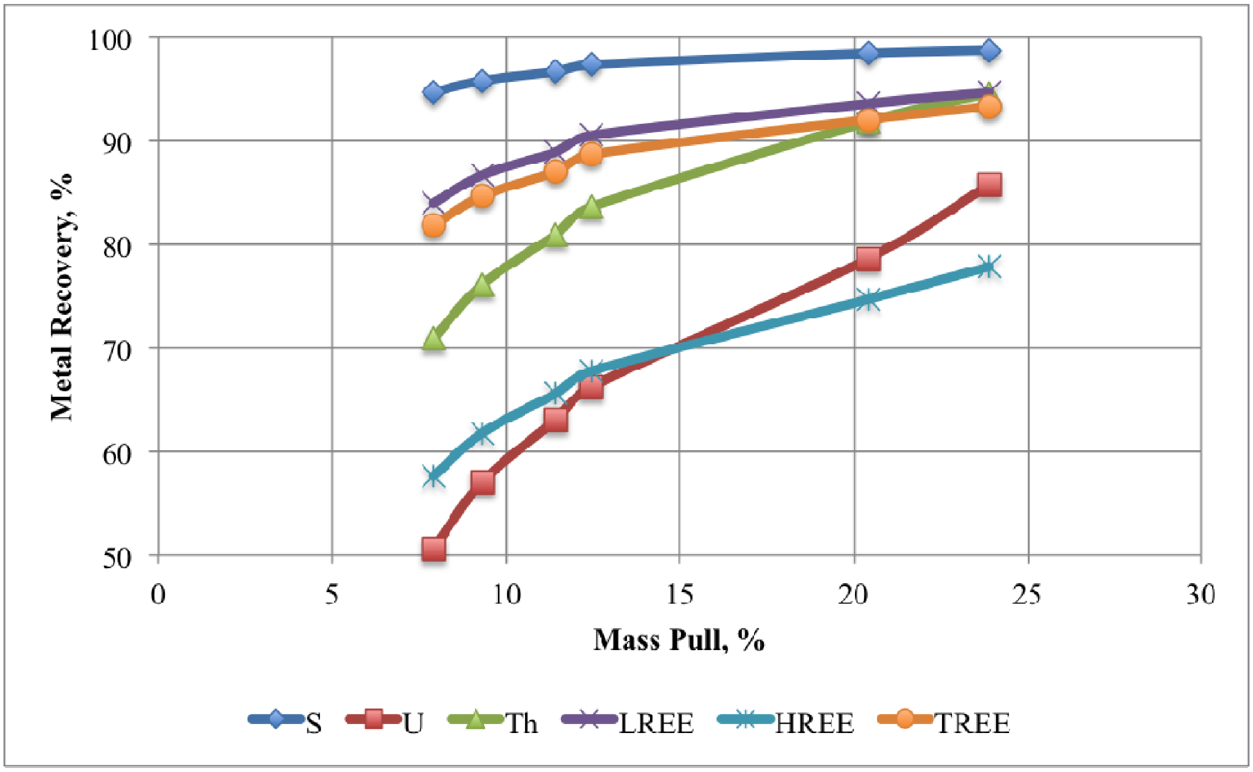

Figure 2. Flotation of Appia ore using LR19 collector.

The LREE and HREE recovery results for a successful beneficiation test (F6) are plotted together with WHIMS and gravity data in Figure 3.

Figure 3 shows that froth flotation performed significantly better at recovering the LREE-bearing minerals which are those requiring an aggressive cracking process. WHIMS performed somewhat better than flotation in recovering the HREE-bearing minerals however that is not too critical given that a tailings leach is reasonably effective at recovering HREE. There may be a case for a hybrid circuit involving flotation and WHIMS or gravity concentration and such possibilities might be investigated at later stages of the project development.

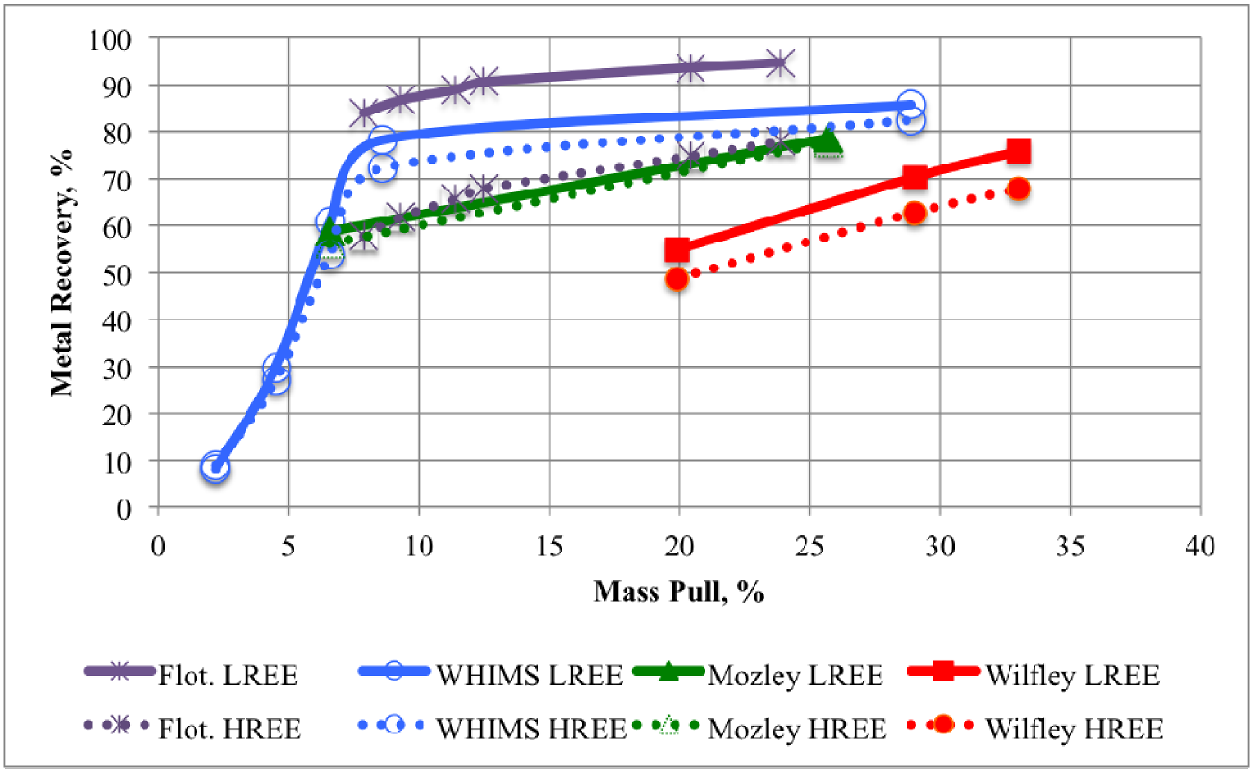

Figure 3. Comparison of beneficiation methods.

Hydrometallurgy

Whole Ore Leaching

Two whole ore leach tests were conducted on ore ground to 80% passing 212 µm and 75 µm (tests AL-1 and AL-2 respectively). In both cases the leach was performed at 80^0 C, 60% solids, with 50 g/L free acid and over 72 h with kinetic sampling. The results for AL-2 are plotted in Figure 4.

The performance of the LREE in test AL-2 (and other tests) indicates LREE precipitation with time. A possible mechanism is the formation of insoluble LREE double sulphates caused by the entry of K and Na into the system by the dissolution of K-feldspar and other minerals. K+Na assays in test AL-2 were 1.3 g/L at the 12 h mark (>90% K, balance Na) and increased to 2.3, 3.3, and 4.1 g/L respectively in the 24, 48, and 72 h samples.

Sc in solids was below the assay detection limit but was found in solution at a level of about 0.002 expressed as a fraction of U assay. Sc caused issues in earlier Elliot Lake REE operations [2] and would need addressing in future plant design.

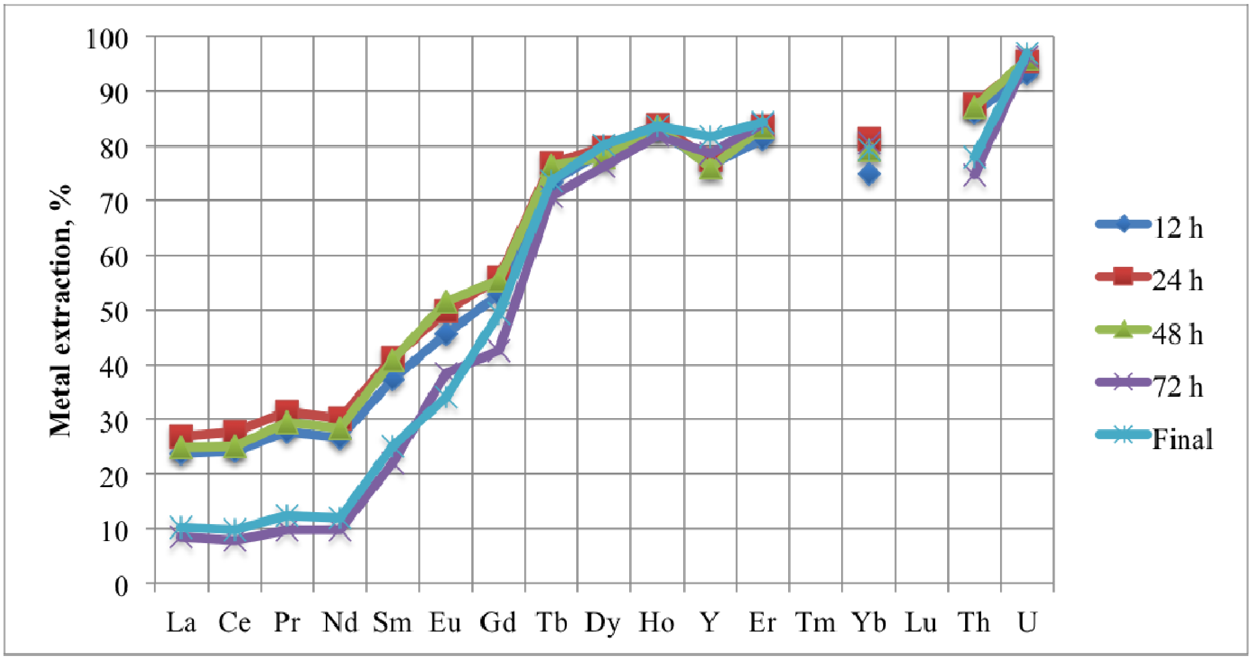

Figure 4. Whole ore leach of Appia ore, 80^0 C, 50 g/L free acid.

Since U leaching seemed to be essentially complete after 48 h, such leach times, or shorter, would be appropriate for maximization of LREE recovery. The acid demand for such leach times were 57 kg/t and 47 kg/t for the coarse and fine grinds respectively.

Flotation Concentrate Leaching

Several different methods of processing the flotation concentrate were investigated including simple atmospheric acid leaching, pressure oxidation in which the pyrite was oxidized to generate lixiviant solution and simultaneously promote metal dissolution, and sulphuric acid baking – a standard way of cracking monazite/bastnaesite minerals.

Agitated Atmospheric Leaching: Flotation concentrate was subjected to a 48 h long, 60% solids, 50 g/L sulphuric acid leach procedure at 80^0 C with kinetic sampling. Not too surprisingly, the U and REE extraction data were very similar to those for the whole ore with about 30% extraction for La and Ce and about 80% for Y and related HREE.

Pug Leaching: In the 1970s, Rio Algom pilot tested the pug leaching of Elliot Lake ore and patented the process [7]. A sample of flotation concentrate was mixed as a paste with sulphuric acid and the resulting pellets held for 24 h at a nominal 80^0 C with moist air passing through the pellet bed. After 24 h, the ore was slurried with water, filtered and the products assayed. Data showed less than 30% U extraction, very low LREE extraction and about 30% HREE extraction.

Pressure Oxidation: SGS was instructed to perform a single pressure oxidation (POX) test on a flotation concentrate containing 814 g/t of U, 5,877 g/t of TREE, and 9.2%S. Test conditions included pre-acidification to pH 1.8 (39 kg/t acid added), a temperature of 210^0 C and an oxygen overpressure of 689 kPa (100 psi). The test was extended over four hours although full oxidation of pyrite and uranium extraction was expected in a shorter period of time. It was speculated that some cracking of refractory REE minerals might also occur given adequate time.

In this test, 88% of the S was oxidized, 98% of the U solubilized, along with 24% of the LREE, and 71% of the HREE. Y extraction was 80% reflecting the close association between U mineralization and Y. Clearly monazite was not cracked during the POX operation.

Acid Baking: Several acid bake tests were performed on various Appia flotation concentrates. Initial tests indicated that a temperature of 200^0 C and an acid addition of 1 t/t concentrate, and a 3 h retention time was satisfactory with an acid consumption of 0.3 t/t, U extraction of 98%, HREE extraction of 90%, and LREE extraction increasing from 60% for La to 90% for Sm.

A pre-leach and acid bake process, simulating a counter-current leach system, was executed in tests AL-7 and AB-6 on a concentrate assaying 780 g/t U and 13,636 g/t TREE obtained from a flotation process (tests F19, F20, and F21) which yielded 10.6% concentrate mass containing 92% of the S, 31% of the U, 79% of the LREE and 50% of the HREE – somewhat inferior results to those of test F6.

The pre-leach required 105 kg/t of acid. The acid bake on the pre-leach residue was done with a 600 kg/t acid addition and at a temperature of 250^0 C for 3 h. The subsequent water leach contained 130 kg/t of free acid which would, in a counter-current system, be more than sufficient for the pre-leach meaning that the fresh acid demand for the pre-leach and bake system is about 600 kg/t of concentrate.

Metal extraction in the AL-7/AB-6 pre-leach and acid bake tests were quite satisfactory as illustrated in Figure 5.

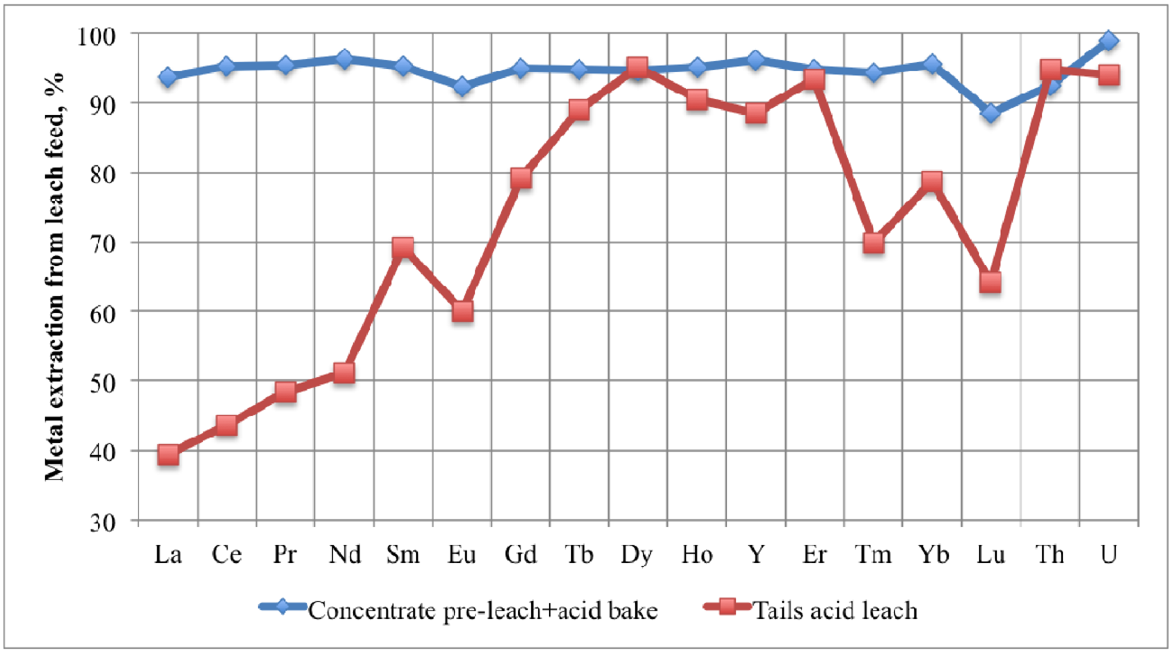

Figure 5. Extraction by pre-leach and acid bake of flotation concentrate and atmospheric leach of flotation tailings

Flotation Tailings Leaching: Samples of the flotation tailings corresponding to the concentrate used in the AL-7/AB-6 pre-leach and acid bake test were leached for 24 h at both room temperature and 50^0 C in dilute sulphuric acid in tests AL-9 and AL-10. The data showed that in both cases metal extraction was substantially complete after just 12 h. Acid demand was about 27 kg/t. The higher temperature leach offered 5% better U extraction and an average of 9% greater REE extraction and so that system was selected. Data are plotted in Figure 5 alongside the extraction data for the concentrate pre-leach and acid bake test.

Solution/Slurry Recovery options and Test Results

In the 1950s and on, efficient U recovery from Elliot Lake leach slurry was readily done using partial neutralization, liquid solid separation ("LSS"), clarification, and strong base ion exchange ("IX") for U extraction. REE were recovered from the IX barren using solvent extraction ("SX") with di-2-ethyl hexyl phosphoric acid ("DEHPA") either directly or after partial removal of ferric iron and thorium by precipitation.

A modern approach to U and REE recovery might include LSS followed by SX for U using a tertiary amine, raffinate solution adjustment, followed by SX for REE using DEHPA or a modern substitute. An alternative approach, offering substantial capital cost savings, would be to dispense with LSS and simply use resin-in-pulp ("RIP") for U as was practiced at many earlier plants, is presently used by Paladin Energy [8], and analyzed and advocated by others [9]. However, to completely eliminate LSS also requires the use of RIP for REE recovery.

Limited testwork was done on post-leach metal recovery. The work showed that neutralization of a clear solution to a pH of 3.5 using MgO would precipitate ferric iron and more than 70% of the Th without significant loss of U or REE. The same procedure using finely ground $CaCO_3$ was far less effective in that although similar levels of ferric iron and Th elimination were obtained, REE losses were significant at pH 2 and were unacceptable by the time pH 3.5 was reached. Limestone precipitation from a slurry, rather than a clear solution could be more effective and will be tested in future work.

A limited amount of IX testwork was done in which a pregnant solution was treated by strong base IX for U recovery and the barren then treated with Lewatit OC 1026 resin for REE adsorption. This macroporous resin has DEHPA incorporated in the resin and so a RIP system analogous to the earlier SX systems could be possible. HREE extraction was high but LREE extraction was low and further work is indicated.

Another option, which was not tested, is the simultaneous extraction of U and the REE by a suitable solvent or resin followed by selective stripping/elution or other means of separately recovering the two products. Further testwork is needed to examine this option and other aspects of U and REE extraction options – both from clear solution using SX and from slurry using RIP.

Flowsheet Options and Overall Recovery

The main flowsheet options available are:

- a simple grind and leach of the Teasdale ore followed by either LSS and SX or RIP for U and REE recovery from solution – sequentially or simultaneously
- a flotation process to recover a high grade concentrate, acid baking of the concentrate and acid leaching of the flotation tailings. This option could be detailed in several ways as follows:
    - separate LSS operations on the acid bake residue and leached tailings and inter-linked SX circuits for U and REE recovery in which weakly loaded extractant from the tailings circuit is passed on to the higher grade concentrate circuit
    - separate inter-linked RIP circuits for the acid bake residue and tailings leach circuits
    - joining the concentrate leach and tailings leach pregnant slurries and recovering U and REE using either LSS and SX or RIP
    - a common U recovery circuit and separate recoveries of dominantly LREE and HREE products from the acid bake and tails leach circuits respectively

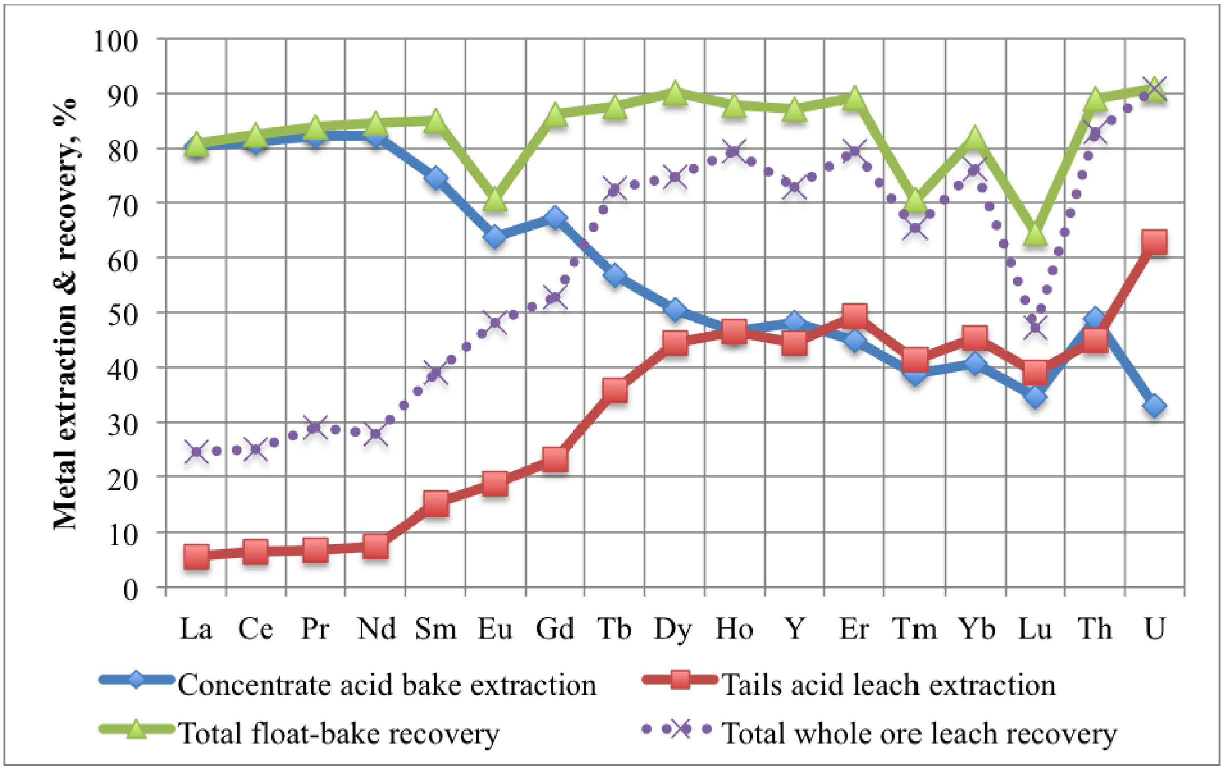

Figure 6. Summary extraction data for float bake and whole ore leach circuits.

The total recovery levels expected from a 36 h whole ore leach on finely ground ore (AL-2), allowing for 5% soluble loss of U and 10% loss of REE, are plotted in Figure 6.

Experimental data for the flotation, acid bake, tailings leach circuit have been combined and are also presented in Figure 6 along with an estimate of the total overall recovery allowing for 5% soluble loss.

Economics

A very preliminary estimate of the capital and operating cost of three process options are presented in Table V. Costs are for the process plant only.

Conclusions

Preliminary testwork and analysis indicates that a flotation – acid bake process route combined with a tailings leach can give high extraction of U and REE from Appia's Teasdale uranium – rare earth deposit. It is believed that planned additional testwork and data analysis will lead to reduced costs and improved recovery.

Table V. Preliminary Production, Capital, and Operating Costs for 7,000 t/d Operation

Parameter	Unit	Leach-Filter U:SX; REE:SX	Float-Bake-Filter U:SX; REE:SX	Leach U:RIP; REE:RIP
Metal recovery				
LREE	t/a	893	2,840	893
HREE	t/a	182	229	182
TREE	t/a	1,075	3,069	1,075
U	t/a	551	551	551
Costs				
Capital cost	M$	$347	$418	$284
Operating cost	M$/a	$75	$110	$74
Operating cost	$/t	$29.21	$43.17	$28.85

Acknowledgements

The mineralogical work was conducted by Tomas Hrstka and Tassos Grammatikopoulos; beneficiation work by Feng Gao, Ben Yu, Yashashree Chaugule, Jason Garbutt, and Dan Lang; hydrometallurgical work by James Brown, Micheal Archer, Krystal Davis; and reports were prepared by Su McKenzie all of SGS. Their efforts are appreciated and acknowledged.

Kurt Breede, Bruce Brady, Gordon Watts and others at WGM are thanked for their contributions. Al MacEachern, formerly of Denison Mines and a consultant to Appia Energy, is also thanked for his input.

We thank company management for their agreement to the release of data.

References

1. Workman, A., and K. Breede, "Report on Geology and Update on Mineral Resources for Appia Energy's Teasdale Deposit, Elliot Lake, Ontario", Watts, Griffis and McOuat Limited, Toronto, Canada, July 2013

2. Goode, J.R., "Canadian Rare Earth and Thorium Recovery Operations. The First 30 Years", *Rare Earths 2012,* ed. J.R. Goode, G. Moldoveanu, M.S. Rayat (West Westmount, Quebec, Canada, Canadian Institute of Mining, Metallurgy and Petroleum, 2012)

3. Hrstka, T., and T. Grammatikopoulos, "The Mineralogical Characteristics of Three Composite Samples from the Elliot Lake Project (prepared for Appia Energy Corp. Project CALR-13849-002)" (SGS Canada Inc. May 8, 2013)

4. Gao, F., and D. Imeson, "Beneficiation Testwork to Assess the Recoverability of Uranium and Rare Earth Elements from the Teasdale Property (prepared for Appia Energy Corp. Project 13849-002 Final Report)" (SGS Canada Inc. June 5, 2013)

5. Grimes, M.E., "Rio Algom Investigations into Preconcentration of Uranium Ore", *Society of Mining Engineers, AIME, Transactions,* 254 (1973), 312 – 318

6. Muthuswami, S.V., et al., "Flotation of Uranium from Uranium Ores in Canada: Part I - Flotation Results with Elliot Lake Uranium Ores Using Chelating Agents as Collectors", *The Canadian Journal Of Chemical Engineering*, 61 (1983), 728 – 744

7. Mather, J.T., "Sulfuric Acid Extraction Of Uranium From Its Ores. United States Patent 4,131,639", Dec 26, 1978

8. Hladun, D., "Startup of the Kayelekera Uranium Mine", *Uranium 2010*, ed. E.K. Lam, J.W. Rowson, E. Özberk, (West Westmount, Quebec, Canada, Canadian Institute of Mining, Metallurgy and Petroleum, 2010)

9. Goode, J.R., and J.A. Brown, "The Michelin Uranium Project, Labrador, Canada: Metallurgical Testwork, Economic Studies And Process Design", *Uranium 2010*, ed. E.K. Lam, J.W. Rowson, E. Özberk, (West Westmount, Quebec, Canada, Canadian Institute of Mining, Metallurgy and Petroleum, 2010)

THE EFFECT OF COMPOSITE LEACHING AGENT ON THE SWELL OF THE WEATHERED CRUST ELUTION-DEPOSITED RARE EARTH ORE

Ruan Chi[1], Zhenyue Zhang[1], Zhengyan He[2], Hui[1] Li, Junxia Yu[1], Zhigao Xu[1]

[1] School of Chemical Engineering & Pharmacy,
Wuhan Institute of Technology, Wuhan 430073, China;

[2] School of Minerals Processing and Bioengineering,
Central South University, Changsha, 410083, China

Keywords: Composite Leaching Agent, Zeta Potentials, Swell of Clay Minerals,
Weathered Crust, Rare Earth Ore

Abstract

The swell of clay minerals in weathered crust elution-deposited rare earth ore is one of the main factors that contribute to landslides and other geological disasters in in-situ leaching of rare earth ores. The effects of the different composite leaching agents on the swelling ratios and swelling kinetic curves of clay minerals were all reviewed to select an efficient leaching agent which could minimize the swelling ratios of clay minerals. Results showed that the best leaching agent was composed of 6% urea, 2.1% NH_4Cl and 0.9% NH_4NO_3. The swelling dynamics model of clay minerals was successfully established as $\delta = A \cdot e^{-B/t}$ where δ is the selling ratio, t is time and A and B are constants. The relationship between the swell ratio and zeta potential of clay minerals in the different leaching agents was also investigated in order to explore the inherent reason causing the swell of clay minerals. It indicated that the swelling ratios of clay minerals were in inverse proportion to the zeta potential of clay minerals.

Introduction

Weathered crust elution-deposited rare earth ore is a unique mineral resource in China with tremendous commercial value. The principal component of the rare earth ore is the clay minerals which account for 40~70% [1-3]. Rare earths are mainly adsorbed on the clay minerals in the form of hydrated or hydroxyl hydrated ions which can be leached by the ion-exchange method. The specific characteristic of the weathered crust elution-deposited rare earth ore make it different to other rare earth ores.

Compared with heap leaching technology, the remarkable predominance of the in-situ leaching technology is because in-situ leaching minimizes damage to the environment. However, clay minerals can swell as they absorb water in in-situ leaching rare earth process which can contribute to landslides and other geological disasters. Cementing materials among the layers can be dissolved by the adsorbed water that can decrease the cohesion of the clay minerals. Furthermore, the dissociation of the hydrogen ion could make the electric charge on the surface of the clay layer more negative that may cause the repulsion effect more intense [4-5]. The two reasons above may account for the swell of the clay minerals.

Currently, many methods are used to prevent the geological disasters by improving the soil body, such as compaction method, chemical amendment, physical amendment, biological amendment, soil replacement and moisturizing method [6]. Among these methods, the chemical amendment is widely adopted in the actual application. However, there are still some problems existed that should be improved and solved. For example, when using lime, a common amendment agent, to modify the soil body, the low cost of lime make it used widely but the effect on the prevention of geological disasters is not so satisfied and the added lime may cause the pollution of underground water and environment [7]; when using potassium chloride to inhibit the swell of soil, a satisfactory effect can be obtained but the introduced impurity and the relatively high cost become an obstacle to wide application [8]. Therefore, it is very necessary to search for a novel anti-swelling agent.

In this study, the effects of different composite leaching agents on the swelling ratios and swelling kinetic curves of clay minerals were all studied to select an efficient leaching agent which could inhibit the swell of clay minerals. An attempt was made to establish a swelling dynamics model. Additionally, the relationship between the swell ratio and zeta potential of clay minerals in different leaching agents was investigated in order to explore the inherent reason causing the swell of clay minerals.

Experimental

All the chemicals in this study were of analytical grade. The experimental weathered crust elution-deposited rare earth ore sample was an original rare earth ore collected from Dingnan County, Jiangxi Province, China. The main chemical composition of the ore sample, passed through 0.078 mm sieve, is listed in Table I.

Table I. The Chemical Compositions of the Ore Sample

Element	SiO_2	Al_2O_3	Fe_2O_3	MgO	K_2O	TiO_2	SO_3	Rb_2O
Content (%)	52.54	28.46	4.64	0.18	4.02	0.34	0.023	0.029
Element	MnO	Y_2O_3	ZrO_2	La_2O_3	Nd_2O_3	CeO_2	Loss	
Content (%)	0.068	0.056	0.064	0.075	0.062	0.055	9.21	

2 g of ore sample which had been treated was subjected to a pressure at 8 MPa for 5 min and the original height of the ore sample was measured using a vernier caliper. Subsequently, the ore sample was placed in the intelligent clay dilatometer (PCY, Xiangtan Xiangyi Instrument CO., LTD) and the anti-swelling agent was injected into the measuring tube. Under 30℃ the height (H_t) and swelling ratio (δ) of the ore sample were monitored for 8 h. The swelling ratio of the ore sample was calculated by the following formula:

$$\delta_t = \frac{H_t - H_0}{H_0} \times 100\% \qquad (1)$$

Where H_t and δ_t is the height and swelling ratio of the ore sample at time t, respectively, and H_0 is original height of the ore sample.

The zeta potential of ore sample in different anti-swelling agents is measured with a zetasizer (Nano ZS, Malvern Instruments Ltd.).

Results and Discussion

The Effect of the Single Anti-swelling Agents on the Swelling Ratio and Zeta Potential

The effect of the anti-swelling agents on the swelling ratio and zeta potential of clay minerals was shown in Figure 1. It is obvious that with the increasing concentration of the leaching agents, the swelling ratios of clay minerals decreased and the zeta potentials of clay minerals increased. The swelling ratios of clay minerals are in inverse proportion to the zeta potentials of clay minerals.

KCl as the earliest anti-swelling agents showed a strong inhibition effect in oilfields [9]. It may be because the ionic radius of K^+ (r=0.133 nm) is similar to the bore radius of hexagonal cavity of Si-O (r=0.13 nm) tetrahedron in the clay minerals. Therefore, once K^+ exchanged H_2O molecule in the hexagonal cavity of Si-O tetrahedron, it would form a closed construction and be hard to be exchanged by other cations. This would prevent H_2O molecules from entering into the cavity [10-12]. However, due to the high cost of KCl, it was unsuitable to be used as an anti-swelling agent in the actual application.

The ionic radius of NH_4^+ is 0.143 nm which is also similar to the bore radius of hexagonal cavity of Si-O tetrahedron in the clay minerals. There was a hypothesis that NH_4NO_3 and NH_4Cl may have the same anti-swelling effects as KCl which is confirmed by the results in Figures 1-3. Consequently, NH_4NO_3 and NH_4Cl could be used as anti-swelling agents to inhibit the swelling of clay minerals.

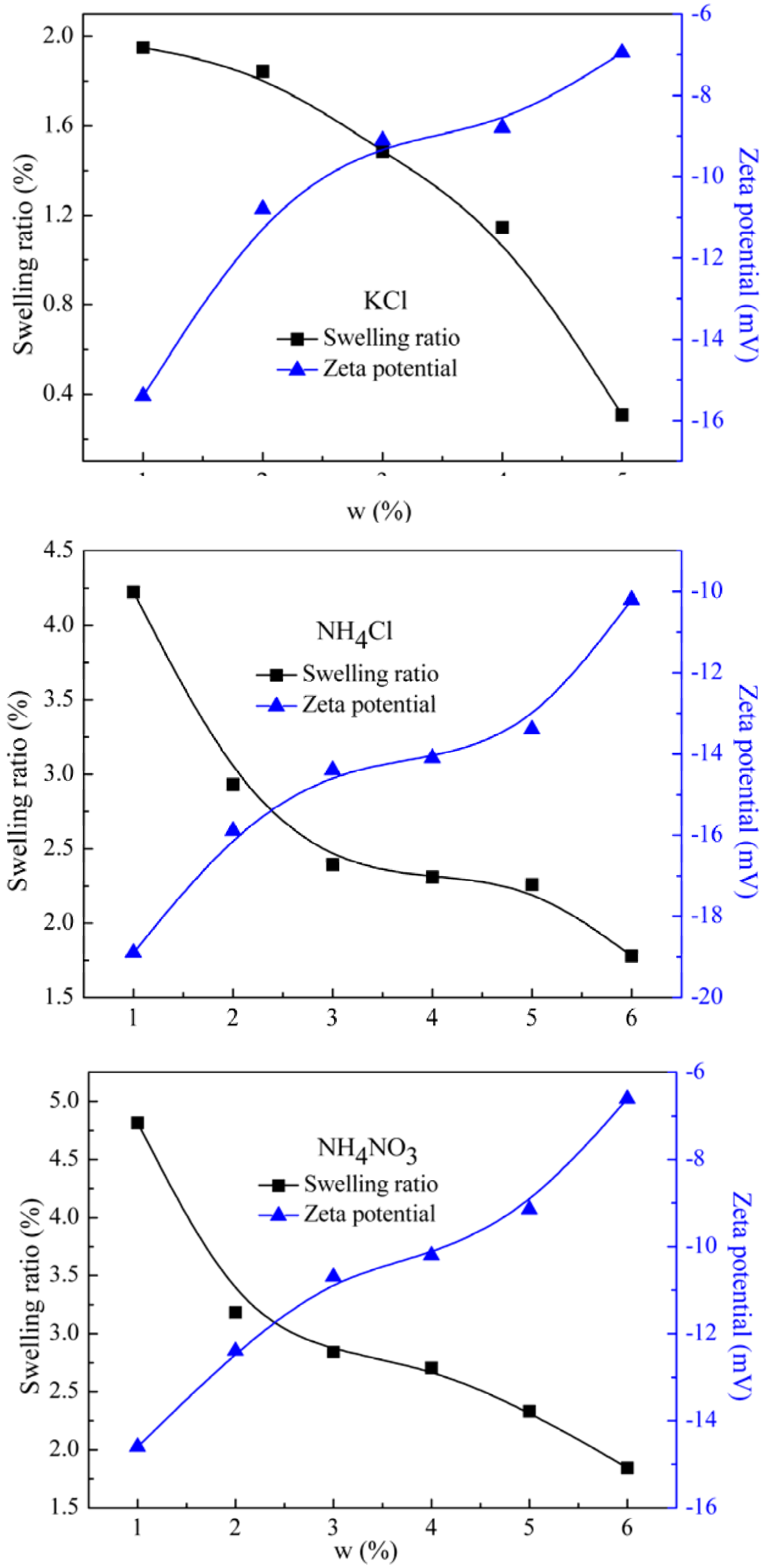

Figure 1. Effect of the Anti-swelling agents on the swelling ratio and zeta potential of clay minerals.

Synergistic Effect of the Binary Anti-swelling Agent on the Swelling Ratio

NH_4NO_3 and NH_4Cl were combined as a binary anti-swelling agent in order to obtain a better inhibition effect on the swelling of clay minerals. Figure 2 showed the synergistic effects of different mass ratio of NH_4Cl/NH_4NO_3 on the swelling of clay minerals when the concentration of the binary anti-swelling agent was fixed at 3%. It can be seen that the optimum mass ratio of NH_4Cl and NH_4NO_3 is 7:3.

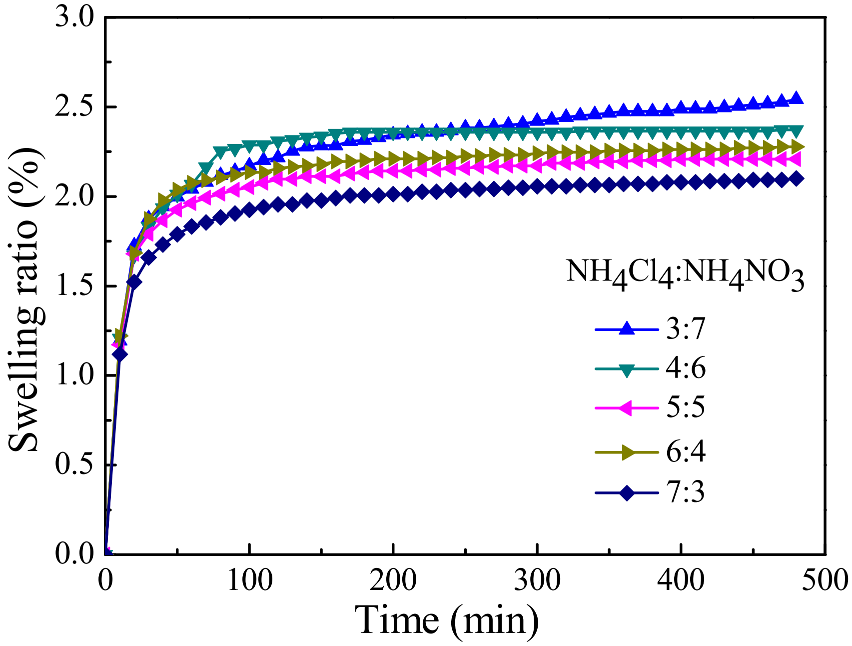

Figure 2. Synergistic effect of different mass ratio of the binary anti-swelling agent on the swelling ratio at 3% total reagent.

Figure 3 shows the effects of different concentration of the binary anti-swelling agent on the swelling of clay minerals when the mass ratio of NH_4Cl and NH_4NO_3 was fixed at 7:3. It indicated that the swelling of clay minerals decreased with the increasing concentration of the binary anti-swelling agent. Consideration of the cost and efficiency of the reagents, the concentration of ammonium salt is commonly controlled at 2%~3% when it is used as leaching agents in situ leaching [13]. Therefore, the concentration of the binary anti-swelling agent at 3% was chosen as a test medium.

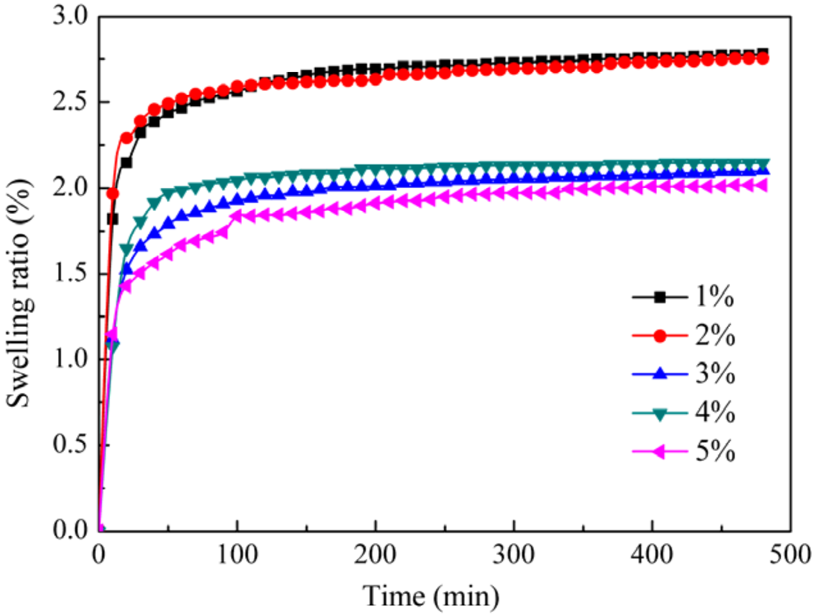

Figure 3. Effect of different concentrations of the binary anti-swelling agent on the swelling ratio - NH_4Cl:NH_4NO_3 fixed at 7:3.

Compared the single anti-swelling agent with the binary anti-swelling agent (in Figure 4), it is obvious that the inhibition effect of the anti-swelling agent is greatly improved after being combined.

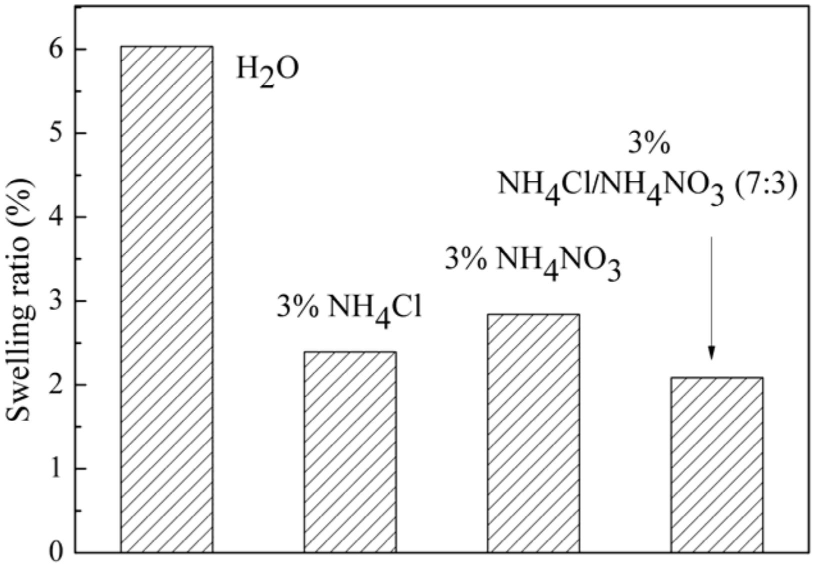

Figure 4. Inhibition effect of the anti-swelling agents on the swelling ratio.

Synergistic Effect of the Ternary Anti-swelling Agent on the Swelling Ratio

According to the results reported by Huang Chun, the NH_2 groups of urea molecules could absorb NH_4^+ specifically to form a complex among the crystal layers of clay minerals that would contribute to inhibit the swelling of clay minerals [8]. Consequently, the binary anti-swelling agent (NH_4Cl/NH_4NO_3) is combined with urea to be a ternary anti-swelling agent. The synergistic effect of the ternary anti-swelling agent with different concentration of urea on the swelling of clay minerals is shown in Figure 5.

It was obvious that the minimum swelling ratio (1.85) of clay minerals can be obtained when the concentration of urea is 6%. Thus, the chosen ternary anti-swelling agent was composed of 6% urea, 2.1% NH_4Cl and 0.9% NH_4NO_3. Comparing the results in Fig. 3 with that in Fig. 4, it can be concluded that the addition of urea would enhance the inhibition capacity of the binary anti-swelling agent (NH_4Cl/NH_4NO_3).

It is well-known that 2% $(NH_4)_2SO_4$ is considered as a good leaching agent and used widely in the actual application of weathered crust elution-deposited ore. The leaching capacities of the studied anti-swelling agents were compared with that of 2% $(NH_4)_2SO_4$. At the same conditions, urea/NH_4Cl/NH_4NO_3, NH_4Cl/NH_4NO_3 and $(NH_4)_2SO_4$ were used respectively to leach the ore samples and the leaching ratios of them were 96.9, 87.0% and 88.7%, respectively. The results indicated that the chosen ternary system could not only inhibit the clay minerals from swelling but also showed high leaching capacities. The chosen ternary system (urea/NH_4Cl/NH_4NO_3) might have potentials for actual application.

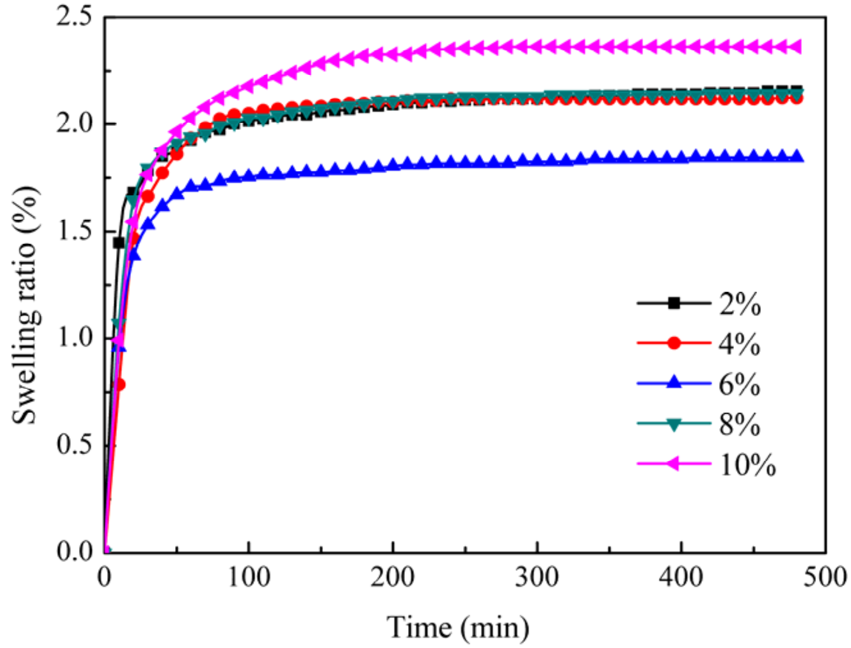

Figure 5. Synergistic effect of the ternary anti-swelling agent with different concentration of urea on the swelling ratio.

Swelling Dynamics Model

From the above swelling dynamic curves, it is obvious that all curves can be divided into two steps, the rapid swelling phase and steady-state phase [4]. A swelling dynamics model was established in order to predict reliably the swelling process of clay minerals. The obtained optimum model is expressed as follows:

$$\delta = A \cdot e^{-B/t} \tag{2}$$

Where δ is the swelling ratio of clay minerals; t is the swelling time of clay minerals; A and B are the constants.

A straight line can be obtained by plotting $\ln\delta$ against t^{-1} with slope and intercept equal to –B and lnA. Using the chosen ternary system (6% urea, 2.1% NH_4Cl and 0.9% NH_4NO_3) as an example, the relationship between the swelling ratio and the swelling time can be presented as in Figure 6. The swelling dynamics model is examined by all the swelling dynamic curves and the correlation parameters are listed in Table II. The high correlation coefficients (R^2>0.9) indicated that the derived swelling dynamics model could describe accurately the swelling process of clay minerals.

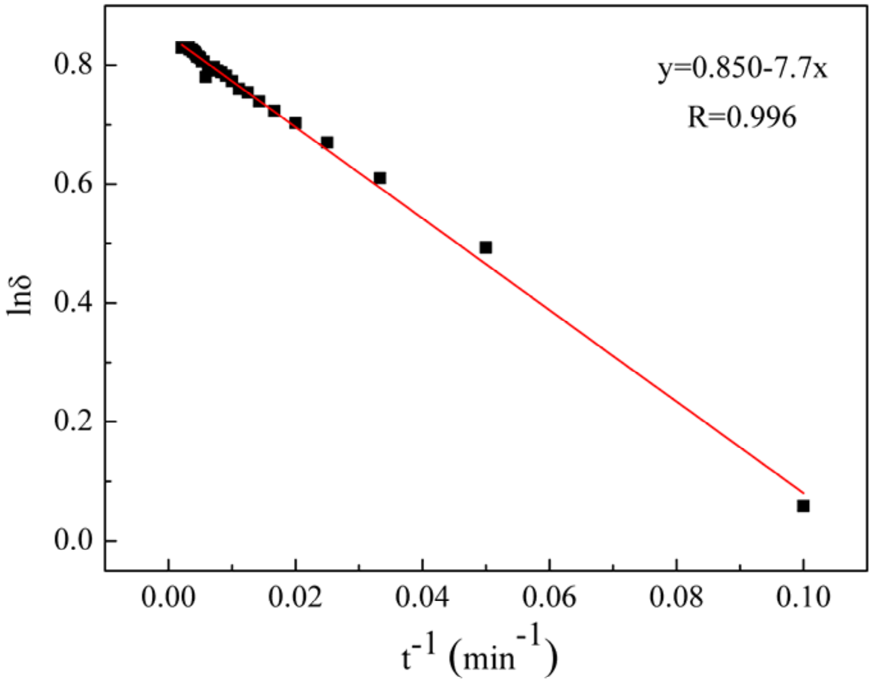

Figure 6. The relationship between swelling ratio and time for the chosen ternary system.

Table II. The Parameters of Swelling Dynamics Model at Different Experiment Conditions (T=30℃)

Experiment Conditions		Coefficients		R^2	Experiment Conditions		Coefficients		R^2
		A	B				A	B	
KCl	1%	1.970	3.310	0.898	CON_2H_4 + 2.1% NH_4Cl + 0.9% NH_4NO_3	2%	2.139	4.425	0.945
	2%	1.843	14.347	0.961		4%	2.205	9.568	0.979
	3%	1.505	9.044	0.940		6%	1.870	6.464	0.995
	4%	1.172	9.197	0.957		8%	2.180	6.734	0.988
	5%	0.324	7.678	0.903		10%	2.416	9.080	0.995
NH_4Cl	1%	4.302	5.411	0.994	NH_4NO_3	1%	4.850	2.200	0.992
	2%	2.897	7.194	0.890		2%	3.150	7.940	0.979
	3%	2.425	6.080	0.982		3%	2.834	6.861	0.980
	4%	2.326	2.493	0.977		4%	2.721	6.687	0.994
	5%	2.223	8.730	0.972		5%	2.366	6.259	0.993
	6%	1.739	4.083	0.850		6%	4.405	6.571	0.944
3% NH_4Cl: NH_4NO_3	3:7	2.458	7.7083	0.937	NH_4Cl: NH_4NO_3 7:3	1%	2.755	4.602	0.952
	4:6	2.411	7.2400	0.983		2%	2.716	3.464	0.944
	5:5	2.220	6.3772	0.990		3%	2.088	6.498	0.984
	6:4	2.288	6.2070	0.996		4%	2.184	6.590	0.983
	7:3	2.088	6.498	0.984		5%	1.980	6.377	0.892

Conclusions

The swelling ratios of clay minerals were in inverse proportion to the zeta potentials of clay minerals. The inhibition capacities of anti-swelling agents in different systems followed the order: single system > binary system > ternary system, and the lowest swelling ratio of clay minerals was obtained using the ternary anti-swelling agents (6% urea, 2.1% NH_4Cl and 0.9% NH_4NO_3). A empirical model of swelling dynamics was established as: $\delta = A\cdot e^{-B/t}$.

Acknowledgements

The work is financially supported by National Natural Science Foundation of China (no. 50974098, 51274152), Program for Changjiang Scholars and Innovative Research Team in University (no. IRT0974).

References

1. Tian Jun, Chi Ruan, and Yin Jing-qun, "Leaching Process of Rare Earths from Weathered Crust Elution-Deposited Rare Earth Ore," *Transactions of Nonferrous Metals Society of China*, 20 (5) (2010), 892-896.

2. Chi Ruan and Tian Jun, "Review of Weathered Crust Rare Earth Ore," *Journal of the Chinese Rare Earth Society*, 25 (6) (2007), 641-650.

3. Chi Ruan et al., "Existing State and Partitioning of Rare Earth on Weathered Ores," *Journal of Rare Earths*, 23 (6) (2005), 756-759.

4. Huang Huaxian and Zhang Chunshun, "Study on Time-Related Characteristics of Expansive Soils Swelling Deformation," *Journal of Hnnnan Unicersitu of Technology*, 23 (4) (2009), 6-10.

5. Yang Hong, Sun Jianrong, and LI Yingquan, "Water-Solubility Macromolecule Solution Applied to Control Clay Swelling," *Coal Science and Technology*, 32 (5) (2004), 58-60.

6. Wang Ming and Han Liwe, "Analysis on Expansion Soil Channel's Landslide and Its Prevention Suggestion," *Journal of Water Resources Architectural Engineering*, 9 (5) (2011), 118-121.

7. Li Zhiqing and Hu Ruilin, "A Modifier to Treat the Landslide of Swelling Earth: China," 200810006959.0. 2008-8-6.

8. Huang Chun, "A Study on the Inhibition of Clay Mineral and the Thermal Stability of Clay Colloid" (Ph.D. thesis, Shandong university, 2003).

9. Dong We, Sun Mingqin, and Chen Lan, "Research and Application of Anti-Clay–Swelling Agent for Acidizing in Oilfield," 9 (4) 2007, 12.

10. Wu Tao et al., "Inhibition of PEG, SDBS and Their Complex on Swelling of Montmorillonite in Aqueous Dispions," *Journal of Shandong University*, 38 (2) (2003), 82-85.

11. E.S. Boek, P.V. Coveney, and N.T. Skipper, "Monte Carlo Molecular Modeling Studies of Hydrated Li-, Na-, and K-smectites: Understanding the Role of Potassium as a Clay Swelling Inhibitor," *Journal of the American Chemical Society*, 117 (50) (1995), 12608-12617.

12. K. Tasaki, "Poly (Oxyethylene)-Cation Interactions in Aqueous Solution: a Molecular Dynamics Study," *Computational and Theoretical Polymer Science*, 9(1999), 271.

13. Huang Chun et al., "Inhibition Behavior of NH^{4+}， Urea and Polyethylene Glycol on Swelling of Montmorillonite," *Acta Chimica Sinica*, 61 (7) (2003), 983-988.

14. Chi Ruan and Tian Jun, Weathered Crust Elution-Deposited Rare Earth Ores (New York, Nova Science Publishers, 2008), 126-127.

A REVIEW ON IRON SEPARATION IN RARE EARTHS HYDROMETALLURGY USING PRECIPITATION AND SOLVENT EXTRACTIONS METHODS

Chen Xia

CanmetMINING/CanmetMINES,
Natural Resources Canada/Ressources naturelles Canada,
555 rue Booth Street, Ottawa, ON, K1A 0G1, Canada

Keywords: Iron, Fe, REE, RE, Rare Earth, Separation, Removal, SX, Solvent Extraction, Precipitation, Hydroxide, Hydrolysis, Jarosite, Hematite, Goethite, Oxalate, Double Salt, Bicarbonate

Abstract

Iron separation from rare earth elements has always been an essential operation in almost all steps of rare earth element recovery and purification processes. As RE^{3+} and Fe^{3+} behave similarly in many operations the separation can sometime be either difficult or cost-inefficient. This article attempts to review the methods and options for removing the iron content within the process, with the focus on the existing or proposed precipitation and solvent extraction technologies. The precipitation of iron from REE solution as iron hydroxide, jarosite, goethite, hematite, or phosphate are briefly introduced. Methods for precipitating REE from solutions leaving iron impurities in the aqueous phase are discussed. Some proposed solvent extraction flow sheets for separating iron from REE are conceptually reviewed in this article.

Introduction

In most hydrometallurgical processes, iron must be removed as waste or separated as a secondary product. Iron control is a mature science with extensive and excellent literature available. The research is especially rich in zinc hydrometallurgy [1,2,3,4,5]. This review will focus on technologies that are used or proposed in the Chinese rare earths metallurgical industry. Due to the limitation on the length of this article, some details, such as operating conditions and figures of flow sheets are excluded. A full version is available as an internal report at Natural Resources Canada, CanmetMINING, Ottawa, Ontario. The technical statements in this article are based on the conclusions in the cited publications and some facts may need to be experimentally verified.

Iron is a common element found in most rare earth ores. It also appears in the intermediate rare earth products at every level of production. Like most rare earth elements (REE), the common valence of iron is +3. This explains the many similarities between iron and REE [6]. In most hydrometallurgical processes, iron is detrimental. It not only contaminates the rare earths but adversely impacts every step of the production process [7,8,9,10,11,]. The iron impurity-tolerance level varies at different production stages, indicating that selecting appropriate iron separation methods for the flow sheet is not a simple task. Typically, the majority of iron reports to iron concentrate stream or rare earths tail in the physical and chemical mineral separation stages [12]. In hydrometallurgy, there are a number of precipitation methods for removing iron, e.g., hydroxide, jarosite, hematite, goethite and phosphate. Some rare earth precipitation methods (i.e., oxalates, carbonates, double salts or fluorides precipitations) are also capable of leaving iron out of the rare earth products. Recent efforts in separating iron are more focused on solvent extraction methods, which may provide better options for large-scale operations in the near future [13].

Physical Separation Methods for Removing Iron

Physical separation is the most important approach for preventing iron from entering the hydrometallurgy circuits. The Baiyunebo mine operation (simplified as Baiyunebo hereafter) utilized magnetic separation to reduce the iron content from 10.1% to 4.9% [14]. Flotation is also an effective way to REE from Ca, Ba and Fe minerals. Usually, a flow sheet combines flotation, gravity separation, electrostatic separation and magnetic separation to obtain a qualified concentrate with rare earth oxides of a grade between 30%~60% [15]. Extensive reviews on physical separation of iron minerals are available in recent publications [16,17].

Precipitation Methods for Iron Removal

As noted earlier, there are a number of precipitation methods for removing iron, which are discussed below.

Hydroxide Precipitation

Through elevating the solution pH to a certain range, Fe^{3+} and many other metallic impurities can be precipitated or co-precipitated. Aeration prior to the precipitation is typically sufficient to oxidize Fe^{2+}. H_2O_2, MnO_2 and $KMnO_4$ are also widely used as oxidants. $KMnO_4$ is sometime preferred when oxidation is required to be controlled quantitatively [18]. The solubility difference between Fe^{3+} and RE^{3+} is the foundation of the iron hydroxide separation process. With the solubility ($-\log K_{sp}$) data of common impurities and REE [19], the initial precipitation pH of metal ions can be predicted [20]. The result indicated that for RE^{3+} to precipitate, the pH shall be generally above 6. Sn^{2+}, Zr^{4+}, $Ti^{4+}$and Fe^{3+} start to precipitate at a pH below 3. Sc^{3+} solubility and initial precipitation pH is similar to that of Al^{3+}. Co-precipitation plays an important role in removing many non-ferrous impurities together with iron. In this article, co-precipitation refers to all possible mechanisms for metallic species to be deposited with iron. Fe and Al can be precipitated in a single step [21]. Si, Mn, U, and Th can also be precipitated together [22,23,24,]. Phosphate anion is removed in this process as iron phosphate, e.g., in the H_2SO_4 acid baking water leach solution, $FePO_4$ is preferentially precipitated at pH 3.5~4.0 before the formation of rare earth phosphates [25].

The settling and filtration of the precipitate is typically difficult. In some cases, an hour-long boiling stage after the addition of alkali is used to enhance the settling rate [18]. The addition of flocculants or surfactants (e.g. sodium butyl naphthalene sulphonate) is another measure for an efficient settling and filtration operation [26]. Rare earth element adsorption onto amorphous iron oxide colloidal or gel is one of the major mechanisms for the co-precipitation valued metals [27]. Elevated temperature will reduce the adsorption of REE as the crystallinity improves and the surface area is reduced. The precipitate with adsorbed rare earths can be re-dissolved with acid followed by an oxalate precipitation which could result in a >98% overall rare earth element recovery [10].

NH_4OH, NH_3 gas, NH_4^+ salts, HCO_3^- salts, are common options for this operation. NH_4OH and NH_3 (gas) are the most popular neutralization agents in the Chinese rare earths industry. NH_3 is used to represent both reagents hereafter. The typical controlled precipitation pH range is 4.5~5.5 [28]. Na_2S is added to bring up the pH to about 5 and precipitate heavy metals as sulfides after the addition of ammonia [28]. The settling and filtration of the produced amorphous precipitate typically requires a flocculant, e.g. PAM (polyacrylamide) at 2~3.5 part per million (weight), or sodium butylnaphthalenesulphonate [26,29]. Ammonia precipitation can be followed by further adding ammonia to adjust the pH to 7.0~7.2 to precipitate heavy rare earth elements (HREE), then to 8.5~9.5 to precipitate all the remaining REE [30]. It should be noted that there are several environmental challenges in the western countries with the use of ammonia and ammonium compounds due to the extreme toxicity to fish and other species.

The advantage of NH_4HCO_3 as the alkali is that this chemical is easier to transport, store and handle than ammonia. Metallic impurities (Al, Fe, Ca, Mg...) are mainly removed in their hydroxide forms. REE may; however, precipitate as carbonate at higher pH. The hydroxide precipitation pH is suggested to be controlled at 4.8~5.0. Iron and aluminum can be mostly removed with Ca and Si partially removed in the process. The Ca^{2+} and Pb^{2+} co-precipitation is more effective in the presence of CO_3^{2-} and HCO_3^- due to the formation of their carbonate salts. The loss of REE is ideally controlled at 2~3%. However, in practice, this number may go up to as high as 10% [31]. Ammonia and ammonium bicarbonate can be used together [32]. NH_3 is used to adjust pH to about 5.0, and then bicarbonate is added to further elevate the pH. In another investigation, it was proposed that ammonia is used to bring the pH up to 4.0~4.5., Ammonium bicarbonate is then added to further adjust pH to 5.0~5.4 [9]. In the study by Yang *et al.*, (2002) the iron removal rate was improved and the REE loss remained below 4.6% [9].

In Baiyunebo, the 2nd generation acid baking process uses milk of lime to precipitate iron. The pH range is controlled at 5.0~5.4 to allow the precipitation of iron and aluminum. Further adjusting the pH to 8.0~9.0 allows the purified REE to precipitate as hydroxides in the presence of crystal seeds [33]. In the caustic decomposition of monazite, the resulting Na_3PO_4 solution contains thorium, uranium and must be treated. In the purification of Na_3PO_4 crystal dissolution leachate, milk of lime is added to precipitate iron and allow U^{4+} and UO_2^{2+} to be co-precipitated [24]. As milk of lime introduce Ca^{2+} ion into the rare earths solutions, the impact of this foreign ion on the following processes must be considered. Rare earth hydroxide can be used as alkali to bring the pH up to 3 before the addition of NH_3. Rare earth carbonate is typically used before the addition of ammonia or ammonium bicarbonate for adjusting pH slowly to 4.0~4.5 [9]. At this pH range, minor amounts of rare earth carbonates remain as solid fine particles. These particles play a role as seeds for iron precipitation. The solution pH is then further adjusted to pH 5.0~5.4 with NH_3, NH_4HCO_3 or hexamethylenetetramine. $CaCO_3$ is a preferred alkali for adjusting pH to about 3.4 and precipitate 99.8% iron from the H_2SO_4 acid baking water leach solution [1]. [Fe]:[P] ratio should be 2~3:1 to allow phosphate to precipitate with iron. Like milk of lime, this chemical introduces Ca^{2+} into the rare earth element solutions. $CaSO_4 \cdot 2H_2O$ as the major calcium species will make the filtration load even higher, and co-precipitate more REE. MgO is more preferable in the practical operations than $CaCO_3$ when removing iron from rare earth H_2SO_4 solution [25] but it is also more expensive and has less impact on the precipitate filterability.

The third generation acid baking process of Baiyunebo, is using $CaCO_3$ or MgO as the alkali, with MgO as the reagent of choice now [25,34]. According to the literature, MgO precipitation produces smaller amounts of precipitate and has lower rare earth element co-precipitation loss. The filtration is also less difficult in comparison to $CaCO_3$ precipitation. A patent described that the calcium or magnesium minerals, hydroxides, or oxides can be thermal-treated to produce calcium or magnesium bicarbonates. The bicarbonate solution is then used to precipitate iron at a lower reagent cost [35].

Oxidative iron precipitation as hydroxide is a proven and versatile technology for separating Fe from rare earths. However, when the solution contains high amount of Ce^{3+}, the Fe^{2+} oxidant may also oxidize Ce^{3+} to Ce^{4+}, and eventually precipitate together with iron hydroxide. One way to minimize this problem is through careful control of the oxidative conditions, i.e., when $KMnO_4$ is used as the oxidant, the Ce^{3+} oxidation can be minimized through accurate control of the amount of oxidant added [18]. Hydroxide precipitation of iron is also limited by the initial iron concentration. High levels of iron (e.g., >5g/L) makes the settling or filtration more difficult and sometime impossible. High iron also increases the loss of rare earths. In recent years, scientific research in iron hydrolysis widened our knowledge of iron hydrolysis procedures. Under hydrothermal conditions, $Fe(OH)_3$ crystallization and α-FeOOH formation are due to a combination of dissolution and precipitation processes, whereas $\alpha\text{-}Fe_2O_3$ particles are formed through dehydration and rearrangement within the primary $Fe(OH)_3$ particles. Raising either pH or the temperature, increases the concentration of soluble iron(III)-containing species and favors the formation of α-FeOOH particles [3,36,37]. The introduction of complexing agents (hydroxy-carboxylic and phosphonic acids or their salts) capable of adsorbing on the surface of the primary $Fe(OH)_3$ particles, reduces $Fe(OH)_3$ solubility, and favors the formation of $\alpha\text{-}Fe_2O_3$ particles. Using these mechanisms to produce larger crystals of iron precipitate will benefit the iron removal process.

Iron Precipitation as Jarosite

In rare earth solutions, Fe^{3+} may form a complex salt upon the addition of Na_2SO_4 at 85-95°C. This method has been reported to be effective for iron removal from a sulfate solution. In HCl solution, iron can be precipitated as jarosite with the addition of sufficient amount of sulfate salts [38]. The crystal is large and the precipitate is easy to settle and filter. An oxidation step is required if any iron exists as ferrous species. Air, oxygen, and H_2O_2 are commonly used for this purpose. The general formula for jarosite-type compounds is $MFe_3(SO_4)_2(OH)_6$, where M can be Na, K, Rb, Ag, Tl(I), H_3O, NH_4, 1/2Pb(II) or 1/2Hg(II). Potassium jarosite is typically the most stable form among these complex salts [39]. Higher concentrations of the REE can be present in the potassium systems without the precipitation of alkali-rare earth sulphate phases, such as $KLa(SO_4)_2 \cdot H_2O$, than is the situation in the corresponding sodium system. However, considering the higher cost of potasium, sodium and ammonium are more frequently used in the Chinese industrial iron control processes [40].

In rare earth solution, this method is implemented at pH values between 1.6 and 1.8 [41]. When jarosite precipitation is used for removing iron from NdFeB barren leachate (after rare earth element oxalate precipitation), the pH is controlled at 2.0~2.5 for 2 hours using NH_4HCO_3. The pH is then controlled at 3.5~4.0 for another 2 hours using NaOH [42]. To facilitate this process, a strict control on the solution pH is critical. In the research of using jarosite precipitation in zinc or copper hydrometallurgy, minor amounts of activated carbon, or $NaNO_2$ was also found beneficial to the overall precipitation performance [43]. After the precipitate is filtered, the crystals can be washed using acid solution to reclaim the rare earths values. A small portion of the precipitate jarosite can be sent back to the precipitation cell to act as seeds for enhancing the crystal growth.

The behavior of rare earths, scandium and uranium incorporation in jarosite (K^+, Na^+, and Pb^{2+}) precipitated from both chloride and sulfate solutions were systematically studied by Dutrizac and Chen [40,44,45,46]. They found that the REE incorporation in jarosite is below 0.3 wt%. Scandium incorporation is significantly higher (2.70 wt%) and the concentration for yttrium; however, is below 0.1 wt%. Uranium does not participate the crystal formation in a significant way. The clear trend observed, however, is that more REE may be deposited when the iron concentration is higher. The aluminum contents may increase the rare earth co-precipitation. Substitution by rare earths can occur in some Al-rich members of the jarosite–alunite group of minerals [44]

The application of jarosite precipitation in rare earth flow sheet is not popular but this process is capable of purifying REE solutions with high iron and sulfate contents. A cited patent described a process in which double salt was used to precipitate REE from an alloy digestion extract followed by further treatment of the barren solution to precipitate iron as jarosite [47]. The process has a longer production circle. Many times, other purification process is required following jarosite precipitation to further reduce the iron impurity level (e.g. 10 ppm (weight)).

Goethite and Hematite Precipitations

Goethite precipitation is also used to precipitate iron from a sulfate or chloride solution. For producing easy-to-filter goethite, the ferric concentration should remain low (e.g. <1g/L, depending on the seeding, temperature conditions). Elevated temperature (typically, 90°C~95°C) is required for acceptable rate of precipitation. Crystal seeds are essential to the formation and growth of goethite crystal as well. Goethite precipitation has also been proposed in REE flow sheet [48]. In the iron separation from NdFeB scrap HCl leachate, goethite precipitation can also be used to precipitate iron, a process for which the optimum pH range is from 3.5 to 4.5[49]. A temperature above 90ºC is not suggested due to the H_2O_2 loss is more significant at >90ºC.

The advantage of goethite precipitation is that the precipitation is fully crystallized and is easy to filter and settle. As, Sb and F are also partially removed together with iron. However, the production circle of goethite process is long and the steam (heat) consumption is high [49].

Hematite is another type of Fe^{3+} precipitate from H_2SO_4 solution. The formation of hematite in an autoclave requires high temperatures and pressures (e.g., 200°C, 1.8MPa). In practice, the iron sulfate solution pH is controlled at 4.0~4.5. No study on the application of hematite precipitation for REE purification was found in the literature.

Iron Phosphate Precipitation

Iron phosphate precipitation is a comparatively newer precipitation method. In zinc hydrometallurgy, this method appeared to be effective (98%~99%) [50]. In addition, the precipitate is easy to settle and filter. The production circle is short and the energy consumption is on the low side in comparison with the other competing processes. Iron phosphate is formed at about pH 2. As REE tend to form phosphate precipitate, adding phosphate for direct removal of iron is not reported by the rare earth industry. At the same acidity; however, iron phosphate ($FePO_4$) precipitates before the formation of rare earths phosphates. Thus, phosphate anion should be able to be used to separate iron and REE. In a test process that was conducted on the purification of rare earths/H_2SO_4 solution at pH 3.5~4.0 with $CaCO_3$ or MgO as the pH regulator the optimum Fe:P ratio was set at 2~3 to 1 [25].

Rare Earths Preferential Dissolution in Acid

REE can be separated from iron by preferential dissolution of REE using an acidic solution at a controlled pH. A patent described a process where REE, iron and some other impurities are precipitated as hydroxide at pH 7. Concentrated HCl is gradually added into the precipitate (hydroxide) reactor. To preferentially dissolve REE leaving iron and other impurities in the residue, the pH is accurately controlled between 4.5 and 4.8 [54]. Preferential dissolution can also be used to separate rare earth oxides and iron oxide. In the processing of NdFeB scrap, a full oxidative roasting step allows all iron to be oxidized into Fe_2O_3. The roasting residue is gradually contacted with HCl. Under a controlled pH range, it is possible to dissolve REE leaving most of the iron in the leach residue [52,53]. Preferential dissolution can also be applied to the Baiyunebo caustic baking product. The high grade (>50% rare earth oxides) concentrate is roasted in the presence of NaOH at 300°C. The residue is mainly hydroxides of various metals. The residue is treated with HCl for selectively dissolve non-cerium rare earths and some Ca residue. Fe, thorium, and cerium and minor portion of REE are left in the solid phase [54]. It must be noted that Ce^{4+} is not behaving like most other REE and may stay in the solid phase with iron during the preferential leach.

Double-salt Precipitation of Rare Earths

Selectively precipitating REE is another approach for separating iron. Double salt precipitation is known for the capacity to recover REE as crystals that are easy to settle and filter. REE form double sulfate salts in sulfate solutions with another metal ion (i.e., Na^+, K^+, or NH_4^+) [55]. Under a properly controlled condition, most impurities are left out of the rare earth double salt. In the double salt precipitation from the monazite with H_2SO_4 acid baking water leach solution at ambient temperatures, when Na_2SO_4:REO ratio is controlled at 4:1, about 98%~99% REE are precipitated as double salt. 1%~2% HREE value is left in the solution. The double salt is determined as $1.3Na_2SO_4 \cdot RE_2(SO_4)_3 \cdot 4H_2O \cdot 0.09Th(SO_4)_2$ [48]. About 50~60% thorium is co-precipitated under this condition.

Below pH 6, iron stays in the solution phase as ferrous sulfate, It is, therefore, beneficial to avoid strongly oxidative condition that oxidizes ferrous species into ferric forms [56]. In the processing of NdFeB scrap, the H_2SO_4 leachate containing Fe and REE also can be separated using double salt precipitation method [57]. In comparison with a double-oxalate precipitation process, the overall Nd_2O_3 recovery in the double salt process is 4% higher (82.1% vs. 78.1%). The iron content in the rare earth oxides product is also lower.

In comparison, the double salt precipitation method is more favorable when the solution iron content is high. Such a solution is not suitable for hydroxide precipitation process. Consequently, the double salt precipitation technology was used in the Baiyunebo first generation acid baking process for isolating REE from iron H_2SO_4 solution [34,58]. This method is regarded in China as an effective and cost-efficient one in small or medium scale production. This process is less attractive in large-scale operations [52,57].

Rare Earths Precipitation as Oxalates or Carbonates

REE-oxalate precipitation is a major method for purifying and recovering REE from either chloride or sulfate solutions (Equation 1).

$$2RE^{3+} + 3H_2C_2O_4 = RE_2(C_2O_4)_3 + 6H^+ \tag{1}$$

According to Equation 1, the precipitation of metal oxalate is largely decided by the reaction pH. The pC-pH diagram of Me-oxalate systems could be used to determine the optimum precipitation pH of oxalate [59]. It was found that higher pH is responsible for higher rare earths precipitation rates. Lower pH is beneficial to the rare earths oxalates purity. Metal impurities co-precipitate with REE-oxalate and contaminate the precipitate; they also consume oxalate by forming oxalate salts and complexes. Rare earths also form double salts with $Al(C_2O_4)_3^{3-}$ and $Fe(C_2O_4)_3^{3-}$ and result in further loss of REE [8]. If the purpose is to obtain REE crystals to produce marketable REO, the solution must be purified in advance using neutralization method, which can remove the majority of the iron.

In the separation of iron from an NdFeB leachate [42], REE are precipitated. Iron in the filtrate can be further treated with various precipitation methods to obtain a by-product. Oxalate precipitate may contain significant impurities; therefore, the double oxalate precipitation method is used to produce a purer Nd_2O_3 product [57]. Another application of oxalate precipitation process is to recover REE lost in the Fe-Al hydroxide precipitate due to the REE solution purification step. This is especially useful when the rare earth element loss is significant.

The oxalic/oxalate precipitation process faces challenges, such as the toxicity of the reagents as well as high reagent consumption which has made it a less popular in China than the bicarbonate precipitation method [13]. Typically, NH_4HCO_3 is used to precipitate rare earths as $RE_2(CO_3)_3$. Iron precipitation as hydroxide with RE-carbonate is possible, especially when the pH is above the optimum level. Therefore, a neutralization precipitation step is typically used to remove the majority of iron before the carbonate precipitation step [10]. Research also indicates that without a proper control, the rare earth element carbonate precipitate is amorphous, which will be difficult in solid-liquid separation. Crystalline precipitation of rare earth element carbonate is possible through controlling the temperature at 20ºC~40ºC, NH_4HCO_3:RE=3.0~3.6:1, rare earth concentration 0.85~1.6 g/L, agitation time 45~90 min, and settling time 9~10 hours [60]. More importantly, an easy-to-settle precipitate can be obtained through removing the majority of impurities with hydroxide precipitation method before the carbonate precipitation [13]. The use of centrifugal solid-liquid separation is also significantly beneficial. The overall Fe and Al removal reached 95% and 98% respectively. The rare earths recovery is close to 100% [8].

Solvent Extraction Methods for Iron Separation

Secondary Carbon Primary Amine Extraction Agent (RNH_2, N_{1923})

N_{1923} is capable of separating thorium and iron from rare earths sulfate solution at low acidity [61]. Both REE and iron are left in the raffinate of the extraction circuit. One option is to add elemental iron to reduce Fe^{3+} to Fe^{2+} in prior to the extraction because Fe^{2+} is not extractable with N_{1923}. Another option is to scrub iron off the loaded organic. The presence of phosphate anion is critical to the success of iron separation from REE. Phosphate anion can be added in the extraction step to reduce the iron loading. In the scrubbing step, H_2SO_4 is used together with H_3PO_4 to ensure all iron is completely scrubbed off. Following N_{1923} iron removal, the REE loaded organic is stripped with HCl. After N_{1923} iron removal, the sulfate anion is further removed from the loaded strip solution through a naphthenic acid (NA) solvent extraction (SX) that will further reduce the iron concentration in the rare earth chloride products.

N, N-di (1–methyl–heptyl) Acetamide (DMHAA or N_{503})

N_{503} is capable of strongly extracting $HFeCl_4$. The solvent extraction is conducted at high acidity under oxidative conditions [62]. H_2O_2 is added to oxidize Fe^{2+} to Fe^{3+} prior to the extraction. The extraction uses 40% N_{503} and is conducted at above 15°C. After scrubbing, the loaded organic phase is stripped with deionized water. N_{503} solvent extraction can also be used in Baiyunebo's H_2SO_4 acid baking leachate for iron removal [63]. Typically, the majority of iron is first removed through a hydroxide precipitation using MgO or $CaCO_3$. After solvent extraction group separation, N_{503} is used to further reduce the iron content and prepare the solution for the following 2–ethylhexyl 2–ethylhexyl phosphate (HEH(EHP), or P_{507}) solvent extraction circuit.

Trialkyl Amine (Alamine-336 or N_{235})

For REE solutions containing high concentration of Ce^{3+}, Alamine-336 is capable of removing iron without a significant loss of rare earths (including Ce). Alamine-336 has strong capacity for extracting iron at high Cl^-- concentration. However, a third phase is easily formed in the process, which makes the process less attractive. In the presence of mixed alcohol (ROH) as the secondary extractant (or phase transfer agent), the emulsification issue is minimized. This SX system is capable of extracting both iron and lead from a REE chloride solution [63]. As iron is extracted as $FeCl_4^-$, the presence of rare earth element chloride in the solution is beneficial to the extraction of both iron and lead.

In another flow sheet, a rare earth chloride solution containing 1 g/L iron and Mn is used as the feed. The extraction rate is higher at higher acidity. NH_4Cl additive also enhances the extraction of iron due to the formation of $FeCl_4^-$ complex anion [65]. The extraction rate increases also with the increase of the feed $RECl_3$ concentration. Nearly all iron can be extracted. The extracted iron (1 g/L) can be easily stripped with water at a 99.4% stripping rate. The raffinate contains REE can be directly sent to the P_{507} circuit for further separation of REE.

When Alamine-336 or naphthenic acid are used individually in SX process for removing iron from REE solutions, the formation of a third phase is sometime limiting the performance of these processes. In Alamine-336 SX, phase separation could be improved by adding mixed alcohol (ROH) or naphthenic acid. However, both assistant solvents will result in a drop of the extraction capacity of Alamine-336. Fundamentally, the negative impact of ROH is more significant than naphthenic acid. Alamine-336, naphthenic acid, and kerosene extraction systems, the presence of excessive chloride anion benefits the formation of $FeCl_4^-$ and increases the extraction rate. REE in the solution phase also accelerated the extraction of iron. After a 7-stage circuit, the iron-containing raffinate is sent to oxalic precipitation and calcination for producing rare earth oxides [66]. The iron content was reduced from 0.58% to $[Fe_2O_3]<10^{-6}$ mol/L. Alamine-336 can also work in a synergistic SX system with tributyl phosphate (TBP). The addition of TBP in Alamine-336 improves the extraction capacity, minimizes the emulsification issue, and allows the iron to be easily stripped from the loaded organic [67].

Di–(2–ethylhexyl)phosphoric Acid (D_2EHPA, HDEHP, or P_{204}), 2–ethylhexyl 2–ethylhexyl phosphate (HEH(EHP), or P_{507}) and Cyanex272

Iron is extractable in organic phosphoric acid extractants, e.g. HDEHP and HEH(EHP). Both are popular extractants for separating rare elements into groups and eventually into individual elements. They can be used to extract rare earth element values from a H_2SO_4 solution leaving impurities (e.g., Fe, Ca, and Mg…) in the raffinate. The feed is mild acidic (pH 4). The organic phase consists of 1.3~1.5 mol/L HDEHP and kerosene. Due to the fact that stripping of HREE from loaded HDEHP is difficult and requires high acidity, this method is still experimental. Similarly, HEH(EHP) can also be used to extract iron. The stripping of iron is quite difficult. Using HDEHP, HEH(EHP) and bis(2,4,4–trimethylpentyl) phosphinic acid (HBTMPP, Cyanex272) in a synergistic solvent extraction system can extract REE from the H_2SO_4 solution. The stripping of HREE becomes much easier in the synergistic system [68]. However, this is a complex extraction system that is still under investigations [69, 70].

HDEHP and (HEH(EHP) also each form synergistic solvent extraction systems with primary amine type and tertiary amine type extractants (phase transfer agents). The benefit is not only the increased extraction performance but also the reduced acid concentration required for stripping the iron from the loaded organic [71].

For purifying the H_2SO_4 rare earth solution produced in the water leach of the Baiyunebo acid baking residue, the conventional technology is to use MgO to precipitate iron and other impurities as hydroxides followed by a N_{503} extraction circuit. A HDEHP and TBP joint flow sheet is patented to replace the current precipitation process [31,72]. The flow sheet still requires a MgO precipitation step at the end of the SX purification process. The amount of MgO required for the operation and the REE loss in the precipitate is reduced significantly. Consequently, the total rare earth element recovery is largely improved. This flow sheet was further enhanced and the new flow sheet completely removed the MgO precipitation step [31].

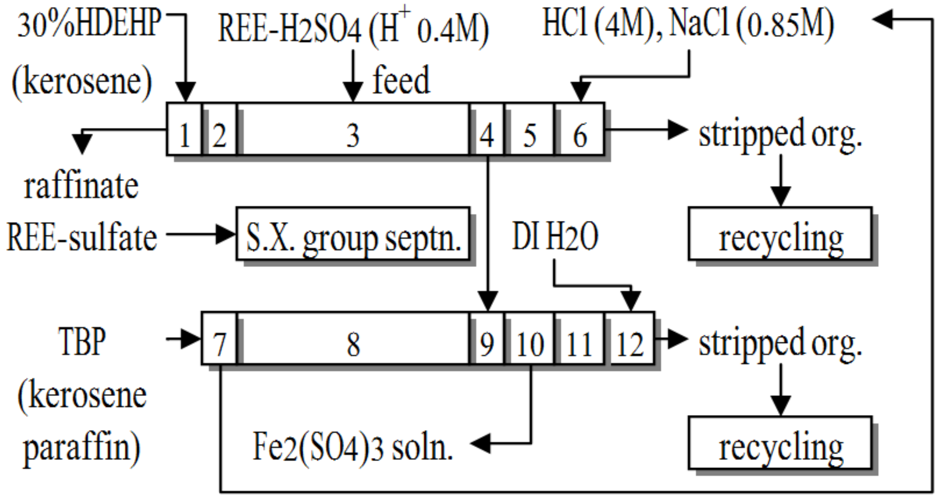

Figure 1. HDEHP and TBP joint solvent extraction for the removal of iron from H_2SO_4 acid baking leachate (II) [31].

As the hydroxide precipitation step is not required before SX, the removal of iron is completely achieved in a continuous SX flow sheet (Figure 1). In the hydroxide precipitation process, the typical loss of REE into the precipitate is from 5% to 10%. The solvent extraction flow sheet can recover 99% REE. Secondly, the precipitation is a batch operation whereas the joined solvent extraction process is continuous thus improving the production rate. Finally, MgO precipitation of iron need another SX process (N_{503}) to further reduce the iron content, the joint process one-step operation does not require another iron removal step. The iron content is reduced to about 10 ppm. The REE recovery is 99.4%.

In HDEHP and HEH(EHP) extractions, it was found that it is the Fe^{3+} that is extractable but not Fe^{2+}. Therefore, by simply reducing the Fe^{3+} to Fe^{2+}, the iron co-extraction will be minimized. This allows both extractants to be used for recovery of total REE leaving iron in the raffinate. Reducing ferric ion can be done though adding reductants or through electroreduction. Hydrogen gas is a reductant for this purpose. Electroreduction is also highly effective. In addition, both methods have potentials to be developed into continuous operations in the solvent extraction circuit [73]. The electroreduction is conducted in cells with iron plate as anode; Ti net as cathode and the cathodic and anodic area are separated with an anion exchange membrane. The SX cell is sealed to avoid Fe^{2+} oxidation by air. The process reduced the iron contents from 126.3 g/L in the feed to 23.4 ppm. The overall rare earth element recovery was above 98%. As the high concentration of iron is as Fe^{2+} in the solvent extraction, the hydrolysis and emulsification issue is avoided.

Cyanex272 is a promising extractant with higher separation factors between REE. Similar to HDEHP, and HEH(EHP), this is a phosphinic acid type extractant. Cyanex272 is weaker acid and a better separating extractant for HREE separation [66]. The solvent extraction performance can be superior than HEH(EHP) solvent extraction systems. In comparison with HEH(EHP), Cyanex272 has lower extraction capacity (about 50%) [70]. Cyanex272 is especially effective on the extraction of scandium. The extraction sequence is: Sc>>Th>Fe>Ln. In comparison with HDEHP and HEH(EHP), Cyanex272 stripping of Fe^{3+}, and Th^{4+} is easier [74,75].

Tributyl Phosphate (TBP) Solvent Extraction Separation of Th/U/Fe

In an HCl matrix, TBP solvent extraction shows very different behavior to the HNO_3 system. The distribution ratio values follow the sequences: $Fe^{3+} > UO_2^{2+} > Th^{4+} > RE^{3+}$. At lower pH range, uranium and iron can be effectively separated from thorium and RE^{3+}. Uranium / iron separation is realized by a reductive solvent extraction based on the enlarged β value of Fe^{2+} and uranium. By adding HNO_3 that react with thorium to form a species that is easily extracted in TBP, Th and rare earth can be separated [76].

Another example of using TBP in the rare earth industry is to purify HCl acid. Industrial grade HCl acid may contain minor amount of iron impurity. One of the ways to purify HCl acid is to use TBP to extract the iron content [76,77].

Dimethylheptyl Methyl Phosphate (P_{350}) Solvent Extraction Separating La-Fe From Other Rare Earth Elements

Dimethylheptyl methyl phosphate solvent extraction can also be used to separate two species from the lanthanum – neodymium rich feed. Fifty percent sulfonated kerosene is used as diluent. The separation factor can be enlarged to about four by adding NH_4NO_3 salting-out agent. The process works well at pH 1~2 without the need for high concentrations of acid [78]. Impurities such as Fe, Ti, Si, Ca and Mg stay in the raffinate with La. This method can produce a purified REE (non-La) product. The iron and La can be separated using various precipitation methods to recovery La [78].

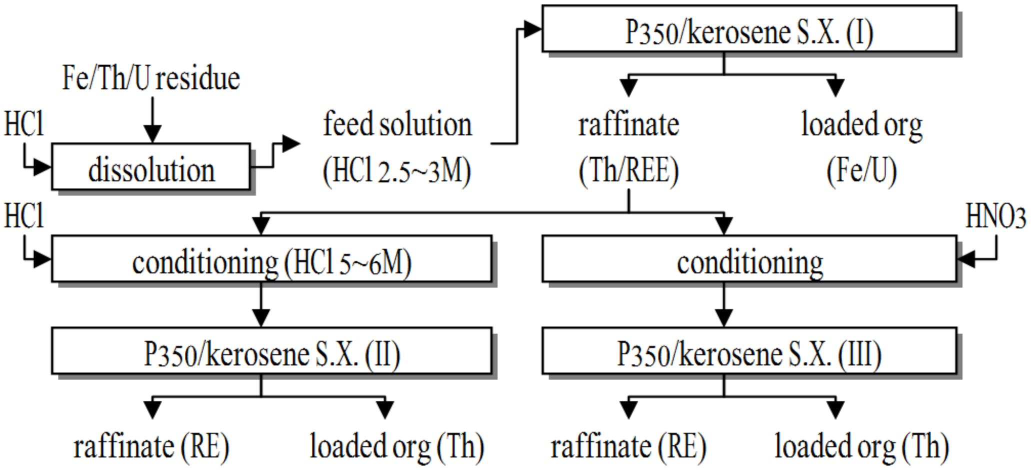

Figure 2. A conceptual flow sheet for iron/thorium/uranium separation using dimethylheptyl methyl phosphate solvent extraction [78].

At 2.5~3 M HCl, dimethylheptyl methyl phosphate could extract all uranium and iron (Figure 2). The loaded organic can be further treated to obtain uranium. The raffinate containing REE and thorium is further separated at 5~6 M HCl with dimethylheptyl methyl phosphate solvent of thorium. Alternatively, by adding HNO_3, the raffinate (REE and thorium) can be processed in dimethylheptyl methyl phosphate solvent extraction for REE – thorium separation. The addition of minor amount of HNO_3 could greatly increase the distribution ratio of thorium in dimethylheptyl methyl phosphate due to the formation of $Th(NO_3)_4$.

Di-(ˉmethyl-heptyl) Methyl Phosphonate (DMHMP) Separation of Rare Earth Element From Impurities

From a feed solution containing 1~2.5 mol/L HCl, DMHMP is capable of extracting iron and uranium leaving REE and thorium in the raffinate [79]. The organic phase consists of 5% TBP, 20% DMHMP and kerosene. In this process UO_2^{2+} is extracted prior to Fe^{3+}. Only 1~2% thorium and the REE enter into the organic. 0.25 mol/L HNO_3 is used to strip 99.77% iron from the organic. The raffinate containing thorium and REE can be further separated in the presence of 1~1.5 mol/L HNO_3 with DMHMP. The HCl-HNO_3 solution can then be treated with DMHMP or TBP to remove HNO_3 and recycle the purified HCl.

Naphthenic Acid (NA) SX

Naphthenic acid is a carboxylic acid, capable of separating many impurities from rare earths. However, the presence of iron may trigger the formation of crud [80]. Naphthenic acid is mostly used on the purification of rare earths solution after a hydroxide precipitation step, where the majority of iron has been removed. This process can also be used to treat the rare earths leachate from ionic adsorption ores. Naphthenic acid also provides an option for the separation of iron in the rare earth recovery from NdFeB scrap.

Iron is one of the most extractable elements in naphthenic acid. The pH required for Fe extraction is significant lower than that for the REE. Almost all iron is extracted at pH 3.8 while only 8% of REE are extracted [81]. In practice, the organic phase contains 20% saponified naphthenic acid, 20% mixed alcohol (ROH) and 60% kerosene. The equilibrium pH is controlled at 3~5. Both Fe^{3+} and Al^{3+} are extracted leaving REE in the raffinate. The Al and Fe contents in the raffinate are both below 1 ppm.

A method using different pH at different solvent extraction stages is proposed for enhanced extraction performance without triggering emulsification. The feed solution pH is adjusted to below 1.5, which could largely avoid the emulsification issue [80]. The last extraction stage has the pH controlled at approximately 3.0. The organic is introduced at stage 1 and 3 (Figure 3).

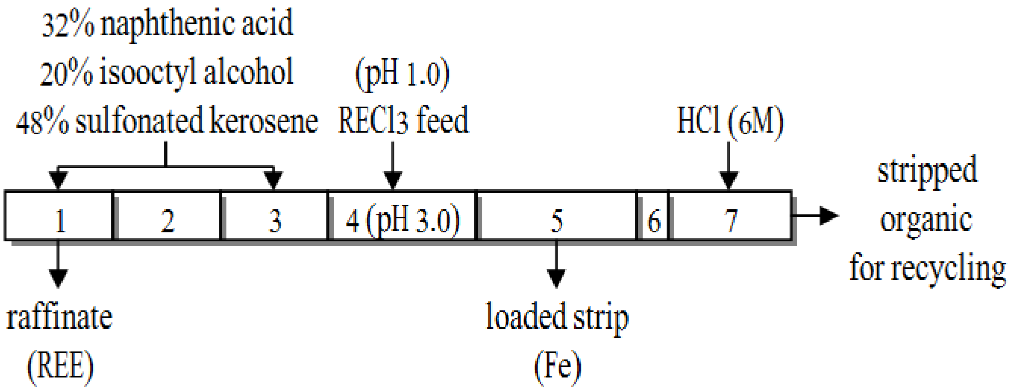

Figure 3. Naphthenic acid solvent extraction for the separation of iron [80].

Naphthenic acid is cheap and widely available and can be looked on as a stable non-toxic extractant. Therefore, it has been popular in rare earth hydrometallurgy. In the separation of REE of low concentration from leachate, naphthenic acid is an especially promising extractant [18]. As a mixture of natural reagents with very complicated and non-uniform compositions, naphthenic acid solvent extraction performance is sometimes unstable. Additionally, the need of high pH (>5) when naphthenic acid is used to extract REE may cause the formation of the third phase. In comparison with naphthenic acid, sec-octyl phenoxy acetic acid (CA-12) is a more stable chemical with simpler composition (i.e., s-C_8H_{17}-$C_6H_4OCH_2COOH$), and lower solubility in water. The crud generation is not significant. A study has suggested using sec-octyl phenoxy acetic acid for the separation of iron with a performance better than naphthenic acid [82].

Benzohydroxamic Acid (BHA) and O-Phthaloyl Hydroxamic Acid (OPHA) Extraction Separation of Iron

In HNO_3 solutions with low total metal content, yttrium, and the REE are strongly extractable with BHA and OPHA. Fe^{3+} is also easily extracted into the organic phase. The loaded organic phase can be stripped sequentially with HCl (0.5 mol/L). REE and yttrium are first stripped leaving Fe^{3+} in the organic [83]. The pH of the HNO_3 rare earth element feed solution is 4.5~4.6. BHA and OPHA are mixed with isooctyl alcohol and kerosene to form the organic phase. The extraction of iron only needs one solvent extraction stage and the rare earth element and yttrium extraction reaches >96% in three stages. The literature; however, does not introduce methods for the stripping of iron. Both BHA and OPHA are chelating extractants. The unit costs of this type of extractant are typically on the high side, making them not widely accepted.

Discussion and Summary

Iron control is an important task and a mature science in hydrometallurgy. In rare earth industry, the conventional approaches include physical separation, iron hydrolysis, and further purification through solvent extraction.

Iron can be separated by precipitating rare earths leaving iron in solutions (e.g., double sulfate salt, oxalate, carbonate, and possibly fluoride precipitations) or precipitating iron while leaving rare earths in the solutions (i.e., iron hydroxide, jarosite, goethite, hematite, and possibly phosphate precipitations). Iron hydrolysis is still the best option when precipitating iron together with many other impurities from a solution containing relatively low levels of iron. Iron precipitation as jarosite, goethite, and hematite also are capable of separating iron from a solution with high iron content. They have the potential to become viable and better iron separation options in the treatment of low-grade REE concentrates. Double salt and oxalate precipitation are popular methods with significant advantages when recovering REE from the leachate containing significant impurities. Ammonium bicarbonate precipitation is a comparatively new option for precipitating REE, and has replaced many oxalate precipitation operations in China due to the lower cost, simpler flow sheet. Precipitation methods are more attractive for medium to small scale production. The equipment and process control are simpler and cheaper. This method is the still the dominant and mature option in practical operations. Most operations require an elevated temperature and a prolonged reaction or settling stage. Further progress on reducing the loss of rare earths, the phase separation difficulties, and the environmental impacts are the topics of future research in this area.

Solvent extraction is a promising alternative to precipitation methods. The obvious advantage is the high overall recovery of metals with a high iron separation rate. The process is continuous and without a major solid-liquid separation step. Several processes have been proposed as improved candidate technologies for large-scale Chinese operations.

Amine type (N-type) extractants (i.e., N_{1923}, N_{503}, and N_{235}) received the most attention and have been used in production. Phosphinic acid type (acidic P-type) extractants (i.e., HDEHP, HEH(EHP) and Cyanex272) are the most popular in the REE separation process. Both REE and iron are highly extractable with these extractants. The stripping and separation of iron is, however, difficult. Neutral P-type extractants are often used in HNO_3 or HCl matrix. In the presence of salting out or self-salting out agents, the extraction capacity is quite large. Tributyl phosphate is used to separate uranium, thorium and REE. For iron separation, one way is to reduce Fe^{3+} to Fe^{2+} to enlarge the separation factor and selectively strip iron. Dimethylheptyl methyl phosphate (P_{350}) can separate lanthanum from non-lanthanum REE in a HNO_3 matrix. Iron follows lanthanum into the raffinate phase. In HCl matrix, iron is extracted with uranium leaving rare earth element and thorium in the raffinate. In the presence of 5% tributyl phosphate, di-(ˉmethyl-heptyl) methyl phosphonate (DMHMP) is capable of extracting iron and uranium leaving REE and thorium in the raffinate. Carboxylic acid extractants are capable of strongly extracting iron at a comparatively mild acidic condition. As a result, emulsification may easily take place due to the presence of iron and aluminium. Together with ROH, naphthenic acid can extract iron leaving rare earth element in the raffinate. The stripping needs strongly acidic solutions. Sec-octyl phenoxy acetic acid (CA-12) is a similar carboxylic acid extractant with more stable performances than naphthenic acid. Chelating extractants are capable to separating iron and REE effectively. The unit cost of this type of extractant is believed to be the major impediment for implementation in the purification processes.

Solvent extraction methods require higher capital investment and may be limited to operations of medium to large scales only. Iron is typically strongly extractable but is also very difficult to strip. The separation of iron and REE is sometime difficult as well. Solutions for this problem include synergistic extraction [84], phase transfer agents [85], joint solvent extraction flow sheet and reductive solvent extraction, etc.

In the selection of a proper iron separation process, the main factors are greener production, higher rare earth element recovery, higher iron removal rate, and lower unit cost. In addition, a flow sheet with less solid-liquid separation and heating requirement is certainly more favorable. The selection of iron separation method is also related to the separation of other impurities, e.g., thorium, uranium, sulfate, chloride, lead, silicate, aluminum, and so on. There is apparently no ideal method to suit all REE processes and the answer lies in a combination of different techniques that would respond to each set of separation constraints and process challenges based on each specific case.

Acknowledgements

Editorial suggestions from Dr. Saviz Mortazavi, Dr. John Kwong, Dr. Bryan Tisch and Zinck Janice at CANMIN are greatly appreciated. Thanks also to John Goode for his technical advices in the writing of this review article.

References

1. Fangqin Yuan et al., "Status and Prospect of Technology for Iron Removal in Zinc Hydrometallurgy," *Multipurpose Utilization of Minerals Resources*, 2011 No.2:30-32.

2. Wenshan Zhang, Chaojun Shi and Guanggui Mei, "Studies on Several Important Methods of Fe Removal from (Zn, Mn, Cu, Ni and Co) Hydrometanurgy," *China Manganese Industry,* 24 (2) (2006), 40-42.

3. V. V. Popov and A. I. Gorbunov, "Hydrothermal Crystallization of Iron(III) Hydroxide," *Inorganic Materials*, 42(3)(2006), 275–281.

4. J.E. Dutrizac and J.L. Jambor, ed., C.N. Alpers, J.L. Jambor, and D.K. Nordstrom, "Jarosites and their application in hydrometallurgy," *Reviews in Mineralogy and Geochemistry. Sulfate Minerals—Crystallography, Geochemistry and Environmental Significance vol. 40* (Mineralogical Society of America, Washington, DC, USA, 2000), 405–452.

5. J.O. Claassen et al., "Iron Precipitation from Zinc-Rich Solutions: Defining the Zincor Process," *Hydrometallurgy*, 67(1)(2002) 87-108.

6. T. Moeller, *The Chemistry of the Rare Earths* (New York, NY: Reinhold, 1963).

7. Liangcai Li, *Rare Earths Extraction and Separation* (China, Inner Mongolia Science and Technology Press, 2011), 99.

8. Tingsheng Qiu et al, "The Current Situation and Trends of the Technology for Impurity Removal of Weathering Crust Ion – Absorbed Type Rare Earth Ores," *Chinese Rare Earths,* 33 (4) (2012), 81-85.

9. Fengli Yang et al., "The Study of Removing Impurity on High-Yttrium Rare earth Carbonatscandium," *Journal of Southern Institute of Metallurgy,* 23 (2) (2002), 15-36.

10. Jinhua Kang, "The Problem of Purifying the Materials Liquid in the Naphthenic Acid - Hydrochloride Acid System," *Journal of Southern Institute of Metallurgy,* 25 (1) (2004), 25-28.

11. Liangcai Li, *Rare Earths Extraction and Separation* (China, Inner Mongolia Science and Technology Press, 2011), 324.

12. Liangcai Li, *Rare Earths Extraction and Separation* (China, Inner Mongolia Science and Technology Press, 2011), 140.

13. Xianping Luo, Youjun Qian, and Changli Liang, "Research Progress and Developing Trend of Rare Earth Extraction from Ionic Rare Earth Leach Solution," *Nonferrous Metals Science and Engineering,*3 (5) (2012), 50-53.

14. Liangcai Li, *Rare Earths Extraction and Separation* (China, Inner Mongolia Science and Technology Press, 2011), 61.

15. Liangcai Li, *Rare Earths Extraction and Separation* (China, Inner Mongolia Science and Technology Press, 2011), 60

16. C.K. Gupta and N, Krishnamurthy, *Extractive Metallurgy of Rare Earths* (CRC Press, 2005), 141.

17. Liangcai Li, *Rare Earths Extraction and Separation* (China, Inner Mongolia Science and Technology Press, 2011), 52-63.

18. Ping Zhang, Fuhua Jiang and Shouci Lu, "To Separate Rare Earth Elements from the Aqueous Chlorinate of Mine Mud by Naphthenic Acid Extraction 1. Removal of Impurities before Extraction," *Chemistry World*, 1999 No.5:269-274.

19. Liangcai Li, *Rare Earths Extraction and Separation* (China, Inner Mongolia Science and Technology Press, 2011), 382.

20. Liangcai Li, *Rare Earths Extraction and Separation* (China, Inner Mongolia Science and Technology Press, 2011), 381.

21. Liangcai Li, *Rare Earths Extraction and Separation* (China, Inner Mongolia Science and Technology Press, 2011), 136.

22. Liangcai Li, *Rare Earths Extraction and Separation* (China, Inner Mongolia Science and Technology Press, 2011), 76.

23. Liangcai Li, *Rare Earths Extraction and Separation* (China, Inner Mongolia Science and Technology Press, 2011), 388-389.

24. Liangcai Li, *Rare Earths Extraction and Separation* (China, Inner Mongolia Science and Technology Press, 2011), 104.

25. Liangcai Li, *Rare Earths Extraction and Separation* (China, Inner Mongolia Science and Technology Press, 2011), 149.

26. Liangcai Li, *Rare Earths Extraction and Separation* (China, Inner Mongolia Science and Technology Press, 2011), 282.

27. Fuhua Jiang et al., "Study of Absorption of Rare Earth Ions with Iron Oxide Gel," *Journal of Wuhan Yejin University of Science and Technology*, 19(1)(1996),

28. Xiufen Li and Ruan Chi, "Study on Removing Impurities in the Exchanged Liquor of Rare Earth Ores," *Multipurpose Utilization of Mineral Resources*, 1997 No.2:10-13.

29. Dexiang He, Liewen Liao and Ruiyuan Xu, "Precipitation of Rare Earths with a Mixed Precipitant," *Chinese Patent*, CN1033976 (A), 1988.

30. Xingchu Qiu et al., "Process for Extracting Rare-Earth from Ion-Type Sulfuric Acid Immersion of Rare-Earth Ore by Liquid Ammonia Deposition", *Chinese Patent*, CN1043685(A), 1988.

31. Xin Zhang et al., "Separating Fe(III) from Rare-Earth Sulphate Leaching Selection Originated in Baotou Rare-Earth Mine with Solvent Extration Method," *Journal of University of Science and Technology Beijing*, 18(1)(1996), 78-83.

32. Yuchuan Feng et al, "A Study of Increasing the Purity of Rare Earth by Precipitation Eliminating Method," *Journal of Jiangxi Science and Technology Normal University*, 4(2006), 115-117.

33. Riping Huang, "Novel Method for Leaching, Impurity Removing and Precipitating Ion Type Rare Earth Ore," *Chinese Patent*, CN101476033(A), 2008.

34. Xiaowei Huang et al., "Development Status and Research Progress in Rare Earth Hydrometallurgy in China," *Journal of the Chinese Rare Earth Society*, 24(2)(2006), 129-133.

35. Xiaowei Huang et al., "Method for Precipitating Rare Earth," *Chinese Patent*, CN101798627(A), 2009.

36. R.M. Cornell, R. Giovanoli, and W. Schneider, "Review of the Hydrolysis of Iron(III) and the Crystallization of Amorphous Iron(III) Hydroxide Hydrate," *J. Chem. Technol. Biotechnol.*, 46(1)(1989), 115–134.

37. M.A. Blesa, and E. Matijevic, "Phase Transformation of Iron Oxides, Oxohydroxides, and Hydrous Oxides in Aqueous Media," *Adv. Colloid Interface Sci.*, 29(3/4)(1989), 173–221.

38. Xueyi Guo et al.,The Thermodynamic and Kinetics of Sodium Jarosite Formation in Chloride Solution," *Journal of Central South University Technology*, 28(1)(1997), 30-33.

39. R.E. Stroffregen, C.N. Alpers, and J.L. Jambor, ed., C.N. Alpers, J.L Jambor, D.K Nordstrom, "Alunite–Jarosite Crystallography, Thermodynamic and Geochronology," *Reviews in Mineralogy and Geochemistry. Sulfate Minerals—Crystallography, Geochemistry and Environmental Significance, vol. 40*(Washington, DC, USA: Mineralogical Society of America, 2002), 453–479.

40. J.E. Dutrizac, "The Behavior of Impurities During Jarosite Precipitation," In: Bautista, R.G. (Ed.), *Hydrometallurgical Process Fundamentals,*Plenum, New York, NY, USA, 1984, 125-169.

41. Liangcai Li, *Rare Earths Extraction and Separation* (China, Inner Mongolia Science and Technology Press, 2011), 391.

42. Wanyan Zhang and Guangyuan Wu, "Experiment of Recovering RE Oxide and Co Oxide from NdFeB Waste," *Jiangxi Nonferrous Metals*, 15(4)(2001), 23-26.

43. Runtian Jiang et al., "Study on Technology of Iron Removal from Acid Leaching Liquid of Copper Sulfate," *Journal of Jinan University (Sci.& Tech.)*, 17(3)(2003), 289-291.

44. J.E. Dutrizac, "The Behaviour of the Rare Earths During the Precipitation of Sodium, Potassium and Lead Jarosites," *Hydrometallurgy*, 73(1)(2004), 11-30.

45. J.E. Dutrizac and J.L. Jambor, "Behaviour of Cesium and Lithium During the Precipitation of Jarosite-type Compounds," *Hydrometallurgy,* 17(1987), 251-265.

46. J.E. Dutrizac and T.T. Chen, "The behaviour of Scandium, Yttrium and Uranium During Jarosite Precipitation," *Hydrometallurgy*, 98(1–2)(2009), 128-135.

47. Jane W. Lyman, and Glenn R. Palmer, "Scrap Treatment Method for Rare Earth Transition Metal Alloys," *US Patent*, US5129945(A), 1992.

48. Yuan Lu, "Carbon Reducting Roast Process of Producing RE Chloride with Mixed RE Concentrate," *Chinese Patent*, CN1384214(A), 2001.

49. Qifa Jian, "A Research on Rare Earths Recovery from NdFeB Scrap," *Jiangxi Nonferrous Metals*, 12(1)(1998), 36-39.

50. Mingmin Dou and Delin Zhou, "A Study on New Technology for Removing Iron by Phosphate," *Nonferrous Metallurgy*, 6(2006), 28-31

51. Xiaonan Liu, "Process for Recycling Trace Rare Earth Produced by Treatment of Waste Residues and Waste Water of Rare Earth Mine", *Chinese Patent*, CN101979335(A), 2010.

52. Jinsong Huang and Meifu Qi, "Review on Recovery Technology of NdFeB Waste Materials," *China Resources Comprehensive Utilization*, 26(11)(2008), 4-5.

53. Yijun Wang et al., "Study and Practice of Selective Dissolution with HCl for the Recovery of RE Elements from NdFeB Scrap," *Rare Metals and Cemented Carbides*, 35(2)(2007), 25-47.

54. Yanhui Xu et al., "Techniques for Clean Smelting and Resource Comprehensive Recycle of Baotou Rare Earth Concentrates," *Journal of the Chinese Society of Rare Earths*, 30(5)(2012), 632-635.

55. Liangcai Li, *Rare Earths Extraction and Separation* (China, Inner Mongolia Science and Technology Press, 2011), 96.

56. Liangcai Li, *Rare Earths Extraction and Separation* (China, Inner Mongolia Science and Technology Press, 2011), 390.

57. Jie Tang et al., "Neodymium Oxide Recovery from Sintered NdFeB Scrap," *Rare Metals and Cemented Carbides*, 37(1)(2009), 9-18.

58. Liangcai Li, *Rare Earths Extraction and Separation* (China, Inner Mongolia Science and Technology Press, 2011), 145.

59. Liangcai Li, *Rare Earths Extraction and Separation* (China, Inner Mongolia Science and Technology Press, 2011), 386-391.

60. Qiying Han, "The Technology of Heavy Rare-earth Carbonate's Crystal Precipitation," *Hunan Nonferrous Metals*, 25(6)(2009), 31-77.

61. Liangcai Li, *Rare Earths Extraction and Separation* (China, Inner Mongolia Science and Technology Press, 2011), 289-292.

62. Yunjin Chen, "A Complete Solvent Extraction Flowsheet for the Recovery of Rare Earth Elements and Cobalt from NdFeB Scrap," *China Resources Comprehensive Utilization*, 2004 No.6:10-12.

63. Liangcai Li, *Rare Earths Extraction and Separation* (China, Inner Mongolia Science and Technology Press, 2011), 150.

64. Xiuli Zhang and Xiong Wan, "The Removal of Fe and Pb From Rare Earth Using N235 - Mixed Alcohol," *Chemical Research And Application*, 11(4)(1999), 435-438.

65. Jun Tian et al., "Separation of Fe from Chlorinated Leaching Solution with N235," *Nonferrous Metals*, 52(2)(2000), 57-60.

66. Xiuli Zhang and Xiong Wan, "Removal of Iron from Rare Earth Using Trialkyl Amine (alamine-336 or N235)-Naphthenic acid (NA)," *Engineering Chemistry & Metallurgy*, 20(1)(1999), 25-28.

67. Ming Liu and Yongmao Zhou, "Removal of Fe(III) from Sulphate Solution by Synergistic Extraction Using Trialkyl Amine (alamine-336 or N235)-Tributyl Phosphate (TBP) Mixed Solvent Systems," *The Chinese Journal of Nonferrous Metals*, 15(10)(2005), 1648-1654.

68. Xiaowei Huang et al., "Synergistic Extraction of Nd3+ and Sm3+ from Sulfuric Acid Medium with D2EHPA-HEHEHP in Kerosene," *The Chinese Journal of Nonferrous Metals,* 18(2)(2008), 366-371.

69. Xiaowei Huang, "An Investigation on the Synergistic Extraction Mechanisms of P204 and P507 or Cyanex272 Mixed-Solvent Systems in H2SO4 Medium," *National Nature Science Foundation of China*,http://www.medsci.cn/sci/nsfc_ab.do?q=414c15353431.

70. Chunfa Liao et al., "Separation of Thulium, Lutetium by Cooperative Extraction Chromatography with Cyanex272-P507 Impregnated Resin," *Journal of the Chinese Rare Earth Society*, 25(2)(2007), 249-252.

71. Shuqiu Yu and Jiayong Chen, "RE-Extraction By Phase Transfer In Extracting of Iron with Acidic Phosphate," *Chinese Patent*, CN1031859(A), 1989.

72. Xin Zhang et al., "Treating Tech. for Baotou rare-earth Mine Sulfuric Acid Baking Extract," *Chinese Patent*, CN1113960(A), 1994.

73. Xuanxu Zhang et al., "On Rare Earth Recovery out of Waste Neodymium, Iron, Boron by Electro-Reduction and 2–Ethylhexyl 2–Ethylhexyl Phosphate (HEH(EHP), or P507) Extraction Separation Method," *Jiangxi Nonferrous Metals*, 23(3)(2009), 30-31.

74. Ruihua Zhang and Hua Tang, "The Application of New Extractant Bis(2,4,4–trimethylpentyl) Phosphinic Acid (HBTMPP, Cyanex272) in Solvent Extraction Separation of Rare Earth Elements," *Jiangxi Nonferrous Metallurgy*, 12(2)(1998), 34-41.

75. Deqian Li, "Bis(2,4,4–trimethylpentyl) Phosphinic Acid Solvent Extraction Rare Earth Element (III), Thorium (IV) and Iron (III)," *Jiangxi Nonferrous Metals*, 10(1)(1996), 29-32.

76. Liangcai Li, *Rare Earths Extraction and Separation* (China, Inner Mongolia Science and Technology Press, 2011), 231.

77. T. Sato, "Liquid-liquid Extraction of Iron (III) from Hydrochloric Acid Solutions by Tributyl Phosphate," *Journal of the Mining and Materials Processing Institute of Japan*, 118(9)(2002), 612-616.

78. Liangcai Li, *Rare Earths Extraction and Separation* (China, Inner Mongolia Science and Technology Press, 2011), 243-244.

79. Dong Zou, "Extraction-Separation Process for U, Fe, Th and Rare Earth Elementents in Monazite," *Journal of Guangdong Non-ferrous Metals*, 2(1)(1992), 16-22.

80. Peijing He, "Study on Removal of Iron and Aluminium from Rare Earth Solution with Naphthenic Acid," 16(2)1995, 19-22.

81. Liangcai Li, *Rare Earths Extraction and Separation* (China, Inner Mongolia Science and Technology Press, 2011), 286.

82. Yanzhi Wang, Shumin Han and Deqian Li, "Performance of Extraction of Fe(III) with Sec-Octylphenoxy Acetic Acid," *Mining and Metallurgical Engineering*, 22(3)(2001), 72-78.

83. Guanghua Liu et al., "An Investigation on Benzohydroxamic Acid (BHA) and O-Phthaloyl Hydroxamic Acid (OPHA) Solvent Extraction of Rare Earths (III) and Fe(III)," *Rare Earth*, 14(2)(1993), 6-8.

84. Chunfa Liao, Yunfen Jiao and Dingfan Qiu, "Characteristics of Adsorbing Heavy Rare Earth Elements with Phosphinic (Phosphoric) Impregnated Resin," *The Chinese Journal of Process Engineering*, 7(2)(2007), 268-272.

85. Shuqiu Yu and Jiayong Chen, "RE-Extraction By Phase Transfer In Extracting of Iron with Acidic Phosphate," *Chinese Patent*, CN1031859(A), 1989.

PROCESS DEVELOPMENT FOR THE SERRA VERDE WEATHERED CRUST ELUTION-DEPOSITED RARE EARTH DEPOSIT IN BRAZIL

Alexandre Rocha[1], Don Schissel[2], Andreas Sprecher[1]
Paulo de Tarso[1], *John R. Goode[3]

[1]Serra Verde Mining LLC
Rua Joaquim Floriano, 466-cj. 2406, CEP 04534-002, São Paolo, SP, Brazil

[2]DJS Group, 1133 Keith Drive, Concord CA 94518, USA

[3]J.R. Goode and Associates
Suite 1010, 65 Spring Garden Avenue, Toronto, Ontario, Canada M2N 6H9
*jrgoode@sympatico.ca

Keywords: Weathered Crust Elution-deposited Rare Earths, Clay, Desorption, Column Leach, Heap Leach, In-Situ Leach, Beneficiation

Abstract

The Serra Verde project has an Indicated Resource of 178 Mt at 0.16% total rare earth oxides (TREO) with 23% as heavy rare earth oxides (HREO - Eu to Lu+Y) and an Inferred Resource of 234 Mt at 0.16% TREO at an 0.1% TREO cut-off grade. The mineralized tonnage is 931 Mt at 0.12% TREO at zero cut-off grade. The REO occur in a shallow clay-bearing saprolite produced by granite weathering.

Tests on numerous samples have shown that more than 50% of the REO, except for Ce, are sorbed on clay and extracted by simple elution processes. Pregnant solutions are clean and yield a product containing up to 40% HREO. Tests also examined the recovery of residual minerals in the leach tailings.

Production-scale recovery systems under study are used at similar deposits elsewhere and include in-situ, heap, and agitated leaching. This paper discusses testwork and development plans for Serra Verde.

Introduction

Mining Ventures Brasil (MVB) controls the Serra Verde property through its subsidiary Serra Verde Mining LLC (SVM). The property consists of 49 unpatented mineral claims and covers an area of 69,814 ha in the northern part of Goias state and extending into Tocantins state, Brazil. The mining town of Minaçu, approximately 260 km north of Brasilia and serviced by regularly scheduled flights, lies about 25 km to the east of the property. Paved road, rail, and hydroelectric power systems are close. The property includes a 900 m long landing strip – a legacy from tin mining operations in the area that terminated in the 1980s. The area of the deposit consists of grassland with small trees and gently rolling hills.

Rare earths were first observed in the Serra Verde area in 1983. MVB, which was formed in 2008, commenced evaluation of the Serra Verde area for its REE potential in 2010. By March 2012, 469 augur holes had tested the saprolite and given encouragement such that 6,297 holes had been completed a year later. In June 2013, Hains Technology Associates prepared a Updated Technical Report [1] to Canadian NI 43-101 standards which will be incorporated into a Preliminary Economic Assessment (PEA) report by August 2013 and will include the resource estimate shown in Table I.

Table I. Mineral Resource Estimate at 0.1% Cut-off Grade – April 5th, 2013 [1]

Target	Resource Classification	Tonnes (Mt)	LREO	HREO	TREO	ZrO_2
			%	%	%	ppm
Córrego Fundo	Indicated	121	0.13	0.04	0.16	711
Areias	Indicated	11	0.11	0.04	0.16	696
Capão Grande	Indicated	36	0.11	0.04	0.16	584
Plateau	Indicated	10	0.15	0.05	0.20	847
Córrego Fundo	Inferred	24	0.12	0.03	0.15	684
Areias	Inferred	39	0.11	0.04	0.14	632
Capão Grande	Inferred	29	0.10	0.04	0.14	672
Plateau	Inferred	142	0.13	0.04	0.17	878
Total	**Indicated**	178	0.12	0.04	0.16	692
	Inferred	234	0.12	0.04	0.16	792

Notes:

1. CIM definitions were followed for Mineral Resources.
2. Other notes as per 43-10 report [1].

The distribution of the REE within the target areas and the resource classifications are presented in Table II.

Geology

The Serra Verde rare earth deposit was enriched in rare earths in three stages from approximately 500 ppm to 2500-4000 ppm TREO. The Pela Ema muscovite albite feldspar granite was intruded 1.8 billion years ago doming the metasediments around the intrusion with accompanying muscovite greisen and tin veining in north-south and northwest trending structures. The protolith granite contains accessary 1-2% TREO bearing monazite and xenotime minerals and background TREO are approximately ~ 500 ppm.

The intrusion of an evolved alkaline (carbonatite?) system at depth 540 Ma ago created broad potassic metasomatism and alteration of the Pela Ema granite. Pegmatitic potassic feldspar veins, biotitite-magnetite veins with TREO-bearing monazite, xenotime, and fergusonite biotite-magnetite veins intrude along pre-existing north-south and north-west structures in the southern portion of the Pela Ema granite and disseminated biotite alter the host granite. Most of the

HREO at Serra Verde are concentrated in the xenotime. Background TREO in these potassic metasomatic zones is ~800-1200 ppm TREO.

Serra Verde occurs within the Amazon-Tocantins laterite belt. Deep tropical weathering occurred from 70-10 Ma with intense peaks at 59, 54, 40, 35, 20, and 15 Ma primarily in the Eocene and Miocene epochs [2]. A 15-20 meters thick lateritic plateau formed with a hard 2-4 m iron-silica duricrust cap and saprolite below. Weak acidic solutions weathered the feldspars in the granite forming kaolinite clays and residual silica in the saprolite. For the past 10 million years stream action has partly dissected the laterite plateau forming the Nova Esperanza colluvium deposits with monazite, xenotime, and fergusonite minerals. Dissection of the plateau in the south at the Pela Ema deposit has exposed at surface a 2-5 meters thick zone of saprolite above the granite "saprock" . This zone is enriched to ~2000-5000 ppm TREO.

Table II. Mineral Resource Estimate at 0.1% TREO cut-off, Mt and g/t – April 5, 2013 [1]

Areas	Indicated				Inferred			
	Córrego Fundo	Areias	Capão Grande	Plateau	Córrego Fundo	Areias	Capão Grande	Plateau
Mass (Mt)	121	11	36	10	24	39	29	142
Element								
Ce	463	398	423	546	439	372	378	470
La	318	293	294	369	284	261	239	309
Nd	178	177	162	219	163	166	150	187
Pr	56	54	51	68	51	50	45	57
Sm	30	33	29	41	28	30	27	33
Eu	2	2	2	3	2	2	2	2
Gd	27	32	28	39	25	28	25	31
Yb	18	23	24	25	17	19	19	21
Dy	28	32	31	40	26	26	28	32
Er	19	23	22	26	17	19	19	22
Ho	6	7	7	8	5	6	6	7
Lu	3	3	3	3	2	3	3	3
Tb	4	5	5	6	4	5	4	5
Tm	3	4	4	4	3	3	3	3
Y	181	219	215	252	164	193	187	211
LREE	1045	955	959	1243	965	879	839	1056
HREE	291	350	341	406	265	304	296	337
TREE	1336	1305	1300	1649	1230	1183	1135	1393
Zr	527	515	432	627	506	468	498	650

Notes: As for Table I. Note that assays are elemental and not as oxide

During the pre-feasibility stage at Serra Verde several 1 tonne composite bulk samples from various areas of the saprolite-colluvium horizon were collected for metallurgical work. At the end of 2012 mineral analyses and head grade assays of the sieved bulk samples indicated that up to 63% of the TREO and yttrium reported to the fine fraction (<600 mesh) consisting of 64-74%

kaolinite. Mineralogical studies confirmed the presence of Ce-depleted monazite and oxidation of Ce to Ce^{4+} forming $Ce^{4+}(Th)O_2$ (cerianite). Supergene weathering released REE from the monazite and xenotime and absorption onto the clays similar to the "ionic clay" rare earth deposits in southern China [3]. Most of the world's HREE are routinely produced from these deposits by in-situ and heap leaching.

Agitated leach and column leach tests on Serra Verde material described in this paper have confirmed high but variable recovery of REO (10 to 90%) using simple desorption techniques, with very low cerium and thorium extraction, from the numerous samples that have been tested.

At the time of writing, the deposit has been defined by 6,300 auger drill holes for a total length of more than 27,000 m. More than 30,000 samples have been assayed for REE, U, Th, multi-element ICP and whole rock analysis. The Pela Ema area in the south of the deposit, and which has been selected for detailed assessment, is defined by 6,590 auger holes with a length of 28,177 m and 28,695 samples [1]. Sixty-eight diamond drill holes totaling 2,010 m have been drilled recently in the Pela Ema area to better define the resource.

Mineralogy

Mariano [4] observed that kaolinite clays at Serra Verde were present in the finer fractions of colluvium and saprolite and also noted cerianite in the saprolite. Ce-depleted REE minerals were observed along with monazite, bastnaesite and xenotime. In late December 2012, Mariano [5] reported on a qualitative test that yielded a positive indication that the clays contained sorbed REE.

SGS [6] completed mineralogical work on Serra Verde samples in early 2013. This showed that the saprolite consists of quartz, feldspar, clays (5 to 14% mass), biotite, and mica. The clays were predominantly kaolinite with minor illite. REE minerals included monazite (mainly LREE but ~1% Y and 7% Th) and xenotime (33% Y, 4% Yb, 4% Dy and 2% Gd). The D_{50} of the REE minerals in the samples subjected to QEMSCAN were generally about 50 µm.

The SGS mineralogical work indicated that the REE minerals were not well liberated and were complex and intergrown. It was indicated that beneficiation of the primary minerals would be difficult. As is discussed below, hydrometallurgical work indicates that about half the REE in Serra Verde ore is sorbed on clays with the balance largely present as primary minerals or partially decomposed minerals.

Beneficiation

Desorption of the REE from the clays will recover about 50% of the REE but the balance remain in the residue following desorption in the form of primary or partially altered minerals. SGS was engaged to undertake very preliminary tests to explore the possibility of recovering the REE remaining in mineral form [7]. Tests included gravity concentration using a Mozley table, wet high intensity magnetic separation (WHIMS), and flotation tests on a sample of -2 mm Serra Verde ore that had been previously column leached for the extraction of clay-sorbed REE [8]. To facilitate handling, the +200 µm material, roughly 50% of the mass at about half head grade, was removed before beneficiation testing. Flotation tests were done using reagents that had been used successfully on other REE projects and were LR19 (a mixture of fatty acid and succinate), Cytec Aero 6493 (an alkyl hydroxamate), LF-P81 (a Chinese hydroxamate) and T610 (a modified salicyl hydroximic acid) with the two last reagents used at 50^0 C.

Results are provided in Figure 1 that presents data on a test feed basis. This shows no REE upgrading using flotation or gravity concentration. However, WHIMS was moderately successful and its use could be further explored in future tests.

The Serra Verde area produced tin in the past and the saprolite is known to contain zircon. SGS followed Zr and Sn deportment in the Mozley and WHIMS tests. Zr and Sn in the test feed was 440 and 75 g/t respectively. It appears that there is the potential to recover residual heavy minerals from the REE leach residue – especially using WHIMS.

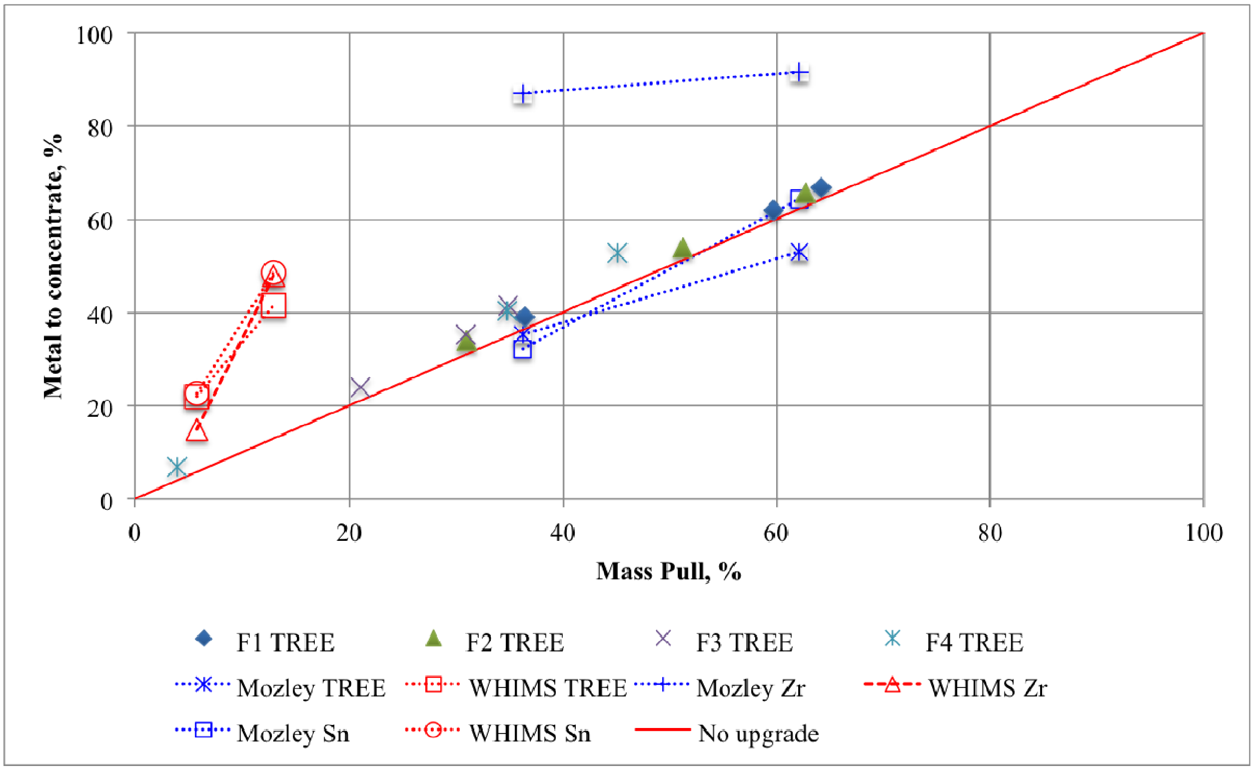

Figure 1. Results of beneficiation work on leach residue - results for REE, Zr, and Sn.

Hydrometallurgy

SGS was engaged to do testwork in January 2013. Seven samples were made available, and quantification of the REE sorbed on clay was prioritized. By late January it was evident that about 50% of the REE in the samples was sorbed on clay. A wide variety of desorption techniques were investigated with a view to better understanding the system and developing a rapid method of evaluating hundreds of samples needed to define recovery for the orebody. Additionally, there was a need to identify a practical desorption system for plant operation, define solution composition and process requirements, and measure environmental parameters.

Some key findings from the preliminary tests were as follows:

- Desorbed at 25% solids with 1 M $(NH_4)_2SO_4$ (AS) at pH 2 and 25^0 C for 2 h, the seven initial samples gave the following ranges in extraction: La – 37 to 59%, Ce – 1 to 13%, Nd – 26 to 48%, Y – 30 to 58%, Th – 1 to 6%, U – 8 to 20%;
- A wrist-action laboratory shaker gave adequate mixing of the 40 g or so of – 2 mm sample in 250 mL Erlenmeyer flasks and could handle six or more at one time;
- Using a composite of the seven it was found that desorption was rapid with a 1 h contact time sufficient;
- With 1 M $(NH_4)_2SO_4$ at pH 2, a temperature of 50^0 C slightly increased the LREE desorbed and co-extracted contaminants but made no difference to the HREE extraction;
- Multi-stage extraction is essential since desorption is a true ion exchange phenomenon;
- NaCl, $(NH_4)_2SO_4$, NH_4Cl are effective eluents;
- $(NH_4)_2SO_4$ was not very sensitive to pH (range 2 to 4) but NaCl performed slightly better at lower pH.

Based on the results of the initial testwork, an analysis of the literature [3, 9], and a review of project needs and available material, a column leach test was undertaken to explore the possibility of heap leaching and generate pregnant solution needed to test REE purification and precipitation. Column feed was a composite of the initial seven samples which was agglomerated with 0.5 M AS solution at pH 3 and loaded into a 25 mm diameter by 1 m h column. Parallel shake flask desorptions were also done. An aggressive 15 $L/h/m^2$ irrigation rate was selected for the column because of the observed rapid desorption rate. The column was run for just 72 h then dismantled, the residue water washed, and all products assayed.

The results of the column leach and the parallel shake flask desorptions are provided in Figure 2. This shows relatively low extraction from the single contact test, better extraction from the two-stage procedure and even better extraction from the column leach. The data highlight the ion exchange nature of the desorption process.

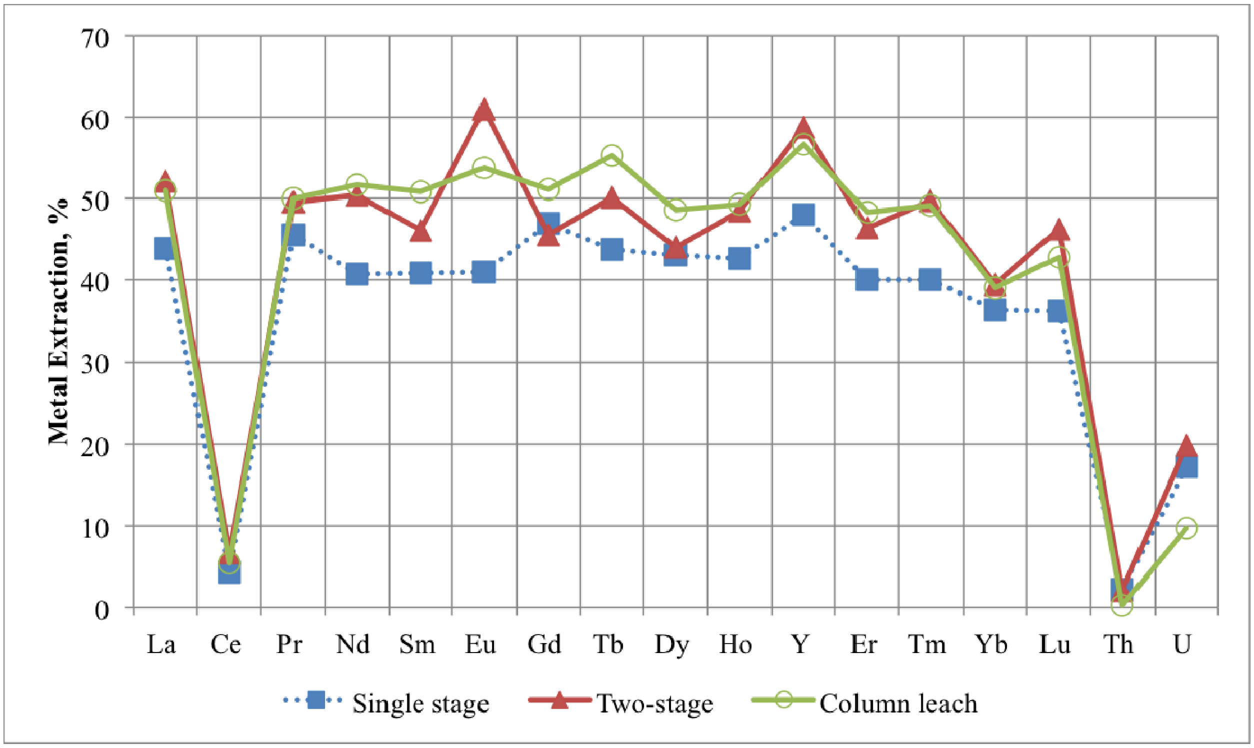

Figure 2. Results of single and two-stage AS desorption and column leach result.

Figure 3 plots extraction against the volume of eluent used in the column leach. Complete desorption of the clays was obtained in 0.6 m^3 of column effluent per 1 t of ore. With a counter-current heap leach system, total pregnant solution volumes of well under 0.5 m^3/t, perhaps as low as 0.3 m^3/t should be achievable – possibly with the injection of additional desorbing reagent.

It should be noted that the column leach process was essentially complete and the clays fully desorbed in just three days of irrigation. The rapid desorption process means that commercial heap leach cycle times will be unusually short and require some imaginative design.

An attempt to conduct a larger-scale column leach failed because adequate irrigation rates could not be attained. This was believed due to the finer feed employed aggravated by poor distribution and extensive packing in the column during loading. The difficulty highlights the importance of excellent agglomeration, binder, and heap construction methods for these high-clay materials. Agglomeration methods and larger scale column tests are being done in Brazil and initial evidence suggests that heap leaching is a viable option.

As part of evaluating the deposit, 66 samples from different areas of the Serra Verde deposit were subjected to standard desorption tests. The samples came from 16 drill holes with each represented contiguous intervals of between 1 an 2 m. Sample head grades varied widely from 616 g/t to 10,609 g/t TREE and averaged 2,023 g/t.

In the standard procedure, 25 g of ore was shaken at 33% solids with the eluent for 30 minutes. The slurry was filtered, then displacement washed three times with eluent (analogous to column leaching) and finally displacement washed with water. Solutions were combined and assayed as well as the filter cake.

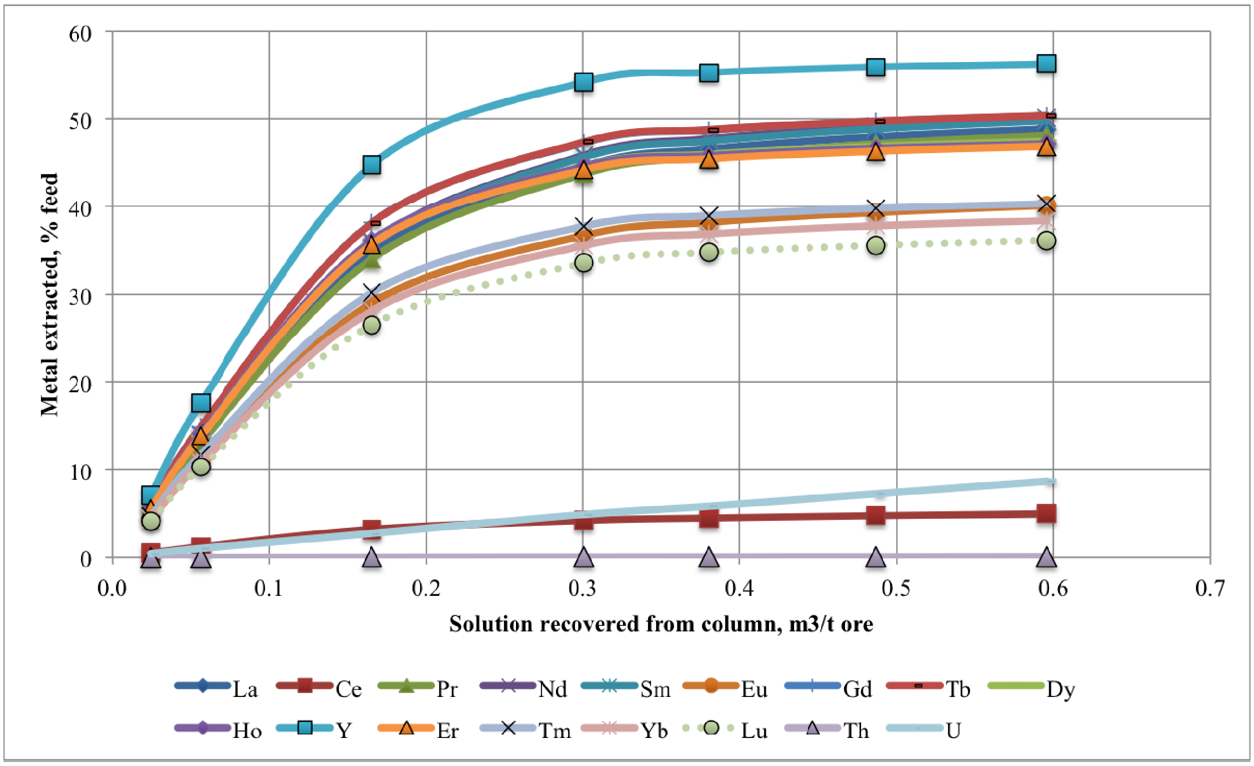

Figure 3. Column leach extraction of REE and cumulative pregnant solution volume.

The first 37 samples were processed in parallel tests using 0.5 M $(NH_4)_2SO_4$ at pH 3 and 1 M NaCl at pH 2. The remaining 29 samples were only processed with the NaCl solution.

Additionally, several samples were processed a first time then the residue reprocessed a second time. Numerous measurements were taken including ORP, terminal pH, filtration times, assays for REE, U, and Th on all products, and Fe, Mg, Ca, Al, P, Mn and Si assays on the leach solutions. Summary extraction results are plotted in Figure 4.

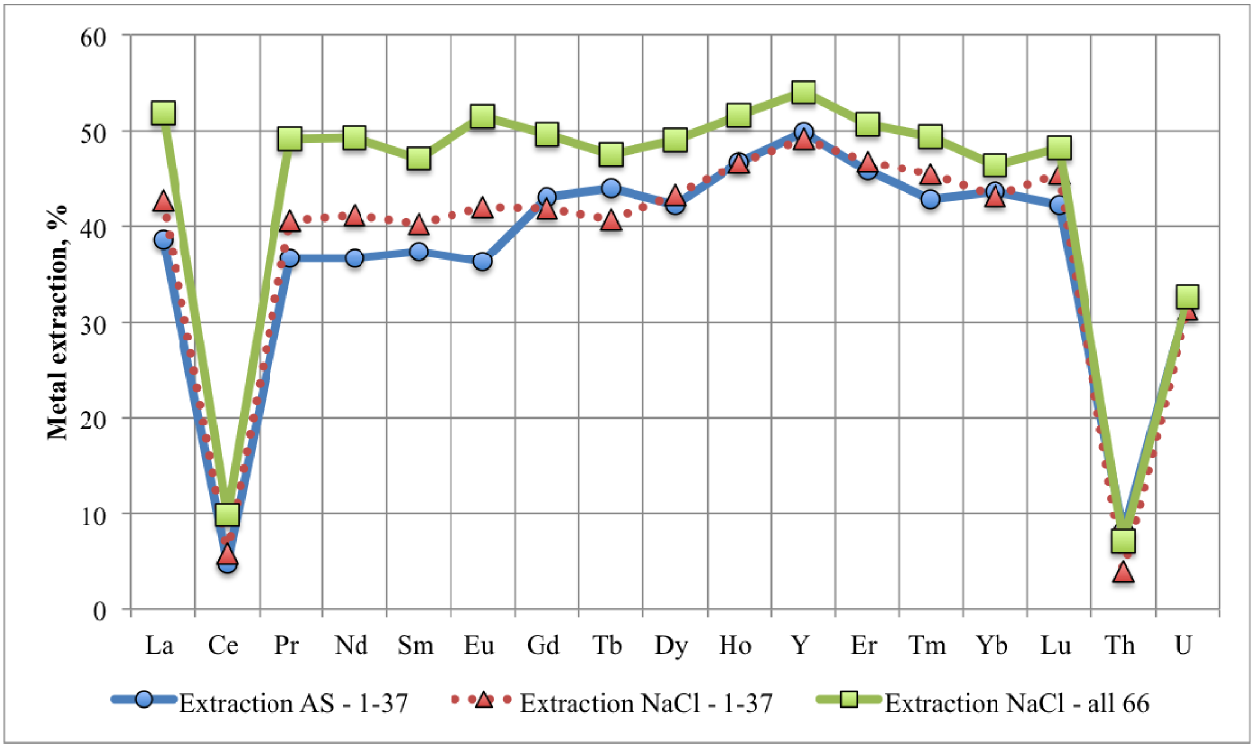

Figure 4. Weighted average extraction results for 66 samples.

Findings include the following:

- REE extractions varied considerably from 90% on some samples to 15% on others.
- The double contact work indicated that an extra 2% (absolute) could be obtained for the LREE and about 1% extra for the HREE.
- The double contact substantially increased Ce and Th extraction – presumably because of cerianite dissolution. Typically, 10% extraction after one contact would increase to about 15% for both elements after a second contact. It is believed this is a kinetic effect but more work will be done.
- In the 37 parallel tests NaCl performed slightly better than $(NH_4)_2SO_4$ (AS) but AS and NaCl were otherwise similar regarding extraction.
- Average extractions weighted according to mass (down-hole interval) and head assay for the parallel 37 tests and all NaCl desorptions are presented in Figure 4.
- The first 37 samples tested with both AS and NaCl happened to generally give lower extractions than the total population of 66 samples.
- Impurity levels in the leach liquors from the desorption tests varied as per the data in Table III which includes, for comparison, data presented by Chi [3] on Chinese leach solutions.

- It can be noted that the impurity levels recorded in Table III can be handled by selective precipitation.

- Various correlations have been examined such as filtration time versus grade and depth, extraction with ore type and lithology and generally weak or no correlation was evident

- Weak correlations between metal percentage extraction and depth show an interesting trend with LREE extraction decreasing with depth but HREE extraction increasing with depth

Table III. Impurity Elements in Pregnant Solutions - % TREE Basis

Impurity levels				Chi [3] - Table 9.2	
	AS 1-37	NaCl 1-37	All NaCl	AS	NaCl
Fe	12	19	15	13	24
Mg	61	59	83	1	2
Ca	103	83	84	13	24
Al	34	39	42	4	7
P	3	3	3	-	-
Mn	2	3	3	4	5
Si	13	12	12	0.4	2
Th	0.4	0.2	0.2	-	-
U	0.9	0.7	0.7	-	-

Interpretation of the data from the 66 samples continues and data from another batch of 113 samples now being processed will be integrated with said data as information becomes available.

Other work has been completed including an investigation of ion exchange as a means of recovering the REE from solution or slurry, counter-current leaching to establish a desorption isotherm, attempts to reduce Ce^{4+} and leach cerianite as a means of increasing the recovery of Ce and other REE, acidic extraction to better desorb REE from the clays and leach precipitated or "colloidal" REE [3], establishment of filtration data, etc. These data will be used to assist in the selection of a processing route for Serra Verde ore.

Possible Development Options

Following upon experience with REE recovery from ionic clays in China, and the recovery elsewhere of uranium, copper, and gold, the emphasis on the commercial recovery of REE at Serra Verde has been placed on heap leaching and in-situ recovery. Larger scale column leach tests are under way and experts in in-situ and heap leach development are being engaged.

An initial objective will be the recovery of a REE chemical concentrate from the leach liquors but clearly further upgrading of the bulk product to refined oxides in Brazil is an ultimate objective. Ways to reach that objective are under study.

Capital and operating costs are now being developed for a facility to mine, leach, precipitate, and separate 5,000 t/a of refined REO – with up to 40% being HREO.

It is possible that a beneficiation process can recover the residual primary mineralization thus doubling the recovery of REE. The beneficiation option will be further investigated once the leach approach has progressed.

Conclusions

Serra Verde Mining has defined a significant rare earth resource in Goias and Tocantins States in Brazil. Since the indication in late 2012 that much of the REE are sorbed on clays, a reasonable idea of the levels of extraction and a commercially viable process system have been generally defined. Work will continue to fully define the process.

The Serra Verde project is rapidly progressing towards development. It is fully expected that it will play a significant role in the supply of REE, and especially HREE, in the next few years.

Acknowledgements

The authors thank and acknowledge Antony and Anthony Mariano, and Nicole Morton and Tassos Grammatikopoulos of SGS for the mineralogical work; Ben Yu who managed the beneficiation work at SGS which was done by Hector Sarne and Marteen Lortie; Niels Verbaan and Mike Johnson who managed the hydrometallurgical testwork which was mainly conducted by Victoria VanderByl. Their diligent efforts are appreciated.

Numerous MVB and SVM staff and contractors who have assisted in defining the resource and assisting with metallurgical, engineering, and economic studies are thanked for their efforts.

We thank company management for their agreement to the release of data.

References

1. Hains Technology Associates, “Updated Technical Report on the Serra Verde Rare Earths Project, Goias, Brasil. Prepared for Mining Ventures Brasil. Report for NI 43-101”, in preparation.

2. G.J. Retallack, “Lateritization and Bauxitization Events”, *Economic Geology*, 2010, v. 105, 655–667.

3. Ru-an Chi and Jun Tian, *Weathered Crust Elution-Deposited Rare Earth Ores* (New York, NY: Nova Science Publishers, Inc., 2008), 1-78.

4. Antony N. Mariano and Anthony Mariano Jr., “Serra Verde Process Testing – Mineralogical Evaluation”, December 21, 2012.

5. Antony N. Mariano and Anthony Mariano Jr., “REE Ion-Adsorbed Clay Test; Serra Verde Saprolite and Mixed Samples”, December 21, 2012.

6. SGS Canada Inc., “An Investigation by High Definition Mineralogy into the Mineralogical Characteristics of Seven Composite Samples from the Serra Verde REE Deposit, Brazil”, January 10, 2013.

7. SGS Canada Inc., “An Investigation into Scoping Level Beneficiation Testwork on a Leach Residue from Serra Verde Ore Samples”, June 17, 2013.

8. SGS Canada Inc. “An Investigation into REE Desorption from Serra Verde Ore Samples – Scoping Level Tests”, June 2013.

9. Jun Tian, Ru-an Chi, and Jing-qun Yin, “Leaching Process of Rare Earths from Weathered Crust Elution-deposited Rare Earth Ore”, *Trans. Nonferrous Met. Soc. China*, 20 (2010) 892-896 166.

CRYSTALLIZATION OF RARE EARTH SOLUTION BY AMMONIUM BICARBONATE

Xian-ping Luo*, You-jun Qian, Xiao-ming Chen, and Chang-li Liang

Jiangxi University of Science and Technology
Ganzhou 341000, China

Keywords: Rare Earth Carbonate Crystal, Rare Earth, Crystallization, SEM

Abstract

In this paper, we will present the results of a study of the influence of chemical factors such as the molar ratio NH_4HCO_3/RE^{3+}，rare earth concentration and aging time on the formation of rare earth carbonate crystal. The molar ratio NH_4HCO_3/RE^{3+}, aging time, the concentration of rare earth and aluminum ion were identified as the major factors affecting the crystallization of rare earth carbonate. These factors were also found to have a significant impact on surface morphology and grain-size of rare earth carbonate, determined by scanning electron microscope (SEM) and Laser particle size analyzer, respectively. The optimum conditions of rare earth carbonate crystallization were determined as follows: the molar ratio NH_4HCO_3/RE^{3+} from 3.5 to 4.0; initial rare earth concentration from 1 to 10 g/L; and aging time of 40 min at room temperature with aluminum ion concentration lower than 50 mg/L.

Introduction

In industry, precipitation is the main method of recovering rare earth elements from leach solutions obtained from weathered crust elution-precipitated rare earth ore [1,2]. Oxalic acid was the initial precipitation agent of weathered crust elution-precipitated rare earth, but the cost is high of oxalic acid precipitation and the oxalic acid residue in the wastewater is harmful to the health of human and environment [3,4]. With the development of rare earth extraction technology, oxalic acid was replaced by ammonium carbonates, for the latter is friendly to environment and has higher selectivity. However, ammonium carbonate precipitation has some defects such as a tendency to form amorphous precipitates, and difficulty in solid-liquid separation.

Crystallization of rare earth carbonate is influenced by many factors, but previous studies mainly focus on empirical research on the precipitation process [5,7]. In recent years, some researchers have proposed the value of pH fall can be taking as a criterion of the rare earth carbonate crystallization characteristics based on the study of the relationship between crystallization process of rare earth carbonate and acidity changes of equilibrium solution [8,10].

In this paper, the influence of molar ratio NH_4HCO_3/RE^{3+}, aging time, the concentration of rare earth, and aluminum ion on the crystallization of rare earth carbonate were studied based on system pH value change, and the morphology and grain-size of rare earth carbonate precipitation were determined by SEM and Laser particle size analyzer, respectively.

Experimental

Samples and Reagent

La_2O_3 was provided by Ganzhou Rare Earth Group Co., LTD, Jiangxi province, China, and the purity of La_2O_3 was 99.9%. $LaCl_3$ solution was prepared by dissolved La_2O_3 in hydrochloric acid. All the chemical reagents used in the experiments were analytical reagent grade, and de-ionized water was used in the preparation of rare earth solution.

Precipitation Experiments

Precipitation experiments were performed at the condition that the stirring rate was maintained at 1000 rpm, and added into 3.4 mL NH_4HCO_3 solution every 5 minutes, and the concentration of NH_4HCO_3 solution is 0.33mol/L, and recorded the pH_{50} (pH_{50} represent the pH value of the system at 5 minutes since the addition of NH_4HCO_3 solution). We have measured the pH values of the system 10 seconds, 20 seconds, 1 minute, 2 minutes, 3 minutes, 4 minutes and 5 minutes after the addition of NH_4HCO_3 solution, and found the pH can maintained constant at 5 minutes (data is not shown in here). Therefore, pH_{50} can be used to characterization the pH of the precipitate system. All the precipitation and ageing experiments were carried out at room temperature 25^0 C. Triplicate experiments were performed under identical conditions.

Analytical Methods

Rare earth concentration was determined by EDTA volumetric titration methods, ammonium bicarbonate concentration was determined by standard acid neutralization titration method. The pH value of the solution was measured with pH meter (PHS-3C). Surface morphology and grain-size of rare earth carbonate was determined by Scanning Electron Microscope (XL30W/TMP) and Laser particle size analyzer (OMEC.LS908), respectively.

Results and Discussion

The influence of the molar ratio of NH_4HCO_3 to RE^{3+} on the crystallization of rare earth carbonate is shown in Figure 1.

It can be seen from Figure 1 that the pH_{50} value increased when the ratio is lower than 0.630, and the pH_{50} value decreased when the molar ratio is in the range of 0.630 to 0.930, then the pH_{50} value maintained quite constant in the ratio range of 0.930 to 3.50, and then the pH_{50} value increased when the ratio is higher than 3.5. The results showed that the rare earth carbonate is easily crystallized under low molar ratio when molar ratio NH_4HCO_3/RE^{3+} is 0.630~3.50, because the pH_{50} value decreasing rapidly and maintained at low level [8,10]. Crystallization of rare earth carbonate is in the inert interval when the molar ratio is greater than 4.0, because the pH_{50} values continue to increase in the ratio range. Meanwhile, the pH value has an inflexion when the molar ratio NH_4HCO_3/RE^{3+} is in the range of 3.50 to 3.780 showed the crystallization is completely. Therefore, the optimum mole ratio of NH_4HCO_3/RE^{3+} to the formation of crystallization of rare earth carbonate is in the range of 3.50~3.780.

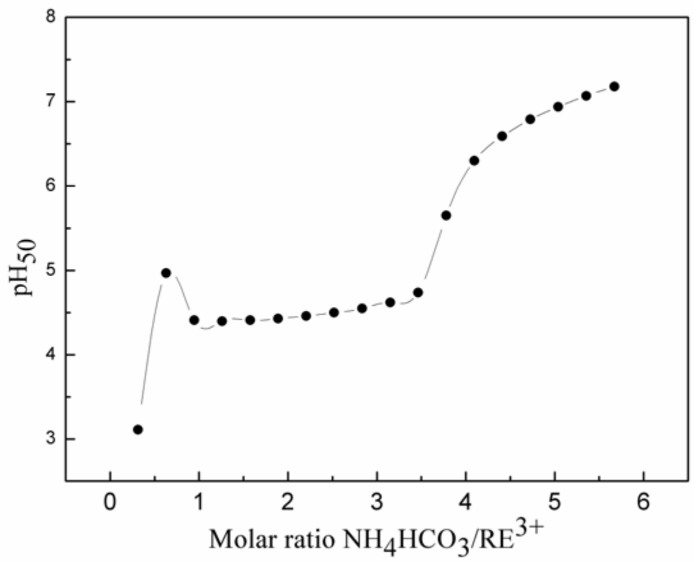

Figure 1. Influence of molar ratio NH_4HCO_3/RE^{3+} on the pH_{50}.

In order to examine the influence of rare earth concentration on rare earth carbonate crystallization, crystallization experiments were carried out under different concentrations of rare earth (0.61 g/L, 1.19 g/L, 4.75 g/L, 9.52 g/L, 12.21 g/L and 15.54 g/L) and the results are shown in Figure 2. The pH_{50} value does not vary very much when the rare earth concentration is 0.61 g/L, which showed that the crystallization speed of rare earth carbonate is slow.

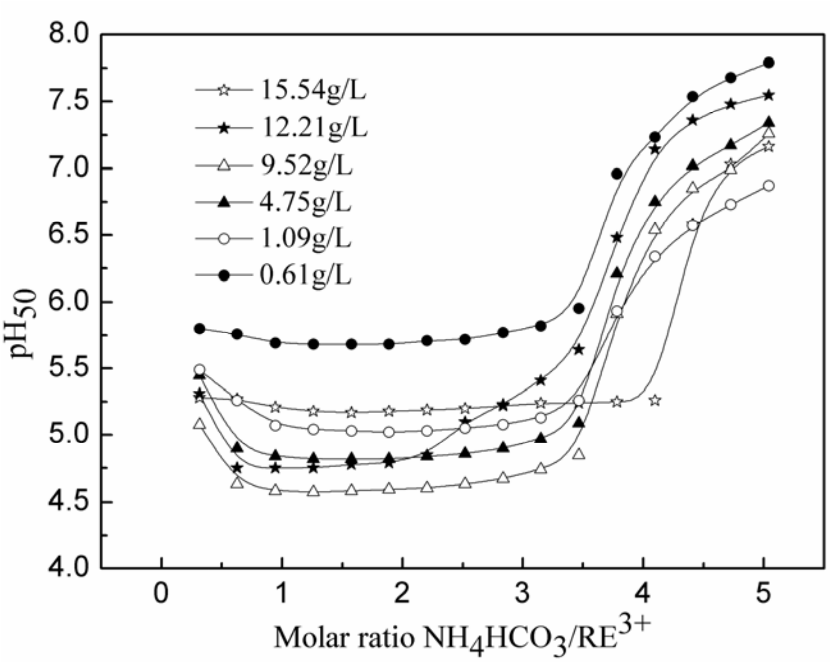

Figure 2. Relationship between pH_{50} and molar ratio of NH_4HCO_3/RE^{3+} under different rare earth concentration.

Crystallization rate is rapid when the rare earth concentration in the range of 1.09 to 12.21 g/mL because the pH_{50} value obviously decreased. It is noteworthy that the active interval of crystallization narrowed down significantly when the concentration is 12.21g/L, which showed the crystallization of rare earth is inhibited under high rare earth concentration. When the concentration is 15.45g/L, the pH value maintained rises in the crystallization, which showed that high concentration will inhibit the transformation of rare earth carbonate crystallization seriously. Optimal rare earth concentration of crystallization is in the range of 1.0g/L to 10.0 g/L.

The influence of rare earth concentration on the grain-size of the crystallization is shown in Figure 3. It can be seen from Figure 3 that the grain-size of the precipitate increased with the increasing rare earth concentration, and reached a maximum at the rare earth concentration of 9.5 g/L. The grain-size of the precipitate decreased when the concentration was higher than 9.5 g/L. The results indicated that the optimal concentration of rare earth is in the range of 5 to 10 g/L.

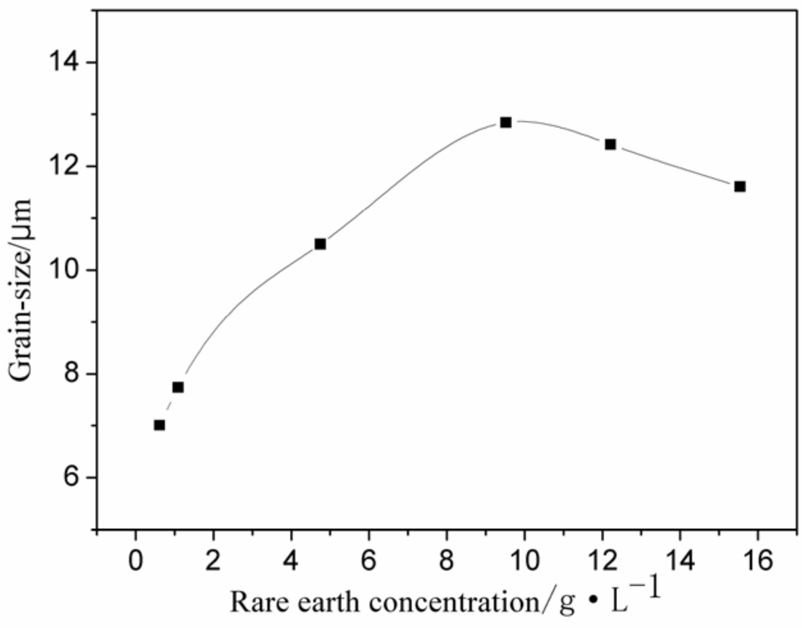

Figure 3. Grain-size analysis of crystallization under varying rare earth concentration.

The influence of aging time on rare earth carbonate crystallization is shown in Figure 4. It can be seen from Figure 4 that the pH value and the precipitate volume decreased with increasing aging time when the aging time is shorter than 40 minutes. The decrease of pH value and volume of precipitate indicates the transformation of amorphous floccules to crystalline precipitate takes place in this period and crystallization is complete when the ageing time is 40 minutes. The results showed that the optimal ageing time should be 40 minutes.

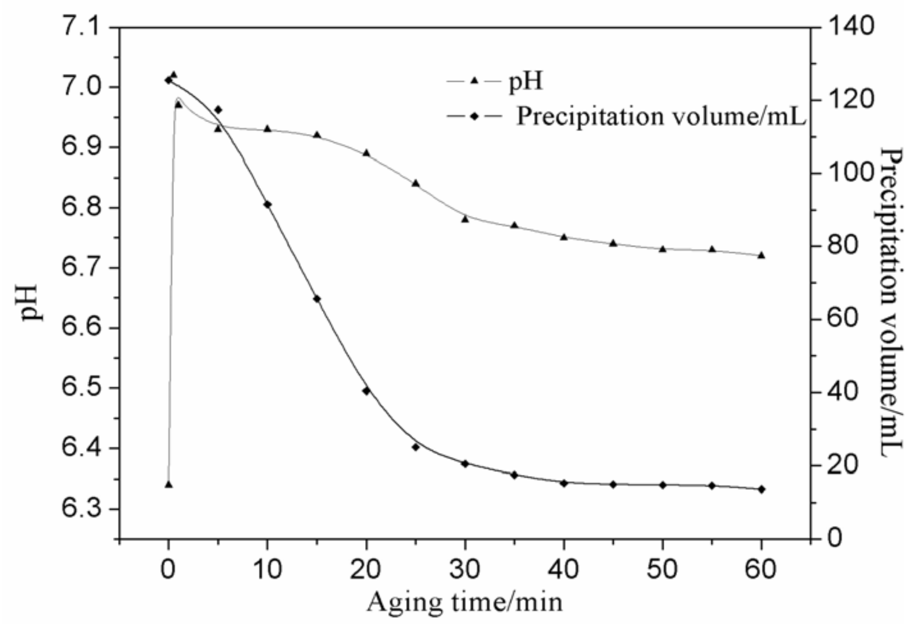

Figure 4. Influence of ageing time on the pH value and the volume precipitate.

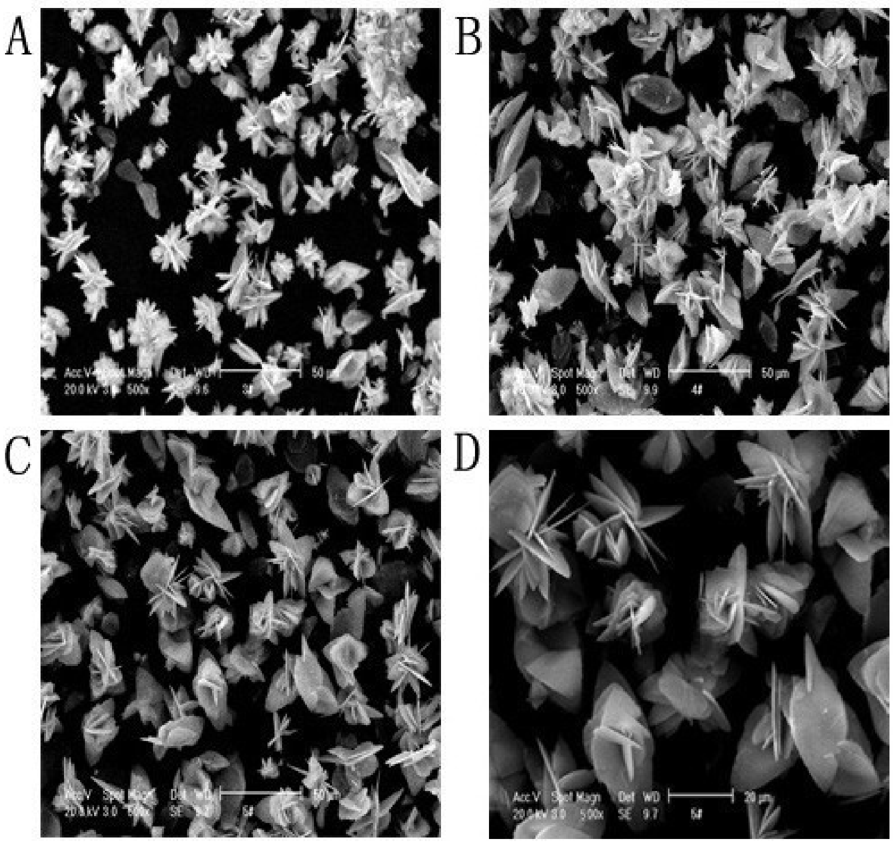

Figure 5. SEM micrographs of the rare earth carbonate precipitate formed under different aging time（Magnified 500 times）, A:0 min, B:5 min, C: 15 min, D: 40 min.

To further understand the influence of ageing time on the crystallization of rare earth bicarbonate, the micrographs and grain-size of the rare earth carbonate precipitate were studied by SEM and Laser particle size analyzer, and the results are shown in Figure 5 and Figure 6, respectively.

It can be seen from Figure 5(A) that the formation of rare earth bicarbonate amorphous precipitate is very rapidly. Rare earth bicarbonate crystals grow with the extending of the ageing time (Figure 5). The analysis of the grain-size of rare earth carbonate precipitate vary with the ageing time confirmed the grain-size increased with the increasing of ageing time (Figure 6). It can be seen from Figure 6 that the crystal grow completely when the ageing time is about 40 minutes for the grain-size increases very little with extension of ageing time. The results indicate the ageing time for rare earth carbonate crystal completion is 40 minutes.

In general, the weathered crust elution-deposited rare earth leach liquor contains a substantial amount of various impurities such as $(NH_4)_2SO_4$ (~2000 mg/L), Al^{3+} (~1000 mg/L), Fe^{3+} (~100 mg/L) and Ca^{2+} (~1000 mg/L), along with a small amount of Fe^{2+}, Pb^{2+} and Mn^{2+} [11, 12]. Described as above, aluminum ion is the primary impurity in leaching liquid of weathered crust elution-precipitated rare earth. In this study, the influence of aluminum ions on the crystallization of rare earth carbonate was studied and the result is shown in Figure 7, and the SEM micrographs and grain-size of rare earth precipitate under different aluminum ion concentration are shown in Figures 8 and 9, respectively.

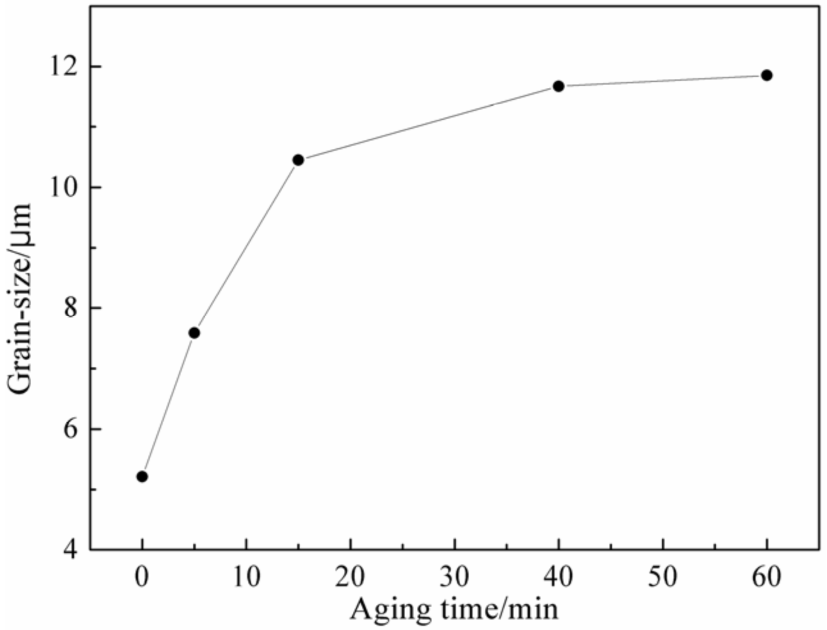

Figure 6. Grain-size of the earth carbonates precipitate under different aging time.

It can be seen from Figure 7 that the crystallization active zone of rare earth carbonate is narrowed down with increasing aluminum ion concentration. The molar ratio of rare earth carbonate crystallization is narrow down to the range of 1.575~3.15 when aluminum ion concentration is about 50 mg/L. As shown in Figure 7, pH_{50} value maintained rise when the concentration of aluminum ion was higher than 200 mg/L, which indicated that rare earth carbonate precipitation cannot spontaneously transform to crystal. The results showed that the existence of aluminum ions in the precipitation system inhibited the crystallization of rare earth carbonate and lead to a narrowing down of the crystallization activity zone. Rare earth carbonate precipitation cannot spontaneously transform to crystallization when the concentration of aluminum ion is higher than 50 mg/L.

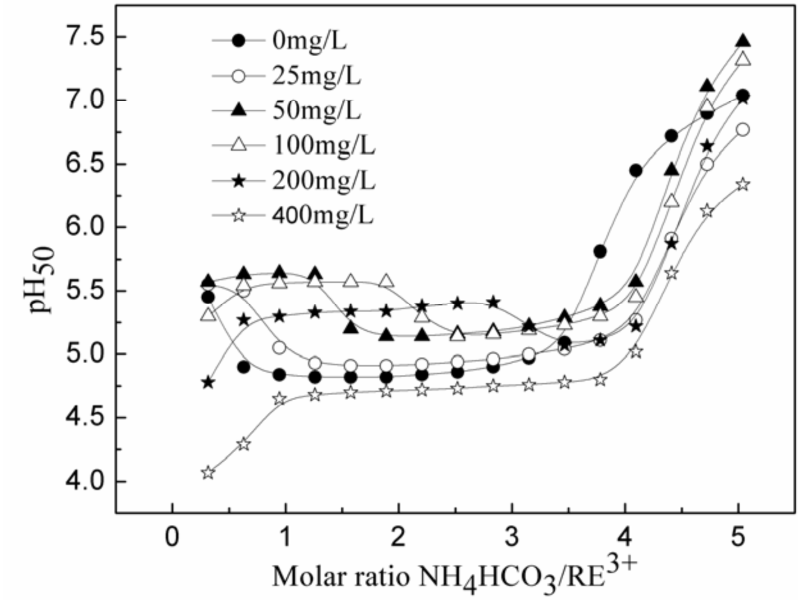

Figure 7. Relationship between pH_{50} and molar ratio NH_4HCO_3/RE^{3+} under different concentration of aluminum ion.

It can be seen from Figure 8 that the presence of aluminum ions has significant influence on the micrographs of rare earth carbonate. The presence of 50 mg/L aluminum ions made the short and thick layered crystal obtained in the absence of aluminum transform to long and thin needle-like structure in the precipitate. The results showed the presence of aluminum ions can inhibit the formation of rare earth carbonate crystal.

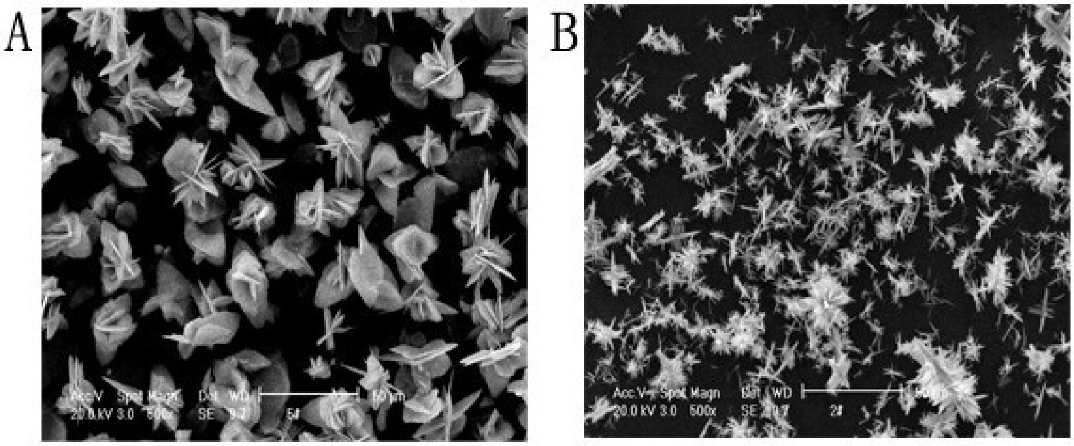

Figure 8. SEM micrographs of precipitate without (A) and with 50mg/L aluminum ion (B).

The influence of aluminum concentration on the grain-size of the precipitate is shown in Figure 9. The results of the analysis of the precipitate grain-size under different concentration of aluminum ion showed that the grain-size decreased rapidly with the increasing of the aluminum ions concentration. The results confirmed the inhibition effect of aluminum ions on the crystallization of rare earth carbonate. The results showed that the aluminum ion has serious inhibition effect when aluminum ions concentration is higher than 50 mg/L.

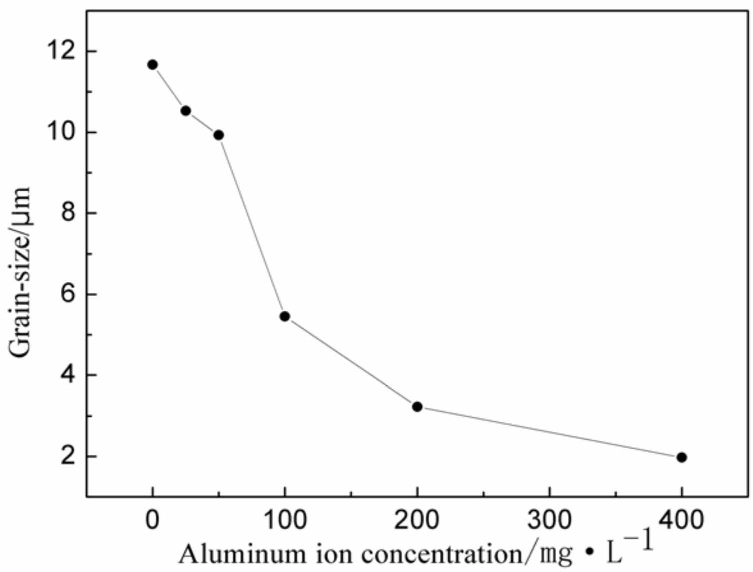

Figure 9. Grain-size analysis of precipitate under varying aluminum ion concentration.

Conclusions

Crystallization experiments showed that the molar ratio of NH_4HCO_3 to RE^{3+} in the range of 3.5 to 4.0 is favor of the formation of rare earth carbonate crystal. The active interval of crystallization is wide when the rare earth concentration is in range of 1 to 10 g/mL, and the grain-size analyze confirmed the maximum grain-size appeared at the concentration of 9.5 g/L. The results of SEM and grain-size of rare earth precipitate under different aging time showed that the complete crystallization needed an ageing time that is not shorter than 40 minutes. The presence of aluminum ions has a significantly inhibiting effect on the crystallization of rare earth carbonate, and amorphous rare earth carbonate precipitate can be formed when the aluminum ions concentration is higher than 50mg/L.

Acknowledgements

The work presented in this manuscript was funded by the National Key Technology R&D Programs under Grant No. 2012BAC11B07, the Program for New Century Excellent Talents in University under grant No. NCET-10-0183 and the Project for Ganpo 555 Excellent Talents.

References

1. Guang X Xu, *Rare Earth* [In Chinese] (Beijing, BJ: Metallurgical Industry Press,

1995)163-175.

2. R.A Chi and J. Tian, “Review of Weathered Crust Rare Earth Ore (In Chinese),”*Journal of the Chinese Rare Earth Society*, 25(6) (2007), 641-650.

3. Y.X Li et al., “Precipitation and Crystallization process of Rare Earth Carbonate (In Chinese),” *The Chinese Journal of Nonferrous Metals,* 1 (1999):1-9.

4. J. Tian et al., “Development progress and Researth Connotation of Green Chemistry of Extraction Process of Rare Earth from Weathering Crust Elution-deposited Rare Earth Ores in China (In Chinese),” *Chinese Rare Earths,* 27(1) (2006), 70-72.

5. S. Liu, R.J Ma, “Preparation of Crystalline Precipitation of Mixed Rare Earth Carbonates (In Chinese),” *The Chinese Journal of Nonferrous Metals*, 8(2) (1998), 331-334.

6. L.Y. Zhang, Z.H. Wu and H.J. Zhang, “Precipitation of the Mixed Crystalline Rare Earth Carbonate (In Chinese),” *Chinese Rare Earths*, 17(3) (1996), 61-63.

7. Y.J. Wang and J.X. Guo, “Study of Precipitation Process for Crystalline Promethium-neodymium Carbonate,” *Rare Earths & Cemented Carbides*, 31(2): (2003),12-14.

8. Z.Y. Gu et al., “Spontaneous Crystallization of Lanthanum Carbonate (In Chinese),” *Chinese Rare Earths*, 22(2) (2001), 7-9.

9. X.Y. Jiao et al., “Study of Crystallization Process during La and $La_2(CO_3)_3$ Precipitation with Sodium Bicarbonate (In Chinese) ,” *Rare Earths & Cemented Carbides*, 145 (2001), 4-8.

10. X.B. He and Y.X. Li, “Crystallization Activity Zone, Crystallization Mechanism and Morphology of praseodymium (In Chinese),” *Journal of the Chinese Rare Earth Society*, 20(2002), 95-98.

11. C. Bazin, K.El-Ouassiti and V. Ouellet, “Sequential leaching for the recovery of alumina from a Canadian clay,” *Hydrometallurgy*, 88 (1–4), (2007), 196–201.

12. Y.X. Li et al., “Precipitation reaction of $RECl_3$ with NH_4HCO_3 and co-precipitation behavior of accompanying impurity ions (In Chinese),” *Chinese Rare Earths*, 20 (2), (1999), 19–22.

LOW TEMPERATURE (T<100°C) REGENERATION OF HCl FROM CHLORIDE LEACHING OF Ca-BEARING MINERALS

Seref Girgin[1], Thomas Feldmann[2], Sebastian Humphrey[1], George P. Demopoulos[2]

[1] BBA Inc., 630 Rene-Levesque Blvd. West, Montreal, QC, Canada, H3B 1S6
seref.girgin@bba.ca

[2] McGill University, 3610 University Street, Materials Engineering Department, Montreal, QC, Canada, H3A 0C5
george.demopoulos@mcgill.ca

Keywords: Hydrochloric Acid Regeneration, Crystallization, Growth Rate, Calcium Sulfate, Operating Cost

Abstract

HCl regeneration is a challenge in the development of any hydrometallurgical chloride processes. This is particularly applicable in the treatment of REE containing carbonate and apatite minerals. The leaching of calcium containing minerals generates a $CaCl_2$ solution. Commonly used pyrohydrolysis does not apply to such $CaCl_2$ solutions for HCl regeneration due to thermodynamic limitations. McGill University has been developing an alternative that regenerates HCl from $CaCl_2$ solutions via stage-wise reaction with H_2SO_4 below 100°C. Besides the regeneration of azeotropic strength HCl, the process offers the potential of generation of commercial $CaSO_4$ products (i.e. gypsum, alpha-hemihydrate). This paper discusses the operating conditions to produce concentrated HCl and $CaSO_4$ compounds with different forms and qualities and briefly addresses the engineering aspects (material balance and process economics) of a conceptual flowsheet.

Introduction

Hydrochloric acid is an important reagent in the metallurgical industry for primary metal extraction and in processing operations, such as steel sheet pickling. For example, the usage of HCl allows effectively leaching sulfidic minerals [1-3], upgrading titani-ferrous slags [4] or the extraction of rare earth metals from apatite based host rock [5-8]. The latter is a calcium fluorophosphates and due to this chemical nature, it is a source of a concentrated spent $CaCl_2$ during the extraction of rare earths.

Other sources of concentrated calcium chloride solutions are HCl based leaching slurries, where the target metal and impurities are separated by stages-wise lime neutralization. One such example is the INTEC nickel process.

Hydrochloric acid is popular in the metallurgical industry due to fast reaction kinetics and the typically high solubility of chloride salts [9, 10]. However, at some point during the extraction process the chloride solution, which is typically concentrated in the tens to hundreds of gram per liter range, needs to be treated. This has to be done for environmental reasons, as the inflow of chlorides into fresh water resources is limited [11], but also for economic reasons, namely cost-saving [12].

The regeneration of HCl from spent chloride solutions can principally be achieved by different methods. These can be grouped into (i) membrane separation, (ii) pyrohydrolysis, (iii) hydrothermal and (iv) crystallization techniques [13-15]. However, not all techniques are applicable to all kinds of feed solutions or feasible on industrial scale. For example, it is possible to produce HCl, simultaneously with NaOH from a NaCl solution via membrane electrolysis. Unfortunately, this process suffers from low current efficiency (~60%), especially at high acid concentration.

In the iron and steel industry large volumes of chloride solutions, originating from steel pickling operations, containing ferrous ions (Fe^{2+}) are treated by the pyrohydrolysis method. This involves the use of a spray roaster or fluidized bed reactor. The iron chloride solution is converted to iron oxide and HCl at high temperatures of 500°C to 800°C [16-19]. A drawback of this regeneration method is the high energy requirement caused by the high temperatures [20]. A less energy intensive regeneration option is the so called “PORI process” or hydrothermal acid regeneration. In this process ferrous chloride solution is oxidized, the resulting ferric chloride is hydrolysed at 150°C to 250°C to HCl and iron(III) oxide [21, 22]. However, this process still requires significant heating due to the elevated temperature.

Treating $CaCl_2$ solutions by pyrohydrolysis is unfortunately thermodynamically very disadvantaged. While the pyrohydrolysis process can be used to regenerate HCl from chloride solutions of Al, Co, Fe, Mg, Mn or Ni, it proves less suitable for $CaCl_2$ solutions [16, 20, 23]. The formation of CaO occurs only at temperatures well above 1000°C to a sufficient extent . Therefore, only crystallization remains an industrially viable option for HCl regeneration. It has been shown that via the simple chemical reaction of calcium chloride solution with sulfuric acid HCl can be easily produced at high strengths via precipitation of only slightly soluble calcium sulfate phases. There are three main phases of $CaSO_4$, namely, Dihydrate (DH or D), hemihydrate (HH or H) and anhydrite (AH or A). The type of calcium sulfate depends on the water content x in the crystal.

$$CaCl_2 + H_2SO_4 + xH_2O \rightarrow 2\ HCl + CaSO_4 \cdot xH_2O \tag{1}$$

This process can be carried out at temperatures well below 100°C and is flexible with respect to the calcium sulfate phase obtained as well as the directly achievable HCl strength [24-28]. Furthermore, it allows the selective production of valuable calcium sulfate α-HH. This calcium sulfate phase can be used as a high-strength building and plaster material with properties superior to conventionally used Plaster of Paris [25, 29-31].

Key parameters of the regeneration process are temperature and water activity. The latter is related to the concentration of HCl and $CaCl_2$. It has been found that especially higher temperatures (50-90°C) at a given concentration will lead to the formation of α-HH [25, 32].

Given the target of a specific HCl concentration to be obtained from the crystallization process, the concentrations of the feed solutions ($CaCl_2$ and H_2SO_4) are only variable to a limited degree.

Even though the chemical reaction of the proposed acid regeneration process is simple and thermodynamic calculations supported its feasibility in principle [26] it is necessary to consider kinetic aspects for design and product quality purposes.

Given the information provided above, the operability of atmospheric HCl regeneration process depends on the quality of $CaSO_4$ precipitates as much as HCl strength. Therefore, it is the objective of this paper to summarize some of the work of McGill Hydrometallurgy group on $CaSO_4$ precipitation and HCl regeneration. The paper presents an overview on some aspects of the crystallization of calcium sulfate phases (stability, reactive crystallization with and without seeding and crystal growth kinetics) with focus on α-hemihydrate due to its technical and economical properties. Furthermore, a detailed mass-balance of the proposed HCl regeneration flow sheet and a preliminary economic evaluation will be presented.

Experimental

Experimental Setup and Procedure

The experimental program covered the testing of the stability of $CaSO_4$ phases, reactive crystallization tests by the reaction of $CaCl_2$ with H_2SO_4 in the absence and presence of seed material and crystal growth kinetics.

The $CaSO_4$ phase stability tests were carried out in 250 mL Erlenmeyer flasks, containing $CaCl_2$/HCl electrolyte solution. The flasks were placed in a water bath that was heated by a thermostatic heater/circulator. The solution temperature was monitored by a temperature probe. Once the desired temperature (80°C±0.5) was reached, $CaSO{\cdot}2H_2O$ was introduced to electrolyte solutions and the slurry was equilibrated.

Samples were withdrawn at certain time intervals during the progress of equilibration of dehydrate crystals and prepared for characterization and analysis. Slurry samples taken for solids characterization were hot filtered, washed with boiled water and acetone and dried at 60°C. This crystal handling procedure [25] was followed to ensure the stability of the produced $CaSO_4$ phases during filtration and especially drying.

The reactive crystallization (precipitation) experiments were performed in a 2 liter glass autoclaveable reactor and the constant solution temperature (80°C) was maintained with a circulating oil bath. The internal temperature was also controlled by a digital thermometer with a precision of ±2°C. The precipitating agent (H_2SO_4) was added to $CaCl_2$-containing solution by a burette with a constant SO_4 addition rate.

All seeded crystallization experiments were carried out at 80°C using hemihydrate seeds. Two types of α-$CaSO_4$ hemihydrate seed material were used; the first one was laboratory-made seed produced by the reaction of 3.5M $CaCl_2$ and 8M H_2SO_4 at 80°C after 4 hours (8 stages of acid addition 4 hours equilibration product) and the other one was commercial HH material produced by the Omega Process [33].

For seed the recycling tests, starting $CaCl_2$/HCl solutions were reacted with 5.32M H_2SO_4 in 8 stages (30 minutes each) and 4 stages (60 minutes each). Fresh seed (100 g/L) was added at the beginning of each series of tests with subsequent tests involving recycling part (100 g/L for 3M $CaCl_2$, 50g/L for 1.5M $CaCl_2$ + 3M HCl) of the product. Laboratory-made α-HH and commercial Omega α-HH were used as seed material.

The crystal growth experiments were conducted in a glass semi-batch reactor allowing for temperature control, reagent addition via peristaltic feed pumps and mechanical agitation. Furthermore, the 2L reaction vessel had baffles to improve mixing conditions. These experiments involved addition of $CaCl_2$ and Na_2SO_4 solutions to ensure an equimolar Ca^{2+} and SO_4^{2-} ion inflow to a seeded background solution mimicking steady state conditions of the acid regeneration process. Sodium sulfate instead of sulfuric acid as a source of sulfate ions for the crystal growth process was chosen in order to not significantly change the acid concentration in the reactor. This method resulted in nearly constant supersaturation conditions during the crystal growth process. Details are reported elsewhere [34].

Characterization Methods

Solution samples from the stability and reactive crystallization tests were subjected to ICP analysis (Thermo Jarrell Ash ICP-AES). The nature of the solid phase was characterized by XRD (Philips PW1710 X-ray diffractometer) and scanning electron microscopy (JEOL 840A or Philips XL30 FEG).

In order to determine the crystal growth rate, volume-based particle size distributions were measured with a Horiba Laser Scattering Particle Size Distribution Analyzer LA-920. Additionally, BET surface area measurements of the seed crystals were undertaken with a Micromeritics Tristar Surface Area Analyzer. Finally, thermodynamic calculations were conducted with the OLI Stream Analyzer [35]. To ensure reproducibility, the growth kinetics experiments were repeated three times and arithmetic averages were employed in the analysis of the data.

Results and Discussion

Stability of Calcium Sulfate Phases

Due to the existence of three different calcium sulfate phases their stability and eventual phase transformations were investigated. The transformation of DH (initial material) to HH and AH was initially studied via a series of stability tests carried out in a wide range of electrolyte composition conditions that were selected with the view of simulating the $CaCl_2$-H_2SO_4 reaction system by considering the change in $CaCl_2$ (decrease) and HCl (increase) concentrations (Table I). The tests were realized at 80°C, where HH metastability is expected [36]. The total chloride concentration was kept constant at 6M, which corresponds approximately to 22% HCl, when HCl is the only reaction product. The data of Table I is based on XRD characterization of the starting, intermediate and final solids. Typical XRD data is shown in Figure 1 illustrating the transformation of DH to HH and AH over time.

Table I. Dihydrate Conversion in Variable $CaCl_2$-HCl Concentrations at 80°C

$CaCl_2$ + HCl, M	Equilibration time, hour					
	0.5	1	2.5	5	18	24
2.5 + 1.0	D	D	D(H)*	D(H)	-	A
2.0 + 2.0	-	-	H	H	A	A
1.5 + 3.0	D(H)	D(H)	D/H**	-	-	A
1.0 + 4.0	H/A	A/H	A	A	A	A
0.5 + 5.0	H/A	A(H)	A	A	A	A
0.0 + 6.0	A	A	A	A	A	A

*Phase in brackets indicates minor amount

**Phases indicated with slash (e.g. D/H) means comparable amounts of both phases

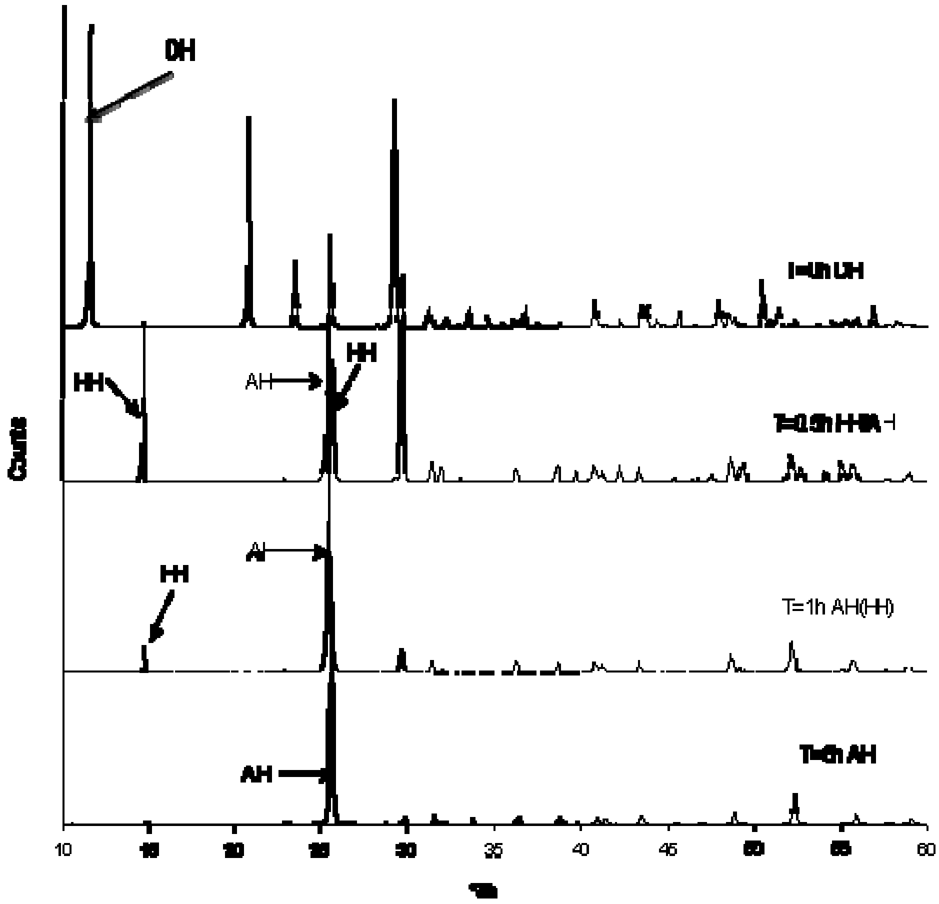

Figure 1. DH-HH-AH conversion with time in 0.5M $CaCl_2$ + 5M HCl solution (80°C).

Solubility estimation of $CaSO_4$ phases provided insight to the stability of those phases. The observed transformations can be attributed to the solubilites of the three $CaSO_4$ phases, which were estimated using the OLI Stream Analyser Software [26, 37]. By comparing the solubilities of the three phases, the relative stability of them can be established. These results showed that AH is the only stable phase in the 1-6M HCl concentration range at 80°C with lowest solubility. DH is metastable at less than 3M and HH is metastable above 3M HCl. Test results confirmed the solubility findings except HH formation was not observed above 3M HCl concentration. This may relate to its very fast transformation kinetics of HH. Hence the production of HH in HCl-H_2O system at 80°C does not appear feasible in the absence of $CaCl_2$ and promotes the formation of AH.

Another solubility estimation example is presented in Figure 2, where solubility of the $CaSO_4$ phases was predicted in the presence of 1.5M $CaCl_2$. The promotion of DH conversion towards HH was confirmed with the analysis of the solubility of these $CaSO_4$ phases in the $CaCl_2$ (1.5M)-HCl system. It can be seen from this Figure that HH becomes metastable above 1M HCl when 1.5M $CaCl_2$ is present.

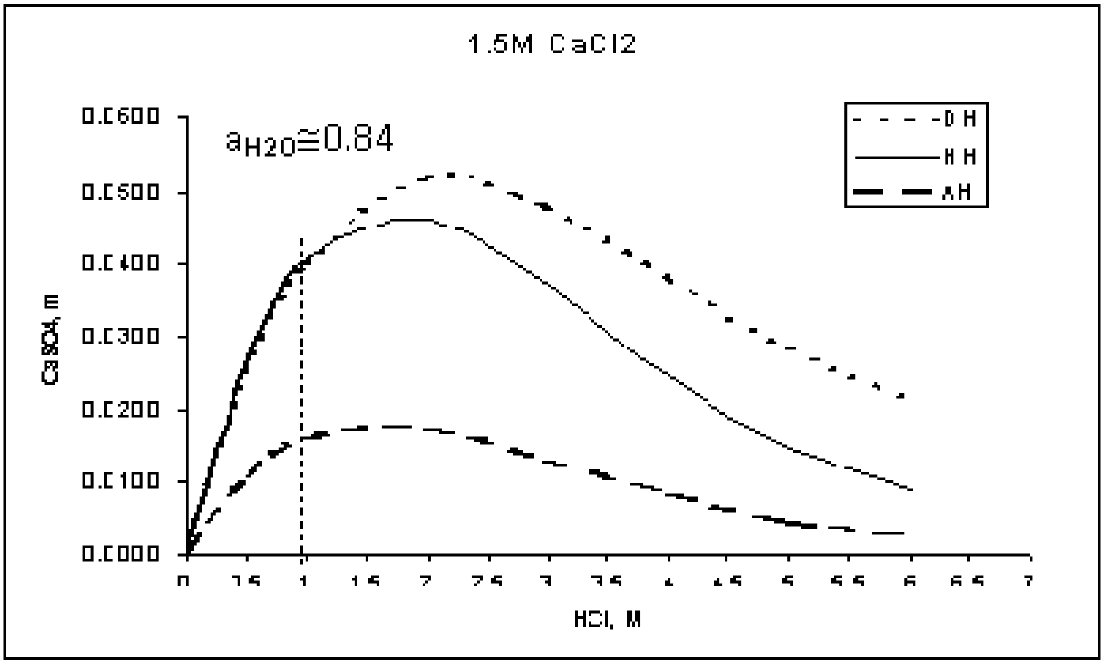

Figure 2. Solubility of $CaSO_4$ hydrates (DH, HH, AH) as a function of HCl concentration in the presence of 1.5M $CaCl_2$ (80°C).

The experimental findings from all stability tests run at 80°C were used to construct dihydrate-hemihydrate-anhydrite kinetics-based stability diagrams. The stability or transition regions of the $CaSO_4$ phases evolved with time.

In an effort to reconcile the generated experimental stability data with the water activity and solubility equilibria of the $CaSO_4$-HCl-$CaCl_2$-H_2O system the diagram of Figure 3 was constructed. In this diagram water activity lines as a function of electrolyte concentration, experimental stability data after 5 hours equilibration and the theoretical DH/HH transition line are plotted. The theoretical transition line was determined by following the points at which DH and HH have the same solubility (refer for example to Figure 2) and indicates a water activity set point of 0.85. There is satisfactory agreement between the experimental stability region of DH and the theoretical DH stability region defined by DH/HH transition line except the conditions that dictate the absence of $CaCl_2$ and presence of high HCl concentration (i.e. above 3M).

Figure 3 suggests the presence of $CaCl_2$ in the regenerated HCl solution in the range of 0.5M in order to ensure the formation of HH. This implies for the practical application of the process, that not all Ca^{2+} should be reacted according to the stoichiometric ratio, but rather a certain percentage needs to remain unreacted as $CaCl_2$

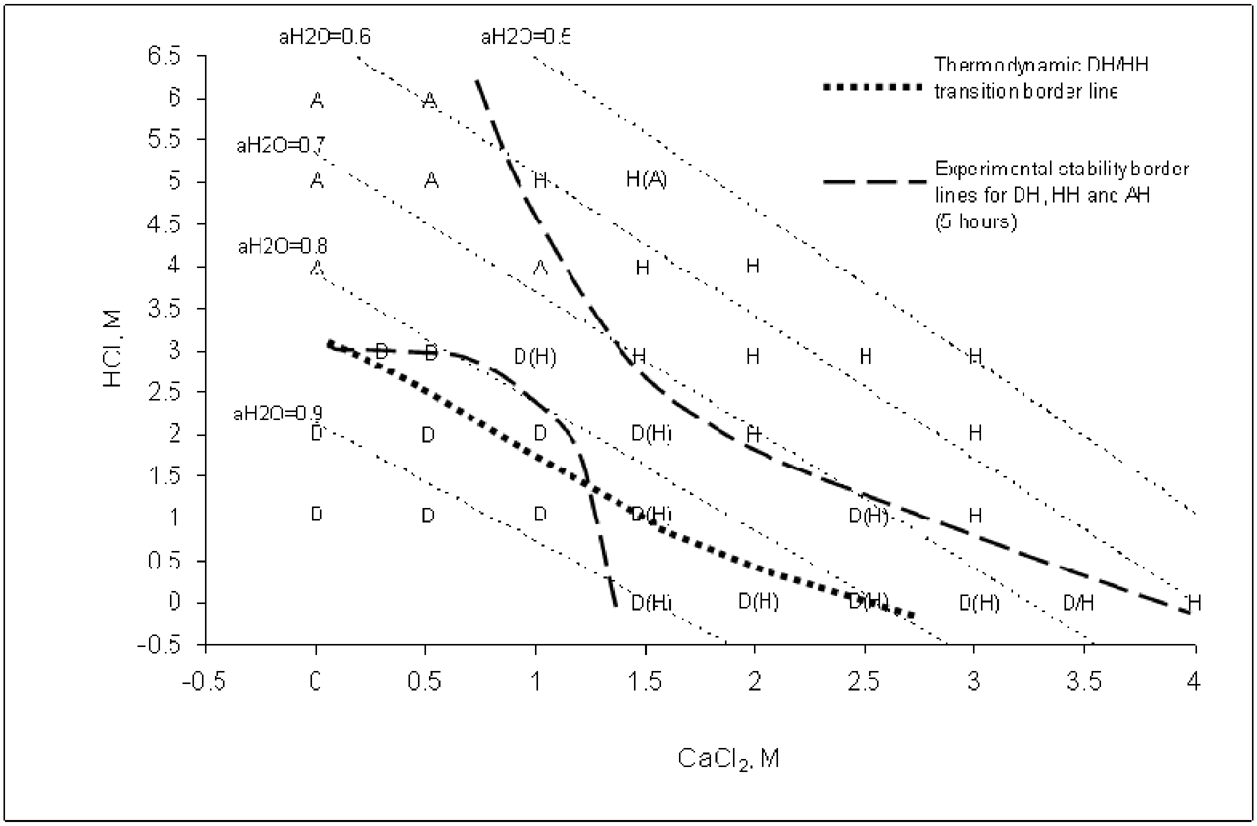

Figure 3. Experimental and theoretical stability regions for $CaSO_4$ hydrates and water activities in $HCl-CaCl_2$ solutions at 80°C (5 hours equilibration time).

Reactive Crystallization of Calcium Sulfate Phases and HCl Regeneration

A series of tests (at 80°C) were conducted at various initial and final $CaCl_2$ / HCl (total $[Cl^-]$ kept constant at 6M) and H_2SO_4 concentrations in order to verify the behavior of $CaSO_4$ phase formation and transformation especially as a function of the sulfate to calcium ratio. Table II summarizes the experimental conditions and the nature of produced $CaSO_4$. Test results confirmed the required levels of HCl and $CaCl_2$ concentrations in the regenerated acid for HH stability. According to Table II, above 3M HCl and 0.5M $CaCl_2$ concentrations favor the metastability of HH. Figure 4 illustrates the significant morphological changes caused by the conversion of DH to HH. The typical plate-like DH morphology is converted to an elongated, acicular crystal shape. This phase transformation was found to follow a dissolution-precipitation based mechanism [32].

Table II. Summary of Preliminary Reactive Crystallization Tests

Initial Solution CaCl$_2$ + HCl, M	Final Solution (Estimated*) CaCl$_2$ + HCl, M	Titrant H$_2$SO$_4$, M	Titrant Volume, mL	Titration/ Equilibration Time, hour	SO$_4$/Ca Ratio	Phase After Equilibration
3.0+0.0	1.45+1.45	2.66	75.0	1/6	0.33	DH
3.0+0.0	0.72+2.90	5.32	75.0	2/4	0.66	α–HH
2.5+1.0	0.36+3.63	5.32	75.0	2/4	0.80	α–HH
2.0+2.0	0.84+3.37	5.32	37.5	1/4	0.50	α–HH
1.5+3.0	0.36+3.63	2.66	75.0	1/4	0.66	α–HH
1.5+3.0	0.42+4.21	5.32	37.5	1/4	0.66	α–HH
1.0+4.0	0.00+4.36	2.66	75.0	1/4	1.00	AH
1.0+4.0	0.00+5.05	5.32	37.5	1/4	1.00	AH
2.0+2.0	0.00+4.36	5.32	75.0	2/4	1.00	AH

*The estimation assumed 100% conversion of added H$_2$SO$_4$ to CaSO$_4$ (aq or solid) and HCl

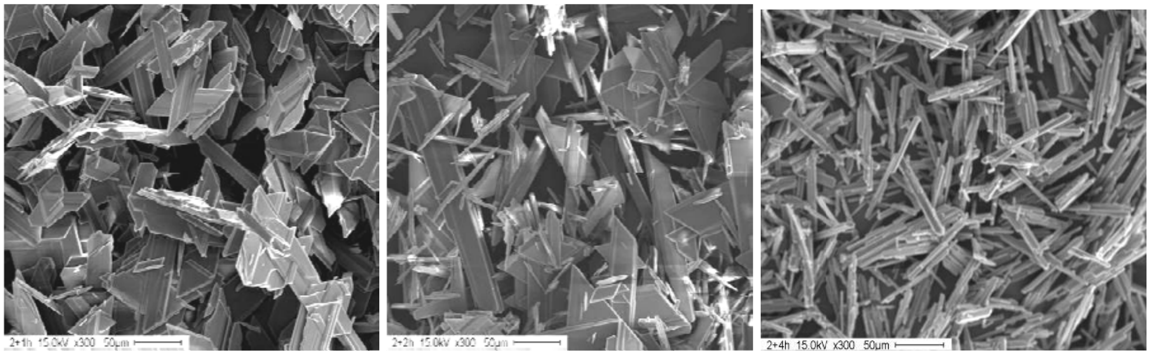

(a) DH (b)DH+HH (c)HH

Figure 4. SEM images of equilibrated solids following the 2 hours titration of 3M CaCl$_2$ solution with 5.32M H$_2$SO$_4$ at 80°C after (a) 1 hr, (b) 2 hrs, (c) 4 hrs.

Time-Dependent Stability Diagram: The results obtained from the reactive crystallization tests were used to construct a time-dependent stability diagram. The nature of CaSO$_4$ obtained after 1, 2 and 4 hour equilibration (following CaCl$_2$ and H$_2$SO$_4$ reaction) was located on CaCl$_2$ vs. HCl plots (Figure 5).

The left-hand side of the continuous line represents the region where HH is unstable. The right-hand side of both the continuous and broken lines represents the region where HH is stable from 1 to 4 hours. Since AH is the only thermodynamically stable phase at 80°C, the material produced within the range of this diagram is going to convert to AH when equilibrium is reached. In terms of metastability of HH, 0.5M CaCl$_2$ and above 5M HCl regenerated acid concentrations is once more found acceptable.

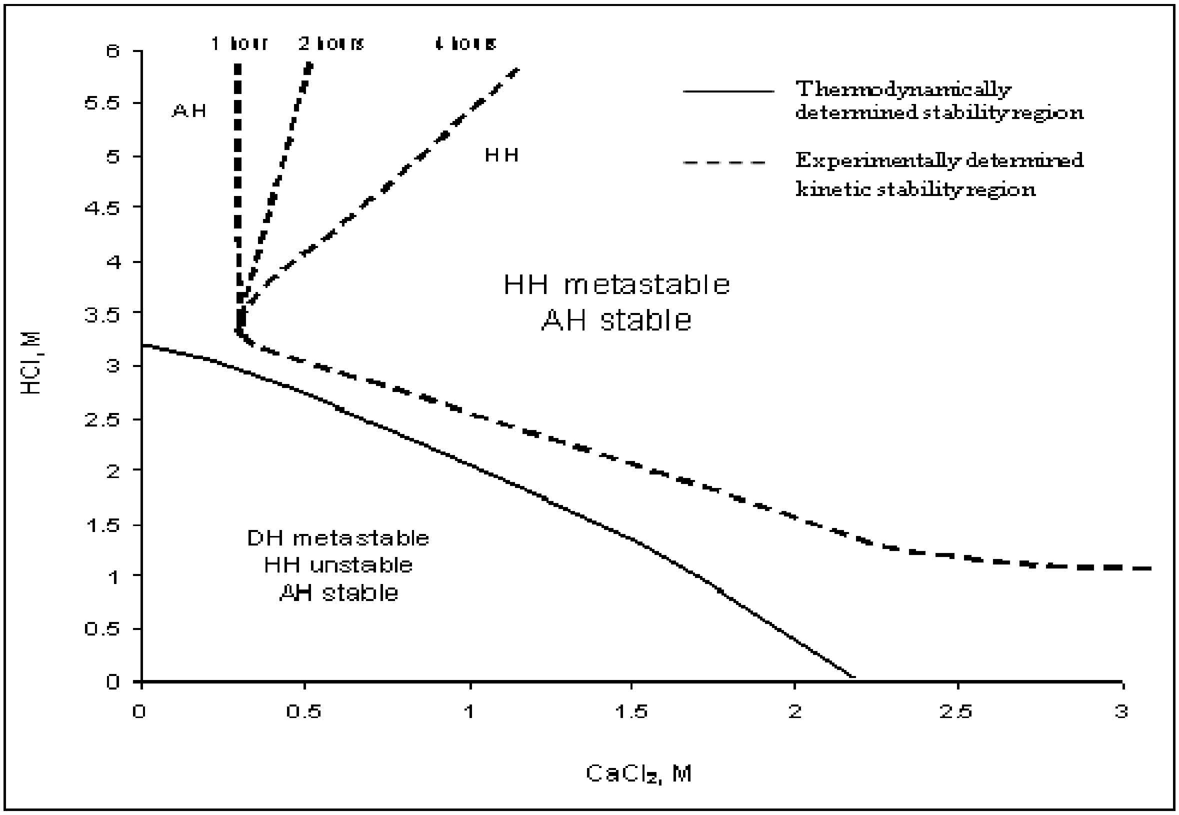

Figure 5. Thermodynamic and time-dependent (2 hours titration+equilibration) stability diagram of HH at 80°C.

Effect of Reaction Extend: The reaction of H_2SO_4 and $CaCl_2$ solution is associated with homogeneous nucleation followed by a growth period. The relative ranges of the nucleation and growth periods will be a function of the method of acid addition. In this section the process system is further analysed by explaining and optimizing the method of H_2SO_4 addition. It becomes evident that the conditions of H_2SO_4 addition (such as acid strength, SO_4/Ca ratio addition rate and continuous vs. staged addition) would influence the supersaturation environment hence the quality of the crystals at different regenerated acid concentrations.

Particle size analysis (Figure 6) of produced HH crystals clearly showed that the crystals grow longer with the extend of the reaction (increasing SO_4/Ca ratio). This was translated to improved filtration rates as well: 1737 kg/m^2/hr for SO_4/Ca = 0.8 vs. 869 kg/m^2/hr for SO_4/Ca = 0.4.

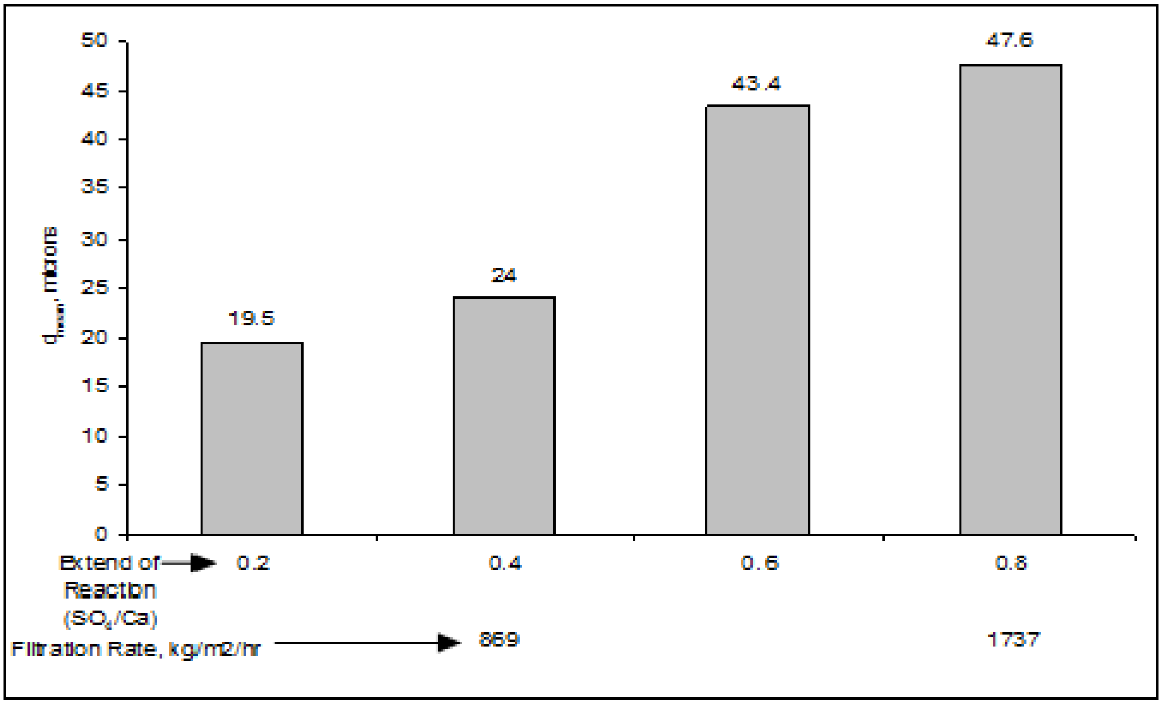

Figure 6. Effect of reaction extent (SO_4/Ca ratio) on mean diameter and filtration rate.

H_2SO_4 Concentration and Step-wise H_2SO_4 Addition: The addition of H_2SO_4 with a concentration above 5.32M (i.e. up to 9M H_2SO_4) was tested to evaluate the opportunities that reduce the amount of dilution water added to the reaction. By doing that it was expected to reduce acid regeneration costs by reducing the water circulating in the circuit that needs to be treated I.e. evaporation) later in the process. The testing of higher H_2SO_4 concentration resulted in the transformation of HH crystals into AH after 4h equilibration, following the reaction. However, no effect was observed on the particle size and filtration rate.

Since the titration of $CaCl_2$ solution with H_2SO_4 - as a laboratory procedure - cannot be scaled-up to real large plant operation, step-wise H_2SO_4 addition procedure was tested to mimic a multi-tank precipitation circuit. The step-wise precipitation tests (4 and 8 steps) are realized by reacting 8M H_2SO_4 with 3.5M $CaCl_2$. The total H_2SO_4 addition time was 4 hours while all products were equilibrated for an extra 2 hours. The SO_4/Ca ratio was 0.8. The products in all cases were found to be HH. Particle size analysis revealed (Figure 7) that the 8-step procedure better approximated the titration procedure than the 4-step one. Therefore, a multi-stage reactor design is expected to give better results in terms of crystal quality and desired regenerated acid concentrations.

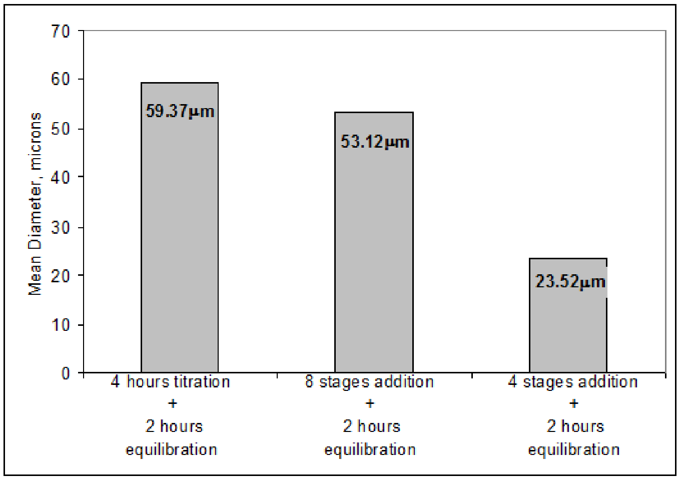

Figure 7. Effect of H_2SO_4 addition procedure on the mean diameter of crystals.

Effect of Seed Loading and Recycling: Seeding is practiced primarily for crystal growth. The amount of seed used is reported more specifically to have 2 important effects in precipitation systems: 1) variations in seed concentration (i.e. solid/liquid ratio) could influence the phase transformation kinetics; and 2) changing the seed concentration could affect the specific surface area, therefore, the number of secondary (surface) nucleation sites and the growth rate [38].

In this part of the work, three seed loadings namely, 25g/L, 50g/L and 100g/L were examined. No hemihydrate-anhydrite transformation was observed during the tests. A quantitative appreciation of the effect of seed loading on crystal size and handling properties is possible by examining the mean crystal diameter and filtration rate data given in Figure 8. According to these data seeding had a profound effect on crystal growth (the volume-based diameter of the crystals increased from around 20 µm to 58-60µm) and a modest negative effect on filtration rate.

SEM images presented in Figure 9 demonstrate the evolution of the seed crystal after 30 minutes and 4 hours of crystallization respectively for 100g/L seed loading.

Test program progressed with the recycling tests in order to determine the upper limit of growth that can be obtained. Recycling was investigated by using 3M $CaCl_2$ initial solution reacted with 5.32M H_2SO_4 in 8 stages. The initial seed and recycled product loadings for 3M $CaCl_2$ were 100g/L (equivalent approximately to the mass of fresh crystal product per run), using lab-made and Omega brand HH seed.

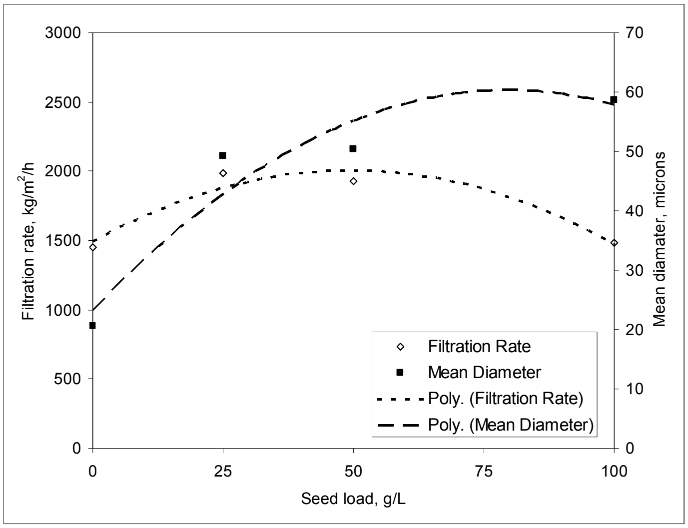

Figure 8. Effect of seed concentration on mean diameter and filtration rate (3M $CaCl_2$ starting solution).

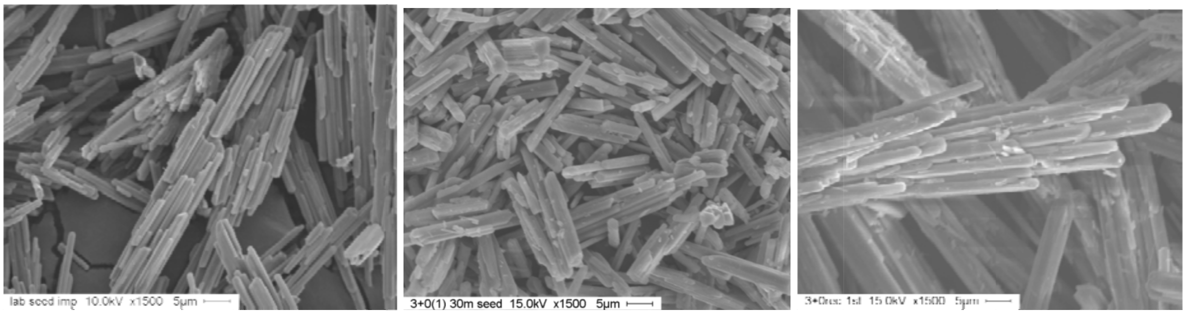

(a) Original Lab-made seed (b) 100 g/L (30 minutes) (c) 100 g/L (4 hours)

Figure 9. Effect of seed loading and crystallization time on crystal morphology (3M $CaCl_2$ starting solution).

SEM images of the crystals obtained from the recycling of commercial Omega seed are presented in Figure 11. Images reveal that the prismatic crystals (original Omega seed) grow along with needle shaped crystals until the 3rd recycle. After that, the disintegration of the prismatic crystals and the growth of needles was observed. This implies that in acidic environments (HCl or H_2SO_4 [39]) the favoured crystal morphology is that of acicular habit.

Test results suggest that, both types of hemihydrate seed underwent no phase change (i.e. conversion to anhydrite) over the 5 recycles with 3M $CaCl_2$ solution. Figure 10 displays SEM images of the growing HH crystals sampled at the end of 1st, and 4th recycle.

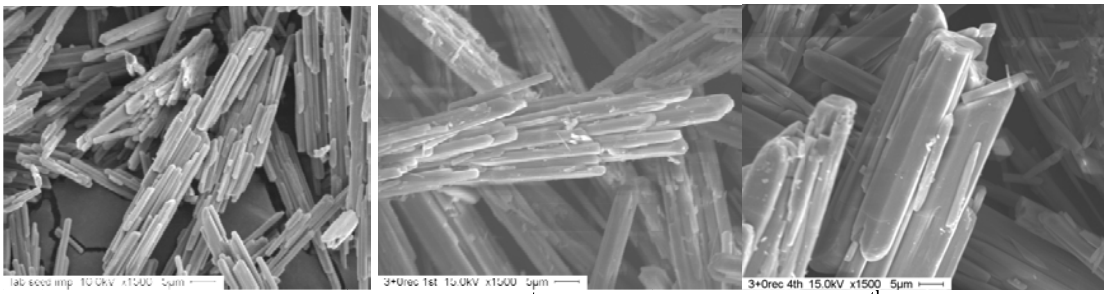

(a) Lab made seed (b) 1st recycle (4 hours) (c) 4th recycle (4 hours)

Figure 10. The growth of lab-made seed at different stages of recycling (3M $CaCl_2$).

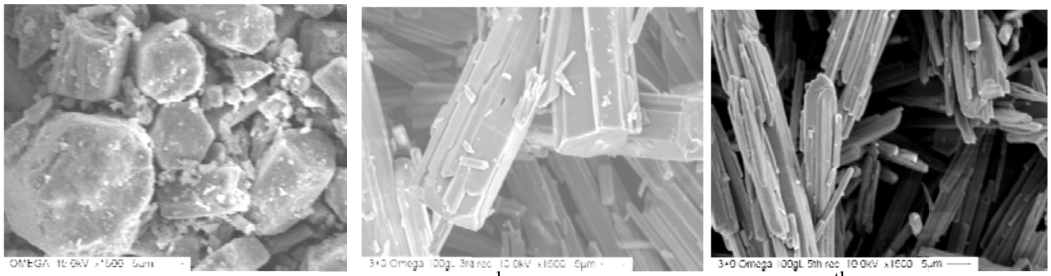

(a) Omega seed (b) 3rd recycle (4 hours) (c) 5 th recycle (4 hours)

Figure 11. Crystal habit changes of Omega seed upon repeated recycling (3M $CaCl_2$).

SEM observations of the recycled crystals for both Lab and Omega seeds were confirmed by the crystal size (Figure 12) and filtration rate measurements (Figure 13). The laboratory made material found to be a better seed option obtained after 2-3 recycles.

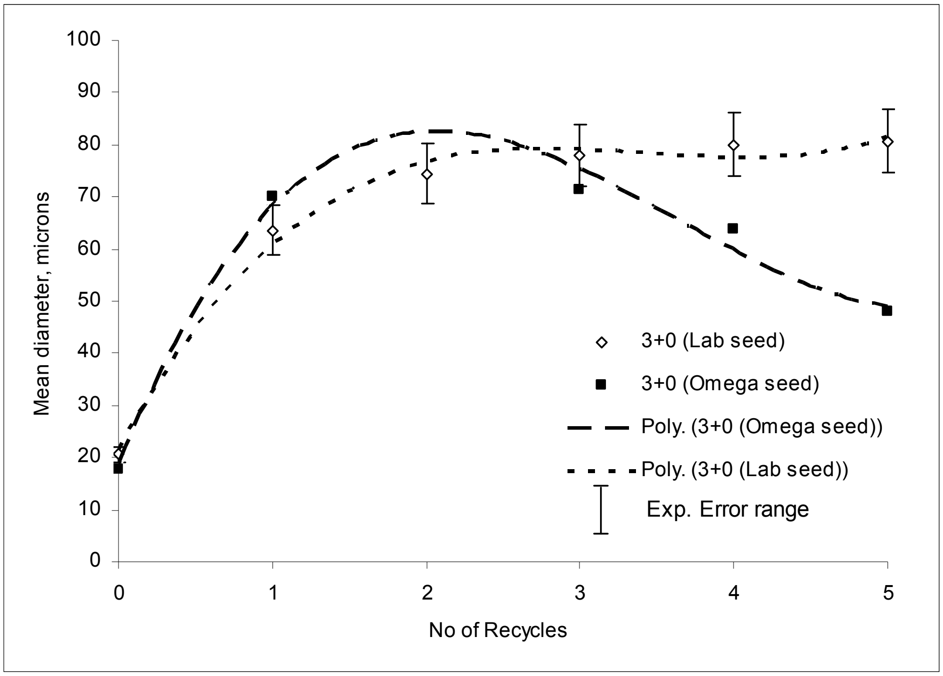

Figure 12. Crystal mean diameter change upon repeated recycling of Lab-made and Omega seed. materials (3M $CaCl_2$, 100g/L seed).

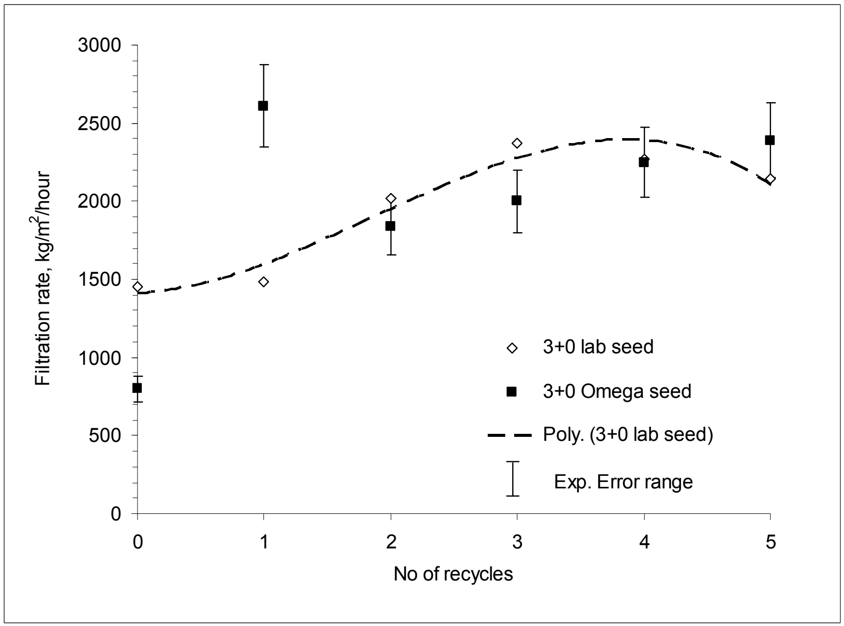

Figure 13. Filtration rate as a function of recycling for different seed materials (3M $CaCl_2$, 100g/L seed).

Crystal Growth of α-Hemihydrate

Determination of Crystal Growth Rates: The crystal growth rate was determined via measurements of the change of particle size over time. For the calculation of the growth rate the measured particle size distributions were fitted to a log-normal probability distribution. The parameters of the fitted distribution were used to calculate the mode of the distribution as a measure of the characteristic length of the particles. The calculation of the mode was done for each of the five samples taken from a single experiment and regressed against time with a linear function. The slope of this function represents the change in particle size with time and hence the crystal growth rate. This approach is schematically described in Figure 14.

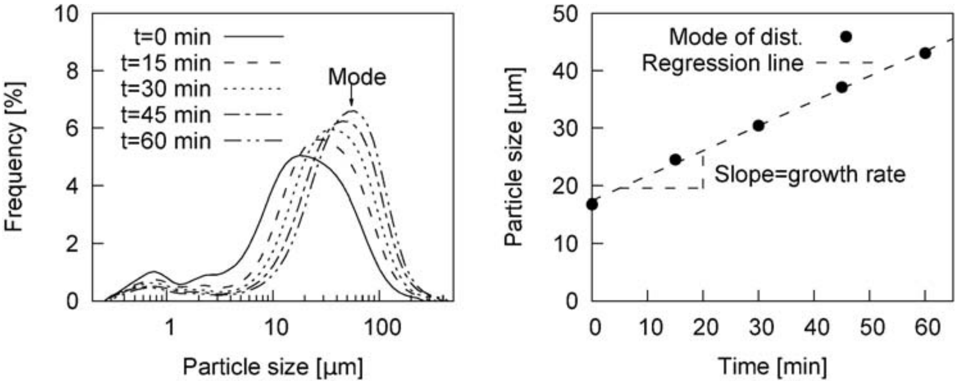

Figure 14. Schematic representation of the derivation of the crystal growth rate from measured particle size distribution data. Example: high $CaCl_2$ condition, T=80°C, specific power input=0.16 W/kg, molar inflow rate=0.3 mol/h [34].

Finally, recognizing that crystal growth predominantly takes place at active surface sites, the measured growth rates were made independent of the specific surface area available for growth by taking into account the initial surface area of the seed crystals (average 0.548±0.072 m^2/g). In the following the results for each of the varied experimental parameters are discussed.

Reagent Inflow Rate: Figure 15 (a) shows the crystal growth rate of HH as a function of the reagent inflow rate. This opens in principle the opportunity for crystal size control via inflow rate regulation. The increase in growth rate with inflow rate is not monotonic. The increase of the reagent inflow rate from 0 to 0.3 mol/h resulted in a nearly linear increase of the crystal growth rate, thereafter reaching a maximum at 0.3 mol/h. At molar inflow rates above 0.3 mol/h the growth rate plateaus. This dependency of the growth rate with increasing molar inflow rate (supersaturation) can be explained on the basis of von Weimarn's second law. It states that for a given crystallization time the average particle size passes through a maximum as a function of initial supersaturation [40-42]. As a consequence the inflow rate corresponds to different initial supersaturation levels; hence explaining the observed behavior of the growth rate as a function of molar inflow rate.

Stirring Rate: In the case of diffusion-controlled processes changes in the stirring rate (expressed as specific power input) should influence the measured crystal growth rate [42]. Experiments done at a molar inflow rate of 0.3 mol/h and a temperature of 80°C showed that a variation of the specific power input did not have any noticeable effect on the crystal growth rate within the range of investigated conditions (see Figure 15 (b)). This behavior is attributed to the turbulent flow regime that characterized the experimental conditions under which the growth of HH crystals was studied (Reynolds numbers of ~15000 to ~60000). These turbulent flow conditions most likely resulted in a reduction of the diffusion boundary layer down to its limiting thickness hence the lack of a noticeable influence of stirring rate.

Temperature: In case of a reaction controlled process; changes of reaction temperature would influence the rate of the process [43]. However, experiments with a reagent inflow rate of 0.3 mol/h and a specific energy input of 0.16 W/kg showed no distinct influence of temperature for either of the two solution types tested (see Figure 15 (c)). Based on the evidence presented above the crystal growth of HH is concluded to be a diffusion controlled linear process under the investigated conditions. A more detailed discussion can be found in a previous publication [34].

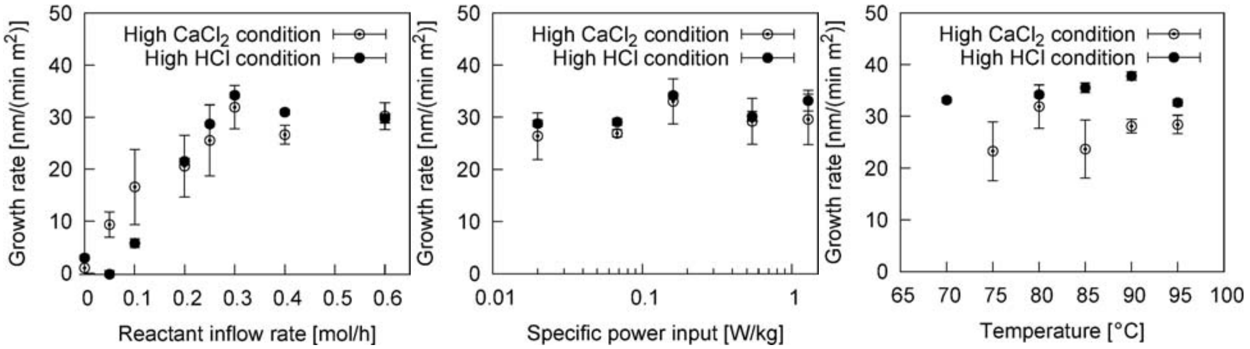

(a) (b) (c)

Figure 15. HH crystal growth rates for High $CaCl_2$ and High HCl condition with (a) variation of inflow rate, (b) specific power input and (c) temperature [34].

Finally, from these results in can be concluded that only the supersaturation is an industrially relevant parameter for the control of the particle size of HH. Temperature and agitation conditions in the reactors need to be monitored and controlled in order to obtain a certain particle size of the resulting crystals and to maintain necessary mixing conditions. From additional research reported elsewhere [32] it was found that lower temperatures led to a relative increase of the metastable lifetime of hemihydrate. This means that the residence time in the reactors can be up to set to up 2 h, if temperature is lowered.

Key Engineering Aspects of the Proposed Continuous Acid Regeneration Process

The crystallization process is preferably carried out in a series of CSTR's. This helps to obtain slurries with a solid density of approximately 10% in each stage, if there is a solid liquid separation step between each stage. If there is no intermediary solid-liquid separation the solid content will be approximately 30 to 35%. An overview of the conceptual flowsheet with the $CaCl_2$/HCl profiles is illustrated in Figure 16.

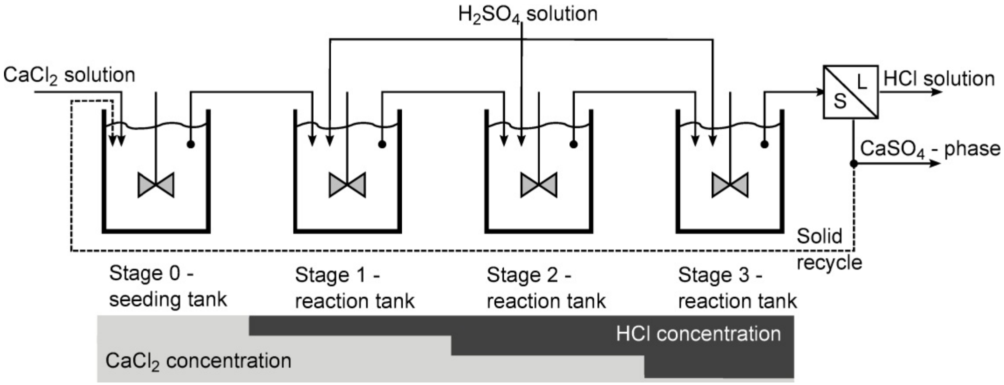

Figure 16. Flowchart of multistage HCl regeneration circuit [32].

A mass balance was performed in METSIM to verify the economic viability of HCl regeneration from spent solution after apatite leaching using sulfuric acid. The objectives of the mass balance were to estimate the levels of dissolved calcium chloride in solution for an apatite deposit associated with rare earth metals, to determine the reagent consumption and energy requirements associated with the regeneration of hydrochloric acid and to assess the economic viability of the HCl regeneration process.

To estimate the economic viability of the HCl regeneration circuit, a mass balance based on the simplified flowsheet shown in Figure 17, consisting of leaching, rare earth precipitation, phosphate precipitation, solution evaporation and hydrochloric acid regeneration, was established.

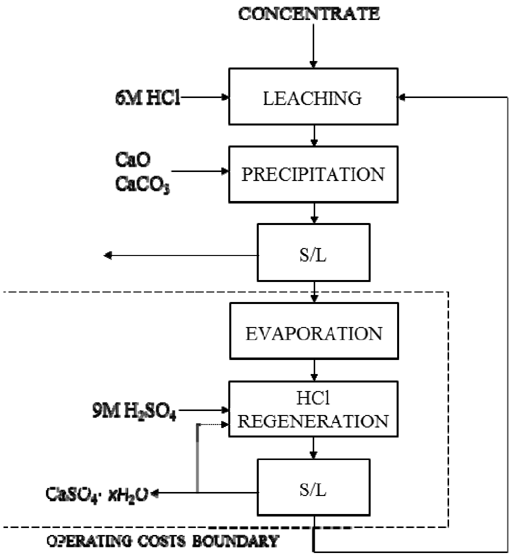

Figure 17. Mass balance and operating cost boundaries.

It was assumed that the process would be treating a concentrate product from a beneficiation circuit. Other basic design criteria used in the simulation are presented in Table III.

Table III. Basic Process Design Criteria

Criteria	**Units**	**Value**
Leach Feed Characteristics		
Phosphate	% P_2O_5	20
Rare Earth	%RO	5
Feed Throughput	t/h	5
HCl Strength		
Fresh	M	6
Recycled	M	6
Sulphuric Acid Strength		
Fresh	M	9
Filtered Calcium Sulfate Percent Solids	%	71

High level operating costs were developed for the evaporation, hydrochloric acid regeneration, solid liquid separation and calcium sulphate handling stages, as outlined in Figure 17. The operating costs were based on the assumption that the plant would be based in North America. These costs were developed per tonne of 6M hydrochloric acid regenerated solution.

Mass-balance and Operating Cost Estimation

The results from the mass balance indicate that $CaCl_2$ levels for this ore type were approximately 2.6 M following the rare earth and phosphate removal steps. The mass balance results for the HCl regeneration circuit are presented in Figure 18.

It was estimated that approximately 15% of the water in the $CaCl_2$ solution would need to be evaporated to produce a solution with a $CaCl_2$ concentration of 3.0M. It was estimated that a solution with a concentration of approximately 3.0M $CaCl_2$ would produce an HCl product with a concentration of 4.7M, depending on the sulfuric acid strength and amount of wash water used. The operating costs developed for the HCl regeneration process include costs for sulfuric acid, equipment maintenance, personnel, electrical power and gypsum handling. It was assumed that evaporation energy would be supplied by electrical power.

A cost of electricity of \$0.12/kWh was used, considered to be on the higher end for North American industrial electricity prices. Equipment maintenance was estimated as a function of the installed mechanical equipment. The cost of gypsum handling was estimated on a per tonne basis. Reagent prices were based on market analysis literature [44], [45] and confirmed via discussions with suppliers. A relatively conservative price of \$150 per tonne of 93% strength sulfuric acid was used for the analysis.

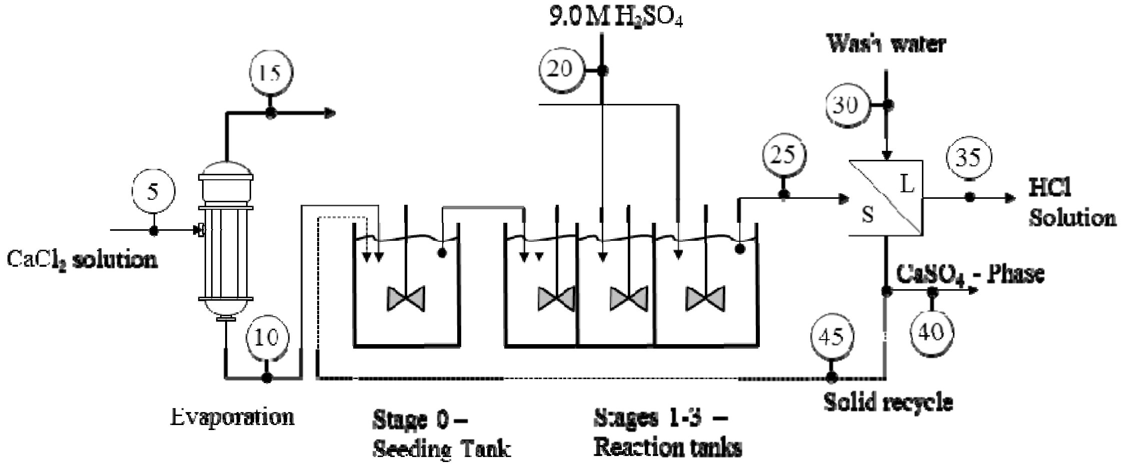

STREAM NUMBER		5	10	15	20	25	30	35	40	45
SOLID	TPH	0.0	0.0	0.0	0.0	4.8	0.0	0.0	2.5	2.3
LIQUID	TPH	7.9	6.7	0.0	2.3	7.6	0.5	6.1	1.0	0.9
GAS	TPH	0.0	0.0	1.2	0.0	0.0	0.0	0.0	0.0	0.0
% SOLIDS	%	0.0	0.0	-	0.0	38.6	0.0	0.0	71.0	71.0
[$CaCl_2$]	M	2.6	3.0	-	0.0	0.4	0.0	0.4	0.3	0.3
[HCl]	M	0.0	0.0	-	0.0	4.7	0.0	4.7	3.3	3.3

Figure 18. Mass Balance Outputs.

The total operating costs for the HCl regeneration circuit were estimated to be approximately \$110 per tonne of 6M hydrochloric acid solution (\$/t HCl) regenerated. The cost of fresh 6.0M HCl was assumed to be about \$300 per tonne for the North America market. The breakdown of the operating costs by area is presented in Figure 19.

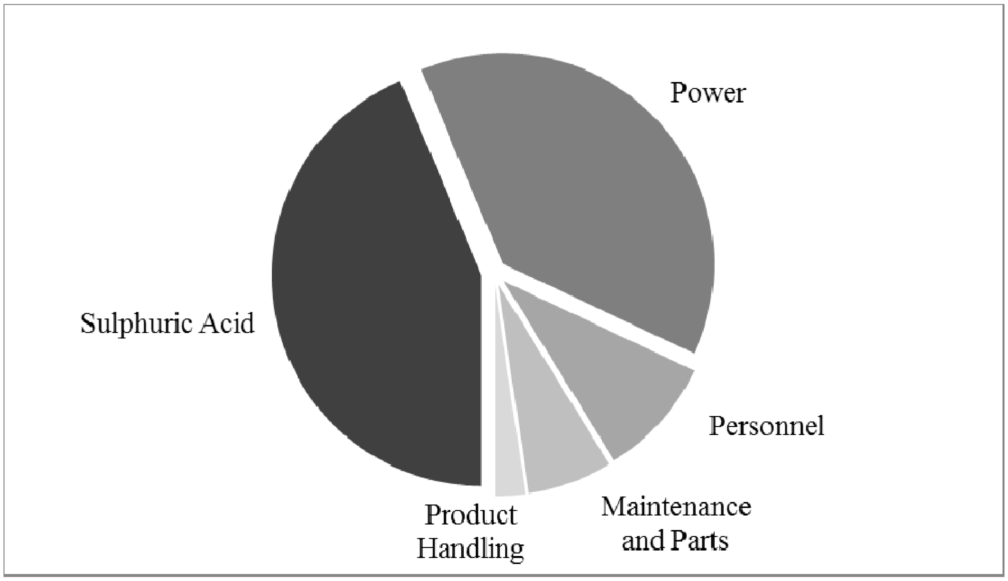

Figure 19. Hydrochloric acid regeneration operating cost breakdown.

Table IV. Sensitivity Analysis Results

Conditions	Inputs				Outputs					
	[$CaCl_2$] - Feed to Regeneration Circuit (M)	[H_2SO_4] Fresh (M)	$CaSO_4$ Recir-culated (%)	$CaSO_4$ Wash Water (m^3/h)	Fresh HCl (t/h)	[HCl] Regen-erated (M)	HCl Regen-erated[1] (t/h)	Cost per t HCl[1] ($/t)	Total Annual Cost HCl[2,3] ($M)	HCl Recovery (%)
Base Case	3	9	100%	0.5	0.8	4.7	4.8	109.7	6.2	85%
Low H_2SO_4 Strength	4.2	5	100%	0.5	0.9	4.9	4.8	129.5	7.1	85%
Low H_2SO_4 Strength, 6.0 M HCl Regeneration HCl Strength	5.6	5	100%	0.5	1.0	6.0	4.8	129.6	7.4	83%
1.0 m^3/h Wash Water	3.0	9	100%	1.0	0.6	4.4	5.0	112.4	6.0	89%
1.5 m^3/h Wash Water	3.0	9	100%	1.5	0.5	4.2	5.1	117.2	6.0	91%
50% $CaSO_4$ Recirculation	3.0	9	50%	0.5	0.8	4.5	4.9	107.0	6.0	87%
0% $CaSO_4$ Recirculation	3.0	9	0%	0.5	0.7	4.7	5.0	102.7	5.7	88%
50% $CaSO_4$ Recirculation, 6.0 HCl Regeneration HCl Strength	4.2	9	50%	0.5	1.0	6.0	4.8	109.5	6.5	83%
0% $CaSO_4$ Recirculation, 6.0 HCl Regeneration HCl Strength	4.2	9	0%	0.5	0.8	6.2	5.0	102.8	6.1	86%

[1] Based on 6.0M HCl equivalent

[2] Total Annual cost includes fresh HCl and HCl regeneration cost

[3] Cost of fresh 6.0M HCl taken to be $300/t

The operating costs are dependent on several variables. Excluding the various costs used as inputs, the main factors affecting the cost are the sulfuric acid strength, wash water in the dewatering stage and the recirculation of $CaSO_4$ - phase crystals. A sensitivity analysis was performed to determine the effect of varying these inputs and the results are presented in Table IV.

The results indicate that the minimum total operating costs occur when under the following conditions: high sulfuric acid strength (9.0M HCl); high wash ratio for $CaSO_4$ dewatering (due to higher HCl recovery); and low or no $CaSO_4$ recirculation. Low $CaSO_4$ recirculation is not considered to be problematic to the process as continuous reactions are considered to be seeded reactors as they always have crystals present. The high wash ratio results in a higher cost per tonne of regenerated HCl, however results in an increase in HCl recovery and resulted in a lower overall HCl cost (considering fresh and recycled HCl).

Conclusions

From the results presented above, which refer to the development of an option for the continuous regeneration of HCl from concentrated $CaCl_2$ solutions via reactive crystallization by H_2SO_4 addition, the following major conclusions can be drawn:

- HCl can be regenerated from spent $CaCl_2$ solutions via the reaction with H_2SO_4. Strength of the regenerated acid depends on the reactant concentrations;

- It is experimentally demonstrated that alpha-$CaSO_4$ hemihydrate can be successfully produced by direct reaction of $CaCl_2$ and H_2SO_4 solutions at 80°C (at atmospheric conditions). DH and HH are metastable in chloride media at 80°C. Their relative kinetic stability depends on the $CaCl_2$ / HCl composition of the solution and reaction time. Increasing HCl concentration favors phase transformation from DH to HH to AH. Increasing $CaCl_2$ concentration on the other hand slows down the conversion of HH to AH;

- 0.5M $CaCl_2$ and 5-6M HCl concentration in the regenerated acid found to be acceptable in terms of produced $CaSO_4$ form (HH) and quality as well as acid regeneration circuit design;

- Seeding and seed recycling was found to lead to the growth of alpha-HH crystals upon staged addition of H_2SO_4 (for maintenance of low supersaturation) into 3-3.5M $CaCl_2$ solution. As a consequence the filtration rate of the crystal slurry was improved;

- The crystal growth rate of α-HH depends on the addition rate of reagents to the process, which is directly linked to the supersaturation. Temperature or stirring conditions did not show a significant influence, leaving a large degree of freedom for process design. It was shown that effective control of the final particle size distribution of the solid product is possible;

- The mass balance and operating cost estimation indicated that for the given conditions, the HCl regeneration circuit appears to be economically viable. The numbers provided were developed based on average conditions for a North American operation and are considered to be generalized;

- The sensitivity analysis indicated that the use of high strength sulfuric acid, high wash ratio for $CaSO_4$ dewatering and little to no $CaSO_4$ recirculation is optimum from an economic point of view;

- All these factors mentioned above are important for the economical and technical operability of the HCl regeneration circuit. The results and assumptions represent the knowhow being developed and actual selected process design should be defined following the execution of continuous integrated pilot tests.

Acknowledgements

The support of NSERC (The Natural Sciences and Engineering Research Council of Canada), and BBA Inc. to the parts of this work is acknowledged.

References

1. Harris, G.B., C.W. White, G.P. Demopoulos, and B. Ballantyne, “Recovery of copper from a massive polymetallic sulfide by high concentration chloride leaching” in *The John E. Dutrizac Symposium on Copper Hydrometallurgy*, eds. P.A. Riveros, D.B. Dreisinger and M.J. Collins, Book 1, 2007, 21–42.
2. C. Allen, C., P. Kondos, S. Payant, G. Van Weert, and A. Van Sandwijk, “Production of zinc oxide from complex sulfide concentrates using chloride processing,” US patent number 6,395,242, May 28, (2002).
3. Lakshmanan, V.I., R. Sridhar, and R. Roy, “Recovery of precious metals from base metal sulfide ores by a hydrometallurgical process” in *TMS 2011 140th Annual Meeting & Exhibition - Symposium Chloride 2011: Practice and Theory of Chloride-Based Metallurgy*, eds. S.N Monteiro, D.E. Verhulst P.N. Anyalebechi and J.E. Pomykala, 2011, 425–432.
4. Borowiec, K., A.E. Grau, M. Gueguin, and J.-F. Turgeon, “Method to upgrade titania slag and resulting product,” US Patent number 5,830,420, Nov.3, (1998)
5. Habashi, F., “The recovery of the lanthanides from phosphate rock,” *Journal of Chemical Technology & Biotechnology*, 35 (1985), 5–14.
6. F. Habashi,F., F.T. Awadalla, and M. Zailaf, “The recovery of uranium and the lanthanides from phosphate rock,” *Journal of Chemical Technology & Biotechnology*, 36, (1986), 259–266.
7. Arafura, Ltd., “Flowsheet Whyalla Rare Earths Complex” company website, retrieved Aug. 2012.
8. Shlewit, H., “Treatment of phosphate rocks with hydrochloric acid,” *Journal of Radioanalytical & Nuclear Chemistry*, 287 (2011), 49–54.
9. R. Winand, R., “Chloride hydrometallurgy,” *Hydrometallurgy*, 27 (1991), 285–316.

10. Muir, D.M., “Basic principles of chloride hydrometallurgy” in *Chloride Metallurgy 2002 - International Conference on the Practice and Theory of Chloride/Metal Interaction*, eds. E. Peek and G. vanWeert, vol. 2, 2002, 759–778.
11. “Canadian water quality guidelines for the protection of aquatic life - Chloride” Canadian Council of Ministers of the Environment, 2011.
12. Brown, C.J., and D.R. Olsen, “Regeneration of hydrochloric acid pickle liquors by crystallization” in *Third International Symposium in Iron Control in Hydrometallurgy*, eds. J.E. Dutrizac and P.A. Riveros, 2006.
13. Regel-Rosocka, M., “A review on methods of regeneration of spent pickling solutions from steel processing,” *Journal of Hazardous Materials*, 177 (2010), 57–69.
14. F. Faverjon, F., G. Durand, and M. Rakib, “Regeneration of hydrochloric acid and sodium hydroxide from purified sodium chloride by membrane electrolysis using a hydrogen diffusion anode-membrane assembly,” *Journal of Membrane Science*, 284 (2006), 323–330.
15. S. Mazrou, S., H. Kerdjoudj, A.T. Cherif, A. Elmidaoui, and J. Molenat, “Regeneration of hydrochloric acid and sodium hydroxide with bipolar membrane electrodialysis from pure sodium chloride,” *New Journal of Chemistry*, 22 (1998), 355–361.
16. Conners, A., “Hydrochloric acid regeneration as applied to the steel and mineral processing industries,” *CIM Bulletin*, 68 (1975), 75–81.
17. Rupay, G.H., and C.J. Jewell, “The regeneration of hydrochloric acid from waste pickle liquor using the Keramchemie/Lurgi Fluidized-Bed Reactor system,” *CIM Bulletin*, 754 (1975), 89–94.
18. [18] A.A. Schuldt, “Regeneration of hydrochloric acid pickle liquor at Stelco’s Hilton Works,” *CIM Bulletin*, 68 (1975), 82–88.
19. Kladnig, W.F., “New development of acid regeneration in steel pickling plants,” *International Journal of Iron and Steel Research*, 15 (2008), 1–6.
20. Steinbach, W., and F. Baerhold, “Comparison of spray roasting and fluidised bed granulation for the recovery of hydrochloric acid from metallurgical processes through pyrohydrolysis,” in *Chloride Metallurgy 2002 - International Conference on the Practice and Theory of Chloride/Metal Interaction*, eds. E. Peek and G. vanWeert, vol. 2, 2002, 643–655.
21. Burtch, J.W.,“Hydrochloric acid from industrial waste streams - The PORI proces,” *CIM Bulletin*, 68 (1975), 96–100.
22. Becze, L., S.J. Höck, and G.P. Demopoulos, “Precipitation of hematite and recovery of hydrochloric acid from concentrated iron chloride solutions by a novel hydrolytic decomposition process,” in *TMS 2011 140th Annual Meeting & Exhibition - Chloride 2011: Practice and Theory of Chloride-Based Metallurgy*, eds. S.N Monteiro, D.E. Verhulst P.N. Anyalebechi and J.E. Pomykala, 2011 529-538.
23. Patoine, N,-C., A. De Mori, K. Borowiec, and C. Coscia, “Pyrohydrolysis of a calcium and magnesium bearing $FeCl_2$ leach liquor,” in *Chloride Metallurgy 2002 - International*

Conference on the Practice and Theory of Chloride/Metal Interaction , eds. E. Peek and G. van Weert, 2002, vol. 2, 699–712.

24. Al-Othman, A.L., and G.P. Demopoulos, "Gypsum crystallization and hydrochloric acid regeneration by reaction of calcium chloride solution with sulfuric acid," *Hydrometallurgy*, 96 (2009), 95–102.
25. Girgin, S., and G.P. Demopoulos, "Production of the high value material alpha-$CaSO_4$ hemihydrate out of spent $CaCl_2$ solutions by reaction with H_2SO_4," in *EPD Congress 2004*, ed. M.E. Schlesinger, 2004, 627–639.
26. Li, Z., and G.P. Demopoulos, "Model-based construction of calcium sulphate phase transition diagrams in the HCl-$CaCl_2$-H2O system between 0 and 100°C," *Industrial & Engineering Chemistry Research*, 45, (2006), 4517–4524.
27. Berrie. J.S., and G.E. Wooley, "Manufacture of calcium sulphate alpha hemihydrate," US patent number 4,120,737, Oct. 17, (1978).
28. Demopoulos, G.P., Z. Li, L. Becze, G. Moldoveanu, T.C. Cheng, and B. Harris, "New technologies for HCl regeneration in chloride hydrometallurgy," *World of Metallurgy - Erzmetall*, 61 (2008), 89–98.
29. Guan, B., Q. Ye, Z. Wu, W. Lou, and L. Yang, "Analysis of the relationship between particle size distribution of α-calcium sulfate hemihydrate and compressive strength of set plaster—Using grey model," *Powder Technology*, 200, (2010), 136–143.
30. T. Koslowski, T., "Calcium sulphate alpha-hemihydrate mfr. by autoclaving dihydrate," German patent 381,651,3 A1, Dec. 8, (1988).
31. . Engert, H.-J., and T. Koslowski, "New gypsum binder Alpha 2000," *ZKG International*, 51 (1998), 229–237.
32. T. Feldmann, T., and G.P. Demopoulos, "Phase transformation kinetics of calcium sulfate phases in strong $CaCl_2$-HCl solutions," *Hydrometallurgy*, 129–130 (2012), 126–134.
33. College, J.W., "The Omega process: Direct conversion of calcium sulphite to alpha hemihydrate," in *6th International Conference on Natural and FGD Gypsum, May 16-19, Toronto*, ed. Process Research ORTECH Inc., 2000, 1–11.
34. Feldmann. T., and G.P. Demopoulos, "The crystal growth kinetics of alpha calcium sulfate hemihydrate in concentrated $CaCl_2$-HCl solutions," *Journal of Crystal Growth*, 351 (2012), 9–18.
35. OLI Systems Inc., "OLI Analyzer Studio - Stream Analyzer v9.0," May-2013. URL: http://www.olisystems.com/new-streamanalyzer.shtml.
36. Martynowicz, E., G.J. Witkamp, and G.M. van Rosmalen, "The effect of aluminium fluoride on the formation of calcium sulfate hydrates," *Hydrometallurgy*, 41 (1996), 171–186.
37. Li, Z., and G.P. Demopoulos, "Development of an improved chemical model for the estimation of $CaSO_4$ solubilities in the HCl-$CaCl_2$-H_2O system up to 100°C," *Industrial & Engineering Chemistry Research*, 45 (2006), 2914–2922.

38. Mersmann, A., *Crystallization technology handbook*, 2nd ed. (New York: Marcel Dekker, Inc., 2001).
39. Ling, Y., “Direct preparation of alpha-calcium sulfate hemihydrate from sulfuric acid,” McGill University, PhD Thesis , 2003.
40. von Weimarn, P.P., “The precipitation laws,” *Chemical Reviews*, 2 (1925), 217–242.
41. Barlow, D.A., J.K. Baird, and C.-H. Su, “Theory of the von Weimarn rules governing the average size of crystals precipitated from a supersaturated solution,” *Journal of Crystal Growth*, 264 (2004), 417–423.
42. Dirksen, J.A., and T.A. Ring, “Fundamentals of crystallization: Kinetic effects on particle size distributions and morphology,” *Chemical Engineering Science*, 46 (1991), 2389–2427.
43. Havlik, T., *Hydrometallurgy - Principles and Applications*. (Cambrigde: Woodhead Publishing Ltd. , 2008).
44. Argus, “Market Analysis,” *CRU - FMB Sulphuric Acid*, (2012), 1–9.
45. Sell, C., “Sulphuric acid - market analysis,” *CRU - Fertilizer Week*, (2012), 1–3.

ASSESSMENT OF VARIOUS PROCESSES FOR RARE EARTH ELEMENTS RECOVERY (I): A REVIEW

*G. Nazari and B. Krysa

Hatch; 2800 Speakman Drive, Mississauga, Canada L5K 2R7
GNazari@hatch.ca

Keywords: Rare Earth Elements, Extraction, Separation

Abstract

In the last few decades, development in the field of rare earth elements (REE) outside China were almost halted due to import of these elements from China. Specialized technologies, equipment, and engineering know-how were allowed to lapse. Since 2009, with a tightening of the export of these elements from China and their reduced availability, other countries have started to look for and develop alternative sources of REE. In this paper, various technologies to extract and recover REE from minerals such as bastnasite, xenotime, and monazite are briefly reviewed. All process steps from leaching and/or decomposition in sulfuric acid, sodium hydroxide, nitric acid, and hydrochloric acid to REE recovery from leachate and separation of these elements in pure form are discussed with an emphasis on the engineering and equipment aspects of process plants required for each flowsheet.

Introduction

Rare earths are a series of 17 elements that have unique chemical, magnetic, and fluorescent properties. They are integral to the functioning of items such as hybrid cars, fluorescent lamps, plasma screens, portable computers, hand-held electronic devices, wind power generators, and optical and medical devices. These elements have largely been ignored until few years ago when they became widely used in smart-phones, computer hard drives, laptops, and plasma screen TVs and many other applications.

In general, there are several methods to extract REE from ore [1, 2, 3]. Due to very low concentration of REE in the ore, the mineral has to be completely dissolved to extract the REE content from the ore. Initially, beneficiation is commonly used to upgrade the ore to higher grade concentrates. The most common hydrometallurgical processes for REE extraction from the ore is acid leaching. REE can be also extracted via sulfation and alkaline decomposition and subsequent leaching in water and acid, respectively.

After dissolution, the next step is to recover REE from leachate. Similarly, there are several processes that are commonly used to recover REE from solution. A well known method for separating REE from pregnant leach solution (PLS) is to precipitate them using oxalic acid [4, 5]. Oxalates of REE are highly insoluble while other metals form soluble complexes with oxalate. Oxalic acid is most commonly used in REE refining plants on purified strip liquors where other impurity metals are of lower concentration and below their oxalate solubility product limit to reduce the consumption of oxalic acid.

Another method for separation and recovery of REE is solvent extraction [6, 7, 8]. Extensive research in this field has been done. The main drawback with solvent extraction is the requirement for large amounts of high-purity solvents that are expensive and toxic and result in the production of hazardous waste. Therefore, the search for new solvents has been a major challenge in solvent extraction process development. Recently, ionic liquids, which are ionic media resulting from the combination of organic cations and various anions, has attracted much attention taking into account their special features such as low-vapor pressure, high viscosity, dual natural polarity, good thermal stability and a wide range of miscibility with water and other organic solvents [9]. Hence many environmental and safety problems associated with organic solvents can be avoided. The application of ionic liquid in solvent extraction in industry is in the early stage of development and requires further study.

In this paper, various processes for extraction, recovery and separation of REE from ore are briefly discussed.

Resources

Rare earth minerals can be categorized into carbonate, phosphate, silicate, and oxide groups. The list of some of the important rare earth minerals is presented in Table I.

Table I. Important Rare Earth Minerals

Minerals	Compositions
Carbonate	
Bastnasite	$(Ce, La, Y)CO_3F$
Phosphate	
Monazite	$(Ce, La, Pr, Nd, Th, Y)PO_4$
Xenotime	YPO_4
Apatite	$Ca_5(PO_4)_3(F, Cl, Oh, Br)$
Silicate	
Allanite	$(Ce, Ca, Y, La)_2(Al, Fe^{+3})(SiO_4)_3(OH)$
Cerite	$(Ce, La, Ca)_9(Mg, Fe^{3+})(SiO_4)_6(SiO_3OH)(OH)_3$
Eudialyte	$Na_{15}Ca_6(Fe, Mn)_3Zr_3SiO(O, Oh, H_2O)_3(Si_3O_9)_2(Si_9O_{27})_2(OH, Cl)_2$
Gadolinite	$(Ce, La, Nd, Y)_2FeBe_2(SiO_4)_2O_2$
Loparite	$\{(Ce, La, Nd, Y)_2FeBe_2Si_2O_{10}$
Oxide Ores	
Euxenite	$(Y, Ce)(Nb, Ta, Ti)_2O_6$
Samarskite	$(Y, Ce)_4(Nb, Ta, Ti)_2O_6$
Fergusonite	$Y(Nb, Ti, Ta)O_4$
Betafite	$(U, Ca, Y, Ce_2(Nb, Ta, Ti)_2O_6(OH)$
Aeschynite	$(Ce, Nd, Y, CA, Fe, Th)(Ti, Nb)_2(O, OH)_6$

A typical heavy mineral sand constituting about 1-2% RE mineral is concentrated by separating it from gangue minerals such as quartz and silicate by physical beneficiation. These minerals may be beneficiated using gravity separation, desliming, magnetic separation, electrostatic separation, and flotation separation techniques [10]. Due to significant differences between specific gravities of RE minerals and the gangue minerals commonly associated with the rare earth minerals such as silicates, gravity separation is commonly used to concentrate RE minerals [10]. Magnetic separation techniques are a common separation step in rare earth mineral beneficiation to eliminate highly magnetic gangue [11]. Electrostatic separation is a beneficiation technique that exploits the differences in conductivity between different minerals to achieve separation [12]. Another common beneficiation process is flotation. This process has the advantage of processing a wide range of fine particle sizes and capability of being tailored to the unique mineralogy of a given deposit [10].

Extraction Techniques

Sulfuric Acid Treatment

Leaching: Sulfuric acid is used to leach phosphate rocks containing rare earth. Reaction 1 occurs at a low ratio of sulfuric acid to the ore, while Reaction 2 represents leaching at a higher acid to ore ratio.

$$Ca_{10}(PO_4)_6F_2 + 2\ H_2SO_4 + 2\ H_2O = 3\ Ca(H_2PO_4)_2.2H_2O + 7\ CaSO_4.2H_2O + 2\ HF \qquad (1)$$

$$Ca_{10}(PO_4)_6F_2 + 10\ H_2SO_4 + 5\ H_2O = 6\ H_3PO_4 + 10\ CaSO_4 + 1/2H_2O + 2HF \qquad (2)$$

It has been found that during the leaching of rare earth minerals with sulfuric acid, lanthanides can become trapped by isomorphous substitution for Ca^{2+} in gypsum leach residue [2]. These losses can be reduced if leaching can be conducted at low temperature and lower concentrations of sulfuric acid [2]. However, the majority of phosphate minerals are too refractory to be dissolved at low temperature.

Sulfation Roasting: Acid roasting, or acid baking, is a major rare earth mineral decomposition process and, therefore, has been reviewed in this section. The general chemistry of the flowsheet and the reaction mechanisms followed by some of the important engineering challenges in the design of a kiln are discussed.

Rare earth elements can be completely extracted into solution by roasting the ore in concentrated sulfuric acid at 180-300°C and then leaching with water [13, 15, 17]. Low grade RE concentrates are usually processed at temperatures lower than 300°C. However, that leads to generation of soluble impurities. Further processing steps are required to remove impurities from the leach solution. High grade rare earth concentrates are often processed at temperatures higher than 300°C to avoid the generation of soluble impurities [17]. However, high temperature roasting leads to greater generation of hazardous exhaust gases such as hydrogen fluoride, sulfur dioxides, sulfur trioxide, and silicon tetrafluoride.

Acid roasting of bastnasite, rare earth oxides, and phosphates can be expressed by following reactions:

$$2\ RECO_3F + 3\ H_2SO_4 = RE_2(SO_4)_3\,(s) + 2HF \uparrow + 2\ CO_2 \uparrow + 2\ H_2O \qquad (3)$$

$$RE_2O_3 + 3\ H_2SO_4 = RE_2(SO_4)_3\ (s) + 3\ H_2O \qquad (4)$$

$$2\ REPO_4 + 3\ H_2SO_4 = RE_2(SO_4)_3\ (s) + 2\ H_3PO_4 \qquad (5)$$

After sulfation roasting, soluble rare earth sulfates are dissolved in water to form soluble rare earth sulfates (Reaction 6). Solubility of the RE sulfates will drop with an increase in leaching temperature [14].

$$RE_2(SO_4)_3\ (s) = RE_2(SO_4)_3\ (aq) \qquad (6)$$

As mentioned earlier, sulfation roasting can be conducted at low and high temperatures. The reaction mechanism during the thermal decomposition process in a kiln up to 500°C has been studied [15]. It has been showed that in addition to Reaction 3 to 5, the following reactions occur in a temperature range of 160 to 225°C.

$$Th_3(PO_4)_4 + 6\ H_2SO_4 = 3\ Th(SO_4)_2 + 4\ H_3PO_4 \qquad (7)$$

$$Fe_2O_3 + 3\ H_2SO_4 = Fe_2(SO_4)_3 + 3\ H_2O \qquad (8)$$

$$CaF_2 + H_2SO_4 = CaSO_4 + 2\ HF\uparrow \qquad (9)$$

$$SiO_2 + 6\ HF = H_2SiF_6\uparrow + 2\ H_2O\uparrow \qquad (10)$$

At a temperature range of 285 to 367°C, insoluble thorium phosphate and thorium pyrophosphate are formed according to Reactions 11 to 14 [15].

$$2\ H_3PO_4 = H_4P_2O_7 + H_2O\uparrow \qquad (11)$$

$$Th(SO_4)_2 + H_4P_2O_7 = ThP_2O_7 + 2\ H_2SO_4 \qquad (12)$$

$$H_4P_2O_7 = 2\ HPO_3 + H_2O\uparrow \qquad (13)$$

$$Th(SO_4)_2 + 4\ HPO_3 = Th(PO_3)_4 + 2\ H_2SO_4 \qquad (14)$$

At temperatures higher than 400°C, ferric sulfate starts to decompose and forms hematite according to Reaction 15 [15].

$$Fe_2(SO_4)_3 = Fe_2O_3 + 3\ SO_3\uparrow \qquad (15)$$

As shown above, at temperatures higher than 160°C, rare earth minerals begin to decompose. By controlling the temperature above 200°C and below 300°C, soluble RE and thorium sulfate are formed. At temperatures higher than 300°C, insoluble thorium phosphate and thorium pyrophosphate are formed. Hence, formation of highly radioactive solid residues is one of the issues of roasting at temperatures higher than 300°C [15]. Generation of sulfur trioxide and insoluble iron compounds are some of the drawbacks of roasting at temperatures higher than 400°C. Sulfur trioxide is difficult to be collected, often passing through wet scrubbers, and needs to be collected electrostatically. In addition, by increasing the temperature higher than 300°C, the decomposition rate of rare earth minerals and the solubility of rare earth sulfates decrease. Roasting between 180°C and 300°C for 2-4 hours is often successful [10, 12, 15].

Due to the generation of potentially hazardous exhaust gases such as hydrogen fluoride gas, sulfur trioxide, silicon tetrafluoride, and carbon dioxide, the vent gas must be collected and treated in a scrubber before being released to atmosphere. It is common to use a water scrubber to capture most of the exhaust gases. A mixed acid containing HF, H_2SO_4, and H_2SiF_6 can be recovered in this initial scrub. A second scrubber using diluted sodium carbonate solution is used to further purify the exhaust gas before it is released.

Due to the importance of sulfation roasting in recovery of REE, some of the important engineering aspects of this process with respect to the design of a kiln and materials selection are discussed briefly.

There are a number of important factors that need to be considered in carrying out the design of a kiln for acid baking rare earth minerals. One of the first and important considerations in selecting a kiln design is determining the handling characteristics of the material which will be feed to the kiln and how these characteristics can be managed. Fineness of feed, corrosivity and toxicity of the feed and reaction products are some of the factors that influence the design of a kiln. Another important decision is in making a choice between a direct fired or an indirect fired rotary kiln. The difference between the two is in the method of introducing the heat.

In a direct fired rotary kiln, the heat is introduced directly into the internals of the rotary kiln, via a stream of hot gas in direct contact with the ore or concentrate. This means there is high heat transfer between the material and the heat. However, it also means that there is more gas exiting the rotary kiln that needs to be processed. This is important due to formation of hazardous exhaust gases in this process.

Contacting the kiln feed with a large amount of gas is another disadvantage of a direct kiln. It can result in overheating of the residue, or a large fraction of the fine particles in the feed can be entrained by the heating gas resulting in a more expensive gas handling system and greater recycle and reheating of the feed material. The larger gas flows also serve to purge sulfuric acid from the kiln which increases acid requirements.

In an indirect fired rotary kiln, the heat comes through the shell of the rotary kiln, and the heat is transferred from the material being in contact with the rotary kiln shell. One of the important advantages to an indirect fired rotary kiln is that the temperature can be controlled along the length of the rotary kiln. Another advantage of using an indirect fired rotary kiln is that there is less exit gas that needs to be processed, because of introduction of lower amount of gas into the rotary kiln. However, due to indirect contact of material with gas and low heat transfer, the size of indirect kiln is larger than that of direct kiln.

Materials of construction for kilns can be selected considering the type of kiln. Direct fired kiln can be constructed of carbon steel. However, the temperature of gas introduced to heat the kiln is very high and strength of carbon steel decreases significantly at temperatures higher than 250°C.

Therefore, refractory lining is required to insulate the carbon steel from the high temperature inside the kiln and protects it from the corrosive material.

Indirect kiln should be constructed of a material with high corrosion resistivity at high temperature. Alloy 686 (nickel, chromium, molybdenum based alloy) shows high resistance to corrosion at elevated temperatures. This alloy has excellent corrosion resistivity in sulfuric acid, hydrochloric, nitric, and hydrofluoric acid media [16].

One of the common risks in design of a kiln is failure to achieve the required process time and temperature parameters. Incomplete sulfation will occur if the residence time is insufficient at the required temperature. To overcome this problem, the kiln set up such as slope and rotation speeds are adjusted. Conversely, excess process temperature and longer residence time than required may lead to formation of insoluble species. As discussed above, as temperature increases above 300°C, decomposition rate of rare earth decreases, more insoluble rare earth sulfates and insoluble thorium phosphates are formed. In direct-fired kiln, co-current kiln configuration, where the burner is at the feed end, may prevent overheating of the material.

Agglomeration and ringing within the kiln is another factor that needs to be considered. The kiln geometry can be selected with a slightly larger aspect ratio (L/D) to reduce the potential for flame impingement on the bed surface and kiln wall. The capability to inject steam at the burner to provide a higher momentum and lower temperature combustion zone can be considered as additional measures to mitigate against problems with ringing or solids agglomeration in a direct fired kiln.

Sodium Hydroxide Decomposition

Bastnasite and rare earth phosphates can be decomposed in concentrated NaOH solutions (>50 wt%) according to Reaction 16 and 17.

$$\mathrm{RECO_3F + 3\ NaOH = RE(OH)_3 + NaF + Na_2CO_3} \quad (16)$$

$$\mathrm{REPO_4 + 3\ NaOH = RE(OH)_3 + Na_3PO_4} \quad (17)$$

At 140°C and a NaOH to RE concentrate ratio of 1.2–1.4, over 90% RE can be decomposed within 5 hours. The reaction time is highly dependent on NaOH concentration. It has been reported that the reaction time can be reduced to less than an hour at 50-60 wt% NaOH solution concentration [17]. In another study, it has been suggested that 40-50 wt% NaOH, 160°C, NaOH to RE concentrate ratio of 2 to1 are the optimum conditions where the reactions are complete in 3 hours [18]. In this process, water soluble phosphates are formed while rare earth elements, thorium and uranium form insoluble hydroxides. The product is a thick paste and is washed, filtered and dried. The cake which contains rare earth hydroxides is dissolved in acid for further separation. The filtrate contains the unreacted NaOH and the phosphorous originally present in the concentrate. Tri-sodium phosphate hydrate crystallizes when it cools down to 60°C. The solid is filtered out and the solution which contains sodium hydroxide is recycled [18].

During the decomposition of bastnasite with caustic, the formation of a refractory film of RE hydroxides on the surface of the mineral which inhibits further leaching can be a problem. The use of mechanical abrasion to maintain leach activity and increase extraction has been suggested [19]. In addition, alkaline decomposition in an oxidizing medium was found to result in a decrease in the recovery of both cerium and the rest of the REE group into solution. Total recovery of the REE into solution does not exceed 30–40% in the presence of an oxidizing agent [20]. Therefore, the presence of oxidizing media must be avoided during alkaline decomposition of rare earth minerals. Refractory linings such as alumina and magnesia in tanks must be used as high temperature caustic soda is highly corrosive.

Hydrochloric Acid Leaching

Another method to dissolve rare earth elements is to use concentrated hydrochloric acid. Bastnasite can be dissolved in concentrated HCl according to the following reaction [17]:

$$3\ RECO_3F + 6\ HCl = 2\ RECl_3 + REF_3 + 3\ H_2O + 3\ CO_2 \qquad (18)$$

Rare earth fluoride precipitates in this step. The solid residue is collected via solid/liquid separation and treated with sodium hydroxide to convert the RE fluoride to rare earth hydroxide [17], which can be recovered by acid leaching:

$$REF_3 + 3\ NaOH = RE(OH)_3 + 3\ NaF \qquad (19)$$

Concentrated HCl can also decompose allanite, cerite and gadolinite. REOs and RE intermediate products can be also dissolved in hydrochloric acid solution.

In chloride media, tanks are usually made of titanium alloys. However, these alloys are not resistant to fluoride in solution. The presence of 20 ppm F^- (ionizable fluoride such as HF or NaF) is enough to cause corrosion as pH falls below 7 [21]. However, metal ions such as Al^{3+} [22] and Cr^{6+}can form a complex with fluoride and effectively inhibit corrosion of titanium alloys. Titanium stabilized palladium or platinum are the most resistant titanium alloys to hydrofluoric acid [23, 24]. In presence of free fluoride in solution, nickel based alloys such as Hastelloy C-276 that has high resistivity in acidic oxidizing/reducing chloride and fluoride media at high temperature can be used [16].

Nitric Acid Leaching

Rare earth silicates such as eudialyte can be decomposed using 30-50% nitric acid.

Rare earth phosphates can be decomposed in nitric acid as shown in Reaction 20 at a temperature of 120-140°C.

$$REPO_4 + 3\ HNO_3 = RE(NO_3)_3 + H_3PO_4 \qquad (20)$$

By increasing the temperature to 180°C, stability of some metal nitrates such as iron and aluminum nitrates decreases. They form a mixed metal hydroxyl phosphates which are insoluble in nitric acid. Therefore, nitric acid can be regenerated by thermal decomposition of the nitrate solution at the final stage after extraction of the REE [20].

Recovery and Purification

After extracting REE from the mineral ore, the most common methods to recover them from solution are solvent extraction and precipitation. The next step after recovery of REE from solution is to separate them. The value of REE products is much greater for selling pure REE separately rather than as a mixed product. Solvent extraction is a conventional method for this purpose.

Solvent Extraction

A major technique for the recovery, purification and separation of rare earth elements is solvent extraction [25]. This technique has several advantages such as simplicity, versatility, and ready adaptability to process scale-up. However, the leach solutions usually contain various and large amount of impurities; therefore more than one extraction circuit with different types of extractants, or a mixture of precipitation and solvent extraction techniques must be employed for primary extraction of the light and heavy rare earths. In addition, the separation of individual rare earth metals through the use of solvent extraction depends on differences in the complex formation ability between each of the rare earth metal and their extractant. Hence, with the chemical properties being so similar for most of the lanthanides, the difference in complexation is very small, which makes the separation of REE difficult [26].

One of the most common acidic extractants used for the separation of REE from leach solution of phosphate concentrates is Di (2-ethylhexyl) phosphoric acid also known as D2EHPA. D2EHPA extracts better from a chloride than from a nitrate medium. D2EHPA may be used either in chloride or sulfate systems both for obtaining rare earth concentrates from complex mixtures and to isolate individual rare earths in high purity. Wang et al. [11] studied the extraction of rare earth from PLS in phosphoric acid media using D2EHPA and showed that the rare earth extraction increases with increasing D2EHPA concentration and reaches 80% with 2.0M D2EHPA. They showed that the extraction efficiency for the elements by D2EHPA is in the order of La<Ce<Pr<Nd<Sm<Gd<Dy<Y which rises with increasing atomic number except for Y. However, by increasing the extractant concentration, removal of impurities by the organic phase is favored which lowers the separation between the lanthanides and impurities [11].

Gupta and Krishnamurthy [27] have studied the extractability of rare earths with TBP from concentrated hydrochloric and nitric acid solutions and showed that extractions with TBP is most effective in nitrate systems. They also showed that the TBP-nitric acid system could be used to separate the trivalent rare earths from one another. TBP can be also used to separate Ce from trivalent rare-earth elements in nitrate-nitric acid solution. Trivalent rare earth nitrate complexes in tributyl phosphate are less stable than cerium complexes [18].

It has also been suggested that the separation of rare earth via solvent extraction can be improved by chemical reactions during extraction [28]. A redox reaction of the metal ion can improve separation since metal ions having different valences behave like different elements with respect to their extractabilities. A complexing reaction with water soluble complexing agents can also improve separation. The separation abilities of the differing metal species are based on a difference in their abilities to form complexes with the agent in the equilibrium case and on a difference in the rates of the complexing reactions in the non-equilibrium situation. For instance, it has been shown that the solvent extraction of Eu from Sm/Eu/ Gd and of Ce from La/Ce/Pr can be improved by using ethylenediaminetetraacetic acid (EDTA) as a complexing agent [26].

In addition to difficulty in separating rare earth elements due to similarity in complexing ability of REE, there are some other limitations to the application of traditional solvent extraction. One limitation is that large volumes of organic solvents are needed, especially when processing dilute solutions, which is not environmentally friendly. Further the method can be tedious and time consuming in those cases where many, many, steps are needed to reach a sufficient level of separation. Another drawback is that with so many mixer settlers required, the method can be difficult to automate and that the liquid phases may form emulsions that at times make it difficult to separate the two phases. High production costs and environmental pollution because of the large amount of organic solvents are some of the drawbacks of solvent extraction [29].

Precipitation

One of the most common methods to recover REE is by precipitation as RE oxalate or sodium RE double sulfates.

Oxalic acid: RE oxalates are highly insoluble, $K_{sp} \approx 10^{-30}$, so oxalic acid can be used to precipitate REE directly from the leach solution [4]. If not too concentrated, Fe(III), Al(III), and Mg(II) form complexes and remain in the solution and do not affect the purity of rare earth precipitate. The solubility of oxalates of Mn, Cu, Pb, Ni, Zn, Co, and Cd increases by increasing the acidity. To avoid their precipitation with the RE oxalates, acidity can be increased during precipitation. However, if pH is too low, then the yield of RE oxalate also decreases [30].

Calcium precipitates with oxalic acid and it is the main problem with the oxalate precipitation method. To avoid calcium co-precipitation, calcium and REE have to be separated before RE oxalate precipitation. The separation of calcium and REE is carried out by precipitation of the calcium from a strong sulfate solution. In a strong sulfuric acid solution (pH 0 to 1), the calcium is precipitated as gypsum. Upon solid liquid separation, gypsum remains in the residue while the filtrate contains the REE. In chloride media, unless the calcium content of the mineral is very low, the oxalate precipitation is not very effective, due to high solubility of gypsum in this medium and co-precipitation of calcium oxalates with the REE. The precipitation of rare earth elements by oxalic acid is shown in Reaction 21 [4, 30]:

$$2\ RE^{3+} + 3\ H_2C_2O_4 + 10\ H_2O = RE_2(C_2O_4)_3.\ 10\ H_2O + 6\ H^+ \qquad (21)$$

Often an oxalic acid addition rate of 1.4-1.5 times the stoichiometric requirement is added to achieve complete rare earth oxalate precipitation [29]. The requirement for such an excess of oxalic acid can be attributed to the reaction of non-RE species such as Fe(III), Al(III), Mg (II), and Ca(II) with oxalic acid. It has been shown that efficiency of oxalic acid precipitation of rare earth elements increases with increasing pH up to 4. However, at a pH higher than 2, co-precipitation of impurities as hydroxide such as $Fe(OH)_3$ and $Al(OH)_3$ can also occur which lowers the purity of the rare earth precipitate. An optimal pH between 1 and 2 maximizes both rare earth element recovery and purity of precipitates [30].

Double Sulfate Precipitation:One of the most widely used precipitation methods is to separate rare earth elements (REE) from acidic solutions by precipitation of sodium double sulfate hydrates ($NaRE(SO_4)_2.xH_2O$) through addition of sodium sulfate [27, 31]. These salts are only slightly soluble in acidic solutions. Double sulfate precipitation results in separations of light-REE and heavy-REE [27]. The different REE can then be separated from each other by converting the double sulfate into an insoluble compound, such as RE-hydroxide.

Rare earths are precipitated in the form of insoluble double sulfate salts at pH 1.5 to avoid ferric hydroxide precipitation. Rare earth double sulfates precipitates, especially light RE precipitates such as La, Ce, Pr, Nd, Pm, Sm, Eu, and Sc, have low solubility in water. Their solubility decreases with increasing temperature and they become highly insoluble in saturated solutions of the alkali metals [32]. The reaction of rare earth sulfate with sodium sulfate can be represented by Reaction 22.

$$Re_2(SO_4)_3 + Na_2SO_4 + 2\ H_2O = Na_2SO_4.(Re_2SO_4)_3.\ 2H_2O \qquad (22)$$

Kul et al. [33] determined the optimum conditions for the precipitation of a rare earth double sulfate salts with sodium sulfate. According to their study, as temperature increases, the rate of RE precipitation increases and the products become more insoluble. However, the rate and level of precipitation of other elements such as Ca, Al, Fe, and Th also increases. Therefore the optimum precipitation temperature of 25-50°C was suggested in that study.

After precipitating rare earth double sulfate, this product needs further processing. Generally, these precipitates are metathesized to rare earth hydroxide by sodium hydroxide. Then hydroxides are dissolved in hydrochloric acid and eventually separated by solvent extraction using DEHPA [33].

Conclusions

In this paper, several hydrometallurgical processes to extract and recover REE have been reviewed. Sulfation roasting has been the major process to extract RE from ore or concentrate. Due to significance of this process, it has been discussed in more detail with respect to the reaction mechanism at various roasting temperature, design of the kiln, and material of construction. The most common processes to recover RE from the leachate are solvent extraction and precipitation.

References

1. Habashi, F., T. Awadalla, and X, Tao, “The hydrochloric acid route for phosphate rock,” *Journal of Chem. Tech. Biotechnol,* 38 (1987), 115-126.

2. Habashi, F., “The recovery of the lanthanides from phosphate rock,” *Journal of Chem. Tech. Biotechnol*, 35A (1985), 5-14.

3. Wang, W., Y. Pranolo, and C.Y. Cheng, “Metallurgical processes for scandium recover from various resources: A review,” *Hydrometallurgy,* 108 (2011), 100-108.

4. Chung, D.Y., et al., “Solubility of rare earth oxalate in oxalic and nitric acid media,” *Journal of Industrial and Engineering Chemistry,* 4 (1998), 277-284.

5. Abreu, R.D., and C.A. Morais, “Purification of rare earth elements from monazite sulfuric acid leach liquor and the production of high purity ceric oxide”. *Mineral Engineering,* 23 (2010), 236-540.

6. Hongtao, C., et al., “Study on separation of rare earth elements in complex system”. *Journal of Rare Earths,* 28 (2010), 116-119.

7. Doyle, F.M., “Direct production of mixed, rare earth oxide feed for high energy product magnets,” (Rare earths and Actinides: Science, Technology and Applications IV, eds. R.G. Bautista and B. Mishra, TMS Warrendale, PA, 2000), 31-44.

8. Thakur, N.V.,“Separation of rare earths by solvent extraction,” *Min. Pro. Ext. Met.,* 21 (2000), 277-306.

9. Zaijun, L., S. Xiulan, and L. Junkang, “Ionic liquid as novel solvent for extraction and separation in analytical chemistry,” *Ionic Liquids: Applications and Perspectives*, (2011), 153-180.

10. Jordens, A., Y.P. Cheng, K.E. Waters, “A review of the beneficiation of rare earth element bearing minerals,” *Minerals Engineering*, 41(2013), 97-114.

11. Wang, L., Z et al., “Recovery of rare earths from wet-process phosphoric acid,” *Hydrometallurgy* 101(2010), 41-47.

12. Higashiyama, Y., and K. Asano, K, “Recent progress in electrostatic separation technology,” *Particulate Science and Technology* 16 (1) (2007), 77-90.

13. Li, D.Q., Y. Zuo, and S.L. Meng, “Separation of thorium(IV) and extracting rare earths from sulfuric and phosphoric acid solutions by solvent extraction method. *J. Alloy.Compd*, 374 (2004), 431–433.

14. Bunzli, G., V. K. Pecharsky. *Handbook on the Physics and Chemistry of Rare Earths*, 2012, 197.

15. Xiuyan, W., et al., “Decomposition reaction kinetics of Baotou RE concentrated with concentrated sulfuric acid at low temperature,” *Rare Metals,* 29(2) (2010), 121-125.

16. High Performance alloys for resistance to aqueous corrosion. www.specialmetals.com

17. Zhang, Z., and C. Edward, “Mineral decomposition and leaching processes for treating rare earth ore concentration,” Conference of Metallurgy (2012), 95-102.

18. Habashi, F., “Extractive Metallurgy of Rare Earths,” Conference of Metallurgy (2012), 51-66.

19. Wantae, K., et al., “Mechanochemical decomposition of monazite to assist the extraction of rare earth elements,” *J. Alloys Compd.* 486 (2009), 610–614.

20. Kuzmin, V.I., et al., “Combined approaches for comprehensive processing of rare earth metal ores,” *Hydrometallurgy,* 129-130, (2012), 1-6.

21. Craig, B., and D. Anderson, Handbook of Corrosion Data, (1995), 440.

22. Corbillon, M.S., M.A. Olazabal, and J.M. Madariaga, “Potentiometric study of aluminum-fluoride complexation equilibria and definition of the thermodynamic model,” *Journal of Solution Chemistry* 37 (2008), 567-579.

23. Nakagawa, M., S. Matsuya, and K. Udoh, “Corrosion behavior of pure titanium and titanium alloys in fluoride containing solutions,” *Dental Materials Journal,* 20 (2001), 305-314.

24. Nakagawa, M., et al., “The effect of Pt and Pd alloying additions on the corrosion behavior of titanium in fluoride-containing environments’” *Biomaterials,* 26 (2005), 2239-2246.

25. Reddy, M.L.P., T.P. Rao, and A.D. Damodaran, “Liquid–liquid extraction processes for the separation and purification of rare earths,” *Miner. Process. Extr. Metall,.*12 (1993) 91-113.

26. Nishihama, S., T. Hirai, and I. Komasawa, “Advanced liquid-liquid extraction systems for the separation of rare earth ions by combination of conversion of the metal species with chemical reaction,” *Journal of Solid State Chemistry,* 171 (2003), 101-108.

27. Gupta, C.K., and N. Krishnamurthy, “Extractive metallurgy of rare earths,” *International Materials Reviews* 37 (1992), 197-248.

28. Nishihama, S., T. Hirai, and I. Komasawa, “Review of advanced liquid-liquid extraction systems for the separation of metal ions by a combination of conversion of the metal species with chemical reaction,” *Ind. Eng. Chem. Res,* 40 (2001), 3085-3091.

29. Wuhua, D., C. Pijia, and Z. Yonhjun, “Extraction of rare earth elements from their oxides using organophosphorus reagent complexes with HNO_3 and H_2O in supercritical CO_2,” *Journal of Rare Earths* 28(2) (2010), 221-226.

30. Chi, R., and Z. Xu, “A Solution Chemistry Approach to the Study of Rare Earth Element Precipitation by Oxalic Acid,” *Metallurgical and Materials Transactions* 30 (B) (1999), 189-194.

31. Abreu, R.D., and C.A. Morais, "Purification of rare earth elements from monazite sulfuric acid leach liquor and the production of high purity ceric oxide," *Minerals Engineering,* 23 (2010), 536-540.

32. Pietrelli, L., et al. "Rare earths recovery from NiMH spent batteries. *Hydrometallurgy* 66 (2002), 135–139.

33. Kul, M., Y. Yopkaya, and I. Karakaya, I, "Rare earth double sulfates from pre-concentrated bastnasite," *Hydrometallurgy* 93 (2008), 129-135.

METALLOTHERMIC REDUCTION OF A RARE EARTH PRECONCENTRATE FOR THE PRODUCTION OF RARE EARTH FERROSILICON ALLOY

Yavuz A. Topkaya, Ahmet Geveci, Serkan Yılmaz

Department of Metallurgical and Materials Engineering,
Middle East Technical University, Ankara, Turkey

Keywords: Rare Earth Ferrosilicon, Bastnasite, Metallothermic Reduction

Abstract

The aim of this study was to optimize the experimental conditions for the production of rare earth ferrosilicon alloy by using a preconcentrate prepared from a bastnasite type of ore located in the eastern part of Turkey. The preconcentrate with 23.5% REO grade was reduced by aluminum together with ferrosilicon in the presence of a basic flux and a rare earth alloy was produced. The optimum conditions of reduction studied were temperature, duration, reducer amounts and the basicity of the slag phase by performing the reduction and smelting in an induction furnace.

Introduction

The term “rare earths” (symbolized as RE or REE) denotes the group of 17 chemically similar metallic elements, including scandium, yttrium, and the lanthanides (Ln).

The rare earths, used as metals, alloys and chemical compounds, have an ever growing variety of applications in the modern technology; Ferrous and nonferrous metallurgy, production of glass and ceramics, the chemical industry, production of permanent magnets, nuclear applications and many more. Rare earth elements, notably cerium and mischmetal have also been used as minor alloying additives for controlling shape of inclusions in cast iron and steel [1].

Although more than 250 rare earth containing minerals are known, about 95% of the rare earths occur in only three minerals; bastnasite ($LnFCO_3$), monazite $(Ce,La,Th,Y)PO_4$ and xenotime (YPO_4).

Rare earth ferrosilicon is an alloy which mainly consists of, as the name implies, mixed rare earth metals, iron and silicon. The alloy is the most extensively used form of rare earths in cast iron and steelmaking technology.

Rare earth ferrosilicon alloy can be produced by two different reduction processes; carbothermic and metallothermic reduction. In carbothermic reduction, carbon is used to extract metal values from the rare earth oxides (REO) [2]. In metallothermic reduction, reducing agents such as CaSi, CaSi together with CaC_2, a metal silicide or silicon and aluminum together with ferrosilicon can be utilized to reduce rare earth oxides. Production of the rare earth ferrosilicon alloy by metallothermic reduction with aluminum and ferrosilicon is the main concern of this study.

Metallothermic reduction with Al and FeSi consists of briefly, reducing rare earth oxides with aluminum and ferrosilicon in the presence of a basic flux at a high enough temperature to melt both metal and slag phases in a suitable crucible and furnace and it is represented by reaction (1) which is given below;

$$3RE_2O_3 + 15Si + 2Al = 6RESi_2 + 3SiO_2 + Al_2O_3 \quad (1)$$

Some previous workers have studied the production of rare earth ferrosilicon alloy by metallothermic reduction, using aluminum and ferrosilicon as the reductants [3 - 6].

The study of Mitchell et al. [3] was based on two important facts to obtain higher metal recoveries; using a highly basic flux to lower the activity of Al_2O_3 in the flux and maintaining this flux at the possible lowest temperature at which the flux is in liquid state.

The process invented by Mitchell et al. [3] was performed in an induction furnace and it consisted of melting down a flux mixture of 90 % CaF_2 and 10 % CaO in a graphite crucible, adding to this mixture rare earth oxide and CaO in 1:1 ratio at a temperature of about 1371 ˚C. The final step was the addition of aluminum and silicon to this mixture in excessive amounts of the theoretically required for the reduction reaction.

In a test carried out by Mitchell et al. [3] 8.2 kg CaF_2 and 0.9 kg CaO were melted as the first step of the process. In the second step 5 kg rare earth oxide and 5 kg CaO were charged into the melt and finally 1.8 kg Si and 2 kg Al were added as the reducing agents. At the end of the test a rare earth ferrosilicon alloy containing 54.14 % by weight rare earth metals with 85 % rare earth metal recovery was obtained.

Morrice et al. [4] indicated that the reactor for their process might be any suitable one capable of generating and maintaining the reaction temperature, but utilizing an induction furnace was advantageous. Also, they found that crucibles made of silicon carbide, boron nitride or graphite could be used as containers for the reactants while emphasizing that using graphite crucible could cause the formation of some calcium carbide.

The process invented by Morrice et al. [4] consists of melting the charge materials in the reaction crucible, holding at a desired temperature for the time period required for completion of the reaction and pouring or tapping the melt into molds. Also separation of the products can be accomplished by allowing the melt to freeze and breaking the slag away from the alloy product.

In a test carried out by Morrice et al. [4] rare earth oxide ore, having 82.5 % by weight of RE_2O_3, in an amount of 227 grams, ferrosilicon having 25% by weight iron, in an amount of 132 grams, aluminum metal in an amount of 68.5 grams, calcium oxide in an amount of 263 grams and magnesium oxide in an amount of 24 grams were placed into a silicon carbide crucible and melted at 1600 ˚C in an induction furnace. After waiting for 30 minutes, the melt was poured into a conical mold and allowed to freeze. Separation of the slag phase was done by breaking it away from the alloy product. Alloy product obtained by such process consisted of 46 % by weight rare earth metals and rare earth metal recovery was 91.5 %.

Marchant et al. [5] conducted their tests in an induction furnace with graphite or densified silicon carbide crucibles. Rare earth oxides prepared from bastnasite flotation concentrates, aluminum turnings and fragments of ferrosilicon and some flux materials such as CaO and MgO were utilized in their process as charge materials.

The charge composition of a test carried out by Marchant et al. [5] consisted of 681 grams mixed rare earth oxides, 309 grams ferrosilicon (78% Si), 182 grams of aluminum, 681 grams of CaO and 45 grams of MgO where CaO and MgO served as the flux and added on top of the other charge materials. The charge materials were melted and held at 1500 ˚C for 30 minutes and then the melt was poured into an iron mold. Separation of alloy product and slag was done by allowing the melt to freeze and breaking the slag away from the alloy product. The rare earth metal recovery of this test was 80 % and an alloy product with 52.6 % by weight rare earth metals was obtained at the end of the test.

Turgay [6] conducted his experiments in an induction furnace using graphite crucibles. Three kinds of rare earth source were utilized in his study; one of them was a bastnasite type preconcentrate with 23.5 % REO grade, the other two sources were rich rare earth oxide concentrates with 81.6% and 94.9 % REO grades. The experiments done with the preconcentrate gave very low rare earth recoveries. Aluminum particles (99.9 %) and ferrosilicon alloy (88 % Si) as reducing agents, lime which was obtained by calcination of $Ca(OH)_2$ or $CaCO_3$, quartz of 99 % purity and fluorspar as the fluxing agents were the other charge materials of the tests carried out by Turgay [6].

Turgay [6] indicated that using excessive amounts of reducing agents was a must for obtaining a high rare earth metal recovery and that reaction temperature should be kept as low as possible at which a molten and fluid slag could be obtained.

In a test carried out by Turgay [6], 44 grams of rich rare earth oxide concentrate (81.6 % REO), 750 % of the stoichiometric amount of aluminum, 112 % of the stoichiometric amount of ferrosilicon and 43.1 grams of lime were utilized as the charge materials. As the first step of the test, the rare earth concentrate was melted in a graphite crucible at 1550 °C, then other charge materials were added together into the crucible and the charge was allowed to react for 30 minutes. After the holding time, crucible was taken out of the furnace and left to cool down. Separation of the metal and slag phases was done by breaking them by a hammer. The alloy product obtained by this procedure consisted of 50.1 % by weight rare earth metals and the rare earth metal recovery was 81.1 %.

Experimental Procedure

In the present experiments, the reduction of the bastnasite type rare earth preconcentrate was carried out by aluminum and ferrosilicon in the presence of a basic flux in an induction furnace using graphite crucibles.

The bastnasite preconcentrate used in this study was produced from an ore sample taken from Beylikahır-Eskişehir region of Turkey. Concentration of this ore was done by attrition scrubbing followed by screening and desliming. For this purpose the ore sample was first ground to -10 mesh (-1.7 mm) and was subjected to attrition scrubbing with a 50% solid concentration for one hour. After screening from 400 mesh and dilution of -400 mesh (-38 microns), classification of the pulp by a series of hydrocyclones was done. A fine bastnasite preconcentrate with a 23.5 % REO grade was obtained on hydrocyclone overflow at the end of such concentration process. The composition of the obtained preconcentrate is given in Table I.

The charge materials were rare earth preconcentrate, aluminum rod pieces (99.9%) about 0.5-1 cm in length and 3 mm in diameter, ferrosilicon containing 73.2 % Si and calcium oxide in powder form as the only fluxing agent.

Table I. Composition of the Preconcentrate

Compound	Weight (%)
La_2O_3	9.01
Ce_2O_3	14.00
CaF_2	35.44
$CaCO_3$	7.24
SiO_2	6.78
Fe_2O_3	7.97
$BaSO_4$	6.12
Al_2O_3	2.38
P_2O_5	2.16
MgO	0.95

At the beginning of all the experiments, 50 grams of preconcentrate was mixed under acetone in an agate mortar with the predetermined amount of CaO. Three spherical agglomerates were made from this mixture to prevent dusting problem that might be encountered during the melting process. The graphite crucible which was closed by a graphite lid was then placed into an induction furnace which had a power output of 41 kW and a melting capacity of 4 kg aluminum and heating process was started. At the center of the lid, there was a hole of about 1 cm in diameter for temperature measurement which was done by an optical pyrometer at about every 1 minute.

After the predetermined reaction temperature was reached, the lid of the crucible was opened and agglomerates were charged into the crucible. Aluminum and ferrosilicon were added to the crucible by a small shovel when agglomerates were melted completely. Holding the crucible at the reaction temperature for a predetermined duration to complete the reaction was followed by taking it out and leaving at room temperature to cool down. The day after, crucible was broke down with a hammer for taking the produced metal and slag phases out. Then, the products were separated from each other by carefully breaking them with a hammer. Flowchart of the experiments is given in Figure 1.

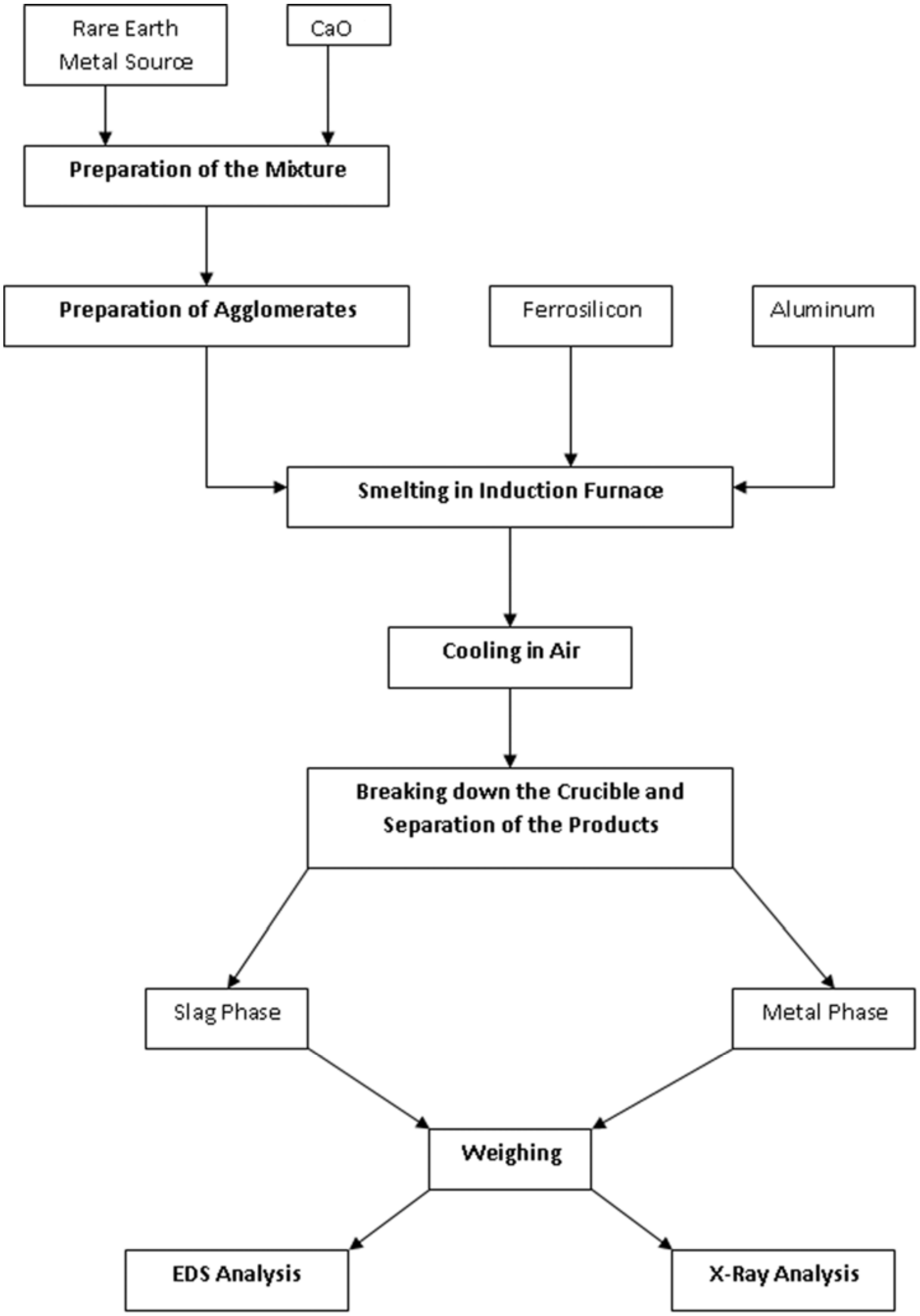

Figure 1. Flowchart of the experiments.

Metal and slag phases were weighed before preparing samples from them for the chemical and Energy Dispersive Spectral (EDS) analyses at the scanning electron microscope (SEM). Rare earth recoveries of the experiments were calculated according to Equation (2) given below;

$$\frac{(\text{Metal wt.})(\text{wt\%RE-metals})_{\text{In metal phase}}}{(\text{Metal wt.})(\text{wt\%RE-metals})_{\text{In metal phase}} + (\text{Slag wt.})(\text{wt\%RE-metals})_{\text{In slag phase}}} \times 100 \qquad (2)$$

The process parameters investigated in the present experiments were basicity (Equation 3) of the slag phase (1.3, 1.65 and 2.0), temperature (1450 °C, 1500 °C and 1550 °C), duration (15, 30 and 45 minutes), amount of aluminum charged (500 %, 550 % and 600 % of the stoichiometric amount required) and amount of ferrosilicon charged (100 %, 112 % and 150 % of the stoichiometric amount required).

$$\text{Basicity of slag} = \frac{\text{CaO(wt.\%)} + \text{BaO(wt.\%)}}{\text{SiO}_2\text{(wt.\%)} + \text{Al}_2\text{O}_3\text{(wt.\%)}} \tag{3}$$

Results and Discussion

Effect of the Basicity of the Slag Phase

To understand the effect of the basicity of the slag phase on the rare earth recovery, three tests were performed. Basicity of the slag phase was adjusted by changing the amount of CaO charged. Basicity of 1.3, 1.65 and 2 were obtained by utilizing 13.04 grams, 17.84 grams and 22.65 grams of CaO, respectively, with 50 grams of rare earth preconcentrate, 3.72 grams of aluminum (600 % of the stoichiometric amount) and 7.57 grams of ferrosilicon (112 % of the stoichiometric amount). Aluminum and ferrosilicon addition were made at 1500 °C and the charge was allowed to react for 30 minutes for each of the experiments. Results of these three experiments are given in Figure 2.

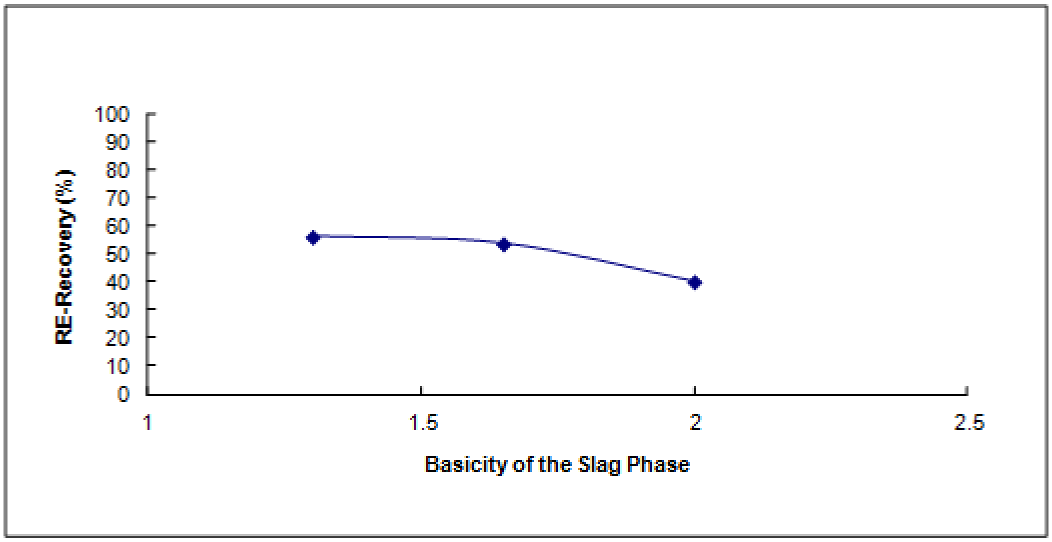

Figure 2. RE-metal recovery vs. basicity of the slag phase.

Recovery of the rare earth metal values slightly decreased from 56.0 % to 53.5 % as the basicity of the slag phase increased from 1.3 to 1.65. Further increment of the basicity to 2 resulted in a high decrease of recovery to 40.0 %.

As mentioned by the previous researchers, a basic flux was necessary for suppressing the activity of Al_2O_3, so that the reduction reaction of the rare earth oxides with Al and FeSi goes to completion as stated by Mitchell et al., [3]. Also it was stated by Morrice et al. [4] that utilizing of the graphite crucible could cause the formation of some calcium carbide.

From the slag viscosity point of view, probably the presence of solid and liquid mixed slag in high basicity region caused more rare earth metal entrapment in the slag than the slag with the basicity ratio of 1.3, since the basicity ratios of the slag phases were adjusted by CaO addition only.

So, it can be concluded that as long as a basic and fluid slag was obtained, basicity of the slag should be kept at a value that prevents the formation of calcium carbide as much as possible.

Effect of the Temperature

In order to understand the effect of temperature, at which the reduction reaction is carried out, on the recovery of rare earth metals as alloy products three tests were made at 1450 °C, 1500 °C and 1550 °C.

50 grams of rare earth preconcentrate was reacted with 600 % of the stoichiometric amount of aluminum and 112 % of the stoichiometric amount of ferrosilicon required for the reduction reaction in all of three experiments. 22.65 grams of CaO was used as the only fluxing agent in all the runs. The charge mixture was allowed to react in furnace for 30 minutes. The results of these three tests are given in Figure 3.

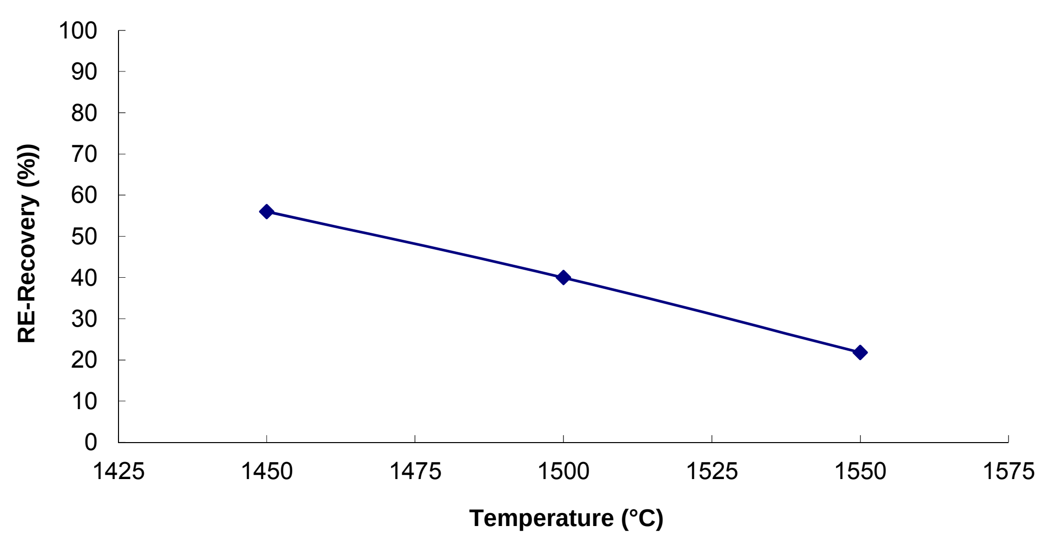

Figure 3. RE-metal recovery vs. reaction temperature.

While temperature increased from 1450 °C to 1550 °C, the recovery of the rare earth metals as alloy product decreased continuously from 56.0 % to 21.8 %. These results showed that the temperature at which the reduction reaction was carried out was highly effective on the recovery of rare earth metals and composition of the alloy product.

Although it is expected that higher temperatures should give better recoveries since the viscosity of slag phase decreases with increasing temperature, the results are not in accordance with this expectation. This fact can be explained by the statement of Mehra et al. [7] which say that even a small decrease in reduction temperature reduces the aluminum losses. Rate of the oxidation of aluminum before reduction reaction increases while working at higher temperatures and results in a higher loss of the reducing agent and therefore a lower recovery of rare earths.

Morrice et al. [4] mentioned in their study that temperatures below 1400 °C were not suitable for the reduction process because of the increasing slag viscosity. Having CaF_2 in the rare earth preconcentrate was an advantage for this study because the existence of CaF_2 made it possible to decrease the temperature to 1450 °C while not vitally increasing the slag viscosity.

It can be said that, to obtain a higher rare earth recovery and better composition of alloy product, temperatures as low as possible which ensure a fluid and low viscosity slag should be utilized for the reduction process.

Effect of the Aluminum Amount in the Charge

To understand the effect of the aluminum amount in the charge, four tests were made with 500 %, 550 %, 600 % and 750 % of the stoichiometric amount of aluminum required for reaction 1.

In all of the experiments, 50 grams of rare earth preconcentrate and 112 % of the stoichiometric amount of ferrosilicon were used with CaO as the fluxing agent, the amount of which was adjusted to set the basicity ratio to 1.3. Aluminum together with ferrosilicon were added to the reaction mixture at 1500 °C and allowed to react for 30 minutes. Results of these four tests are given in Figure 4.

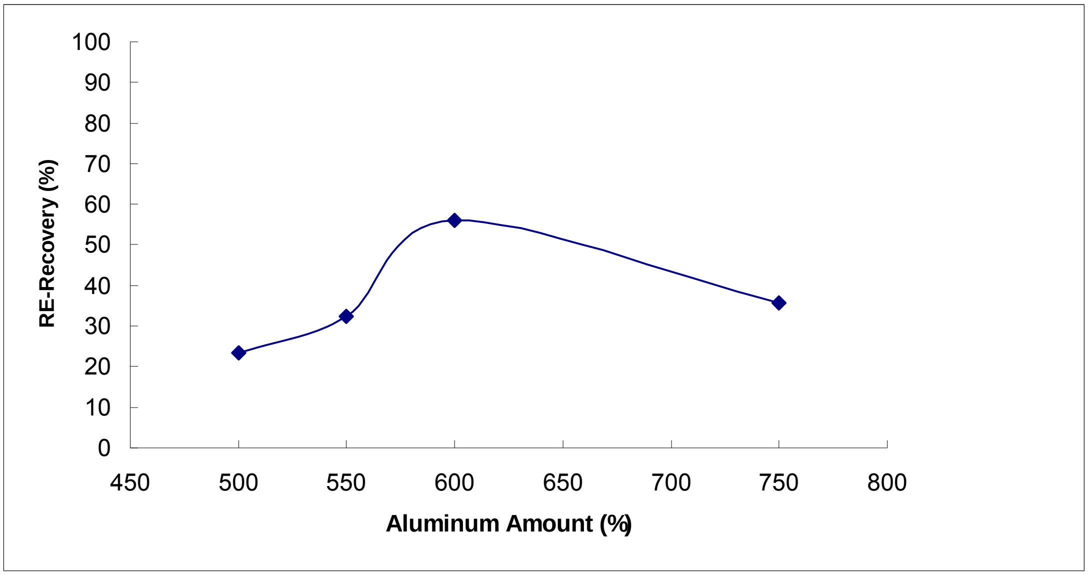

Figure 4. RE-metal recovery vs. % aluminum addition of the stoichiometric amount.

Recovery of the rare earth metal values increased from 23.3 % to 56.0 % with the increasing amount of aluminum addition from 500 % to 600 % of the stoichiometric amount. Further increment in the amount of aluminum to 750 % of the stoichiometric amount resulted in a decrease of the rare earth metal recovery to 35.6 %.

At high temperatures, a significant amount of aluminum is oxidized before the reduction reaction. As it was mentioned by the previous workers Mitchell et al., [3]; Morrice et al., [4], the amount of aluminum to be charged should be in excess of the stoichiometric amount to compensate the aluminum losses due to oxidation. On the other hand, Mitchell et al. [3] indicated in their study that the alloying reactions became less efficient as the Al_2O_3 content (activity) increased and would stop at some point. Also, Morrice et al. [4] pointed out in their study that 700 % of the stoichiometric amount of aluminum was the upper limit to obtain a better recovery of rare earth metals. In the study of Turgay [6], 600 % of the stoichiometric amount of aluminum was found to be the optimum value to obtain a better recovery and alloy composition since the recovery began to decrease over this amount of aluminum and since the aluminum amount in the alloy product showed a considerable increase (4.0%) as the amount of aluminum reached to 700 % of the stoichiometric amount. The results of the present study are in accordance with the aforementioned ones.

It can be concluded from the above discussion that the aluminum amount should be in excess of the stoichiometric amount to compensate the aluminum losses due to oxidation while keeping the Al_2O_3 activity as low as possible in slag phase. Six times of the stoichiometric amount of aluminum seems to be the best choice from the recovery and alloy composition points of view in the current slag composition.

Effect of the Ferrosilicon Amount in the Charge

To understand the effect of ferrosilicon amount charged on the rare earth recovery and alloy composition three tests were made with the 100 %, 112 % and 150 % of the stoichiometric amount of ferrosilicon.

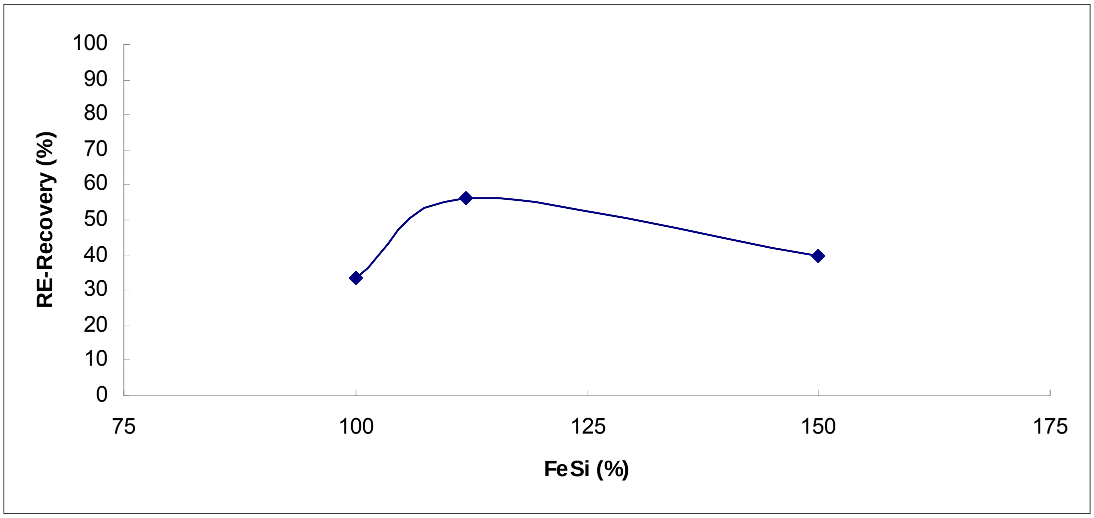

Figure 5. RE-metal recovery vs. % FeSi addition of the stoichiometric amount.

50 grams of rare earth preconcentrate, 600 % of the stoichiometric amount of aluminum and CaO amount of which was adjusted to set the basicity ratio of slag phase to 1.3 were used with the

predetermined amounts of ferrosilicon. Ferrosilicon was added at 1500 °C together with aluminum and duration was set to 30 minutes in each of the tests. The results of these three tests are given in Figure 5.

Rare earth metal recovery increased from 33.5 % to 56.0 % while amount of ferrosilicon addition increased from 100 % to 112 % of the stoichiometric amount. Further increment in the amount of ferrosilicon to 150 % of the stoichiometric amount resulted in a decrease of the rare earth metal recovery to 39.7 %.

As reported in the previous studies by Marchant et al., [5] and Turgay [6], the ferrosilicon amount charged should be in excess of the stoichiometric amount required for reaction (1). From the SiO_2 activity point of view, ferrosilicon usage over 112% of the stoichiometric amount resulted in an increase of SiO_2 activity in slag phase while preventing the completion of reaction (1) and decreasing the rare earth metal recovery as alloy product.

Effect of the Duration

In order to observe the effect of duration on rare earth metal recovery, three tests were realized with 15, 30 and 45 minutes of duration. In all of the runs 50 grams of rare earth preconcentrate was utilized as the rare earth metal source. CaO amounts were adjusted to set the basicity ratio of the slag phases to two. 600 % aluminum and 112 % ferrosilicon of the stoichiometric amounts were added into the charge which consisted of rare earth preconcentrate and CaO at 1500 °C. Results of these three tests are given in Figure 6.

From Figure 6, it is seen that rare earth metal recovery was the highest (47.6 %) with 15 minutes of duration period. Then, it showed 7.6 % decrease to 40.0 % as the interval extended to 30 minutes, and on extending the duration period further to 45 minutes, the recovery dropped sharply to 20.6 %.

Some of the calcium in lime reacts with the graphite crucible and forms calcium carbide. Formation of calcium carbide decreases the basicity of the slag which resulted in higher activity of Al_2O_3 and SiO_2, therefore affected the reaction thermochemistry adversely. The effect of calcium carbide formation became more pronounced at longer time intervals, namely 30 and 45 minutes of duration period. Results of the tests are in accordance with the studies of Morrice et al. [4] and Turgay [6] who also mentioned about the formation of calcium carbide while using graphite crucibles.

Apart from the results of these tests, extending the duration period over 15 minutes results in consumption of more energy and decrease in productivity, which are economically unfavorable. 15 minutes of duration period was found to be the optimum for completion of the reduction reaction while keeping the formation of calcium carbide as low as possible.

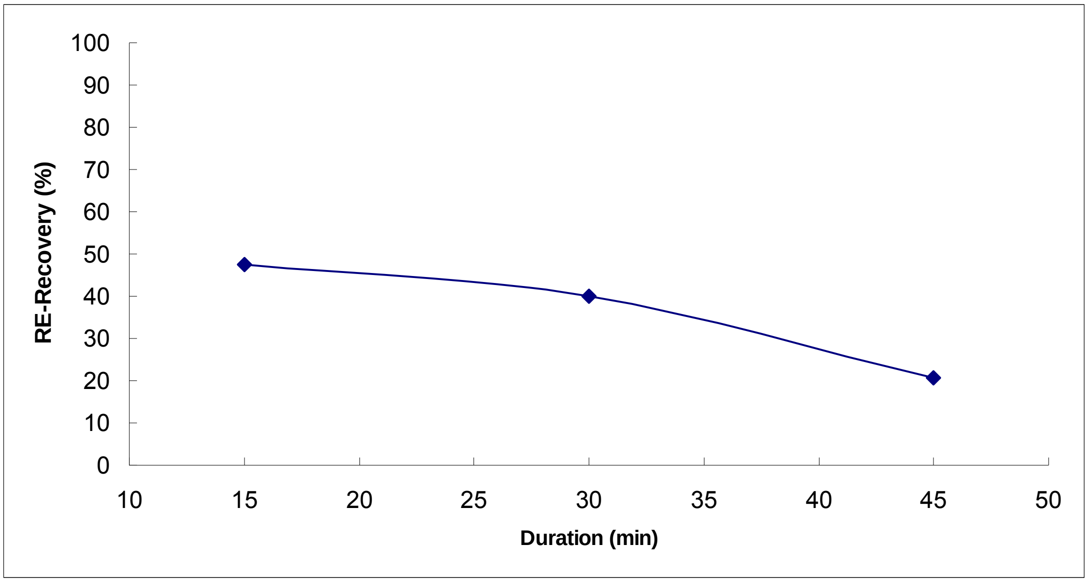

Figure 6. RE-metal recovery vs. duration.

Experiment Performed Under the Optimum Conditions Determined

After realizing several experiments, it was found that utilizing 600 % aluminum of the stoichiometric amount and 112 % ferrosilicon of the stoichiometric amount with a slag basicity ratio of 1.3 and a holding time of 15 minutes at 1450 °C were advantageous for production of rare earth ferrosilicon alloy from rare earth preconcentrate.

A final experiment was conducted to apply the findings and obtain the highest rare earth recovery. 50 grams of rare earth preconcentrate was utilized with the optimum values of the parameters which are given above. Results of the test are given in Table II.

Table II. Results of the Test Performed Under the Optimum Conditions

Composition of the alloy product (wt. %)				RE-metal recovery (%)
RE's	***Si***	***Fe***	***Al***	
39.3	37.5	19.3	3.9	57.7

Conclusions

In this research work, the optimization of conditions of metallothermic reduction of rare earth preconcentrate was studied. The following conclusions were drawn considering the experimental results:

1. As long as a basic and fluid slag was obtained, the basicity of the slag should be kept at a value that prevents the formation of calcium carbide as much as possible since utilizing graphite crucibles cause the formation of calcium carbide.

2. To obtain a higher rare earth recovery and better composition of alloy product, temperatures as low as possible which ensure a fluid and low viscosity slag should be used for the reduction process.

3. Aluminum amount should be in excess of the stoichiometric amount to compensate the aluminum losses due to oxidation while keeping the Al_2O_3 activity as low as possible in slag phase. Six times of the stoichiometric amount of aluminum seems to be the best choice from the recovery and alloy composition points of view.

4. Utilizing the ferrosilicon in excess of the stoichiometric amount was found advantageous to obtain a better rare earth metal recovery up to a point where the increasing SiO_2 activity started to reduce the rare earth metal recovery. In this study, 112 % of the stoichiometric amount of ferrosilicon gave the highest recovery.

5. In order to achieve satisfactory rare earth metal recoveries, allowing the reduction reaction of rare earth oxides to occur for 15 minutes was found advantageous.

6. In order to increase rare earth metal recoveries in metallothermic reduction of rare earth preconcentrate, reducing agents such as CaSi should be tried as future work.

References

1. Gupta, C.K., N. Krishnamurthy, “Extractive Metallurgy of Rare Earths”, *International Materials Reviews*, (1992), 197-248.

2. Staggers, J.O., “Rare Earth Metal Silicide Alloys”, U.S. Patent No. 4.018.597, 1977.

3. Mitchell, A., J.R. Goldsmith, J.M. Gray, “Preparation of Rare Earth and Other Metal Alloys Containing Aluminum and Silicon”, U.S. Patent No. 4.108.645, 1978.

4. Morrice, E., J.D. Marchant, “Process for the Preparation of Rare Earth Silicon Alloys”, U.S. Patent No. 4.135.921, 1979.

5. Marchant, J.D., E. Morrice, B.P. Herve, M.M. Wong, “Preparing Rare Earth Silicon Iron Aluminum Alloys”, U.S.B.M, R.I. 8445, 1980.

6. Turgay, O., “The Optimization of Experimental Conditions for Production of Rare Earth Ferrosilicon Alloy”, (M.Sc. thesis, Middle East Technical University, 2003).

7. Mehra, O.K., S. Singh, J.S. Sehra, T.S. Krishnan, D.K. Bose, C.K. Bose, “Extractive Metallurgy of Rare Earths – Developmental Work at the Bhabha Atomic Research Center”, Materials Science Forum, (1988), 73-88.

PREPARATION OF RARE EARTHS OXIDE BY SPRAY PYROLYSIS

Bian Xue, Wu Wenyuan

School of Materials & Metallurgy,
Northeastern University,
Shenyang 110819, China

Keywords: RECl3; RE2O3; Spray Pyrolysis

Abstract

Rare earths oxide is precipitated by oxalic acid or ammonium acid carbonate in RECl3 solution, and the problem is polluted by discharge of waste water containing NH4+ or C2O42-. If the output of REO is 120000 ton, 18900 ton (NH4)2CO3 are used, and 4800 ton CO2 and 12900 ton NH4+ are discharged. The preparation of RE2O3 can also be used the method of metals chloridate spray pyrolysis. But the study of this method without agent (as acetic acid, citric acid, mixed acid and et al) is less reported. In this paper, the thermodynamic feasibility of RE2O3 preparation by RECl3, and the effect parameters of temperature, time on the conversion ratio of RE2O3 are studied. The conversion ratio of RE2O3 reach 90% at 700~900℃. The results can supply a new method of RE2O3 preparation.

RE have been increasingly used in the field of chemical engineering, metallurgy, nuclear energy, optical, magnetic, luminescence and et al[1]. RE_2O_3 is a important product which is prepared by oxalic acid or ammonium acid carbonate precipitation in $RECl_3$ solution, and it is a main problem that the environment can be polluted by discharge of waste water containing NH_4^+ or $C_2O_4^{2-}$[2]. If the output of La_2O_3 is 4000 ton (If the output of REO is 120 thousand ton.), 6300 ton $(NH_4)_2CO_3$ are used, and 1600 ton CO_2 and 4300 ton NH^{4+} are discharged. For those problems, the methods of coprecipitation and low-temperature combustion synthesis are studied, but the waste water also exists for organic precipitant addition [3, 4].

Metals oxide preparation using metals chloridate pyrolysis was used to recovery HCl on steel industry [5-7], and this method is also used to prepare Al_2O_3, TiO_2, MgO and et al [8-10]. The preparation of CeO_2, La_2O_3, Nd_2O_3 et al can also be used this method, but the agents as acetic acid, citric acid, mixed acid and et al should be added in $RECl_3$ solution[11-13]. The study of the preparation of La_2O_3 by $LaCl_3$ without agent is less reported. The thermodynamic feasibility of RE2O3 preparation by RECl3, and the effect parameters of temperature, time on the conversion ratio of RE2O3 are studied. The conversion ratio of RE2O3 reach 90% at 700~900℃. The results can supply a new method of RE2O3 preparation.

Experimental

Materials

$RECl_3$ crystal was prepared by $RECl_3$ solution evaporation. The oxyhydrogen gas was supplied by oxyhydrogen machine, and the fundamentals of this machine were water electrolysis.

Experimental Process

The schematic plan of experimental equipments was shown in figure 1. The experimental process was as follows: firstly, $RECl_3$ crystal was put in a crucible and pushed in alundum tube. Secondly, the different flux oxyhydrogen gas was enkindled, and the samples were calcined at different temperature. Finally, the crystal structures and the micro-pattern of the products were investigated by X-ray diffractometry (XRD, X'pert PRO DY2198) and scanning electron microscopy(SEM, SUPER35). The roasted temperature was determined by infrared temperature meter.

The content of Cl and La elements was tested by ICP, and the conversion ratio of RE_2O_3 (%) $=(C_{La}-C_{Cl}/3)/C_{La}$. Which C_{La} and C_{Cl} was the mole content of La and Cl in products.

Results and Discussion

Thermodynamics Analysis of Roasted Process

In order to further estimate the possibility of the reaction, the thermodynamic theory was used to calculate the standard Gibbs free energy change of RECl3 reacted to RE2O3. The relation equations of standard generating Gibbs free energy and temperature $\Delta G_T^\theta = \Delta H_T^\theta - \Delta S_T^\theta \times T$ of the products and the reactants, where In the equations, ΔH_f^θ and ΔS_f^θ are the standard phase change heat and standard mol entropy at 298K, and a, b, c, and d are temperature coefficients of heat capacity.

$$\Delta H_T^\theta = \Delta H_f^\theta + a(T-298) + \frac{1}{2}\times 10^{-3} b\left(T^2 - 298^2\right) - 10^5 c\left(\frac{1}{T} - \frac{1}{298}\right) + \frac{1}{3}\times 10^{-6} d\left(T^3 - 298^3\right) \tag{1}$$

$$\Delta S_T^\theta = \Delta S_f^\theta + a(\ln T - \ln 298) + 10^{-3} b(T-298) - \frac{1}{2}\times 10^5 c\left(\frac{1}{T^2} - \frac{1}{298^2}\right) + \frac{1}{2}\times 10^{-6} d\left(T^2 - 298^2\right) \tag{2}$$

The relations of standard Gibbs free energy change and temperature were calculated and shown in table I.

The results are shown that chemical reaction free energy of chloride of La, Ce, Pr and Nd which have the water of crystallization, and comparing with La, Ce, Pr and Nd, and know that the temperature of direct roasting reaction have the order that $CeCl_3 < PrCl_3 < NdCl_3 < LaCl_3$.

Table I. The Function of ΔG^0 and T of the Reaction of Rare Earth Chloride and Water

No.	Reaction equations	ΔG^0 / J•mol^{-1}	Temperature Range / K	$T_{\Delta G0=0}$/K
1	$2LaCl_3(s)+3H_2O(g) =La_2O_3(s)+6HCl(g)$	398.7-0.41T	298-1128	980
2	$2LaCl_3(l)+3H_2O(g) =La_2O_3(s)+6HCl(g)$	200.1-0.18T	1128-2085	1128
3	$2CeCl_3(s)+3H_2O(g)+1/2O_2 (g)=2CeO_2(s)+6HCl(g)$	-37.4-0.22T	298-1090	Easy reaction
4	$2CeCl_3(l)+3H_2O(g)+1/2O_2 (g)=2CeO_2(s)+6HCl(g)$	-128.0-0.13T	1090-1300	1090
5	$2PrCl_3(s)+3H_2O(g)+1/2O_2(g) =2PrO_2(s)+6HCl(g)$	146.0-0.29T	298-1059	510
6	$2PrCl_3(l)+3H_2O(g)+1/2O_2(g) =2PrO_2(s)+6HCl(g)$	9.73-0.11T	1059-1300	1059
75	$2NdCl_3(s)+3H_2O(g)=Nd_2O_3(s)+6HCl(g)$	338.8-0.40T	298-1032	850
8	$2NdCl_3(l)+3H_2O(g)=Nd_2O_3(s)+6HCl(g)$	227.1-0.26T	1032-1947	1032

The Parameters of RE2O3 Conversion Ratio

When we study the parameters of RE2O3 conversion ratio, the CeCl3 is selected. The effect of temperature and concentration of CeCl3 solution on CeO2 conversion ratio are shown in figure 1 to 2.

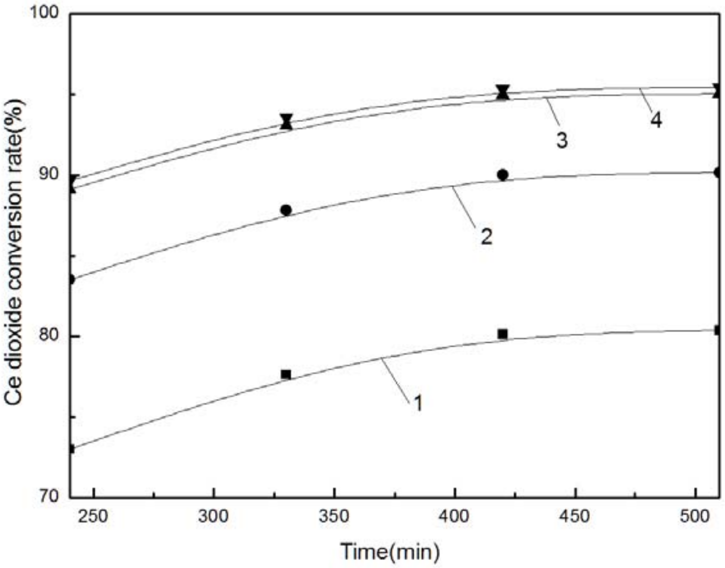

1-750℃，2-850℃，3-950℃，4-971.5℃

Figure 1. Temperature on the influence of cerium dioxide conversion.

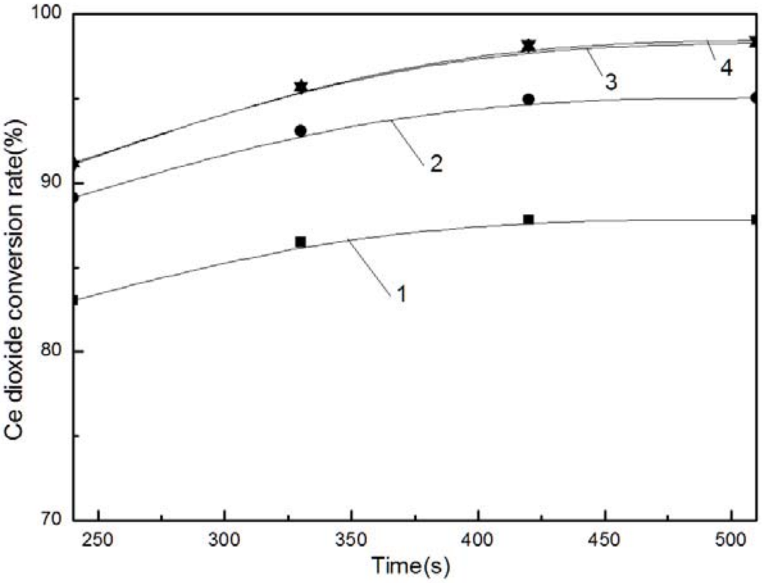

1-130 g/L，2-200 g/L，3-270 g/L，4-278.75 g/L

Figure 2. Ce dioxide concentration conversion relation graph.

The optimal condition of Roasting temperature for 950℃ and liquid concentration for 270g/L the conversion ratio of CeO_2 is 98.4%.

The Analysis on Phase of Products

XRD analysis and SEM images of the products are shown in figure 3 and 4, and it demonstrate that the percent conversion of CeO_2 products will get higher at the optimal condition baking

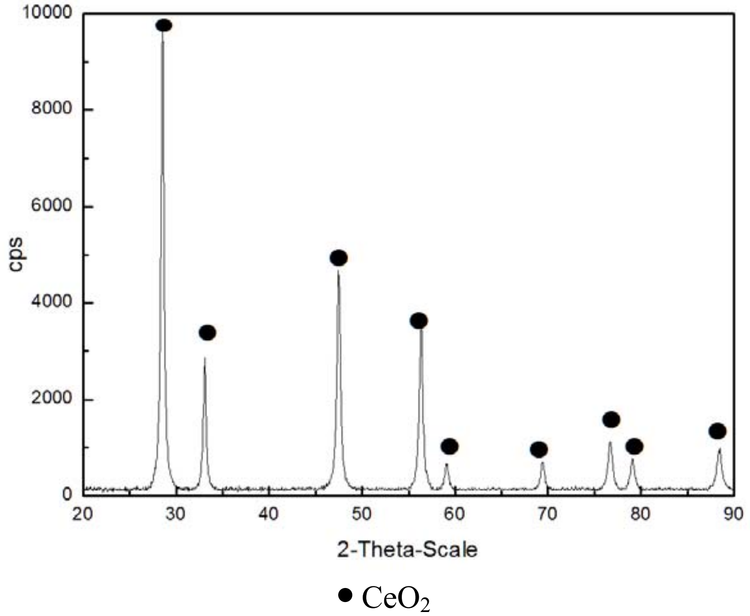

Figure 3. X ray diffraction of products.

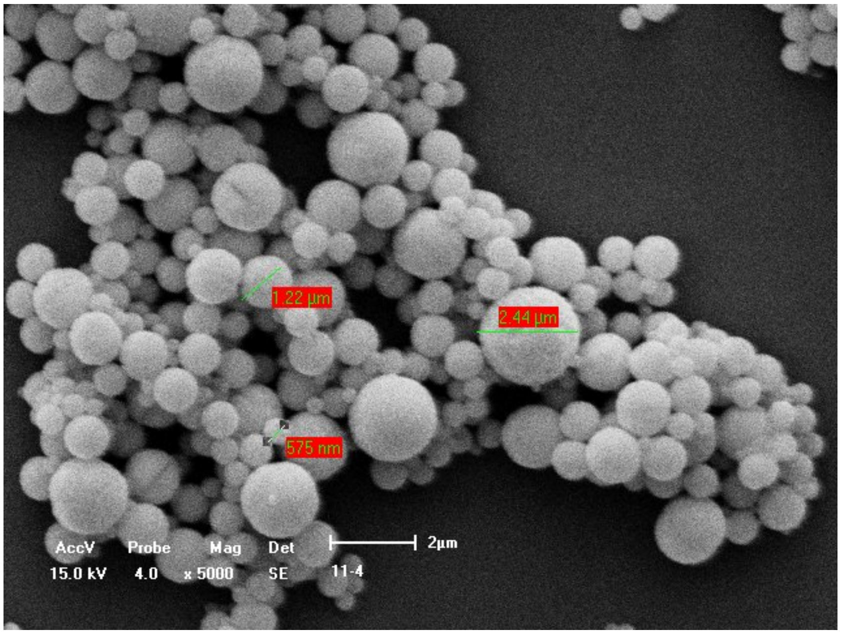

Figure 4. SEM of products.

conditions- roasting temperature for 950℃ and liquid concentration for 270g/L , when the baking conditions cannot meet the optimal condition , the higher the temperature, feeding speed and material liquid concentration are the higher the conversion rate and quality of products.

Conclusion

Calculated the chemical reaction free energy of chloride of La, Ce, Pr and Nd which have the water of crystallization, and comparing with La, Ce, Pr and Nd, and know that the temperature of direct roasting reaction have the order that $CeCl_3<PrCl_3<NdCl_3<LaCl_3$. The free energy of liquid chloride is smaller than solid chloride. It have been demonstrated from that the conditions of thermokinetics would valid if dynamic roasting way of rare earth chloride actualized.

When Roasting temperature is 950℃，liquid concentration is 270g/L, the conversion rate of CeO_2 can amount to 98.4%.

Acknowledgement

The study is support by Key Projects in the National Science & Technology Pillar Program during the Eleventh Five-year Plan Period(2012BAE01B02), Project supported by the National Natural Science Foundation of China (51104040, 51274060).

Reference

1. Xu Guangxian. Rare Earths[M] Beijing: Beijing: Metallurgical Industry Press, 1995.

2. Wu Wenyuan. Rare Earths Metallurgy[M]. Beijing: Chemical Industry Press, 2005.

3. Zhong Liang, Zheng Yuwen. New Preparation Method of Superfine Lanthanum Oxide[J]. Guangdong Chemical Industry, 2010, 37(12): 41-42.

4. Zhang Hiarei, Chu Gang, Zhou Li, Zeng Liying. Preparation of Nanometer Lanthanum Oxide Powder by Low-temperature Combustion Synthesis Method[J]. Journal of Synthetic, 2010, 39(5): 1286-1291.

5. Hong Yuntao, Qiao Liang, Liu Xinhua. Application of Ruthner-spray hydrochloric acid regeneration technology in cold rolling[J]. Modem Chemical Industry, 2005，25(1):48-50.

6. Zhou Haiping, Qiu Zumin, Qiu Junming. Progress in preparation of iron oxide by using three-wastes[J]. Chemical Industry and Engineering Progress, 2007, 26(2): 173-179.

7. Amiri M. C. Characterization of iron oxide generated in ruthner plant of pickling unit in moba rakeh steel complex[J]. Mater Sci Technol, 2003, 19(6): 596-598.

8. Wang Yanhua. Research on Recovery of Synthetic Rutile Leaching Liquor[J]. Iron Steel Vanadium Titanium, 2008, 29(3): 35-40.

9. Pramod S. Patil. Versatility of chemical spray pyrolysis technique[J]. Materials Chemistry and Physics, 1999, 59: 185-198.

10. Tsunenori Watanabe, Yoshihisa Miki, Takeo Masuda, Hiroshi Deguchi, Hiroyoshi Kanai, Saburo Hosokawa, Kenji Wada, Masashi Inoue. Synthesis of γ- Ga_2O_3 - Al_2O_3 solid solutions by spray pyrolysis method[J]. Ceramics International, 2011, 37: 3183-3192.

11. Hee Sang Kang, Jong Rak Sohn, Yun Chan Kang, Kyeong Youl Jung, Seung Bin Park.The characteristics of nano-sized Gd-doped CeO_2 particles prepared by spray pyrolysis [J]. Journal of Alloys and Compounds, 2005, 398: 240-244.

12. Lin Liu, Gap-Yong Kim, Andrew C. Hillier, Abhijit Chandra. Microstructural and electrochemical impedance study of nickel–Ce0.9Gd0.1O1.95 anodes for solid oxide fuel cells fabricated by ultrasonic spray pyrolysis[J]. Journal of Power Sources, 2011, 196: 3026-3032.

13. Xu Huarui, Gao Wei, He Bin, Gu Hongchen, Yuan Weikang. Synthesis of Solid Spherical CeO2Particles by Spray Reaction[J]. Chinese Rare Earths, 1999, 20(6): 29-31.

STUDY ON THE DECOMPOSITION OF MONAZITE AND BASTNAESITE BY $Ca(OH)_2$-NaOH

Bian Xue, Xue Shoufeng, Jia Zhongshuai and Wu Wenyuan

School of Materials & Metallurgy,
Northeastern University, Shenyang, Liaoning 110004, China

Keywords: Mixed Rare Earth Concentrate; Roasting; $Ca(OH)_2$-NaOH

Abstract

The decomposed process of bastnaesite, monazite and mixed rare earth concentrate in $Ca(OH)_2$-NaOH is studied by means of TG-DTA method. The relationship among decomposition ratio, roasting temperature, and $Ca(OH)_2$-NaOH addition is studied by the quadratic regression orthogonal analysis, and then the regression equation is obtained. when the temperature is 630℃, the quantity of $Ca(OH)_2$ is 23%, the quantity of NaOH is 15% , and 30 min, the decomposition rate of rare earth concentrate is 98.1%.

The mixed rare earth concentrate is the paragenesis mineral that is composed of bastnaeaite and monazite (mixed concentrate is shortened form of mixed rare earth concentrate in the following paper), and it is important resource to extract the element of rare earth. The constituent of this mineral is complex, and it is hard to treat. Now, the widely used decomposition method has sulfuric acid decomposition, but this method releases the off-gases of SO_2 and HF, and the off-gases are hard to recycle respectively. NaOH also can decompose the mineral, but firstly the calcium should be removed in this process. Used this method to roast the mixed concentrate ore, the by-products such as NaF and Na_3PO_4 should be removed by wash, and producing waste water also influences the environment. In resent years, it is report that the methods of Na_2CO_3 roasting[1-3], NH_4Cl roasting[4], CaO roasting[5,6] and machine ball milling[7,8] can all make fluorine exist in solid phase product, and these methods can restrain the waste gas that contains fluorine. In this paper, in the basis of studying mixed concentrate decomposed by CaO-NaCl[5,9,10], $Ca(OH)_2$-NaOH is selected to decompose mixed concentrate. The purpose is to reducing roasting temperature, and makes the method approach the request of commercial process, and supplies the theoretical supposing for clean decomposition of mixed concentrate.

Experiment

Experiment Materials

The mixed concentrate is supplied by concentration plant of steel-industry in Baotou. The granularity of mineral is below 0.043mm, and the color is grey, and chemical constitution is arrayed in Table I, and the other reagents in the experiment are analytically pure.

Table I. The Constitutions of Mixed Concentrate

Constitutions	RExOy	CaO	SiO_2	T_{Fe}	P_2O_5	F
Content/%（mass）	51.66	13.15	1.38	2.46	8.74	9.83

Experiment Process

According to scheme of regression-orthogonal designing, mixed concentrate, $Ca(OH)_2$-NaOH are mixed in mortar. Then the steel-boat loaded mixed ore, which is put into oven, and roasts one hour. BT119 temperature controlling device is used to control temperature, and accuracy standard is 0.2 levels. In the determination process of decomposition ratio, the decomposition ratio of rare earth concentrate is instead by the oxidize ratio of Ce. Document[4] considers that Ce is trivalent in rare earth ore, so if Ce^{4+} is determined, it must be decomposed outgrowth. The content of Ce^{4+} is determined by ferrous ammonium sulfate calibration. Before determination, Ce^{3+} is oxidized to Ce^{4+} by perchloric acid. The calculation formula is $Ce^{4+}/\Sigma(Ce^{3+}+Ce^{4+})$=ratio decomposition(%). SDTQ600 thermal analyzer is used in differential thermal analysis, and the atmosphere is static nitrogen, and warming-up speed is 10℃/min, and the range of temperature is from room-temperature to 900℃. The roasted products are analyzed by mean of XRD.

Regression-orthogonal Designing

Temperature, $Ca(OH)_2$-NaOH addition and roasting time are selected as the studying object. Table II is encode table of four factors and twice regression orthogonal experiment, at the same place, $\gamma=1.414$. The regression orthogonal experiment schemes and the decomposition ratio results are arrayed in Table III. The regression equation is obtained with the results of table III calculated by mathematical statistics.

$$Y=73.583+2.559825x_1+4.513063x_2+9.995201x_3+3.563765x_4-0.8875x_1x_2-0.325x_1x_3-0.15x_1x_4+0.125x_2x_3-0.2x_2x_4-0.2125x_3x_4-0.9575(x_1^2-0.8)+1.2425(x_2^2-0.8)+2.13625(x_3^2-0.8)-2.3075(x_4^2-0.8) \tag{1}$$

There into, $x_1=Ca(OH)_2$ addition(%)；x_2=NaOH addition (%)；x_3=Temperature(℃)；x_4=time(min)F check of regression equation is as follows:

$S_{total}=3701.898$

$S_{regression}=2905.384$

$S_{remain}=S_{total}-S_{regression}=796.514$

$F=(S_{regression}/14)/(S_{remain}/10)=2.605$

$F=2.605>F^{(0.05)}_{[14,10]}=2.6$，Equation is conspicuous at 0.1 level. It is shown that the effect of experiment factors on decomposition of mixed concentrate can be described by this equation.

Table II. Encode of Factors

Factors	$Ca(OH)_2$ （wt%）	NaOH （wt%）	Temperature （℃）	Time （min）
Numbers	X_1	X_2	X_3	X_4
Base levels（0）	20	10	500	30
Change ranges（Δ_j）	7.07	7.07	106.08	14.14
Up levels（+1）	22.93	12.93	543.92	35.86
Down levels（-1）	17.07	7.07	456.08	24.14
Up asterisk arm（+γ）	30	20	650	50
Down asterisk arm（-γ）	10	0	350	10

Table III. The Results of Experiments

NO.	1	2	3	4	5	6	7	8	9	10	11	12	13
Decomposition ratio（%）	77.5	74.2	62.8	59.0	71.0	67.3	58.0	53.1	76.3	73.0	61.7	56.8	67.7
NO.	14	15	16	17	18	19	20	21	22	23	24	25	
Decomposition ratio（%）	62.8	52.0	47.0	70.0	51.9	75.2	55.5	98.1	38.7	71.5	45.0	66.0	

Results and Discussion

The Heat Decomposing Process of Mixed Concentrate

In order to study the effect of $Ca(OH)_2$-NaOH in the roasting process, TG-DTA experiments are performed in different mixed ratios. The text results are shown in Figure 1. The XRD analysis are shown in Figure 2.

According to the test results from 25℃ to 900℃, the following conclusions are obtained:

(1) In the 350-480℃ temperature range, there presents the decomposition reaction of Banstnaesite and oxidation reaction of Ce:

$$CeCO_3F=CeOF+CO_2\uparrow \tag{2}$$

$$2CeOF+Ca(OH)_2+1/2O_2=CaF_2+2CeO_2+H_2O\uparrow \tag{3}$$

(2) at 500-660℃, $Ca(OH)_2$ has ability to decompose of monazite and rare earth oxyfluoride, and the reaction is as follows:

$$2CePO_4+3Ca(OH)_2+1/2O_2=Ca_3(PO_4)_2+2CeO_2+3H_2O\uparrow \tag{4}$$

$$CaF_2+3Ca_3(PO_4)_2= 2Ca_5(PO_4)_3F\downarrow \qquad (5)$$

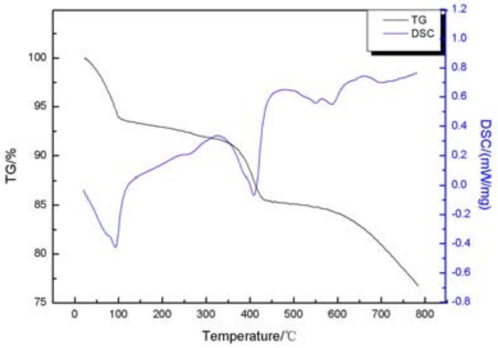

Figure 1. The TG-DSC curve.

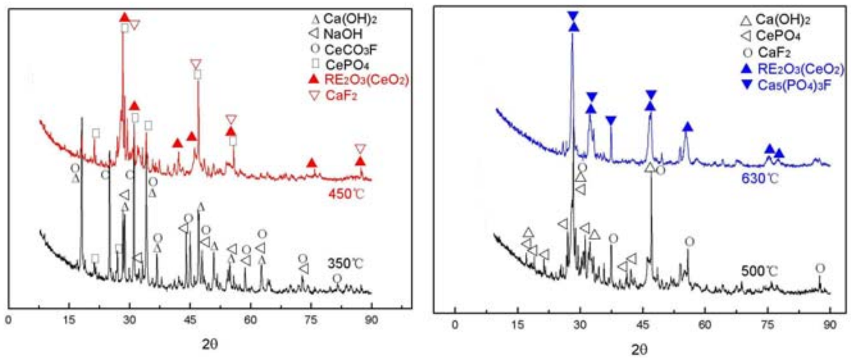

Figure 2. X ray diffraction of different temperature.

Effect of Parameters on Decomposition Ratio

The effect of parameters on decomposition ratio are studied, and the results are shown in figure 3 to 5.

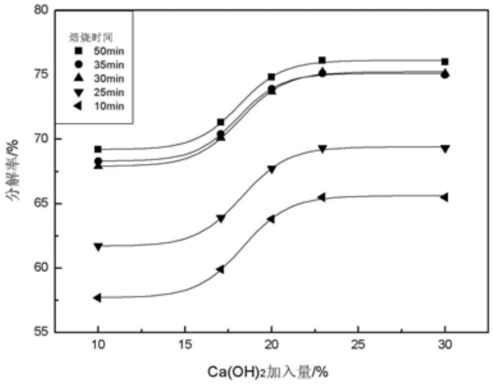

Figure 3. The scheme of relationships between rare earth concentrate decomposition rate and weight of $Ca(OH)_2$.

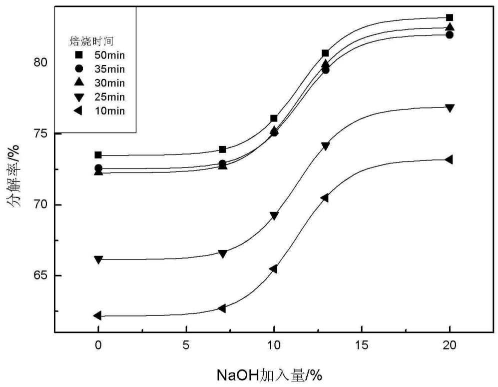

图 4 NaOH-分解率关系图

Figure 4. The scheme of relationships between rare earth concentrate decomposition rate and weight of NaOH.

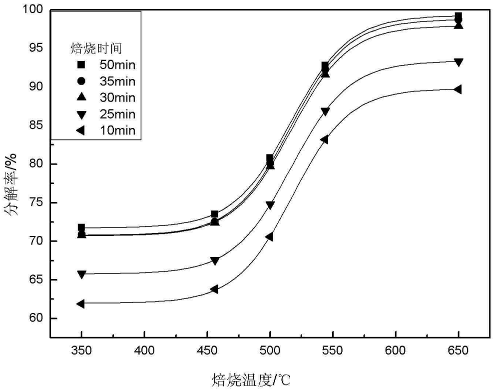

图 5 温度-分解率关系图

Figure 5. The scheme of relationships between rare earth concentrate decomposition rate and temperature.

The purpose of roasted mixed concentrate by $Ca(OH)_2$-NaOH is further reducing the roasting temperature. Synthesized above analysis, under the precondition of the decomposition ratio above 98%, the conditions that roasting temperature is 630℃, and Ca(OH)2 addition is 23%, and NaOH is 15%, and roasting time is 30min are optimum.

Conclusions

1. The process of the mixed rare earth concentrate decomposed by $Ca(OH)_2$-NaOH is studied by means of TG-DTA method. The results show that after adding of $Ca(OH)_2$-NaOH, the decomposition process of the mixed rare earth concentrate is divided into two stages. Firstly, $REFCO_3$ is decomposed and cerium oxyfluoride is decomposed by CaO and cerium is oxidized at 350-480℃, secondly, monazite are decomposed by CaO and CaF_2 in minerals at 500-660℃.

2. The relationship among decomposition ratio of mixed rare earth concentrate, roasting

temperature, $Ca(OH)_2$-NaOH addition, and roasting time is studied by the quadratic regression orthogonal analysis, and then the regression equation is obtained. The optimization conditions are confirmed as that roasting temperature is 630℃, and $Ca(OH)_2$ addition is 23%, and NaOH is 15%, and roasting time is 30min, and the decomposition ratio is 98.1%.

Acknowledgement

The study is support by National Basic Research Program of China (973Program) (2012CBA01205), Key Projects in the National Science & Technology Pillar Program during the Eleventh Five-year Plan Period(2012BAE01B02), Project supported by the National Natural Science Foundation of China (51104040, 51274060).

References

1. Zhang Guocheng, Huang Xiaowei. Comment of Smelting Technology of Bastnaesite[J*], Rare Metals*, 1997, 21 (3):193~199.

2. Qiao Jun, Liu Zhaogang, Ma Ying ect. Study on Roast Reaction Kinetics of Baotou Concentrate of Rare Earths[J*]. Journal of Rare Earths*, 1999, 17(1): 86-89.

3. Wu Wenyuan et al. Study on Decomposition Reaction of Monazite and Bastnaesite Mixed Rare Earth with Sodium Carbonate[J]. *Journal of Rare Earths*, 2001, 19 (Supplement): 61~64.

4. Shi Wenzhong, et al. Recovery of Re from Rare Earth Concentrate with Ammonium Chloride Roasting[J*]. Journal of Henan University* (Natural Science), 2002, (4): 45~49.

5. Chen Xudong, Wu Wenyuan, Sun Shuchen, et al. Study of Roasting Decomposition of Mixed Rare Earth Concentrate in CaO-NaCl[J]. *Chinese Rare Earths*, 2004, (25): 32-35.

6. Yu Qing-chun. Technological Research on Roast of Baotou Rare Earth Concentrate Added by Calcium Oxide[J]. *Chinese Rare Earths*, 2002, 23(2): 13-15.

7. Jin Pingzhang, Frank J. Lincoln. The decomposition of monazite by machemical milling with calcium oxide and calcium chloride[J]. *Journal of Alloys and Compounds*, 1994, 205: 69~75.

8. Sun Peimei, Li Honggui, Li Yunjiao et al. New Technology on Decomposition of Monazite by Mechanical Activation and Caustic Decomposition[J]. *J.Cent.Southuniv.Technol*, 1998, 18(1): 36-38.

9. Wu Wen-yuan, Hu Guang-yong, Sun Shuchen et al. Decomposition Reaction of Mixed Rare Earth Concentrate and Roasted with CaO and NaCl[J]. *Journal of Rare Earths*, 2004, (2): 210-214.

10. Xu Guangxian. Rare Earth, 2nd version[M]. *Beijing: Metallurgical Industry Press*, 1995, 382.

Rare Earth Element Separation

ADVANCES IN SOLVENT EXTRACTION AND SEPARATION OF RARE EARTHS

*Deqian Li, Yan Bai, Xiaoqi Sun, and Shuzhen Liu

State Key Lab of Rare Earth Resource Utilization, Changchun Institute of Applied Chemistry
Chinese Academy of Sciences, Changchun 130022, China
*ldq@ciac.jl.cn

Keywords: Rare Earths, Solvent Extraction, Separation, P507, HAB

Abstract

This paper introduces briefly what our lab has been studying on new extraction systems and separation of REs in recent years, which includes:

1. New systems superior in separating heavy REs with P507;
    (1) The solvent extraction of rare earths from chloride solution has been investigated using mixtures of P507 and P204, Cyanex 272, Cyanex 302, and Cyanex 301.
    (2) P507-isooctanol (ROH)-REs new system.
2. Two-solvent (HAB) extracting system that is superior in separating Y(III) to HA.

Introduction

The rare earth separation process exploited by our laboratory using HEHEHP (P507) and naphthenic acid (HA) solvent extraction has been applied widely in China. This process provides industrial production of all the individual RE with purities of up to 99.99%. However, the industrial practice indicates that there are some problems in the process [1]. Consequently to explore some new extractants or extraction systems superior to P507 and naphthenic acid has been interesting for many researchers.

This paper introduces briefly what our laboratory has been studying on new extraction systems and separation of REs in recent years.

Results and Discussion

Superior New System for Separating Heavy REs with P507

Up to now an extraction system generally superior to P507 has not been discovered. However, the extracting and stripping acidities of HEHEHP remain high, and it is still difficult to strip the heavy rare earths.

New system excelled P507 separates heavy REs has four routes:

(1) Keep P507 structure, augmenting steric hindrance of alkyl chain such as PT-2 [2]. Figure 1 represented isopropylphosphinic acid 1-hexyl-4-ethyloctyl ester (HHEOIPP, PT-2) with high steric hindrance, pKa=5.49, separation selectivity of adjacent heavy REs(III) exceeds P507.

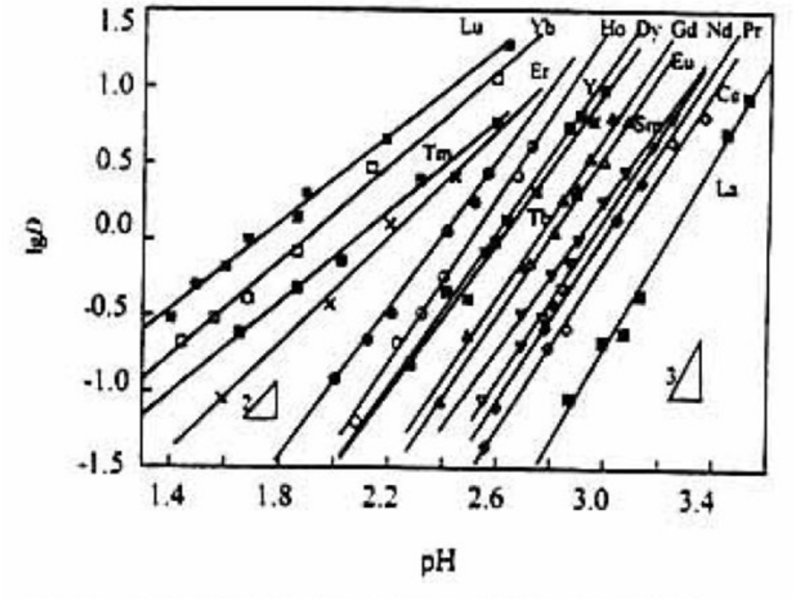

Figure 1. The effect of pH on the extraction of rare-earth ions from chloride solution by PT-2.

(2) Change P507 structure, with two alkyl groups attached to phosphorus atom such as Cyanex 272.[3] Bis(2,4,4-trimethylpentyl)phosphinic acid (Cyanex 272, HBTMPP), is a high steric hindrance di-alkyl phosphinic acid, pKa=6.37, average separation factors β of adjacent RE(III)=3.24 as shown in Figure 2.

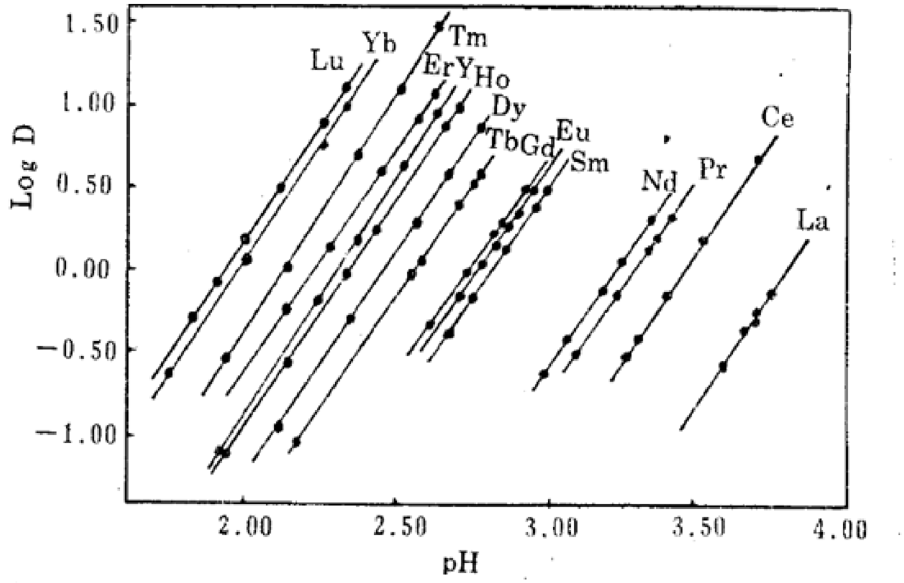

Figure 2. Cyanex 272 – HCl - REs extraction curves.

Separation selectivity and stripping capability for heavy REs decreases in the order: C272 > PT-2 > P507/ C272 > P507 > P204.

(3) Extracting REs using mixtures (HDP) [4].

The solvent extraction of REs from chloride solution has been investigated using mixtures (HDP) of P507 and P204, PT-2, Cyanex272 (C272), C302, C301. Extractability results are summarized in Figure 3, which shows the $pH_{1/2}$ (the pH where extraction is 50%) against the lanthanide atomic number.

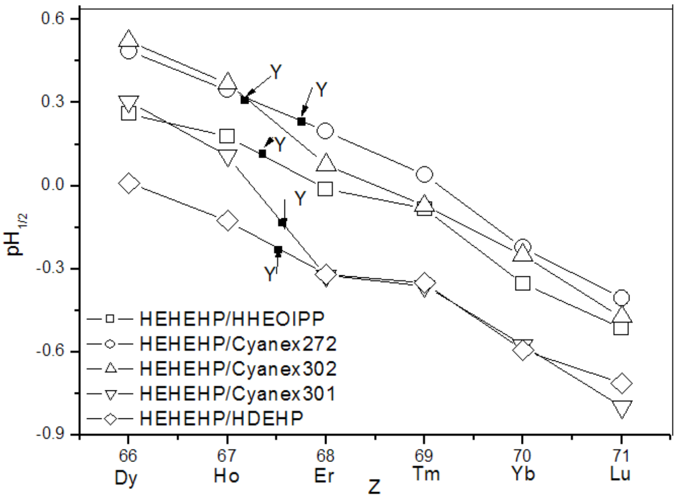

Figure 3. The relationship between the values of $pH_{1/2}$ and lanthanide atomic number *Z*.

Extractability decreases in the order: P507/P204 > P507/C301 > P507/PT-2 > P507/C302 > P507/C272. Stripping data are illustrated in Figure 4.

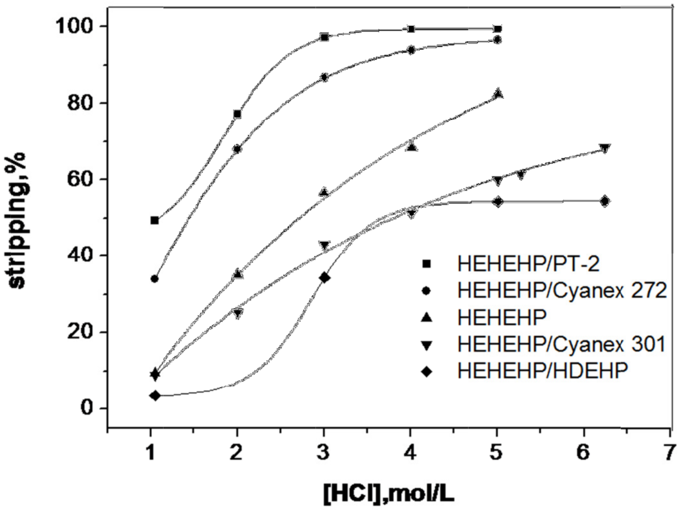

Figure 4. Stripping capability of P507/PT-2, P507/C272, P507, P507/C301 and P507/P204.

Results show that the extractability of the selected extractants for REs decreases in the order: P507/P204 > P507/C301 > P507/PT-2 > P507/C302 > P507/C272, and the value of the $pH_{1/2}$ decreases across the series Dy to Lu. It is interesting to note that these mixtures have higher selectivity and hence potential for commercial application, P507/C272 has been applied to separate heavy REs.

(4) P507-iso-octanol (ROH)-REs new system [5].

Recently, it was discovered by our team that P507 containing iso-octanol as modifier could not only improve the stripping ratio, but also heightened the selectivity among some adjacent REs. This new extraction system is superior to P507 for separating heavy REs and it may be applied in industrial practices.

ROH can form hydrogen bond with P507, thereby reducing extractability and increasing separation selectivity of heavy REs. Table I gives comparative separation factors for P507 and the new system. Stripping data are provided in Figure 5.

Table I. Separation Factors β of P507-isooctanol (ROH)-REs New System

System	$\beta_{Tm/Er}$	$\beta_{Yb/Tm}$	$\beta_{Lu/Yb}$
P507	3.64	2.40	1.81
P507+10%ROH	4.31	3.55	1.78
P507+20%ROH	5.49	3.18	1.67
P507+30%R0H	—	2.9	1.74

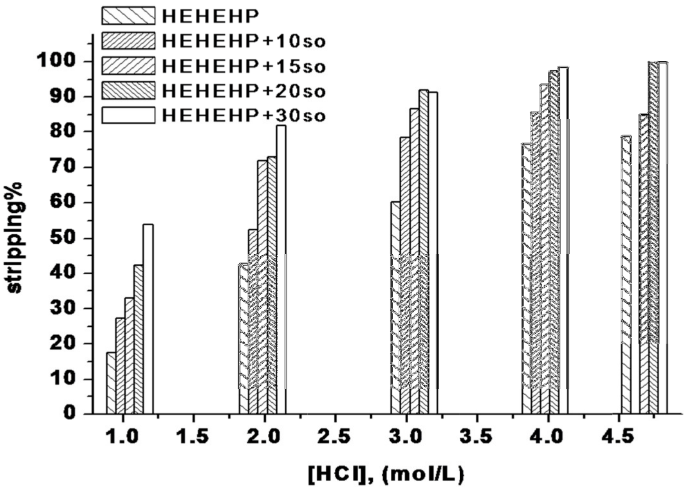

Figure 5. Stripping Yb with HCl in P507-ROH.

Figure 5 shows that, for example, 3.0M HCl gives 60% stripping from P507 but 92% from P507-20%ROH.

Two-solvent Extracting System (HAB) Superior in Separating Y(lll) with HA

Sec-octylphenoxy acetic acid (CA-12) is a kind of organic carboxylic acid extractant developed by SIOC, CAS. Comparing with HA, CA-12 has several advantages including stable composition, slow solubility, and resistance to emulsification during extraction.

The extractability of CA-12 for Y was found to be the lowest in all REs and Y was easier to be separated from light and middle RE than HA. However, the separation of Y from heavy REs (HRE) is very difficult using CA-12. In order to obtain highly purified Y, a novel system was developed by our lab for separating yttrium. This system was named as HAB two-solvent extracting system. In the HAB system, the separation coefficients between yttrium and other REs are greater than 2 as indicated in Table II

Table II. The Distribution Ratio (D) and Separation Coefficients (β) of HRE in CA12-TBP and HAB System

System	D						β				
	Ho	Y	Er	Tm	Yb	Lu	Ho/Y	Er/Y	Tm/Y	Yb/Y	Lu/Y
CA12-TBP	0.883	0.507	0.851	0.685	0.642	0.546	1.74	1.68	1.35	1.27	1.08
CA12-P204-TBP	1.28	0.79	1.25	1.2	1.4	1.4	1.62	1.58	1.52	1.77	1.77
CA12-P507-TBP	1.21	0.808	1.35	1.72	3.1	3.98	1.5	1.66	2.12	3.84	5.17
CA12-C272-TBP	1.11	0.775	1.31	1.96	4.01	5.13	1.43	1.69	2.53	5.17	6.62

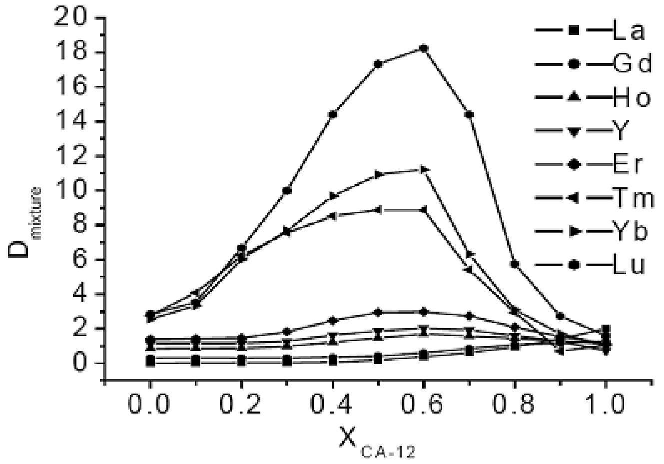

Figure 6. Synergistic extraction of REs with CA12-C272 [7].

The Synergistic extractability decreases in the order: Lu >Yb >Tm >Er >Y as was expected.

Separation processes for yttrium using CA12-TBP and HAB (CA12-C272) were compared [6] and as defined in Table III and Figure 7 with results shown in Table IV.

Table III. Parameters of Process in Fractional Extraction Simulation
Y2O3 /REO= 67.4% in Feed

System	Organic phase	Feed	Scrub acid
CA12-TBP	0.70M CA12 and 15% TBP, saponification rate=90%	1. 0 M RECl3	3.0M HCl
HAB-TBP	0.68M CA12, 0.12M C272 and 15% TBP, saponification rate=90%	1.1 RECl3	3.0M HCl

Table IV. Y_2O_3 Products from CA12 and HAB Circuits

Ingredients	CA12, %	HAB, %
Y_2O_3	99.47	99.94
La_2O_3	0. 026	<0.001
CeO_2	0. 022	0.002
Pr_6O_{11}	<0. 002	0.002
Nd_2O_3	0. 003	0.008
Sm_2O_3	0. 010	<0.001
Eu_2O_3	<0. 002	<0.001
Gd_2O_3	<0. 002	<0.001
Tb_4O_7	<0. 002	<0.001
Dy_2O_3	0. 051	<0.001
Ho_2O_3	0. 068	0.009
Er_2O_3	0.130	0.032
Tm_2O_3	0. 024	<0.001
Yb_2O_3	0.170	<0.001
Lu_2O_3	0. 016	<0.001

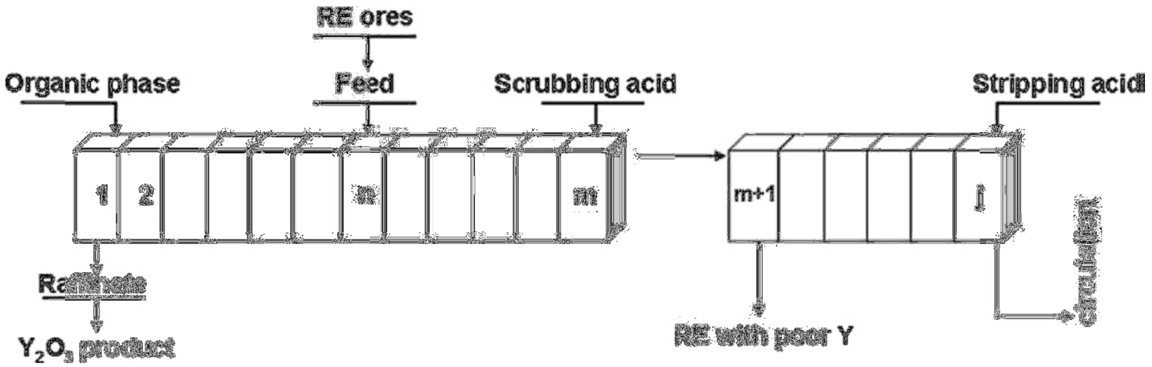

Figure 7. Y separation process using HAB.

Comparing the Y_2O_3 products from the CA12 system and HAB system, as shown in Table IV, Y_2O_3 product with a purity of 99.94% was obtained by HAB extraction from Ion-absorbed-type rare earth (IATRE) minerals which was higher than by CA12 extraction. The total recovery of Y was about 95%.

Conclusion

This paper introduces briefly what our laboratory has been studying on new extraction systems and separation of REs in recent years, which includes:

1. New system superior in separating heavy REs than P507;

2. HAB two-solvent extracting system superior in separating Y(lll) than HA.

A Y separation process using HAB gave a purity of 99.94% and total recovery of about 95% from IATRE minerals, which was higher than obtained by CA12 extraction.

Acknowledgements

The project was supported by the State Key Project of the Foundation Research (2004CB719506).

References

1. Li, D.Q., “Chemical Engineering Problems in Hydrometallurgical Industry of Rare Earths”. *Progress in Chemistry,* 7(3) (1995), 209-213.

2. Lu, J., S.L. Meng, D.Q. Li and W.Z. Ye, “Extraction of Lanthanides with 1-hexyl-4-ethyloctyl Isopropylphosphonic Acid”. *Journal of the Chinese Rare earth*, 17 (Spec. Issue) (1999), 72-74.

3. Zhang, X.F., and D.Q. Li, “Extraction of Rare Earths (lll) With Cyanex272”. *Chinese Journal of Applied Chemistry*, 10(4) (1993), 72-74.

4. Wang, X.L., W. Li, S.L. Meng and D.Q. Li, “The Extraction of Rare Earths using Mixtures

of Acidic Phosphorus-based Reagents or Their Thio-analogues“, *J Chem Technol Biotechnol* , 81: (2006), 761-766.

5. Wang, X.L., “The Separation and Purification of Rare Earths in the Double Acidic Phosphorus-based Reagents System or Room Temperature Ionic Liquids System”. (Ph.D. thesis, Changchun Institute of Applied Chemistry, Chinese Academy of Sciences, 2008).

6. Wang, Y.L, W.P. Liao and D.Q. Li, “A Solvent Extraction Process with Mixture of CA12 and Cyanex 272 for the Preparation of High Purity Yttrium Oxide from Rare Earth Ore”, *Separation and Purification Technology*, 82(2011), 197-201.

7. Sun, X.B., J.M. Zhao, S.L. Meng and D.Q. Li, “Synergistic Extraction and Separation of Yttrium from Heavy Rare Earths using Mixture of Sec-octylphenoxy Acetic Acid and Bis (2,4,4-trimethylpentyl) Phosphinic Acid”, *Analytica Chimica Acta* 533 (2005), 83–88.

APPLICATION OF [A336][P507]/[P204] ON HIGH SELECTIVE EXTRACTION AND SEPARATION OF RARE EARTHS(III) FROM MECHANISM TO TECHNIQUES

J. Chen,* L. Guo, Y. Deng, D. Li

State Key Laboratory of Rare Earth Resources Utilization,
Changchun Institute of Applied Chemistry, Chinese Academy of Sciences,
5625 Renmin Street, Changchun 130022, PR China
*jchen@ciac.jl.cn

Keywords: Rare Earth, Ionic Liquid Extractant, Separation

Abstract

To address the concerns about the low utilization of rare earth resources and environmental pollutions, especially the tailings containing radioactive thorium in China, we invented a type of new ionic liquid extractants (ILE), such as [trialkylmethylammonium] [di-(2-ethylhexyl)orthophosphinate] ([A336][P507]) and [trialkylmethylammonium] [di-2-ethylhexylphosphinate] ([A336][P204]). A systematic investigation of ILEs on RE extraction was conducted. The effects of aqueous equilibrium pH, different acid medium (HNO3, HCl, H_2SO_4), extractant concentration, salting-out agent concentration, and stripping property were investigated. According to separation factors (β), [A336][P507] and [A336][P204] were suitable for the separation of heavy REs(III) in nitrate medium and the separation of light REs(III) in chloride medium. In nitrate medium the β values were Tm/Er (3.36), Yb/Tm (7.92) and Lu/Yb (8.55), respectively, when [A336][P204] was used as extractant. In chloride medium the β were Nd/Pr (9.52) and Sm/Nd (4.70), respectively, when [A336][P507] was used as extractant. The extraction mechanism for the high selectivity of RE(III) was discussed. Further improvement and potential application of [A336][P507] in RE(III) separation was recommended. Based on the separation results of ILE on RE extraction, a two-step decomposition of Bayan Obo RE concentrate process was developed to reduce the radioactive thorium waste residue and improve the utilization of RE, thorium, F and P values. A new separation technique of heavy RE from ion-absorbed RE deposits was also developed to meet the demand for heavy RE in laser crystals.

Introduction

Rare Earths (REs) are composed of scandium, yttrium, and the lanthanides. The similar configuration of RE(III) with small difference of 4f electron and radius makes the separation of REs, especially adjacent elements, very difficult. The worldwide REs resource estimate is about 88 million tons. About 27million tons of RE resources are in China accounting for 30.68% word reserve according to US Geological survey mineral commodity in 2009. The majority of the REs resources including Bayan Obo mixture mine, Bastnasite, and southern ion adsorption deposits are in Batou, Sichuan, Shandong and southern five provinces, especially Jiangxi. As one of the most important strategic and critical mineral resources, REs are important for luminescence, electronics, magnetism, catalysis, metallurgy and ceramic industry. As shown by Figure 1, the industrial value chain of REs can be extended from the upstream RE separation and purification, to the midstream of RE functional materials and the downstream of commercial products.

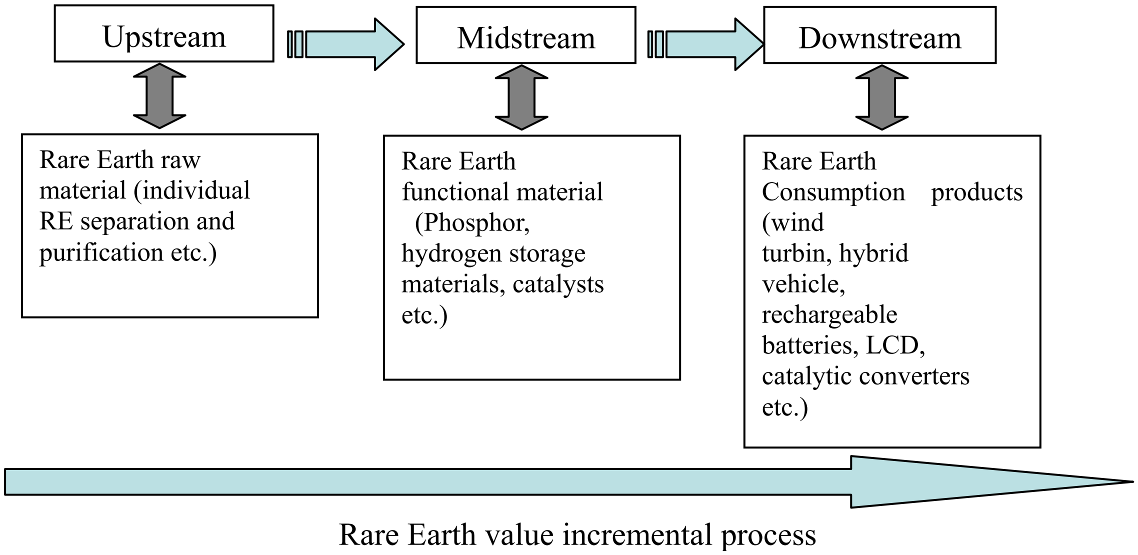

Figure 1. Complete rare earth industrial value chain demonstration.

RE Industry Environmental Pollution and Protection in China

REs separation industry in China has experienced fast growth in the last decades. Great progress and contributions have been made in China in countercurrent extraction theories, novel separation techniques, and industrial applications[1]. However, the environmental pollution issues associated with the RE resources excessive exploitation and metallurgy are becoming a great concerns in recent years. The concerns was endorsed by the white paper of Rare Earth Situation and Policy in China published in 2012 [2]. The environmental pollution occurs in almost every aspect of the RE processing industry in China. Examples include exhaust gas containing F and S, waste water containing high levels of NH3-N or salt, and tailings containing radioactive thorium in the processing of Bayan Obo mixture ore of bastnasite and monazite. As well, in the processing of ion adsorption RE deposits, $(NH_4)_2SO_4$ used in leaching has resulted in serious environmental damage to mountains, plants, and underground water. To protect the resources and environment and to reduce the amount of wastewater production, “Emission Standards of Pollutants from Rare Earths Industry (GB26451-2011)” was issued by China's Ministry of Environment Protection (MOP) in 2011 [3]. The emission standards of all the main pollutants are much morestrict, especially for the control of NH3-N, COD, heavy metals in water discharge. To meet the demand for REs and also environmental protection, more efficient green separation technologies for REs extraction and separation is great of interest in China.

Technology Background of Environmental Pollution

What are responsible for the environmental pollution and low efficiency of RE resources utilization include: (1) the release of NH_4^+ or Na^+ from the saponification of P507

(2-ethylhexyl phosphoric acid mono(2-ethylhexyl) ester) and acid extractant by $NH_3.H_2O$ or NaOH etc., (2) the low extractive efficiency of P507 for Ce(IV) with F and P together in H_2SO_4 system, the low separation factor β for part of adjacent RE elements such as Pr/Nd (1.55) and Yb/Lu(1.81), and the high stripping acid consumption (≥ 5mol/L) for partly stripping of heavy RE Tm/Yb/Lu, (3) the waste gas containing F and S and waste residue containing radioactive thorium due to the high temperature roasting of Bayan Obo RE concentrate using H_2SO_4, Therefore, more efficient decomposition method and/or successive extraction technologies will be important to the integral clean separation of Bayan Obo rare earth and south ion-adsorption rare earth.

Ionic Liquids Extractant Synthesis and Application

Ionic Liquids Extractant (ILE) Definition and Structure

The criteria of a high efficient extractant include: high efficiency and selectivity, high stability, low cost, low toxicity, low acid and base consumption, and no NH3-N and salts discharge, etc. The bifunctional ionic liquid extractants (Bif-ILEs, or ILEs) are composed of organic cation and anion. They represent a kind of environmentally friendly green solvents and are widely used as extractants in metal separation and extraction [4]. The neutral bifunctional ionic liquid extractants (Bif-ILEs) provide a new choice for REs separation.

This paper will focus on the application of [A336][P507]/[P204] on high selective extraction and separation of Rare Earths(III). The chemical structure of [A336][P507] is shown in Figure 2.

Ionic Liquids Extractant Design and Synthesis

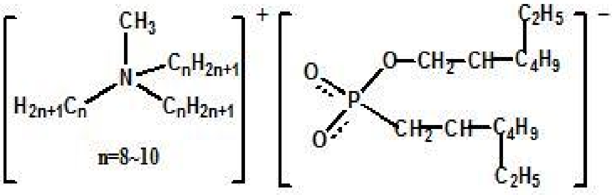

Figure 2. Chemical structure of [A336][P507].

The design of ILE originated from ionic liquid active pharmaceutical ingredient (IL-API) such as Lidocainium Docusate. Rogers et al. [5] first found that the physical, chemical, and biological properties of an IL-API drug can be controlled by changing the cation or anion of IL. This provided a new method and concept for the designing of a drug in comparison with covalent modification. We further apply the method on ionic liquid extractant (ILE), and synthesized the first ILE of [A336][P507] by neutralizing acidic organophosphorus extratant P507 using weak basic quaternary ammonium extractant Aliquat 336 [6]. Both P507 and Aliquat 336 are important industrial RE extractants. Especially P507 is the only extractant for individual REs separation except the separation of yttrium by another carboxylic acid extractant aphthenic acid in China.

Extraction Mechanism of ILE on RE(III)

The extraction mechanism of ILE, [A336][P507], for RE(III) is quite complicated [7]. It involves the extraction of inorganic acid of HNO_3 (equation 1) and the competitive neutral complex extraction of RE salt, $RE(NO_3)_3$, (equation 2).

$$[A336][P507]_{(O)} + H^+ + NO_3^- = [A336][P507] \cdot HNO_{3(O)} \tag{1}$$

$$3[A336][P507]_{(O)} + RE^{3+} + 3NO_3^- = RE(NO_3)_3 \cdot 3[A336][P507]_{(O)} \tag{2}$$

It should be noted that [A336][P507] is quite different from the simple mixing of Aliquat 336 and P507 [8]. The partition coefficience, D, in [A336][P507] is much higher than the mixture of Aliquat 336 and P507. In Table I, the comparison of [A336][P507] with other acidic and neutral extractants showed its excellent extraction ability[9]. The selectivity of ILE for the light RE in HNO_3 and the heavy RE in HCl in terms of separation factors β of Pr/Nd and Yb/Lu are 4 times of P507[10].

Table I. The Comparison of ILE with Available RE Extractant

Type	Extractants	Mechanism	Notes
Ionic liquid extractant	[A336][P507] [Tricaprylmethyl ammonium][di-(2-ethyl hexyl)orthophosphinate]	Neutral complex	No saponification, no NH3-N release; extraction ability and selectivity close to P507; lower acidity（pH range) for both extraction and stripping ; Lower water solubility.
Organic acid extractant	P507 2-ethylhexyl phosphoric acid	Cation exchange	Saponification; high acidity(3~4M) for extraction and stripping; HRE is hard to be stripped completely; good RE selectivity; NH3-N or salts released.
Weak Base extractant	Aliquat336 Tricaprylmethyl ammonium chloride	Anion Exchange	To enhance the RE separation by adding SCN- or DTPA complexing agent.
Neutral phosphate extractant	TBP Tributyl phosphate Cyanex923 Alkylated phophine oxide	Neutral complex Neutral complex	High extraction acidity; high water solubility. High extraction ability; high price.

[A336][P507] is a pure stable compound with single component. It is easily dissolved in organic solvent like kerosene. The partition coefficience, D, increases with the atom number from la(III) to Lu(III) in all acid medium of HNO_3, HCl, and H_2SO_4. [A336][P507] shows high efficiency and selectivity for the RE(III) extraction in all HNO_3, HCl, and H_2SO_4 systems. The extraction ability of RE(III) in different acidic media follows the order of: HNO_3>HCl> H_2SO_4. This is consistent with the anion hydration energy: ($\Delta G_{NO3^-}°$= -314 kJ/mol, $\Delta G_{Cl^-}°$= -340 kJ/mol, $\Delta G_{SO42-}°$= -1103 kJ/mol). Higher acid and base consumption for RE separation increase the production cost and environmental pollution, and ILE shows high extraction and stripping efficiencies at low acidity[9].

The extraction and separation of Ce(IV) and F are encouraging. The extraction ability of six extractants at chosen acidity follows as the order of: [A336][P507] > [A336][P204] > Cyanex923 > P204>P507>TBP [11].

Application of ILE in RE Separation

Table II lists the ILE important features as high efficient extractant. The potential application of ILE on the RE resource utilization and green separation is conducted, and the new separation techniques of Bayan Obo RE concentrate and South ion adsorption RE deposit in China are developed in our laboratory. [12]

Table II. ILE Important Features as High Efficient Extractant

Standards for high efficient extractant	ILE [A336][P507] features
High efficiency	E%, [A336][P507]>P507>TBP
High selectivity	β, [A336][P507]> P507
high stability	Multiple recycle and reuse; solubility<50ppm
Low cost	170CNY(28USD)/Kg
low toxicity	low toxicity similar to P507 and Aliquid336
low acid and base consumption	low acid and base usage
No NH3-N and salts released et al.	No NH3-N and salts released et al.

Figure 3 shows the proposed two-step decomposition process of the Bayan Obo rare earth concentrate. The advantages of the new process include: (1) The Two-step roasting of Bayan Obo ore will reduce consumption of NaOH and effectively recover all main valuable elements such as RE, Th, F, P. As well, the amount of waste residue can be reduced to 5%. (2) Th can be separated effectively with 90% recovery and 99% purity using primary amine N1923 (a methyloctadecyl amine in China). The recovered Th can be further upgraded to nuclear reactor fuel. (3) F and P can be recovered separately in each step with over 90% recovery. Diluted NaOH can be reused to dissolve the monazite tailing at the second stage. (4) The separation of Ce(IV) and F with Th(IV) and RE(III) in the H_2SO_4 leaching solution can be conducted in Cyanex923 and [A336] [P507]. The separation of Ce(IV) with other RE(III) will reduce the process loading, simplify the separation process, and lower the cost.

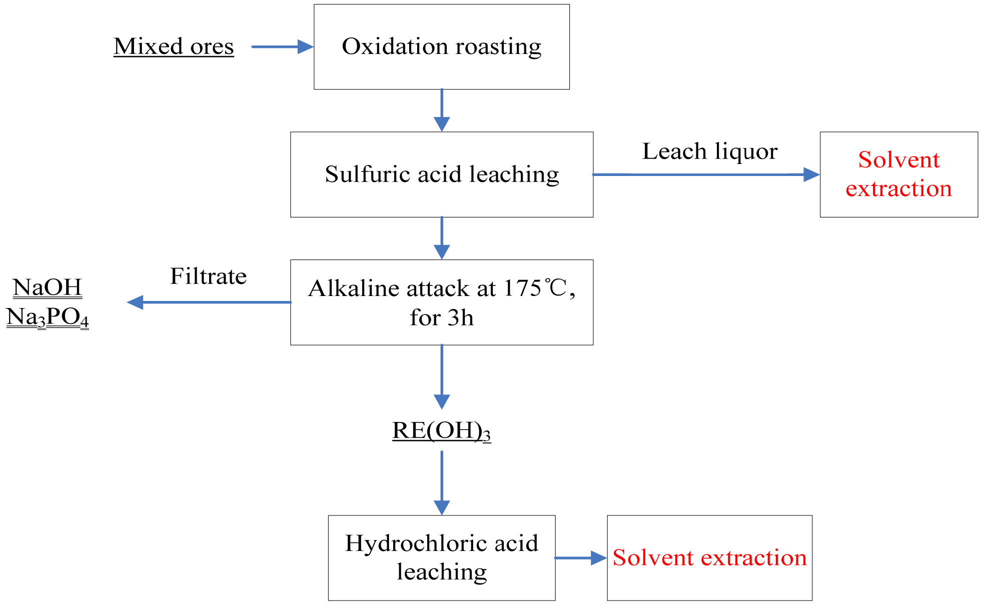

Figure 3. Two-step decomposition process of Bayan Obo RE concentrate.

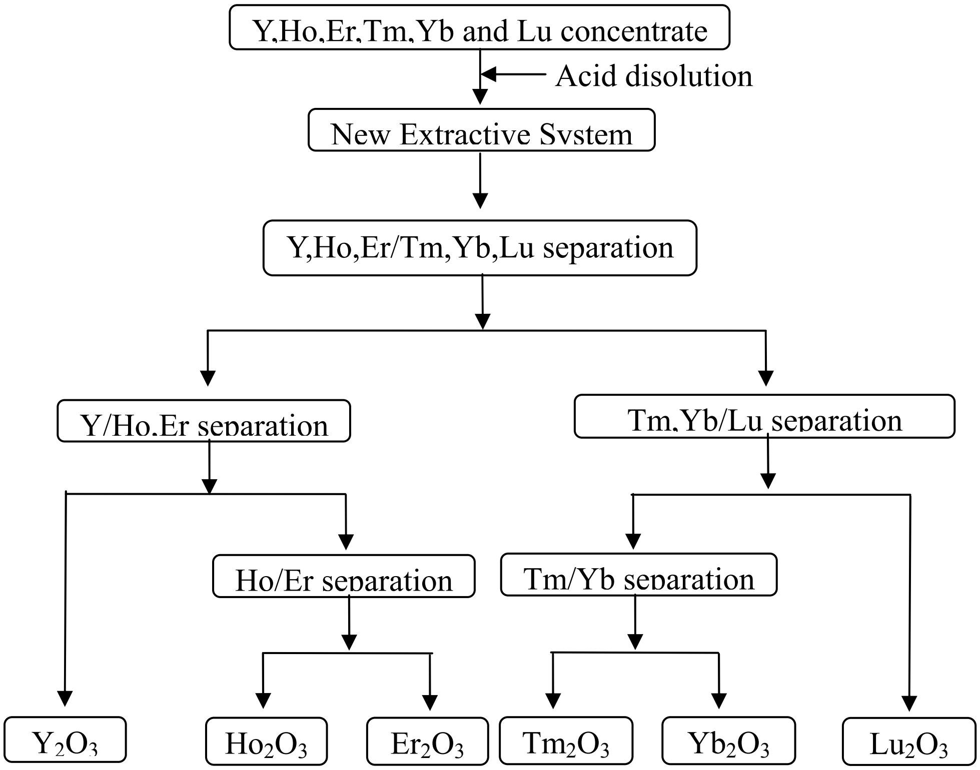

Figure 4. The integration technology of heavy RE separation from ion-absorbed RE deposits.

Another important application is the integration technology of heavy RE separation from ion-adsorption RE deposits [13, 14]. Its advantages are : (1) increased separation factor β of

HREand low stripping acid (< 5M), (2) complete stripping with low acid and alkaline consumption, (3) closed recirculating system of organic phase.

Summary

The results showed that ILE is an important extractant by non- chemical bond preparation, and a useful supplement to organic synthesis of extractants. The main extraction mechanism of ILEs was inner synergistic neutral complexing, and significantly changes the mechanism of P507, which is a typical cation exchange process. ILEs also showed high extraction to Ce(IV)-F, and high extraction selectivity for Pr/Nd, Yb/Lu et al.

The two-step decomposition of Bayan Obo ore and integrated separation of HRE for Southern ion-adsorption RE deposits were invented, and this will provide theoretical basis and technical supporting to meet the new national RE industry pollutants discharge standards.

References

1. Xu, G., *Rare Earth* (Beijing, Metallurgical Industry Press, 1995), 8-24.
2. Information Office of the State Council of the People's Republic of China White Papers of the Chinese Government 2012, Foreign Languages Press, 2012.
3. Ministry of Environmental Protection & The State Administration of Quality Supervision Inspection and Quarantine, *Emission Standard of Pollutants from Rare Earth Industry* (The People's Republic of China national standard), GB26451-2011, 201.1
4. Liu, Y., J. Chen and D. Li, "Application and perspective of ionic liquids on Rare Earths green separation," *Sep. Sci. Technol.*, 47 (2012), 223-232.
5. Hough, W.L., and R. D. Rogers, "Ionic liquids then and now: From solvents to materials to active pharmaceutical ingredients," *Bull. Chem. Soc. Jpn.*, 80 (2007), 2262-2269.
6. Sun, X. et al., "An engineering-purpose preparation strategy for ammonium-type ionic liquid with high purity," *AIChE J.,* 56 (2010), 989-996.
7. Sun, X. et al., "The inner synergistic effect of bifunctional ionic liquid extractant for solvent extraction," *Talanta*, 81 (2010), 1877-1883.
8. Belova, V.V., et al., "Solvent extraction of some lanthanides from chloride and nitrate solutions by binary extractants," *Hydrometallurgy*, 97 (2009), 198–203.
9. Yang, H., et al., "Recovery of rare earth elements from simulated fluorescent powder using bifunctional ionic liquid extractants (Bif-ILEs)," *J. Chem. Technol. Biotechnol.*, 87 (2012), 198-205.
10. Chen, J., et al., "An extraction and separation method of rare earth elements," PCT/CN/2012/082448 (2012, 09, 29).

11. Zhang, D., et al., “Extraction and recovery of Cerium(IV) and Fluorine(I) from sulfuric solutions using bifunctional ionic liquid extractants,” *Chem. Eng. J.*, 179 (2012), 19-25.

12. Chen, J., et al., “A processing method of decomposition of Baotou rare earth ore China patent application,” CN200310018072.4(2013, 01, 17).

13. Li, D., et al., “The separation process of rare earth elements for adding modifier,” ZL200510016682.6 (2005, 04, 05).

14. Chen, J., L. Guo and Y. Deng, “Extraction and separation method of rare earth elements,” CN 201210093082.X (2012, 03, 31).

SIMULATION OF THE SEPARATION OF RARE EARTH ELEMENTS WITH A VIEW TOWARD ECONOMIC PROCESS OPTIMIZATION

C. Bazin[1], C.B-Chapleau[1], M. Ourriban[2]

[1]: Dept Mining, Metallurgy and Materials Engineering,
Laval University, Quebec, QC, Canada

[2]: IAMGOLD Corporation, Longueil, QC, Canada

Keywords: Rare Earth Elements, Separation, Solvent Extraction, SX, Simulation

Abstract

The separation of rare earth elements is currently carried out by solvent extraction applied to an aqueous solution that contains more than 10 valuable elements of different prices. The economics of the separation process may lead to the production of individual rare earth oxides of various purities or the production of a composite of different elements sold for further separation. This paper describes the use of a simulator to study the economics associated with the operation of a separation plant for rare earth elements. The simulator incorporates modules to simulate the separation of light and heavy rare earth elements as well as the separation of light elements into individual compounds.

Introduction

Rare earth elements (REE's) refer to group of elements with atomic numbers ranging from 57 to 71. Scandium and yttrium are also considered as members of the REE's family. These elements are usually divided into light (La to Nd [1]), middle (Sm to Gd) and heavy (Tb to Lu, including Y) REE's. The REE's are mostly used for the production of permanent magnets and electronic devices [2-7]. Processing of REE's ore or of recycled materials leads to a solution [4,5,6,7] that may contain more than ten (10) REE's that need to be separated into individual compounds. The separation of REE's in the aqueous solution is the last step prior to metallurgy in the production of these elements.

There are few REE's separation plants around the world [6] and the documentation on the operation of these plants is very lean. General flow sheets for Rhône-Poulenc [4, 7, 8] in France, Mountain Pass in California [4, 8, 9, 10], Yao Lung in China [11] and Udyogamandal [12] in India are available but operating data is seldom available in the literature. Simulation is a possible approach to develop knowledge about a given process operation. However although the importance of simulation for the control and optimization of REE's separation plants is recognized as strategic [13] few papers were presented on the subject [14, 15]. This paper describes a prototype for the simulation of a REE's separation plant that is initially developed to facilitate learning about this process but which could ultimately be used for process design, optimization and control. The paper consists of 4 sections. The first section describes the general REE's ore processing flow sheet. The second section deals with the solvent extraction process used for the separation of REE's. The following sections describe the simulator and show its application for process optimization.

REE's Ore Processing and Element Separation

The main minerals that carry REE's are monazite and bastnasite [1, 4, 10]. Xenotime [1] and clays [4] are also a source of REE's. This section reviews the basic steps of processing ore and minerals to obtain the REE's.

Ore Processing and Production of a REE's Solution

Flotation and magnetic separation are the usual techniques used for processing rare earth ores to produce a concentrate of monazite and/or bastnasite [3, 10]. The REE's mineral concentrate contains between 60 and 70% of rare earth oxides (REO's). The recovery of REO's in concentrate varies between 40 and 80% [3]. Depending of their nature the concentrates of REE's minerals follow various processing routes that lead to the extraction of the REE's into an aqueous solution [5, 16]. The processing scheme is shown in Figure 1.

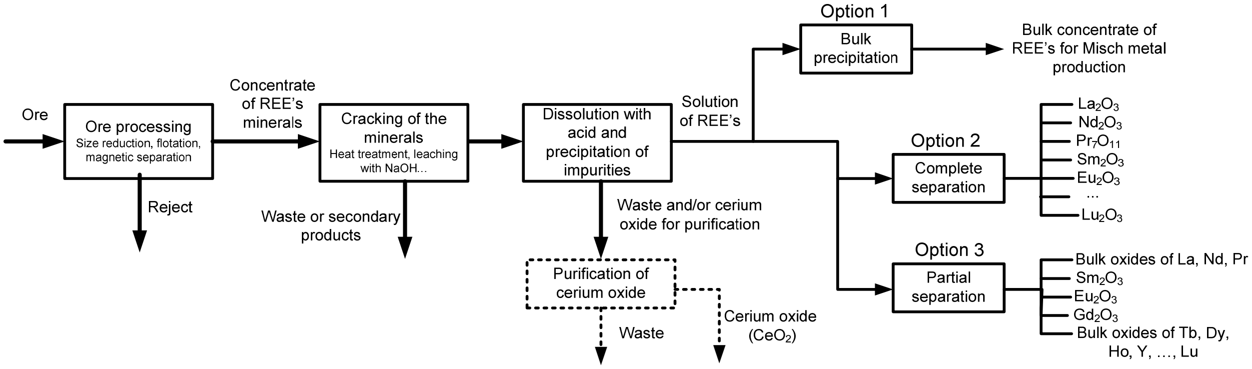

Figure 1. Processing of the REE's ore and separation into products.

Separation of the REE's in the Aqueous Solution

The REE's in the aqueous solution can be precipitated to obtain a bulk REE's product that can be used for the production of Misch metal [4]. The REE's can also be separated into individual oxide, carbonate or chloride products of the elements or precipitated as a bulk concentrate of neighbor REE's that can be sold to another separation plant (see Figure 1). MolyCorp Mountain Pass initially treated a bastnasite ore to produce individual oxides of europium, samarium and gadolinium and bulk concentrate of lanthanum, neodymium and praseodymium oxides sent to another separation plant. This paper is concerned with the separation of REE's from the solution.

The separation of REE's is industrially carried out using solvent extraction [7, 8, 9, 10, 14]. The strategy for the separation of REE's varies from plant to plant [4]. A possible separation scheme is shown in Figure 1. The separation may begin at the mineral cracking and dissolution stage where cerium is oxidized to tetravalent cerium and precipitated as CeO_2 that can be further purified [10, 12]. The Ce free aqueous solution follows the process shown in Figure 2. The solution is firstly processed to separate the light REE's (La-Nd) from the heavy ones (Sm to Lu+Y). Lanthanum is then separated from neodymium and praseodymium that can subsequently be separated or precipitated as a bulk product. The heavy REE's solution feeds a separation circuit where the samarium, europium and gadolinium (SEG) are separated from the heavier REE's [10].

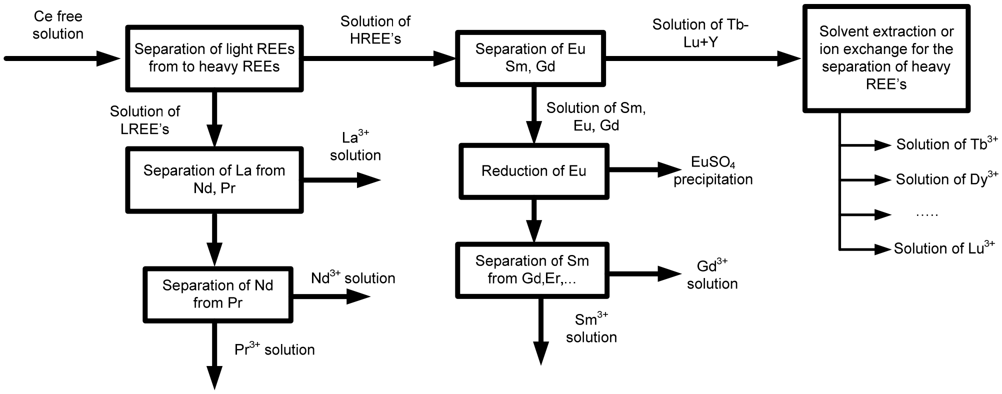

Figure 2. Separation strategy for REE's.

Simulation Procedure

Although some models exist for the simulation of solvent extraction processes for oxide copper ores few authors reported the development of mathematical models for the separation of REE's using solvent extraction [14, 15, 16]. The model proposed here predicts the steady state conditions of a circuit of batteries of mixer-settlers. The steady state simulator assumes that chemical equilibrium is reached within each mixer-settler of the circuit, i.e. that the mixing and separation times are sufficient to reach the equilibrium condition of the mass transfer between the aqueous and organic phases as:

$$Re_{i;Aq}^{3+} + 3(H_2X_2)_{Org} = Re_i(HX_2)_{3\,Org} + 3H_{Aq}^{+} \tag{1}$$

$$Re_j(HX_2)_{3\,Org} + Re_{i;Aq}^{3+} = Re_i(HX_2)_{3\,Org} + Re_{j;Aq}^{3+} \tag{2}$$

The symbol Re^{3+}stands for a trivalent ion of any REE's. The organic radical of the extractor is noted X. In this case, D2EHPA exists as dimmers when dissolved in organic solvents of low polarity. This last exchange (Eq. 2) is negligible when the concentration of the free extracting agent is large but may become important [18] for operation under a reflux [2, 8, 9]. The reaction of Eq. 1 proceeds until an equilibrium is reached between the reactants and the products, i.e.:

$$K_{Re} = \frac{\left[H_{Aq}^{+}\right]_{Eq}^{3}\left[Re(HX_2)_{3\,Org}\right]_{Eq}}{\left[Re_{Aq}^{3+}\right]_{Eq}\left[(H_2X_2)_{Org}\right]_{Eq}^{3}} \tag{3}$$

The simulation procedure is based on the equilibrium constants (K_{Re}) describing the mass transfer [14]. The equilibrium constants need to be obtained from laboratory tests using synthetic or plant REE solutions. The separation factors reported in the literature [4, 19] can be used to obtain preliminary estimates of the equilibrium constants.

Simulated Circuit

The simulator developed here is based on the processing of a bastnasite ore to produce a solution that feeds the separation plant. The light and heavy REE's are separated in a primary circuit and then the light REE's are separated into individual oxides. The separation of REE's above neodymium is not yet incorporated in the simulation.

Reconstruction of the Feed Solution

The REE mineral of the processed ore is assumed to be bastnasite with the composition given in Table I. The processing circuit is similar to the former Mountain Pass circuit [10, 14, 22]. The assumed gangue minerals are identified in Table I. The REE's content of the bastnasite is adjustable as well as of the concentration of the gangue minerals to simulate the processing of various ore types. The feed preparation follows the sequence shown in Figure 3. After a size reduction of the ore a bastnasite concentrate is produced by flotation. The characteristics of the concentrate are estimated using selectivity curves [22]. For instance a 72% bastnasite recovery leads to a concentrate assaying 60%REO for an ore with a bastnasite content of 10% or 7.5% total REO.

Table I. Example of the Reconstruction of the Feed Solution to a Separation Plant [22]

Solution Feed Reconstruction

Bastnasite composition	% REO/TREO
La2O3	32,500
Ce2O3	50,027
Pr2O3	4,000
Nd2O3	12,500
Sm2O3	0,600
Eu2O3	0,105
Gd2O3	0,200
Tb2O3	0,017
Dy2O3	0,027
Ho2O3	0,009
Er2O3	0,015
Tm2O3	0,002
Yb2O3	0,006
Lu2O3	0,001
Y2O3	0,053
*ThO2**	*0,100*

*: Not REE but considered in the calculation of %REO

Plant data	
Circuit ore througput (t/h)	50
Strong acid flow (l/min)	90
Wash water flow (l/min)	90
Target bastnasite recovery (%)	**72%**
Cerium conversion (III)-->(IV)	97%

Solids residues from leaching	
t/h	1,6
CeO2	84,2%

Ore processing plant feed and products

Minerals	Formula	Ore	Flot. conc.	Weak leach conc.	Calcined minerals	Heat treated conc
	Solids (t/h)	50,0	4,5	3,5		2,8
Bastnasite	ReFCO3	10,0%	80,3%	96,7%	ReFCO	97,2%
Calcite	CaCO3	14,0%	5,8%	0,7%	CaO	0,5%
Dolomite	MgCa(CO3)2	60,0%	11,5%	1,5%	MgCaO2	1,0%
Ankarite	Ca(FeMg)(CO3)2	10,0%	1,7%	0,3%	Ca(FeMg)O2	0,2%
Silica	SiO2	6,0%	0,7%	0,9%	SiO2	1,1%
	Total REO(%)	*7,5%*	*60,1%*	*72,4%*		*91,0%*

Adjustable parameters

	% diss. In weak acid	LOI	% diss in strong acid
Bastnasite	5,0%	20,0%	87,0%
Calcite	91,0%	44,0%	98,0%
Dolomite	90,0%	47,7%	97,0%
Ankarite	86,0%	42,0%	95,0%
Silica	0,0%	0,0%	5,0%

Solution to separation plant

Flow rate	l/min	180
Total REO	g/l	107
La^{3+}	g/l	57,309
Ce^{3+}	g/l	2,638
Ce^{4+}	g/l	0,000
Pr^{3+}	g/l	7,061
Nd^{3+}	g/l	22,139
Sm^{3+}	g/l	1,069
Eu^{3+}	g/l	0,187
Gd^{3+}	g/l	0,358
Tb^{3+}	g/l	0,031
Dy^{3+}	g/l	0,049
Ho^{3+}	g/l	0,016
Er^{3+}	g/l	0,027
Tm^{3+}	g/l	0,003
Yb^{3+}	g/l	0,011
Lu^{3+}	g/l	0,002
Y^{3+}	g/l	0,086
Fe^{3+}	g/l	0,200
Th^{4+}	g/l	0,162
Ca^{2+}	g/l	2,035
Mg^{2+}	g/l	0,633
Si^{2+}	g/l	0,070

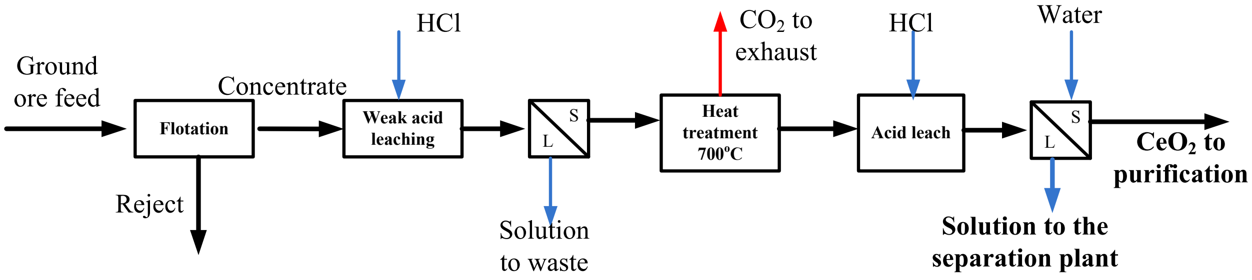

Figure 3. Preparation of the pregnant solution for the separation plant.

The flotation concentrate is then leached with a weak acid to dissolve some of the entrained carbonate gangue minerals and a heat treatment is applied to the leached concentrate to obtain the feed to the leaching circuit. An example of the solution feed reconstruction is presented in Table I. The ore feed rate to the processing plant is assumed to be 1200 t/d (50 t/h) with a bastnasite content of 10%. The solution that advances to the separation plant contains 107 g/l of REO a value that is consistent with the former Mountain Pass operation [10] solution feed concentration. The algorithm to generate the solution feed is still under development. For the moment it provides a flexible way to study the sensitivity of the separation plant to changes in the composition of the input solution following disturbances in the operation of the mineral processing and cracking plant.

Flow Sheet of the Simulated REE Separation Plant

The simulated flow sheet of the REE separation plant is shown in Figure 4. The light and heavy REE's are firstly separated in the *primary circuit*. The solution of light REE's contains La, Pr, Nd and some Sm and flows toward the *lanthanum circuit*. The lanthanum circuit produces the feed to the Pr/Nd separation circuit and a solution for the production of the lanthanum oxide. The current simulation algorithm does not incorporate the Sm-Eu-Gd and heavy REE's separation. The configuration proposed in Figure 4 is based on the few descriptions that it was possible to find in the literature dating of the 1990's.

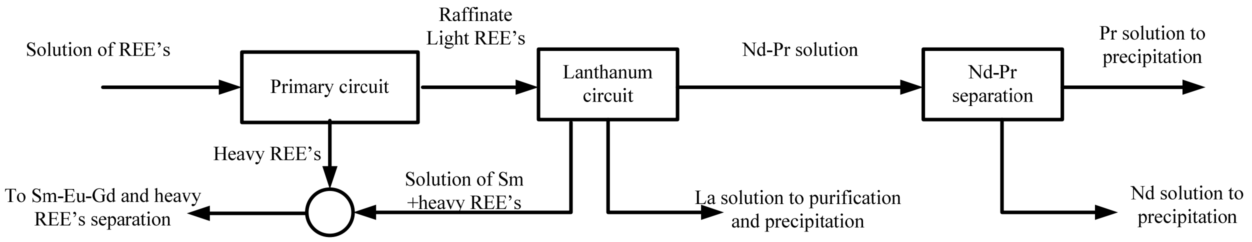

Figure 4. General layout of the simulated REE's separation circuit.

Reagents and Reagent Additions: The organic phase used in the circuits consists of di(2-ethylhexyl) phosphoric acid (D2EHPA) in solution of various concentrations in kerosene. The extracting agent is not saponified [16] but the simulator is built so that controlled addition of a NaOH into each mixer-settler of an extraction battery is possible in order to reduce the impact of the acidification of the aqueous solution following the transfer process (see Eq. 1). A bleed system can be operated for each organic stream to handle the crud [20]. Hydrochloric acid and NaOH solutions of various strengths of are used for scrubbing, stripping and pH adjustment.

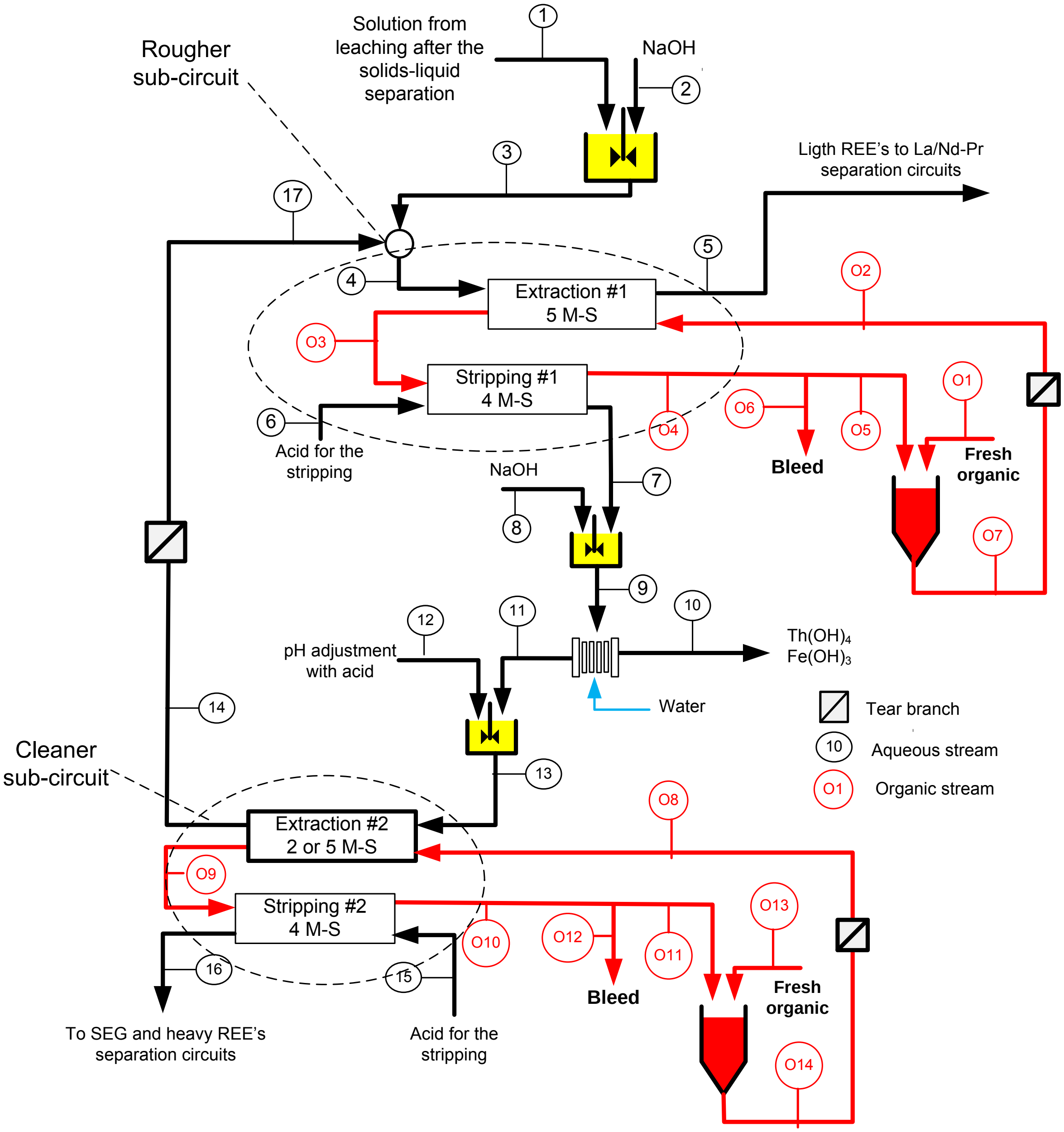

Figure 5. Primary separation of light and heavy REE's.

<u>Primary Circuit:</u> The primary circuit used to separate the light and heavy REE's is shown in Figure 5 [14]. The circuit consists of the two sets of extraction/stripping batteries identified as the rougher and cleaner sub-circuits. The first extraction/stripping battery or rougher sub-circuit produces an impure solution of heavy REE's that is reprocessed in a second set of extraction/stripping batteries. The raffinate of the first extraction/stripping battery (stream 5 of Figure 5) flows to the lanthanum circuit while the pregnant strip solution (stream 7 of Figure 5) is sent to a Fe-Th precipitation circuit. The Fe-Th free solution (stream 11 in Figure 5) is cleaned in the cleaner sub-circuit. The raffinate of this sub-circuit is returned to the first sub-

circuit (stream 14 in Figure 5) while the loaded solution from the stripping battery (stream 16 of Figure 9) contains the heavy REE's.

Lanthanum Circuit: The lanthanum circuit shown in Figure 6 separates lanthanum from the neodymium and praseodymium. The pH of the solution that flows from the primary circuit is firstly adjusted and the solution is combined with the discharge of a scrubbing battery to feed the extraction battery. The raffinate of the extraction battery advances to the La precipitation circuit shown in Figure 7. The loaded organic phase is scrubbed to remove some lanthanum and cerium and the scrubbed organic phase is stripped a first time to recover Nd and Pr in a solution (stream 9 of Figure 6). The organic phase is then stripped a second time with a stronger acid to recover some samarium and other heavy REE's that are returned to the SEG solution of the primary circuit. As indicated earlier, since we don't have access to detailed separation plant flow sheets, actual plant flow sheets could be different from the flow sheet of Figure 6.

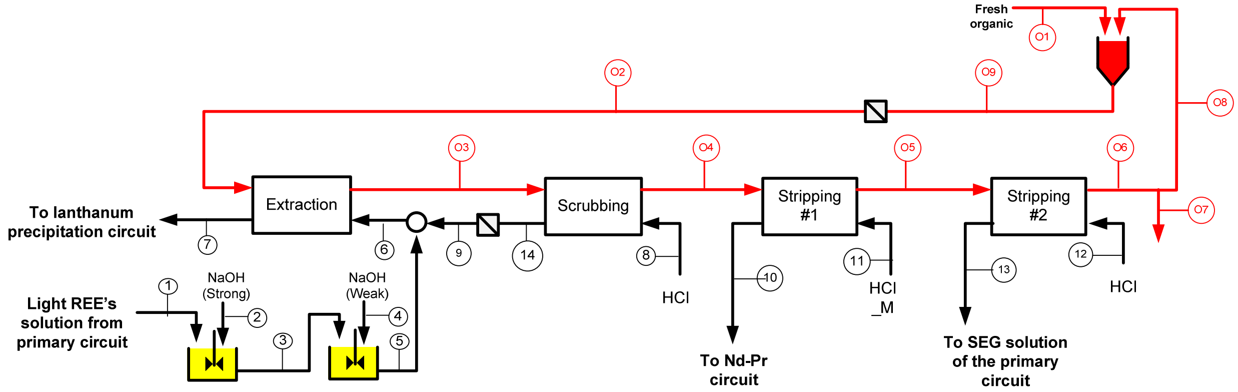

Figure 6. Lanthanum circuit.

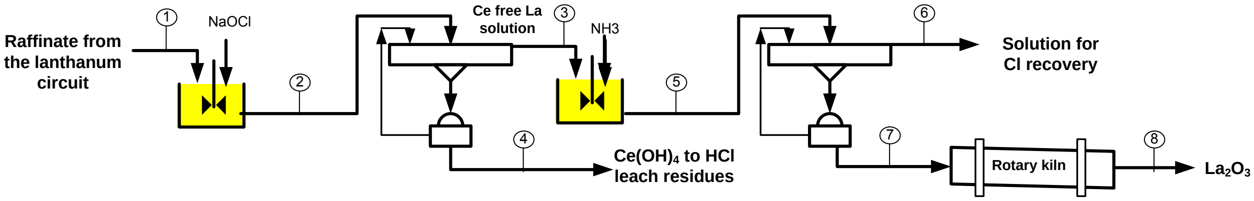

Figure 7. La-Ce precipitation circuit.

Pr-Nd Separation Circuit: The simulated Pr/Nd separation circuit is shown in Figure 8. The circuit consists of three (3) sub-circuits with the configuration shown in Figure 9. The first sub-circuit operates a primary separation of the neodymium from the praseodymium. The other two sub-circuits upgrade the solutions released by the primary circuit. The literature provides very little information on industrial Pr/Nd separation circuits which may indeed differ from the circuit of Figure 8. The Pr/Nd primary circuit (see Figure 8) is fed by the pregnant solution from the first stripping battery of the lanthanum circuit. The feed solution is combined with the raffinate from the Nd upgrading sub-circuit and the pregnant strip solution from the Pr upgrading circuit. The primary Pr-Nd separation circuit produces a raffinate enriched in Pr and a pregnant solution from a stripping stage that is enriched in Nd. The two streams are then processed in their respective upgrading circuits that produce the solution for the precipitation of the praseodymium and the neodymium oxides.

The configuration of the sub-circuits used for the primary separation and upgrading of the Pr and Nd solutions is shown in Figure 9. The sub-circuit of Figure 9 corresponds to the primary Pr/Nd separation circuit but the upgrading sub-circuits have the same configuration. The feed solution to the sub-circuit is firstly combined with the raffinate from the scrubbing battery and the pH is adjusted with caustic soda before being processed in the extraction battery that produces a Pr rich raffinate and a Nd enriched organic phase. The separation between the elements is marginal since the Nd/Pr separation factor is close to 1.0 [19]. Some water in the raffinate of the extraction battery is evaporated and a portion of the concentrated raffinate is returned to the extraction battery as a reflux. The loaded organic is scrubbed with a weak acid combined with a portion of the pregnant solution from the stripping battery (see Figure 9). The upgraded Pr and Nd solutions are processed in a similar way than the lanthanum solution, i.e. the cerium is precipitated before the precipitation and heat treatment of the precipitated REE hydroxide.

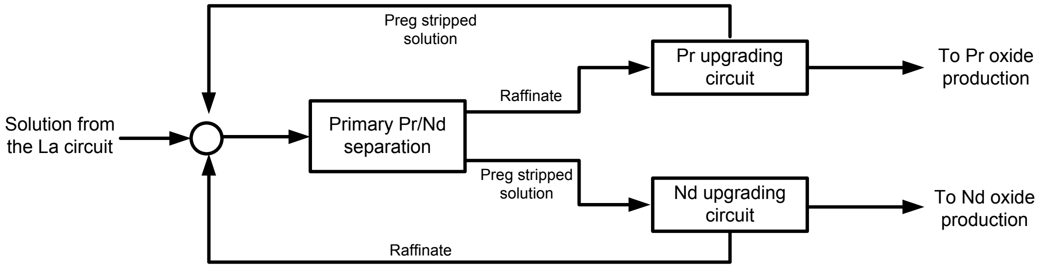

Figure 8. Proposed Pr/Nd separation circuit.

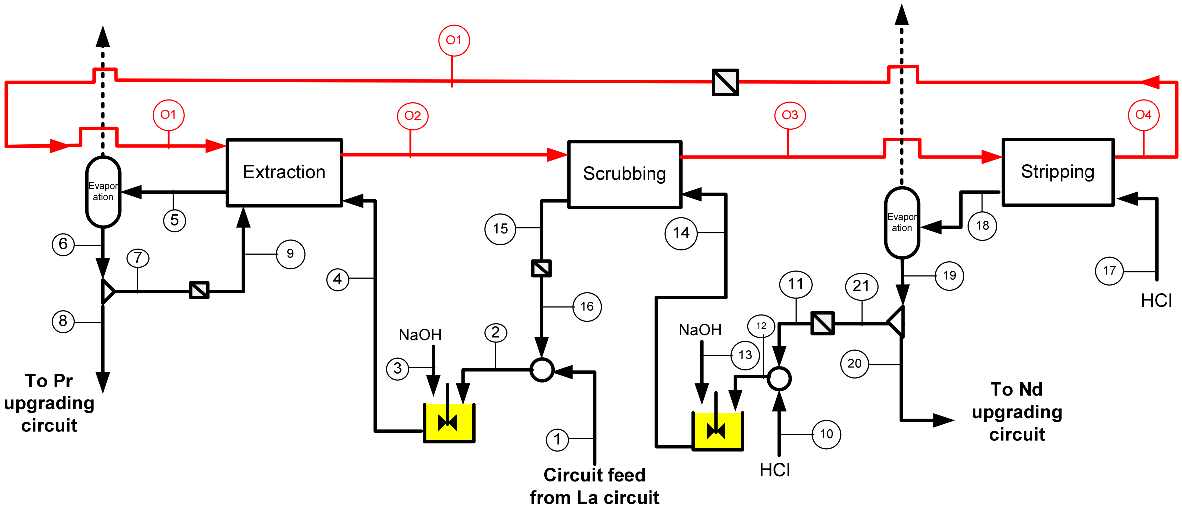

Figure 9. Primary sub-circuit for Nd/Pr separation.

Simulation Results

Even if the simulated circuit is incomplete as there is no separation of the SEG and heavier REE's the simulator already allows the manipulation of many operating and design variables. Indeed the number of mixer-settlers in each battery can be adjusted as well as the flow rates and compositions of the organic phase, the flow rates and concentrations of the scrubbing and stripping acids, the target pH in the batteries, the degree of solution evaporation when required and the proportion of reflux when used in a circuit [18]. The simulator uses estimates of the equilibrium constants deduced from the separation factors found elsewhere [19].

Economic Index

The revenues associated with the material flowing in a stream k are calculated using:

$$E_k = F_{A;k} \sum_{i=1}^{N} B_{i;k} \varphi_i x_{i;k} P_i \frac{60}{1000} \tag{4}$$

The calculated revenues flow is expressed in \$/h and refers to stream k. The volume flow rate (L/min) of the aqueous solution in stream k is noted $F_{A;k}$, the concentration (g/L) of the ith REE is $x_{i;k}$ and φ_i converts the concentration of an element into the corresponding oxide concentration. The variable $B_{i;k}$ takes a value of 1.0 if element i is profitable in stream k and 0.0 if the element is not. For instance the lanthanum, cerium, neodymium and praseodymium do not generate revenues in the stream feeding the SEG separation circuit. On the other hand all REE's in the raffinate of the primary circuit generate revenues as the heavy REE's (Sm and above) can return to the SEG circuit via the lanthanum circuit (see Figure 6). The price of the ith REO is noted P_i and the oxide prices used here [21] are given in Table II. An empirical model described elsewhere [22] is used to account for the purity of the produced oxide. Since most of the cerium is removed before the separation circuit its value is not accounted for in the economic analysis although it would be used in subsequent studies. The proposed revenues flow is a simplification of a global optimization index that should indeed account for the costs associated with the consumption of acids, bases and organic phases and energy required for solution evaporation. A ratio of two revenue flows is used to estimate an economic recovery associated with the operation of a circuit. For instance the economic recovery associated with the operation of the primary circuit is given by the ratio of the sum of revenues flow with the light REE's and the heavy REE's to the revenues flow in the feed. A 100% economic recovery is obtained for a perfect separation of the elements toward payable products.

As an example the revenues flow calculated using Eq. 4 for the solution feeding the separation circuit with the flow rate and the composition of the solution given in Table I is 41100\$/h. The neodymium accounts for 51% of this value, followed by praseodymium with 18% and 18% for the lanthanum. Europium accounts for 8% of this value, and the other elements share the remaining 6%.

Table II. REO Prices of April 2013 [21]

Oxide	$/kg	Oxide	$/kg
La2O3	10,00 $	Dy2O3	*625,00 $*
CeO2	20,00 $	Ho2O3*	*400,00 $*
Pr6O11	82,00 $	Er2O3*	*400,00 $*
Nd2O3	75,00 $	Tm2O3*	*400,00 $*
Sm2O3	23,00 $	Yb2O3*	*400,00 $*
Eu2O3	1 400,00 $	Lu2O3*	400,00 $
Gd2O3	45,00 $	Y2O3	35,00 $
Tb4O7	1 150,00 $		

* : Value assumed as non available in the literature

Preliminary Economic Optimization of OHE REE's Separation Circuit

The optimization process used here is sequential i.e. the operation of the primary circuit is firstly adjusted followed by the lanthanum circuit and the Pr/Nd separation circuit. Unlike a global optimization process the procedure followed here lead to a sub optimal solution.

Optimization of the Primary Circuit: The application of the optimization procedure to the primary circuit for the separation of light and heavy REE's (Figure 5) is summarized in Table III. Since the light REE's (La, Ce, Pr, Nd) do not generate revenues when in the heavy REE's solution stream the operation of the circuit should maximize their rejection toward the raffinate. The heavy REE's that follow the light REE's could still be recovered in the lanthanum circuit. Some of the tested operating conditions for the primary circuit are presented in Table III with the economic recovery. The tested conditions of Table III encompass modifications of the organic to aqueous (O/A) flow rates in the batteries and the number of mixer-settlers in the batteries of the circuit. As expected results show that the economic optimum is achieved by maximizing the

Table III. Optimization of the Primary Separation Circuit (Figure 5)

	Rougher sub-circuit				**Cleaner sub-circuit**						
	Extraction battery		**Stripping battery**		**Extraction battery**		**Stripping battery**		**Recovery (%)**		
Case	Ratio O/A	Numb M-S	Ratio O/A	Numb M-S	Ratio O/A	Numb M-S	Ratio O/A	Numb M-S	Heavy REE's	Light REE's	Revenues ratio (S_{Prm})
A	0,95	5	15,4	4	2,33	3	7,5	4	94,4	99,8	99,6
B	0,85	5	13,9	4	2,33	3	7,5	4	93,1	99,8	99,6
C	1,07	5	17,3	4	2,33	3	7,5	4	95,4	99,8	99,6
D	0,93	5	11,9	4	1,76	3	7,5	4	96,0	99,9	99,7
E	0,97	5	18,5	4	2,85	3	7,5	4	92,6	99,8	99,6
F	**0,95**	**7**	**15,4**	**4**	**2,33**	**3**	**7,5**	**4**	**96,8**	**99,9**	**99,7**
G	0,95	3	15,4	4	2,33	3	7,5	4	87,9	99,7	99,4
H	0,95	5	15,4	3	2,33	3	7,5	4	93,9	99,8	99,6
I	0,95	5	15,4	5	2,33	3	7,5	4	94,7	99,8	99,6
J	0,95	5	15,4	4	2,33	3	6,3	4	94,6	99,8	99,5
K	0,95	5	15,4	4	2,33	3	10,0	4	91,6	99,9	99,8
L	0,95	5	15,4	4	2,07	3	6,7	4	90,8	99,9	99,8
M	0,95	5	15,4	4	2,59	3	8,3	4	94,6	99,7	99,3

Ratio O/A : Ratio of organic to aqueous phase flow rate
Numb. M-S: Number of mixer-settlers in the battery

recovery of light REE's (cases D, F, K and L in Table III). The selected operating conditions for the primary circuit correspond to case F that is found to be a good compromise between the recovery of light and heavy REE's. The 96.7% recovery of heavy REE's is consistent with the reported 96% recovery of europium from the former Mountain Pass plant [4, 10].

Optimization of the Lanthanum Circuit: The solution that feeds the lanthanum circuit comes from the optimized primary circuit (case F of Table III). The optimum operating conditions of the lanthanum circuit should be a compromise between the elimination of the lanthanum from the pregnant Pr/Nd solution and the recovery of praseodymium and neodymium. Increasing the recovery of lanthanum to the raffinate stream leads to an increase Pr/Nd losses to that stream. Increasing the recovery of Pr/Nd to the pregnant solution from stripping would lead to an increase loss of lanthanum to the stream and a subsequent contamination of the Pr and Nd oxides by lanthanum. Ideally the lanthanum circuit should use a similar configuration than the primary circuit with a roughing stage followed by a cleaning one (see Figure 5).

Some of the tested conditions for the optimization of the lanthanum circuit are reported in Table IV. The optimum condition corresponds to case J with a 98% economic recovery. These conditions lead to a 91.2% recovery of neodymium and praseodymium that are the elements that carry most of the solution potential revenues. A better Pr/Nd recovery could have been achieved at the expenses of a higher concentration of lanthanum in the solution feeding the Pr/Nd separation circuit which would ultimately contaminates the praseodymium oxide product. The lanthanum oxide produced after cerium removal contains 98.4% La_2O_3, 1.1% Pr_6O_{11} and 0.6% Nd_2O_3. The revenues flow of the lanthanum oxide is 7360$/h. The solution feeding the Pr/Nd separation circuit contains 2.19, 23.1 and 78.6 g/L of La, Pr and Nd compared to a lanthanum circuit feed composition of 48.4, 5.94 and 18.6 g/L respectively.

Optimization of the Pr/Nd Separation Circuit: The optimization of the Pr/Nd separation circuit was the most challenging and frustrating step of the process. In 1980 Poirier [7] made the following comment:

> *'I think that once you know how to separate neodymium from praseodymium you can separate any elements'*

The statement is certainly true as it was not possible, even by simulation, to achieve an acceptable separation of praseodymium and neodymium using the circuit configuration shown in Figure 9. It would have probably been necessary to repeat the upgrading process two or three other times to achieve an acceptable separation. This would have required reprogramming of the simulator which was not possible at the time of writing the paper. The handling of the circulating loads between the sub-circuits of Figure 9 also becomes problematic. A change of acid from hydrochloric to nitric acid with a switch to a TBP extracting agent instead of D2EHPA could have helped as TBP provides slightly better separation factors for Pr and Nd than D2EHPA [13]. This was not attempted here.

The praseodymium oxide produced after removal of cerium and precipitation of the remaining elements of the raffinate solution from the Pr upgrading circuit contains 5.8% La_2O_3, 35.4% Pr_6O_{11} and 58.8% Nd_2O_3. The neodymium oxide obtained after removal of cerium and precipitation of the elements of the Nd upgrading circuit pregnant strip solution contains 0.0% La_2O_3, 10.8% Pr_6O_{11}, 89.1% Nd_2O_3 and 0.1% Sm_2O_3. The recovery of praseodymium to its oxide is 93% while the neodymium recovery to its oxide is below 45% which is unacceptable since this element carries most of the value of the Pr/Nd solution. The circuit's economic recovery is 35% but this figure can be improved by adding more stages of upgrading for both elements. The simulated Pr/Nd circuit consists of more than 60 mixer-settlers and the separation of praseodymium and neodymium is still unacceptable. This number of units is however in agreement with the large number of mixer-settlers reported to be used in REE's separation plants [7, 10]. Subsequent simulation work will be directed toward the development of a circuit that can achieve a better separation of the praseodymium and of the neodymium.

Table IV. Optimization of the Lanthanum Circuit (see Figure 6)

	Extraction battery		**Scrubbing battery**		**Strip Pr/Nd**		**Strip heavy REEs**					**Revenues**
	Ratio	Numb	Ratio	Numb	Ratio	Numb	Ratio	Numb	**Recovery (%)**			**ratio**
Case	O/A	M-S	O/A	M-S	O/A	M-S	O/A	M-S	La	Pr/Nd	Heavy	**S_{la} (%)**
A	0,85	13	8,2	10	4,2	5	8,4	5	98,0	92,3	41,1	97,9
B	0,87	13	8,4	10	4,3	5	8,6	5	96,8	97,8	40,1	99,1
C	0,83	13	8,0	10	4,1	5	8,2	5	98,8	86,9	39,5	96,3
D	0,79	13	7,7	10	3,9	5	7,8	5	99,8	75,8	38,7	94,2
E	0,81	13	7,8	10	4,0	5	8,0	5	99,5	81,1	40,3	97,6
F	0,85	13	8,1	10	4,2	5	8,4	5	98,6	90,8	40,9	97,4
G	0,85	12	8,1	10	4,2	5	8,4	5	98,6	91,0	40,9	97,6
H	0,85	14	8,1	10	4,2	5	8,4	3	98,7	90,2	41,8	97,7
I	0,85	13	8,1	11	4,2	5	8,4	5	98,7	90,9	41,8	97,8
J	**0,85**	**13**	**8,1**	**12**	**4,2**	**5**	**8,4**	**3**	**98,7**	**91,2**	**41,8**	**98,0**

Ratio O/A : Ratio of organic phase flow rate to aqueous phase flow rate
Numb. M-S: Number of mixer-settlers in the battery

Conclusion

The separation of rare earth elements is a process that is not thoroughly described in the literature. Most of the available literature dealing with REE separation plant operations describes the general principle of the operation with practically no details about the circuit operation. This paper presented the bases of a simulator for the separation of rare earth elements. The simulator uses the chemical equilibrium constants of the mass transfer equation between the organic and aqueous phases in a mixer-settler to simulate the steady state operation of a solvent extraction plant.

The simulated process studied in this paper starts with a Ce-free solution prepared by HCl leaching a heat-treated bastnasite concentrate. The light and heavy REE's are separated and then the light REE's are separated into oxides of lanthanum, praseodymium and neodymium. The simulator does not yet incorporate the separation of SEG and heavier REE's but it already provides a flexible way to learn about the REE separation process by allowing the study of the effect of the pH, flow rate of the organic phase, stripping and scrubbing acids as well as the concentration of these reagents and the number of mixer-settlers in the various batteries of a solvent extraction circuit. An illustration of the application of the simulation to the optimization of the circuits for the preparation of the light REO is presented in the paper. Simulation clearly points out the difficulty associated with the separation of praseodymium and neodymium.

References

1. Habashi, F. 2012. "Extractive metallurgy of rare earths", *In Rare Earths, Proc. of the 51th CIM Conf. of Metallurgists*, Eds J.R. Goode et al. (Niagara Falls, Canada: CIM 2012) 54-67.

2. De Logiviere, X., "Terres rares: enjeux économiques et principales applications". *Techniques de l'Ingénieur*, in 158 (2013), Éditions TI, 249 rue de Crimée, 75019 Paris.

3. Zhang, J., and C. Edwards, 2012. "A review of rare earth mineral processing technology", *44th Annual Can. Mineral Processors Operators Conf.*, (Ottawa, Can: CIM 2012), 79-102.

4. Gupta, C.K., and N. Krishnumurthy, *Extractive metallurgy of rare earths*, (Boca Raton, FL.: CRC Press, 2005).

5. Koch, D.F.A., "Rare earth extraction and separation", *Materials Australasia*, 19-4 (1987) 12-15.

6. Goode, J.R., 2012. "Canadian Rare earth and thorium recovery operations: The first 30 years", *In Rare Earths, Proc. of the 51th CIM Conf. of Metallurgists*, Eds J.R. Goode et al. (Niagara Falls, Canada: CIM 2012) 31-47.

7. Poirier, P., "New developments in rare earth markets", *4th industrial minerals international congress*, (Atlanta, Georgia, 1980) 205-209.

8. Rydberg, J., et al., 2004. *Solvent extraction: Principles and practice*, (New-York: 2nd Edition, Marcel Dekker Inc, 2005).

9. Ritcey,G.M., and A.W. Ashbrook, *Solvent Extraction: Principles and applications to process metallurgy Part II,* (Amsterdam: Elsevier Scientific Publishing Company, 1979).

10. Mackey, T.S., "Recent development in USA rare earth technology", *In Advances in Mineral Processing*, (Ed. P. Somasundaran: SME, Littleton, CO, 1986) 509-530.

11. Zhang, B.Z, et al., "Rare earth industry in China", *Hydrometallurgy*, 9 (1982), 205-210.

12. Narayanan, N.S., et al., "Processing of monazite at the rare earth division", Udyogamandal. *Materials Science Forum*, 30 (1988), Trans Tech Publications, Switzerland, 45-56.

13. Maestro, P., and A. Lévêque, "Terres rares", *Techniques de l'ingénieur,* J6630 (1993).

14. Bazin,C., et al., "Simulation of the industrial separation of rare earth elements by solvent extraction", *SME Annual Meeting*, (Preprint 13-008, Denver, February: 2013) 26-28.

15. Nishihama, S., et al., "Selective extraction of Y from a Ho/Y/Er mixture by liquid-liquid extraction in the presence of a water-soluble complexing agent", *Ind. Eng. Chem. Res.*, 39 (2000), 3907-3911.

16. Thakur, N.V., et al., “Separation of neodymium from lighter rare earths using alkyl phosphonic acid”, PC 88A, *Hydrometallurgy*, 34 (1993), 99-108.
17. Zhang, J., and C. Edwards, “Mineral decomposition and leaching processes for treating rare earth ore concentrates”, *In Rare Earths, Proc. of the 51th CIM Conf. of Metallurgists*, Eds J.R. Goode et al. (Niagara Falls, Canada: CIM 2012) 95-102.
18. Bao, D.S., et al., “Processing route for direct production of mixed rare earth metal oxides by selective extraction”, *Patent WO/2000/047785* (2000).
19. Quan, C.H., et al., “Separation factors of rare earths for D2EHPA and Ionquest in various diluents”, *Rare Earths, Resources, Science, Technoloogy and application*, Eds. R.G. Bautista and N. Jackson (The Minerals, Metals and Materials Society: San-Diego,CA, 1992) 271-281.
20. McCallum,T., et al., “Crud processing improvements using Acorga CB™ 1000 crud busting agent”, *SME Annual Meeting*, (Preprint 13-122, Denver, CO, 2013).
21. http://www.metalprices.com
22. Bazin, C., and C. Boudrias-Chapleau, “Simulation and optimization of rare earth separation circuits”, *In preparation*, 2014.

SOME PROCESSING OPTIONS FOR THE REMOVAL OF CRITICAL IMPURITIES FROM MULTI-SOURCE CONCENTRATES FEEDING A RARE EARTHS REFINERY

V. Yahorava*, A. C. du Preez, M. H. Kotze

Mintek, Hydrometallurgy Division, 200 Malibongwe Drive, Ranburg, South Africa
E-mail: olgay@mintek.co.za

Keywords: Rare Earths Refinery, Critical Impurities, Precipitation, Solvent Extraction, Ion Exchange

Abstract

Processing and refining of rare earth elements are of pronounced interest in the world outside China. New refineries (Molycorp and Lynas), are fed from world class deposits and hence have relatively stable feed compositions. However, smaller REE deposits or projects most probably would not be able to install and operate individual refineries cost effectively. This spawned the concept of centralized refineries, which would treat and refine intermediate rare earth element products or concentrates from different producers. Concentrates or intermediate products from different mines could vary significantly in composition, thus introducing a large variation in the impurities and their levels over the life-time of a centralized refinery. Various purification circuits might have to be installed before the actual refinery. Limited information is available on the behaviour of impurities and processing options to remove them effectively. The current paper identifies the most critical impurities in the refining of rare earth elements from chloride medium, as well as options for their removal/elimination using various techniques.

Introduction

In recent years the global demand for rare earth elements (REE) increased, hence a relatively large number of processing and exploration projects have been initiated [1]. One of the primary reasons for this is that although China flooded the market with REE for a number of decades, they have recently withheld supplies to countries outside of China and hence they became an unreliable, international REE supplier.

In order to develop a new REE refinery, the following aspects have to be taken into account:

- Sufficient feed material should be treated to render the facility economically attractive. The amount of feed material required would be dependent on the basket value of the feed to the refinery;

- Capital investment, including infrastructure and community developments, could be relatively high depending on the products to be produced, and hence its complexity;

- A REE refinery producing many refined products requires a relatively high-technology design and operation. The level of this would be determined by the product specifications;

- Products to be produced could vary, depending on market changes;
- A holistic approach would generally have to be implemented, where waste streams, including radioactive waste, have to be considered carefully.

Only a few of the new projects may fulfil all the criteria, thus the concept of centralized refineries, which would treat and refine intermediate REE products or concentrates from different producers, was developed.

The basic principle of a centralized refinery would be to receive physically upgraded concentrates or intermediate REE precipitates or products from various mines. There are various REE minerals, including xenotime that is enriched with Y and heavy REE, bastnaesite containing mainly light REE, synchysite that could be enriched with Ce, Nd or Y, while monazite containing primarily Ce, La, Nd and Sm [2]. The gangue minerals of each deposit are unique, and this would introduce complexity into a REE refining plant. Hence, it would be critical for any centralized REE refinery to have the potential feed materials accurately quantified over the life of the plant or at least for the first 5-10 years of operation.

The current paper gives an overview of the most crucial impurities associated with REE ores and also highlights the complexity of developing a suitable flowsheet for the preparation of a REE refinery feed.

Identification of Critical Impurities in Rare Earths Refining

Refining of REE is usually conducted in hydrochloric (Molycorp, Lynas, Indian REE, Chinese Refineries) or nitric acid medium (Silmet, Kashka REE Plant, Rhodia) [3-5]. Solvent extraction (SX), sometimes in combination with ion exchange (IX), is typically used for separation. In this paper the focus will be on the impact of critical impurities on REE refining from HCl medium via SX and approaches for their elimination.

Table I. Impurities Associated with the Main REE Minerals

Mineralogy	Description	Main impurities
Bastnaesite	REE fluorocarbonate	F^-
Monazite	REE phosphate	Th, U, PO_4^{3-}
Aeschynite	$(REE,Ca,Fe,Th)(Ti,Nb)_2(O,OH)_6$.	Th, Ti, Nb, Fe, Ca
Loparite	REE, Nb, Ta, Ti oxide	Nb, Ta, Ti
Zircon	REE, Zr oxide	Si, Hf, Zr
Xenotime	Y phosphate	As, Th, Si, Ca, U
Apatite	REE phosphate	F^-, Ca, U, Th, Fe, PO_4^{3-}

The conventional solvent used in REE refining is 2-ethylhexyl phosphonic acid mono-2-ethylhexyl ester (EHEHPA), which is well-known under the following trade names: PC88A (Daihachi Chemicals), Ionquest 801 (Rhodia), and P507 (China). EHEHPA is a typical chelating, cation exchange extractant.

Table I gives an indication of the variety of REE minerals and the associated impurities. Impurities that would be introduced by apatite and zircon are also given as an example of the importance of gangue minerals.

Impurities can be of anionic or cationic nature depending on their speciation in the specific leach liquor. The main anionic impurities are fluorides, chlorides, sulphates, and phosphates, of which the most critical ones are fluorides, phosphates and sulphates. Fluorides and phosphates form insoluble species with REE (see Table II). For separation of REE, a typical SX plant would require strict pH control and neutralization is usually done with NaOH or NH_4OH/NH_3. In the presence of sulphates in the refinery liquor, formation of sparingly soluble double REE sulphates ($Na(NH_4,K)REESO_4 \cdot nH_2O$) can occur.

Table II. Solubility Constants of REE Phosphates, Fluorides and Double REE Sulphates

Element	Phosphates [6]	Fluorides [7]	Sulphates
	pK_{sp}		In saturated K_2SO_4 solution, g/L [8]
Y	25.0		46.85
La	25.7	20.5	-
Ce	26.2	19.8	
Pr	26.4	18.8	-
Nd	26.2	19.8	-
Sm	n/a	n/a	0.5
Dy	n/a	18.1	-

Moreover, fluorides, phosphates and sulphates form complex species with REE, i.e.:

- $REEF^{2+}$ [7, 9];
- $REEHPO_4$+ and $REEH_2PO_4^{2+}$;
- $REESO_4^{+}$ and $REE(SO_4)^{2-}$ [10,11].

If an anionic impurity is present in the refinery feed liquor in significant quantities and forms complexes with REE, the extraction behaviour and process parameters might change significantly. For example, the presence of sulphate ranging from 0.15 to 0.7 M, was found to result in a depression of the distribution coefficient in particular for the light rare earths which extract at pH >1 for 1 M EHEHPA in ShellSol D60. In the presence of sulphates pH_{50} for lanthanum was shifted up to 0.7 pH units relative to extraction from chloride medium (individual REE concentrations were not specified) [12]. It also was reported, that when the fluoride concentration was over 2 g/L emulsification of the organic phase could occur [13].

In an attempt to identify the impurities that would most likely interfere during the solvent extraction processes employed for REE separation, a pH vs extraction test was performed with 30 % (v/v) EHEHPA (PC88A) in an aliphatic diluent (Shellsol D70). A synthetic chloride solution, with the composition specified in Table III, was used. Only chloride salts were used as a source of elements (excluding Th and U where standard solutions in HNO_3 medium were used). The solution contained 1.5 M HCl and a total background chloride concentration of about 3.5 M.

Table III. Composition of Synthetic REE and Impurities Solution

Element	Concentration (g/L)	Element	Concentration (g/L)
La	21.16	Mn	0.10
Ce	42.00	Al	0.10
Pr	4.29	Mg	1.00
Nd	15.78	Ca	1.00
Sm	2.72	U	0.05
Eu	0.54	Th	0.05
Gd	2.24	Zr	0.05
Dy	1.48	Fe	0.10
Yb	0.66	Cu	0.05
Ho	0.32	Cr	0.05
Tb	0.39	Co	0.05
Y	7.50	Ni	0.05
Lu	0.08	Zn	0.05
Tm	0.09	Cd	0.05
Er	0.75	Pb	0.05

Results achieved for extraction vs pH are presented in Figure 1.

The main cationic impurities which were extracted more selectively or together with REE, and hence could potentially cross-contaminate products of the refinery were:

- Th^{4+}, Zr^{4+}, UO_2^{2+}, which were extracted preferentially to REE and could potentially foul the organic phase, requiring special regeneration procedures [14-16];
- Ferric ion, which was co-extracted with the heavy REE such as Lu and Yb, would require a high acid concentration strip (such as 6 M HCl) to be employed and could contaminate individual REE products in the final stages of refining;
- Aluminium and zinc, which cross-contaminated fractions of both the light and middle REE fractions and, when present in high quantities, could increase organic phase capacity requirements. Also, aluminium was reported to be responsible for the formation of cruds and emulsions in SX circuits when extraction capacity of EHEHPA for Al exceeded 5 g/L during operation at pH ~ 2 [17];
- Ca, Mg, Cu, Mn, Pb, and Si, which had no or an insignificant effect on the separation of REE, however, if present in high quantities, could cause difficulties with viscosity, phase separation, crud and emulsion formation [18, 19].

The level of impurities in the feed solution to the refinery and specifications of the REE products would ultimately determine the technology to be used and its position (before or after refining in the individual REE fractions) in the flow sheet.

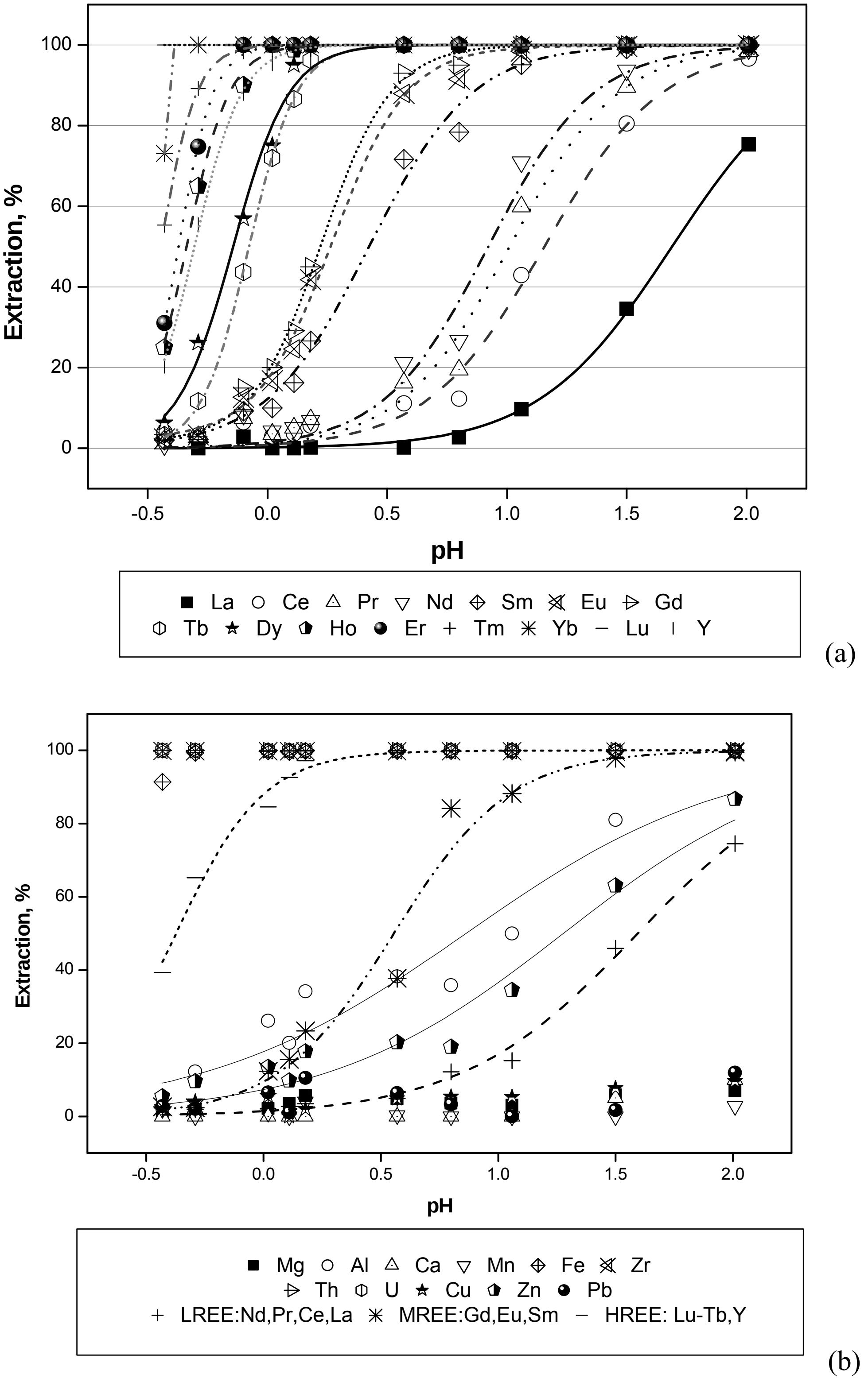

Figure 1. pH vs extraction isotherms for REE (a) and impurities (b).

Generalized Approach for Processing of REE Concentrates

A simplified flow sheet used for the treatment of the concentrates of the major REE minerals is presented in Figure 2.

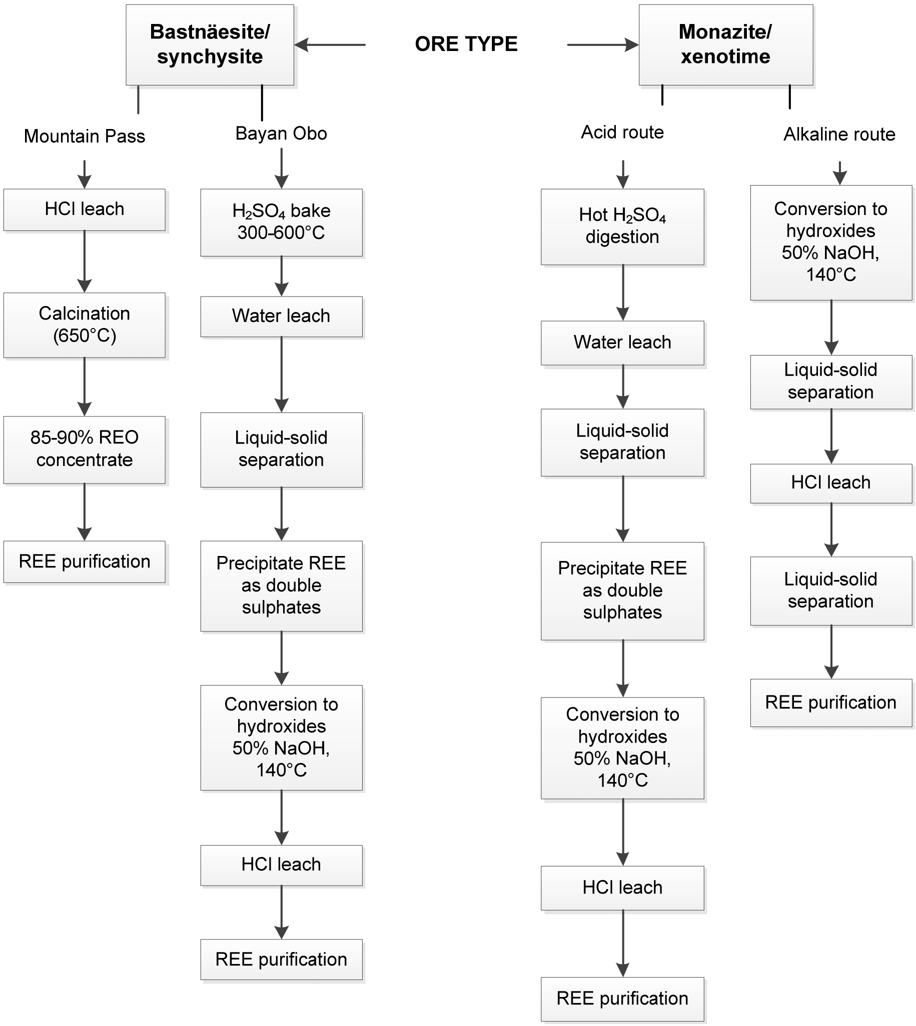

Figure 2. Examples of processing routes for separation of individual REE from major REE-bearing minerals [20].

It is typical for any conventional processing route to have a step of REE conversion into hydroxides. The process is called either depending on the type of REE concentrate (physical or chemical). REE concentrate is treated with 50% m/m NaOH solution at 140°C under atmospheric pressure. The residue is subsequently washed in order to remove new species formed. Cracking of the REE compounds and rejection or partial elimination of some impurities occurs under caustic leach conditions [21, 22].

$$Al(OH)_3 + NaOH = NaAlO_2 + 2H_2O \quad (1)$$

$$SiO_2 + 2\ NaOH = Na_2SiO_3 + H_2O \quad (2)$$

$$Zn(OH)_2 + 2\ NaOH = Na_2Zn(OH)_4 \qquad (3)$$

$$REEOH(F,PO_4,SO_4) + x\ NaOH = x\ NaF,\ Na_3PO_4,\ Na_2SO_4 + REE(OH)_3 \qquad (4)$$

Once the REE and associated impurities are present in the form of hydroxides, various approaches can be chosen for further purification.

Rare Earths Hydroxide Re-dissolution

Curves for pH vs degree of re-dissolution were generated for the dissolving of an intermediate REE hydroxide product (see composition in Table *IV*) in HCl at 20°C are presented in Figure 3.

Table IV. Composition of Intermediate REE Hydroxide Product

Element	La	Ce	Pr	Nd	Sm	Eu	Gd	Y	Dy
Concentration, %	18	23	1.3	3.9	0.2	0.02	0.09	0.5	0.03
Element	Ho	Er	Tm	Yb	Lu	Tb	Sc	TREE	
Concentration, mg/kg	31	101	22	49	11	89	0.05	47%	
Element	Na	Al	Si	S	Ca	Ti	Cr	Mn	Fe
Concentration, %	0.4	4.2	0.2	0.1	0.9	0.2	0.2	1.3	5.2
Element	Co	Ni	Cu	Zn	As	Cd	Th	U	
Concentration, %	0.08	0.21	0.13	0.18	0.34	0.04	0.05	0.2	

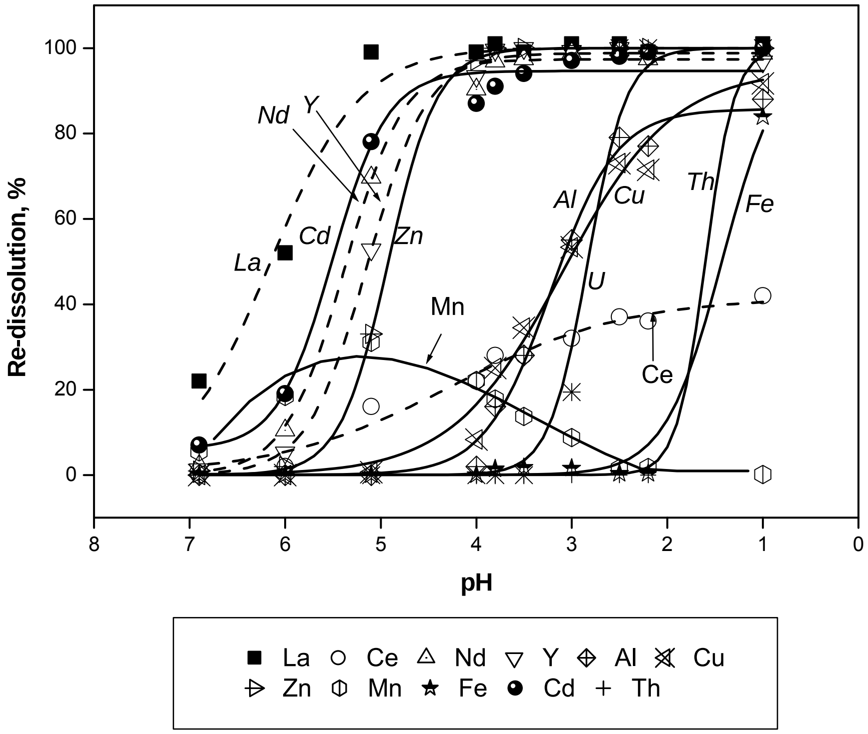

Figure 3. Re-dissolution of REE hydroxides and associated impurities vs pH in HCl medium.

The intermediate REE product was formed during REE precipitation from a leach liquor with 20 % m/m CaO slurry up to final pH of 8.5. Re-dissolution behaviour of the major REE is reported, namely, La, Ce, Nd and Y. The behaviour of some impurities was omitted in order to simplify the graph.

Re-dissolution of a sample of the intermediate REE hydroxide product was performed without the addition of reductant like SMBS or alcohol [23], which resulted in incomplete re-dissolution of cerium. The requirement of reductant addition to recover cerium, if needed, is governed by the type and amount of impurities present in the intermediate hydroxide product as well as by precipitation and drying conditions of such a product, as high pH values and elevated temperatures promote oxidation of cerium [8].

The sample used for evaluation of selective re-dissolution contained relatively high Mn and Ce values (see
Table IV). During re-dissolution test work the ORP of the slurry (with reference to Ag/AgCl) increased from 316 to 1080 mV with decreasing pH. The behaviour of Mn and Ce couple in this specific case was puzzling and has to be evaluated further. Presumably, Mn^{2+} started to re-dissolve at pH <6 and then due to oxidation to Mn^{4+} by Ce^{4+}, precipitated as MnO_2.

REE and impurities were re-dissolved in the following order:

Mg > La > Cd > Nd >Y> Zn ≈ Co ≈ Ni > Ce* >> Cu > Al > U > Fe, Th > Si, Ti, Cr*

*- in liquor were found in quantities close to detection limit

The composition of the liquors obtained after re-dissolution at pH 3.8 and 1.0 (for enhanced cerium re-dissolution) is given in Table V.

Table V. Composition of Re-dissolution Liquor

Major	Eh	La	Ce	Nd	Y	Al	Fe	Ca
pH 3.8, g/L	723	28.5	9.8	5.8	0.8	1.0	0.1	0.9
pH 1.0, g/L	1068	28.7	14.9	5.8	0.8	5.7	6.8	4.5
Minor	Mg	Co	Ni	Zn	Cu	Th	U	Mn
pH 3.8, mg/L	348	132	264	316	52	0	0.0	350
pH 1.0, mg/L	347	144	287	336	191	165	844	2

Re-dissolution at pH 3.8 of the intermediate sample allowed complete rejection of the following impurities: Th, U, As, Si, Ti, Cr, with almost complete elimination of Fe, Al and Cu. However, Zn, Ni, Cd and Co (of which Ni and Co are not shown on the graphs) followed the REE during re-dissolution. Further polishing of Zn, Ni, Cd, Co, and a portion of Al, Fe and Cu might be required.

In the case of this specific sample bulk re-dissolution with addition of a reductant might be required if complete recovery of cerium was targeted, this might change re-dissolution behaviour of impurities.

Rejection of Impurities via Precipitation

Precipitation is usually employed for the removal of relatively high levels of impurities. This option is usually attractive due to relatively easy implementation, low CAPEX and OPEX, simplicity of the operation and the absence of difficulties associated with such methods as solvent extraction (fire hazard, big environmental issues, etc.). However, precipitation has the following disadvantages which have to be accounted for if this option is considered for the removal of impurities from REE solutions, namely:

- Strict control of the process parameters is required;
- Losses of valuable metals (REE) due to co-precipitation;
- Polishing of an impurity to ppb levels might not be possible without major losses of the valuable metals.

The following precipitation procedures are usually applied for selective removal of impurities or selective REE precipitation:

- Precipitation with neutralizing agents (NaOH, NH_4OH, CaO, MgO, $CaCO_3$ as solution/slurry);
- Precipitation of base metal impurities with sulphides;
- Precipitation of Th, U, Zr as phosphates;
- Selective precipitation of REE as oxalates; and
- Removal of excessive concentrations of alkaline earth metals as sulphates.

Hydroxides and Carbonates

Various reagents could be used to precipitate a mixed intermediate REE hydroxide. Some of the potential hydroxide precipitation reagents were evaluated at 30°C. The results are presented in Figure 4.

CaO and MgO were added as 20 % m/m slurries, NaOH as 2 M and ammonia as 37 % solution. Precipitation of REE with 2 M Na_2CO_3 solution was also evaluated. The composition of the solution used for precipitation test work is given in Table VI. The pH value was gradually increased up to 9-10 and intermediate solution samples were taken at various pH values.

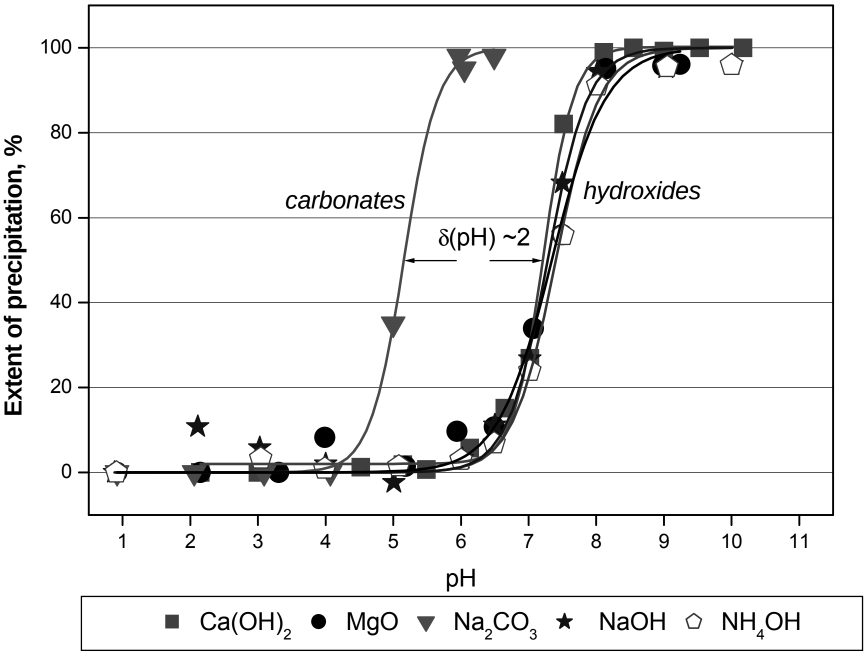

Figure 4. Precipitation of REE with various neutralizing agents.

Table VI. Composition of REE Chloride Solution used for Comparison of Different REE Hydroxide Precipitation Reagents and Carbonate Product, mg/L

Na	Mg	Al	K	Ca	Fe	Sr	Total REE
2653	129	10	849	71249	86	245	1024

There was no difference in the precipitation trends of the REE hydroxides with the various precipitants under the test conditions used. However, the reagent that was used, had an influence on the grade of the formed REE precipitate. In the case of sodium and ammonium hydroxides, the total REE content in the precipitate was ~40%, while the grade of REE hydroxide formed after neutralization with $Ca(OH)_2$ was lower at 33.9%. This was most probably due to unreacted lime (as the precipitate formed contained 9.1% Ca reporting to the solids).

It is well-known that MgO reactivity decreases at pH>6-6.5. In order to minimize Mg deportment into REE hydroxide a strict control of the precipitation procedure should be applied. It is advisable to precipitate REE up to pH 6.5 with MgO and then use lime (in the form of a 20 % m/m CaO slurry) to increase the pH value to 8.5-9.0.

When Na_2CO_3 was used for REE carbonate precipitation, complete REE removal was observed at 2 pH units lower than for REE hydroxides precipitation. The precipitate formed contained 50% Ca (feed solution had ~72 g/L Ca) and only 1 % REE.

The composition of the solution used for evaluation of the behaviour of various impurities and REE during precipitation as hydroxides (with 20% m/m CaO slurry) and carbonates (with 2 M Na_2CO_3) is given in Table VII.

Table VII. Composition of Leach Solution Containing Impurities and REE, mg/L

Mg	Al	Ca	Cr	Mn	Fe	Ni	Cu	Th	U	Si	Total REE, g/L
0.3	2.0	5.7	0.04	0.06	0.82	0.06	2.8	0.6	0.08	0.1	**46.4**

Precipitation behaviour of impurities and total REE vs pH is shown in Figure 5. Comparison of pH_{50} values for precipitation of individual impurities and REE with lime and carbonates is given in Table VIII.

Table VIII. pH50 Values for Precipitation of impurities and REE as Hydroxides and Carbonates

	Mg	Mn	Co	Ni	REE	Cu	Si	Al	Cr	Fe	Th
hydroxides	9.4	7.6	6.8	6.8	6.9	4.5	4.2	4.2	4.2	4.2	4.3
carbonates	9.4	6.7	5.8	6.2	4.8	4.43	2.3	2.0	2	1.6	1.6
ΔpH_{50}	0	0.9	1	0.6	2.1	0.07	4.2	2.2	2.2	2.57	2.7

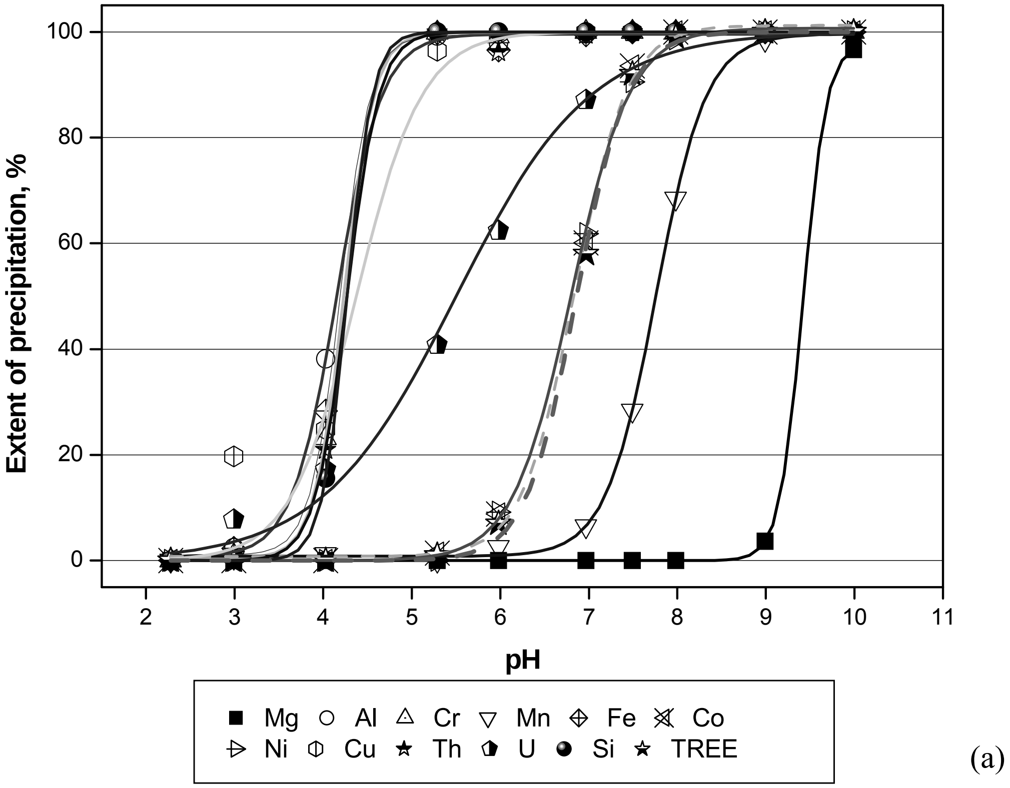

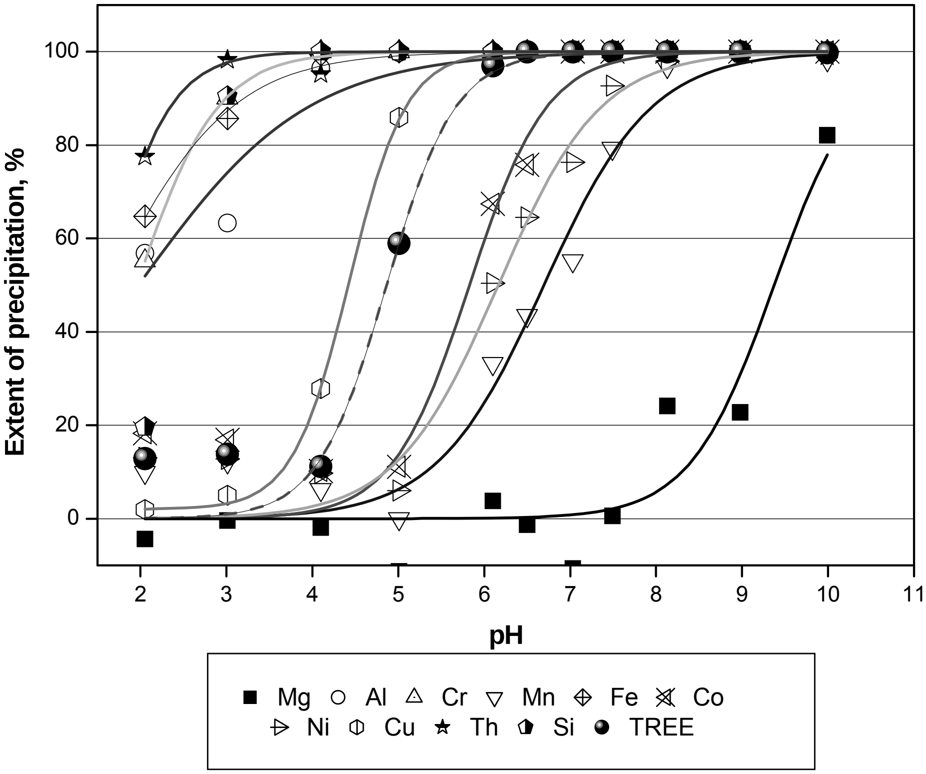

(b)

Figure 5. Precipitation of impurities and REE as (a) hydroxides and (b) carbonates.

The pH_{50} values for precipitation shifted into a more acidic region when carbonate was used as precipitating agent instead of lime (see Table VIII). The relatively large difference in precipitation behaviour of hydroxides and carbonates of the REE and various impurities indicates that it would be beneficial to use limestone ($CaCO_3$) in order to neutralize excess acid and precipitate impurities such as Th, Fe, Cr, Si, Al at pH~3-3.5. These impurities could then be removed and the REE precipitated as hydroxides at pH 8-8.5.

Phosphates

One of the known approaches for the removal of some impurities is precipitation of these as phosphates. Solubility constants of various critical elemental phosphates are given in Table IX [24, 25].

Properly controlled precipitation (phosphate addition and pH control) should allow minimizing Zr, Th and U deportment to the REE streams. Treatment of Th hydroxides with phosphoric acid or phosphates is used for stabilization of thorium wastes in the environment [26].

Table IX. Solubility Product Constants (Ksp) of Some Phosphates

Compound	**K_{sp}**
$Zr_3(PO_4)_4$	132
$Th_3(PO_4)_4$	79
$(UO_2)_3(PO_4)_2$	47
$CePO_4$	23
$LaPO_4$	22
YPO_4	25
$AlPO_4$	18
$FePO_4$	22

Oxalates

Oxalate precipitation is a well-known analytical procedure to recover pure rare earths from solution. Along with Th, Ca, Sr and Ba, the REE form the most insoluble oxalates. REE precipitation as oxalates can partition between the rare earths on the one hand and Si, Mn, Fe, Cu, Al and Zn on the other [22]. However, strict control of oxalic acid addition should be in place in order to avoid co-precipitation of impurities [27]. Fluorides and phosphates usually are co-precipitated with REE oxalates, thus, their presence in the feed liquor has to be avoided.

Currently, this method is not an attractive option for intermediate REE product production due to its high costs.

Sulphides

A combination of neutralization and sulphide addition (using NaSH) was reported to be applied successfully for simultaneous removal of aluminium (90%) and Cu, Pb, Zn, etc from REE liquor [28]. Solubilities of base metal sulphides as well as some REE are given in Table X.

Based on this information Cu, Pb, Zn, Co and Ni could be removed as sulphides.

Alkaline Earth Metals Removal

Excessive concentrations of Ca, Sr and Ba in REE chloride liquors could be removed by precipitation as sulphates (see solubility constants in Table XI).

Radioactive Ra is removed by co-precipitation with $BaSO_4$. Lead could also be removed as a sulphate.

Precipitation Summary

The selection of a precipitation agent should be governed by the composition of the leach liquor. It has to be noted that the presence of sulphates, fluorides and phosphates in some cases could interfere with selective impurity removal, especially when pH is a critical parameter.

Table X. Solubility Product Constants (Ksp) of Some Sulphides [29]

Formula	pK_{sp}
CoS	20
CuS	35
FeS	17
MnS	10 (amorphous) 13 (crystalline)
NiS	19
ZnS	24
Al_2S_3	7
La_2S_3	13
Ce_2S_3	10
PbS	27
Y_2S_3	moderately water and acid soluble

Table XI. Solubility Product Constants (Ksp) of Some Sparingly Soluble Sulphates [29]

Formula	pK_{sp}
$BaSO_4$	10
$CaSO_4$	4
$SrSO_4$	6
$RaSO_4$	10
$PbSO_4$	8

Solvent Extraction

Impurities such as Cu, Ni, Co, Zn, Fe, Al, U, Th, Zr, Ca, Mn, Mg, etc. have to be dealt with during the processing of REE, and selective removal of these is crucial when targeting high purity REE products. Various solvent extractants can be employed for this purpose. Some examples are briefly described.

Organophosphorous Acids

It is generally accepted that the commercial separation of the rare earths is best accomplished by use of organophosphorous acid extractants. Commercially available extractants of this type include di-(2-ethylhexyl) phosphoric acid (DEHPA), 2-ethylhexyl 2-ethylhexyl phosphonic acid (PC-88A, Ionquest 801) and 2,4,4-trimethylpentyl phosphinic acid (Cyanex 272) [30]. These extractants are also employed for various base metal extractions such as cobalt from nickel sulphate, separation of zinc from impurities such as copper and cadmium, the recovery of uranium and vanadium, and extraction of thorium [31].

Preliminary studies on the extraction of REE (100 g/L total REE) from a simulated chloride solution containing some impurities using 30 vol.% PC-88A in Shellsol D70 were done at Mintek. Results were presented at the beginning of the paper in Figure 1. pH_{50} values (the pH at which 50% of the metal originally in the feed solution was extracted) achieved for each element present in the liquor are listed in Table XII.

The strong extraction of Zr^{4+}, Th^{4+}, UO_2^{2+} and Fe^{3+} (pH_{50} values of lower than -0.4) indicated that these metals would be extracted together with the heavy rare earth fraction (pH_{50} values between <-0.4 and -0.24) under the test conditions employed.

Table XII. Extraction of Metals from REE Chloride Solution Spiked with Impurities by 30 vol.% PC-88A in Shellsol D70 at Ambient Temperature

Metal ion	pH_{50}	Metal ion	pH_{50}
Zr^{4+}, Fe^{3+}, Th^{4+}, UO_2^{2+}	<-0.4	Nd^{3+}	0.94
Ca^{2+}, Mg^{2+}, Mn^{2+}	>2.0	Pr^{3+}	1.00
Zn^{2+}	1.30	Sm^{3+}	0.38
Al^{3+}	1.06	Eu^{3+}	0.25
Cu^{2+}, Cd^{2+}, Ni^{2+}, Co^{2+}, Cr^{3+}	>2.0	Gd^{3+}	0.29
Y^{3+}	-0.31	Ho^{3+}	-0.24
La^{3+}	1.69	Yb^{3+}	<-0.4
Ce^{3+}	1.14	Lu^{3+}	<-0.4

However, a SX purification circuit could be designed in order to extract Zr^{4+}, Th^{4+}, UO_2^{2+} selectively and possibly Fe^{3+} from the REE. The stripping of these metals would have to be investigated and optimised in order to separate them efficiently from the co-extracted rare earths. According to the literature, Th and Zr could be stripped selectively from DEHPA by sulphuric acid after stripping of REE with 3.5 M HCl [14, 15]. The main drawback of removing these impurities with PC88A is the low acidity required for selective extraction.

Bulk extraction of REE with PC88A would allow rejection of alkaline earth metals and base metals like Cu, Cd, Ni, Co and Cr.

Mintek performed some scouting test work on behaviour of impurities and some REE during extraction with various organophosphorous reagents from chloride medium. Two synthetic solutions were prepared with equimolar amounts of impurities (Feed 1) and REE (Feed 2) in ~3 M chloride background. These compositions are given in Table XIII.

Table XIII. Average Feed Composition

Feed 1: Impurities		Feed 2: Rare Earths	
Element	Concentration, g/L	Element	Concentration, g/L
Al	0.5	La	2.2
Cu	1.2	Ce	2.0
Fe	1.0	Pr	1.3
Mn	1.0	Nd	1.4
Th	4.4	Gd	2.6
U	6.4	Dy	1.7
Zn	1.2	Ho	2.5
Zr	1.7	Y	1.5

Equilibrium distribution curves (S-curves) for pH versus extraction were generated to determine the possibility of selective extraction of impurities or bulk REE extraction while rejecting most impurities. A comparison of pH vs extraction curves achieved for impurities and REE with 20 vol.% DEHPA, PC88A and Cyanex 272 in Shellsol A150 at ambient temperature is shown in Figure 6 and Figure 7, respectively. The pH_{50} values achieved for impurities and REE are summarized in Table XIV.

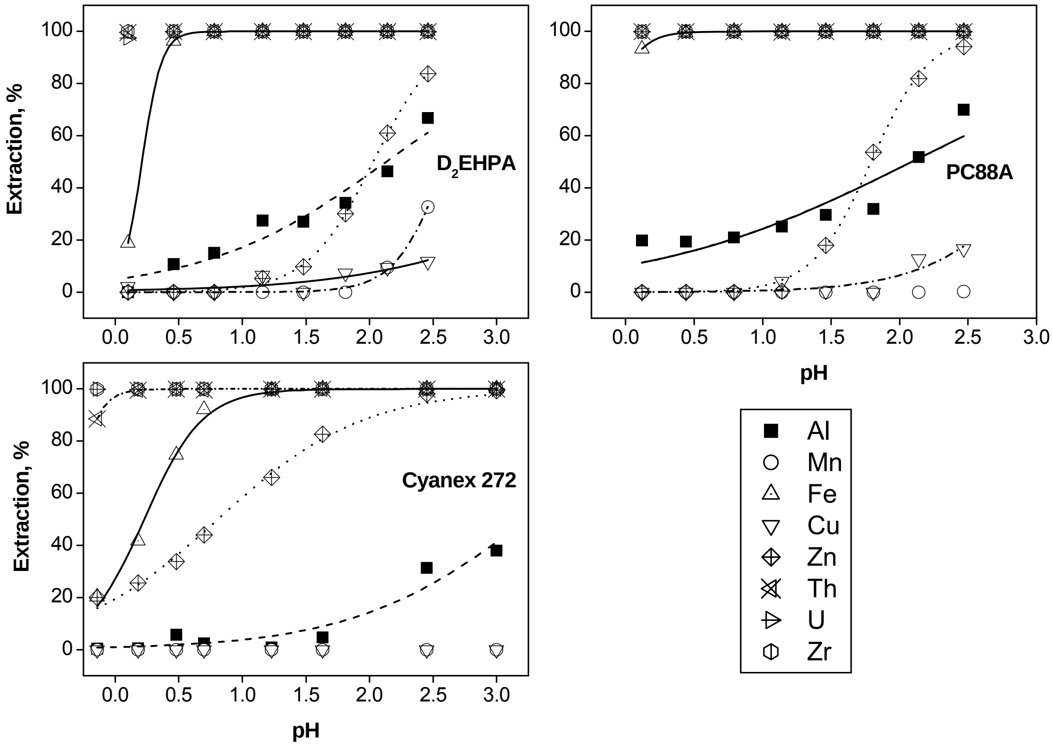

Figure 6. Extraction of some impurities using various organophosphorous reagents of 20 vol % concentration from chloride liquor at ambient temperature.

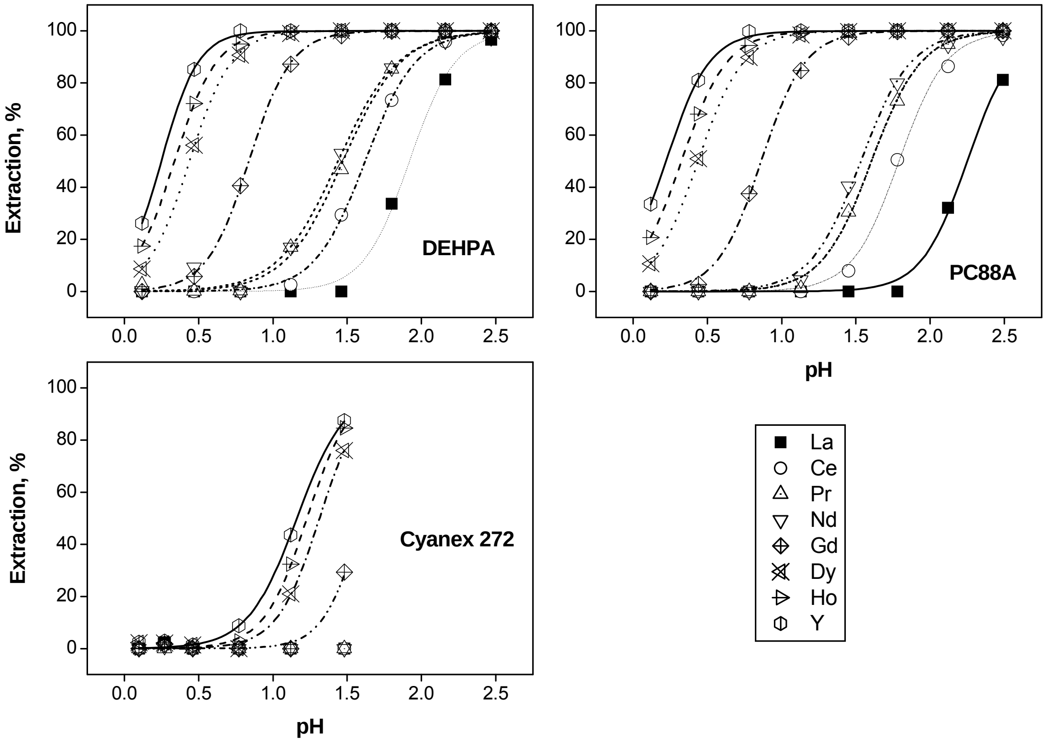

Figure 7. Extraction of some REE using various organophosphorous reagents of 20 vol % concentration from chloride liquor at ambient temperature.

Table XIV. pH_{50} Values for Some Impurities and REE Using Different Organophosphorous Reagents (20 vol% in ShellSol D50)

Impurity	pH_{50} value			Rare earth	pH_{50} value		
	DEHPA	PC88A	Cyanex 272		DEHPA	PC88A	Cyanex 272
Al	2.20	2.11	>3.0	La	1.92	2.25	>1.48
Mn	>2.46	>2.47	>3.0	Ce	1.62	1.79	>1.48
Fe	0.24	<0.00	0.26	Pr	1.47	1.61	>1.48
Cu	>2.46	>2.47	>3.0	Nd	1.44	1.53	>1.48
Zn	2.02	1.77	0.84	Gd	0.84	0.86	>1.48
Th	<0	<0	<-0.14	Dy	0.44	0.44	1.31
U	<0	<0	<-0.14	Ho	0.34	0.33	1.23
Zr	<0	<0	<-0.14	Y	0.25	0.22	1.16

Extraction of REE by organophosphorous reagents was shifted into a more basic pH region in the following order: DEHPA → PC88A → Cyanex 272. The trend in impurities behaviour varied for some elements, for example, extraction of Fe, Th, U and Zr followed similar trends as REE while Zn was extracted more efficiently with Cyanex 272 at a lower pH value than with PC88A or DEHPA. This anomaly will have to be confirmed before any final conclusions can be drawn.

All organophosphorous reagents tested showed selectivity for Th, U and Zr over REE. Removal of these impurities with Cyanex 272 might be beneficial due to easier stripping. It was reported that Cyanex 272 could be employed successfully for selective uranium and thorium separation from REE [32, 33]. According to the pH_{50} values achieved it might also remove ferric selectively.

Bulk extraction of REE with organophosphorous reagents could allow rejection of alkaline earths metals as well as some base metals due to the relatively large difference in pH_{50}.

Carboxylic Acids

Extractants of the carboxylic type are not as widely used as their organophosphorous counterparts, but has found some application in the hydrometallurgical processing of various metals, including base metals and REE [34]. From a practical point of view, these reagents are relatively inexpensive and readily available. The order of metal extraction depends to some extent upon the identity of the carboxylic acid but, in general, decreases through the series:

$$Zr^{4+} > Fe^{3+} > Th^{4+} > Al^{3+} > UO_2^{2+} > Cu^{2+} \approx Pb^{2+} \approx Y^{3+} \approx Ln^{3+} > Cd^{2+} \approx Zn^{2+} > Ni^{2+} > Co^{2+} \approx V^{2+} > Mn^{2+} \approx Fe^{2+} > Ca^{2+} > Sr^{2+} > Ba^{2+} > Mg^{2+}$$

(where Ln^{3+} denotes the trivalent lanthanides) [34].

It is therefore indicated that the removal of some impurities such as U, Zr, Fe, Th and Al could be possible from REE solutions prior to separation of the latter.

The values for pH_{50} for the extraction of some metals (0.05 M) from nitrate solutions (1.0 M) by Versatic 10 and naphthenic acids (0.50 M each, two commercially available carboxylic acids) in xylene at 20ºC are given in Table XV [34].

Table XV. Extraction of Some Metals by 0.50 M Solutions of Carboxylic Acids in Xylene at 20ºC

Metal ion	pH_{50}		Metal ion	pH_{50}	
	Versatic 10 acid	Naphthenic acid		Versatic 10 acid	Naphthenic acid
Fe^{3+}	1.84	1.83	Ce^{3+}	5.65	4.72
Sc^{3+}	2.81	2.71	Nd^{3+}	5.54	4.61
Th^{4+}	2.84	2.34	Gd^{3+}	5.36	4.52
UO_2^{2+}	3.41	3.48	Ho^{3+}	5.22	4.51
Al^{3+}	3.53	3.35	Yb^{3+}	5.05	4.53
Cu^{2+}	4.01	3.77	Mn^{2+}	6.75	6.20
Y^{3+}	5.32	4.64	Ca^{2+}	7.42	6.64
La^{3+}	5.80	4.86	Mg^{2+}	8.11	7.43

It can be seen that Fe, Th, U and Al could possibly be extracted (pH_{50} values from about 1.84 for Fe to 3.53 for Al) without co-extraction of the REE (of which pH_{50} values start from about 4.53 for Yb^{3+} using naphthenic acid and 5.05 when using Versatic 10 acid) under conditions used. In previous studies with carboxylic acids, it was found that there were negligible differences in the pH_{50} values for extraction of some metals (Co, Ni, Cu, Zn, Pb, Cd, Al and Fe^{3+}) from sulphate, chloride or nitrate solutions [35]. In principle, this could be further optimised and applied to real REE feed solutions in the required medium and operating conditions.

The results of test work recently performed at Mintek using a simulated feed solution containing about 100 g/L total REE and some impurities (see Table XVI, relative concentrations of various REE was the same as in Table III) in chloride medium using 20 vol.% naphthenic acid in ShellSol D70 are summarised in Table XVII and presented in Figure 8.

Table XVI. Composition of the Liquor Used for Naphthenic Acid Performance Evaluation

Elements, g/L															
Total REE	Th	U	Zr	Fe	Al	Cr	Mn	Co	Ni	Cu	Zn	Cd	Pb	Ca	Mg
100	0.2	0.2	0.2	0.5	0.5	0.05	0.1	0.1	0.1	0.1	0.1	0.05	0.05	1	1

Table XVII. Extraction of Metals from Chloride Solution by 20 vol.% Naphthenic Acid in ShellSol D70 at Ambient Temperature

Metal ion	pH_{50}	Metal ion	pH_{50}
Zr^{4+}	1.34	Nd^{3+}	4.28
Fe^{3+}	1.96	Pr^{3+}	4.32
Th^{4+}	2.14	Sm^{3+}	4.06
Al^{3+}	3.32	Eu^{3+}	4.08
Cu^{2+}	3.23	Gd^{3+}	4.17
Y^{3+}	4.37	Ho^{3+}	4.20
La^{3+}	4.58	Yb^{3+}	4.03
Ce^{3+}	4.44	Lu^{3+}	4.04

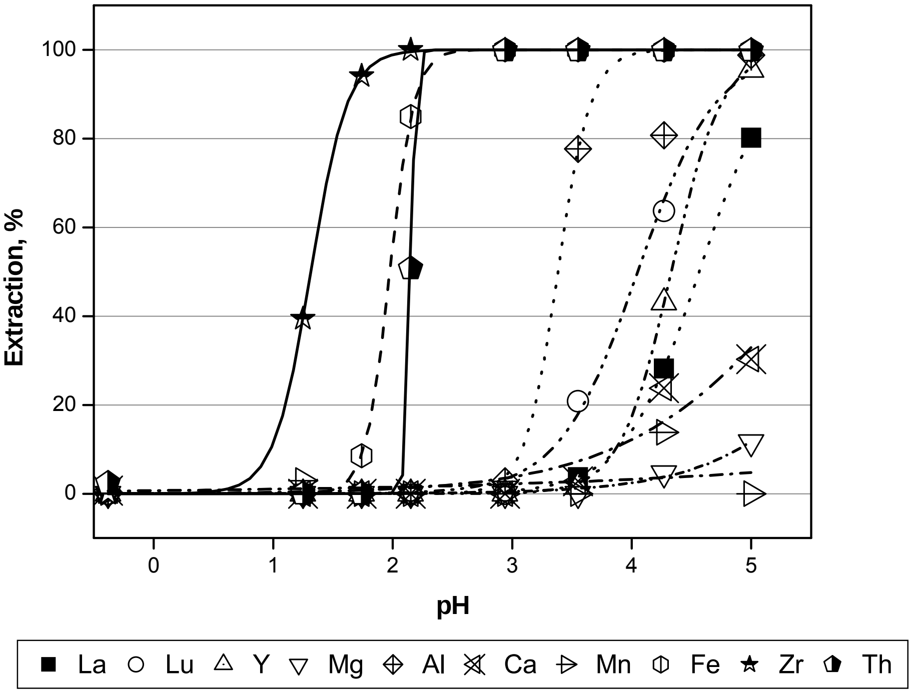

Figure 8. Extraction of some impurities and REE using 20 vol % naphthenic acid from chloride liquor at ambient temperature.

Metal impurities such as Zr, Fe^{3+}, Th, Al and Cu were more strongly extracted (with pH_{50} values between 1.34 and 3.23) than the most strongly extracted REE, namely Lu (with pH_{50} value of 4.04). The pH_{50} values for Mg, Ca, Mn, Co, Ni, Zn, Cd and Pb were >5.0, which could indicate that these metals would not interfere in the REE separation process.

Although this could indicate a possible separation between certain impurities and REE in the specified solution, crud formation and slow phase separations were observed during the test work which made the application of these systems questionable.

Ion Exchange

Cation and Anion Exchangers

Separations of REE and impurities with a straightforward ion exchange (simple cation or anion exchange) are based on the difference in complex formation by the impurity metals and REE. For example, Fe, Zn and Cu can form anionic complexes $FeCl_4^-$, $ZnCl_3^-/ZnCl_4^{2-}$ and $CuCl_3^-/CuCl_4^{2-}$, at HCl or chloride concentration of 0.1-0.5 M, while REE form cationic complexes ($MeCl_2^+$, $MeCl^{2+}$) even in 2-4 M HCl [36].

Strong acid cation-exchangers have been used for the separation of Th^{4+} from REE and other metals in analytical practice [37, 38, 39]. The principle of selective elution was applied. The majority of the base metals and rare earths adsorbed by the resin can be eluted with 3-5 M HCl, while Th can be eluted with 10 M HCl or 3 M H_2SO_4, as well as with 5 M HNO_3, ammonium oxalate, ammonium carbonate or ammonium sulphate solutions.

The potential of the removal of some impurities represent as anionic complexes with anion exchange resins was confirmed by Mintek. During screening of various resins for either selective REE upgrade or selective impurities removal (chloride liquor, pH 3.5, total REE 2.9 g/L, 8 g/L Ca, 2.1 g/L Al, 1.3 g/L Mn, 0.1 g/L Fe, 1.2 g/L Sr, 0.13 g/L Zn) it was identified that a strong base anion exchange resin possessed minimal adsorption capacity for REE and base metals present in solution. Only 1 g/L Zn was loaded onto the resin phase at 4 mg/L in the barren in this specific screening test. Zinc adsorption by anion exchange resin presumably occurred due to the tendency of Zn to form $ZnCl_3^-$ and $ZnCl_4^{2-}$ complexes under the conditions tested.

However, extraction of impurities as anionic complexes with anion exchange resins from chloride liquor would be a challenging approach, as speciation of the elements would be strongly dependent on total chloride and element concentration, ionic strength of the liquor and pH.

Chelating Ion Exchangers

For the removal of U, Th, Fe(III), Cr(III), Cu, Ni, Co, Mn from REE chelating ion exchangers with various functional groups including phosphinic, phosphonic, phosphate, iminodiacetate, aminophosphonic, and carboxylic groups could be used [39, p. 121]. Typically the ion exchange approach has been applied for analytical purposes and limited information is available in the public domain with regard to impurities removal from high tenor REE chloride liquors (>>5 g/L total REE).

Ion exchangers with phosphonic acid functional groups effectively absorb REE(III), U(VI) and Fe(III). It was stated that U(VI) and Th(IV) could be separated selectively from REE using phosphonic ion exchangers such as Duolite ES-63 and Purolite S-950 by both the frontal analysis technique and elution with mineral acids [39 p. 121, 40]. In order to elute uranium from aminophosphonic Amberlite IRC 747 it was treated with 2 BVs of 1 M NH_4OH followed by 1 M Na_2CO_3 [41].

Mintek conducted some scouting test work to evaluate various resins for the selective removal of impurities from various rare earths solutions. It was identified that:

- Conditions for selective impurity removal with commercially available ion exchange resins were highly dependent on liquor composition and have to be optimized for each system;
- Selectivity for Th, U, Zr and Fe over REE can be achieved at pH values <<1 with aminophosphonic resin S950 and resins impregnated with DEHPA and Cyanex 272 (Lewatit OC1026 and TP272);
- High selectivity usually implies requirement for a complexing eluting agent or procedure (EDTA, citric acid, combination of eluting agents, etc.).

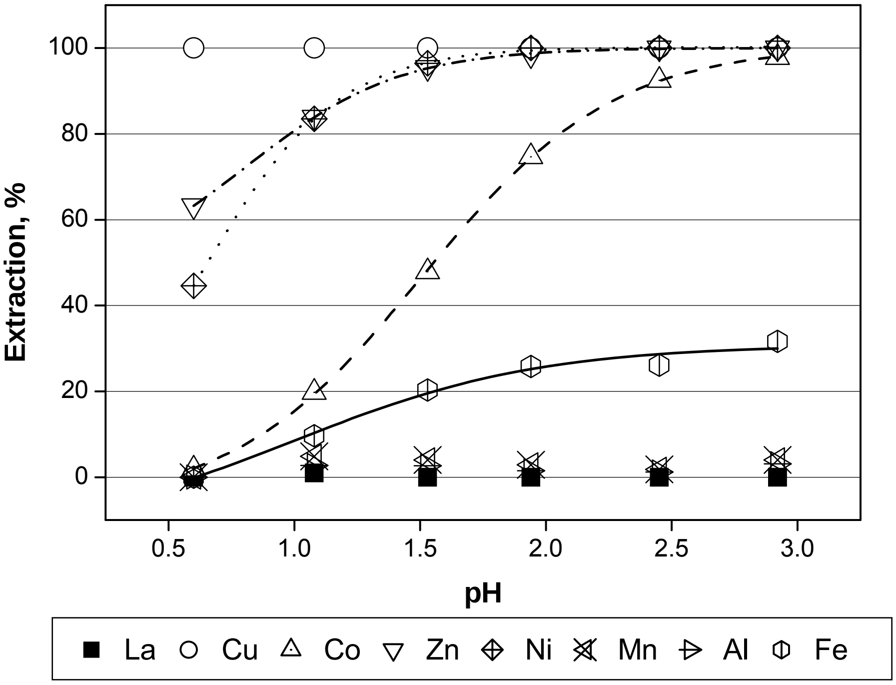

Figure 9. pH vs extraction for base metals impurities and lanthanum with chelating ion exchange resin.

During test work done at Mintek, an ion exchange chelating resin was identified which could be selective for Cu, Zn, Ni and Co over REE. Extraction equilibrium data (S-curves) generated using chloride solution containing about 50 mg/L each of Cu, Co, Zn, Ni, Mn, Al, Fe and 20 g/L La and this commercially available ion exchange resin, is presented in Figure 9.

It can be seen that selective removal of Cu, Zn, Ni and Co could be achieved without extraction of REE. The elution procedure for this resin is fully established and used in practice for other applications where selective Cu and Ni recovery are done.

Solvent Impregnated Resins

There is a number of commercially available solvent impregnated resins (SIRs), which potentially could be used for the removal U, Th, Zr and Fe from REE liquors to very low levels (<0.1 mg/L), namely, Lewatit OC1026 (DEHPA impregnated resin) and Lewatit TP272 (Cyanex 272 impregnated resin) [42].

Eichrom produces special types of resins for analytical separations of REE and selective extraction of radioactive elements [43]:

- RE Resin and TRU Resin consist of 1 M octyl(phenyl)-N,N-diisobutylcarbamoyl-methylphosphine oxide (CMPO) in tributyl phosphate(TBP) coated on an inert methacrylic polymeric support. The difference between these two products is in CMPO ratio (RE Resin has higher content).
- Ln Resin contains di(2-ethylhexyl) orthophosphoric acid (HDEHP) and is used for REE separation in nitric acid medium
- TEVA and UTEVA resins containing an aliphatic quaternary amine and diamyl-amylphosphonate are used for selective recovery of actinides.

Eichrom resins are used for analytical and environmental purposes only. Their application in metallurgical practice has to be evaluated. Typically, these products have high costs and often have to be incinerated in order to recover the selectively extracted element. Also, it should be mentioned that SIRs are characterized by lower adsorption capacity and can have shorter lifetime compared with the common ion exchange resins [39 p. 127].

Conclusions

Separation of rare earths elements (REE) is a difficult task. Removal of impurities prior to REE refining could also be challenging. A centralised REE refining facility would receive concentrates from various sources and, hence, should be able to handle numerous impurities. Various approaches applicable for the removal of the main impurities in a pre-refining purification plant are summarized in the Table XVIII.

Table XVIII.

Impurities	Treatment with caustic	REE Selective Re-dissolution	Precipitation	Solvent Extraction	Ion Exchange
Fluorides, sulphates, phosphates	140°C, 50 % NaOH	-	as insoluble species (i.e. $CaSO_4$)	-	-
Th, Zr, U, Fe^{3+}	-	pH>3, optimum temperature	phosphates/ hydroxides/ carbonates	Organophosphorous reagents	Phosphorous containing reagents Special resins (TEVA, UTEVA)
Al	140°C, 50 % NaOH (+Zn & Si)	pH>4, optimum temperature (+Cu)	hydroxides/ carbonates	-	-
Cu, Pb, Zn, Co, Ni	-		sulphides, hydroxides (for Cu)	Bulk REE extraction (except for Zn) with organophosphorous reagents	Chelating resin (Pb was not evaluated)
Ca, Mg, Ba, Sr	-		sulphates	Bulk REE extraction with organophosphorous reagents	-

Development of an appropriate flowsheet for the pre-purification of a REE refinery feed is a complex and challenging target. It is governed by a feed composition and final products specifications, but also associated costs, REE losses, and implications that it might have on the downstream refining process and costs.

In order to develop a suitable flowsheet for the pre-purification of a REE refinery feed, the following aspects would have to be considered:

- Identify the sources and compositions, especially with regards to impurities, of intermediate REE products that would feed the REE refinery for at least 5-10 years;
- Implement an effective quality control system for the intermediate REE product;
- Develop suitable operating windows for the different impurity removal unit operations;
- A qualified research and development team should form a part of centralized refinery in order to effect troubleshooting when required;

- Comprehensive understanding of the process economics and how it could be optimised with variations in the market requirements, as well as accepting other intermediate products for processing.

References

1. The IMC Consortium “Eliminating the Rare Earth Industry Bottleneck” by P. Wong , G. Hatch November 2012, retrieved from http://mric.jogmec.go.jp/kouenkai_index/2012/briefing_121109_4.pdf

2. Retrieved from http://en.wikipedia.org/wiki/Rare_earth_mineral

3. N. V. Thakur “Separation of Rare Earths by Solvent Extraction”, *Mineral Processing and Extractive Metallurgy Review: An International Journal*, Vol. 21 (2000), 277-306.

4. S.B. Castor, J.B. Hedrick “*Rare earth elements*”, Industrial Minerals and Rocks: Commodities, Markets, and Uses, 7th edn, Society for Mining, Metallurgy, and Exploration, Littleton, CO (2006) 769–792.

5. Chu Yong Cheng, K. Soldenhoff, M. Vaisey “Development of a solvent extraction process for the production of pure neodymium oxide from synthetic Mt Weld Process liquor”, *Proceedings of the International Solvent Extraction Conference*, (2002), 1082-1088.

6. H. Liu, R. H. Byrne “Rare Earths and Yttrium Phosphate Solubilities In Aqueous Solution”, *Geochimica et Cosmochimica Acta*, Vol. 51 (1997), 1625-1633.

7. A. A. Migdisov, A.E. Williams-Jones, T. Wagner “An Experimental Study Of The Solubility And Speciation Of The Rare Earth Elements (III) In fluoride- And Chloride-Bearing Aqueous Solutions At Temperatures Up To 300°C”, *Geochimica et Cosmochimica Acta* 73 (2009) 7087–7109.

8. *Chemistry and technology of rare and scattered elements* Part II. Ed by K. Bolshakov, Moscow, 1976, P. 360.

9. *Lanthanide and Actinide Chemistry* by Simon Cotton, John Wiley & Sons, 30 Jan 2007 - Science –P. 280.

10. Eunyoung Kim, K. Osseo-Asare “Aqueous stability of thorium and rare earth metals in monazite hydrometallurgy: Eh–pH diagrams for the systems Th–, Ce–, La–, Nd– (PO_4)–(SO_4)–H_2O at 25 °C”, *Hydrometallurgy*, 113-114 (2012), pp. 67–78.

11. A. A. Migdisov, A.E. Williams-Jones “Pectrophotometric study of Nd(III), Sm(III) and Er(III) complexation in sulfate-bearing solutions at elevated temperatures”, *Geochimica et Cosmochimica Acta*, Vol. 72 (2008) pp. 5291–5303.

12. M. Fainerman-Melnikova, E. Hio, K. Soldenhoff “Impact of Sulphate Medium on the Extraction Of Rare Earths With Organophosphorous Reagents”, *Proceedings of the International Solvent Extraction Conference,* (2011), Chapter 3, 7 p.

13. Z. Yongqi et al. “Study On Thorium Recovery From Bastnaesite Treatment Process”, *J. Of Rare Earths*, Vol. 30, No. 4 (2012), 374–377.

14. B. R. Reddy, et al. “Solvent Extraction of Zirconium(IV) From Acidic Chloride Solutions Using 2-Ethyl Hexyl Phosphinic Acid Mono-2-Ethyl Hexyl Ester (PC-88A)”, *Hydrometallurgy*, 72 (2004) 303-307.

15. S. Muthuchamy, et al. “Application of Solvent Extraction Technique For The Separation Of Rare Earths, Thorium And Uranium”, *Proceedings of the International Symposium on Solvent Extraction,* (2002), 511-523.

16. US7282187 B1 “Recovery of Metal Values”, 2007.

17. WU Wenyuan, et al. “Formation Mechanism of Micro Emulsion On Aluminum And Lanthanum Extraction In P507-HCl System”, *J. Of Rare Earths*, Vol. 28, (2010), 174-178.

18. B. Grinbaum “An Integrated method for Development and Scaling up of Extraction Processes”, Published in “*Ion Exchange and Solvent Extraction*”, Y. Marcus, A. Sangupta (eds.), vol. 15, Elsevier, 2002.

19. G. Miller “Contamination Management in Solvent Extraction Plants”, *2011, Ni-Co-Cu Contents, ALTA Proceedings,* (2011), 218-232.

20. “Rare Earth Elements”, British Geological Survey, November 2011. www.mineralsuk.com

21. E. P. Lokshin, et al. “Desulfation of Rare-Earth Concentrates”, *Russian Journal of Applied Chemistry*, Vol. 79, (2006), 534-538.

22. “Extractive Metallurgy of Rare Earths” by C.K.Gupta, N. Krishnamurthy, 2005, CRC Press, 522 P.

23. US 3111375 “Process For Separation of Thorium, Cerium And Rare Earths Starting From Their Oxides And Hydroxides”, 1963.

24. E. Kim, K. Osseo-Asare “Aqueous stability of thorium and rare earth metals in monazite hydrometallurgy: Eh–pH diagrams for the systems Th–, Ce–, La–, Nd– (PO_4)–(SO_4)–H_2O at 25 °C”, *Hydrometallurgy*, (2012), 67–78.

25. X. Liu, R.H. Byrne “Rare Earth And Yttrium Phosphate Solubilities In Aqueous Solution”, *Geochem. Et Cosmochem. Acta*, V. 61, (1997), 1625-1633.

26. US 5403565 “Thorium phosphates prepared by insolubilization of soluble thorium compounds”, 1995.

27. R. Chi, Z. Xu “A Solution Chemistry Approach to the Study of Rare Earth Element Precipitation by Oxalic Acid”, *Metallurgical and Materials Transactions B*, V. 30B, (1999), 189-195.

28. C. Ruan, et al. “Recovering RE from leaching liquor of rare earth ore by extraction”, *Transactions of Nonferrous Metals Society of China*, (1995), 36–40.

29. “Analytical Chemistry Handbook” by J. Lurije, Moscow, 1971, 456 P. (in Russian)

30. F.M. Doyle, et al. “Direct Production of Mixed, Rare Earth Oxide Feed for High Energy-Product Magnets in Rare Earths and Actinides”, *Science, Technology and Applications IV*, (2000), 31-44.

31. M.J. Nicol, et al. “Comprehensive Coordination Chemistry, The Syntheses, Reactions, Properties and Applications of Coordination Compounds”, Ed. Sir Geoffrey Wilkinson, FRS, Volume 6, Applications, 1987, pp. 792-802.

32. B. Rajeswari, et al. “Role of Cyanex-272 As An Extractant For Uranium In The Determination Of Rare Earths by ICP-AES”, *J. of Radioan. & Nuclear Chem.*, Vol. 254, (2002), 479–483.

33. Eskandari Nasab, et al. “Determination of optimum process conditions for solvent extraction of thorium using Taguchi method”, ., Vol. 287, N 1, 2011, pp. 239-245.

34. J.S. Preston “Solvent extraction of metals by carboxylic acids”, *Hydrometallurgy*, (1985), 171-188.

35. A.W. Fletcher, et al. In “Solvent Extraction Chemistry of Metals”, London, 1965, p. 359.

36. Rimskaya-Korsakova, et al. “Concentration Of Lanthanides During Analysis Of Natural Sulphides”, *Herald of Moscow University*, N 2, *Chemistry*, V. 42, No 4, (2001), 255-269. (in Russian).

37. G. Guo, et al. “Separation and Continuous Determination Of The Light Rare Earth Elements And Thorium In Baotou Iron Ore By A Micro-Column”, *J. Radioanal. Nucl. Chem.*, Vol. 281, (2009), 647-651.

38. Han Suk Choi, Young Gu Ha “Ion-Exchange separation of Thorium in Monazite*”, J. of the Korean Chemical Society*, Vol.5, (1961), 56-59.

39. “Ion Exchange Technologies” edited by Ayben Kilislioğlu, Intech, 2012, 366 P.

40. N. Tjaart N., P. van der Walt, D. Coetzee “Distribution Coefficients And Ion Exchange Behaviour Of Some Elements With Purolite S-950 In Hydrochloric Acid”, *Fresenius J Anal Chem*, V. 356, (1996), 420-424.

41. US 20120125158 A1 “Method for the Recovery of Uranium from Pregnant Liquor”, 2012.

42. I. Yuanming, et al. “Separation Of Rare Earths From Zinc, Calcium, And Magnesium With P507 Levextrel Resin”, *Proceedings of the 2nd International Conference on Rare Earths Development and Application*, V. 1, (1991), 22-26.

43. Eichrom Technologies, Products. Retrieved from http://www.eichrom.com/eichrom/products/

44. TRISKEM INFOS, N2, December 2008. Retrieved from http://www.triskem-international.com/iso_album/binder_tki2_en.pdf

SEPARATION OF RARE EARTH SUBCLASSES BY USING HIGHLY SPECIFIC SOLID PHASE EXTRACTION COLUMNS

*Richard Hammen[1], John Hammen, Chris Hammen, and Jack Lifton[2]

[1]IntelliMet LLC
425 N. Fifth Street, Unit 5
Missoula, MT 59802 USA
*rich.hammen@gmail.com

[2] Jack Lifton, LLC
31126 Country Bluff
Farmington Hills, MI 48331

Keywords: Rare Earth Elements, Purification, Separation, Solid Phase Extraction, Solvent Extraction

Abstract

Separated rare earth element (REE) products are conventionally produced by solvent extraction and ion exchange technologies. Solid Phase Extraction (SPE) has been developed as a logical extension of SX and IX engineering. SPE columns have both the fast equilibration kinetics of SX, and the operating advantages of solid ion exchange columns. REE purification columns with SPE resins are capable of capturing REE ions from solution in seconds. The enhanced kinetics also effect rapid equilibrations of different REE ions, thus enabling separation and purification in minutes. We report data on the use of SPE columns to separate RE elements in a Pregnant Leach Solution obtained from Bokan Mountain ore. The PLS is directly processed through two-stage SPE columns to produce subclasses of Ce/La, Pr/Nd, Sm/Eu/Gd, Y, and heavy REE. The separation is carried out in four pairs of columns wherein a lead column in each pair makes a bulk separation from the purified leach solution while an amplifier column further separates the rare earths eluted from the lead column into subclass fractions. The process for screening ligands and amplifier column eluants is described. The combination of the fractions eluted from the amplifier columns into the five target subclasses is also discussed.

Introduction

Today, rare earth elements find important application in many emerging technologies including electronics and related fields. This has led to an increasing demand for individual rare earth chemicals of high purity as well as purified mixed rare earth products. Separating the rare earth elements (REE) into individual and mixed products is a significant technical challenge. The current state-of-the art uses solvent extraction (SX) technology for separating individual rare earths or groups of rare earths from mixed rare earth solutions originating from the leaching of ores. Ion exchange, which is relatively slow and expensive, is still used for ultra-purification of the desired “light” rare earths (LREE), or for the recovery and purification of higher atomic numbered, “heavy” rare earths (HREE). While solvent extraction is a common unit operation applied in different hydrometallurgical separations, the SX technology available today for RE separation is complex and relatively costly mainly because hundreds of stages are needed across many separation steps to separate the REE into saleable products and IX is often needed for further purification.

The mining, production, and purification of Rare Earth Elements (REE) is essentially a chemical separation process incorporating a series of standard hydrometallurgical unit operations. In general, REE ores are first concentrated if possible using standing mineral processing techniques such as flotation or magnetic separation. Depending on the mineralogy, some ores require chemical and thermal pretreatment to render them amenable to acid attack. The prepared ores or concentrates are contacted with mineral acid solutions to leach the REE from the ore into a pregnant leach solution (PLS). Leaching is not selective, and depending on the ore, other inorganic elements can be dissolved into the PLS including uranium, thorium, iron, manganese, other transition metals, alkali earths, silicon, iron, aluminum, and zirconium. In order to produce commercially saleable purified REE products, the REE substances must be separated from these impurities. The economic value of the impurities is low and, in some cases as with uranium and thorium, the environmental liability can be quite high. Separation of some of the impurity elements such as aluminum can pose significant technical challenges requiring additional processing steps.

The hydrometallurgical separation of REE's is accomplished by selective partitioning of one element between two phases. This is commonly done using a combination of processing techniques such as chemical precipitation and solvent extraction, where the PLS is mixed with an organic (hydrocarbon) solution [1] of metal-selective complexing reagents, known as the extractant. The application of SX to the separation and purification of REE becomes particularly laborious and expensive adding to process complexity and capital costs.

The Solid Phase Extraction (SPE) columns that were tested in this work are designed to have the rapid chemical equilibration kinetics advantage of SX while maintaining the engineering advantages of IX and so be an improvement over conventional REE purification technologies. The SPE columns for molecular and ionic separations are manufactured as a nano-composite material that called "Spiderweb"™. This material was conceived [2,3] to overcome a fundamental physical limitation of conventional ion exchange resins. Resin-based ion exchange products are constrained by the rate limiting diffusion of metal ions from the bulk solution phase to the interior of the resin beads where ion exchange actually occurs. Spiderweb media, on the other hand, are thinly cross-linked networks of polymers supported *between* solid material – like a spider web strung between large boulders (see Figure 1). Metal-selective ligands are tethered to the Spiderweb so that they are directly in the solution flow path and away from the stagnant surface. This enables the metal-chelating groups to quickly entrap metals ions, which now have access to a wide array of openly available binding sites. Metal ions are captured with residence times of seconds allowing higher flowrates than in conventional IX. Elution also occurs in seconds with low volumes of eluant. The Spiderweb Solid Phase Extraction (SPE) technology, at a very basic level, improves the process efficiency and economics of metal recovery. We believe that it represents a fundamentally new development in chemical separations, wherein the tethered ligands attached to the Spiderweb behave with near-solution-phase kinetics while maintaining the engineering advantage of being bound to a solid support substrate.

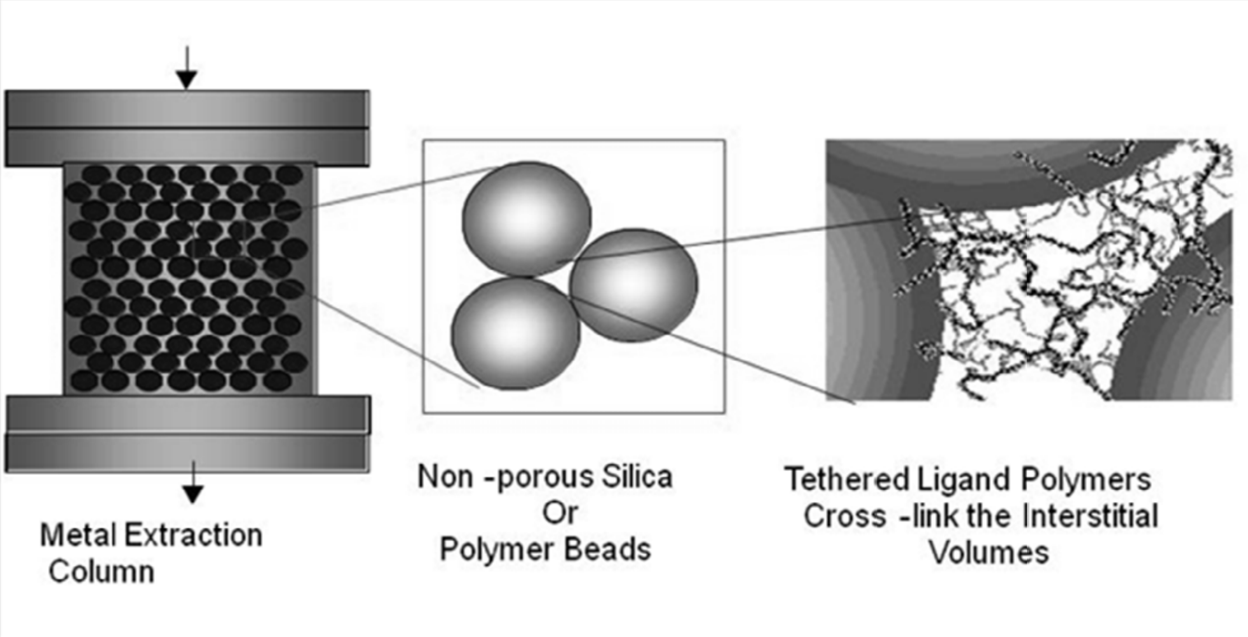

Figure 1. Conceptual diagram of the Spiderweb SPE columns used for metal capture.

The metal-binding kinetics of SPE materials are over an order of magnitude more rapid than the equilibration kinetics characteristic of ion exchange resins in use today. The SPE extraction columns that are used in the testwork described below are manufactured with REE selective ligands immobilized in columns. Application of “Spider Web” resin columns for the REE extraction and purification of REE has the following attributes and advantages:

- Rapid (seconds) metal adsorption and equilibration kinetics providing near quantitative levels of metal recovery to allow high processing speeds with unprecedented productivity per cubic meter of resin;
- A radically smaller system footprint relative to solvent extraction;
- An range of possible chelating ligand chemistries that can give *high* and *differential* association constants for the rare earths, to allow their selective extraction in the presence of other typical impurity elements. Binding strengths for the individual rare earths vary by as much as 10,000 across the series. This enables the differential release (elution) and therefore separation of these ions after they have been extracted away from the impurity elements;
- A suite of uranium-specific ligands that has been developed to attain low parts-per-billion (ppb) levels for radioactive elements in environmental treatment of process water effluents.

The expected smaller footprint of an IntelliMet REE separation plant using SPE technology and the lower number of operating stages compared to SX, should lead to simpler plant startups, and lower capital and operating costs as compared to current operating practices.

Our group has been working on the application of the solid phase extraction technology to the separation of rare earth elements from a PLS generated from the leaching of Bokan ore. Preliminary results were reported in an earlier paper [4]. This contribution reports on further development of the separation scheme and results achieved wherein the SPE columns are first used to separate REE, as a group, from the impurity elements in the PLS, and then clean mixed RE solution is passed through an initial series of columns to further separate the RE's into five relatively enriched "sub-classes"; Heavy, SEG, Y, Didymium, and CeLa.

Experimental

Metal binding, displacement, and elution tests were carried out with PLS solutions with ore obtained from deposits under development. The representative solutions were pumped through bench scale columns varying in volume from 1.66 to 325 mL. The flow rates through the columns ranged from 1 to 4 Bed Volumes (BV) per minute. Solutions were assayed for metal ion content by a photodiode array UV-visible spectrometer, atomic absorbance or by inductively coupled plasma (ICP) spectroscopy.

Data and Discussion

Selective Class Recovery of Light and Heavy Rare Earth Elements

Processing of the sample of high grade ore (4.2% REE + Y) from Ucore's Bokan Mountain deposit was described previously [4]. Essentially, the ore was crushed, ground to a P80 or 185 µm, and leached in 30% nitric acid at a pulp density of 20% solids at 90ºC for 8 h. The leach residue filtrate (PLS) (0.25 bed volumes) was processed through an IntelliMet SPE column at a rate of 60 BV/h with an immobilized ligand that chelates Fe(III) and Th(IV) ions. Column effluent fractions were collected and the metals analyzed by ICP. The first fractions that passed through the column (the flowthrough) were composited with the criterion that the composite solution should contain >98% of the REE. The loaded column was eluted with a solution of ammonium citrate. Good separation was achieved. Over 90% of the Th and U were removed from the flowthrough solution with only 2% loss of the feed RE's. Elution of the loaded U was complete. The eluate would be disposed of as radioactive waste.

The flowthrough, neutralized to pH 2 with concentrated ammonium hydroxide (and labeled PLS2), was then passed through a second SPE column with RE element separation ligands. Three BVs of PLS2 was injected into the SPE column. The column was rinsed with 1.0 BV of water and then eluted with 1.0 BV of 1.0 M acetic acid. The injection and rinse water column effluent fractions were pooled to make fractions labeled "Flowthrough" and "Eluate". Fresh PLS was then used to strip any remaining REE and provide the feed solution for separation Column 1; thus creating a cyclic process with Column 1 producing a strong binding waste stream and Column 2 producing a weak binding waste stream and the purified REE stream where the REE concentration had been upgraded from the original leach solution. Figure 2 shows a schematic diagram of the process.

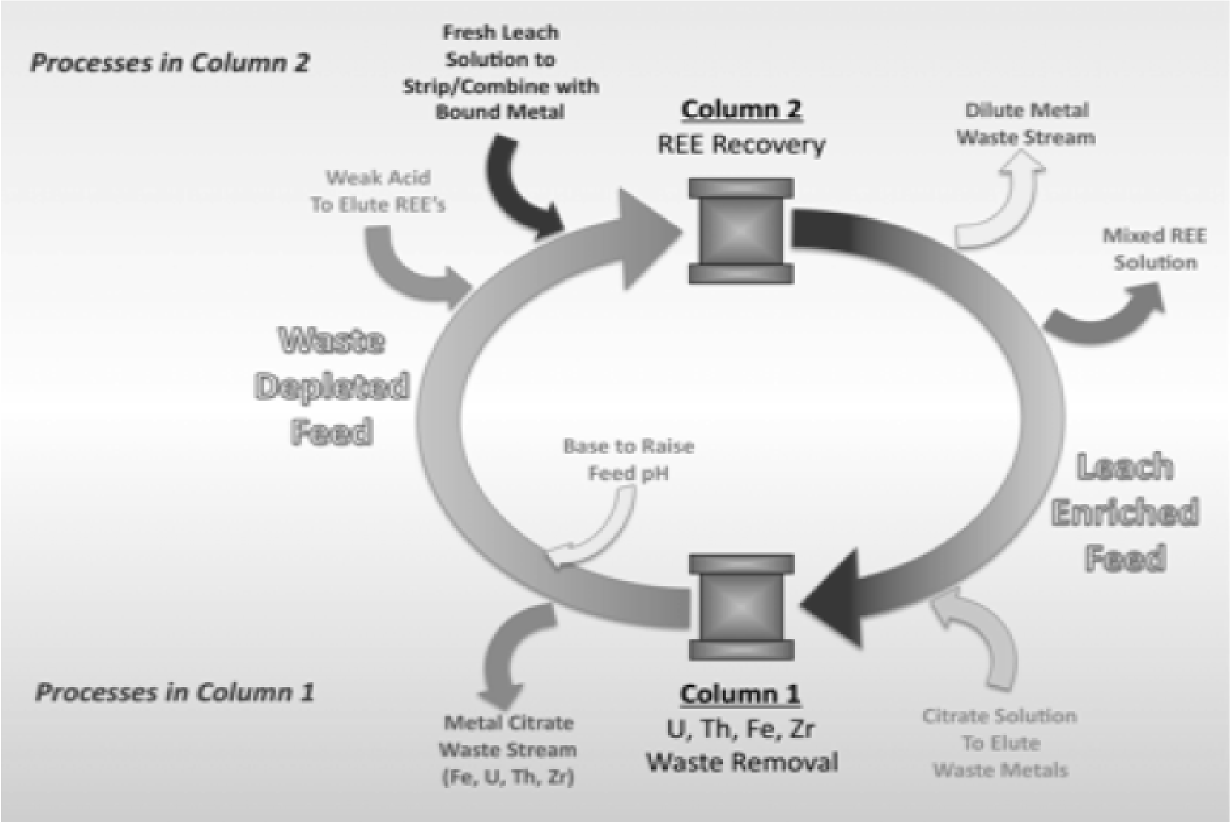

Figure 2. The process diagram of the two-column REE class separation process used with Bokan ore.

The process continues with the separation of the rare earths into subclasses (rare earth elements chemically similar to each other, and generally adjacent on the periodic table) which can then be further separated into individual elements. Subclass enrichment testwork has been carried out to divide the rare earths into a rough "cut" of five rare earth subclasses (CeLa – cerium + lanthanum, didymium – praseodymium + neodymium, yttrium, SEG – samarium, europium and gadolinium, and Heavy – terbium, dysprosium, holmium, erbium, thulium, ytterbium, and lutetium, with terbium and dysprosium being of particular interest). The goal is to produce subclass fractions enriched in the targeted subclass and depleted in the other four subclasses. This is in contrast to trying to simply show maximum enrichment factors using SPE, where larger loading volumes would have been needed to reach equilibria. As these were the first process development stages, the amount of metal processed per cycle was also considered so as to limit the overall number column steps to ultimately produce high purity single element products with high recovery.

The ultimate intention is to feed the products of these subclass separations into subsequent processing hubs, further separating the elements into more refined subclasses, and eventually into individual elements. Compared to trying to separate individual rare earths from the feed one by one, using such a branched separation scheme to produce successively purer subclasses, reduces the number of purification steps downstream to individual element products. As well, some of the subclass products are already saleable commodities. A similar strategy is used in the solvent extraction separation of rare earths but the aim of the application of SPE technology is to attain these separations with simpler equipment and fewer individual processing stages.

Column Process for Subclass Separation

The acetic acid mixed REE stream produced by the Class Separation process was passed into a series of four “lead” separator columns which progressively depleted the Heavies (Column 1), SEG (Column 2), Didymium (Column 3), and CeLa (Column 4) subclasses. Each column retained a greater proportion of the subclass it was targeted to extract so that the flowthrough solution was progressively depleted down the battery of columns. The loading flowrate was 60 BV/h. The loaded column train was eluted progressively with a weak acid. Lighter rare earths bind relatively weakly compared to heavy rare earths, so lights elute from the columns ahead of heavies. The eluate streams from each lead column were then passed into a second “amplifier” column, one for each of the four lead columns. This amplifier further retarded the heavy rare earths relative to the light rare earths so again, a stream enriched in lights emerges before the heavies come off the loaded amplifier columns. Each rare earth concentrator column / amplifier column pair produced multiple product streams enriched to different degrees in the target subclasses. So, streams enriched in a particular subclass were in some cases, produced by more than one column pair. Rare earths were precipitated to oxides from these various subclass streams and stream oxide products were combined for each subclass type from the different column pairs. These enriched subclass precipitates can then be releached to provide enriched and more concentrated feed solution streams for subsequent processing hubs.

Optimization of Loading Volume for Heavy Concentration by Column 1

A large number of ligand formulations were screened for their capacity to bind the REEs from the acetic acid feed solution and enrich them relative to one another. From these results, a short list of three ligands was selected and columns with these ligands were loaded (at 60 BV/h) with varying volumes of feed solution, 8, 12, 24, 32, and 48 BVs. The results, summarized in Table I, are reported as the percent of metal extracted (and eluted) relative to the metal in the input stream, in other words, the percent recovery.

The target for Column 1 was upgrading of the heavies subclass. Therefore, the ligand selected to be used for Column 1 was the one that showed the highest relative enrichment of Heavies over SEG. A secondary criterion was being able to process a reasonable amount of solution while maintaining a good level of separation. Based on these criteria, Ligand 3 with a loading volume 24 BVs was selected for Column 1. Similar screening processes were used to pick the ligand chemistry for Columns 2 and 3 with the conditions being the enrichment of SEG:Didymium and Didymium:CeLa, respectively. The ligand for Column 4 was selected for its capacity to remove the remaining REEs from the feed solution to produce a barren stream fully depleted of REE.

Table I. Comparison of recovery performance of three selected ligands considered for Column 1

	BV Passed	Subclass Recovery (extracted)				
		CeLa	Didymium	Y	SEG	Heavy
LIgand 1	8	50%	76%	83%	90%	95%
	12	36%	63%	73%	82%	91%
	24	8%	16%	35%	41%	62%
	32	5%	11%	22%	29%	47%
	48	3%	8%	14%	17%	32%
LIgand 2	8	11%	28%	46%	46%	71%
	12	10%	24%	43%	41%	67%
	24	4%	6%	21%	17%	39%
	32	2%	3%	12%	10%	26%
	48	0%	1%	2%	2%	5%
LIgand 3	8	33%	59%	73%	78%	90%
	12	15%	25%	46%	54%	71%
	24	14%	34%	46%	55%	72%
	32	4%	11%	23%	23%	46%
	48	2%	6%	15%	13%	31%

Selection of Ligand and Elution Conditions for Amplifier Columns

Following the selection of the "lead" columns, different ligands were screened for application in theamplifier column, This was done by eluting the lead column with 10 BVs of dilute acid which was fed directly into the "amplifier" column to obtain further separation of the fractions during the elution of the amplifier columns producing two or more product streams. Figure 3 shows the subclass separation amplifier column elution data as the percent of mass of each subclass group in a fraction produced. The curves show the percent mass of each subclass extracted by the secondary amplifier column as a function of the number of bed volumes of lead column eluate fed to the secondary column.

Amplifier Ligand 6 was selected to be used with Column 1 because it achieved a higher separation between the Heavy and SEG sub-classes. This same process was repeated to select the amplifier ligands for Columns 2 to 4 with the criteria being high separation between the neighboring sub-classes and significant mass recovery in each fraction.

Elution of the loaded amplifier column by different acids was tested for each of the selected Column-Amplifier Ligand sets Figure 4. shows the results from a few of the acids screened in the test program for elution of the Column 1 amplifier column. Hydrochloric acid was selected as the eluting acid to maximize the mass of lighter REEs eluted before the heavy REEs which reported primarily in the 7th BV. The output of this process produced two different streams; one enriched with HREE while the other was predominantly didymium. Again, this process of screening eluant acids for the amplifier columns was repeated for Columns 2 to 4.

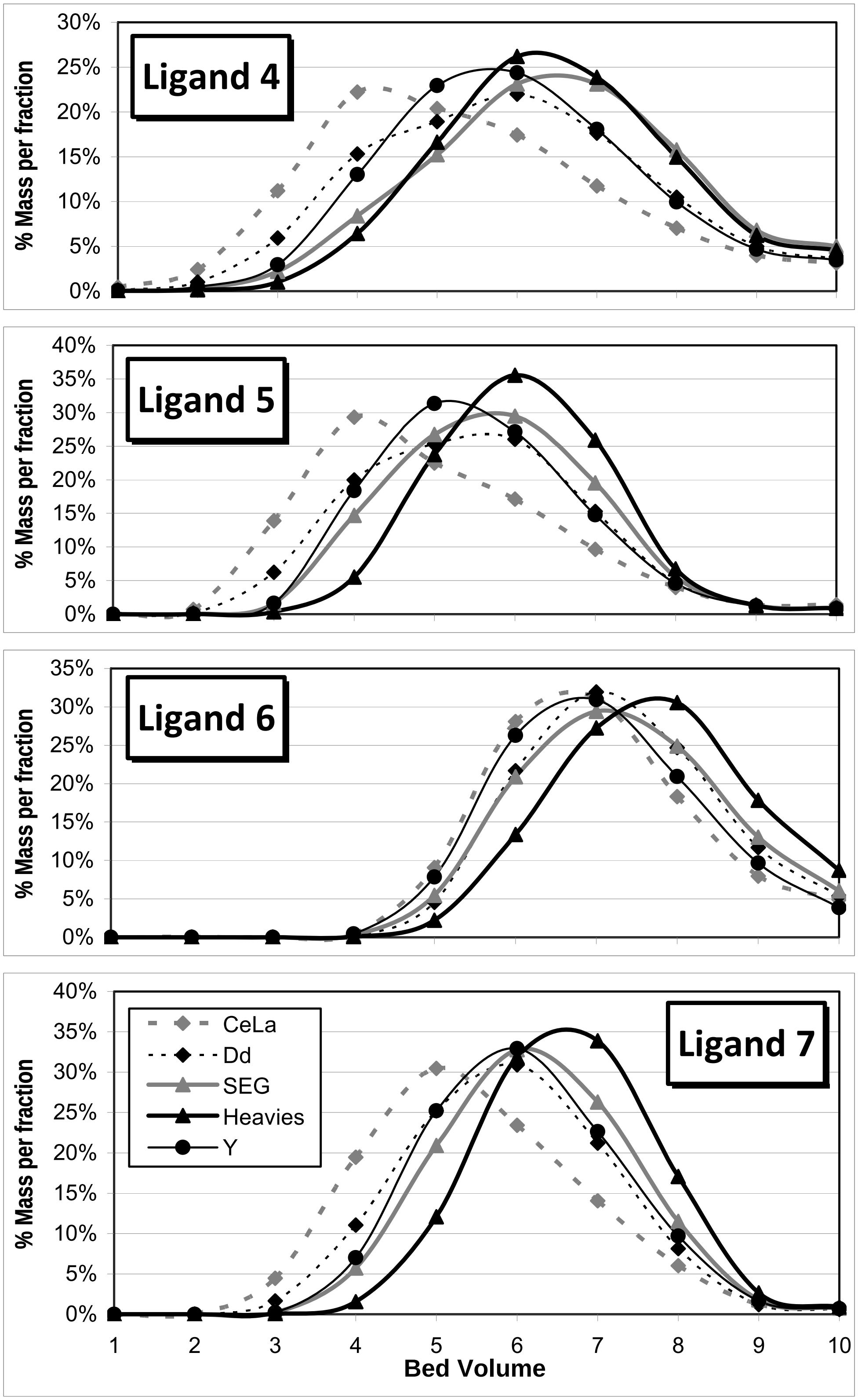

Figure 3. Screening of column 1 amplifier column ligands.

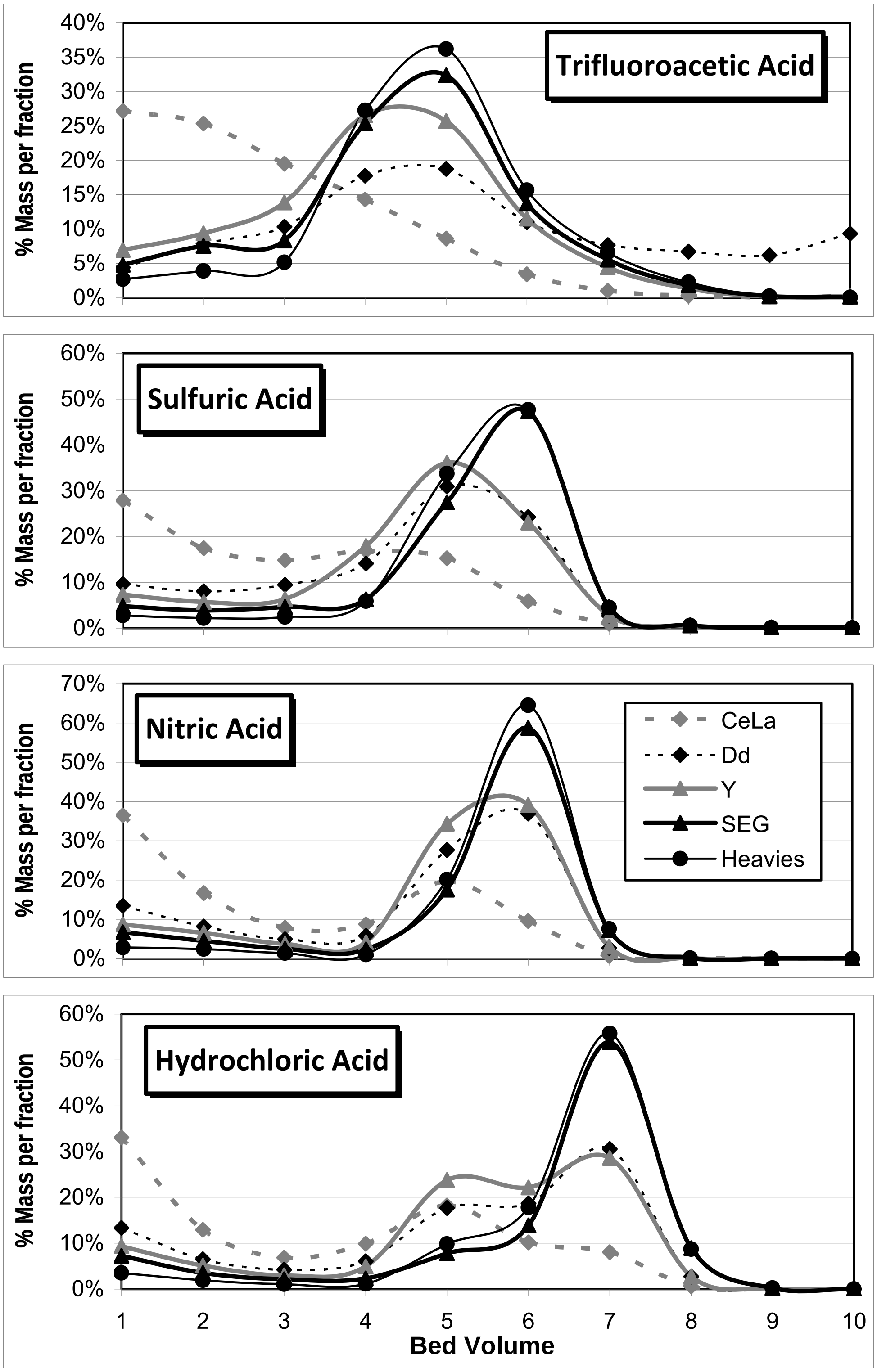

Figure 4. Screening of acids for elution of column 1 amplifier column.

Column Scale-Up and Repeated Cycles

After the selection of ligands and acid eluents, larger column sets (12.5-25 mL) were prepared and the solutions processed over multiple cycles. For ease of detection, the remaining aluminum in the solutions was used as a marker for the REEs to ensure that there was little variation between cycles. Figure 5 is a trace of the output aluminum concentration from Column 1 during the cycle testing. Aluminum concentration is plotted in the three different output streams, the flowthrough (barren), the didymium eluate and the heavies eluate. The totals do not add up to 100% because a portion of the solution was recycled during the process.

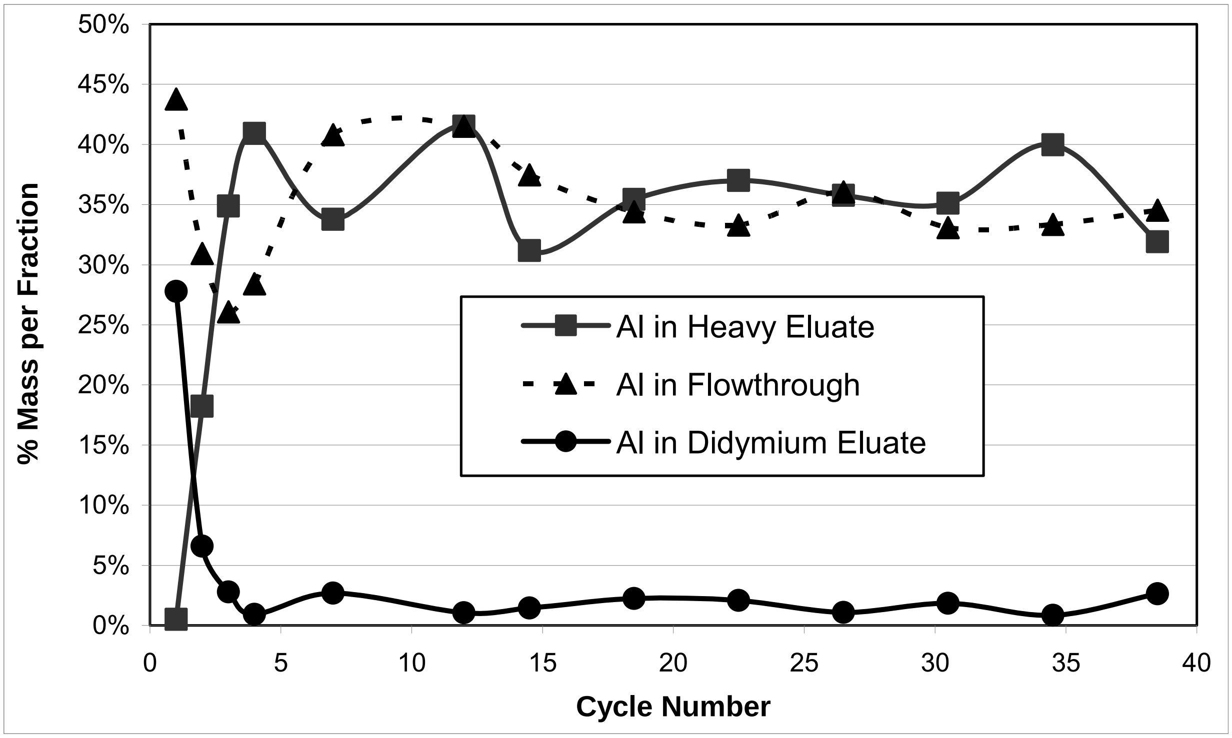

Figure 5. Variation of aluminum recovery in Column 1 output streams over successive cycles.

It can be seen that aluminum recoveries were changing during the first four cycles as the columns equilibrated to the process conditions. After that, the aluminum reported in each fraction varies within ±5% of an average from cycle to cycle indicating that the results were consistent and reproducible from cycle to cycle once steady-state had been reached.

Solution Outputs From SPE Columns

The operation of four column sets consisting of a lead and amplifier column in each set produced a total of 11 output streams, contributing to five final subclass products. These streams, arranged according to concentrator column, are shown in Table II, with metal contents (in mg/L) given for each stream:

Table II. Output Streams From Subclass Enrichment Process (concentrations in mg/L)

Concentrator Column	**Heavy**		**SEG**			**Didymium (Dd)**				**CeLa**	
Output Product	***Heavy***	***Dd***	***SEG***	***Y***	***Dd***	***SEG***	***Y***	***Dd***	***CeLa***	***Dd***	***CeLa***
TREE+Y	1647	1043	337	1283	857	399	2065	2961	806	482	265
Total Subclasses											
CeLa	232	466	48	217	293	71	888	812	487	217	218
Dd	350	273	101	296	231	125	538	975	204	160	35
Y	454	176	57	397	205	61	505	599	87	60	11
SEG	281	85	83	156	73	105	84	395	22	37	1
Heavy	330	43	47	218	55	38	50	179	6	8	0
Individual Elements											
La	21	72	4	26	47	10	158	115	115	32	72
Ce	211	395	44	191	246	61	731	698	371	186	146
Pr	41	37	15	53	54	19	139	169	62	33	12
Nd	309	235	86	242	177	106	400	806	142	127	24
Y	454	176	57	397	205	61	505	599	87	60	11
Sm	142	45	43	74	38	52	44	190	13	19	1
Eu	14	3	5	8	3	6	3	19	1	1	0
Gd	124	37	35	74	31	47	37	186	9	16	0
Tb	26	4	6	18	5	6	4	22	1	1	0
Dy	157	23	25	105	27	22	24	98	4	5	0
Ho	26	3	4	21	5	3	5	17	0	0	0
Er	65	9	7	45	12	5	13	31	2	1	0
Tm	8	0	1	4	1	0	1	2	0	0	0
Yb	45	3	4	21	4	1	3	9	0	0	0
Lu	4	0	0	2	0	0	0	1	0	0	0

REE elements were then precipitated from these eluate solutions solutions using calcium oxide, ammonium hydroxide, sodium phosphate, or oxalic acid). The precipitates of one type (eg. SEG from both SEG and Didymium columns) were combined to produce the five subclass enriched products. For the feed ore that was tested, the anticipated production of each of the five enriched subclass products at the planned mining rate and the relative compositional breakdown of each of the five products is given in Table III

Table III. Relative Compositions and Expected Production of the Five Enriched Subclass Products

	Product Production (kg/d)					
	Heavy	SEG	Y	Dd	CeLa	Total
	928	214	350	1298	520	3311
	Product Composition (wt%)					
La_2O_3	1.3%	1.6%	4.8%	5.4%	22.9%	6.7%
CeO_2	13.1%	14.2%	25.8%	32.8%	53.6%	28.6%
Pr_6O_{11}	2.5%	4.6%	5.5%	5.8%	5.3%	4.7%
Nd_2O_3	18.3%	25.4%	18.4%	25.0%	10.9%	20.2%
Y_2O_3	29.2%	17.6%	28.9%	17.6%	6.1%	20.3%
Sm_2O_3	8.4%	12.6%	3.7%	4.8%	0.7%	5.6%
Eu_2O_3	0.8%	1.4%	0.3%	0.4%	0.0%	0.5%
Gd_2O_3	7.2%	10.4%	3.6%	4.4%	0.4%	4.9%
Tb_4O_7	1.6%	1.7%	0.8%	0.5%	0.0%	0.8%
Dy_2O_3	9.1%	6.6%	4.3%	2.1%	0.2%	4.3%
Ho_2O_3	1.5%	1.0%	0.9%	0.3%	0.0%	0.7%
Er_2O_3	3.8%	1.7%	1.9%	0.7%	0.1%	1.7%
Tm_2O_3	0.4%	0.2%	0.2%	0.0%	0.0%	0.2%
Yb_2O_3	2.6%	0.9%	0.8%	0.2%	0.0%	0.9%
Lu_2O_3	0.2%	0.1%	0.1%	0.0%	0.0%	0.1%

Enrichment Factor

The goal of each processing step in metal refining is to increase the ratio of the valuable product relative to impurities. The enrichment factor for each subclass was calculated as follows:

$$EF = (\text{wt of class in product/TREO in product}) / (\text{wt of class in feed/ TREO in feed})$$

As shown in Table IV, the measured enrichments relative to the feed solution for this step of SPE processing ranged from 1.34 (for Didymium) to 5.96 (for CeLa). Due to sampling and process optimization procedures, recovery of all the REE throughout testing was incomplete. Therefore, the enrichment factor values shown were calculated using the feed composition obtained by adding up all the product streams, rather than from the original feed assay.

Table IV. Enrichment Factors Obtain in Subclass Enriched Products

Mixed Oxide Product	Heavy	SEG	Y	Didymium	CeLa
Upgrading Ratio[1]	2.51	2.63	1.60	1.34	5.96

[1] relative to feed assay calculated from products

Conclusions

Continuing work on the application of the Spiderweb solid phase extraction technology for the separation of rare earths has been undertaken with encouraging and positive results. After an initial separation from base metals and impurities, the results have demonstrated the separation of the clean rare earths feed solution produced by the first impurity removal step into enriched fractions or subclasses. Cleaned solution was successfully processed through a series of four separation columns to produce five enriched subclass products. Each separation column consists in fact, of a pair of columns, one for the primary extraction and a second amplifier column which further separates the eluate from the primary column into two or more streams. The amplified RE product streams are precipitated and similar precipitates combined to yield five enriched subclass products. These five subclass products represent a significant separation and upgrading of the original mixed rare earths as found in the ore leach solution.

Test protocols have been developed and applied for selection of the best ligands for the primary and secondary separations. Additional work has also identified which mineral acid provides the best elution in the amplifier columns with a view to producing good separations. For example HCl has been selected as the eluant for the first extraction amplifier column. These procedures can be applied to work that will be carried out on further separation within the subclass products.

The data presented demonstrates the potential for SPE to be used to produce upgraded rare earth product streams. Significant enrichments have been attained in relatively few processing steps as compared to conventional technologies. The value of the products increases as the degree of enrichment increases and the SPE process remains open to further improvements from identification of more selective ligands. The greater the enrichment per processing step, the fewer the number of steps required to obtain a saleable material. It is envisaged that such a process, with relatively few stages, could be carried out at the mine site to 1) provide more enriched and thus higher value products to be sent to a processing facility (which might not otherwise be built at the remote locations) and 2) mitigate the need for an expensive bulk oxalic acid precipitation of all the REE.

Additional testing is under way to further purify the subclass products and incorporate the results to model a REE separation facility utilizing SPE.

Rapid extraction kinetics allows the SPE process to operate in relatively small SPE columns for a given throughput. This should enable the construction and operation of REE separation plants with lower capital and operating costs than those using currently available technology. Application of SPE technology also opens the door to the potential production of intermediate enriched products at the minesite.

References

1. Lee, M-S., Lee, G-S., Lee, J-Y., Kim, S-D., Ahn, J-W., & Kim, J-S. Solvent extraction of Gd from chloride solution with PC88A. *Materials Transactions, 46*(2) (2005), 259-262.

2. Hammen, R., & Hammen, J. "Composite Matrices with Interstitial Polymer Networks", United States Patent 6,946,070 (2005).

3. Hammen, R., & Hammen, J. "Composite Matrices with Interstitial Polymer Networks", United States Patent 7,201,844 (2007).

4. Lifton, J., & Hammen, R. "The State Of The Art In Separating And Purifying The Heavy Rare Earths: Solvent Exchange, Ion Exchange, And Solid Phase Extraction, Which Is The

Optimal Process?", 51st Annual Conference of Metallurgists COM 2012, Niagara Falls, ON, CA (2012).

HIGH PURITY SAMARIUM ACETATE FROM MIXED RARE EARTH CARBONATES

Carlos A. da S. Queiroz[1], José A. Seneda[1]
Walter dos R. Pedreira[2] and Mari E. de Vasconcellos[1]

[1]Instituto de Pesquisas Energéticas e Nucleares - IPEN / CNEN - SP
Av. Professor Lineu Prestes, 2242 – CEP: 05508-000 – São Paulo – SP
mstela@ipen.br
[2]Fundação Jorge Duprat Figueiredo de Segurança e Medicina do Trabalho
Rua Capote Valente, 710 – CEP: 05409-002 - São Paulo - SP.

Keywords: Samarium, Acetates, Rare Earth Metals

Abstract

A simple and economical chemical process for the production of highly pure samarium acetates is discussed. The raw material, which was used in the form of rare earth carbonates was produced industrially from the chemical treatment of Brazilian monazite. Ion exchange chromatography was performed using a strong cationic resin that is typically employed in water treatment processes to fractionate rare earth elements (REE) without the use of retention ions. Under these conditions, 99.9% pure Sm_2O_3 was eluted using the ammonium salt of ethylenediaminetetraacetic acid (EDTA) at a controlled pH. The EDTA-samarium complex was transformed into samarium oxide, which was subsequently dissolved in acetic acid to obtain the samarium acetates. Molecular absorption spectrophotometry was used to monitor the samarium content during the proposed process, and sector field inductively coupled plasma mass spectrometry was used to certify the purity of the samarium acetates. Typical samarium acetates obtained from the proposed procedure contained the following contaminants in micrograms per gram: Sc (20.90); Y (11.80); La (3.36); Ce (1.87); Pr (1.28); Nd (2.98); Eu (17.70); Gd (84.30); Tb (1.41); Dy (1.92), Ho (2.85); Er (1.49); Tm (2.96); Yb (19.90); Lu (1.18). The high-purity samarium acetates produced in the present study can be used as an alternative to imported products in research and development applications.

Introduction

Samarium is currently used in many applications, such as catalysts, lasers and metal alloys. For instance, samarium-cobalt alloys are used to prepare magnets that are resistant to demagnetization. Samarium is also employed to absorb neutrons in nuclear reactors and is used in sensitizers matches, optical glasses and carbon arc lamps. In medicine, samarium is used in the form of radioactive Sm_{153} to produce radiopharmaceuticals, which are used to reduce bone pain in patients with cancer. Moreover, new compounds containing samarium have been investigated as drugs. In Brazil, the extraction of rare earth metals occurs during the industrial exploitation of monazite. Herein, we use mixed rare earth carbonates depleted in cerium and lanthanum from the monazite processing industry to obtain high-purity Sm_2O_3, via ion exchange chromatography.

Monazite is a heavy mineral composed of REE phosphates and thorium. Monazite occurs as an accessory constituent to granites, gneisses and pegmatites, as well as sands from the decomposition of the aforementioned rocks [1]. In Brazil, monazite is found in riverbeds located in Bahia, Minas Gerais, Goias and Mato Grosso, and the beaches off the coast of Bahia, Espirito Santo and Rio de Janeiro, which contain 25% to 30% o monazite. Other minerals present in monazite include quartz, zircon, ilmenite, magnetite and rutile [2-4]. The present procedure for the separation of samarium was carried out using raw material from the separation of thorium and rare earths in monazite. Fractional precipitation and ion exchange chromatography were employed to obtain high-purity samarium oxide. Molecular absorption spectrophotometry and sector field inductively coupled plasma mass spectrometry (SF ICP-MS) were used to ensure the quality of the samarium oxide and samarium acetates, respectively.

At IPEN-CNEN/SP, the separation of rare-earth metals is performed to meet internal demands in other research areas[5-14].

EXPERIMENTAL

Starting Raw Materials

A representative aliquot of commercial rare earth (RE) carbonates (17% Sm_2O_3) was used. Hydrochloric acid, acetic acid, the ammonium salt of ethylenediaminetetraacetic acid (EDTA) and all other reagents were of analytical grade. Solutions of RE chlorides were prepared by dissolving the RE carbonates in hydrochloric acid. Solutions of RE chlorides with a RE_2O_3 concentration of 10 g L^{-1} were filtered to remove insoluble products.

Loading the Resin and Eluting the Rare Earth Metals to Obtain 20%-93% Pure Sm_2O_3

Rare earth chlorides solutions with a concentration of 10 g L^{-1} were pumped into a system of columns filled with a strong cationic resin, which is typically used as a resin for water treatment and that is easy to obtain in the Brazilian market. Subsequently, the resin was rinsed with deionized water. REEs in the resin were eluted with EDTA solution at pH 3.5- 4.0. The effuent was collected in fractions, from which the oxalates were precipitated and converted into oxides. Ion exchange-system 1 contained several columns connected in series, including 3 columns with a lenght of 1.4 meters and a diameter of 12 cm and 4 columns with a length of 1.0 meter each and a diameter of 5 cm. In this way, samarium oxide with a purity of 20% to 93% was obtained.

Loading the Resin and Eluting the REEs to Obtain ≥ 99.9% Sm_2O_3

Several fractions (20%-93%) were combined to obtain 100g of oxide yelding a 65% Sm_2O_3 concentrate, and the combined fractions were dissolved in hot 1:1 HCl. The resulting solution was diluted to 10 g L^{-1} of 65% Sm_2O_3. Subsequently, this solution was percolated in another ion exchange system containing 5 columns with a length of 1 meter and a diameter of 5 cm, which were connected in series and filled with a strong cationic resin. The same resin used in the previous section was employed in the second ion exchange system, and an EDTA solution at pH 3.5-4.0 was used to elute the REEs. As a result, Sm_2O_3 with a purity of 99.9% was obtained. A block diagram of this process is presented in Figure 1.

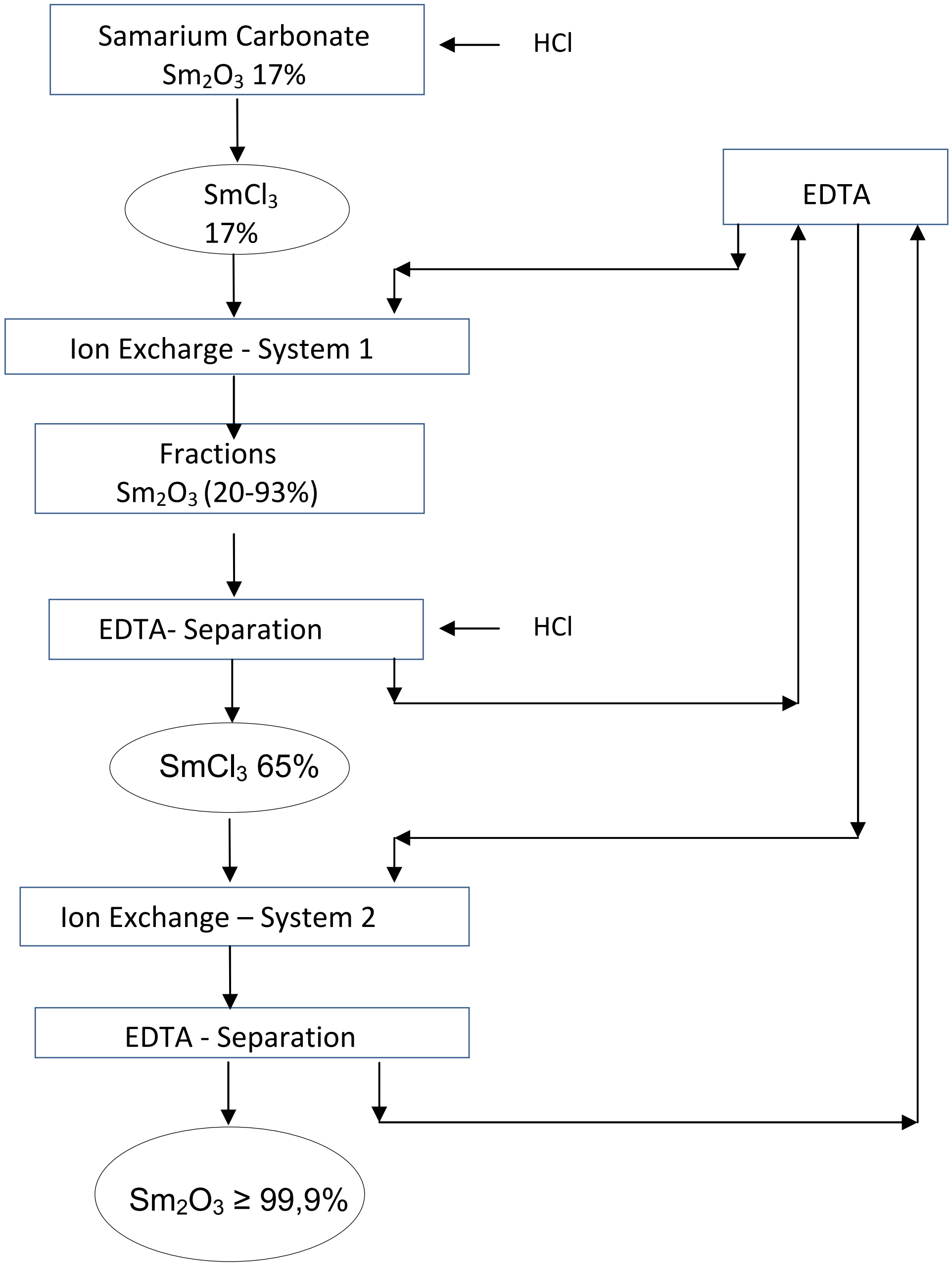

Figure 1. Procedure for the preparation of pure samarium acetates for use in P&D at IPEN-CNEN/SP.

Production of High Purity Samarium Acetates

For the preparation of highly pure samarium acetates, samarium oxide with a purity greater than 99.9% was obtained using the procedure previously described. In the experimental procedure samarium oxide was added to acetic acid and the resulting solution was heated to evaporate excess acid. Subsequently, the formation of samarium acetate crystals was achieved. The resulting material was characterized by SF ICP-MS to determine the quality of the samarium acetates.

Characterization and Analytical Control of the Proposed Process

Molecular absorption spectrophotometry and sector field inductively coupled plasma mass spectrometry (SF ICP-MS, Element, Finningan MAT Bremen, Germany) were used to ensure the quality of the samarium oxide and the samarium acetates, respectively. This technique provided accurate results and reproducible contaminant values in the µg $^{-1}$ range.

Results

Table I shows the elution conditions and mass balance in enriched samarium from RE carbonates (17% Sm_2O_3) using ion exchange-system 1. Various fractions with a samarium oxide content between 20% and 93% Sm_2O_3 were obtained. Several fractions were combined to btain a 65% Sm_2O_3 concentrate, which was used in ion exchage-system 2 to increase the purity to ≥ 99.9% Sm_2O_3. Samarium acetates were prepared using 99.9% pure samarium oxide, the REE content of which is shown in Table II.

Table I. Ion Exchange - System 1. Elution and Mass Balance of Enriched Samarium From Mixed Rare Earth Carbonates (17%Sm_2O_3). Eluent: EDTA Solution-Acetic Acid-NH_4OH at pH 3.5-4.0. Elution Rate: 8 ± 2 mL/minute

Fraction	pH	Time (h)	Oxide (g)	Oxide Color	Sm_2O_3 (%)
1	3.5	583	623	-	-
2	4.0	30	30	White	-
3	4.0	24	14	White	20
4	4.0	48	30	yellow	26
5	4.0	96	88	yellow	35
6	4.0	24	30	yellow	45
7	4.0	24	27	yellow	60
8	4.0	48	46	yellow	76
9	4.0	24	31	yellow	93.5
10	4.0	48	50	yellow	93
11	4.0	24	30	yellow	93.4
12	4.0	48	42	yellow	93
13	4.0	96	121	brown	72

Table II. Rare Earth Impurities Present in Samarium Acetate. Sector Field Inductively Coupled Plasma Mass Spetrometry (SF ICP-MS)

Element	$Sm(CH_3COO)_3$ (µg.g^{-1} +/- σ)
Y	11.80 +/- 0.20
Sc	20.90 +/- 0.22
La	3.36 +/- 0.81
Ce	1.87 +/- 0.70
Pr	1.28 +/- 0.80
Nd	2.98+/- 0.80
Sm	……………
Eu	84.30 +/- 0.90
Gd	15.40 +/- 0.40
Tb	1.41+/- 0.50
Dy	1.92 +/- 0.50
Ho	2.85+/- 0.10
Er	1.49 +/- 0.70
Tm	2.96 +/- 0.10
Yb	19.90 +/- 0.60
Lu	1.18 +/- 0.50

Conclusions

Using cationic ion exchange chromatography, highly pure samarium oxide was obtained as an eluent, without the retention of ions and EDTA solution at pH 3.5-4.0. Moover, high-purity samarium acetates were produced.

High-purity samarium acetate can be used as an alternative to imported products employed in research and development applications. Further studies on the synthesis and chemical characterization of the samarium acetates by thermogravimetry, X- ray diffraction and infrared spectroscopy will be published in due course.

Acknowledgements

The Authors dedicate this work to Professor Alcidio Abrão PhD, to whom we owe a great deal of our professional experience, for always valuable suggestions, teachings, support and mainly for the friendship. We Thank You, wherever you may be!

We thank to IPEN/CNEN-SP and FAPESP for financial support.

References

1. Alcídio Abrão, *Química e tecnologia das terras raras* (Série: Tecnologia Mineral n.66, CETEM/CNPq) 1994.

2. Elbert V.Viera, Fernando F. Lins, *Concentração de minérios de terras raras* (Série: Tecnologia Mineral n.73, CETEM) 1997.

3. W. R. Pedreira et al. “Trace amounts of rare earth elements in high purity samarium oxide by sector field inductively coupled plasma mass spectrometry after separation by HPLC”. *Journal of Alloys and Compounds*, 418 (2006), 247-250.

4. D. C. Stwart, P. Kato, “Analysis of rare earth mixture by a recording spectrophotometer”. *Anal. Chem.*, 30 (1958), 164-174.

5. C. A. S. Queiroz, e A. Abrão, “Separação de cério e fracionamento das terras raras a partir dos cloretos mistos”. *In: Vicentini, G. e Zinner, L. B., Coord., Química dos lantanídeos e actinídeos. Anais do VI Simpósio Anual da ACIESP, São Paulo, ACIESP, Publicação ACIESP* N 36-1 (1986), 200-224

6. C.A.S. Queiroz, A. Abrão, “Obtenção de neodímio e lantânio de alta pureza a partir de uma mistura de cloretos de terras raras”. In: Vicentini, G. e Zinner, L. B., Coord.,Química dos lantanídeos e actinídeos. Anais do VIII Simpósio Anual da ACIESP, São Paulo, ACIESP *Publicação ACIESP* N 44-1 (1984), 57-75.

7. C.A.S. Queiroz, A. Abrão, “Obtenção de gadolínio e samário puros a partir de uma mistura de carbonatos de terras raras por troca iônica”. *In: Vicentini, G. e Zinner, L. B., Coord., Química dos lantanídeos e actinídeos. Anais do X Simpósio Anual da ACIESP, São Paulo, ACIESP Publicação ACIESP* N 50-1(1986), 33-45.

8. C.A.S. Queiroz, A. Abrão, “Alguns aspectos do controle analítico aplicado ao processo de separação das terras raras”. *In: Vicentini, G. e Zinner, L. B., Coord., Química dos lantanídeos e actinídeos. Anais do XIV Simpósio Anual da ACIESP, São Paulo, ACIESP Publicação ACIESP N* 68-1 (1990), 157-89.

9. L.C.P.E. Reino, A. R. Lordello, “Determinação de elementos lantanídeos em óxidos puros de lantânio, de samário e de gadolínio por espectrometria de emissão com plasma”. São Paulo, Instituto de Pesquisas Energéticas e Nucleares, *IPEN-Pub*-317 (1975).

10. W.R. Pedreira et al., ”Quantification of trace amounts of rare earth elements in high purity gadolinium oxide by sector field inductively coupled plasma mass spectrometry (ICP-MS)”. *Journal of Alloys and Compounds*, 374 (2004), 129-132.

11. C.A.S. Queiroz et al., “Synthesis and thermoanalytical characterization of samarium peroxocarbonate”, *Journal of Alloys and Compounds*, 374 (2004), 401-404.

12. M. E. de Vasconcellos et al., “Sequential separation of the yttrium-heavy rare earths by fractional hydroxide precipitation”, *Journal of Alloys and Compounds*, 374 (2004), 405-407.

13. M. E. de Vasconcellos et al., “Solubility behavior of rare earths with ammonium carbonate and ammonium carbonate plus ammonium hydroxide: precipitation of their peroxicarbonates”, *Journal of Alloys and Compounds*, 451 (2008), 426-428.

14. S.M.R. Rocha et al., “Influência do lantânio na estabilidade térmica de aluminas”, In: *XVIII CEBCIMAT*, (2008), 544-549.

Rare Earth Elements in Advanced Materials

INORGANIC FUNCTIONAL MATERIALS FOR ENVIRONMENTAL PROTECTION

Nobuhito Imanaka

Professor, Osaka University, President, The Rare Earth Society of Japan
Department of Applied Chemistry, Faculty of Engineering, Osaka University
2-1 Yamadaoka, Suita, Osaka 565-0871 Japan
imanaka@chem.eng.osaka-u.ac.jp

Keywords: Rare Earth Oxides, Nitrogen Oxides, Catalyst, Catalytic Decomposition

Extended Abstract

Nitrogen oxides (NO_x) are harmful to the environment as well as human beings. Among various NO_x removal methods, direct catalytic decomposition into non-toxic N_2 and O_2 is one of ideal ways, because the process is simple and any reductants are not necessary. The predominant NO_x species in the emitted gas at elevated temperatures is thermodynamically stable nitrogen monoxide, NO. Therefore, the research should be directed on the NO direct reduction.

Rare earth oxides hold three phases as shown in Figure 1. The lighter lanthanides have A-type phase. In contrast, the heavier lanthanides hold C-type phase. The intermediate oxides are stable to hold B-type phase. Among three phases, C- type phase is the most loose in its structure and seems to have suitable pores to absorb gas species, like NO.

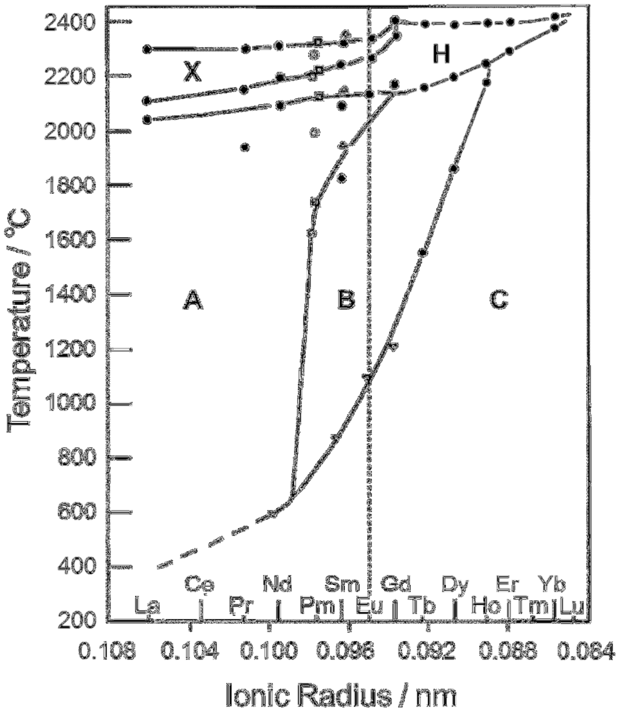

Figure 1. Polymorphic transformation for the lanthanoid sesquioxides [1].

The C-type cubic crystal structure possesses large interstitial open space in its structure with oxide anion vacancies, O^{2-}, which plays a significant role in the direct NO decomposition, and the catalytic activity can be enhanced by partial substitution of the trivalent rare earth cation sites with lower divalent Ba^{2+} ions to produce further oxide anion vacancies.

Here, yttrium oxide (Y_2O_3), which is one of thermally stable C-type cubic oxides, was employed as the fundamental oxide, and the Y^{3+} ion was partially substituted with $Tb^{3+/4+}$ to promote the direct NO decomposition activity by the additional redox characteristics of terbium ion.

On the present $(Y_{0.69}Tb_{0.30}Ba_{0.01})_2O_{2.99+x}$ catalyst, complete purification, that means 100 % NO decomposition into non-toxic N_2 and O_2, was sucessfully realized at 900 °C as presented in Figure 2. Furthermore, the NO decompsotion activity was maintained as high as 64 %, even in the presence of 10 vol% O_2 at 900 °C.

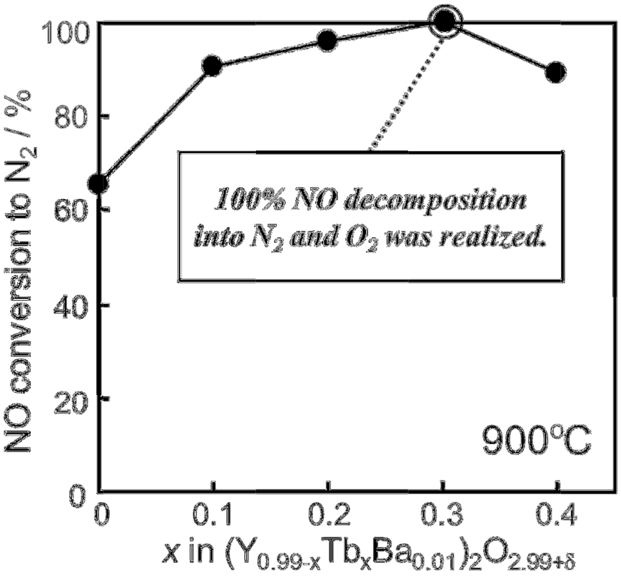

Figure 2. Dependence of the NO conversion to N_2 at 900 °C on the $(Y_{0.99-x}Tb_xBa_{0.01})_2O_{2.99+\delta}$ catalysts (NO 1 vol%, He balance, W/F = 3.0 g s cm^{-3}) [2].

References

1. G. Adachi and N. Imanaka, *Chem. Rev.*, 98 (1998), 1479.

2. S. Tsujimoto, K. Mima, T. Masui, and N. Imanaka, *Chem. Lett.,* 39 (2010), 456

TWO EXOTIC AND UNIQUE FAMILIES OF RARE EARTH INTERMETALLIC COMPOUNDS

*K.A. Gschneidner, Jr.[1,2], A. Provino[1,3], P. Manfrinetti[1,3], V.K. Pecharsky[1,2], and Y. Mudryk[1]

[1]Ames Laboratory
Iowa State University
Ames, IA 50011-3020, USA
*cagey@ameslab.gov

[2]Department of Materials Science and Engineering
Iowa State University, Ames, IA 50011-2300

[3]Department of Chemistry
University of Genova
16146 Genova, Italy

Keywords: Rare Earth Intermetallic Compounds, Ductile Intermetallic Compounds, Fibrous Intermetallic Compounds, Ductility; Brittleness

Abstract

The rare earth metals form two unique, one of a kind, families of intermetallic compounds. One family crystallizes in the simple cubic CsCl, B2-type structure with 2 atoms in the unit cell; while the second family has the complex orthorhombic $Nd_{11}Pd_4In_9$-type structure with 48 atoms in the unit cell. The first family, the RM compounds with the B2-type structure, where R is a rare earth metal and M = Cu, Ag, and Au, are ductile phases. Some non-rare earths containing B2 phases have also been studied and most were found to follow the criteria for ductility/brittleness established by the RM phases. The second family, the $R_{11}M_4In_9$ phases where M = Ni, Pd and Pt, form a fibrous microstructure. The microstructure is self-assembled directly from the melt (whether rapidly or slow cooled) and is probably due to the large aspect ratio of 6.0 for the *b*/*c* lattice parameter ratio and the very short In-In bonds in the *a*-*b* plane which give rise to kinetic hindrance during solidifying and prevent the crystal from growing in the *a* and *b* directions.

Introduction

There are several rare earth intermetallic compounds which are well known because they are commercially important and play critical roles in many applications. These include: (1) the $Nd_2Fe_{14}B$ and the $SmCo_5$-Sm_2Co_{17} families of high strength permanent magnets which are used in electric motors, spindles for computer hard drives, magnets for cell phone speakers, MRI (magnetic resonance imaging) units, direct drive wind turbines, etc.; (2) nickel metal (La) hydride rechargeable batteries ($LaNi_5H_x$) which are used in hybrid automobiles, such as the Prius; and (3) Terfenol ($Tb_{0.3}Dy_{0.7}Fe_{1.9}$), the giant magnetostrictive material, which is used in magneto-mechanical sensors and ultrasonic transducers [1]. There are, however, tens of thousands of other rare earth intermetallic compounds which are obscure and have no claim to fame. There are a few others which fall in-between these two groups – LaB_6 as an electron gun; $PrNi_5$ as a low temperature magnetic coolant to reach a record working temperature of 22 μK when used in tandem with Cu metal; $Gd_5(Si_{1-x}Ge_x)_4$ and $La(Fe_{1-x}Si_x)_{13}$ as giant magnetocaloric effect materials for near room temperature cooling [1]. Today we wish to describe two families of intermetallic compounds which will be famous for their exotic behaviors: the ductile CsCl, B2-type RM intermetallic compounds, and the fibrous $Gd_{11}Ni_4In_9$ prototype of the $R_{11}M_4In_9$ family (where M = Ni, Pd, Pt) of intermetallic compounds.

Ductile RM Compounds

Most intermetallic compounds are intrinsically brittle, but a few compounds can be made ductile: by alloying; changing the composition away from the truly stoichiometric ratio of the two (or three) components; inducing a martensitic transformation to make the compound ductile; testing at high temperatures approaching the melting point, or in zero-humidity atmosphere [2]. So it was quite a surprise when ten years ago a family of rare earth intermetallics was reported to be ductile, with some ductilities greater than 20% at room temperature [2]. All of these RM (where R = a rare earth element which includes Sc, Y and the lanthanide metals and M = a group 10 [Ni, Pd, Pt] or group 11 [Cu, Ag, Au] metals) compounds have the B2 CsCl-type structure. The RCu, RAg and RAu compounds which form the cubic CsCl B2-type structure are ductile, however, some of the RCu and RAu phases form either the orthorhombic B27 FeB-type structure or the orthorhombic B_f CrB-type structure, and a few form both the B27 and B_f structures, and none of these are ductile. The ductile B2 compounds are: RCu for R = the heavy trivalent lanthanides, Sc and Y; RAg for R = any trivalent rare earth metal; and RAu for R = a small size rare earth metal, i.e. Er-Lu, and Sc. The ScM phases with M = Ni, Pd and Pt are ductile. To date only 19 RM B2 phases have been found to be ductile out of ~160 known RM phases with this structure.

Of the hundreds of thousands of intermetallic compounds, one may ask why these 19 rare earth compounds are so unique to exhibit ductility – what makes them special. For one thing, all of the ductile phases have the B2 cubic CsCl structure. When considering the mechanical behavior of metallic phases, the material needs to have at least five independent slip systems for any significant ductility – this is known as the von Mises criterion. *Of all the crystal structures of stoichiometric intermetallic compounds only the B2 satisfies the von Mises criterion* [3]. But there are several hundred intermetallics with the B2 structure, yet only 24 (19 RM + 5 non-rare earth containing compounds) are known to be ductile. Thus satisfying the von Mises criterion is a necessary but not sufficient condition. About four years ago Gschneidner et al. [3] supplied the answer. The authors used a global semi-empirical alloy theory approach and first principles calculations to show that the *d*-band electrons must lie well below the Fermi level of the RM B2 cubic CsCl-type compounds. This is the second a necessary requirement. That is, these compounds exhibit ductility when the bonding electrons are predominately *s* electrons and have no *d*-bonds, thus permitting the R and M atoms to move past one another with little or no difficulty when dislocations easily glide during plastic deformation. For the 10 known brittle RM intermetallics the authors showed that there is a significant fraction of directional *d*-bonds which must be broken to allow the R and M atoms to move past each other.

Some of these authors, Russell *et al.* [4] predicted the MgAg, CdAu, ZnAu and CuPd were ductile intermetallics and experimentally this has been confirmed for the first three compounds, but no experimental data were available for CuPd. The following phases AlFe, AlNi, AlRu, AlPd, AlPt and TiCo were predicted to be brittle, but only the first two have been found to be brittle, and no experimental data was available for the last four. The *d*-electron correlation does not hold for either ZrCo and ZnCu, the first was predicted to be brittle and the latter to be ductile, but experimentally just the opposite behaviors were observed.

The von Mises criterion/*d*-electron presence or absence at the Fermi level model correctly predicts the ductile/brittle behavior of 34 of the 36 B2 intermetallics examined for which experimental data exist – a reliability of 94%. That is, the discovery of the existence of ductility in intermetallic compounds is like the proverbial finding of the needle in a haystack.

Fibrous Intermetallics

More recently we have found that a complex rare earth containing intermetallic compound formed a fibrous microstructure when cooled from the melt [5], see Figure 1. A variation of the usual cooling rates used to cool samples from the molten state does not have much of an effect on the fibrous structure. Fibers are formed regardless whether a sample is arc-melted or cooled in a furnace by turning off the power. That is, these are self-assembled fibrous intermetallic compounds. The cross-section thickness of the fiber will, however, vary with the rate of cooling – the more rapid the cooling the thinner the fibers. The fiber cross-section varies from 0.1 μm to 20 μm, and the length from 1 to 40 mm. The microfibers grow along the short *c*-axis which is orthogonal to the *a*-*b* plane; the growth of the fibers is parallel to an unidirectional temperature gradient. One can also grow large grains by slowly freezing the alloy as during a Bridgman growth process.

The lattice parameters of the orthorhombic $Gd_{11}Ni_4In_9$ are: $a = 14.48$, $b = 21.74$, and $c = 3.65$ Å. The large disparity of the *a*- and *b*- axis with respect to the *c* axis, which results in an aspect ratio of ~6 (between the *c* and *b* axis) and also a very short In-In bond distance in the *a*-*b* plane (2.968 Å vs. 3.251 Å for pure In metal), leads to kinetic hindrance in which the atoms do not have sufficient time to arrange themselves to form the correct structure giving rise to the fibrous microstructure. As one would expect, the mechanical, magnetic and electrical properties are strongly anisotropic. For example, the electrical resistivity is ~100 μΩ·cm measured parallel to the fiber direction and 184 μΩ·cm perpendicular to the fibers. This compound orders ferrimagnetically at 86 K, and exhibits spin reorientation transitions at 46 and 10 K. $Gd_{11}Ni_4In_9$ is a reasonably soft magnet: an applied field of ~1 kOe is sufficient to align the spins in the fiber direction, but 30 kOe is required orthogonal to the fibers. The respective saturation magnetic moments are 6.1 and 4.8 μ_B/Gd atom, which are less than the theoretical value of 7 μ_B/Gd atom, indeed confirming that this compound is a ferrimagnet with some moments antiparallel to each other.

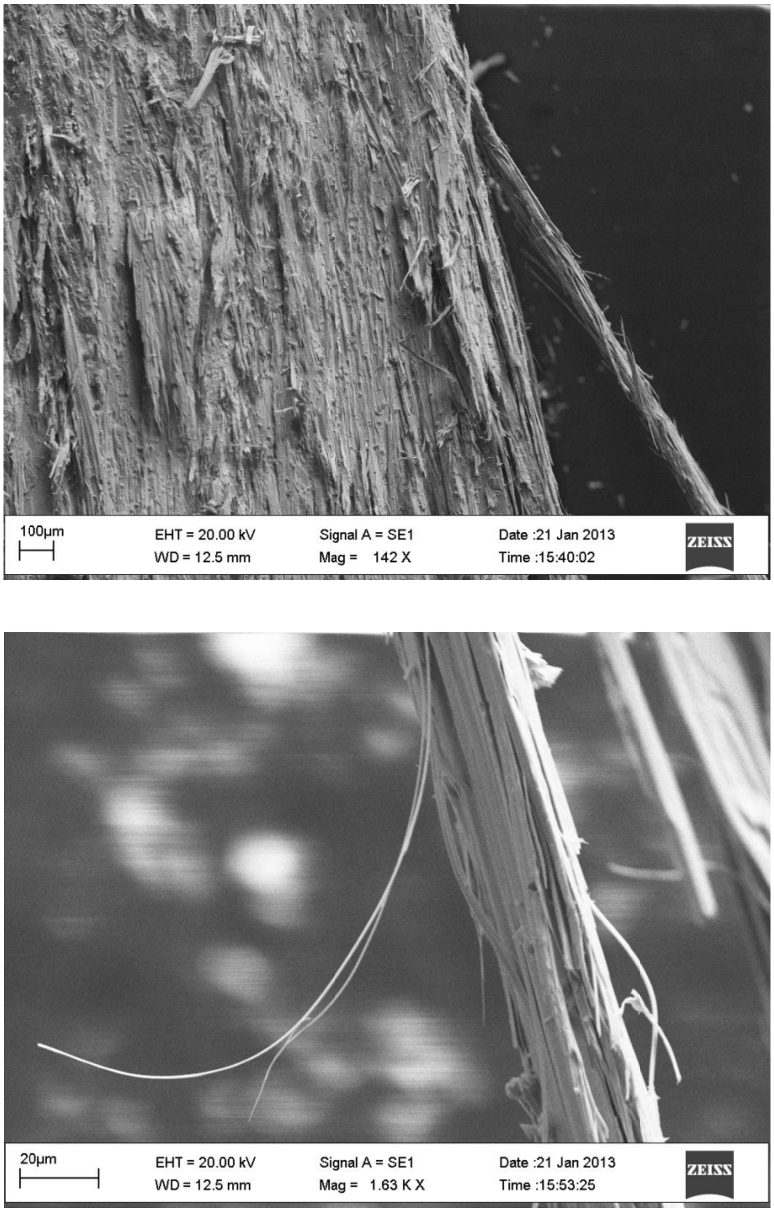

(a)

(b)

Figure 1. SEM photographs of the $Gd_{11}Ni_4In_9$ fibers from an arc-melted ingot taken at two magnifications.

There are a number of other rare earth 11:4:9 isostructural compounds which also form a fibrous microstructure. These include: $R_{11}Ni_4In_9$ for R = Y, La-Nd, Sm, Gd-Tm and Lu; $R_{11}Pd_4In_9$, where R = Nd and Gd; and $Gd_{11}Pt_4In_9$ [5]. As far as we are aware these are the first reported intermetallics to form a fibrous microstructure directly from the melt. Metallic fibers have been prepared by other means, but all of these processes are time consuming and expensive. This discovery may open new avenues of both basic and applied research opportunities.

Acknowledgements

The research carried out at the Ames Laboratory was supported by the U.S. Department of Energy, Office of Basic Energy Science, Division of Materials Sciences and Engineering. The Ames Laboratory is operated for the U.S. Department of Energy by Iowa State University under Contract No. DE-AC02-07CH11358. A.P. is grateful to University of Genova, Italy for support for a one-year fellowship abroad.

References

1. Gschneidner, K.A., Jr. et al., "Rare Earth Intermetallics – A Fertile Field for New Discoveries," *Rare Earths 2012*, *Proceedings of the 51st Annual Conference of Metallurgists of CIM (COM2012)*, eds. J.R. Goode, G. Moldoveanse, M.S. Reyat, (Westmount, Quebec: Canadian Institute of Mining, 2012) 275-280.

2. Gschneidner, K.A., Jr. et al., "A Family of Ductile Intermetallic Compounds," *Nature Materials,* 2, (2003), 587-590. doi:10.1038/nmat958.

3. Gschneidner, K.A., Jr. et al., "Influence of the Electronic Structure on the Ductile Behavior of B2 CsCl-type AB Intermetallics," *Acta Materialia,* 57, (2009) 5876-5881. doi: 10.1016/j.actamat.2009.08.012.

4. Russell, A.M., et al., "Progress in Understanding the High Ductility of Rare Earth B2 (CsCl-type) Intermetallics," *TMS 2008, 137th Annual Meeting & Exhibition, Collected Proceedings*, (Warrendale, PA: The Minerals, Metals, Materials Society, 2008), 587-606. http://knowledge.tms.org.

5. Provino, A., et al., "$Gd_{11}Ni_4In_9$: A Self-assembled Fibrous Intermetallic Compound," submitted for publication.

CORROSION PROTECTION MECHANISMS OF RARE-EARTH BASED INHIBITORS IN AEROSPACE COATINGS

William G. Fahrenholtz and Matthew J. O'Keefe

Department of Materials Science and Engineering and the Materials Research Center
Missouri University of Science and Technology, Rolla, MO 65409 United States

Keywords: Rare-earth Compounds, Cerium, Praseodymium, Corrosion Protection Mechanism

Background

The corrosion protection mechanisms were studied for conversion coatings and paint primers containing rare-earth corrosion inhibitors on aluminum alloys used in aerospace applications. Rare-earth compounds have demonstrated the potential to be environmentally benign corrosion inhibitors. As such, they are potential replacements for chromate-based coatings. Chromates are robust inhibitors that provide protection to a variety of metal alloys in several different types of coatings. In contrast, alternative inhibitors only protect a limited number of alloys or can only be incorporated into a specific coating formulation. The purpose of this presentation is to review recent results focused on the mechanisms by which cerium-based conversion coatings and praseodymium-based inhibitors in epoxy-polyamide primers protect high strength aluminum alloys from corrosion.

Cerium-based Conversion Coatings

Pioneering research by Hinton revealed that cerium-based conversion coatings (CeCCs) could be deposited spontaneously from aqueous solutions and that the coatings provided significant corrosion protection to high strength aluminum alloys.[1,2] Subsequent research has extended the research to other substrates and revealed details of the deposition mechanism.[3-6] Hinton discovered that CeCCs acted as cathodic inhibitors based on selective deposition on intermetallic particles, but few other studies examined the mechanisms by which CeCCs protected cracks or damaged areas in the coatings.

Missouri S&T has investigated the corrosion protection mechanisms of CeCCs deposited on aluminum alloy 2024-T3 and 7075-T6 substrates using a spontaneous spray process.[7] Corrosion protection mechanisms were deduced by characterizing coatings before and after exposure to ASTM B117 salt spray testing.[8-910] These studies revealed that cerium species present in coatings were nearly insoluble.[11] Hence, the corrosion protection provided by CeCCs is different than the mechanism for conventional chromate-based coatings, which involves dissolution, transport, and reaction of inhibiting species. Instead, CeCCs appear to protect through a combination of mechanisms that includes acting as a barrier to chloride ion attack and responding electrochemically by forming a reaction layer between the CeCC and the underlying substrate (Figure 1).[12,13]

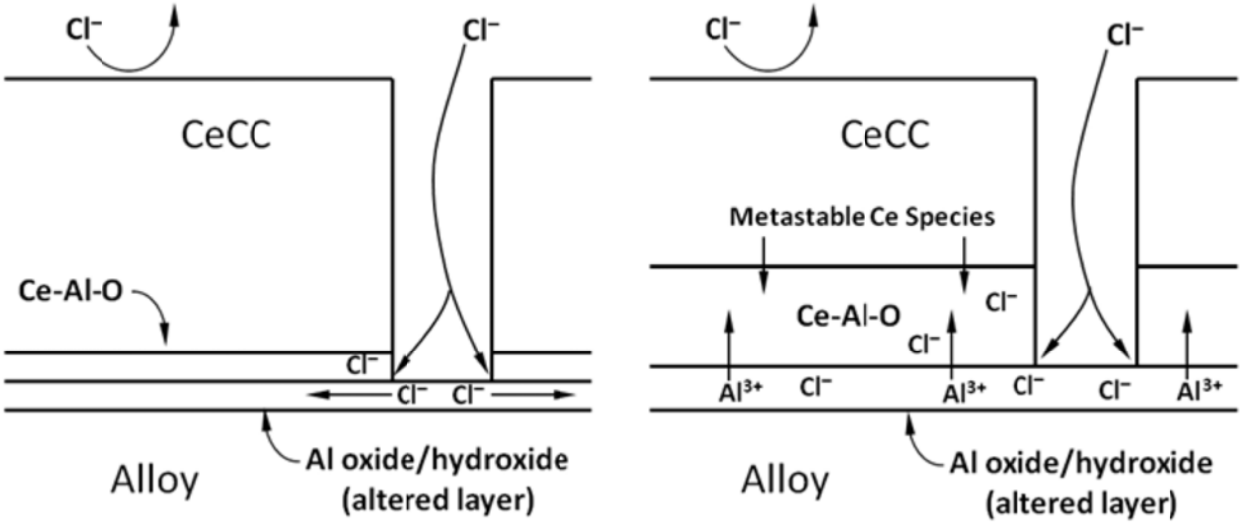

Figure 1. Schematic representation of the formation of reaction layer containing Ce, Al, and O at the interface between a CeCC and an aluminum alloy substrate during exposure to chloride ions taken from Reference 13.

Praseodymium-based Inhibitors in Epoxy-polyamide Primers

A praseodymium-based inhibitor package was developed at Missouri S&T [14,15] and has been licensed for commercial use. The inhibitor is added to the coating as Pr_2O_3, but hydrates to $Pr(OH)_3$. When the coating is damaged and the underlying metal is exposed, Pr species dissolve from the coating and transport to the site of attack. The coating has a relatively low pH due to the presence of the acid extender, which allows the Pr species to dissolve. After transport to the site of attack, the Pr species precipitate as a hydroxycarbonate phase near intermetallic particles where the local pH is relatively high.[16]

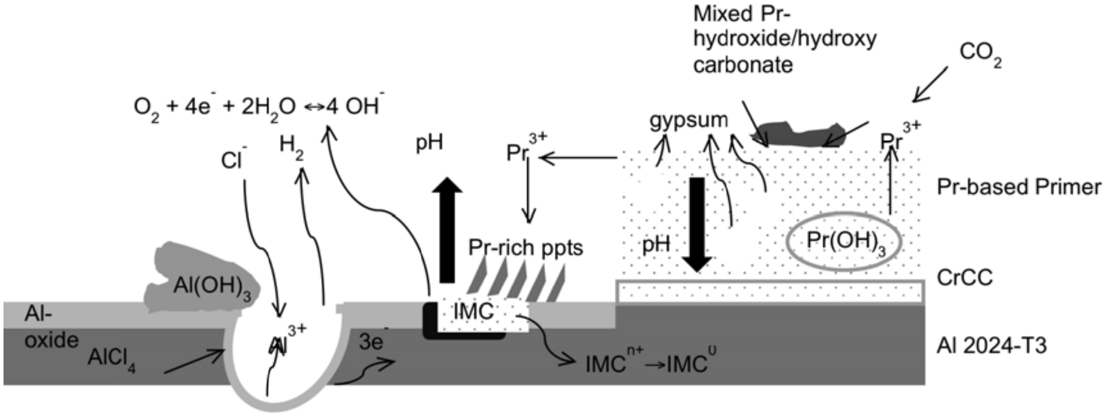

Figure 2. Schematic representation of the corrosion protection mechanism for epoxy-polyamide primers containing a praseodymium-based corrosion inhibitor from Reference 16.

Summary

Rare-earth compounds function as corrosion inhibitors in conversion coatings and paint primers. For CeCCs, the coatings inhibit corrosion by acting as a barrier between the aluminum alloy substrate and the corrosive species as well as providing electrochemical protection due to the formation of an interfacial reaction layer containing Ce, Al, and O. In contrast, Pr-based inhibitors in organic primers provide corrosion protection by dissolving from the coating, transporting to the sight of attack, and precipitating as a praseodymium hydroxycarbonate phase.

References

1. Hinton, B.W.R., D.R. Arnott, and N.E. Ryan, “The Inhibition of Aluminum Alloy Corrosion by Cerous Cations” Materials Forum, 7 (1984) 211-217.

2. Hinton, B.R.W., D.R. Arnott, and N.E. Ryan, “Cerium Conversion Coatings for the Corrosion Protection of Aluminum”, Materials Forum, 9 (1986) 62-173.

3. Palomino, L.E.M., I.V. Aoki, H.G. de Melo, “Microstructural and Electrochemical Characterization of Ce Conversion Layers Formed on Al Alloy 2024-T3 Covered with Cu-Rich Smut” Electrochimica Acta, 51 (2006) 5943-5953.

4. Decroly, A. and J-P. Petitjean, “Study of the Deposition of Cerium Oxide by Conversion on Aluminum Alloys” Surface Coatings Technology, 194 (2005) 1-9.

5. Hughes, A.E., J.D. Gorman, P.R. Miller, B.A. Sexton, P.J.K. Paterson, and R.J. Taylor, “Development of Cerium-based Conversion Coatings on 2024-T3 Al Alloy

6. After Rare-Earth Desmutting”, Surface and Interface Analysis, 36 (2004) 290-303.

7. Wang, W., F. Jiang, and F. Wang, “Cerium Chemical Conversion Coating for Aluminum Alloy 2024-T3 and its Corrosion Resistance”, Corrosion, 60 (2004) 237-243.

8. Pinc, W.R., P. Yu, M. O’Keefe, and W. Fahrenholtz, “Effect of Gelatin Additions on the Corrosion Resistance of Cerium Based Conversion Coatings Spray Deposited on Al 2024-T3,” Surface and Coatings Technology, 203(23) (2009) 3533-3540.

9. Pinc, W., D. Heller, W. Fahrenholtz, M. O’Keefe, “Electrochemical and Structural Changes in Cerium Based Conversion Coatings During Exposure to Salt Spray,” ECS Transactions, 25 (2010) 3-17.

10. Heller, D.K., W.G. Fahrenholtz, and M.J. O’Keefe, “Chemical and Structural Analysis of Subsurface Crevices Formed During Spontaneous Spray Deposition of Cerium-Based Conversion Coatings,” Materials Characterization, 62(11) (2011) 1071-1075.

11. Joshi, S., B.L. Treu, M. O’Keefe, and W.G. Fahrenholtz, “Characterization of Cerium-Based Conversion Coatings on Al 7075-T6 Deposited From Chloride and Nitrate Salt Solutions,” Journal of the Electrochemical Society, 158(3) (2011) C88-C93.

12. Joshi, S., E.A. Kulp, W.G. Fahrenholtz, and M.J. O'Keefe, "Dissolution of Cerium from Cerium-based Conversion Coatings in 0.1 M NaCl Solutions," Corrosion Science, 60 (2012) 290-295.

13. Pinc, W.R., "Characterization of the Corrosion Protection Mechanism of Cerium-Based Conversion Coatings on High Strength Aluminum Alloys," PhD Dissertation, Missouri University of Science and Technology, 2010.

HYDROPHOBICITY OF RARE-EARTH OXIDE CERAMICS AND THEIR TECHNOLOGICAL IMPACT

Gisele Azimi[1], Rajeev Dhiman[1], Hyuk-Min Kwon[1], Adam T. Paxson[1], Kripa K. Varanasi[1]

[1] Department of Mechanical Engineering, Massachusetts Institute of Technology,
Cambridge, MA 02139, USA

Keywords: Rare-earth Oxide, Hydrophobic Ceramic, Dropwise Condensation, Water Repellency

Abstract

Robust hydrophobic materials can have broad applications in various industries including energy, water, and transportation. Existing durable materials such as metals and ceramics are generally hydrophilic and require polymeric modifiers to render them hydrophobic, but these modifiers deteriorate in harsh environments. Therefore, robust hydrophobic surfaces have been difficult to realize and their widespread applicability has been limited. Here we demonstrate that all rare-earth oxide ceramics, ranging from ceria to lutetia, are intrinsically hydrophobic. We attribute this behavior to their unique electronic structure that minimizes polar interactions with interfacial water molecules. To demonstrate their technological potential, we show dropwise condensation, water repellency, and sustained hydrophobicity after exposure to high temperature, steam, and abrasive wear. Since these ceramics are intrinsically hydrophobic, they can preserve their hydrophobicity even after damage at the surface. Hence, we envision that this class of robust hydrophobic materials will have far-reaching technological potential in various industrial applications.

Introduction

Over the past decades a significant body of theoretical and experimental work has been devoted to understanding interfacial water. It is known that common ceramics and metals tend to be hydrophilic, as their surfaces are known to have a large number of polar sites due to coordinative unsaturation [1-8]. For example, pristine alumina has a large number of polar sites originating from unsaturated aluminum and oxygen atoms that act as Lewis acid and base sites, respectively [6-8]. The aluminum atoms at the surface are electron-deficient, with six electrons in their three sp^2-hybrid orbitals. Therefore, to achieve a full octet of electrons these atoms form a hydrogen bond with interfacial water molecules, resulting in a hydrophilic hydration structure, as sketched schematically in Figure 1a [5].

In contrast, metal atoms in rare-earth oxides (REOs) have a different electronic structure where the unfilled $4f$ orbitals are shielded from interactions with the surrounding environment by the full octet of electrons in the $5s^2p^6$ outer shell [5]. Consequently, these metal atoms would have lower tendency to form a hydrogen bond (HB) with interfacial water molecules. Hence, water molecules next to the surface cannot maintain their hydrogen-bonding network and instead would be expected to orient such that one HB vector points towards the surface while the remaining three point away from the surface as shown in Figure 1b [5]. This orientation is reminiscent of a hydrophobic hydration structure [9,10], and we therefore anticipate rare-earth oxides to exhibit hydrophobic wetting properties. Indeed, we observe water droplets to bead up on a smooth neodymia surface (Figure 1b), in contrast to alumina (Figure 1a) [5].

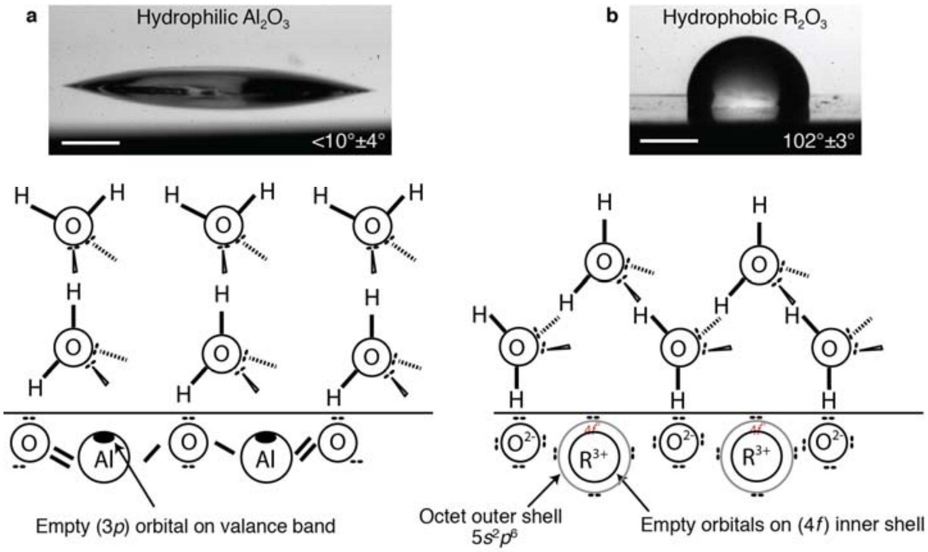

Figure 1. Schematic of the orientation of water molecules and the associated wetting properties of a surface. (a) Hydrophilicity and schematic of water molecules' orientation next to alumina surface (using different scales for the surface and water molecules). (b) Hydrophobicity and schematic of water molecules' orientation next to a rare-earth oxide surface (surface and water molecules not to scale).The photograph shows water droplet beading up on a smooth neodymia surface. The scale bars are 1 mm [5].

Experimental

To validate our hypothesis on the hydrophobicity of REOs, we synthesized their entire series from cerium oxide to lutetium oxide, except promethium oxide, as it is radioactive. We dry-pressed their powders into disk pellets, and sintered the green bodies in a tube furnace in a dry air environment. Sintering temperatures were determined based on the melting point of each REO and ranged from 1400 °C to 1650 °C [5].

Results and Discussion

We characterized the wetting properties of the sintered pellets by measuring contact angles of three probe fluids (water, ethylene glycol, diiodomethane) and quantifying the polar component of surface free energy using the van Oss-Good-Chaudhury approach [11]. The sintered pellets were polished to a mirror finish to minimize the effect of roughness on contact angle measurements. As hypothesized, all the rare-earth oxides are hydrophobic: water contact angles range between 100° and 115° (see Figure 2). In addition, the polar component of surface free energy for all rare-earth oxides was found to be negligible as shown in Figure 2. Moreover, there is minimal variation in the wetting properties over the entire series, which is consistent with the previously reported similarities in other physiochemical properties of rare-earth elements and their compounds [5].

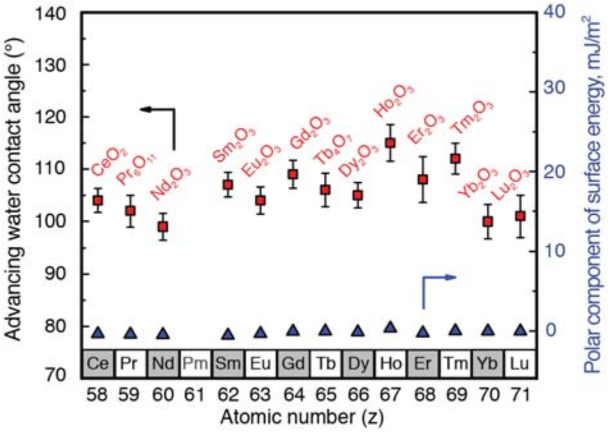

Figure 2. Measured advancing water contact angle (left axis) and the polar component of the surface free energy (right axis) of sintered rare-earth oxides [5].

To highlight the technological potential of this class of hydrophobic ceramics, we conducted steam condensation, water droplet impingement, high-temperature exposure, and abrasive wear experiments on these ceramics and demonstrated dropwise condensation, complete water droplet bounce-off, and sustained hydrophobicity after high-temperature exposure and abrasion [5].

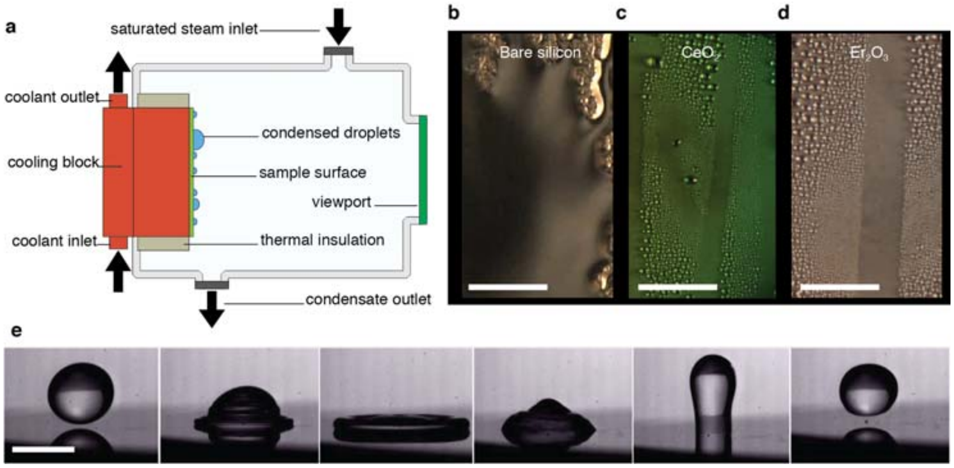

Figure 3. Steam condensation and water repellency on smooth REO substrates. (a) Condensation chamber schematic. (b) Filmwise condensation on a bare silicon substrate. (c) and (d) Dropwise condensation on CeO_2 and Er_2O_3 sputtered silicon wafers. The scale bars are 5 mm. (e) Sequential photographs of water droplet impinging (V = ~1.2 m/s) on a smooth silicon wafer sputtered with a thin layer of ceria (~200 nm). The scale bar is 2.5 mm [5].

For steam condensation experiments, we exposed smooth silicon wafers sputtered with a thin layer (~200-350 nm) of rare-earth oxides to saturated steam in a controlled environment condensation chamber. Figure 3a shows a schematic of the condensation chamber. Since these surfaces are hydrophobic, condensation occurred in the dropwise mode in contrast to the filmwise mode on a bare silicon surface (see Figure 3b-d). The dropwise mode of condensation yields significantly higher heat transfer coefficients than the filmwise mode. Our experiments show that the rare-earth oxides are sufficiently hydrophobic to promote dropwise condensation, and also result in departing drop sizes that are smaller than those exhibited on typical dropwise promoters, such as oleic acid and gold, by greater than 30%, and thus are expected to yield higher heat transfer coefficients. As another example of the hydrophobicity of rare-earth oxides, we show that water droplets impinging on a smooth ceria surface completely rebound, leaving the surface dry (see Figure 3e) [5].

Conclusion

In summary, we show that rare-earth oxides over the entire lanthanide series are intrinsically hydrophobic. These materials could be applied as coatings at large scales using a wide variety of ceramic processing techniques including thermal sprays and colloidal processing. We therefore envision hydrophobic rare-earth oxide ceramics help realize the technological potential of hydrophobic surfaces by addressing some critical aspects of robustness [5].

References

1. Quéré, D.,"Non-sticking drops." *Rep. Prog. Phys.* 68 (2005) 2495–2532.
2. Bocquet, L., and E. Lauga, "A smooth future?" *Nature Mater.* 10 (2011) 334–337.
3. Quéré, D.,"Wetting and roughness." *Annu. Rev. Mater. Res.* 38 (2008) 71–99.
4. Liu, K., and L. Jiang, "Metallic surfaces with special wettability." *Nanoscale* 3 (2011) 825–838.
5. Azimi, G., R. Dhiman, H. Kwon, A.T. Paxson, and K.K. Varanasi, "Hydrophobicity of rare-earth oxide ceramics, *Nature Mater.* 12 (2013) 315–320.
6. Kung, H.H., *Transition Metal Oxides: Surface Chemistry and Catalysis* (New York, NY: Elsevier, 1989), 53-57.
7. Drzymala, J.,"Hydrophobicity and collectorless flotation of inorganic materials." *Adv. Colloid Interface Sci.* 50 (1994) 143–185.
8. Hass, K.C., W.F. Schneider, A. Curioni, and W. Andreoni, " The chemistry of water on alumina surfaces: reaction dynamics from first principles." *Science* 282 (1998) 265–268.
9. Giovambattista, N., P.G. Debenedetti, and P.J. Rossky, "Effect of surface polarity on water contact angle and interfacial hydration structure." *J. Phys. Chem. B* 111 (2007) 9581–9587.
10. Stirnemann, G., P.J. Rossky, J.T. Hynes, and D. Laage, "Water reorientation, hydrogen-bond dynamics and 2D-IR spectroscopy next to an extended hydrophobic surface." *Faraday Discuss.* 146 (2010) 263–281.
11. Good, R.J., "Contact angle, wetting, and adhesion: a critical review." *J. Adhes. Sci. Technol.* 6 (1992) 1269–1302.

UNDERSTANDING THE STRUCTURAL STABILITY OF RARE-EARTH CONTAINING PYROCHLORE-TYPE OXIDES FOR NUCLEAR WASTE SEQUESTRATION APPLICATIONS BY X-RAY SPECTROSCOPY

Esther Rani Aluri and Andrew P. Grosvenor*

Department of Chemistry,
University of Saskatchewan,
Saskatoon, SK, Canada, S7N 5C9

*andrew.grosvenor@usask.ca

Abstract

With the continued use of nuclear reactors to supplement civilian power needs, appropriate technologies need to be developed to deal with radioactive waste [1]. Current strategies for waste management include incorporating waste elements in silica glasses or placing spent nuclear fuel bundles in casks [1,2]. An alternative strategy is to heat a mixture of waste elements and appropriate binary metal oxides to high temperature to form a crystalline, ordered oxide structure that incorporates the waste elements, especially actinide elements, in distinct crystallographic positions [1,3]. The pyrochlore-type structure has received considerable attention as a potential nuclear wasteform owing to its compositional flexibility, enhanced resistance to structure damage caused by radioactive decay, and the high concentration of actinides that can be substituted into these materials [1,3]. Pyrochlore-type oxides can be represented by the following formula, $A_2B_2O_7$, where the A atoms are found in an 8-coordinate site while the B atoms are found in a 6-coordinate site [1].

For a crystalline oxide to be considered as a potential nuclear wasteform for long-term storage of radioactive elements, it must remain crystalline for thousands of years [1]. Radioactive decay of incorporated actinide elements can lead to structural damage, resulting in the crystalline material potentially transforming to an amorphous phase [1,3,4]. As such, it is necessary to understand how a structure responds to the radioactive decay of incorporated actinide elements. Investigating actinide-containing materials can be difficult owing to the radiotoxicity of these materials; however, actinide simulator elements such as rare-earth (RE) elements can be used instead, and bombarding the materials using a beam of high-energy heavy ions can simulate the effect of radioactive decay on a material [1,3,4]. Along with acting as an actinide simulator, rare-earth elements are also used in the nuclear industry as neutron absorbers and can be incorporated in burnable poisons for in-reactor applications, and in wasteforms to stabilize the material [5,6]. In this study, it is shown how X-ray absorption near-edge spectroscopy (XANES) can be used to investigate the structural stability of rare-earth titanate and stannate pyrochlore-type oxides ($RE_2Ti_2O_7$, $Gd_2Ti_{2-x}Sn_xO_7$; RE = Sm, Gd, Yb).

The $RE_2Ti_2O_7$ and $Gd_2Ti_{2-x}Sn_xO_7$ oxides were synthesized by combining stoichiometric quantities of binary oxides (RE_2O_3, TiO_2, SnO_2) and heated at 1400 °C until phase purity was reached. To simulate structural damage of the materials by radioactive decay, sintered pellets were bombarded (implanted) using a beam of 2 MV Au^{1-} ions produced using the 1.7 MV Tandetron accelerator located at Interface Science Western, University of Western Ontario. The effect of ion implantation on the materials was investigated by collecting XANES spectra using

beamlines located at the Canadian Light Source and Advanced Photon Source synchrotron radiation facilities. High-energy XANES spectra are generally bulk sensitive; however, the 2 MV ion beam used in this study penetrates up to a maximum depth of 450 nm. Decreasing the angle of incidence between the X-ray beam and the surface of the material increases the surface sensitivity of the spectra, enabling an investigation of the implanted near-surface region [4]. This technique, referred to as Glancing-angle XANES (GA-XANES), has been used here to study the structural stability of $RE_2Ti_2O_7$ and $Gd_2Ti_{2-x}Sn_xO_7$ pyrochlore-type oxides.

First-row transition-metal XANES spectra are very sensitive to changes in the local coordination environment, especially K-edge spectra in which a 1s electron is excited into either unoccupied 3d (pre-edge) or 4p (main-edge) conduction states. The pre-edge (1s → 3d) region in Ti K-edge XANES spectra is particularly sensitive to these changes [7]. The pre-edge peak intensity from Ti in a 6-coordinate environment is very weak, and it increases in intensity significantly with decreasing coordination number [8]. Ti K-edge XANES spectra were collected from all $RE_2Ti_2O_7$ materials studied before being exposed to the ion beam (Fig. 1a). Examination of both the pre-edge and main-edge regions of the spectra confirmed that Ti was present in a 6-coordinate site. This observation is important as it is known that the A- and B-site atoms can undergo antisite disorder in the pyrchlore-type structure as the ionic radius ratio between the A and B atoms (r_A/r_B) decreases and approaches 1.46 [1,8]. Below a r_A/r_B ratio of 1.46, the material is more likely to adopt the disordered, defect fluorite structure [1,8].

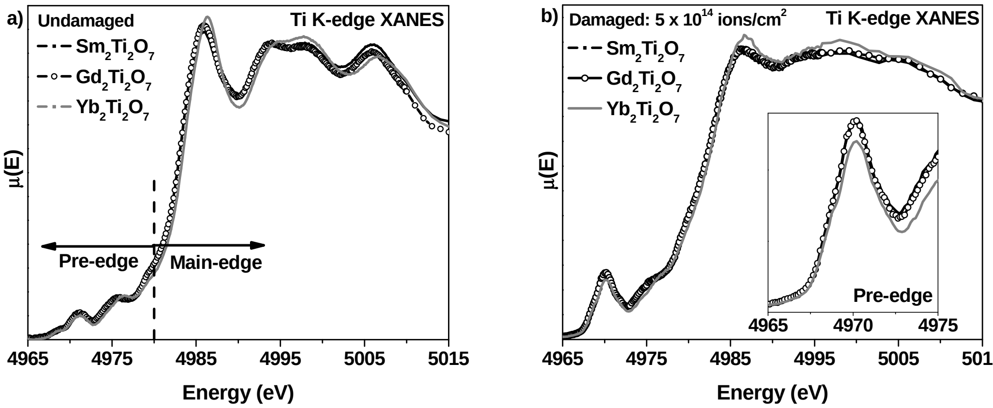

Figure 1. (a) Ti K-edge XANES spectra from $RE_2Ti_2O_7$ (RE = Sm, Gd, Yb). All three spectra are indicative of Ti being located in the 6-coordinate B-site. (b) Ti K-edge GA-XANES spectra from $RE_2Ti_2O_7$ after being implanted by a 2 MV Au^{1-} ion beam to a dose of 5 x 10^{14} ions/cm^2. The X-ray attenuation depth was 450 nm for each spectrum. A lower pre-edge peak intensity in the spectrum from $Yb_2Ti_2O_7$ shows that this material is less susceptible to radiation induced structural damage compared to $Sm_2Ti_2O_7$ and $Gd_2Ti_2O_7$.

After implanting the $RE_2Ti_2O_7$ materials to a dose of 5 x 10^{14} ions/cm^2 using 2 MV Au^{1-} ions, Ti K-edge GA-XANES spectra were collected using a glancing angle that resulted in the X-ray beam penetrating the surface of the material up to a distance of 450 nm (Fig. 1b). After implantation, the pre-edge peak in the Ti K-edge spectra from each material showed that the local coordination environment around the Ti atoms decreased from 6 in the undamaged materials to a mixture of 6- and 5-, and possibly 4-coordinate Ti in the damaged materials. Examination of these spectra from $Sm_2Ti_2O_7$, $Gd_2Ti_2O_7$, and $Yb_2Ti_2O_7$ showed that the susceptibility of the materials to becoming amorphous because of radioactive decay decreased as the RE element was changed from Sm or Gd to Yb. This result is consistent with previous transmission electron microscopy studies, and is a result of $Yb_2Ti_2O_7$ transforming from the ordered, pyrochlore structure to the disordered, defect fluorite structure instead of becoming amorphous [3]. As the r_A/r_B radius ratio is lower in $Yb_2Ti_2O_7$ than in $Sm_2Ti_2O_7$ or $Gd_2Ti_2O_7$, the cations are more likely to undergo antisite disorder, which leads to the transformation of the structure [3].

The r_A/r_B ionic radius ratio decreases in $Gd_2Ti_{2-x}Sn_xO_7$ with increasing Sn concentration while the metal-oxygen bond covalency increases [9]. It has been suggested previously that the degree of covalency of the metal-oxygen bonds in a material can affect the ability of the material to remain crystalline when implanted by high-energy ion beams [1]. Examination of $Gd_2Ti_{2-x}Sn_xO_7$ materials by XANES confirmed that the Sn-O bond becomes more covalent with increasing Sn concentration [9]. Pellets of these materials were implanted to a dose of 5 x 10^{15} ions/cm^2 with Au^{1-} ions and studied by GA-XANES. Examination of Ti K- and Sn L-edge GA-XANES spectra showed that these materials become more susceptible to radiation induced structure damage with increasing Sn content (Fig. 2). The increased covalency of the Sn-O bond results in an increase in the energy required to disorder the Sn atoms in the 6-coordinate (A) site into the 8-coordinate (B) site [10]. This leads to the material becoming more likely to become amorphous because of radiation induced structure damage instead of transforming from the pyrochlore structure to the defect-fluorite structure [10]. Comparison of GA-XANES spectra from ion implanted $RE_2Ti_2O_7$ and $Gd_2Ti_{2-x}Sn_xO_7$ surfaces has shown the importance of ionic radii and bond covalency to the ability of a material to resist radiation induced structure damage.

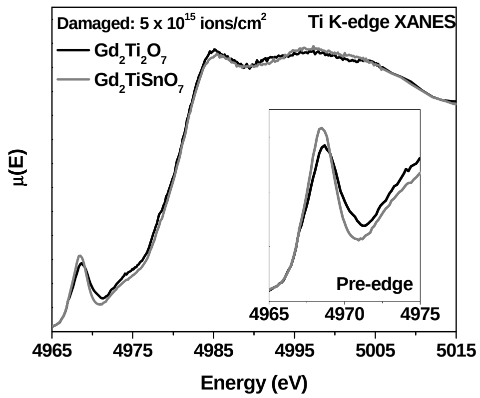

Figure 2. Ti K-edge GA-XANES spectra from $Gd_2Ti_{2-x}Sn_xO_7$ (x = 0, 1) after being implanted by a 2 MV Au^{1-} ion beam to a dose of 5 x 10^{15} ions/cm^2. The X-ray attenuation depth was 100 nm for each spectrum. An increase of the pre-edge peak intensity on going from $Gd_2Ti_2O_7$ and Gd_2TiSnO_7 indicates that $Gd_2Ti_{2-x}Sn_xO_7$ becomes more susceptible to radiation induced structure damage with increasing Sn concentration.

References

1. Ewing, R.C., W. J. Weber, J. Lian, “Nuclear waste disposal – pyrochlore ($A_2B_2O_7$): nuclear waste form for the immobilization of plutonium and “minor” actinides”, *Journal of Applied Physics*, 95 (2004), 5949 – 5971.

2. Loiseau, P., D. Caurant, O. Majerus, N. Baffier, C. Fillet, “Crystallization study of (TiO_2, ZrO_2)-rich SiO_2-Al_2O_3-CaO glasses”, *Journal of Materials Science*, 38 (2003), 843 – 852.

3. Lian, J., J. Chen, L. M. Wang, R. C. Ewing, J. M. Farmer, L. A. Boatner, K. B. Helean, "Radiation-induced amorphization of rare-earth titanate pyrochlores", *Physical Review B*, 68 (2003), 134107.

4. Reid, D.P., M. C. Stennett, B. Ravel, J. C. Woicik, N. Peng, E. R. Maddrell, N. C. Hyatt, "The structure of ion beam amorphized zirconolite studied by grazing angle X-ray absorption spectroscopy", *Nuclear Instruments and Methods in Physics Research B*, 268 (2010), 1847 – 1852.

5. Mandal, B.P., P. S. R. Krishna, A. K. Tyagi, "Order-disorder transition in the $Nd_{2-y}Y_yZr_2O_7$ system: Probed by X-ray diffraction and Raman spectroscopy", *Journal of Solid State Chemistry*, 183 (2010), 41 – 45.

6. Kim, H.S., C. Y. Joung, B. H. Lee, S. H. Kim, D. S. Sohn, "Characteristics of $Gd_xM_yO_z$ (M = Ti, Zr or Al) as a burnable absorber", *Journal of Nuclear Materials*, 372 (2008), 340 – 349.

7. Walker, J.D.S., J. R. Hayes, M. W. Gaultois, E. R. Aluri, A. P. Grosvenor, "A case for oxygen deficiency in $Gd_2Ti_{2-x}Zr_xO_7$ pyrochlore-type oxides", *Journal of Alloys and Compounds*, 565 (2013), 44 – 49.

8. Subramanian, M.A., G. Aravamudan, G. V. S. Rao, "*Oxide pyrochlores – A review*", Progress in Solid State Chemistry, 15 (1983), 55 – 143.

9. Aluri, E.R., A. P. Grosvenor, "*An X-ray absorption spectroscopic study of the effect of bond covalency on the electronic structure of* $Gd_2Ti_{2-x}Sn_xO_7$", 15 (2013), 10477 – 10486.

10. Panero, W.R., L. Stixrude, R. C. Ewing, "*First-principles calculation of defect-formation energies in the* $Y_2(Ti, Sn, Zr)_2O_7$ *pyrochlore*", 70 (2004), 054110.

DYSPROSIUM-FREE MELT-SPUN PERMANENT MAGNETS

David Brown, Wu Zhensheng, He Feng, David Miller and Jim Herchenroeder

Magnequench Technology Centre
01-19 The Galen, 61 Science Park Road, Singapore 117525

Keywords: Permanent Magnets, NdFeB, Dy-free, Melt-spun, Grain Size

Abstract

Melt-spun NdFeB powders can be formed into a number of different types of permanent magnet for a variety of applications in the electronics and automotive industries. The melt-spinning process produces powder with a fine, uniform array of nano-scale $Nd_2Fe_{14}B$ grains. These powders can be net-shape formed into isotropic polymer-bonded magnets or hot formed into fully dense magnets. This paper discusses the influence of heavy rare-earth elements and microstructure on the magnetic performance, thermal stability and material cost of NdFeB magnets. It is demonstrated that melt-spun nanocrystalline NdFeB magnets are less dependent on heavy-rare-earth elements for high-temperature performance than the traditional 5-10 μm grain-sized sintered NdFeB magnets. In particular, hot-pressed melt-spun magnets are an attractive, low cost solution for applications that require thermal stability up to 175-200°C.

Introduction

There are many factors that govern the successful application of permanent magnets. Traditionally high remanence (B_r) and maximum energy product (BH_{max}) have been a priority. However, enhanced intrinsic coercivity (H_{ci}), good thermal stability and alloy cost have become increasingly important. Melt-spun NdFeB magnets offer particular advantages with respect to these latter three considerations.

NdFeB can be rapidly solidified by pouring a stream of molten alloy on to a high-speed rotating quench wheel. The resulting flake-like powder is approximately 30 μm in thickness, mechanically brittle, extremely chemically stable and magnetically isotropic [1, 2]. Figure 1 shows SEM images of this melt-spun powder and the $Nd_2Fe_{14}B$ grain structure within each single flake, at a magnification of 70,000 times. These $Nd_2Fe_{14}B$ grains are arranged isotropically, and are near-spherical with diameters of 50 nm.

Polymer-bonded Magnets

Most applications of melt-spun NdFeB powder are for isotropic polymer-bonded magnets with BH_{max} between 40 and 80 kJ/m^3. These are typically cured compacts of between 60 and 80 vol % NdFeB powder in an epoxy- or nylon-based resin. These magnets can be net-shape formed into intricate parts, like thin-walled rings for spindle motors in drive systems [3]. Bonded NdFeB magnets are significantly stronger than sintered ferrite magnets (BH_{max} ~ 30 kJ/m^3) but weaker than sintered NdFeB magnets (BH_{max} ~300 kJ/m^3). Therefore, to compete with the high flux density of sintered NdFeB magnets, melt-spun powders need to be fully densified by hot pressing and crystallographically orientated by hot deformation processes.

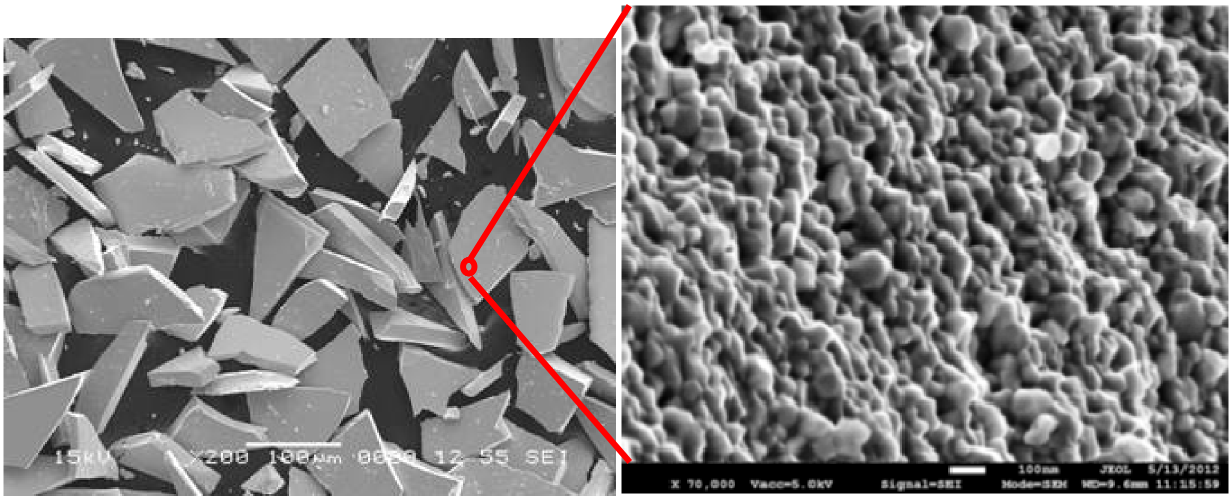

Figure 1. Images of the melt-spun NdFeB powder and internal nano-scale grain structure.

Hot-pressed Magnets

Melt-spun powder, with compositions where the rare-earth component is over 28 wt%, can be hot pressed into fully dense, isotropic magnets. The powder is first cold compacted into a low-density perform (~65% with respect to the density of $Nd_2Fe_{14}B$), coated with a lubricant and then pressed to full density at ~750 °C under a load of approximately 100 MPa. Figure 2 illustrates the microstructure of a hot-pressed magnet at two different magnifications. At low magnification, on the left, the as-spun flakes can be observed to align perpendicular to the pressing-force direction in the densified structure. The 50,000 times magnification image to the right reveals the nano-scale $Nd_2Fe_{14}B$ grains within each individual flake. These $Nd_2Fe_{14}B$ grains are similar to those observed in the as-spun material, albeit slightly larger at 80-100 nm.

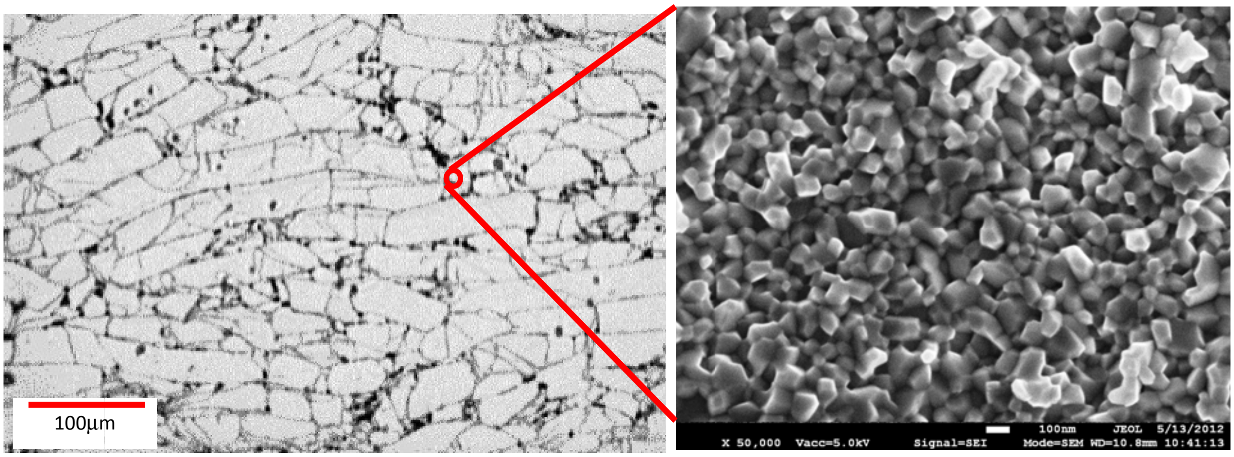

Figure 2. Hot pressed magnet microstructure.

Hot-deformed Magnets

Fully dense compacts can then be hot deformed (e.g. extruded or die-upset) to produce anisotropic, high-energy magnets. Hot deforming NdFeB creates much greater crystallographic alignment, and therefore much higher B_r (>1.2 T) and BH_{max} (~300 kJ/m^3) in the aligned direction of the magnet. Figure 3 illustrates the hot-deformed magnet microstructure at two magnifications. At low magnification on the left side, the original melt-spun flake structure can be seen in flattened, elongated form, flowing perpendicular to the force direction. At 30,000 times magnification the individual $Nd_2Fe_{14}B$ grains appear as 50 x 500 x 500 nm platelets having undergone a preferential grain-growth mechanism during deformation [4]. These $Nd_2Fe_{14}B$ grains have their magnetically preferred c-axes aligned perpendicular to the grain-growth direction and the magnet now exhibits strongly anisotropic magnetic performance in the vertical direction.

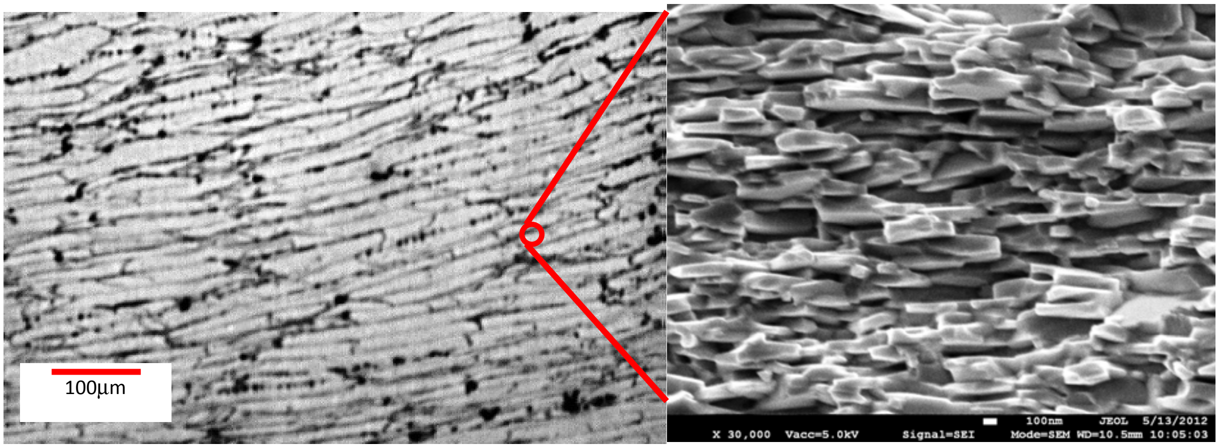

Figure 3. Hot deformed magnet microstructure, showing the $Nd_2Fe_{14}B$ grains at x 30,000 mag.

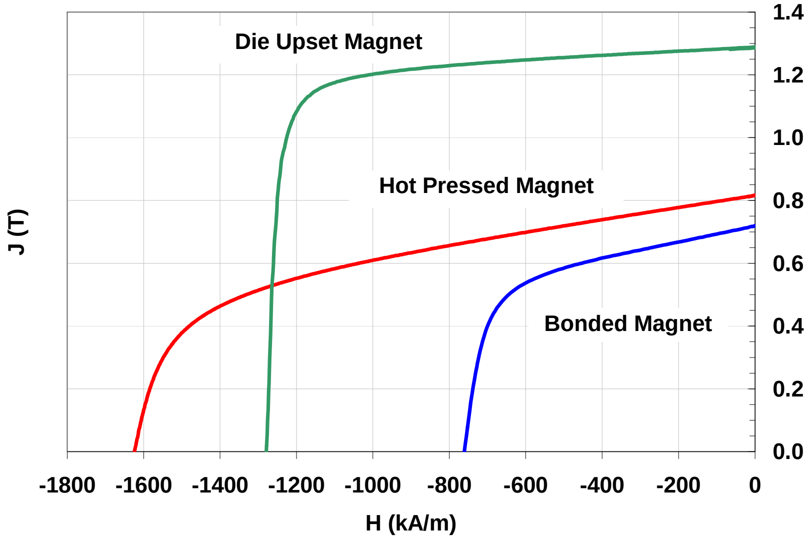

Figure 4. Comparison of melt-spun NdFeB magnet demagnetization curves.

Figure 4 illustrates the relative magnetic performances of polymer-bonded, hot-pressed and hot-die-upset melt-spun magnets. The transition from isotropic to anisotropic performance can be seen by comparing the hot-pressed sample (BH_{max} = 120-140 kJ/m^3) with the die-upset sample (BH_{max} = 240-360 kJ/m^3), and the microstructural images in Figures 2 and 3.

Recent Developments with Hot-pressed and Hot-Deformed Magnets

Over the last 20 years, hot-extruded melt-spun material has enjoyed considerable commercial success in the form of radially aligned ring magnets. These anisotropic ring magnets are commercially available in a wide range of sizes (minimum outer diameter of 5 mm, heights of up to 80 mm, wall thickness >1 mm) and can be found in a number of applications from micro-motors to automotive power-steering devices [5, 6]. Recently, both hot-pressed and hot-deformed melt-spun magnets have become more competitive with the traditional sintered NdFeB magnets, as they are less reliant on expensive heavy-rare-earth elements (Dy and Tb) for higher H_{ci} [7].

Sintered NdFeB magnets dominate the NdFeB industry, representing approximately 90% of all NdFeB magnet material produced. These magnets are manufactured by a number of companies and are produced in large-scale batches, in contrast with the net-shaped magnets produced from melt-spun material. The microstructure of sintered NdFeB magnets is composed of 5-10 μm grains, which is much coarser than those of melt-spun magnets, as shown in Figure 5. Well-made sintered NdFeB magnets benefit from a high degree of crystallographic alignment and resulting high BH_{max}. Therefore, key development areas for melt-spun magnets have been (1) maximizing magnetic performance, (2) maintaining high thermal stability, and (3) using zero or minimal amounts of costly Dy and Tb.

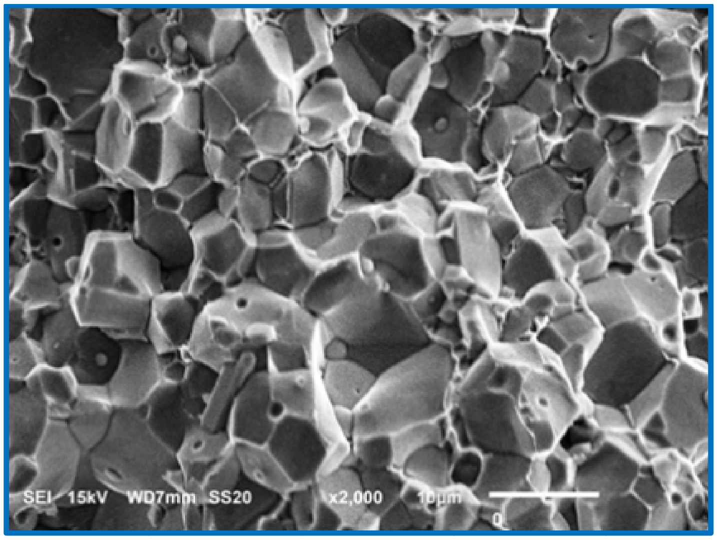

Figure 5. The typical grain structure in sintered NdFeB magnets.

1. Increasing Remanence of Hot-Deformed Magnets

Die-upsetting is one variation of the hot-deformation technique. The ranges of magnetic properties achieved by melt-spun anisotropic die-upset (MQ3) and isotropic hot-pressed (MQ2) materials are illustrated in Figure 6. The alloy composition tends to dictate the position of a particular magnet on this chart [8, 9]. Generally, some Dy is required for MQ3 magnets to exceed an H_{ci} of 1450 kA/m and MQ2 magnets to exceed H_{ci} values of 1750 kA/m.

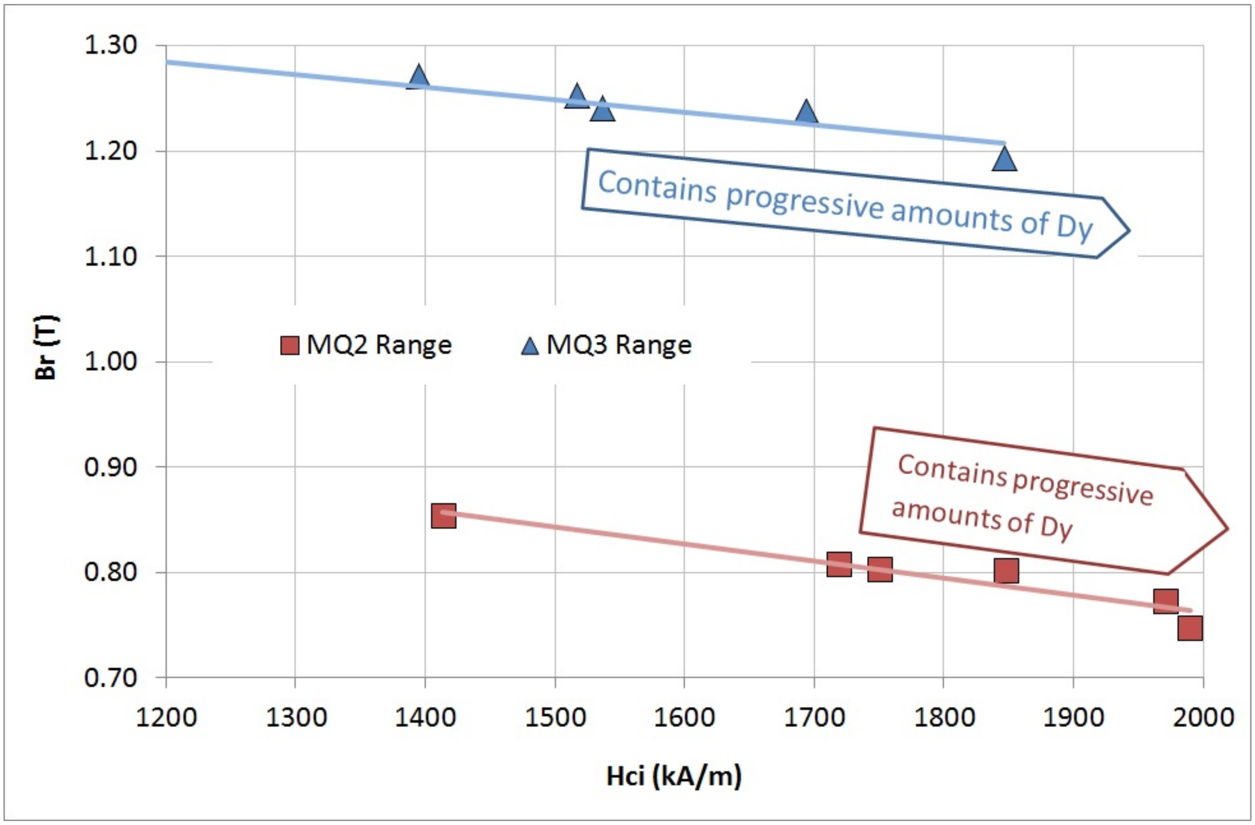

Figure 6. Magnetic performance range of die-upset (MQ3) and hot-pressed (MQ2) magnets.

If the B_r of these magnets is to be maximized the following equation has to be considered:

$$B_r = M_s \,.\, d/d_o \,.\, (1-V_{nonmag}) \,.\, f_\varphi \qquad (1)$$

where M_s is saturation magnetization , d/d_o is magnet density over theoretical density, V_{nonmag} is the volume fraction of non-magnetic phases and f_φ is the degree of alignment of magnetic phase.

A typical die-upset alloy has a composition based on 30Nd-69.1Fe-0.9B (wt.%) and has between 8 and 10 vol % of non-magnetic grain-boundary phase. Unfortunately, this level of V_{nonmag} is necessary to facilitate the die-upsetting process [4]. So the main focus of B_r improvement for die-upset magnets has to be through greater crystallographic alignment (f_φ).

This can be achieved by upsetting the magnet to a higher degree [2]. Typically, a magnet is upset by 60%. This is to say, the isotropic preform part starts with a surface area (**A_s**), which undergoes a 60% increase during the upsetting process to yield a new surface area (**A_f**), as expressed by:

$$\%\ \text{Upset} = 100\%\ \text{x}\ (A_f - A_s) / A_f \qquad (2)$$

Figure 7 illustrates the effect of increasing the degree of upset on a popular grade of die-upset magnet (MQ3-39-50). The hot-pressed preform magnet has the highest H_{ci} and near isotropic performance, while the die-upset magnets exhibit increasingly higher B_r and BH_{max} with progressively higher degrees of upset. The microstructure becomes increasingly aligned with higher upsetting, although there is an associated loss in coercivity.

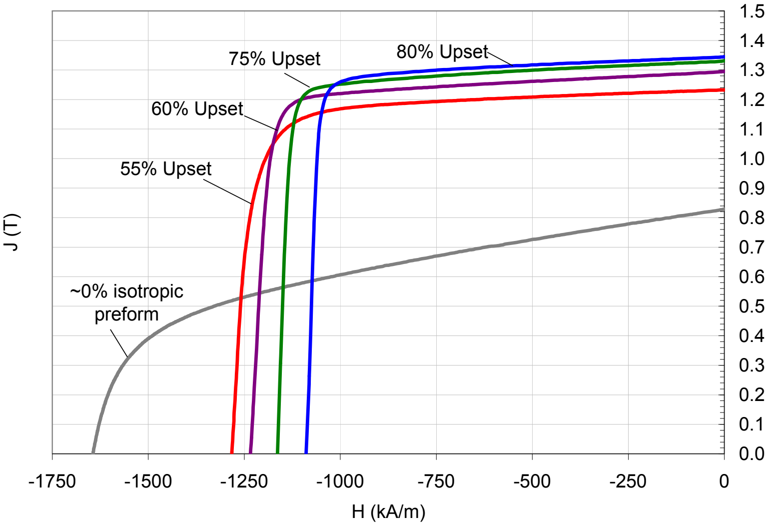

Figure 7. Demagnetization curves of MQ3-39-50 magnets with various degrees of upset, or crystallographic alignment.

2. Effect of Dy Substitution for Nd on Magnet Coercivity

Permanent-magnet devices that operate at elevated temperatures tend to need higher H_{ci} magnets so that stable performance is maintained in operation. As indicated in Figure 6, magnets with H_{ci} >1450 kA/m at 25 °C tend to need some amount of Dy in their composition. Heavy-rare-earth elements like Dy and Tb are partly substituted for Nd in the $Nd_2Fe_{14}B$ lattice and the magnetocrystalline anisotropy (H_A) of the magnet is substantially increased.

Figure 8 illustrates the demagnetization curves of three die-upset NdFeB magnets with 0, 2.6 and 4 wt% Dy. The H_{ci} is seen to increase proportionally with the Dy level, and at some expense in B_r. The Pc or load-line represents the point on the curve that a particular magnet will operate at in an open-circuit application, and is also related to the magnet's dimensional proportions. For example, short and wide magnets operate at lower Pc values and are more easily demagnetized, especially if the load-line crosses over the knee of the demagnetization curve.

A more practical illustration of how Dy, and the associated H_{ci}, affects the high-temperature stability of a magnet involves measuring the flux loss suffered by a magnet when it is exposed to a certain temperature for a certain time. Figure 9 charts the flux lost by MQ3 magnet samples of the three compositions (Dy = 0, 2.6 and 4.0 wt.%) operating at the three load-lines (Pc = 0.5, 1.0 and 2.0), after being held at temperatures between 25 and 175 °C for 1 hour.

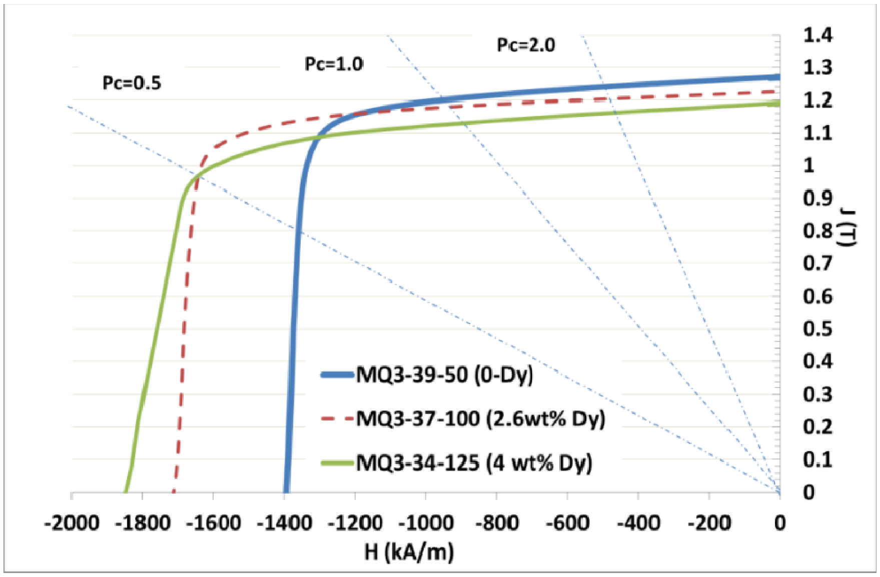

Figure 8. Demagnetization curves of MQ3 magnets with various levels of Dy.

The load-lines are related to magnet samples of different dimensional proportions. These MQ3 magnets were all 24.6 mm in diameter but the Pc=0.5 samples were 5.2 mm tall, Pc=1.0 samples were 9.3 mm tall, and the Pc=2.0 samples were 16.2 mm tall.

Figure 9 shows how magnets with more Dy exhibit less flux loss after being exposed to elevated temperatures. The shorter samples (Pc=0.5) were particularly affected by the elevated temperatures as these magnets were effectively operating on or beyond the knee of the demagnetization curve (Figure 8).

3. Effect of Microstructure of Magnet Coercivity

The previous figures have demonstrated the dependence of H_{ci} on the amount of Dy present. The microstructure of a magnet can also influence the way that the magnet resists demagnetization. Melt-spun magnets have the advantage of a nano-scale grain structure, where the individual $Nd_2Fe_{14}B$ grains are close to the dimensions of a magnetic domain and can resist domain movement via the intricate array of grain boundaries. In contrast, the coarser microstructure of sintered magnets has less of a grain boundary network to resist magnetic domain movement and reversal.

The performance and composition of MQ3 and sintered magnets have been compared to illustrate the effect microstructure on magnet H_{ci}. A variety of sintered grades from N35 to N45 (with H, SH and UH suffixes) were purchased from the market and compared to grades of die-upset MQ3 magnets. Figure 10 charts the H_{ci} of these samples against the amount of Dy in their composition. Most MQ3 samples have no Dy and H_{ci} values between 1250 and 1450 kA/m, while on average, the sintered samples need 2.5 wt% Dy to achieve the same H_{ci} level. The trend lines for these two types of magnet illustrate die-upset magnets have an advantage in H_{ci}.

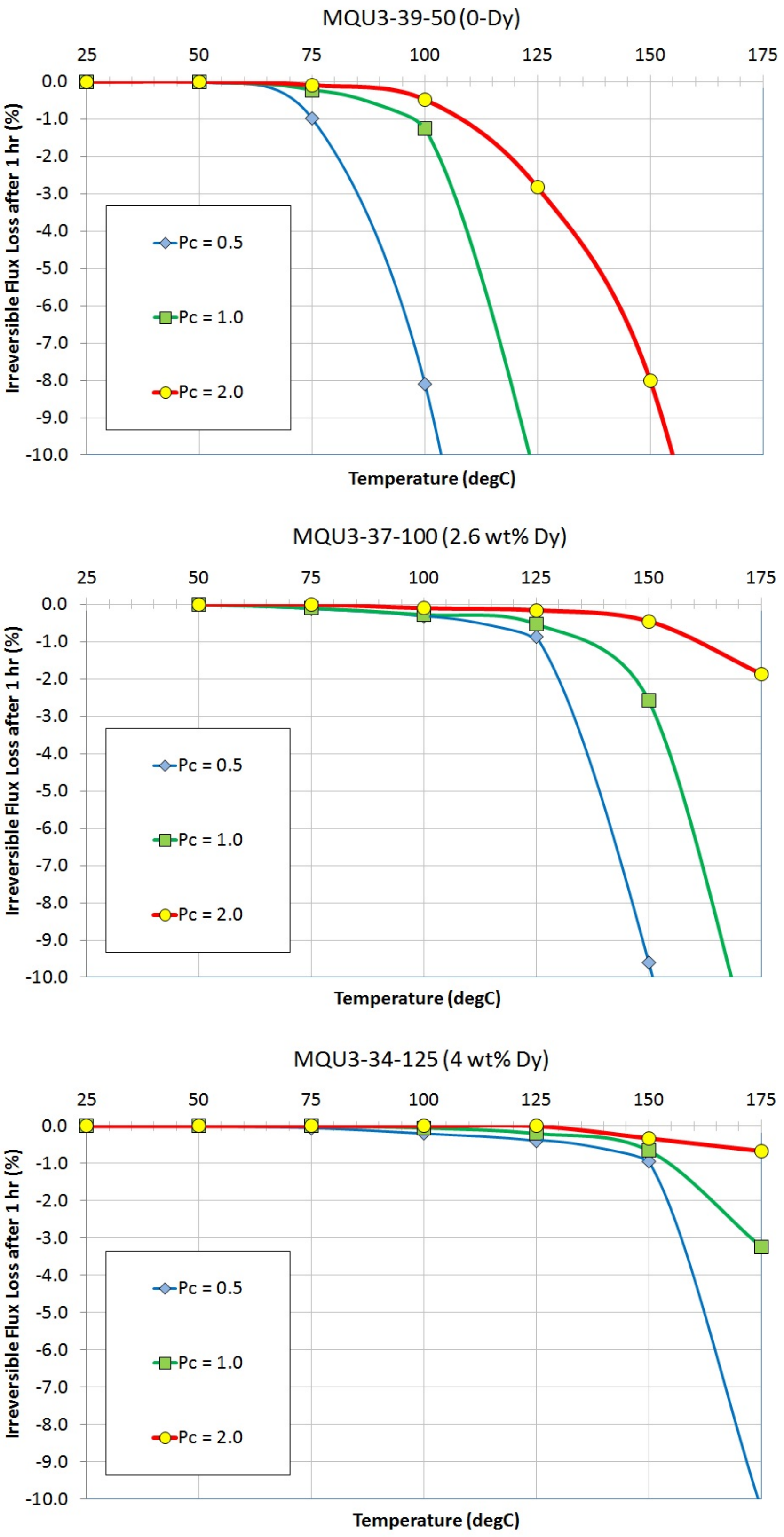

Figure 9. Effect of Dy content on ageing performance of MQ3 magnets.

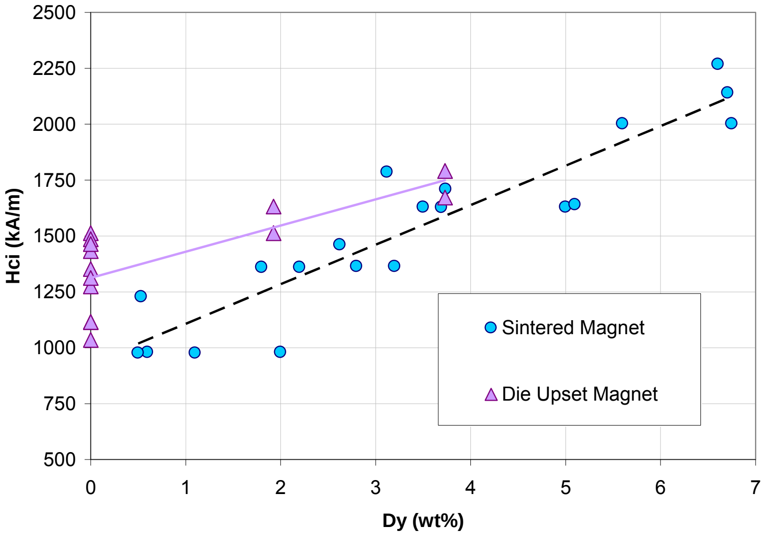

Figure 10. Coercivity of sintered and die-upset magnets with various levels of Dy.

Figure 11 compares the room-temperature demagnetization curves of Dy-free sintered, MQ3 and MQ2 magnets. A contrast in remanence and coercivity can been seen between the three types.

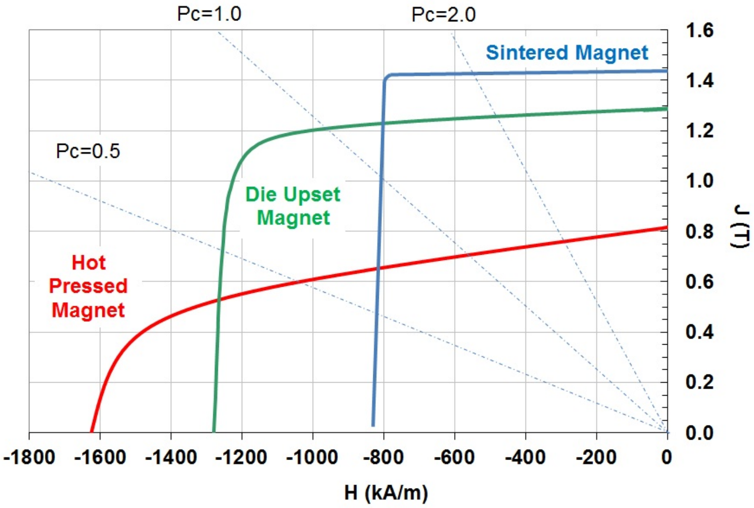

Figure 11. Demagnetization curves of the three types of Dy-free magnets.

Flux-ageing loss performance of these three types of Dy-free magnet is compared in Figure 12. Pc=0.5, 1.0 and 2.0 samples of these magnets were exposed to temperatures up to 175 °C for 1 hour and the observed flux losses were plotted against the exposure temperatures. These graphs show that Dy-free Pc=2.0 sintered magnets should not be operated above 75 °C to avoid severe flux loss, while the die-upset Pc=2.0 magnets can be operated up to 100 °C and the hot-press magnets up to and beyond 175°C without serious flux loss. The principle reason for this difference in thermal stability is the scale of microstructure. The sintered magnet exhibits 5-10 µm $Nd_2Fe_{14}B$ grains, while the die-upset magnet contains 50 nm x 500 nm x 500 nm $Nd_2Fe_{14}B$

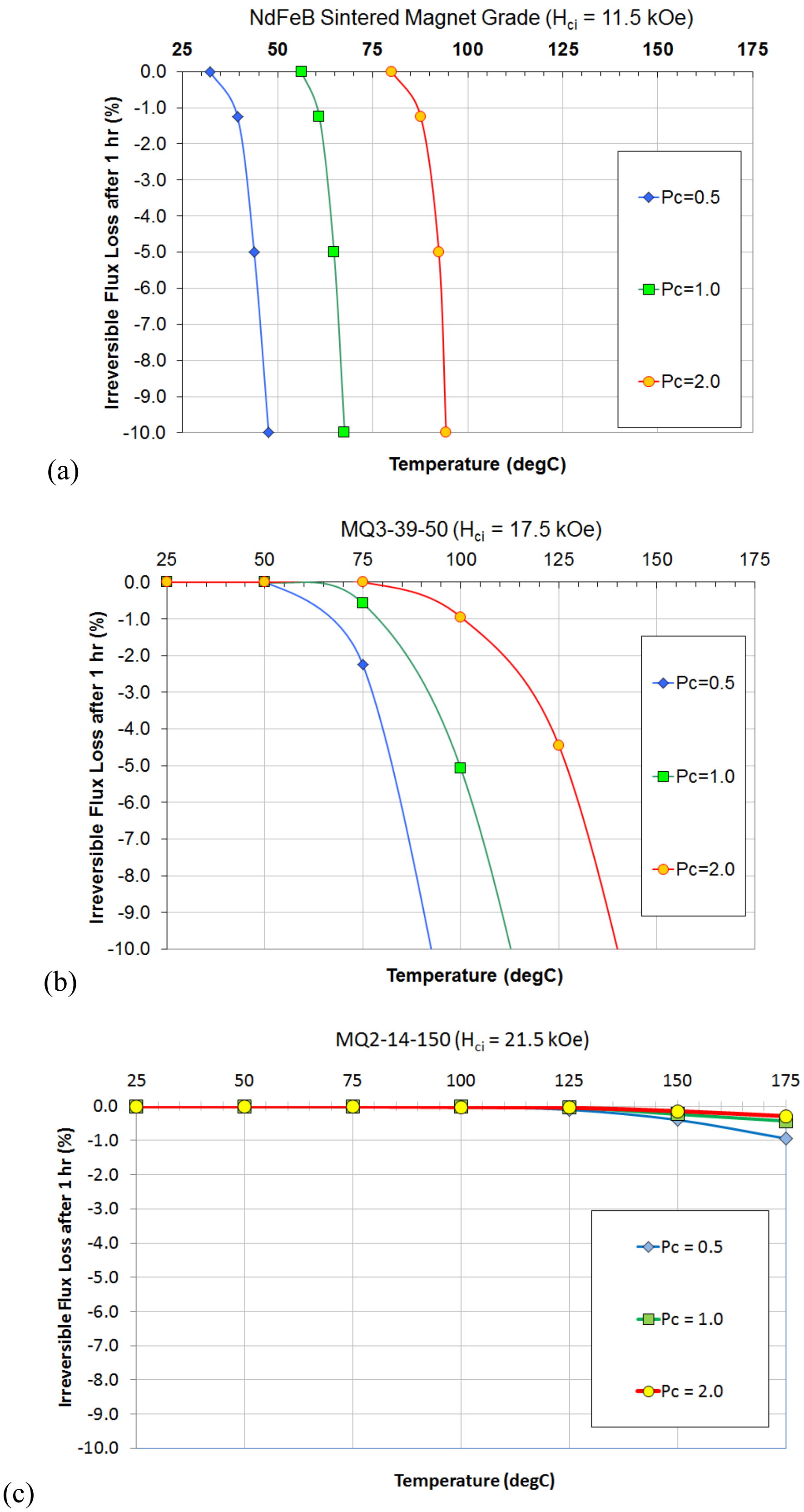

Figure 12. Flux-ageing loss behaviour of Dy-free (a) sintered, (b) MQ3, and (c) MQ2 magnets.

platelet grains, and the hot-pressed magnet contains 80-100 nm near spherical $Nd_2Fe_{14}B$ grains. This advantage in microstructure can be used to avoid having costly heavy-rare-earth elements in the alloy to control magnet thermal stability. The MQ2 magnet has the finest scale microstructure and these magnets and can be operated at extremely high temperatures without the need for any Dy in the alloy.

Summary

Having discussed the influence of heavy-rare-earth elements and microstructure on the magnetic performance and thermal stability of NdFeB magnets it is possible to see that melt-spun magnets offer an advantage. The fine nano-scale $Nd_2Fe_{14}B$ grain structures in hot-pressed and hot-deformed magnets yield higher H_{ci} and greater thermal stability than similar compositions in the coarser grained sintered magnet form. Therefore, melt-spun magnets, and in particular the hot-pressed MQ2 version, can provide a low-cost solution for permanent-magnet devices that require exceptional thermal stability.

References

1. Herbst, J.F., and J.J. Croat, J. Mag. Magn. Mat. Vol. 100, (1991) 57.
2. Croat, J.J., IEEE Trans. Mag., Vol. 25, no. 5, (1989) 3550.
3. http://www.mqitechnology.com
4. Grunberger, W., Proceedings of the 15th International Workshop on Rare-Earth Magnets and Their Applications. Dresden, Germany, 1998, 333.
5. http://www.daido-electronics.co.jp/
6. Yoshikawa, Y., et al, IEEE Trans. Magn. 35, (1999) 3268.
7. Sagawa, M., et al., J. Appl. Phys. 55, (1984) 2083.
8. Brown, D. et al J. Appl. Phys. 109, (2011) 07A742.
9. Kirchner, A., et al., *IEEE Trans. Magn.*, vol. 36, no. 5, (2000) 3288.

THE USES OF RARE EARTH ELEMENT ACTIVATED MICROMETER AND NANOMETER SIZED PHOSPHOR PARTICLES IN MODERN TECHNOLOGY

Jack Silver, George R. Fern, Terry G. Ireland, Paul Marsh, Mohd Ghazli and Xiao Yan

Centre for Phosphor and Display Materials, Wolfson Centre for Materials Processing, Brunel University, Uxbridge, Middlesex UB8 3PH, UK;

Keywords: Phosphors, Phosphor Synthesis, LED Phosphors

Abstract

An overview of the uses of rare earth element activated phosphor particles in modern technology is presented herein. Different kinds of phosphors are introduced where they are relevant, including down and up converting photoluminescent phosphors (emitting in the UV, visible or infra-red regions of the electromagnetic spectrum), cathodoluminescent phosphors, radioluminescent phosphors scintillators), electroluminescent phosphors and long after glow storage phosphors. Examples cover the displays and lighting industries, security applications (marking objects and currency) and as probes for marking bio-molecules. The main rare earth elements used for particular phosphor applications are emphasised and why particular oxidation states are useful for applications in LED lighting. Methods of both laboratory and industrial scale phosphor synthesis are briefly reviewed and illustrated including mass production of phosphor nanoparticles. Factors affecting phosphor stability/performance and the needs, methods and problems encountered in coating particular types of phosphor particles (to protect from atmospheric/environmental degradation) are partially reviewed.

Introduction

Rare Earth activated phosphors have been used in the lighting and display industry for over 80 years. The first fluorescent lamps were commercialised in the late 1930's, black and white TV appeared soon after and colour TV was widespread in the 1960's [1]. The phosphors used in these applications had to be tailored for their role and depended on specialized chemical manufacturers to produce them. In the last 60 years, research on phosphors and solid state luminescence has blossomed. Concomitant with advances in solid-state physics and optical spectroscopy, research on phosphors has led to their development as important industrial/technological materials. Phosphors have found widespread use in the lives of people all over the world.

Phosphors can be defined as solid materials manifesting luminescence, luminescence being the conversion of energy into light.

In display technology the constraints on energy provision are:

light as in	*Photo*luminescence
an electric field as in	*Electro*luminescence
cathode rays as in	*Cathodo*luminescence

So What is a Phosphor?

Phosphors may be defined as solid materials showing luminescence. Phosphors essentially consist of very pure inorganic materials doped with suitable ions called *activators*.
The activator is usually present in concentration levels varying from a few parts per million to one to five percent of the *host lattice*. Often, additional ions act as charge compensators or donors in the lattice. These are termed *co-activators*.

How Do Phosphors Emit Light?

Essentially, when an ion is in an excited state it reverts to its ground state by either:

(a) Emitting photons, (or visible light), and/or

(b) Emitting phonons, e.g. lattice vibrations

The probability of de-excitation is given by:

$$\begin{array}{ccccc} \text{Probability of} & = & \text{Probability of} & + & \text{Probability of} \\ \text{de-excitation} & & \text{radiative} & & \text{non radiative} \\ & & \text{de-excitation} & & \text{de-excitation} \\ P_{\text{de-ec}} & = & P_{\text{rad}} & + & P_{\text{non-rad}} \end{array}$$

For optimum performance a lattice must be chosen where $P_{\text{non-rad}}$ is minimised,
Typical 1/e emission life times for rare earth element activator ions in seconds are:

Eu^{3+} $(4f \leftarrow 4f)$ $\sim 10^{-4}$-10^{-2}
Tb^{3+} $(4f \leftarrow 4f)$ $\sim 10^{-4}$-10^{-2}
Ce^{3+} $(5d \leftarrow 4f)$ $\sim 3\text{x}10^{-8}$
Eu^{2+} $(5d \leftarrow 4f)$ $\sim 8\text{x}10^{-7}$

The emission of light from inorganic solids is often split into two categories which are related to the lifetime of the activator: Phosphorescence: emission having lifetimes > ca. 1 µs.

Fluorescence: emission having lifetimes < ca. 1 µs.

Phosphor Synthesis in Industry

The synthesis and characterization of inorganic phosphors has been subject to intensive research since the beginning of the last century. Due to its industrial importance most of this work has been carried out in industry and is not available in the public domain. One of the best ways to access such knowledge of phosphor manufacturing methods for industrial phosphors is to consult specialist books written by people who have spent much of their lives working in the phosphor industry rather than research journals; we therefore refer the reader to the well-known texts by Ropp [2–4]. In industry, almost all phosphors were synthesized by solid state reactions between very pure inorganic compounds at high temperature. Clearly, it is impossible to discuss every aspect of phosphor synthesis from its inception to present day in this paper so we will be brief in covering phosphor preparation. Most industrial syntheses for almost all phosphors still use solid state reactions between very pure inorganic compounds at high temperature. Such methods usually lead to micrometre sized phosphor particles. These methods of phosphor synthesis can be divided into two distinctly different types of reactions:

1. The first involves introducing the activator ions into an existing host material;

2. The second involves the synthesis of the host material and the simultaneous incorporation of the activator during firing.

The main drawbacks of these predominantly solid state methods are:

a) hat the distribution of the activators in the host lattice may not be even, as the precursors are not mixed on the atomic scale;

b) That particle growth cannot be easily controlled, and involves milling and sieving.

In recent years, with the needs for phosphors for high-definition display screens and for color-converting LEDs, attention has turned to addressing these drawbacks by studying methods of homogeneous precipitation and utilizing particle growth methods developed for other industrial uses.

The structures of most of the host lattices used to prepare phosphors have been described by Wells [5] and others [6]. The host lattice will determine the coordination environment of the dopant atom, which usually influences its emission behaviour. The influence of different site geometries for the dopant is apparent in the emission spectrum of $SrY_2O_4:Eu^{3+}$, which consists of two kinds of Eu^{3+} emission bands that are assigned to Eu^{3+} ions in the Sr site and the Y site [7]. The general properties of luminescent materials have been discussed in a number of texts [1–4, 8–10]. Full synthetic details of most phosphors can be found elsewhere [1–4, 10].

The traditional micrometre sized phosphor particles have until the last few years been the only size of phosphors widely available and are still the mainstay of the phosphor industry. However in the last twenty years interest has grown in the properties and potential applications of nanometre sized phosphor particles.

Nanophosphor Synthesis and Mass Production

To address the history of nanometre sized phosphor particles it is convenient to consider that cubic yttrium oxide doped with europium ($Y_2O_3 : Eu^{3+}$) which has been an important red industrial phosphor since its first discovery in the early 1960's for both television and lighting applications[11]. Since the first reports on quantum confined effects in nano-particle zinc sulphide based phosphors by Bhargarva and co-workers [12-17], there has been a flurry of interest into the properties and uses of many traditional phosphors in nano-particle (or nanometre sized crystalline) form. Nanocrystalline phosphors are thought to have more perfect lattices [18] and therefore fewer bulk defects compared to conventional micron size phosphor particles. Emission studies of, for example, $ZnS:Mn^{2+}$ have provided evidence that the intrinsic luminescence efficiency of the doped phosphors can be dramatically improved if the particle size is reduced to nanodimensions; in addition, lifetime shortening of the excited state has been reported [12,13,15]. These workers also reported on the preparation and optical spectroscopy of Eu and Tb doped Y_2O_3 [19].

Herein we concentrate primarily on cubic nanocrystalline $Y_2O_3:Eu^{3+}$, as this is the industrially important phase. Firstly we discuss the practical synthetic methods of producing nanocrystalline cubic europium doped yttria particles that can easily be scaled up for industrial production.

Apart from the drive of curiosity to understand the properties of nanocrystalline cubic $Y_2O_3:Eu^{3+}$ there are a number of important reasons that have pushed this research forward. To appreciate this and the need for new phosphor materials two questions must be asked and answered. These are: (a) Why new synthetic methods? (b) What is the driving force from industry? The answers include:

That in the last ten years there was demand from the market place and hence industry for both high resolution and high efficiency phosphors for flat panel displays (FPD) and field emissive displays (FED), and these were prime movers in the development of phosphors that perform at low voltages. Such FPD's and FED's were then thought to have widespread uses in advanced technological, commercial and domestic applications. For FED's in particular phosphors that perform at low voltages and are made up of small ideally spherical particles (0.1µm to 1.0µm) are of particular interest because they offer the possibility of brighter cathodoluminescence (CL), high definition, and much improved screen packing. Unfortunately technology moved faster than the research and LCD and Plasma displays dominated the market and other flat panel displays missed the bus. Nevertheless it is worth considering the methods used for the chemical synthesis of nanocrystalline cubic europium doped yttria particles. Nanocrystalline europium doped yttria particles have been synthesised using a wide variety of methods that have given rise to nanoparticles or nanocrystallites of different size regimes. The methods used to form nanocrystalline europium doped yttria particles can be divided into five categories. These are:- (a) Solution methods; (b) Aerosol Spray methods; (c) Chemical vapour techniques; (d) Combustion methods; (e) Synthesis of novel structures.

Of these methods some of the solution methods and aerosol spray methods are in some cases able to be scaled for industrial applications, and in addition industry uses techniques based on chemical vapour methods for mass production.

(a) Solution Methods (suitable for industrial use)

The homogeneous precipitation of phosphors from solution offers the possibility of facile mixing in of the dopant into the host lattice at the atomic level without depending on high temperature diffusion. This can however often involve the initial preparation of a phosphor precursor lattice such as in the most versatile method for preparing Y_2O_3:Eu^{3+} nanocrystalline phosphor which is the urea precipitation method. This method has been pioneered for phosphor application [20-33]. It is based on synthetic methods developed for the preparation of other metal oxides for a variety of uses (none phosphor uses) [24]. This method shows promise for industrial scale production and was indeed patented early for this reason.

This approach provides more effective control over stoichiometry in the final product. It also allows good control over phosphor morphology which, for example, has facilitated the generation of spherical particles (Figure I) which we have shown will pack well in small pixel areas for high definition display screens [20-32]. In addition the size of the final phosphor particle can be controlled by manipulating solution conditions in the precipitation process [29, 30, 32].

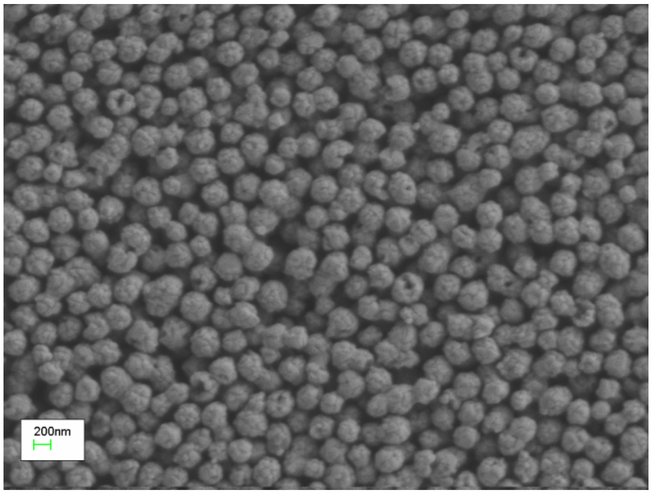

Figure 1. Spherical particles of Y_2O_3:Eu.

It was previously assumed that there was a lower limit to the particle size that could be used in practical display application [34]. Therefore, industrial phosphors were optimised with a particle size range of about 5-10µm. It was thought that a dead layer, which may be several microns thick, would invariably exist at the surface of the phosphor. Many synthetic processes, especially those using fluxes, yielded not only phosphors with even larger particlesizes, but also with a large range in particle size distribution. Probably the greatest change over the last few years is the recognition on the roles that particle size and morphology play in influencing phosphor properties [34]. Clearly, the particle shape and size will affect the screen properties and the efficiency of the final layer used in the display screen. However, the morphology may also affect the absorption of the incident electron and resultant photons as well as determining the path the light takes in leaving the phosphor thus affecting screen production. Similarly, the effects of crystallite boundaries must also be taken into consideration. Using the urea homogeneous precipitation method the synthesis of spherical phosphor powders of cubic-Y_2O_3:Eu^{3+} (Figure 1) the standard red cathode ray phosphor is facile [22-24].

(b) Aerosol Spray Methods (suitable for industrial use).

Spray pyrolysis is said to have a number of advantages in the preparation of metal oxide based phosphor particles for applications in displays and fluorescent lamps [35]. The phosphor particles prepared by this method have spherical morphologies uniform size and were non-aggregated [36-39]. However although these particles have sub-micron size and many attractions in new types of flat panel displays, they have the problem of poor luminescence characteristics due to many defects and scattering of emitted light. In our hands working with industry for scale up of nanophosphor particles we have had luminance up to 50%of bulk and even higher when the particles are given further treatments.

(c) Chemical Vapour Synthesis, (CVS).

Nanocrystalline europium doped yttria particles have been synthesized using a chemical vapour technique [40]. Y_2O_3:Eu^{3+} (NPs) were prepared in a tubular flow reactor by CVS using tris(tetramethyl-heptaanedionato) yttrium $Y(C_{11}H_{19}O_2)_3$ as the precursor for the host lattice and tris(tetramethyl-heptaanedionato) europium $Eu(C_{11}H_{19}O_2)_3$ for the europium doping. The powder was characterised using x-ray diffraction, transmission electron microscopy, and ultraviolet spectroscopy. The Y_2O_3:Eu^{3+} nanoparticles(NPs) crystallised in the cubic structure with an average particle size of only 10 nm. The reflection, excitation, and emission spectra were reported. These nanoparticles manifested blue shifted absorption bands with respect to coarse grained material [40]. Variations of this method of phosphor production have been scaled successfully by industry and ranges of rare earth element doped phosphor nanoparticles are available in bulk.

Phosphors for Lighting

Now we know what a phosphor is and how it can be made let us look at some applications of rare earth element activated phosphors for lighting summarised in Table I [1,9].

Many phosphors used for lighting depending on application (such as those used to colour change blue LEDs) are expensive selling for over £1000 per kilo, so we have also included starting precursor materials. This is to indicate which pure rare earth inorganic precursors are needed in the market place in bulk. The red and blue phosphors used in fluorescent lamps both contain europium as the activator though the red are based on Eu^{3+} cations, whereas the blue contain Eu^{2+} cations, The red phosphor that dominates the international market in both strip and compact fluorescent lamps is cubic Y_2O_3:Eu^{3+}.

$(Sr,Ca,Ba)_5(PO_4)_3Cl$:Eu^{2+} and $BaMg_2Al_{16}O_{27}$:Eu^{2+} are two main classes of blue-emitting phosphors found in these fluorescent lamps. The ratio of Ca:Ba:Sr of the former phosphor changes from manufacturer to manufacturer in order to optimize the emission spectrum according to their lamp design. For the latter phosphor, partial replacement of Ba by other alkaline earth metals and small deviation from the formulated composition are also introduced by various manufacturers to optimize the performance.

Table I. Rare Earth Element Activated Phosphors Used as Lamp Phosphors

Phosphor (formula)	Precursors	Uses
Y_2O_3:Eu^{3+}	$(Y,Eu)_2(C_2O_4)_3$	In fluorescent lamps but originally developed as a red emitting phosphor for colour television in 1959.
YVO_4:Eu^{3+}	$(Y,Eu)_2(C_2O_4)_3$,V_2O_5	Red emitting phosphor used in blends with halophosphate phosphors for specific lamp colours.
YVO_4:Dy^{3+}	Y_2O_3,Dy_2O_3	Can be used for calibration of optical equipment for quantum efficiency measurements.
$Sr_5Cl(PO_4)_3$:Eu^{2+}	$SrHPO_4$,$SrCO_3$,$SrCl_2$,Eu_2O_3	Blue emitting phosphor for high brightness fluorescent lamps
$BaMg_2Al_{16}O_{27}$:Eu^{2+}	$3MgCO_3.Mg(OH)_2.3H_2O$, $BaCO_3$,Al_2O_3,$EuCO_3$	As above and as blue for plasma television

There are three kinds of green-emitting phosphors used. These are: $CeMgAl_{11}O_{19}$:Ce^{3+}:Tb^{3+}, $LaPO_4$: Ce^{3+}:Tb^{3+} and $GdMgB_5O_{10}$: Ce^{3+}:Tb^{3+}, All three contain cerium and terbium activators in the M^{3+} state.

Rare Earth Element Activated Phosphors for Light Emitting Diodes (LEDs)

There are a number of different approaches that can be used to generate white light from LEDs or a combination of colour conversion phosphors and LEDs (pcLEDs) [41-44]. The approach used is dependent on the desired application. This is because there is a trade-off between the colour rendering index (CRI) and the luminous efficacy. Four of these different approaches for achieving white light are given below, along with an assessment of their relative CRI *versus* luminous efficacy attributes.

(a) A combination of red, green and blue LEDs may be used. Drawbacks arise from differential ageing of the LEDs, poor CRI of the white light (due to narrow wavelength ranges of emissions) and the ‘green window’. However, the luminous efficacy is relatively high, because of the absence of colour conversion phosphors and the quantum deficit that they necessarily introduce.

(b) A pcLED consisting of a blue LED and two colour conversion phosphors; that are excited by the blue light and emit at green and red wavelengths[41, 42]. Here as only a single LED is needed there is no problem with differential ageing of the LEDs. The green and red emitting phosphors can have broad emission bands, so the CRI is higher than for (a), above. Here a quantum deficit is involved, thus overall luminous efficacy of the pcLED is lower than for (a).

(c) A pcLED consisting of a blue LED and a single colour conversion phosphor, which emits in the yellow-orange region. This common approach uses only one phosphor. The phosphor emission has to cover as broad a wavelength range in the orange-yellow region as possible to achieve a CRI in the 70-80% range. This approach leads to missing emission wavelengths in the red and between the LED and phosphor emissions, so a maximum CRI of only around 80% is achievable. Though the CRI is less than what can be obtained for (b), above, the luminous efficacy can be higher as the total quantum deficit is lower than for (b).

(d) A pcLED consisting of a UV LED and three phosphors, (emitting in the blue, green and red regions of the visible spectrum). This approach is referred to as 'colour by neutral' and it can achieve a higher CRI than (a)-(c), above, because the three phosphor emissions can cover the whole visible region. Unfortunately, there is a trade-off in luminous efficacy, which is lower than for (a)-(c), above, due to the high quantum deficit.

All the phosphors used in the last three approaches have to be broad band and very efficient. These conditions have led to all LED colour converting phosphors used to date being based on cerium cations present as Ce^{3+}, or europium cations present as Eu^{2+}.

There are many phosphors used to convert LED light to the visible for approaches (b)-(d) above, but space permits only a few types to be covered here.

Yttrium aluminium garnet doped with cerium, (Formula = $Y_3Al_5O_{12}$:Ce known as YAG:Ce), has been used widely as the phosphor of choice for approach (b) above. Many phosphors based on this structure have found use in the LED industry. These include YAG:Ce,Pr, (Y,Gd)AG:Ce, TbAG:Ce (known as TAG:Ce) and LuAG:Ce, (though the latter two are very expensive as they contain terbium and lutetium). These expensive phosphors are used to allow patenting. In Figure 2 normalised emission spectra of $(Y_{1-a}Gd_a)_3Al_5O_{12}$:Ce phosphors (where a = 0.3-0.6), under 468nm excitation are presented, in actual fact as the Gd% is increased the intensity of the emission decreases so although the spectrum moves to the red which is desirable there is a playoff with efficiency.

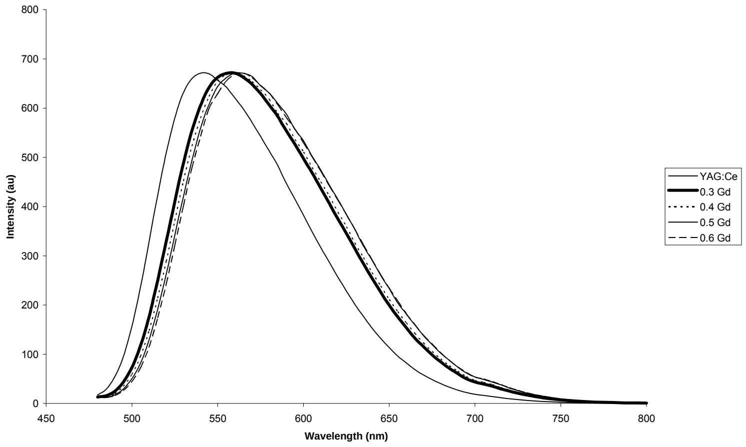

Figure 2. Normalised emission spectra of $(Y_{1-a}Gd_a)_3Al_5O_{12}$:Ce phosphors (where a = 0.3-0.6), under 468nm excitation.

Other phosphors used with blue LEDs include strontium thiogallate doped with europium, $SrGa_2S_4:Eu^{2+}$, which has absorption bands in the UV and visible regions stretching from 508 nm to below 265 nm [43]**.** It emits in the green region of the visible spectrum with a wavelength maximum at around 535 nm and a FWHM of 50 nm (see Figure 3) [45].

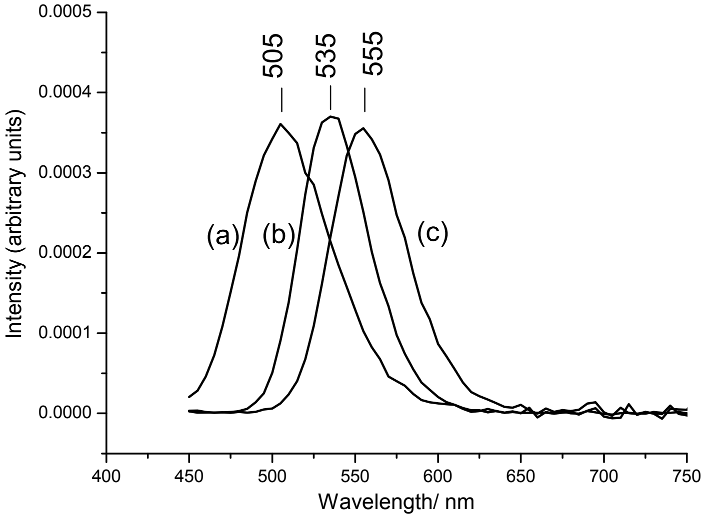

Figure 3. Emission spectra of (a) $BaGa_2S_4:Eu$, (b) $SrGa_2S_4:Eu$, and (c) $CaGa_2S_4:Eu$ (for all the Eu activator concentration was 4 mol %). These phosphors were excited at 430 nm.

This phosphor is an efficient converter of blue light to green, having a theoretical limit of luminous efficacy of ca. 500 lm/W when excited with 470 nm light which is better than YAG:Ce though its temperature properties are not as good as the latter. In fact $SrGa_2S_4:Eu^{2+}$ is one of a family of phosphors based on $MGa_2S_4:Eu$ (M = Sr, Ca, Ba, or a mixture of these elements). These phosphors are difficult to prepare pure and are currently out of favour as LED colour convertors.

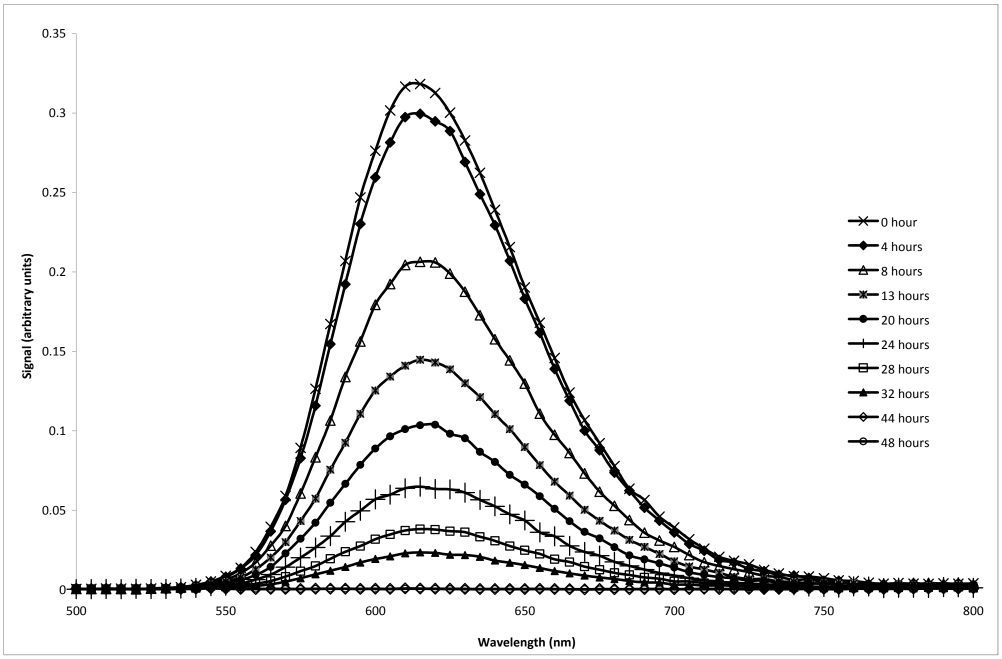

Figure 4. PL spectra of SrS:Eu^{2+} before and after accelerated ageing at 80% relative humidity and 50°C (over a time period of 48 hours).

There are a number of red emitting phosphors currently used as blue LED colour convertors including $Sr_2Si_5N_8$:Eu^{2+} (6 mol %). A sample we prepared was shown to have an efficiency of 47lm/W when excited at 470 nm [42]. This low value is largely due to the fact that the photopic eye response curve decreases in the red region of the spectrum; indeed the theoretical maximum luminous efficacy of this $Sr_2Si_5N_8$:Eu red emitting phosphor is calculated to be only 135 lm/W when exciting at 470 nm. This phosphor has the advantage over the red emitting SrS:Eu^{2+} phosphor (see figure 4), which can also be excited at 470 nm, that it has much better stability to moisture and oxygen. SrS:Eu^{2+} needs to be given a protective coat [46] (usually a metal oxide coating or a coating of SiO_2) if it is to be used as a color converting phosphor for LEDs. Currently there is still a great deal of research and development going on in both new and existing color converting phosphor for LEDs for both display and lighting applications.

Rare Earth Element Activated Phosphors for Displays

A number of rare earth doped phosphors are still used in CRTs for special applications such as ultrafast screens (see Table II) [47]. Until the last few years the most common colour displays were based on the CRT and the phosphor used for the red was Y_2O_2S:Eu^{3+} which was used continuously since the late 1960's as the red emitting phosphor of choice though some still used Y_2O_3:Eu^{3+} until the middle 1970's.

Table II. Display Phosphors

Phosphor Formula	Precurser	Use
$Ca_2MgSi_2O_7$:Ce	$CaCO_3$, $3MgCO_3.Mg(OH)_2.3H_2O$, SiO_2,$Ce(NO_3)_3.6H_2O$	Flying spot scanners and other devices where a very fast decay is desired (ultraviolet emitting (380 nm) phosphor). Still useful devices where fast displays are needed.
$Gd_2O_2S:Tb^{3+}$	$Gd_2O_3:Tb_{0.075}$,S	Green emitting (544 nm) phosphor for display screens and old colour television at high current densities better than other green phosphors
$La_2O_2S:Tb^{3+}$	$La_2O_2S:Tb^{3+}$	As above for $Gd_2O_sS:Tb^{3+}$ but not quite as bright it emits at 547 nm.
$Y_2O_2S:Tb^{3+}$	Y_2O_3,Tb_4O_7,S	This phosphor has many emission lines in the blue green and red areas of the electromagnetic spectrum depending on Tb^{3+} concentration and screens made from it have a whitish appearance
$Y_3Al_5O_{12}:Ce^{3+}$	$(Y_{0.988},Ce_{0.012})_2(C_2O_4)_3.3H_2O$, Al_2O_3	Yellow emitting (526 nm) phosphor decay time in nanoseconds. Fast Scopes.
$Y_2SiO_5:Ce^{3+}$	$Y_2O_3:Ce_{0.055}$,H_2SiO	Deep blue (centered at 415 nm) emitting phosphor screen used wherever a very fast decay is needed such as flying spot scanners
Y_2SiO_5:Tb	$Y_2O_3:Tb_{0.075}$,H_2SiO_3	Projection colour television tubes needing high brightness maintenance.

Plasma TVs and Display Screens

Plasma display panels (PDPs) can be defined as flat-panel information-display devices where the pixels consist of small gas-discharge cells that radiate visible light directly or emit luminescence produced by phosphors. In the latter, the phosphors are excited by ultraviolet light produced by the gas discharge controlled individually in each cell.

Table III. Vacuum UV excited Rare Earth Cation doped Phosphors

Blue-emitting phosphors	Green-emitting phosphors	Red-emitting phosphors
$BaMg_2Al_{14}O_{24}:Eu^{2+}$	$BaMg_2Al_{14}O_{24}:Eu^{2+}$, Mn^{2+}	$YVO_4:Eu^{3+}$
$Ba_3(PO_4)_2$ Eu^{2+}	$CeMgAl_{11}O_{19}:Tb^{3+}$	Y_2O_3: Eu^{3+}
$SrMg(SiO_4)_2:Eu^{2+}$	$Y_3(Al, Ga)_5O_{12}:Ce^{3+}$	$YP_{0.65}V_{0.35}O_4:Eu^{3+}$
$Sr_3(PO_4)_2:Eu^{2+}$		YBO_3: Eu^{3+}
$Sr_5Cl(PO_4)_3$: Eu^{2+}		
$Y_2SiO_5:Ce^{3+}$		

A number of vacuum UV excited rare earth cation doped phosphors have been reported since the mid-1970s [48]; these are presented in Table III.

Although plasma displays are still on the market and a flexible display won an award at SID this year it is likely that apart from specialised uses they will likely be phased out in the next few years. The phosphors for these displays have never been perfected although the plasma industry has led to much research and development on them.

Backlighting Displays

In the first generations most LCD displays were backlit by ultrathin fluorescent tubes, but are now mainly backlit by LEDs either white containing phosphors as laid out under LEDs for lighting or blue LEDs lighting screen containing green and red emitting quauntum dots, The latter quantum dots do not use rare earth elements.

Rare Earth Element Activated Phosphors for Security Applications

Stamps printed with phosphor-containing inks were first introduced in Great Britten in 1959 [49]. From the beginning by optically reading these phosphor marks allowed high-speed automatic sorting and verification at a rate of 30,000 letters per hour.

Other countries including the U.S., Germany, and Japan also use phosphorescent inks in printing of all kinds of postage stamps [49]. In the countries cited above, the phosphor prints on the stamps are hardly distinguishable by the human eye. This is an additional useful function of phosphor mark, which makes it effective for the preservation of secrecy and the prevention of forgery.

Infrared up-conversion phosphors activated with Yb^{3+} and Er^{3+} ions have been used for marking (secretly for a number of years). Yb^{3+} cations have an excited state in the near-infrared region (~970 nm), and efficiently sensitizes the Er^{3+} ion, which emits red and green luminescence as a result of up-conversion processes. The Yb^{3+} cations are particularly useful for this since they have strong infrared absorption bands and exhibit little concentration quenching. Up-conversion phosphors are inefficient and need high-intensity excitation; this is a serious demerit for their use in marking. Another rare earth cation that has been suggested for this use is Nd^{3+}[49] .

Other Applications of Rare Earth Element Activated Phosphors

There are many other applications for Rare Earth Cation activated phosphors but space permits only the more important industrial applications to be discussed herein.

Detection of Diode Laser Light

Up-conversion phosphors can be used to detect infrared diode laser light. Examples include $Y_{0.8}Er_{0.2}F_3$ phosphors in the 0.8-μm region, for $Y_{0.78}Yb_{0.20}$,$Er_{0.02}F_3$ phosphors in the 1.0-μm region, and for $25ErCl_3$-$75BaC_{l2}$ phosphors in the 1.5-μm region [50-53]. Since the rare-earth ion absorption spectra are relatively insensitive to the host lattices, the applicable wavelength regions are not so different for different hosts.

Luminous Paints

There are two types of luminous paints: radioluminous paints and phosphorescent paints [54]. Only phosphorescent paints use rare-earth cation activators. These paints glow in the dark for a while after absorption of light, such as sunlight or man-made light. As the absorption-emission cycle can be repeated many times it is necessary to use phosphorescent paints in areas where there is an excitation light source.

Some of the known rare earth element activated long phosphorescent phosphors are listed in Table IV. The most used phosphors for phosphorescent paints are those that are most readily seen by the human eye, these include $SrAl_2O_4:Eu^{2+}$, and $SrAl_2O_4:Eu^{2+},Dy^{3+}$.

Table IV. Phosphors for Phosphorescent Paints Containing Rare Earth Metal Activators

Composition	Luminescence color	Luminescence wavelength at peak (nm)
$CaAl_2O_4 :Eu^{2+},Nd^{3+}$	Blue	440
$Sr_2MgSi_2O_7:Eu^{2+,} Dy^{3+}$	Blue	470
$Sr_4Al_{14}O_{25}:Eu^{2+}, Dy^{3+}$	Blue-green	490
$SrAl_2O_4:Eu^{2+}$	Green	520
$SrAl_2O_4:Eu^{2+},Dy^{3+}$	Green	520
$CaS:Eu^{2+},Tm^{3+}$	Red	650
Y_2O_2S:Eu,Mg,Ti	Red	625

New Phosphor Materials Containing Multiple Rare Earth Activators for Applications in Security and Other Fields: It is possible to combine two or more rare earth cations into the same lattice, where they may interact under for example up-conversion excitation, but not under downconversion excitation [55]. Such phosphors may find use in the security fields.

Rare Earth Cation Activated Phosphors as Probes for Biological Applications

In the last few years a plethora of phosphor nanoparticles have been used as labels for biological molecules. Many of these phosphor nanoparticles contain rare earth element cations and though useful are not yet mass produced for these applications.

A new method of preparing such phosphor nanoparticles to be used as labels for biological molecules for visualising in transmission electron microscopes has recently been reported [56]. This method uses a quartz wool substrate to immobilise nanometre sized phosphor precursor particles enabling them to be fired at high temperature without sintering/-agglomeration. The nanometre sized phosphor particles are easily removed from the substrate by re-dispersion into liquid for subsequent use.

Conclusions

Rare earth element doped phosphors will continue to find application in the marketplace in many different areas including lighting displays and security markets in the next ten years or more, and are expected to remain in use in lighting for much longer.

Acknowledgements

We are grateful to the Department of Trade and Industry (UK) for substantial financial support in the form of DTI and TSB Technology programmes “Nano-phosphor” under the Nano/Micro Initiative and the “Novelels” and “Activel” part of the Photonics and Electronics programme, as well as the EPSRC and TSB for “Converted” under the Photovoltaics Challenge. We are also grateful to the DTI and Enfis Ltd for a KTP project.

References

1. Shigeo Shinoya , William M. Yen, eds., “*Phosphor Handbook”*. (London, UK: CRC Press, 1998), 1-921.

2. Richard C. Ropp, *The Chemistry of Artificial Lighting Devices.* (Amsterdam, NL: Elsevier, 1993), 1-664.

3. Richard C. Ropp, *Luminescence and the Solid State.* (Amsterdam, NL: Elsevier, 1991), 1-453.

4. Richard C. Ropp, *Luminescence and the Solid State.* (Amsterdam, NL: Elsevier, 2004), 1-711.

5. Alexander F. Wells, *Structural Inorganic Chemisty,* 4th edn. (Oxford, UK: Clarendon Press, 1975), 1-1095.

6. Markku Leskel and Lauri Ninisto, (1986) “Inorganic Complex Compounds 1,” *Handbook on the Physics and Chemistry of Rare Earths,* ed. K.A. Gschneidner Jr, L. Eyring, (Amsterdam, NL: Elsevier, 1986), 203-334.

7. S.-J. Park, et al., “Structure and Luminescence of SrY_2O_4:Eu.” *J. Electrochem. Soc.,* 146 (1999), 3903-3906.

8. George F.J. Garlick, *Luminescent Materials.* (Clarendon, Oxford 1949), pp 1–254.

9. William M. Yen, Shigeo Shinoya, and Hajimo Yamamoto, eds., *Phosphor Handbook*, 2nd edn. (London, UK: CRC Press, 2007), 1-1051.

10. William M. Yen, and Marvin J. Weber, *Inorganic Phosphors, Compositions, Preparation and Optical Properties* (London, UK: CRC Press, 2004), 1–475.

11. Jack Silver, "Metal Compounds as Phosphors," *Comprehensive Coordination Chemistry II: The Synthesis, Reactions, Properties and Applications of Coordination Compounds*, ed. J. A. McCleverty, (New York, NY: Pergamon Press, 2003), Vol. 9. 9.15, 689-717.

12. R.N. Bhargava et al., "Optical properties of manganese-doped nanocrystals of ZnS," *Phys. Rev. Lett.,* 72 (3) (1994), 416-419.

13. R.N. Bhargava, D. Gallagher, and T.J. Welker, "Doped nanocrystals of semiconductors-a new class of luminescent materials," *J. Lumin,* 60 &61 (1994), 275-280.

14. T.A. Kennedy et al., "Symmetry and electronic structure of the Mn impurity in Zn nanocrystals," *Phys. Rev. B,* 52 (1995), 14356-14359.

15. D. Gallagher et al., "Homogeneous precipitation of doped zinc sulfide nanocrystals for photonic applications," *J. Mater. Res,* 10 (1995), 870-878.

16. R.N. Bhargava, "Doped nanocrystalline materials-Physics and applications," *J. Lumin,* 70 (1-6) (1996) 85-94.

17. E. Goldburt, and R.N. Bhargava, "Doped nanocrystalline phosphors for lowvoltage displays," *J. Electrochem. Soc., Proc.,* 95-25 (1996), 368.

18. M.A. Hines, and P. Guyot-Sionnest, "Synthesis and characterisation of strongly luminescing ZnS-capped CdSe nanocrystals," *J. Phys. Chem,* 100 (1996), 468-471.

19. E. Goldburt, and R. N. Bhargava, "Terbium-doped nanocrystalline phosphors," *J. SID,* 4 (4) (1996), 365.

20. Y. Nishisu, and M. Kobayashi, "Particulate fluorescent material of $(Y_{1-X}$"$Eu_X)_2O_3$ and process of preparing same." *U.S. Pat.* (1995), 5413736.

21. Y. D. Jiang et al., "Synthesis and characterisation of Y_2O_3:Eu^{3+} powder phosphor via a Sol-Gel technique," *J. Mater. Res,* 13 (10) (1998), 2950-2955.

22. A. Vecht et al., "Submicron spherical phosphors for FED applications," *SID 98. Digest,* 29 (1998), 1043-1047.

23. A. Vecht et al., "Engineering phosphors for field emission displays," *J. Vac. Sci Tech. B,* 17 (1999), 750-757.

24. X. Jing et al., "Control of Y_2O_3:Eu spherical particle phosphor size, assembly properties, and performance for FED and HDTV," *J. Electrochem. Soc,* 146 (12) (1999), 4654-4658.

25. X. Jing et al., "Optimisation of Grain size and percentage Europium dopant in Y_2O_3:Eu Spherical Particle Phosphor Luminescence from Nanoparticles." (Paper presented at 5th International Conference on the Science and Technology of Display Phosphors, San Diego, USA, 8-10 November 1999), 297-300.

26. M.I. Martinez-Rubio et al., “Effect of EDTA on Controlling Nucleation and Morphology in the Synthesis of Ultrafine Y_2O_3:Eu Phosphors.” *Electrochemical and Solid State Lett,* **2000**, (3) (2000), 446-449.

27. A. Vecht et al., “Factors Affecting Efficiency in Submicron Phosphors: Implications for Screens for High Definition Displays,” *SID 00 Digest,* 31 (2000), 15-17.

28. J. Silver et al., “Yttrium oxide upconverting phosphors. 3. Upconversion luminescent emission from europium-doped yttrium oxide under 632.8 nm light excitation,” *J. Phys. Chem. B.*105 (2001), 9107-9112.

29. M.I. Martinez-Rubio et al., “A New Application for Microgels: Novel Method for the Synthesis of spherical particles of the Y_2O_3:Eu Phosphor Using a Copolymer Migrogel of Nipam and Acrylic Acid,” *Langmuir,* 17 (2001), 7145-7149.

30. M.I. Martinez-Rubio et al., “A Synthetic Method for the Production of a range of particle sizes for Y_2O_3:Eu Phosphors Using a Copolymer Migrogel of Nipam and AMPS.” *J. Electrochem. Soc,* 149 (2) (2002), H53-H58.

31. D. Ma et al., “Y_2O_3:Eu Nanophosphor,” *SID’97 Digest,* 28 (1997), 423-426.

32. J. Silver et al., “A Novel Synthetic Method for the Controlled Production of Particle Desired Size for Y_2O_3:Eu Phosphor using Copolymer Microgels of NIPAM.” *SID Digest*, 33 (2002), 393-396.

33. Y.S. Her, E. Matijevic, and W. R. Wilcox, “Continuous Precipitation of monodisperse yttrium basic carbonate powders. III. Kinetics,” *J. Mater. Res,*7 (1992), 2269-2272.

34. J. Silver et al., “Light Emission from Solids and its Relevance to the Modern Display Electronics and Photonics Industries,” *Proceedings of SID@EID '00, London, 21st-23rd November* 2 (2000), 1-49.

35. Y.C. Kang et al., “The effect of metal carbonate fluxes on the crystallinity morphology and photoluminescence characteristics of Y_2O_3:Eu phosphor in spray pyrolysis,” *J. Mat. Sci. Lett,* 19 (2000), 1225-1227.

36. Y.C. Kang et al., “Gd_2O_3:Eu phosphor particles with sphericity, submicron size and non-aggregation characteristics,” *J. Phys. Chem. Solids,* 60 (3) (1999), 379-384.

37. Y.C. Kang et.al., “Luminescence characteristics of Y_2SiO_5:Tb phosphor particles directly prepared by the spray pyrolysis method,” *J. Electrochem. Soc,*146 (3) (1999), 12271230.

38. Y.C. Kang, Y. S, Chung, and S. B. Park, “Submicron-size $BaAl_{12}O_{19}$: Mn phosphor particles with spherical morphology,” *J. Mat. Sci. Lett,* 18 (1999), 779-781.

39. Y.C. Kang et al., “Preparation of nonaggregated Y_2O_3:Eu phosphor particles by spray pyrolysis method,” *J. Mater Res,* 14 (6) (1999), 2611-2615.

40. A. Konrad et al., “Chemical vapor synthesis and luminescence properties of nanocrystalline cubic Y2O3:Eu,” *J. Appl. Phys.,* 86 (6) (1999), 3129-3133.

41. Jack Silver, and Robert Withnall, “Colour Conversion Phosphors for LEDS”, Chapter 3 in *Luminescent Materials and Applications,* Ed. A. Kitai, (John Wiley & Sons, 2008) 75-109.

42. R. Withnall et al., “Experimental and theoretical luminous efficacies of phosphors used in combination with blue-emitting LEDs for lighting and backlighting,” *Journal of the SID,* 16 (2) (2008), 359-368.

43. J. Silver et al., “White light production from blue LEDs: The synthesis of small particle YAG:Ce type phosphors for solid state lighting,” *Chinese J. Electron Dev*, 21 (2008), 197-200.

44. J. Silver, R. Withnall, and A. Lipman, “Measurements of luminous efficacies of conversion phosphors for blue emitting LEDs,” *Chinese J. Electron Dev*, 21 (2008), 381-384.

45. C. Chartier et al., “Photoluminescence of Eu^{2+} in $SrGa_2S_4$,” *J. Lumi,* 111 (2005), 147-158.

46. R. Withnall et al., “Accelerated Ageing Studies of $CaS:Eu^{2+}$ and $SrS:Eu^{2+}$ Phosphors,” (Paper presented at the International Displays Workshop Annual Meeting December 2012, Kyoto, Japan.). *Proc. IDW/AD’12,* (2012), 1727-1729.

47. Shuji Inaho, and Takashi Hase, “Phosphors for cathode-ray tubes,” eds. W. M, Yen, S, Shinoya, H. Yamamoto, *Phosphor Handbook*, 2nd edn. (London, UK, CRC Press, 2007). Chapter 6, 607-618.

48. Takehiro Kojima and Takayuki Hisamune, “Phosphors for plasma display.” eds. W.M. Yen, S, Shinoya , H. Yamamoto, Phosphor Handbook, 2nd edn. (London, UK, CRC Press, 2007). Chapter 10 (1-4) 735-745.

49. Atsushi Suzuki, “Other Phosphors,” eds. W. M, Yen, S, Shinoya , H. Yamamoto, Phosphor Handbook, 2nd edn. (London, UK, CRC Press, 2007). Chapter 12 (4-6) 819-822.

50. J. Ohwaki, and Y. Wang, “Infrared to visible upconversion of Er^{3+} doped in a chloride matrix,” *Jpn. J. Appl. Phys*, 31 (1992), L1481-L1483.

51. Y. Wang and J. Ohwaki, High efficiency infrared to visible upconversion of Er^{3+} in $BaCl_2$,” *J. Appl. Phys*, 74 91993), 1272-1278.

52. J. Ohwaki, and Y. Wang, “Efficient 1.5 µm to visible upconversion in Er^{3+}-doped halide phosphors,” *Jpn. J. Appl. Phys*, 33 (1994), L334-L337.

53. Yoh Mita, “ Other Phosphors,” eds. W. M, Yen, S, Shinoya , H. Yamamoto, Phosphor Handbook, 2nd edn. (London, UK, CRC Press, 2007). Chapter 12 (1) 775-783.

54. Yoshihiko Murayama , “ Other Phosphors,” eds. W. M, Yen, S, Shinoya , H. Yamamoto, Phosphor Handbook, 2nd edn. (London, UK, CRC Press, 2007). Chapter 12 (2) 785-792.

55. X. Yan et al., “Contrasting behaviour of the co-activators in the luminescence spectra of $Y_2O_2S:Tb^{3+},Er^{3+}$ nanometre sized particles under UV and red light excitation,” *Nanoscale*, 5 (2013), 1091-1096. A. Salimian et al., “A novel method for the preparation of non-agglomerated nanometre *sized pa*rticles of lanthanum phosphate phosphors utilising a high surface area support in the firing process,” *J. Mater. Chem*, 22 (2012), 21529-21532.

LUMINESCENT LANTHANIDES: PAST, PRESENT AND FUTURE

Andries Meijerink

Debye Institute for Nanomaterials Sience,
Departement of Chemistry
Utrecht University

Keywords: Luminescence, Lanthanides, White LED, Solar Cells, Spectral Conversion, Economics

Extended Abstract

Lanthanides are found in luminescent materials in every home. Since first introduced in 1963 with the application of Eu^{3+} emission in color TVs, the unique optical properties of lanthanides have led to technological developments which have promoted the widespread use of rare earth-based phosphors in (compact) fluorescent tubes, flat displays, white light LEDs, medical imaging, lasers, fiber amplifiers, anti-counterfeiting labels and more. Following a brief update on the status of the various current applications, this paper provides a focused outlook on the future, including new materials for spectral conversion for higher efficiency solar cells, scintillators for medical imaging and homeland security and warm white LEDs, causing a revolution in lighting. New opportunities, challenges and limitations for new luminescent materials for solar cells, medical imaging and white light LEDs are discussed. The opportunities and challenges in the field of rare earth luminescence, including the implications of a transition to LED-lighting for the rare earth market are put into context.

Lanthanide ions are typically trivalent (Ln^{3+}) and have a $4f^n5s^25p^6$ electron configuration with n=0-14. The partly filled 4f shell is responsible for the unique optical and magnetic properties of lanthanide ions. The energy levels of the various lanthanide ions are given in the so-called Dieke diagram. The trivalent ions may be doped in different host materials, varying from fluorides to oxides, depending on the application. There is no Stokes' shift for the sharp line emission and this results in the strongly reduced vibrational energy losses. The large variety of absorption and emission wavelengths, the independence on the host materials and the low vibrational energy losses make lanthanides ideal ions for spectral conversion and in almost all artificial light sources the light emission originates from lanthanide ions.

A potential new area of application is in spectral conversion for solar cells. State-of-the-art commercial crystalline Si (c-Si) solar cells dominate the market and have energy efficiencies around 15%. The main energy losses (over 70%) are related to the spectral mismatch.[1] IR photons with energies lower than the bandgap are not absorbed while for photons with energies exceeding the bandgap, the excess energy is lost as heat during the fast thermalization. Two methods are capable of reducing spectral mismatch losses: upconversion and downconversion.[2] In case of upconversion, two infrared photons are 'added up' to give one higher energy photon that can be absorbed. The opposite process, downconversion, involves 'cutting' of one high energy photon into two lower energy photons. This process can reduce

energy losses related to thermalization. In Figure 1, the potential efficiency gain for solar cells through up- and downconversion is shown.

Recent research on downconversion reveals that potential downconversion couples are (Er^{3+}, Yb^{3+}), (Nd^{3+}, Yb^{3+}) and (Pr^{3+}, Yb^{3+}) [3, 4]. The potential and challenges for the application of downconversion materials will be discussed, including the search for a good absorber (sensitizer) for downconversion couples. Upconversion materials have already been used to enhance the efficiency of solar cells. Recently, the efficiency of upconversion materials has improved and internal quantum efficiencies above 10% have been reported for new upconversion materials, e.g. $Gd_2O_2S:Er^{3+}$, under moderate excitation densities [5]. The progress in the development of efficient upconversion materials may also trigger new applications for IR to NIR upconversion materials, e.g. for anti-counterfeiting.

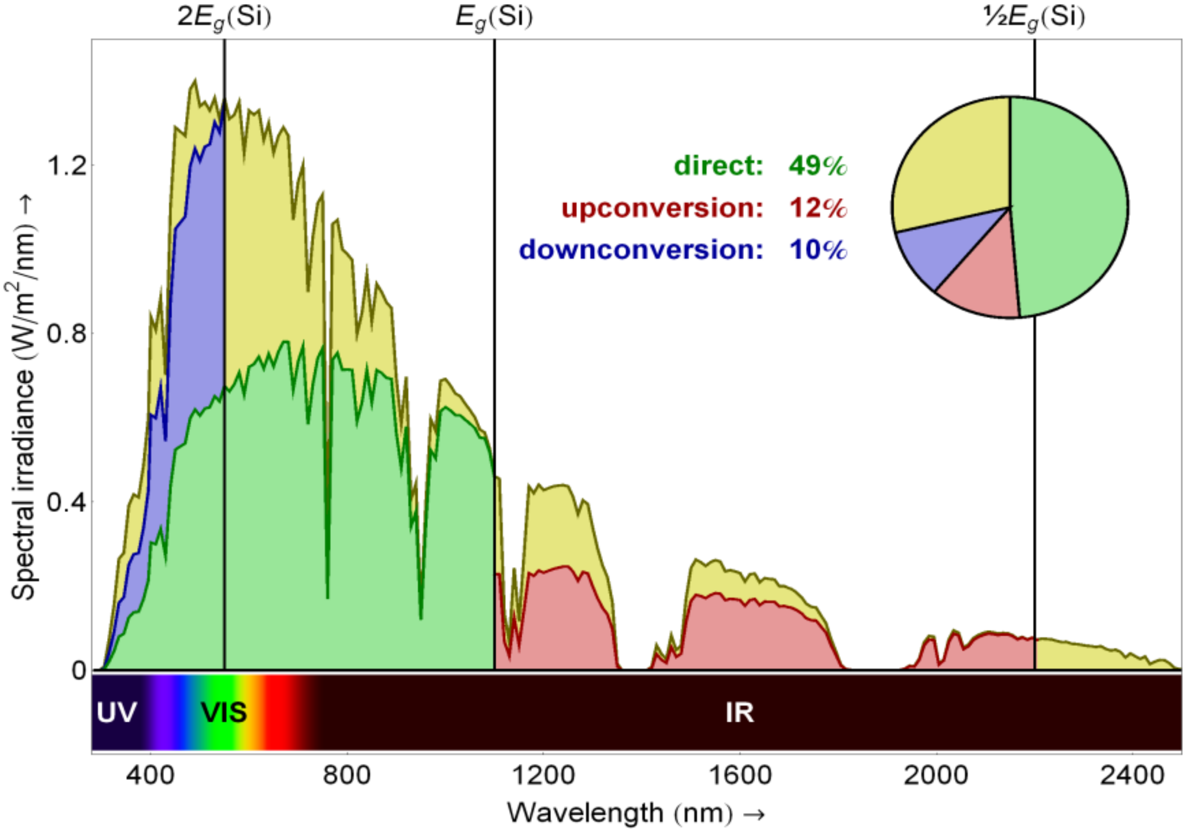

Figure 1. Potential efficiency gain for c-Si solar cells through the application of upconversion of IR photons (adding *two* sub-bandgap photons to *one* supra-bandgap photon) and downconversion (splitting *one* high energy blue/green photon into *two* NIR photons).

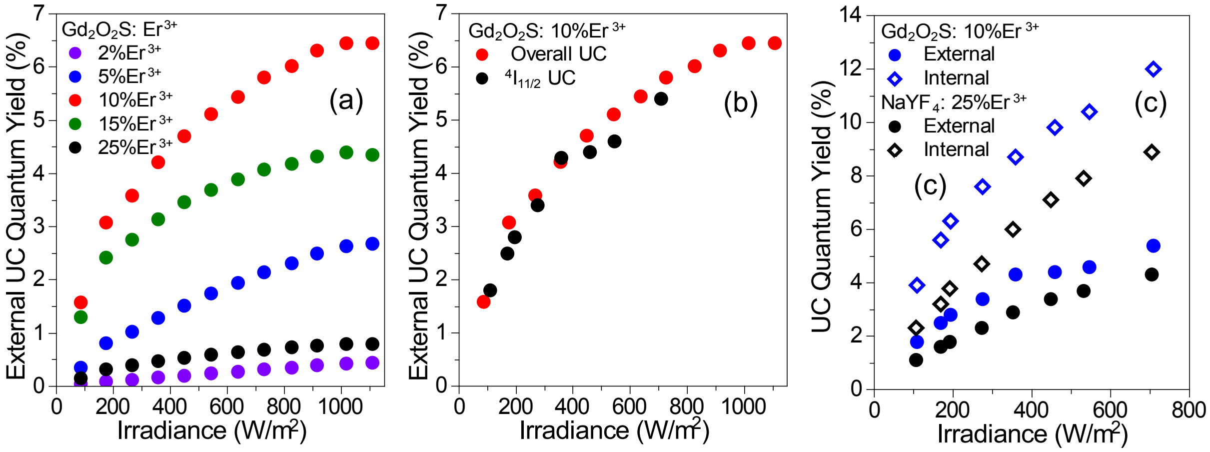

Figure 2. (a) External UC quantum yield of Er^{3+}-doped Gd$_2$O$_2$S for 2, 5, 10, 15 and 25% doping concentrations measured at different irradiances at 1510 nm. (b) Comparison between the total and $^4I_{11/2}$ external UC quantum yields in Gd$_2$O$_2$S: 10%Er^{3+} (c) Power dependence of the external and internal $^4I_{11/2}$ UC QY in Gd$_2$O$_2$S: 10%Er^{3+} and β-NaYF$_4$: 25%Er^{3+}.

A second area with new opportunities for lanthanide doped luminescent materials is in the field of scintillators. Scintillators convert high energy x-rays or γ-rays into flashes of light that are detected by light detectors. Fast and efficient conversion is crucial for high resolution medical imaging (PET- and CT-scanners) and homeland security (discrimination between radioactivity from K and U). In the past decades, great effort was made to develop efficient and fast scintillators to detect ionizing radiation. At present, the best combination of stopping power, light yield, and decay time is achieved by Ce^{3+}-doped materials [6]. New materials involve Pr^{3+}-activated LuAG. This high density (6.7 g/cm^3) material exhibits good properties such as fast scintillation response of about 20 ns and a prospective light yield of up to 40,000 photons/MeV. Ce-doped halides (e.g. LnBr$_3$:Ce^{3+}) form another class of scintillators with a superior energy resolution and efficiencies close to 100 000 photons/MeV [7]. The use of lanthanide doped scintillators is expected to increase. Especially the application of the heavy Lu-ion is crucial in scintillators and may boost the need for Lu, one of the rarest rare earths.

The third application will change the lighting market more rapidly than ever before. The development of white light LEDs (w-LEDs) has started a revolution in lighting that has not ended yet. In the next ten years a transition from incandescent lamps and compact fluorescent lighting to white light emitting LEDs is anticipated [8]. With an increased energy efficiency and a long operation life time, w-LEDs form an attractive energy efficient alternative for incandescent lamps and (compact) fluorescent tubes.

An important issue for the home lighting market is however the color rendering. Blue LEDs combined with the yellow emitting YAG:Ce phosphor generate cool white light which is not considered suitable for home application in most regions in the world. To generate warm white light orange/red emitting phosphors have been developed and a variety of Eu^{2+} doped (oxy)nitride materials is presently applied in warm white LEDs [9]. The improved color temperature comes at a cost: the lumen/W output is reduced by the spectral width of the Eu^{2+}

emission band which causes a substantial fraction of the emitted light to be at wavelengths beyond 630 nm where the reduced eye sensitivity causes a significant reduction of the lumen/W efficacy. The search for a narrow band red phosphor which can be excited in the blue spectral region has so far not resulted in the ideal narrow band red emitter. The search for narrow band red emitters to realize warm white LEDs while maintaining a high lumen/W efficacy is generally recognized as one of the main remaining challenges in solid state lighting, together with increasing the efficiency of the LED-chip under high power operation. (Zn,Cd)Se quantum dots can serve as a narrow band emitter, but is expensive and requires a remote concept.

Lanthanides may provide a good alternative for the development of a better narrow band red phosphor for blue excitation. Successful development will give any lighting company a strong advantage in the extremely competitive field of solid state lighting. A significant increase in the lumen/W output can be realized if an efficient narrow band red phosphor is developed. The lumen/W performance is one of the crucial parameters in the sales of w-LEDs and an increased lumen/W efficacy will immediately boost the sales. The LED market is rapidly growing and revenues are expected to exceed 20 G$ in five years (see Fig. 4). The implications of the transition from (compact) fluorescent tubes to w-LEDs as an energy efficient light source are also important for the rare earth market. In a fluorescent tube, typically ~ 1 g of rare earth phosphor is used. In a w-LED less than 1 mg is used. Overall, the volume of rare earth phosphors may decrease two orders of magnitude with the transition from fluorescent tubes to w-LEDs.

Finally, the use of lanthanides, and specifically Europium, for anti-counterfeiting will be discussed. The Euro banknotes that came out in 2002 relied on the emission from Eu^{2+} and Eu^{3+} under UV excitation [10]. In May 2013 new banknotes were introduced with a more complicated protection scheme. The emission under short wavelength UV (254 nm) and long wavelength UV (360 nm) is different and at least three different Eu^{3+}-doped materials have been identified. The secrets of the different luminescent materials in the new Euro banknotes will be unveiled as a final demonstration of the widespread use of luminescent lanthanides.

In conclusion, the importance of lanthanides for spectral conversion continues to increase, both in the traditional area of light emitting devices (lamps, displays) and new areas (solar cells, homeland security, 3D medical imaging, lasers, information transfer and storage, afterglow materials, anti-counterfeiting etc.). The high efficiency of the emission and the flexibility in spectral range and time response give lanthanides unique optical properties for a wide range of applications. The supply risk of lanthanides will affect different areas in a different manner. For lighting the transition to w-LEDs will strongly reduce the overall volume of lanthanides used, while for other application (e.g. scintillators) a large increase in the demand for specific lanthanides is foreseen.

References

1. Richards, B.S., “ Luminescent layers for enhanced silicon solar cell performance: Down-conversion”, *Sol. En. Mat. Sol. Cells* 90, 2329-2337 (2006).

2. Trupke, T., M.A. Green, P. Würfel, "Improving solar cell efficiencies by down-conversion of high-energy photons", *J. Appl. Phys.* 92, 1668 (2002); "Improving solar cell efficiencies by up-conversion of sub-band-gap light", J. Appl. Phys. 92, 4117.(2002)

3. van der Ende, B., L. Aarts and A. Meijerink, "Near-Infrared Quantum Cutting for Photovoltaics", *Adv. Mater.*, 21**,** 3073-3077 (2009).

4. van der Ende, B., L. Aarts and A. Meijerink, "Lanthanide ions as spectral converters for solar cells", *Phys. Chem. Chem. Phys.* 11, 11081 (2009).

5. Martín-Rodríguez, R., S. Fischer, A. Ivaturi, B. Froehlich, K.W. Krämer, J. C. Goldschmidt, B. S. Richards, A. Meijerink, "Highly efficient IR to NIR upconversion in Gd_2O_2S: Er^{3+} for photovoltaic applications", *Chem. Mater.*, in press

6. Ogino, H., A. Yoshikawa et al. "Growth and scintillation properties of Pr-doped $Lu_3Al_5O_{12}$ crystals", *Journal of Crystal Growth* 292, 239–242 (2006)

7. van Loef, E.V.D., P. Dorenbos, C.W.E. van Eijk, K. Kramer, H.U. Gudel, "High-energy-resolution scintillator: Ce^{3+} activated $LaBr_3$", *Appl. Phys. Lett.* 79 1573 (2001)

8. "Charge of the LED brigade", *The Economist*, Aug 20, 2011

9. Zeuner, M., S. Pagano and W. Schnick, "Nitridosilicates and Oxonitridosilicates: From Ceramic Materials to Structural and Functional Diversity", *Angew. Chemie. Int. Ed.* 50, 7754 (2011).

10. Meijerink, A., and J. F. Suyver, "Europium beveiligt de €uro", *Chemisch2Weekblad* 4, 12 (2002).

LIQUID–FREE MECHANOCHEMICAL PREPARATION OF RARE EARTH METAL ORGANIC FRAMEWORKS

Niraj K. Singh,[1] Shalabh Gupta,[2] Meenakshi Hardi,[1] V. K. Pecharsky,[2] Viktor P. Balema[1]

[1]Aldrich Materials Science, Sigma Aldrich Corp., 6000 N. Teutonia Avenue, Milwaukee, WI, 53209, USA
[2] The Ames Laboratory, Iowa State University, Ames, IA, 50011, USA

Keywords: Metal Organic Frameworks, Mechanochemical Synthesis, Luminescent Materials

Extended Abstract

Metal organic frameworks (MOFs) are hybrid inorganic-organic crystalline materials with intrinsically high porosity. MOFs have attracted significant attention due to applications as luminescent materials, advanced gas absorbers, sensors, etc.[1] Rare earth based MOFs are best known for their excellent luminescence properties.

Although the first report on mechanochemical synthesis of organic compounds dates back to 2002 [2], the synthesis of MOFs using this approach was not reported until 2006.[3] Since then there has been intense research activity on MOFs synthesis using this approach.[1] Till 2012, all the reported mechanochemical synthesis of MOFs involved liquids which were either added externally to assist grinding or were generated in-situ as by-products.[4]

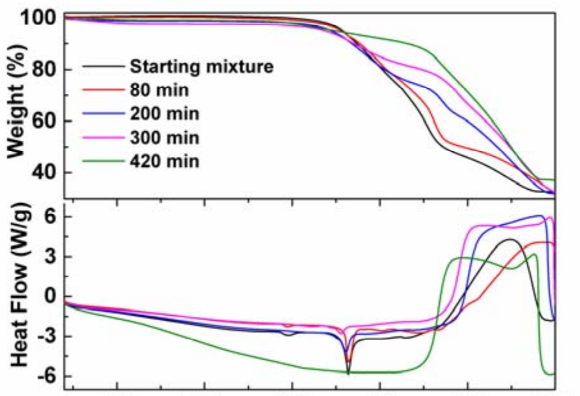

Figure 1. The thermogravimentric analysis (TGA) and differential scanning calorimetric (DSC) data of 1:1 mixture of yttrium hydride and trimesic acid milled for various durations.

In the present study, we report on the mechanochemical synthesis of rare earth based MOF using metal hydrides as precursors. By performing the differential scanning calorimetric (DSC) measurements of the precursors (trimesic acid and yttrium hydride) milled for various durations (see Figure. 1), we unambiguously demonstrate that MOFs can be synthesized through a true solid state process and liquids can be excluded completely. Also, the variations in the latent heat associated with melting of trimesic acid in the reaction mixtures milled for varying durations reveal a linear dependence of the mechanochemical reaction on milling time (Figure. 2). Possible mechanism of mechanochemical transformation along with the effect of variations in the milling conditions (using SPEX vs. Retsch mill) will be discussed.

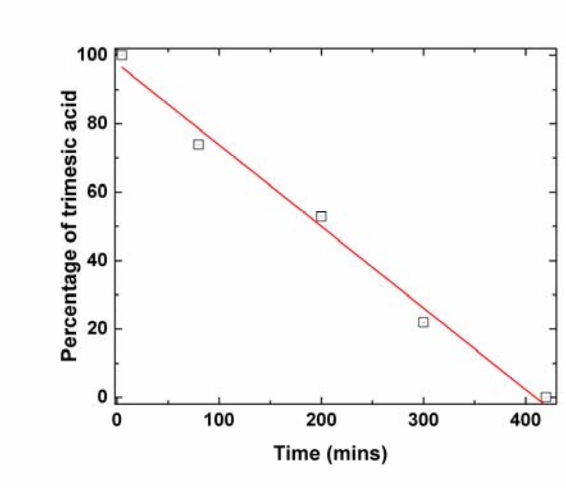

Figure 2. The degree of conversion of trimesic acid as a function of time during ball milling of 1:1 mixture of yttrium hydride and trimesic acid.

References

1. S. L. James et al., Chem. Soc. Rev. 2012, 41, 413

2. V. P. Balema et al., Chem. Commun., 2002, 724.

3. A. Pichon et al., CrystEngComm., 2006, 8, 211.

4. N. K. Singh et al., Chem. Commun., 2013, 49, 972.

EFFECT OF DEPOSITION TEMPERATURE AND OXYGEN PRESSURE ON HYDROPHOBICITY OF CERIA THIN FILMS GROWN BY PULSED LASER DEPOSITION

Sin-Pui Fu, Jelani Hannah and Jeremiah T. Abiade

Laboratory for Oxide Research and Education (LORE)
Department of Mechanical and Industrial Engineering
University of Illinois at Chicago,
Chicago, IL, USA, 60607

Keywords: Hydrophobicity, Cerium Dioxide, Pulsed Laser Deposition

Introduction

Cerium dioxide, CeO_2 belongs to group of rare-earth oxides (REOs). In past decades, ceria has been studied widely because of its attractive properties, such as high hardness [1], high thermal stability [2], high wear resistance [3], wide band gap (3.6eV), high chemical stability [4], high transparency [5], high refractive index [6] and good adhesion [2]. Because of these characteristics, ceria has been widely used in solid oxide fuel cells [7], gas sensors [8], electrochromic smart window devices [9], for corrosion protection [10] and catalysis [11].

A recent report suggests that the entire REO series is intrinsically hydrophobic [12]. This effect has been attributed to the oxides' electronic structure, which affects the surface polarity and resulting interaction with water molecules. REO materials have unfilled 4f inner orbital electron shell, which are shielded from interaction with the surrounding environment by the full octet of electrons in the $5s^2p^6$ outer shell. Hydrophobicity is believed to arise because water molecules have only one OH^- vector preferentially pointing to the surface with the other three forming hydrogen bonds with other water molecules. In contrast, the water molecules in contact with a hydrophilic surface have one electron lone-pair pointing preferentially outward from the surface [13]. Consequently, REO materials have lower tendency to exchange resulting in a hydrophobic surface.

Ceria thin films can be fabricated by several methods, such as spray pyrolysis [14], ion-beam assisted deposition [15], thermal evaporation [16], radio frequency magnetron sputtering [17], plasma-enhanced chemical vapor deposition [18], sol-gel method [19], electron spray assisted vapor deposition [20] and pulse-laser deposition (PLD) [21]. In this study, ceria thin films were deposited by pulsed-laser deposition method. PLD is a simple process that allows low processing temperatures with the potential of accurately reproducing the stoichiometry of the target.

We have investigated the wetting characteristics of ceria thin films prepared at different substrate temperatures and at variable oxygen pressures using pulsed laser deposition. X-ray photoelectron spectroscopy (XPS), atomic force microscopy (AFM) and goniometer contact angle measurements were used for characterization. We will discuss the effect of varying these deposition parameters on the wetting behavior of ceria thin films.

Experimental Procedures

Ceria thin films were deposited on the silicon substrates by PLD method. The substrates were ultrasonically cleaned in acetone for 10 minutes at room temperature. A CeO_2 (99.99% purity) target was used during the laser deposition. The target was rotated and rastered during laser ablation to reduce pitting on target. The chamber was pumped to a base pressure of ~ 1 × 10^{-6} torr using a turbo-molecular pump. PLD depositions were performed using a KrF excimer laser operating at 248nm in the temperature range from room temperature to 700℃ at the oxygen partial pressures of 5 × 10^{-2}torr, 3 × 10^{-2}torr and without oxygen. The Si substrates were placed on the holder with 7.2 cm away from the target. The laser frequency, number of pulses and laser energy was 5Hz 5000 laser pulses and 410mJ laser energy respectively.

The AFM (Asylum MFP-3D-SA) scans were carried out to measure the surface roughness. Goniometer contact angle measurement was used to measure the surface contact angle. The constant of volume water droplets of 4µm ml were dropped on the dry ceria thin films at room temperature to control the size of the droplets.

Results and Discussion

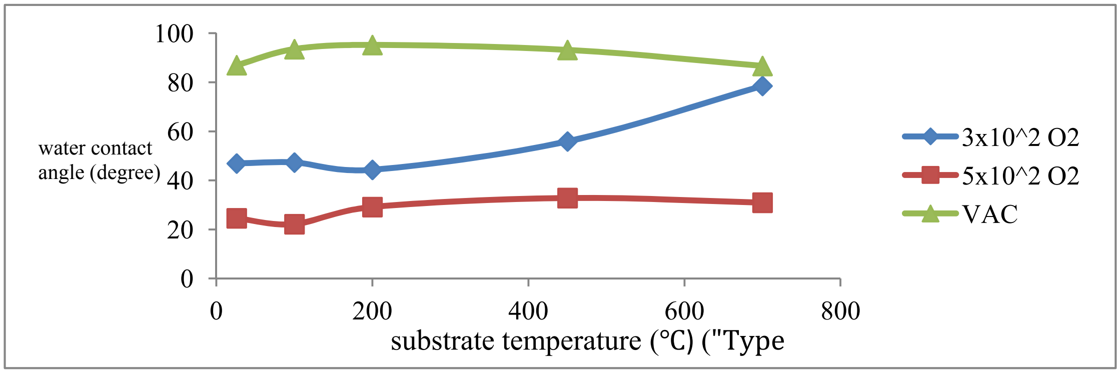

Figure 1. Contact angle vs. substrate temperature at different oxygen pressures.

Wetting Behavior

Figure 1 shows the water contact angle on CeO_2 thin films. The samples were divided into three different groups. The samples were grown in vacuum and at oxygen pressures of $5x10^{-2}$ torr and $3x10^{-2}$ torr. The water contact angle decreases with an increase in the oxygen pressure. The contact angle for samples grown using oxygen pressures of $5x10^{-2}$ torr varies from ~ 25 degrees to ~ 33 degrees for substrate temperatures from room temperature to 700 ℃. For oxygen pressures of $3x10^{-2}$ torr, the contact angle varies from ~ 47 degrees to ~ 73 degrees for substrate temperatures up to 700 ℃. The highest contact angles were measured for samples grown in vacuum, varying from ~ 87 degrees to ~ 95 degrees as the substrate temperature is increased to 700 ℃. On the other hand, the contact angle was only dependent on the substrate temperature for the samples grown in an oxygen pressure of $3x10^{-2}$ torr.

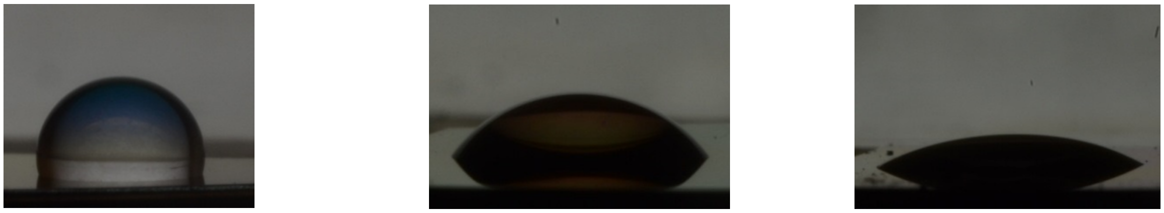

Figure 2. Wetting of water on CeO$_2$ thin films: sample 3 (left), sample 8 (middle) and sample 13 (right).

The dependence of the contact angle on the deposition parameters is clearly depicted in figure 2. The wetting characteristics can be tailored from hydrophobic to hydrophilic by varying the oxygen pressure and/or substrate temperature. The left image in figure 2 was obtained for a sample deposited in vacuum and at 200 ℃, the contact angle decreased (middle image) as the oxygen pressure was increased to 3x10^{-2} torr, decreasing further (right image) as the oxygen pressure was increased to 5x10^{-2} torr.

AFM Characterization

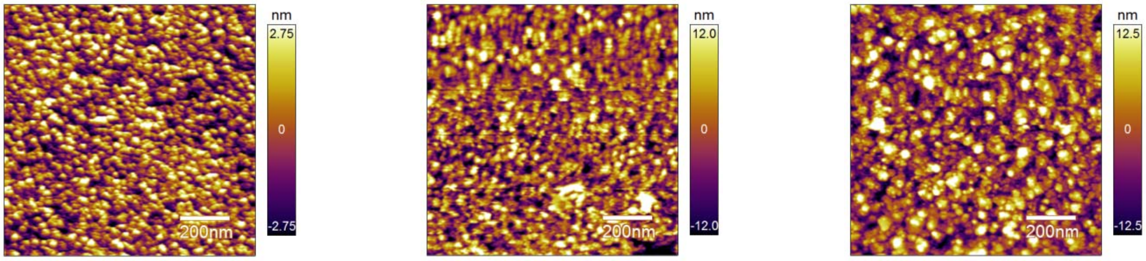

Sample 3 Sample 8 Sample 13

Figure 3. AFM scans for samples depicted in figure 2.

Figure 3 shows the surface roughness measured by atomic force microscopy on the samples depicted in figure 2. The root mean square surface roughness varied from was 4.6 nm, 4.9 nm, and 1.1 nm, respectively, for sample 8, sample 13, and sample 3.An increase in surface roughness was observed with an increase in oxygen pressure. The morphology of ceria thin films in figure 3 show the ceria thin films have been changed by different oxygen pressures.

Summary and Conclusion

Ceria (CeO$_2$) thin films were deposited by PLD at different substrate temperatures and oxygen pressures. The oxygen pressure during film deposition influences the wetting behavior. Reducing the oxygen pressure increases the water contact angle on the CeO$_2$ films. The substrate temperature did not have a pronounced effect on the wetting characteristics, with a dependence being observed only at intermediate oxygen pressures. AFM characterization was used to analyze the surface morphology. The surface roughness increased as the oxygen pressure increased. The results show that the wetting characteristics of thin films can be tailored from hydrophilic to hydrophobic by varying the substrate temperature and amount of oxygen present during film growth.

References

1. Tsukuma, K., M. Shimada, "Strength, Fracture Toughness and Vickers Hardness of CeO2 Stabilized Tetragonal ZrO2 Polycrystals," *Journal of Materials Science*, 20 (1985), 1178-1184.

2. Beie, H.J., A.Gnorich, "Oxygen Gas Sensor Based on CeO2 Thick and Thin Film," *Sensors and Actuators B*, 4 (1991), 393-399.

3. Mangam, V., S. Bhattacharya, K. Das, S. Das, "Friction and Wear Behavior of Cu-CeO2 Nanocomposite Coating," *Surface & Coating Technology*, 205 (2010), 801-805.

4. Stroosnijder, M.F., V. Guttmann, T. Fransen, J. H. W. de Wit, "Corrosion of Alloy 800H and the Effect of Surface Applied CeO2 in a Sulfidizing Oxidizing Carburizing Environment at 700 degree-C", *Oxidation of Metals,* Vol. 33, Nos. 5/6, 1990.

5. Elidrissi, B., M. Addou, M. Regragui, C. Monty, A. Bougrine, A. Kachouane, "Structure and Optical Properties of CeO2 Thin Film Prepare by Spray Pyrolysis", *Thin Solid Films*, 379 (2000), 23-27.

6. Balakrishnan, G., S. Triqura Sundari, P. Kuppusami, P. Chandra Mohan, M.P. Srinivasan, E. Mohandas, V. Ganesan, D. Sastikumar, "A Study of Microstructural and Optical Properties of Nano-crystalline Ceria Thin Film Prepared by PLD," *Thin Solid Films*, 519 (2011), 2520-2526.

7. Joacobs, G., E. Chenu, P. M. Patterson, L. Williams, D. Sparks, G. Thomas, B.H. Davis, "Water-Gas Shift Comparative Screening of Metal Promoters for Metal Ceria System and Role of the Metal," *Applied Catalysis A: General*, Vol. 258, issue 2, 20 (2004), 203-214.

8. Izu, N., W. Shin, N. Murayama, S. Kanzaki, "Resistive Oxygen Gas Sensors Based on CeO2 Fine Powder Prepared Using Mist Pyrolysis," *Sensors and Actuators B,* 87 (2002), 95-98.

9. Ozer, N., "Optical Properties and Electrochromic Characterization of Sol-Gel Deposited Ceria Films," *Solar Energy Materials & Solar Cells,* 68 (2001), 391-400.

10. Montemor, M.F., R. Pinto, M. G. S. Ferreria, "Chemical Composition and Corrosion Protection of Silane Films Modified with CeO2 Nanoparticles," *Electrochimica Acta,* 54 (2009), 5179-5189.

11. Zhong, L.S., J.S. Hu, A.M. Cao, Q. Liu, W.G. Song, L.J. Wan, "3D-Flowerlike Ceria Micro/Nano Composite Structure and Its Application for Water Treatment and CO Removal," *Chem. Mater,* 19 (2007), 1648-1655.

12. Azimi, G., R. Dhiman, H.M. Kwon, A.T. Paxson, K.K. Varanasi, "Hydrophobicity of Rare Earth Oxide Ceramics," *Nature Materials,* 20 Jan 2013.

13. Giovambattista, N., P.G. Debenedetti, P.J. Rossky, “Effect of Surface Polarity on Water Contact Angle and Interfacial Hydration Structure,” *J. Phys, Chem. B,* 111 (2007), 9581-9587.

14. Patil, B.B., S.H. Pawar, “Structural, Morphological and Electrical Properties of Spray Deposited Nano-crystalline CeO2 Thin Film,” *Journal of Alloys and Compounds,* 509 (2011), 414-420.

15. Al-Robaee, M.S., K. Narasimha Rao, S. Mohan, “Influence of Substrate Temperature on the Properties of Oxygen-Ion Assisted Deposited CeO2 Film,” *Journal of Applied Physics,* 71 (1992), No. 5,

16. Guillou, N., L.C. Nistor, H. Fuess, H. Hahn, “Microstructural Studies of Nanocrystalline CeO2 produced by Gas Condensation,” *NanoStructured Materials,* 8 (1997), 545-557.

17. Wakiya, N., M. Yoshida, T. Kiguchi, K. Shinozaki, N. Mizutani, “RF-Magnetron Sputtered Heteroepitaxial YSZ and CeO2/ YSZ/ Si (001) thin films with Improved Capacitance Voltage Characteristics,” *Thin Solid Films,* 411 (2002), 268-273.

18. Barreca, D., A. Gasparotto, E. Tondello, C. Sada, S. Polizzi, A. Benedetti, “Nucleation and Growth of Nanophasic CeO2 Thin Films by Plasma-Enhanced CVD,” *Chemical Vapor Deposition,* 9 (2003), No.4 .

19. Schem, M., T. Schmidt, J. Gerwann, M. Wittmar, M. Veith, G.E. Thompson, I.S. Molchan, T. Hashimoto, P. Skeldon, A.R. Phani, S. Santucci, M.L. Zheludkevich, “CeO2 Filled Sol-Gel Coating for Corrosion Protection of AA2024-T3 Aluminum Alloy,” *Corrosion Science,* 51 (2009), 2304-2315.

20. Wei, M., D. Zhi, K.L. Choy, “Electrostatic Spray Assisted Vapour Deposition and Structural Characterization of Cerium Oxide Films on Biaxially Textured Ni Tapes,” *Materials Letters,* 60 (2006), 1519-1523.

21. Balakrishnan, G., S.T. Sundari, P. Kuppusami, P.C. Mohan, M.P. Srinivasan, E. Mohandas, V. Ganesan, D. Sastikumar, “A Study of Microstructural and Optical Properties of Nano-crystalline Ceria Thin Film Prepared by PLD,” *Thin Solid Films,* 519 (2011), 2520-2526.

EXPLORING THE CHEMICAL SPACE FOR RARE-EARTH ADDITIONS TO OPTIMIZE AEROSPACE ALLOYS

*Patrick H.J. Mercier[1] and John R. Rodgers[2]

[1]National Research Council Canada, NRC Energy, Mining and Environment Portfolio, Ottawa, Ontario, Canada
*patrick.mercier@nrc-cnrc.gc.ca

[2]Toth Information Systems, Ottawa, Ontario, Canada

Keywords: Materials Informatics, Rare Earth Elements, A*ab Initio* Calculations, Aerospace Alloys

Abstract

We have embarked upon building a database of the calculated physical, electrical, optical and magnetic properties of known rare earth element (REE) alloys and compounds using computational methods. These methods, in materials research, offer powerful tools to provide fundamental understanding of the behaviors of materials and to support the selection and design of materials that meet application requirements. With advances in computational science and information technology in recent years, materials research and development are shifting from the empirical approaches to the design to achieve optimal functionality based on integrated computational-prediction and experimental-validation methods. REE additions to non-ferrous metal alloys improve their physical and mechanical properties, resulting in lightweight and high strength alloys with special application in the aerospace industry. Physical property results will be presented on (i) a number of binary REE-alloys families and (ii) on the use of rare-earths in improving the mechanical properties of lightweight alloys.

Introduction

The development of modern aerospace alloys necessitates a constant search for new metallic materials with specific property profiles. Ultra high-temperature materials are critical to the development of next generation propulsion systems and hypersonic spacecrafts. Advances in the performance and efficiency of these propulsion systems are strongly dependent on the development of lighter, more durable high-temperature materials. Military technologies place increasing demand on materials operating in extreme service environments—high-stress, high-strain and temperature (high/low); corrosion and oxidation, heat flux. Operation of military equipment in these environments results in complex material degradation phenomena, such as creep, fatigue, fracture, or oxidation. Hence, materials requirements for these operations, and the substantial technological payoff for improved materials performance, are providing much of the impetus for fundamental research on metals, alloys, ceramics and composites. Intermetallic compounds provide a good starting set for the developments of aerospace structural materials for high-temperature/high-strength applications (HT/HS). In this regard there is now much greater interest in rare-earth metals, including yttrium and scandium, in the aerospace industry, that have significant application in the design of new structural alloys. Basic properties of primary importance for many of the aerospace applications are: density – for developing light-weight materials; melting temperature – for the knowledge of high-temperature stability, alloy fabrication and diffusion; and elastic modulus – for the knowledge of the mechanical properties.

A major topic of research on these materials is the continuing requirement to develop materials that have improved property profiles for strength at increasing temperatures, particularly for aerospace and space applications, where component materials having high specific strength (strength per unit density) and high specific stiffness (elastic modulus per unit density) are necessary. Here we cover the materials selection, for high-temperature/high-strength applications, by the calculation of intrinsic properties starting from their crystal structures. The use of certain structure-insensitive properties such as elastic moduli (E) and specific gravity (ρ) to identify suitable starting single-phase candidate materials (binary intermetallic compounds) have been employed. These calculations, based on density functional theory, provide a fast and efficient method to explore chemical, structure and property space in a combinatorial manner. Regularities and systematics, using structure-property relations, within structural families will identify suitable candidate materials. The informatics methods described here can be used in designing new materials for military application, particularly for the efficient search of chemical space for candidate materials. This results in reducing the time and cost for material development cycle. These "Materials Informatics" approaches enable the exploration of chemical and property space to aid the prediction and property optimization of candidate materials.

Materials informatics [1] approaches, then, provide an effective way to interpret and use materials properties data in the selection and design of materials and products. Combinatorial materials science (CMS) is an "experimental" approach to quickly analyze materials and to test for their physical and structural properties. It aims at discovering new materials using a combination of high-speed chemical synthesis, high-throughput screening, fast data-storing, data screening, and information processing.

Methods

For this study, physical properties such as elastic tensors (and the properties derived from them) and specific gravities (densities) have been calculated for binary intermetallic compounds from the crystal structure database CRYSTMET1 [2] using lattice, composition and structure type data. The elastic tensors were calculated using the method of Le Page and Saxe [3] using density functional theory (DFT) *ab initio* calculations with VASP [4]. When lattice information and composition was available, but no atomic co-ordinates, the model crystal structures were calculated with VASP using the structure type data. For binary intermetallic compounds the highly preferred structure types NaCl (B1), Cu_2Mg (C15), $AuCu_3$ (L10), CsCl (B2),with the preferred stoichiometric ratios of 1:1, 1:2, 1:3 were studied.

For materials selection a systematic design-oriented, five-step approach was used: (1) establishing design requirements, (2) material screening, (3) ranking, (4) researching specific candidates and (5) applying specific cultural constraints to the selection process. At the centre of this approach are the performance indices (i.e. particular combinations of material properties). In this study we are interested in intermetallic compounds for which (1) no experimental property data are known, and (2) the crystal structure of the material might or might not be known.

Here we have applied the systematic approach for the screening of suitable HT/HS compounds. The properties used are ones that are not significantly altered by processing or very slightly altered by small changes in alloy composition. These properties are the Young's modulus (E), the melting temperature T_m and the specific gravity or density (ρ). The elastic constants of a material are basic physical properties that are insensitive to heat treatments, deformation and microstructure. This insensitivity makes them useful for understanding the bonding of solids, including the role of crystal structure. For example, for aerospace application the importance of weight reduction is a requirement. For such light-weight materials the elastic properties give the stiffness of a material and when normalized by the specific gravity (ρ) give the specific stiffness E/ ρ.

Results and Discussion

The authors will present at the conference complete calculations for a number of binary REE-alloys families as well as results for ($Ti_{1-x}REE_x$) or ($Al_{1-x}REE_x$) binary systems screened for potential applications as aerospace alloys.

References

1. Rodgers, J.R., and W. Beres, "Design, Modelling, Lifing and Validation of Advanced Materials in Extreme Military Environments", NATO-AVT-187, Biarritz, France, October 2012.

   White, P.S., J.R. Rodgers and Y. Le Page, "CRYSMET: a database of structures and powder patterns of metals and intermetallics", *Acta Crystallogr. B,* 58 (2002), 343-348.

2. Le Page, Y., and P. Saxe, "Symmetry-general least-squares extraction of elastic data for strained materials from *ab initio* calculations of stress", *Phys Rev. B*, Volume 65 (2002), 104104.

3. VASP- Vienna Ab Initio Simulation Package: G. Kresse, Thesis, Technische Universiät Wien 1993; G. Kresse and J. Hafner, Phys. Rev. B 48, 13115 (1993); G. Kresse and J. Hafner, Phys. Rev. B 49, 14251 (1994).

Recycling of Rare Earth Elements

A REVIEW OF THE RECYCLING OF RARE EARTH METALS

C.J. Ferron[1], P. Henry [2]

[1] HydroProc Consultants, Peterborough, Ontario

[2] Jean Goldschmidt International, Brussels, Belgium

Keywords: Rare Earth Recycling, Permanent Magnets, Ni-MH Batteries

Abstract

Although rare earth metals are more abundant than their name would indicate, disruptions of their supply chain has occurred recently, and it is no surprise that the US Department of Energy DOE and the EU Commission have listed several of them as critical for their role as materials essential for a clean society.

This paper briefly reviews the major uses for rare earth metals and identifies the potential sources of scrap for recycling. The paper then describes the various processes developed to recycle rare earth-containing scraps, such as spent Ni-MH batteries, magnets, catalysts, polishing powders and phosphors, with case studies taken from industrial practice and research work.

Success of recycling efforts depend not only on adequate technical advancements but also requires the overcoming of non-technical challenges comprising amongst others logistics (collection, transportation), and an appropriate political and legal frame.

Introduction

The rare metals, to the contrary of what their name implies, are relatively abundant in the earth crust, with each of their being more plentiful than silver, and four of them (cerium, lanthanum, neodymium, and yttrium) being more plentiful than lead. Their combined crystal abundance is around 200 ppm. Rare earths are also found in concentrations higher than 10% REO in over 70 minerals, with the most commercially significant being monazite, bastanaesite, and xenotime, together with ion adsorption clays and apatite[1].

Rare metals are relatively well distributed but their production is dominated by China. The recent tightening of export quotas for rare earths by China has resulted in price spikes and supply issues for rare earths consumers around the world. Because of the widespread use of rare earths in a clean energy economy, in particular magnets for wind turbines, automobile magnets, rechargeable batteries, and phosphors for lighting, the US Department of Energy DOE has listed eight of the rare metals in the critical range in the short term (2015), and five in the medium term (2025), both regarding the risk of supply and their importance to clean energy[2]. Similarly, the European Union EU has also included the rare metals in their list of materials critical to its future development [3]. As a consequence, more and more efforts are being dedicated to examine the feasibility of recycling rare earths from the manufacturing process scrap (primary scrap) and from the used components (EOL scrap). This paper will first briefly review the major usages of rare earths in order to identify areas where recycling could play a significant role, and then review processes that are in use commercially or are being proposed to recycle the rare earths (RE).

Recycling Opportunities - Major Rare Earth Usages

Commercial application of the rare earths started in 1903 with the patenting of a pyrophoric alloy (70% mischmetal, 30% iron) by Von Welsbach. Since then, industrial applications of rare earths, used individually or in mixtures have increased significantly.

Table I summarises the principal usages of the rare earths from an economic point of view, while Table II presents typical compositions of important products and Table III summarizes the principal RE usages a from tonnage point of view [4, 5].

Table I. 2008 REO Consumption

REO Uses	% Total	
	By Volume	By Value
Catalysts	20	5
Glass	10	2
Polishing powders	12	4
Metal alloys	18	14
Magnets	21	37
Phosphors	7	32
Ceramics	6	3
Other	6	3

Table II. Typical Composition of Potential Recycling Feeds

Potential Recycling Feeds	Typical Composition (%)
Catalysts	
Fluid Cracking	3.5 REE (mostly La, +Ce, Pr, Sm)
Auto. Converter	<3.5 REO (mostly Ce)
Styrene	6-12 CeO2
Permanent Magnets	
SmCo	Sm 18-30; Co 50; Fe < 20; Cu 8; Zr 4; Gd<9.
NdFeB	Fe 50-60; Dy 1-2; Nd 20-30; B 1; C0 4; Pr <7 .
Rechargeable Batteries	
Ni-MH	Ni 48; Co 3.5; Fe 13; La 15; Ce 1; Pr 3; Nd 10; Sm 0.3.
Polishing Powders	Ce 40-65; La 1-6; Nd 0.1-0.7; Si 5-10; Pb 1-2; Fe 1-2
Alloys	Mg 2-3 Y or La; Ferroalloy 1-4 Y; Superalloy 0.3-1.3 Y; <1 La
Mischmetal	Ce 50-60; La 20-30; Nd 2-14; Pr 5-8.
Glass	Decol. (0.65 CeO_2); Stabil. (< 2.5 CeO_2); Colour. (< 5% RE).
Phosphors	Red 60 Y_2O_3+3 Eu_2O_3; Green 30 Tb; Blue 10 Eu

Table III. Estimate of 2008 Worldwide Usage of REE, in Metric Tonnes and Percentages

End Uses	CeO_2		La_2O_3		Nd_2O_3		Y_2O_3		Pr_6O_{11}		Dy_2O_3		Gd_2O_3		SmO		Tb_6O_7		Eu_2O_3		Other	
	t	%	t	%	t	%	t	%	t	%	t	%	t	%	t	%	t	%	t	%	t	%
Auto Catalytic Converters	6,840	90.0	380	5.0	228	3.0	-	-	152	2.0	-	-	-	-	-	-	-	-	-	-	-	-
Ceramics	840	12.0	1,190	17.0	840	12.0	3,710	53.0	420	6.0	-	-	-	-	-	-	-	-	-	-	-	-
Catalyst	1,980	10.0	17,800	90.0	-	-	-	-	-	-	-	-	-	-	-	-	-	-	-	-	-	-
Glass Additives	7,920	66.0	2,880	24.0	360	3.0	240	2.0	120	1.0	-	-	-	-	-	-	-	-	-	-	480	4.0
Alloys	5,980	52.0	2,990	26.0	1,900	16.5	-	-	633	5.5	-	-	-	-	-	-	-	-	-	-	-	-
Battery Alloys	4,040	33.4	6,050	50.0	1,210	10.0	-	-	399	3.3	-	-	-	-	399	3.3	-	-	-	-	-	-
NdFeB Magnets	-	-	-	-	18,200	69.4	-	-	6,140	23.4	1,310	5.0	525	2.0	-	-	53	0.2	-	-	-	-
Phosphors	990	11.0	765`	8..5	-	-	6,230	69.2	-	-	-	-	162	1.8	-	-	414	4.6	441	4.9	-	-
Glass Polishing	10,700	65.1	5,170	31.4	-	-	-	-	574	3.5	-	-	-	-	-	-	-	-	-	-	-	-
Other	2,930	39.0	1,430	19.0	1,130	15.0	1,430	19.0	300	4.0	-	-	75	1.0	150	2.0	-	-	-	-	75	1.0
Total	42,200	32.7	38,700	29.9	23,900	18.5	11,600	9.0	8,740	6.8	1,310	1.0	762	0.6	549	0.4	467	0.4	441	0.3	555	0.4

The Recycling of Rare Earth Catalysts

Rare earths catalysts constitute two major groups: fluid cracking catalysts (FCC) or automobile converter catalysts.

Fluid Cracking Catalysts: are used in petroleum refineries to convert heavy hydro-carbons into lighter fractions. During the operation, the catalyst becomes contaminated with carbon. This poisoned catalyst is regenerated and blended with fresh catalyst until it is deemed spent. Spent catalyst is considered hazardous waste. To the best of the author's knowledge, the REO content of spent catalyst is not presently recovered.

Automobile Catalytic Converters: In this application, the REO's are used mostly to protect the actual catalysts (Pt, Pd, Rh) whose intrinsic value in 2008 was 20 times higher than that of the REO's. As such, automobile catalytic converters are recycled to recover almost exclusively their PGM's values. Such recycling processes typically involve a smelting operation during which the REO’s are slagged off and not recovered.

Styrene Catalysts: [40] To the author’s best knowledge, the REO content is not recovered.

The Recycling of Rare Earth Permanent Magnets

Several types of permanent magnets have been developed over the years, but the rare earth based permanent magnets are amongst the highest producers of magnetic energy [1], as illustrated in Table IV.

Table IV. Typical Permanent Magnetic Material

Material	Average maximum energy product (MGOe)
Hard ferrite	3.5
NdFeB	35
SmCo	22
AlNiCo	8
Pt-Co	10

Commercial applications include computer hard disks, motors in cordless tools, automobile auxiliary features motors, wind-mill turbines. Permanent magnet scraps are generated during the fabrication of the magnet (manufacturing scrap) or at the end-of-life of the magnet (E-O-L scrap). Same E-O-L magnets are just demagnetized, and their recycling could just be to re-magnetize the magnets. In all other cases, a recycling process should be considered.

Over the last 20 years, numerous studies have been dedicated to the recycling of permanent magnet scrap, either the sludge produced during the manufacturing of the magnets, or the end-of-life (EOL) material itself. It is important to remember that the material to be recycled could be oxidized and will normally contain additional material, such as organics (adhesive, machining oil) or other metals (nickel,...), and this could influence the process selection. Moreover, the overall objectives of the recycling operation must be clearly defined. For example, is the goal to recover the REE's as a blend or separate, as metals or as oxides? Various process have been proposed, as schematically illustrated in Figure 1.

Both routes offer advantages and disadvantages. The processes recovering the REE's directly as metals offer the significant advantages of avoiding the energy-intensive step of the reduction to metal, but they normally generate a blend of metals that could only be recycled for the same use. The other group must undergo an oxidation step (to dissolve/evaporate) the REE's, followed then by a reduction step (to produce the metal), but their separation from solution and the final reduction to metal is commonly practiced in the industry, and the integration of such processes into existing facilities would seem relatively easy.

Group 1: Recycling of the REE’s as Salts

Acid Dissolution of the Magnets: The dissolution of the magnet using typical inorganic acids (HCl, HNO_3, H_2SO_4) is relatively straightforward but non-selective and fairly concentrated leach solutions are generated that will contain large amounts of iron, and, during the leach, large volumes of hydrogen are generated. The presence of organics might also cause some problems. Once the magnets are dissolved (relatively quickly for sludges, but quite longer for full magnets, unless they are shredded or granulated) and filtered, a fairly concentrated leach solution is available for metal recovery. Such a solution could assay 100-120 g/L Fe, 40-60 g/L REE, 4-6 g/L Co.

RE Metal Recovery From the Acidic Leach Solution: Numerous processes have been suggested to recover the REE's from magnet leach solution as discussed in recent reviews [6, 7, 8], and their differences revolve around the separation of iron from the REE's. The various processes could be classified as follows:

- selective precipitation of REE's by double salt, HF or oxalic acid, followed by iron removal (jarosite precipitation [11] or SX with naphtenic acid [9].

- solvent extraction of iron using N5O3, followed by solvent extraction for Nd/Dy and for cobalt [10].

Processes suggested by the USBM [11], Chen [9] and Shen [10] are illustrated in Figure 2, 3 and 4.

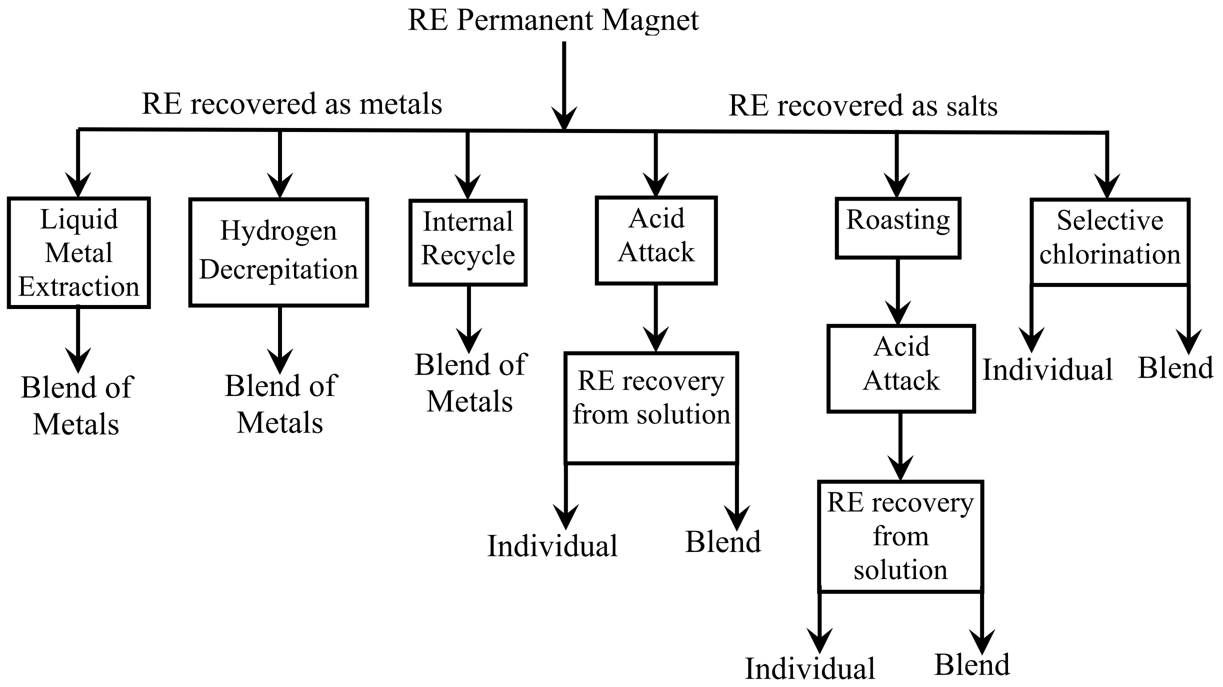

Figure 1. Simplified flow charts of various process options to recycle RE permanent magnets.

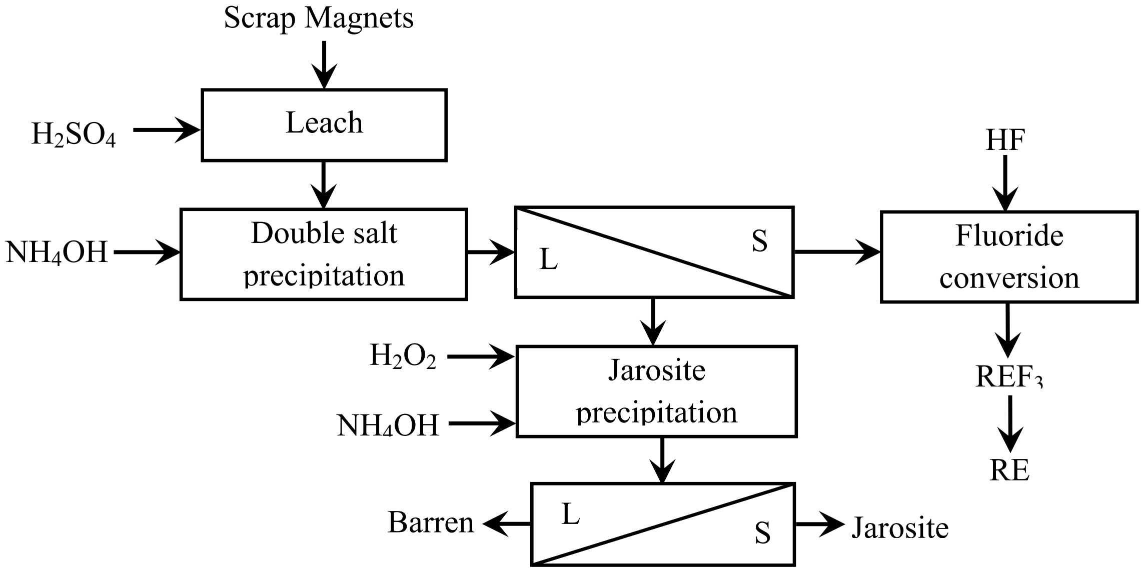

Figure 2. Simplified process flowsheet to recycle scrap magnet [11].

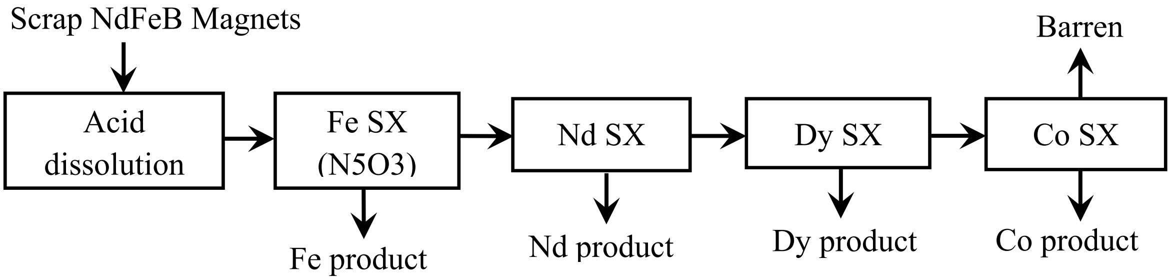

Figure 3. Simplified process flowsheet to recycle scrap NdFeCo magnet .[9].

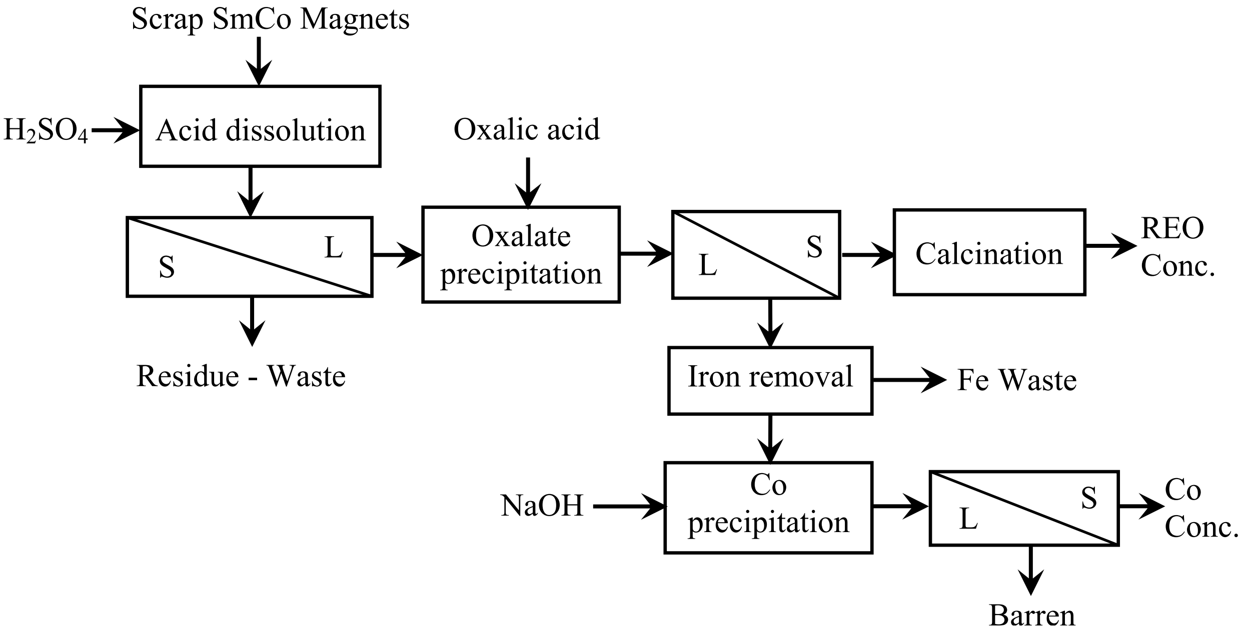

Figure 4. Simplified process flowsheet to recycle scrap SmCo magnets. [10].

To alleviate the problem of the separation from large quantities of iron, it has also been suggested to submit the magnet scrap to an oxidative roasting step prior to acid dissolution, to minimize the amount of iron dissolved during the acid leach and therefore simplifying the subsequent separation steps [12]. The proposed process is illustrated in Figure 5.

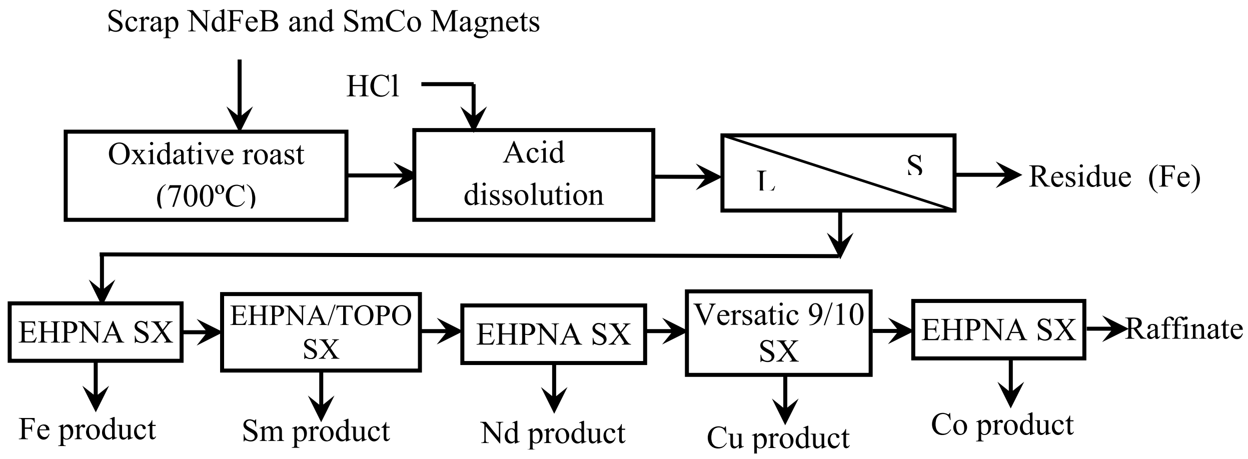

Figure 5. Simplified process flowsheet to recycle NdFeB and SmCo scrap magnets [12].

As can be seen, fairly complex processes involving numerous SX circuits with various organics are being proposed. Recent research has also taken non-conventional directions. One of such new promising routes involves the use of ionic liquids (low vapour pressure, non-flammable). The process investigated by researchers from the University of Leuven, Belgium, can be summarized as shown in Figure 6.

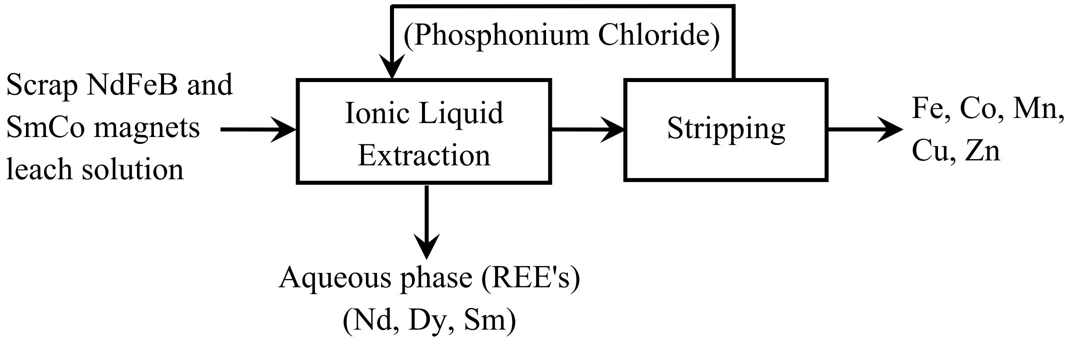

Figure 6. Simplified process flowsheet to recycle magnet scrap using Ionic Liquids [13].

Another process developed by Japanese researchers [14] also indicates the potential of separating iron from the rare earth metals by a two-stage electrodeposition from ionic liquids (choline-based).

Selective Chlorination: Selective chlorination processes have also been developed to recycle scrap magnets. In one instance, ferrous chloride is added to NdFeB scrap (at 800-1000ºC) to recover most of the rare earths as high purity chloride mixture condensate [6]. In another, aluminum chloride is added to SmCo scrap, and high purity samarium and cobalt chlorides are recovered separately in the condensates [7].

Group 2: Recycling of the REE's as Metals

The most attractive process would obviously be to recycle directly the spent magnets (after disassembly) to a re-melting stage, with possibly slagging off some impurities, and re-adjusting the composition with the addition of fresh components. Most of the time this is not possible and other routes have to be considered.

Rare Earth Metals Recycling Through Liquid metal Extraction: Ames Laboratory had developed, in the past, a process to separate La from Ni using liquid Pb-Zn metal [15]. The process was later expanded to separate (Nd + Dy + Pr) from (Fe + Co) in NdFeB magnets [16]. It is based on selective distribution of the REE`s within the molten metal (Mg) while the base metals (Fe + Co) are not soluble in the molten metal. It can be illustrated in Figure 7

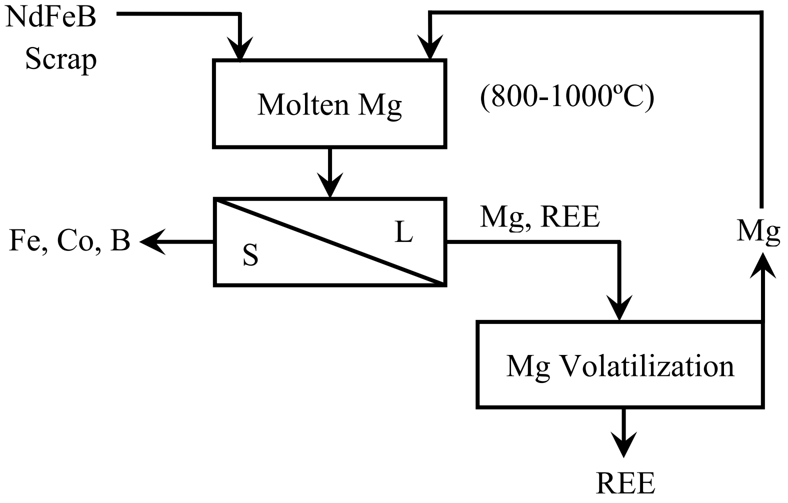

Figure 7. Simplified process flowsheet - to recycle REE`s from NdFeB magnets using liquid magnesium.

Laboratory results have indicated that the material properties of the recycled metals compare favourably with fresh materials.

Rare Earth Metals Recycling using Hydrogen Decrepitation Techniques.

The University of Birmingham (UK) has developed the hydrogen decrepitation process (HD), which could be applied to the recycling of rare metals from SmCo and NdFeB permanent magnets [17].

Hydrogen decrepitation is well known for breaking RE alloys into powder. The process is based on preferential penetration of hydrogen into RE rich grain boundaries (up to 0.4% wt.) in the material, with an associated volume expansion. The RE rich grains break away from the material to form a fine powder within a few hours, that can be removed by screening. Recent work [18] has indicated that by blending the decrepitated material with Nd hydride (1at %), the magnetic properties of the magnet were maintained.

The Recycling of Rare Earths from Alloys (Ni-MH Batteries)

This area has seen a flurry of activity over the last few years due to the development of rechargeable batteries for consumer goods and for electric (EV) and hybrid (HEV) vehicles. Not surprising to see large manufacturing companies leading the way in the development of recycling processes and public announcements have been made by companies such as Honda [19], Mitsubishi [20], Hitachi [21], Dowa [22] , Rhodia/Solvay in partnership with Umicore [23].

Figures 8 and 9 illustrate the processes developed by Umicore and Chinese Researchers, respectively.

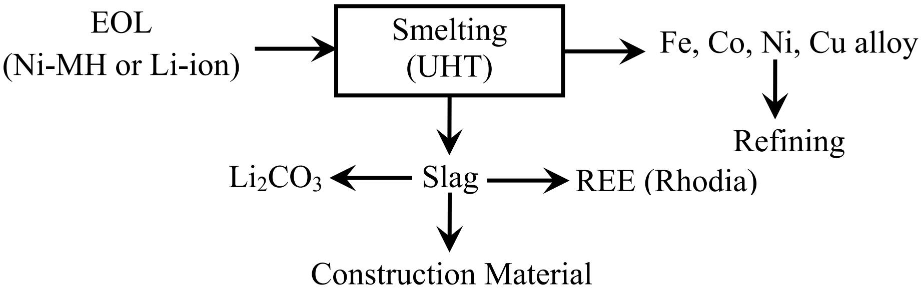

Figure 8. Simplified process flowsheet of Umicore UBR Plant [24].

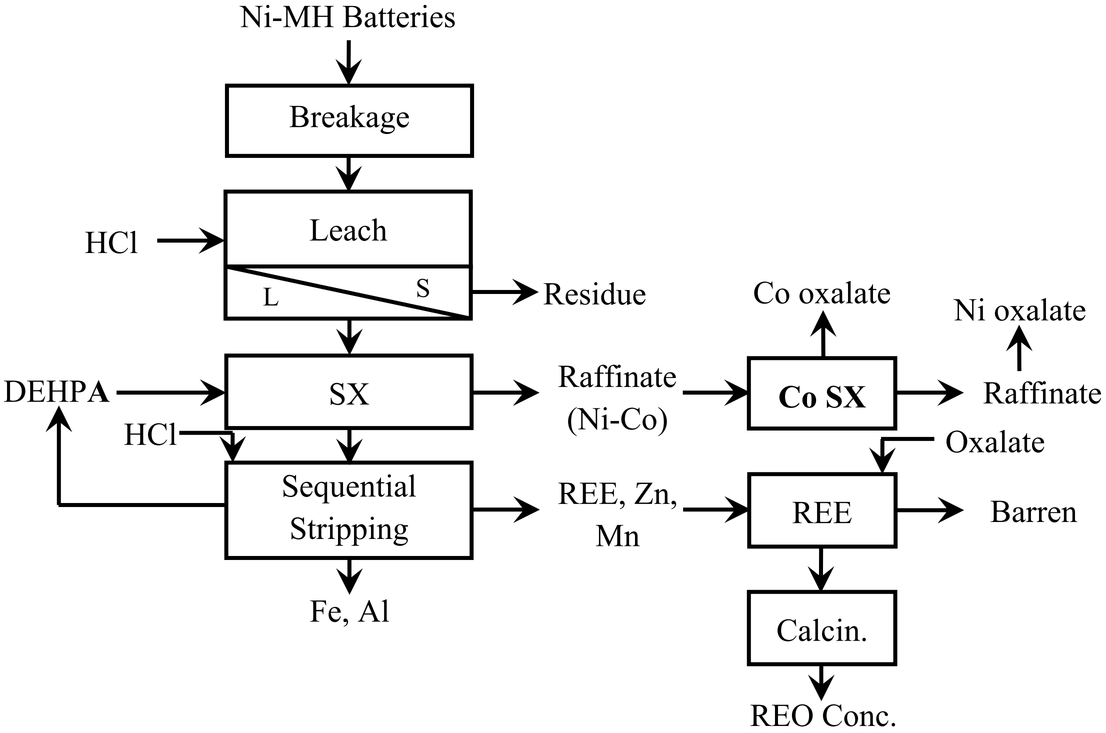

Figure 9. Simplified process flowsheet to recycle cobalt from Ni-MH batteries [25].

The Umicore Battery Recycling (UBR) division can process up to 7000 tonnes per year of batteries through their ultra-high-temperature (UHT) patented process. On the other hand, Chinese scientists have developed a fully hydrometallurgical process. [25]

A simplified version of Honda new recycling plant (Spring 2012) is presented in Figure 10.

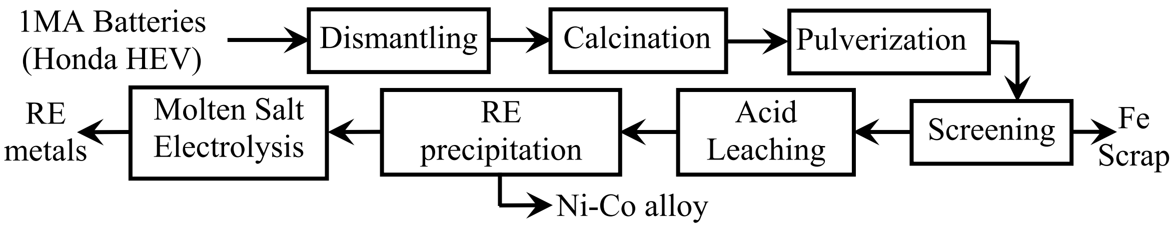

Figure 10. Simplified process flowsheet of Honda Plant [19].

Both the RE metals and the Ni-Co alloy are to be re-used to manufacture new IMA batteries.

The Recycling of Rare Earths from Phosphors

RE-based phosphors are used in various applications such as triphosphor fluorescent lamps, cathode ray tubes (CRT), liquid crystal displays (LCD), and others.

Rare earths used in these applications are high-value, and several processes have been developed [8, 26-29]. Examples of process to treat specific phosphors are presented in Figures 11 and 12.

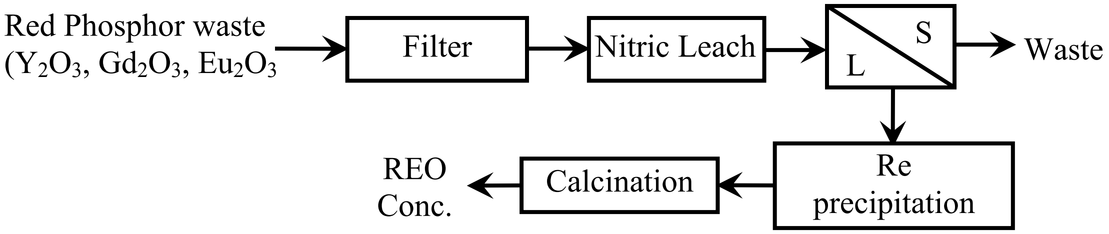

Figure 11. Simplified Process Developed by Matsushita Electronics Corp. [27].

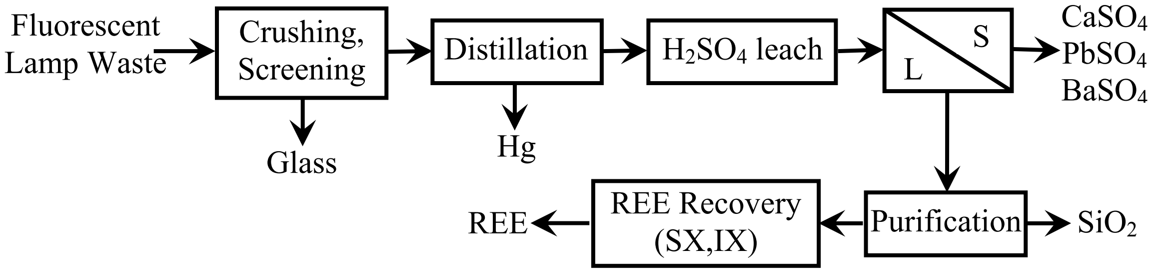

Figure 12. Simplified process to recover REE`s from fluorescent lamp waste [28].

The Recycling of Rare Earths from Other Sources

Research has also been carried out in other areas where rare earth containing waste are produced, such as glass polishing [30], garnets (gadolinium-gallium garnets GGG [31]) and overall electronic waste [32-34].

In 2012, Hydrometal SA processed 250 tons of polishing sludges through its recycling plant in Engis, Belgium [30]. The sludge consisted of 40-65% Ce, 1-6% La, 0.1-0.7% Nd, with major impurities Si (5-10%), Fe, Pb, Zn at 1-2% each, all in oxide form. The process developed and operated by Hydrometal can be illustrated in Figure 13.

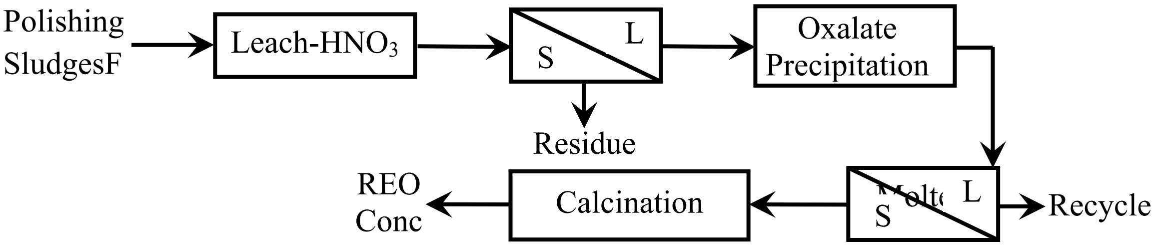

Figure 13. Schematic flow diagram of Hydrometal process to treat polishing sludges.

The Recycling of Rare Earths - Are We There Yet?

After this far from exhaustive review of the technical efforts to recycle rare earths from various scraps, the question arises as to the extent of recycling actually occurring in our world. A recent United Nations report [35] indicated that the average recycled content (RC), defined as the percentage of scrap metal in the total metal input to metal production was <1% for 9 of the rare earths and between 1 and 10% for 6 others, as compared to >50% for lead and between 25 and 50% for other metals such as Fe, Al, Cu, Co, Ni. The recycling rate of metals clearly does not depend just on the value of the metal to recycle, and is clearly low for rare earths. Recent metal price hikes have likely improved these statistics, at least as long as the high prices are sustained.

If we try to assess the size of the rare earth recycling business from a literature review (and we acknowledge that not all information is public, plants can be operating or shut down, and language barriers are complicating the exchange of information), we arrive at the following picture for RE recycling plants:

- Rhodia/Solvay has announced the opening of two RE recycling plants for Ni-MH batteries (Partnership with Umicore), and for low-energy light bulbs in St. Fons and La Rochelle.

- Honda is recycling its own Ni-MH batteries at a capacity of 400 tonnes/year, producing 24 T RE/yr. with a recovery of 80%.

- Mitsubishi has developed equipment to dismantle permanent magnets from air conditioners and washing machines capable of treating 120 units/h. and directly recycle the RE magnet

- Hitachi has developed equipment to recover RE magnets from air conditioners and disk drive (1 air conditioner ~ 30g REE) and capable to process 100 units/h. to provide about 60 T RE/yr. (10% of their needs)

- Ganzhou Recycle Hi-Tech Co Ud is operating a plant that recycles 8000 T/yr. of magnet scrap resulting in 2000 T REO/yr. production [36].

- Umicore UBR plant can process 1000 T/yr. of batteries (Li-ion plus Ni-MH), with the RE component recovered by Rhodia/Solvay.

- Hydrometal S.A. has been recycling glass polishing sludges and magnet sludges in its plant in Engis (Belgium) and has recycled ~1200 T REO since 2011.

- Showa Denko KK has built a recycling plant in Vietnam to recycle permanent magnet scraps and capable of covering 10% of their needs, or 800 T RE/yr.

This list indicates recent technical efforts to recycle RE but these efforts must be sustained and further increased. Without minimizing the technical challenges ahead of some new developments, challenges to further improve the recycling rates of the RE from their major scraps are mostly non-technical, and include the collection of the scrap, the dismantling of the RE-containing part if needed ("upgrading") and transportation to the recycling plants [37, 38].

Drivers to enhance the recycling rate of rare earths, in addition to economics, are sustainability, stewardship, strategic (lowering dependence on foreign sources), and these three latter factors are difficult to quantify financially but should be part of the overall economic equation. Environmental effects of recycling RE (by not having to mine primary ores) should also be considered and Life Cycle Assessment (LCA) should be routinely carried out [8, 39].

Conclusions

Significant technological advances are being made to recycle rare earths from various scraps, and a few commercial recycling plants are now operating. To further improve the recycling rate of the rare earths, efforts should be directed to improve the logistics (collection, dismantling, transporting) of bringing the RE scraps to processing centres pre-existing or to be constructed.

In many cases, to balance the economics, “soft” incentives such as strategic independence from foreign sources, sustainability and stewardship must be considered, with possible use to enforced legislation.

References

1. Roskill Information Services Ltd., *The Economics of Rare Earths and Yttrium,* Twelfth Edition, 2004.

2. US Department of Energy, "2011 Critical Materials Strategy Summary".

3. European Commission, "Critical Raw Materials for the EU," (Report of the ad-hoc Working Group on defining critical raw materials, 2010).

4. USGS, "Rare Earth Elements - End Use and Recyclability," (Scientific Investigations Report 2011 - 5094).

5. Kingsnorth, D.J., "Rare Earths: Facing New Challenges in the New Decade," (Paper Presented at SME Annual Meeting, 2010 Phoenix, Arizona).

6. Anderson, C.G., C.D. Anderson and P.R. Taylor, "The Extractive Metallurgy of Rare Earths Recycling," (Magnetics 2012, March 2012, Orlando, Florida).

7. Xu, T., and H. Peng, "Formation Cause, Composition Analysis and Comprehensive Utilization of Rare Earth Solid Wastes," *Journal of Rare Earths*, Volume 27, No. 6, Dec. 2009.

8. Binnemans, K. et al., "Recycling of Rare Earths: A Critical Review," *Journal of Cleaner Production*, 51 (2013), 1-22.

9. Chen, Y., "Recovery of Rare Earth and Cobalt in NdFeB Slag by Full Extraction Process," (China Resources Comprehensive Utilization), 2004, 6.

10. Shen, X., Y. Hou, "Utilization of Magnet Scraps," Jiangsu Chemical Industry, 2003, 31(3).

11. Lyman, J.W., G.R. Palmer, "Recycling of Neodymium Iron Boron Magnet Scrap," US Bureau of Mines, RI 9481, 1993.

12. Niinae, M., et al., "Hydrometallurgical Treatment of Rare Earth Magnet Scrap," *XIX International Mineral Processing Congress*, 1995, Volume 2, 229-233.

13. Farrell, I., "Recycling Rare Earth Elements using Ionic Liquids," March 2013, http://www.rsc.org/chemistryworld/ 2013/03.

14. Ishii, M., M. Matsumiya and S. Kawakami, "Development of Recycling Process for Rare Earth Magnets by Electrodeposition Using Ionic Liquids Media," *ECS Trans*., 2013, Volume 50, Issue 11, 549-560.

15. Ellis, T.W., F.A. Schmidt and L.L. Jones, "Methods and Opportunities in the Recycling of Rare Earth Based Materials," US DOE, Ames Laboratory IS-M796.

16. Westenhaus, B.,"Recycling Magnets to Extract the Rare Earth Metals," http://oilprice.com/metals/commodities/recycling.

17. Pearson, J., "Rare Earth Magnetic Cycling Method," University of Birmingham, http://gtp.autm.net/technology/view/15658.

18. Zakotnik, M., et al, "Multiple Recycling of NdFeB - Type Sintered Magnets," *Journal of Alloys and Compounds*, Elsevier, 469 (2009) 314-321.

19. Honda, "World's First Commercialization of Rare Earth Elements Recycling," http://www.honda.co.jp/environment/face/2012/case17.

20. Mitsubishi Electric, "Environment - How Are Rare Earth Magnets Being Recycled?," http://www.mitsubishielectric.com/company/.

21. Clenfield, J., M. Yasu and S. Biggs, "Hitachi Leads Rare Earth Recycling Efforts as China Cuts Access to Supply," http://www.bloomberg.com/news/2010-12-08/Hitachi.

22. Dowa, Kosawa Holdings, http://www.nytimes.com/2010/10/05/business/global

23. Recycling Today Staff, "French Firm Targets Rare Earth Metals for Recycling," http://www.recyclingtoday.com/

24. Umicore Battery Recycling, http://www.batteryrecycling.umicore.com.

25. Zhang, P., et al., "Hydrometallurgical Process for Recovery of Metal Values from Spent Nickel-Metal Hydride Secondary Batteries," Hydrometallurgy, Elsevier, 50 (1998), 61-75.

26. Tunsu, C., T. Retegan and C. Ekberg, "Sustainable Processes Development for Recycling of Fluorescent Phosphorous Powders - Rare Earths and Mercury - A Literature Report," (Chalmers University of Technology, Gothenburg, Sweden, 2011.

27. Otsuka, S., and Y. Okabayashi, "Method for Reclaiming Rare Earth Fluorescent Substances," U.S. Patent 3,506,585, April 14, 1970).

28. Otto, R., A. Wojtalewicz-Kasprzak, "Method for Recovery of Rare Earths from Fluorescent Lamps," U.S. Patent 7,976,798 B2, July 12, 2011.

29. Weltevreden, E.R.,, C. Klauber and C. Vernon, "The Modern Rare Earth Mine; on the Possibilities of Recycling CRT's," (Presented at Rare Earths 2012, COM 2012, Niagara, Ontario, Canada).

30. Henry, P., S. Lamotte and J.M. Bier, "Recycling of Rare Earth Materials at Hydrometal (Belgium), (Rare Earths 2013, COM 2013, Montreal, Quebec, Canada, to be published).

31. E. Gusset, "Recovery and Separation of Gadolinium and Gallium," U.S. Patent 4,198,231, April 15, 1980.

32. Laarmann Group, "Urban Mining for Rare Earth Elements With Laarman," http://www.laarmann.info/urban-mining.htm/

33. Resende, L.V., and C.A. Morais, "Recovery of Europium and Yttrium from Electronic Scrap," (Paper presented at Rare Earths 2012, COM 2012, Niagara, Ontario, Canada).

34. Grabas, K., et al., "Recovery and Characterization of Lanthanides from Electronic Waste Recycling," (Paper presented at Rare Earths 2012, COM 2012, Niagara, Ontario, Canada).

35. United Nations (UNEP), "Recycling Rates of Metals," (a status report, 2011).

36. Ganzhou Recycle Hi-tech Co: http://www.jxgda.com/En

37. U.S. EPA, "Rare Earth Elements: A Review of Production, Processing, Recycling and Associated Environmental Issues", EPA 600/R-12/572, December 2012/www.

38. Schüler, D., et al, "Study on Rare Earths and Their Recycling," (OKO-Institute V., Darmstadt, Jan. 2011).

39. Hagelüken, C., "Metal Recycling: Make Technology, Service and Business odel Design Match/Match Design," (Presented at Umicore, VTT Seminar from Sustainable Mining to Eco Design, 2012, Helsinki).

40. Hirano, T., “Dehydrogenation of Ethylbenzene over Potassium-promoted Iron Oxide Containing Cerium and Molybdenum Oxides”, Applied Catalysis, Vol. 28, Dec 1986, 119-132.

RECYCLING OF Nd FROM Nd PERMANENT MAGNET USING LIQUID Mg SOLVENT

Jordan Zampini[1], Yonghwan Kim[2], Marie-Aline Van Ende[1] and *In-Ho Jung[1]

[1]McGill University, 3610 University Street, Montreal, Canada H3A 0C5
*in-ho.jung@mcgill.ca

[2]Korea Institute of Industrial Technology, Song-do, Incheon, South Korea 406-840

Keywords: Nd Permanent Magnet, Recycling, Selective Extraction

Extended Abstract

Scrap neodymium boron magnet material is a valuable source of Nd for recycling. The magnet material is a ternary alloy of Nd, Fe and B with a nominal formula $Nd_{0.12}Fe_{0.76}B_{0.06}$. The kinetics of extraction of Nd from Nd magnets was investigated by dissolution of Nd magnet powders in molten Mg at 973 K, 1023 K and 1073 K. Pre-crushed Nd magnet powders with three different particle sizes (5 mm, 1.5 mm and 0.5 mm in diameter) were used in the experiments. During the dissolution of Nd magnet material, molten Mg was sampled for up to 60 min. The evolution of the Nd concentration in molten Mg at 1023 K with holding time is plotted in Fig. 1 for the three powder sizes. Although higher Nd extraction rate was expected with smaller Nd magnet particles, the results show the opposite behavior. The extraction rate of Nd surprisingly increases with increasing the particle size. In order to understand this, the chemical composition of the pre-crushed particles was obtained using ICP (Inductive Coupled Plasma) technique and the internal structure of a pre-crushed particle was examined by Scanning Electron Microscopy (SEM). As seen in Fig. 2, it was found that oxygen concentration increases sharply with decreasing Nd magnet material particle size. The internal microstructure of a pre-crushed particle analyzed by SEM shows that the oxygen is mainly bonded with Nd, which might form Nd_2O_3 oxide.

Why the oxygen content in the Nd magnet particle increases with decreasing particle size can be explained by the formation of Nd oxide phases during mechanical crushing. A greater mechanical force was applied to crush the particles to smaller size, creating larger surface area, which induced more oxidation of the Nd magnet . Once such Nd oxides are formed, their reduction by molten Mg would be difficult. Therefore, the total Nd concentration in liquid Mg from the dissolution of smaller size particles after 60 min is lower than that of larger size particles for the same duration. It is known that the extraction of Nd occurs by penetration of liquid Mg through the grain boundaries of the Nd magnet.[1] Therefore, the lower Nd extraction rate observed with smaller particles results from the more significant blockage of liquid Mg penetration by the formation of Nd oxides.

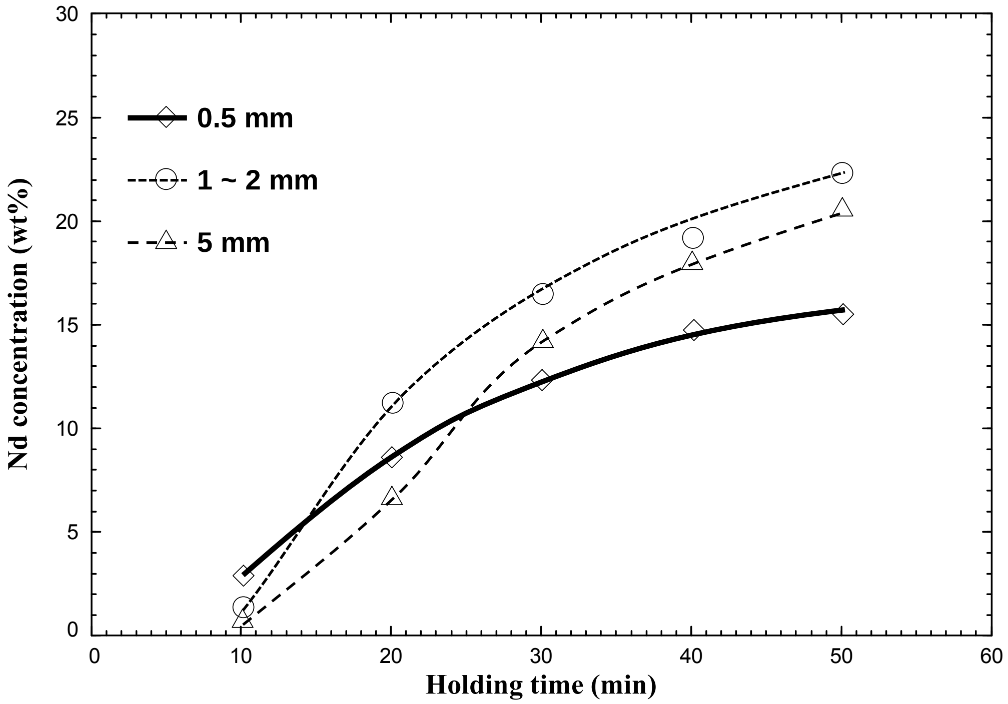

Figure 1. Effect of time and particle size on Nd extraction by molten Mg at 1023 K.

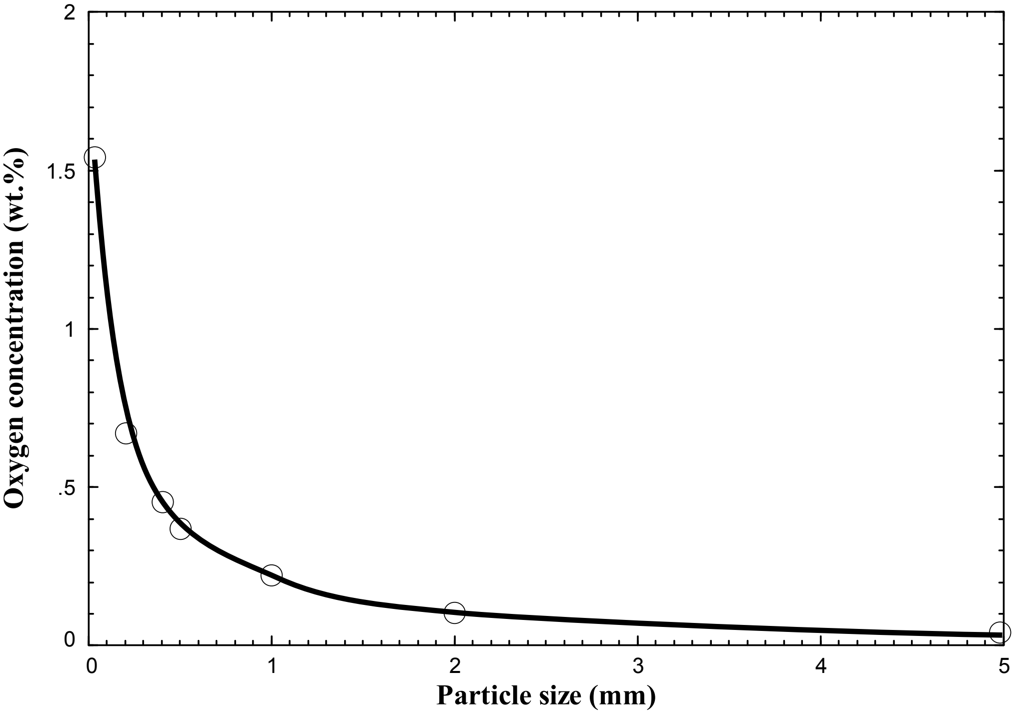

Figure 2. Effect of crushed particle size on oxygen content of Nd magnet materials.

The extraction process was simulated using a kinetic model linked to an accurate thermodynamic database recently developed by the present authors [2]. Fig. 3 shows the thermodynamic phase calculations for the chemical reaction between Mg and Nd magnet. According to the phase diagram, when the solid Nd magnet is reacted with liquid Mg above 700 °C, Nd can be selectively dissolved into molten Mg, leaving the two other magnet constituents Fe and B in a solid form such as solid Fe (BCC) and Fe_2B. Theoretically, a maximum of about 80 g of Nd magnet can be dissolved into 20 g of molten Mg for the extraction temperatures above 700 °C. Of course, the Nd extraction becomes faster with increasing temperature, but it is recommended to keep the temperature below 900°C to avoid significant oxidation of Mg.

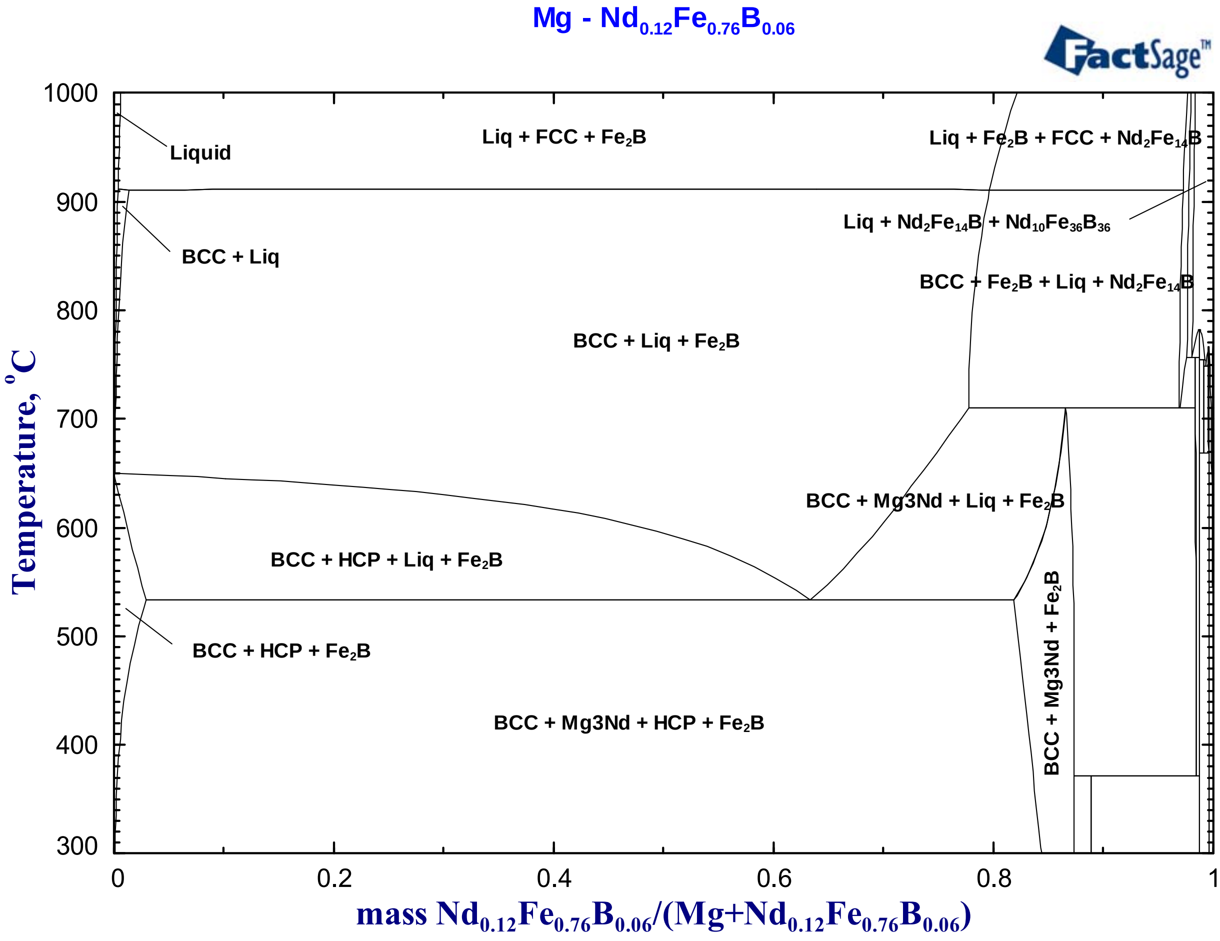

Figure 3. Calculated phase diagram between Mg and Nd magnet ($Nd_{0.12}Fe_{0.76}B_{0.06}$) from the thermodynamic database [2].

References

1. Chae, H.J., Y.D. Kim, B.S. Kim, J.G. Kim and T.-K. Kim, “Experimental investigation of diffusion behavior between molten Mg and Nd-Fe-B magnet”, *J. Alloys Compd.* (2013), in press.

2. Van Ende, M.A., and I.-H. Jung, “Critical thermodynamic evaluation and optimization of the Fe-B, Fe-Nd, B-Nd and Nd-Fe-B systems”, *J. Alloys Compd.* 548 (2013), 133–154.

RECYCLING OF RARE EARTH MATERIALS AT HYDROMETAL (BELGIUM)

Philippe Henry[1], Sabine Lamotte[2], Jean-Michel Bier[3],

[1] Managing Director, [2]RD Manager, 3 Project Manager
SA HYDROMETAL
Rue du Parc Industriel 3
4480 Engis Belgium

Keywords: Hydrometallurgy, Non-Ferrous Metals, Recycling, Rare Earth Residues, HYDROMETAL

Abstract

HYDROMETAL is using suitable technology to reintroduce lost metal units into the industrial cycle, thereby saving resources and energy while keeping the environment cleaner. Since 2010, Hydrométal has started the recycling of RE (Rare Earth) units from wastes generated by the RE refining industry in Europe and has decided to initiate new recycling projects for the RE recovery from magnets industry or glass industry. Two case studies of recycling of materials during the last two years in our integrated hydrometallurgical facility (Hydrométal) in Belgium are discussed:

1. Recycling of Cerium from polishing sludges;

2. Recycling of Neodymium-Samarium-Dysprosium from magnets industry.

What is Hydrométal?

Hydrométal SA (Engis, Belgium) is a subsidiary of Jean Goldschmidt Int. SA (JGI) in Brussels. JGI is mainly involved in metal trading activities. In the eighties, JGI acquired the leaching circuit of a Belgian electrolytic zinc refinery located in Engis, a few kilometers south of Liège. Hydrométal is well connected by water, rail and road from its central location in the industrial region of Liege, in the heart of Europe. The operation covers an area of 5 hectares and received in 1993 an additional license to process and recycle toxic and hazardous waste. Figure 1 shows a picture of the entrance of the plant. In this paper we will discuss two case studies thereby presenting an overview of the broad possibilities of metal recycling at Hydrométal.

Hydrométal's business is focused on the recycling of complex materials loaded with non-ferrous metals. Feed materials to the plant consist mainly of residues generated by industrial activities of Hydrométal's suppliers and clients. These feeds arrive in the form of fumes, drosses, slags, sludges, dusts, ashes, cements, filter cakes, spent catalysts, complex alloys, turnings, grindings, manufacturing rejects and the like.

Figure 1. Entrance of Hydrométal.

The complex non-ferrous metals residues that are treated may contain Cu, Zn, Ni, Co, Ge, Pb, Sn, Cd, Se, Te, Bi, As, Ag, Au (and other precious metals) and originate from all over the world. They are converted into simpler, purer metal compounds such as cements, salts or concentrates, both in solid form or in solution. These products are thereafter used as feed materials for plants in the metallurgical or chemical industries. Hydrométal also produces refined metals, such as high purity Sn (up to 99.999 %). Since 2010, Hydrométal diversified its activity into recycling of materials containing rare earths. For example, in 2012, Hydrométal recycled more than 1% of the refined REO capacity in the world.

All surface run-off and waste process liquors are collected and recycled at the front end of the various re-pulp or leach processes. Additionally, a fully automated effluent treatment facility is treating the acidic or alkaline waste waters produced in Hydrométal's various treatment facilities in order to fulfil the last IPPC rules. The resulting filter cakes are often recycled internally to recover otherwise lost metal values.

Hydrométal has treated some 75,000 WMT of raw material in 2012.

Rare Earth Recyling at HYDROMETAL

RE have been defined as critical materials by the EU Commission (1). This is mainly due to the high supply risk and dependence on China deliveries. Actually, China is producing more than 90% of the global world production while it only possesses 40% of the estimated reserves. So China is mining and extracting RE and is specialised in the refining and/or separation of RE but also a specialist in the production of RE as individual elements (oxide, salt) and in the production of RE magnets, phosphors (2). The tightness in quota export for the last years causes serious problem for EU companies. So it is important to start an efficient recycling program to reduce our dependency to the Chinese deliveries.

For several years, intensified research projects have been started in order to promote efficient recycling of RE from complex materials and mainly from permanent magnets, lamp or CRT phosphors, FCC catalysts, glass polishing powders and metal hybride batteries (3,4). In order to benefit from this RE booming price opportunity, Hydrométal started to recycle different kinds of sludges loaded with Ce, La, Nd and Dy in 2010. Hydrométal also started a R&D program which turned into a practical recycling process, concerning either the recycling of sludges from magnets industry or the recycling of Re from glass polishing powders.

Case Study: Recycling of Rare Earth from Polishing Sludges

Polishing sludges treated at Hydrométal typically consist of cerium (40-65%), lanthanum, (1-6%) and neodymium (0.1-0.7%), with zinc (1-2%), iron (1-2%), lead (1-2%), silica (5-10%). The elements are mainly present as oxide. A specific flowsheet (see Figure 2) has been developed at Hydrométal to treat these materials and to separate them into a RE concentrate and Zn-Fe bleed. For the past two years at Hydrométal, polishing sludges have been treated from several other sources (glass or crystals producers).

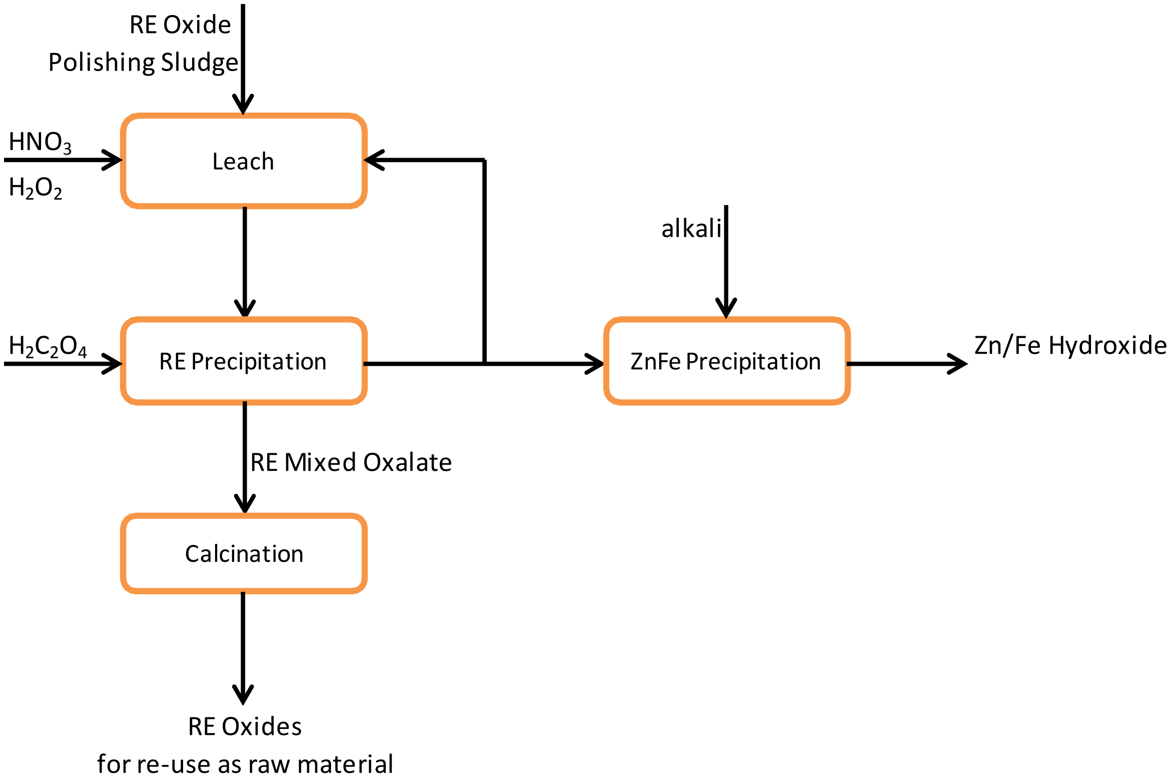

Figure 2. Schematic flow diagram – treatment of polishing sludges at Hydrométal.

Nitric acid is used to leach the sludges and produce a rare earth (RE) solution containing more than 15% RE. Nitric acid is used as it promotes the good leachability for Rare Earth elements and selective towards silica and alumina. Most of the feed material is oxidised and a small quantity of hydrogen is used to get optimum Ce-La recovery yield. This consumption is not more than the stoechiometric required quantity to reduce Ce^{4+} to Ce^{3+}. The temperature needs to be maintained at 80°C or higher in order to favour optimum reagent diffusion into the silica matrix but also obtain practical filtration characteristics. The reaction is monitored by ORP control to avoid any trace of Ce^{4+}. This permits the use of stainless steel as a reactor material. Zinc and iron are also leached and it is hence necessary to use oxalic acid to recover a RE concentrate with the following analysis (see Table I):

Table I. Rare Earth Concentrate

	Ce	La	Zn	Fe	SiO2	Pb
%	35-45	1-4	<0.1	<0.1	< 0.1	<0.1

The solution obtained after oxalate removal is reused at the leaching step and bled to remove Zn and Fe by precipitation as mixed hydroxide. The oxalate concentrate is then calcined externally in a rotary kiln to produce a new quality RE concentrate which can be used in the production of new quality of polishing sludge.

Case Study: Recycling of Nd-Sm-Dy from Magnets Industry

The magnet industry is generating complex wastes loaded with Fe-Nd-Dy but also Co-Sm depending on the type of magnet application. The material received at Hydrométal is pre-calcined externally at 650°C to remove some of the organic binders and is subsequently processed as dry oxidic material.

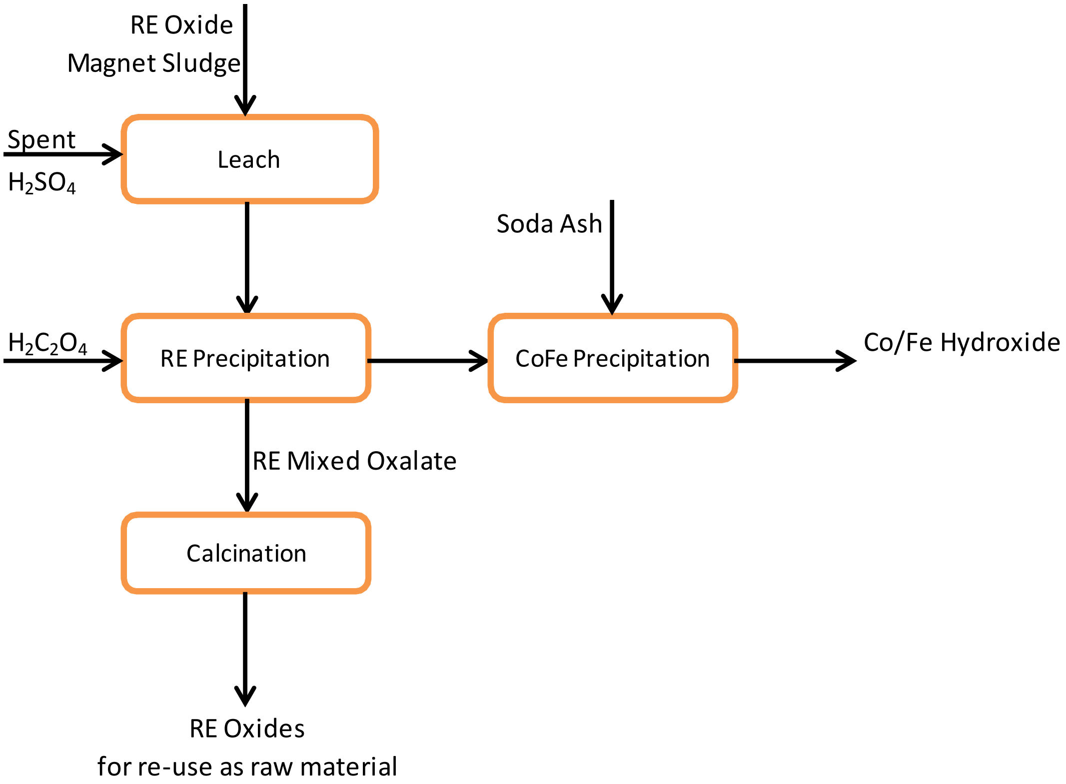

Figure 3. Schematic flow diagram of magnets sludges treatment at Hydrométal.

Hydrométal has developed and is applying a new process (Figure 3) to recover two concentrates:

1. Fe-Co concentrate by using caustic soda precipitation;

2. REO concentrate by using selective oxalate precipitation of Rare Earths.

In this case, spent sulphuric acid (from battery recycling) is used to leach the raw material and produce a rare earth (RE) solution containing more than 10% RE plus cobalt and iron. Cheap recycled sulphuric acid can be used as there is no trace of Ce^{3+} which tends to be insoluble at high sulphate concentrations, contrary to Nd-Dy-Sm which are soluble at our level in this media. The temperature in the stainless steel leach reactors is maintained at 50°C which has been determined to be the maximum optimum temperature for good recovery yield. Oxalic acid is used to recover a RE concentrate with the following analysis (see Table II):

Table II. Rare Earth Concentrate

	Nd	Dy	Sm	Fe	Co	SiO2
%	15-35	1-7	10-20	<2	<1	<0.1

The Fe-Co contained in the oxalate filtrate is then precipitated with soda ash to recover Co and Fe as hydroxides. The oxalate concentrate of RE is subsequently calcined to produce a high grade RE concentrate which can be used in the production of RE salts after additional refining. Tests have also been performed externally to produce new alloys directly suitable for the reuse in the magnets production.

Conclusions

Hydrométal is treating a wide range of complex metal residues. It has at its disposal various hydrometallurgical techniques such as consecutive leaching, cementation and precipitation, along with more specialized techniques such as solvent extraction, ion exchange and electrowinning which have been installed during the last years. Many of the treatments use residual reagents from the chemical industries.

Since 2010, Hydrométal has diversified its activities to recycle valuable Rare Earth material. Beside spent catalysts, sludges, Hydrométal has also treated significant quantities of polishing sludges and wastes from the magnet industry to recover Ce, La, Nd, Dy, Sm as valuable oxides but also Co, Fe as valuable by-product salts. Rare Earth recycling at Hydrométal accounted in 2012 for > 1% of total REO refined in the world.

References

1. European Commission : Report of the Working Group on Defining Critical Raw Materials, 2010.

2. Xu, T., Yan Wang, Baotou Research Institute of Rare Earth, “Processing and Utilisation of Rare Earth Wastes”, *Critical Metals Conferenc*e, MetalEvents, London, 18-19th March 2013.

3. Feron, J., Philippe Henry, “A Review of the Recycling of Rare Earth Metals,” COM Montreal, 2013, to be published.

4. Binnemans, K., et al., “Recycling of Rare Earths: a Critical Review”, *Journal of Cleaner Production* 51 (2013), 1-22.

EXTRACTION OF CERIUM AND LANTHANUM FROM SPENT GLASS POLISHING AGENT

Alexander Poscher, Stefan Luidold and Helmut Antrekowitsch

Chair of Nonferrous Metallurgy
University of Leoben, Franz-Josef-Straße 18, 8700 Leoben, Austria

Keywords: Glass Polishing, Abrasive Materials, Cerium Dioxide, Recovery

Abstract

Cerium dioxide is frequently used as an abrasive material in the glass industry. The field of application includes the technique of CMP (chemo-mechanical polishing/planarization) which is also used for wafer processing in semiconductor production. The aim of this work was the development of a process for the recovery of cerium and lanthanum from a spent glass polishing slurry which had previously been dried and calcined. The material of interest contains approximately 56% Ce and 7% lanthanum as well as contaminants like silicon, zinc, sodium, calcium and lead, whereas 79% of all cerium exists as CeO_2. 21% of the element is bound in compounds similar to fluorbritholite and monazite. The first step of our process suggests a combined leaching of the calcined material by hydrochloric acid and the reduction agent hydrogen peroxide due to the fact that cerium exists in the residue in its tetravalent state. Furthermore, research was conducted producing a Ce/La oxide (>99%) which can be reused for the production of a polishing agent.

Introduction

The use of polishing compounds based on rare earth elements is widespread in the production of optical lenses or in wafer processing nowadays. According to Schüler et al. [1] the worldwide demand for rare earths in the glass and ceramics industry was about 33-42 kt in 2008, which represented 30% of the global production. Nevertheless, the mechanisms of polishing or planarization are not completely understood. Klemm and Smekal [2] stated in the early 1950s that the planarization of a glass surface is mainly caused by the abrasive impact of grains, concluding that the polishing process can be performed by the use of any kind of grinding material simply regarding the grain size. Today it has become clear that the polishing process is much more complex than it was first thought. In his work, Kaller [3] published a three-step model which takes tribochemical aspects during the rubbing process into account and considers interactions between exposed lattice defects on the fractured surface of the polishing grains and the glass substrate. Additionally the model includes a dissolution step of rubbed-off parts from the glass substrate forming an aqueous silicate solution. A nearly identical description of the above mentioned scheme is given by Steigerwald [4]. It is illustrated that a chemical reaction has to take place between the polishing slurry and the glass surface which was investigated by the measurement of weight loss of the substrate versus the polishing rate given in microns per minute.

Beside the complex fundamentals of the chemistry of the polishing process, the techniques used are diverse. A short overview of different operations used is given in [5].

Nonetheless, polishing agents are manufacturing materials and as it was stated above, quite a large amount of rare earths - especially cerium dioxide and lanthanum oxide is therefore consumed by the glass industry. During the glass processing the slurries get enriched by a number of elements depending on the chemical composition of the glass, of which some (esp. Si, Zn, Na) could affect the product quality adversely. As a result the abrasives have to be replaced and due to the lack of recycling processes the material is disposed of in special landfills. However, some applicable technologies are known from literature, as described by Kato et al. [6]. Their investigations dealt with an alkaline treatment of a polishing powder waste containing about 22.1% CeO_2, 17.8% La_2O_3 and almost 25% Al_2O_3 together with 12.6% SiO_2 as impurities. The experiments for the removal of the contaminants took place under different operating conditions concerning the temperature, alkali ratio and sodium hydroxide concentration. It could be found from the authors that the extraction conditions for silicon dioxide and alumina should be 50-60°C, using a NaOH solution concentration of 4 mol/kg and 1 kilogram of alkaline solution to treat 1 kg of waste slurry [6]. The treatment of the remaining alkaline solution includes the precipitation of hydroxysodalite at 80-100°C [7]. Further research was done by Kim et al. [8] applying froth flotation combined with a solution of oxalic or citric acid for the removal of bits of broken glass and the flocculant (poly-aluminium chloride) present in the raw material whereas the operation was carried out under ultrasonic conditions. The remaining glass was dissolved using sodium hydroxide at pH = 11.5 followed by a thermal treatment of the resulting slurry at 600°C in a rotary kiln. Sulfuric acid was applied for solubilization and the resulting solution was mixed with sodium sulfate for selective precipitation of the trivalent rare earths as double sulfates. Cerium remained in the aqueous phase, whereas no separation experiments for the element were performed [8].

In our work we would like to present a process for the recovery of cerium and lanthanum from a spent glass polishing slurry by hydrochloric acid leaching followed by the addition of hydrogen peroxide. Results for precipitation experiments are also presented using oxalic acid.

Recycling Concept

The recycling concept developed at the Chair of Nonferrous Metallurgy at the University of Leoben is based on three operation steps (Figure 1).

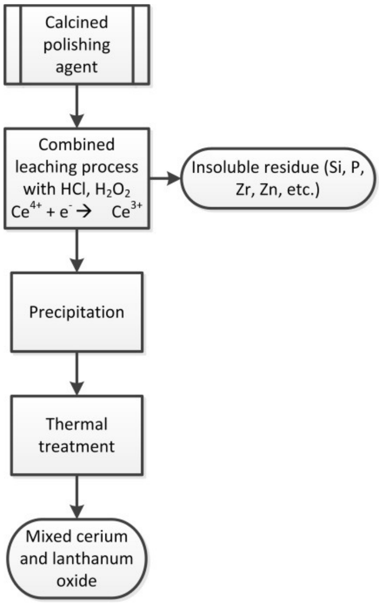

Figure 1. Flowsheet of the recycling concept.

Initially it was important to extract all valuable metals into an aqueous hydrochloric solution. As it is shown later in this paper, sufficient extraction rates can only be achieved by the simultaneous addition of hydrogen peroxide to the leaching liquor. This is due to the fact that 79% of the cerium present in the raw material exists in its tetravalent stage as CeO_2 and is partly (21%) embedded in complex compounds which are similar to fluorbritholite, $Ca_2(Ce,Ca)_3(SiO_4,PO_4)_3(F,OH)$ and monazite, $CePO_4$. After a precipitation of the lanthanides by oxalic acid, the mixed oxalates were converted to their oxides by a thermal treatment and analyzed by XRF. Based on the chemical analysis of the won oxidic products mass balances were calculated to determine the yield of cerium and lanthanum in each trial. In order to visualize the results and the influence of the precipitation parameters, concentration and amount of oxalic acid, on the yield of cerium and lanthanum a statistical analysis of the experimental results was done using the computer program MODDE 7.

Experimental

The leaching experiments were carried out in a three-neck round-bottom flask using a condenser at the top in order to keep the volume of the leaching solution at a constant level. A burette was applied for the addition of hydrogen peroxide (30 wt.-%), as well. Figure 2 shows the schematic experimental set-up for all leaching experiments.

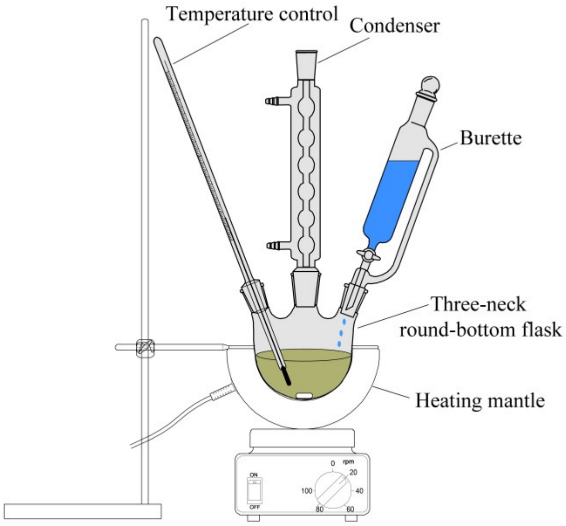

Figure 2. Schematic drawing of the experimental set-up in the leaching step.
(Figure drawn with ACD/ChemSketch)

For each experiment 50 grams of a dried and calcined polishing agent were used. Its XRF analysis is shown in Table I.

Table I. XRF Analysis of the Calcined Polishing Agent

Element	wt.-%	Element	wt.-%
Ce	56.0	Zr	1.0
La	7.2	Al	0.7
Si	5.2	Pb	0.1
P	1.0	Ca	0.8
Zn	1.5	Na	0.9

The hydrochloric acid leaching was carried out using different amounts of acid (136.7, 273.5 and 547 g) of variable concentrations (16, 21 and 32%), to represent liquid-to-solid (L/S) ratios of approximately 2.7, 5.5 and 11. The standard test mode for the leaching experiments (Table II) includes the addition of hydrochloric acid solutions and water (except experiments 6, 8 and 9) to the waste polishing agent, a heating period to the required temperature and the subsequent addition of 100 g hydrogen peroxide within the first ten minutes on temperature. Detailed conditions of the experiments are shown in Table II, whereas the marked trials differ from the above described test mode as it is explained beyond the table.

However, as it is shown later in the results the acid concentration, the liquid-to-solid ratio as well as the use of hydrogen peroxide have a great influence on the leaching operation. Nevertheless, the pregnant solutions for precipitation originated in previous leaching experiments performed with 50 g of polishing agent, 273.5 g of 32 wt.-% HCl while 100 g hydrogen peroxide solution were added within the first 10 min at 80°C (experiment 9). After a solid-liquid separation by filtration using frits of mesh 0.010 to 0.016 mm, the obtained solution was adjusted to 500 mL with deionized water, homogenized and transferred to 2000 mL beakers where the precipitation took place under continuous agitation of 300 rpm and drop-wise addition of different amounts (30, 40, 50 g) and concentrations (50, 62.5, 80 g/L) of oxalic acid solutions. The applied amounts of acid represent excess of 0, 34 and 67%, calculated for the achieved extraction rates into the solution of 97% of Ce, 70% of La and 54% of Zn present in the raw material. Before carrying out the experiments zinc was assumed to co-precipitate. Therefore, its content in the raw material was considered in the stoichiometric calculation for the demand of oxalic acid. Nevertheless, the final product exhibits only insignificant amounts of the element. A white solid was produced by further filtration and drying at 120°C for at least 12 h and subsequent conversion of the RE oxalates to their oxides at 750°C for 6 h. The resulting red-brown solid was examined by XRF analysis in order to calculate the mass balances for the described process and identify the optimum precipitation parameters. The worksheet used for the experiments was designed by MODDE 7 and included 11 precipitation experiments.

Table II. Leaching Experiments

Nr.	m pol. agent [g]	m HCl 32% [g]	m HCl 10% [g]	m H_2O [g]	m H_2O_2 [g]	T [°C]	t_{leach} [h]
1	50.0	136.7	0	136.7	0	80	4
2*	50.0	136.7	0	136.7	0	80	4
3	50.0	136.7	0	136.7	100	80	4
4	50.0	136.7	0	136.7	100	95	4
5	50.0	136.7	0	136.7	100	80	8
6	50.0	136.7	0	0	100	80	4
7**	50.0	136.7	0	136.7	100	80	4
8	50.0	136.7	136.7	0	100	80	4
9	50.0	273.5	0	0	100	80	4
10	50.0	273.5	0	273.5	100	80	4

* dropwise addition of hydrochloric acid over total leaching time

** dropwise addition of hydrogen peroxide over total leaching time

Results and Discussion

The leaching experiments which were performed under different conditions (temperature, concentration and amount of acid) pointed out that a hydrochloric acid leaching without the use of hydrogen peroxide as a reducing agent for cerium dioxide leads to insufficient extraction rates (Figure 3).

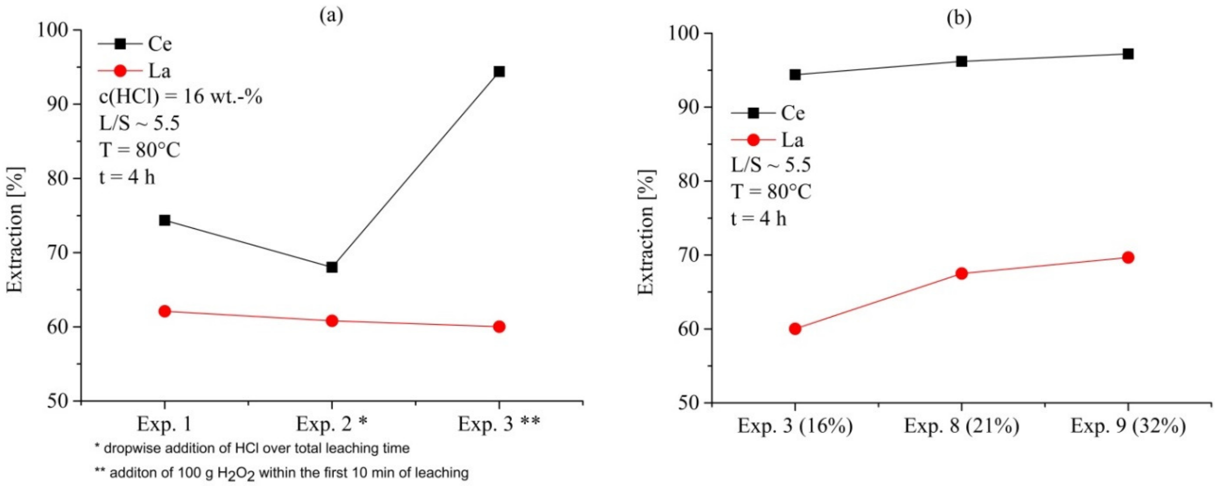

Figure 3. Influence of H_2O_2 addition (a) and acid concentration (b) on the extraction of cerium and lanthanum.

The difference in the extraction of cerium and lanthanum using 16 wt.-% hydrochloric acid with and without hydrogen peroxide is shown in Figure 3a, whereas Exp. 3 represents the addition of H_2O_2. Additionally, an increase in HCl concentration at a constant L/S ratio results in higher extraction rates, especially of lanthanum (Figure 3b). The influence of temperature on the yield of extraction was investigated by two tests. As can be seen in Figure 4a, the extraction of lanthanum slightly increases if using higher temperatures and an acid concentration of 16 wt.-%.

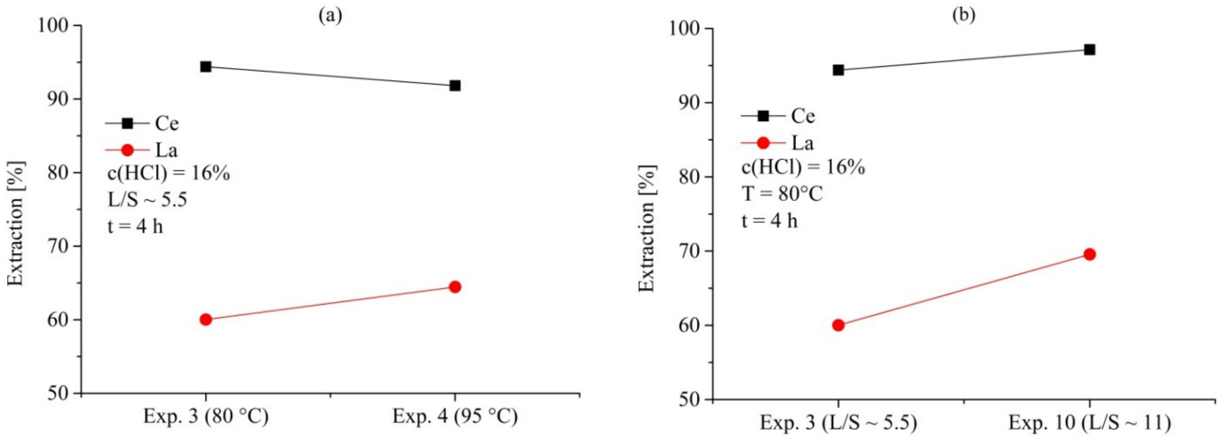

Figure 4. Influence of temperature (a) and L/S ratio (b) on the extraction of cerium and lanthanum.

In contrast to this, the leaching of cerium decreases while the utilization of rising L/S ratios (Figure 4b) leads to higher extraction rates of both Ce and La but the yield is comparable to the extraction rate achieved in Exp. 9. Nevertheless, the acid consumption in Exp. 10 is double that of Exp. 9, so that the latter was used as the standardized leaching procedure for the investigation of the precipitation step. As it was mentioned, 11 precipitation experiments were carried out whereas the produced solids (Ce/La oxalate) were calcined and analyzed by XRF. Based on the data of the mass and chemical composition of the leaching residue and the final oxidic product mass balances were calculated and the yields of cerium and lanthanum together with the parameters of the precipitation (amount and concentration of oxalic acid) were fed to the computer program MODDE 7 to create a mathematical model for the dependence of the different parameters on the yield, and to fit the experimental data by multiple linear regression. Therefore it is possible to decide which parameters are of statistical significance resp. it allows the detection of experimental outliers. In the case of cerium and lanthanum precipitation from real leaching liquors (similar to Exp. 9), the statistical evaluation indicated that in the case of cerium, the precipitation is dependent on the concentration and amount of oxalic acid added (Figure 5).

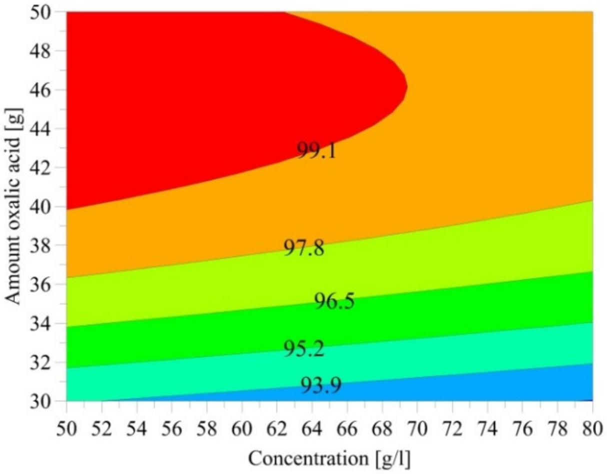

Figure 5. Influence of the concentration and amount of oxalic acid added on cerium yield.

As it was found, the influence of the concentration on the precipitation is not as strong as the effect of the amount of oxalic acid on the process. In contrast to this, the mathematical model for the description of lanthanum precipitation leads to the graph shown in Figure 6.

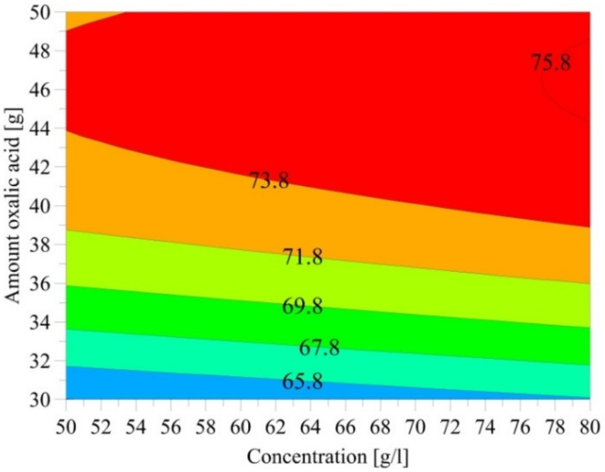

Figure 6. Influence of the concentration and amount of oxalic acid on lanthanum yield.

It indicates that the formation of a lanthanum oxalate is strongly influenced by the amount of oxalic acid added, but there is again little effect from the concentration. The results presented in Figure 5 and 6 can be expressed by two quadratic equations (1, 2) which include the parameters of the precipitation step, whereas “C” stands for the concentration of oxalic acid in gram per liter and “A” represents the amount of the precipitation agent in grams. The interaction parameter $C \cdot A$ as well as the quadratic term C^2 are not considered due to their statistical insignificance.

$$\text{Ce yield} = 53.1794 - 0.0479475 \cdot C + 2.13356 \cdot A - 0.023107 \cdot A^2 \tag{1}$$

$$\text{La yield} = -11.1726 + 0.0641254 \cdot C + 3.53126 \cdot A - 0.0380075 \cdot A^2 \tag{2}$$

However, it has to be considered that the equations are just valid in the ranges of 30 to 50 g of oxalic acid solution and 50 to 80 g/L concentration.

A typical XRF analysis of a thermally treated oxalate is shown in Table III. The chemical composition indicates a rather pure mixed RE oxide with less than 1% of contaminants, whereas iron-, zirconium-, calcium- and silicon oxide form the main impurities.

Table III. Representative XRF Analysis of an Oxide Product

Oxide	wt.-%
CeO_2	90.73
La_2O_3	8.57
ZrO_2	0.08
Fe_2O_3	0.074
CaO	0.07
SiO_2	0.04

Conclusions and Recommendations

The research explained here showed that cerium and lanthanum extraction from the spent glass polishing agent is possible using a combined leaching by hydrochloric acid and hydrogen peroxide. High acid concentrations (32%) seemed to be applicable for the leaching of cerium with good yields (>97%). Lanthanum could not be extracted in the same way as cerium. One reason for this phenomenon might be the low solubility of lanthanum and fluorine compounds in hydrochloric media under the chosen conditions. The best yields concerning the extraction of cerium and lanthanum from the spent glass polishing agent can be found for L/S ratios of 5.5, which refer to approximately 273.5 g of 32 wt.-% HCl and the subsequent addition of 100 g H_2O_2 at 80°C and a leaching time of 4 hours.

In the case of cerium yield the subsequent precipitation showed a dependency on the amount of oxalic acid used but there was no significant influence found concerning the concentration of the precipitation agent. In contrast to this, the formation of lanthanum oxalate is affected by both adjusted parameters. Due to the experimental results and the mathematical model high acid concentrations combined with an excess of oxalic acid lead to good La yields. The present investigations showed that it is essential for a quantitative precipitation to use between 40 (~27%

excess of oxalic acid compared to the precipitated mass of cerium and lanthanum oxide) and 50 g of oxalic acid for a solution which was won by the leaching of 50 g of the examined input material. Nevertheless, it has to be considered that the insignificant coefficients which were removed from the model equations (1 and 2) may be of significance if the experimental design gets extended. However, the experimental data and the resulting statistical analysis and models enable an estimation of parameters which influence the process of precipitation.

Another possible way for precipitation and to reduce oxalic acid consumption might be a selective cerium precipitation by an oxidizing treatment and pH adjustment. All the trivalent cerium ions should be transferred to their tetravalent state through an oxidizing agent like hydrogen peroxide or potassium permanganate after raising the pH value of the leaching liquor. Due to the lower basicity of Ce(IV) a cerium hydroxide, which is almost free from lanthanum can be directly separated from the solution, whereas the remaining La^{3+} ions can be precipitated again by the use of oxalic acid. The major challenges of this process will be to inhibit the precipitation of contaminants during the raising of the pH value. On the one hand, the separation of impurities originating from the leaching liquor is possible, while on the other hand the use of any other kind of oxidant than H_2O_2 results in the addition of further foreign cations which might cause problems, but further investigations have to be done in this field.

Acknowledgements

The authors want to thank the Austrian Research Promotion Agency (FFG) and the Federal Ministry of Economy, Family and Youth (BMWFJ) for the financial support of this work.

References

1. Schüler et al., “Study on Rare Earths and Their Recycling”, (*Final Report for The Greens/EFA Group in the European Parliamen*t, Öko-Institut e.V., 2011).

2. Klemm, W. and A. Smekal, “Über den Grundvorgang des Polierens von Gläsern”, *Naturwissenschaften*, 29, (1941), 688-690.

3. Kaller, A. “The Basic Mechanism of Glass Polishing”, *Naturwissenschaften*, 87 (2000), 45-47.

4. Steigerwald, Joseph M., Shyam P. Murarka, and Ronald J. Gutmann, *Chemical Mechanical Planarization of Microelectronic Material*s (New York, Wiley-VCH, 1997), 130 ff.

5. Bouzid, D., N. Belkhie, and T. Aliouane, “Optical glass surfaces polishing by cerium oxide particles”, *IOP Conf. Series: Materials Science and Engineering* 28 (2012), 1-6.

6. Kato, K., T. Yoshioka, and A. Okuwaki, “Study for Recycling of Ceria-Based Glass Polishing Powder”, *Industrial and Engineering Chemistry Research*, 39 (2000), 943-947.

7. Kato, K., T. Yoshioka, and A. Okuwaki, “Study for Recycling of Ceria-Based Glass Polishing Powder II-Recovery of Hydroxysodalithe from the 700Alkali Waste Solution

Containing SiO_2 and Al_2O_3", *Industrial and Engineering Chemistry Research*, 39 (2000), 4148-4151.

8. Kim , J.-Y. et al., "Recovery of cerium from glass polishing slurry*", Journal of Rare Earths* 29 (2011), 1075-1078.

RECYCLING OF RARE EARTH ELEMENTS FOR THE SYNTHESIS OF PERMANENT MAGNET ALLOYS

R.T. Ott*, L.L. Jones, K.W. Dennis and R.W. McCallum

Ames Laboratory (USDOE)
Ames, IA 50011
*rtott@ameslab.gov

Keywords: Rare Earths, Permanent Magnets, Recycling

Extended Abstract

With the increasing implementation of rare earth (RE) magnets in critical energy technologies, securing additional supplies of rare earth elements via recycling has become increasingly important. Here we discuss using liquid Mg to recover RE elements from magnet scrap. The process entails placing crushed sintered magnets (2-4 mm in size) in a mesh box that is surrounded by Mg, which is melted in an induction furnace. After the appropriate processing temperature and time have been achieved, the liquid Mg-RE alloy that forms from the diffusion of the RE elements out of the magnet pieces into the liquid phase, the liquid is poured into a mold to separate it from the remaining magnet scrap. The high-purity RE elements are then recovered from the Mg-RE alloy by vacuum distillation. Using this process, we have recovered RE metals with purities > 98%. Furthermore, we have demonstrated this recycling process on commercial grade magnets for batch sizes up to 4 kg. From the rare earth elements that are recovered from the scrap magnets, we have synthesized permanent magnet alloys. The composition of the recovered RE alloy, which is a mixture of Nd, Pr and Dy, was measured by Inductive Coupled Plasma Spectroscopy (ICP) and then alloyed with Fe and B via arc melting and then melt spun to make a permanent magnet alloy based on the $RE_2Fe_{14}B$ composition. For comparison, a permanent magnet alloy of identical composition (with the exception of impurities incorporated during the recycling process) was prepared from high-purity non-recycled RE metals. To investigate the effectiveness of the process, the intrinsic magnetic properties of the alloys synthesized from the recycled RE elements were compared with those of permanent magnet alloys synthesized from pure RE elements, Figure 1. It is important to note that the composition and microstructure of the permanent magnet alloys synthesized in this study were not tailored in order to optimize the extrinsic properties (e.g., BH_{max}).

From the results shown in Table I, we see that the saturation magnetization and the anisotropy field of the permanent magnet alloy synthesized from recycled RE metals are reasonably close to those measured for the alloy containing non-recycled RE metals. The results suggest that RE metals recovered by the liquid Mg extraction process can be used to synthesize permanent magnets without a significant degradation in the intrinsic magnetic properties. The small decrease in the intrinsic properties of the alloys containing the recycled RE metals could be due to the incorporation of impurities (e.g. Ni) during the recycling process.

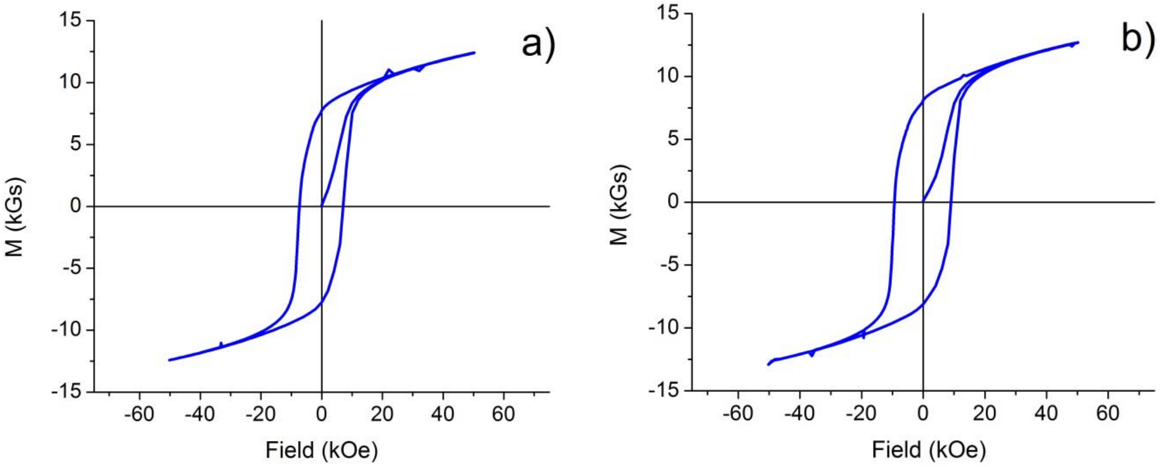

Figure 1. Magnetic hysteresis curves for permanent magnet alloys prepared from (a) recycled and (b) non-recycled rare earth metals.

Table I. Comparison of Intrinsic Magnetic Properties for Permanent Magnet Alloys containing Recycled and Non-recycled Rare Earth Metals

Property	Recycled RE metals	Non-recycled RE metals
Saturation Magnetization (M_s)	13.6 kGs	14.0 kGs
Anisotropy Field (H_a)	68.6 kOe	70.7 kOe

Author Index

Rare Earth Elements

COM CIM ICM 2013
CONFERENCE OF METALLURGISTS
MET SOC

Hosted by MS&T13

October 27-31, 2013 | Montreal, Canada

Rare Earth Elements Symposium
Speakers & Organizing Committee Directory

COM 2013
CONFERENCE OF METALLURGISTS
MET SOC
Hosted by MS&T13
October 27-31, 2013 | Montreal, Canada

Organizing Committee

Ian M. London P.Eng. (Met), MBA
Market Development Advisor
Avalon Rare Metals Inc.
CANADA
ianlondon@rogers.com

Co-Chair

Ian London has been actively engaged in the rare earth/rare metals sector for seven years. In addition to addressing market and project development initiatives, Ian established Avalon's University Outreach Initiative and Corporate Social Responsibility Roadmap in 2011. Ian was also one of the original editors for *RareMetalBlog* and *RareMetalApps.* Ian chaired the Organizing Committee for the inaugural REE Symposium at COM12.

Ian brings an extensive career in corporate management, international marketing and project management. His 40 years of industry experience includes terms as President & CEO of Ontario Hydro International Inc. and CEO of Process Products Limited. Ian has served on several new technology and alternative energy company boards. Ian has been sought after speaker on the emerging rare earth sector and corporate social sustainability.

Ian earned his Metallurgical Engineering degree from McGill University and an MBA from the Schulich School of Business.

Mandeep Singh Rayat, MSc, MBA
CANADA
rayat.mandeep@gmail.ca

Co-Chair

Mandeep Singh Rayat served as Communications and Investor Relations Associate at Avalon Rare Metals, playing a key role in producing Avalon's first Sustainability Report and expanding its strategic academic partnerships. Mandeep has a diverse educational background with undergraduate degrees in Chemical Engineering and Economics from the University of Western Ontario, a Master's in Chemical Engineering from the University of Toronto, and an recently an MBA from the Schulich School of Business at York University.

Organizing Committee

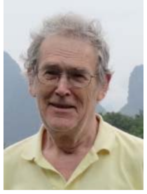

John R. Goode
Consulting Metallurgist
J.R. Goode and Associates
CANADA
jrgoode@sympatico.ca

John Goode started working in the rare earth industry in 1967 at Rio Algom's uranium-rare earth-thorium production facilities in Elliot Lake, Ontario. John joined Kilborn Engineering in Toronto in 1976 where he eventually became Vice President, Mining and Metallurgy. With Kilborn, John was responsible for numerous rare earth projects including design and early operation of a new rare earth recovery plant for Denison Mines in 1985, and due diligence on several rare earth separation plants in China for AMR (later NeoMaterials) in 1993.

John joined Barrick Gold Corporation in 1994 and established and managed its Beijing operations for the following four years before returning to Canada and establishing a metallurgical consultancy. John has recently provided metallurgical and engineering input to rare earth projects in Greenland, Brazil, and Canada.

In-Ho Jung, PhD
Associate Professor,
William Dawson Scholar, Gerald Hatch Faculty Fellow Mining and Materials Engineering,
McGill University
CANADA
in-ho.jung@mcgill.ca

In-Ho Jung joined the Department of Mining and Materials Engineering at McGill University in 2007, following his career as a senior researcher at RIST (Research Institute of Industrial Science and Technology), South Korea. His expertise is Computational thermodynamic database development and Applications to material design and process design. He has authored/co-authored more than 150 journal papers and conference papers, and holds over 20 patents. He is also co-developer of the thermo-chemical software, FactSage (www.factsage.com), which is one of the most well-known software packages in computational thermodynamics.

In-Ho also served as Organizing Committee for the inaugural REE Symposium at COM12.

Georgiana Moldoveanu
Post-Doctoral Fellow
University of Toronto
CANADA
georgiana.moldoveanu@utoronto.ca

Georgiana Moldoveanu graduated in 1993 from University of Bucharest (Romania) with a BSc in Chemistry and worked for three years as a formulation chemist at the Centre for Macromolecular Materials and Membranes. She then pursued post-graduate studies at McGill University, Department of Materials Engineering, where she earned her MEng (1999) and PhD (2005) in the field of Hydrometallurgy.

In May 2009 she joined the Department of Chemical Engineering and Applied Chemistry at University of Toronto as a Postdoctoral Fellow. As a senior member of the Aqueous Process Engineering and Chemistry Group, she manages research projects focused on three areas: rare earths hydrometallurgy, gypsum scale control in industrial streams and water purification via forward osmosis.

Her work in the field of rare earths involves collaboration with industry partners to design and optimize an integrated flowsheets covering all steps of the production process, from ion-exchange leaching to selective precipitation of REE intermediates and final oxide production.

Dimitri Psaras, PhD
Vice President of Technology
Molycorp
USA
dimitri.psaras@molycorp.com

Dimitri Psaras currently holds the position of Vice President of Technology of Molycorp Chemicals and Oxides business and serves on the Board of Directors of Zibo Jiahua Advanced Materials Resources Co., Ltd. His responsibilities include leading the Molycorp R&D and Technology groups at ZAMR (China), JAMR (China), NEO Europe (UK), NEO Singapore (Singapore) and SILMET (Estonia). These groups develop and commercialize novel, advanced value-add rare earth based technology products.

Dimitri earned his Ph.D. from the University of Connecticut in 1985. He has gained increasing responsibilities in the R&D sector successively at the laboratories of AIRCO BOC (1985-1989), Degussa (1989-1994) and Rhône-Poulenc/Rhodia's rare earth business group (1994-1999). He joined AMR Technologies Inc. in 1999 as Vice President of Technology where he established the company's Research and Development groups at the ZAMR and JAMR facilities. He was also instrumental in establishing the AMR Nanotechnology Centre (UK) in 2000 and the Electronics R&D Laboratory in Singapore in 2002.

COM 2013
CONFERENCE OF METALLURGISTS
MET SOC
Hosted by MS&T13
October 27-31, 2013 | Montreal, Canada

Organizing Committee

Niels Verbaan
Principal Metallurgist
SGS Minerals Services, Lakefield
CANADA
niels.verbaan@sgs.com

Niels Verbaan joined SGS Minerals in 2000 and has worked on numerous projects involving hydrometallurgical processing of nickel laterites, silver/indium deposits, zinc oxides, secondary materials as well as rare earths. Since 2008, Niels primary focus has been on testing of various processing options of rare earth deposits. Niels specializes in the management of long term hydrometallurgical projects including flowsheet design and operation of complex integrated pilot plants.

Niels has a Master of Science degree in Raw Material Processing from Delft University in the Netherlands and a Master of Engineering degree in Hydrometallurgy from McGill University in Montreal.

Jack Zhang, PhD, P.Eng.
Senior Metallurgist
Saskatchewan Research Council
CANADA
zhang@src.sk.ca

Jack Zhang is a Senior Metallurgist in Mineral Processing and Hydrometallurgy at the Saskatchewan Research Council (SRC). His areas of focus include applied R&D and contract testing for uranium, potash, rare earth, diamond, gold, base metals, and mine water treatment. He has previously served as a Plant Metallurgist of Cameco Corporation and Process Engineer of SINOPEC.

Jack earned his Bachelor's Degree in Chemical Engineering from the Shandong University of Technology and PhD from the University of Saskatchewan.

Christopher Wildman
Administrative Co-Ordinator
Avalon Rare Metals Inc.
CANADA
cwildman@avalonraremetals.com

Christopher Wildman graduated from York University with a BA Spec. Honours in Economics in 2011. Prior to returning to his studies, Chris served as General Manager of Hockley Valley Brewing Company in Orangeville, Ontario. He has been with Avalon Rare Metals Inc. since 2012 as an Administrative Coordinator in the Finance Department.

Speakers Directory

C.K. Asnani
Director (Technical) & Member, Board of Directors
Indian Rare Earths Ltd.
INDIA
asnani@irel.gov.in

Invited Speaker

C. K. Asnani is a chemical engineer with over 26 years of professional experience in chemical process plants. Presently, Asnani is with Indian Rare Earths Ltd., which is under the administrative control of the Government of India. IREL is in the business of beach sand mining, mineral separation and value addition by chemical processing. It is a producer of high purity rare earths from monazite.

Asnani has developed several innovative processes, which have resulted in doubling production, savings in chemicals and energy consumption as well as minimization in generation of waste. He is recipient of several awards including the 'IIChE National Award for Excellence in Process Development' and 'Excellence in Science and Technology' Award from the Ministry of Government of India.

Gisele Azimi PhD, P.Eng.
Postdoctoral Associate
MIT
USA
gazimi@mit.edu

Gisele Azimi is a Postdoctoral Associate within Professor Kripa Varanasi's research group in the Department of Mechanical Engineering at the Massachusetts Institute of Technology. Her research involves both experimental and fundamental investigations and falls at the intersection of solid-sate chemistry and materials science, thermodynamics, transport phenomena, and surface engineering. More specifically, she is focused on developing a fundamental understanding of materials chemistry and their interactions at the molecular level to design new materials with desired properties.

Gisele received her PhD in Chemical Engineering from the University of Toronto, where she investigated precipitation fouling in hydrometallurgical processes. Her PhD research also involved a mechanistic and kinetic investigation of the transformation between calcium sulphate hydrates and polymorphs using solid-state characterization techniques.

Claude Bazin, P.Eng., MSc, PhD
Professor
Laval University
CANADA
Claude.bazin@gmn.ulaval.ca

Claude Bazin graduated with a Bachelor degree in Metallurgical Engineering at Laval University in 1980. He obtained a PhD from Laval in 1991. During his studies he worked with Quebec Iron and Titanium and Brunswick Mining.

From 1987 to 1990, Claude worked for Brunswick Mining and Smelting (Noranda) as Research Engineer and Process Control Engineer, before accepting the position of Senior Metallurgist in the Heath Steele concentrator in New Brunswick.

In 1992 Claude accepted the position of Professor at Laval University.

David N. Brown, PhD
Senior Research Scientist
Molycorp Magnequench
SINGAPORE
david.brown@molycorp.com

David Brown has been working in the rare earth permanent magnet field for over 15 years. David is currently a senior research scientist at Molycorp Magnequench in Singapore. He is an active member of the permanent magnet research community and regularly presents work on rapidly quenched Nd-Fe-B type magnet topics.

Previous to his career in permanent magnet materials, David worked in other fields of applied materials science, including clean-melting of Ni-based superalloys, reactive-gas processing technology and investment casting of gas turbine components.

David has a PhD in Metallurgy from the University of Birmingham, UK.

Speakers Directory

Ruan Chi
Professor
Wuhan institute of technology
CHINA
rac@mail.wit.edu.cn

Ruan Chi joined the Wuhan Institute of Technology in Hubei province as "Chutian scholar program" distinguished professor in 2003 ultimately becoming Assistant to the President and the Chief of Scientific Research Division.

Chi's career has included Visiting Scholar with the Department of Chemical and Materials Engineering at the University of Alberta, Canada (1997), Senior Scientist to CVT Apotex Inc., Canada (1999), returning to University of Alberta as a researcher in 2002.

Chi has completed more than a dozen successful national research projects on rare earths, published two academic monographs -- "Rare earth ore beneficiation and extracting technology" and "The Weathered Crust Elution-Deposited Rare Earth Ores", published nearly 200 academic papers of which 59 have been catalogued by SCI and EI, and applied for 18 national (8 already authorized). Chi earned his Bachelor's degree from Fujian Normal University, a Master's degree in Inorganic Chemistry from Inner Mongolia University, and his PhD Mineral Engineering from Central South University in 1991.

Ji Chen
Professor, RE Metallurgist
Changchun Institute of Applied Chemistry, Chinese Academy of Sciences
CHINA
jchen@ciac.ac.cn

Ji Chen is a professor at Changchun Institute of Applied Chemistry (CIAC), Chinese Academy of Sciences (CAS). He was selected as a "Hundred Talents" person and appointed as a professor in CIAC in 2004. He has published more than 90 peer-reviewed papers, received over 800 citations and filed 30 patents, of which 18 were authorized. His research interests include advanced separation materials, such as ionic liquids, green separation chemistry and clean techniques for rare earth and heavy metal elements.

Chen received his BS degree from Tianjin University in 1994, and obtained PhD from CIAC, CAS, in 1999. He has 5 years' postdoctoral experience in Institute of Process Engineering of CAS, Kanazawa University in Japan and the University of Alabama in USA.

Steve Constantinides
Director of Technology
Arnold Magnetic Technologies
USA
SConstantinides@ArnoldMagnetics.com

Steve Constantinides is Director of Technology at Arnold Magnetic Technologies Corporation, a global manufacturer of magnets, magnetic materials and precision magnetic assemblies.

Steve's experience includes 12 years with Corning Inc. involved with glass ceramics, combustion systems design and manufacturing management systems. He then joined tungsten carbide manufacturer GTE Valenite and was responsible for modernization and operation of over 40 vacuum and atmosphere furnaces. In 1988 he joined Crucible Magnetics as Manager of Technology and Quality Assurance for Neo, Samarium Cobalt and Alnico magnets. For the last 21 years, Steve has performed process and product development, manufacturing engineering and project management for Arnold Magnetic Technologies.

Hendrix Demers
Post Doctoral
Materials Science and Engineering
McGill University
CANADA
hendrix.demers@mail.mcgill.ca

Hendrix Demers is a postdoctoral in the Department of Material Engineering at McGill University, Canada since 2012.

Hendrix received his Bachelor of Science in Physics at the University of Sherbrooke, Canada, a Master's of Engineering (Mechanical) at the University of Sherbrooke, Canada and his PhD in Mining and Materials Engineering at the McGill University, Canada. Before joining McGill Hendrix was a postdoctoral fellow at Universite de Sherbrooke and at College of Nanoscale Science and Engineering University at Albany, SUNY. He is involved in the field of microscopy and microanalysis by working on x-ray fluorescence quantification algorithm, microanalysis of insulators and development of the microcalorimeter x-ray detector.

He is also author of a world-renowned research program 'Win X-Ray' on imaging simulation and complete of the X-ray spectrum software for the scanning electron microscope. This Monte Carlo software aims at helping SEM users in their X-ray microanalyses, metrology applications and also in more advanced applications such as electron beam lithography.

Speakers Directory

Yuefeng Deng
Assistant professor, RE Metallurgist
Changchun Institute of Applied Chemistry
Chinese Academy of Sciences
CHINA
yfdeng@ciac.ac.cn

Yuefeng Deng started working in the rare earth separation field in 2005 with Prof. Chen Ji's group at the Changchun Institute of Applied Chemistry, Chinese Academy of Sciences. His current research interests focus on separation chemistry and applied chemistry, mainly concerning the application of green functional materials in extraction of rare earths and heavy metals.

Deng obtained his BS degree (2002) and MS degree (2005) from the College of Chemistry at Jilin University, Changchun, China.

Invited Speaker

Jürgen Eckert, Prof. Dr.-Ing.
Director
IFW Dresden
GERMANY
j.eckert@ifw-dresden.de

Jürgen Eckert is an internationally recognized expert in the metallurgy of advanced metallic material design, equilibrium and non-equilibrium processing techniques via microstructure-property relations, and technology transfer for industrial applications. He is the holder of several patents in the areas of materials science and processing technology: metallic glasses and composites, nanostructured high-strength materials, strength and plasticity improvement, hard magnetic materials, superconducting materials, surface modification, intermetallic compounds, porous bulk materials and hybrid structures. Jürgen is associate editor of the *Journal of Materials Research*.

Jürgen is the Director of the Institute for Complex Materials and since 2013, Scientific Director of the Leibniz-Institute for Solid State and Materials Research Dresden, Germany. He is also Full Processor and Chair for Materials Synthesis and Analysis at the Technical University Dresden, Germany.

Jürgen earned his degree in Materials Science at the Friedrich-Alexander University Erlangen-Nürnberg.

William G. Fahrenholtz
Curator's Professor
Missouri University of Science and Technology
USA
billf@mst.edu

Bill Fahrenholtz is a Curators' Professor of Ceramic Engineering in the Department of Materials Science and Engineering at the Missouri S&T (formerly University of Missouri-Rolla). He earned his BS and MS degrees in Ceramic Engineering at the University of Illinois at Urbana-Champaign, and completed his PhD in Chemical Engineering at the University of New Mexico (1992).

At Missouri S&T, Bill has received seven campus-wide faculty excellence awards, teaching awards, and a prestigious CAREER award from the National Science Foundation. He was elected a Fellow of the American Ceramic Society in 2007. Bill's current research focuses on the processing, characterization, and mechanical testing of advanced structural ceramics for use in environments with extreme thermal loads, mechanical forces, and/or chemical reactivities. Bill has published over 100 papers in peer-reviewed journals and given over 30 invited presentations. He has also been Principal Investigator or Co-Principal Investigator on nearly 50 grants from sources including the National Science Foundation, and the Air Force Office of Scientific Research.

D. Grant Feasby, MSc
Specialist, Mining and Environment
SENES Consultants
CANADA
gfeasby@senes.ca

Grant Feasby has 40 years' experience in the mining, minerals and metallurgy sectors specializing in providing metallurgical operations and environmental for uranium, rare earth, gold, silver, base metal and bauxite mining.
Grant has recently worked with mine professionals and aboriginal people in assessing environmental and social aspects of uranium, rare earth and tin-thorium- uranium resource development in Canada and other countries.

Grant has worked in a several countries for mining companies and international regulatory agencies as well as banks and insurance companies, frequently on the subject of the management of mineral-sourced radioactivity. Before joining SENES he was the environmental manager for large scale gold and bauxite operations in South America. In the recent past he managed Canadian national research programs on Acid Rock Drainage and Uranium Mine Tailings.

Grant earned his Metallurgical Engineering degrees from Queens University.

Speakers Directory

Cesar Joe Ferron
VP Technology
Molycorp/HydroProc
CANADA
joe.ferron@molycorp.com

Joe Ferron graduated as Metallurgical Engineer from the University of Louvain, Belgium in 1974, and earned his PhD in Mineral Engineering and Chemical Metallurgy from Columbia University, New York in 1988.

Joe spent 6 years as Research Assistant at the Louvain University, and 4 years as Principal Engineer at the R&D Center of Gecamines of the DRC. In 1988, Joe joined Lakefield Research of Canada where he held the positions of Manager Hydrometallurgy and Vice President Metallurgical Technology. In 2002, Joe was awarded the Sherritt Hydrometallurgy Award.

Since 2004, he has worked simultaneously as Consultant (HydroProc Consultants) and presently, as Vice President Technology with Molycorp Rare Metals Division.

Sin-Pui Fu
Ph.D. Student
University of Illinois at Chicago
USA
fusinpui@gmail.com

Sin-Pui Fu has worked on various projects related to CeO2 thin films since 2011 when he joined the Laboratory for Oxide Research & Education (LORE).

Fu earned his Bachelors of Science in Mechanical Engineering from University of Illinois at Chicago in 2012, where he is now working on his PhD.

Seref Girgin, PhD
Metallurgist
BBA Inc.
CANADA
seref.girgin@bba.ca

Seref Girgin has been working in the Mineral Processing and Hydrometallurgy fields since 1998. Seref holds a Mining Engineering degree from the Mining/Mineral Processing Engineering Department of Istanbul Technical University in Turkey. He started his career working as a research assistant in the same department while he was working on the solvent extraction of uranium during his master`s thesis. In 2001, he started his PhD studies at McGill University, hydrometallurgy group and conducted research on the crystallization of alpha-gypsum out of chloride solutions and HCl regeneration.

After graduation in 2006, Seref has developed expertise in the non-ferrous extractive metallurgy field during his employment at COREM, where he was the leader of the extractive metallurgy team that focused mostly on precious metals and chloride metallurgy. He joined the BBA's operation support team, Mining and Metals Department in 2011. Seref has since been working on the development of hydrometallurgical chloride processes and development and support for gold processing operations.

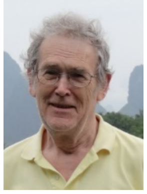

John R. Goode
Consulting Metallurgist
J.R. Goode and Associates
CANADA
jrgoode@sympatico.ca

John Goode started working in the rare earth industry in 1967 at Rio Algom's uranium-rare earth-thorium production facilities in Elliot Lake, Ontario. John joined Kilborn Engineering in Toronto in 1976 where he eventually became Vice President, Mining and Metallurgy. With Kilborn, John was responsible for numerous rare earth projects including design and early operation of a new rare earth recovery plant for Denison Mines in 1985, and due diligence on several rare earth separation plants in China for AMR (later NeoMaterials) in 1993.

John joined Barrick Gold Corporation in 1994 and established and managed its Beijing operations for the following four years before returning to Canada and establishing a metallurgical consultancy. John has recently provided metallurgical and engineering input to rare earth projects in Greenland, Brazil, and Canada.

Tassos Grammatikopoulos
Senior Mineralogist
SGS Canada Inc
CANADA
tassos.grammatikopoulos@sgs.com

Tassos Grammatikopoulos has a M.Sc from Acadia University, Canada and a PhD from Queen's University in Kingston in geology.

Tassos joined Lakefield Research in 1997 as mineralogist and later a senior mineralogist. Tassos became an assistant professor in Economic Geology at the University of Patras, Greece in 2003, re-joining SGS in 2007 as a senior mineralogist.

Tassos has worked on a number of REE deposits worldwide. He has a number of publications on PGM, gold, base metals, REE and industrial minerals.

Invited Speaker

Andrew Grosvenor
Associate Professor
Department of Chemistry,
University of Saskatchewan
CANADA
andrew.grosvenor@usask.ca

Andrew Grosvenor received his B.Sc. and M.Sc. degrees from the University of Western Ontario, and his PhD from the University of Alberta. He completed a one-year postdoctoral fellowship at McMaster University before joining the University of Saskatchewan in 2009 where he has since led the solid-state chemistry group.

The research group that Andrew leads is primarily focussed on the development and examination of metal oxides for the sequestration of nuclear waste elements. This research program involves the synthesis of new and known materials, and the examination of these materials by X-ray diffraction and X-ray spectroscopy. Rare-earth elements play a prominent role in this research program because of the ability of these elements to act as actinide simulator elements, and because of the neutron absorption capabilities of some of these elements.

Invited Speaker

Karl A. Gschneidner Jr.
Distinguished Professor
Ames Laboratory,
Iowa State University
USA
cagey@ameslab.gov

Karl Gschneidner is an Anson Marston Distinguished Professor in the Department of Materials Science and Engineering at Iowa State University; a Senior Metallurgist of the Ames Laboratory, U. S. Department of Energy; and Chief Scientist of CMI. He was the founding Director of the Rare-Earth Information Center from 1966 to 1996.

Karl received a BS degree from the University of Detroit and his Ph.D. from Iowa State University (1957).

Karl is considered the world's foremost authority of rare earth science, technology, application and utilization, and is known as "Mr. Rare Earths." He has published over 509 papers, holds 15 patents (plus 4 pending), and given 324 invited presentations. He retired in 2011 as the founding and senior editor of the 41 volume series of the Handbook on the Physics and Chemistry of Rare Earths.

He was elected to the National Academy of Engineering in 2007 for "contributions to the science and technology of rare-earth materials", and has received over 25 awards and honors.

Jiayi Guan
Chemical Engineer
Avalon Rare Metals Inc.
CANADA
jguan@avalonraremetals.com

Jiayi Guan received her undergraduate degree from the University of Toronto's Chemical Engineering and Applied Chemistry program. Her interest in mining developed while working an internship at Xstrata Copper's Kidd Concentrator. During this time Jiayi lead a team to develop a preliminary process package for Vale to recover copper, cobalt and nickel from converter slag for her final year design project. The project went on to win the Department of Chemical Engineering's Sustainability Energy Plant Design award for that year. She also earned the Quadra FNX Mining Ltd. Scholarship during this time, awarded to students with an Environmental minor based on strong academic achievement, with preference going to students who demonstrate an interest in the mining industry.

Jiayi joined Avalon Rare Metals in June 2012 as a Chemical Engineer and has been working on both the Thor Lake and Separation Rapids projects. She is currently anticipating getting her Masters in Engineering in 2014 in Mechanical and Industrial Engineering at the University of Toronto.

Speakers Directory

Richard Hammen, PhD
President and CEO
IntelliMet LLC
USA

Richard Hammen is a graduate of Stanford University, and attended graduate school at the University of Wisconsin where he studied under one of the leaders in modern organic synthesis. Richard did postdoctoral research at UCLA, and worked at the Molecular Biology Institute at UCLA and the Stanford Research Institute where he witnessed the growth and development of the bio-tech industry.

After directing the chemistry laboratory at the NASA Jet Propulsion Laboratory, Richard was a founding employee of Vestar, a bio-tech company in Pasadena, California with roots at CalTech. A pioneer in Solid Phase Extraction technology, Richard has developed innovative new technologies in recombinant protein production and purification.

Richard is also an advisory board member at Ucore.

Invited Speaker

Dr. Ir. Sri Harjanto
Associate Professor
Department of Metallurgy and Materials Engineering, Universitas Indonesia
INDONESIA
harjanto@metal.ui.ac.id

Sri Harjanto has research interest in waste processing from metallurgical process and extractive metallurgy of common and rare metals/rare earths. He earned his Dr. Eng. in Metallurgical Process Engineering from Institute of Multidisciplinary Research for Advanced Materials, Tohoku University, Japan at 2002. He then joined Venture Business Laboratory, Akita University as postdoctoral fellow for 3 years.

Sri Harjanto began his work in rare metals and PGM in 2005, during his postdoc at Akita University. At Universitas Indonesia, he develops several research collaborations on rare metals and rare earths processing. He also teaches minerals processing and extractive metallurgy of ferrous and non-ferrous for undergraduate and graduates students. He published his works in many national and international journals, book chapters and monograph.

Zhengyan He
Ph.D. Candidate
Central South University
CHINA
Hezhengyan_1988@sina.com

Zhengyan He earned her Bachelor's degree in Chemical Engineering and Technology in 2009 and Master's degree in Applied Chemistry in 2012 from Wuhan Institute of Technology.

In her Master studies, He sought to determine an efficient leaching agent which could inhibit the swell of clay minerals and prevent landslides and other geological disasters in the in-situ rare earth leaching process.

Since September 2012, He has been a PhD candidate actively engaged in kinetic studies on the heap leaching of rare earth from the Weathered Crust Elution-deposited Rare Earth Ore in Central South University.

Philippe Henry
Managing Director
SA Hydrometal
BELGIUM
phenry@hydrometal.be

Philippe Henry has been actively engaged in the rare earth/rare metals recycling for seven years.

Philippe brings an extensive career in recycling project management, international trading and plant management. His 20 years of industry experience includes terms as plant manager and managing director of SA Hydrometal and as director of SA Jean Goldschmidt International, a well known company active in the trading and recycling of complex materials.

Philippe earned his Chemical Engineering and PhD degrees from Polytechnic University of Louvain-la-Neuve in Belgium.

Speakers Directory

Invited Speaker

Nobuhito Imanaka
Professor
President, The Rare Earth Society of Japan
Osaka University
JAPAN
imanaka@chem.eng.osaka-u.ac.jp

Nobuhito Imanaka earned his B.E. (1981) and M.E. (1983) degrees in Applied Chemistry from Osaka University. He then obtained a Ph.D. degree from Osaka University in 1986. He has joined the faculty at Osaka University since 1988 and now he is Full Professor. His main research fields include rare earths and functional materials such as solid electrolytes, catalysts, and chemical sensors, etc.

Nabuhito has received various awards, including the Ichimura Science Award in 2005, Inoue Science Award in 2008, and Yazaki Science Award in 2009.

Keynote Speaker

Marian Campbell Jarvis
Assistant Deputy Minister, Minerals and Metals
Natural Resources Canada
CANADA

Marian Campbell Jarvis was appointed Assistant Deputy Minister, Minerals and Metals Sector, Natural Resources Canada in June, 2013. Previously, she held the post of Director General in the Earth Sciences Sector, where she was responsible for the Polar Continental Shelf Program, the Climate Change Impacts and Adaptation Program, as well as a number of international files and policy issues, including leading for NRCan on the Government of Canada Northern Strategy.

Prior to this, Marian developed strategic policy at Human Resources and Skills Development Canada, Health Canada and the Privy Council Office.

Originally from Vancouver, B.C., Marian has an undergraduate degree in Canadian Studies and a Master's degree in Public Administration.

Frank Johnson, PhD
Senior Engineer
GE Global Research
USA
johnsonf@ge.com

Frank Johnson joined GE Global Research in 2005 as a Materials Scientist in Ceramic and Metallurgy Technologies. His current research focuses on the development of magnetic materials for power generation, distribution, and conversion technologies. Frank's area of expertise is the structure-processing-property relationships of crystalline, nanocrystalline, and amorphous soft magnetic alloys, rare-earth permanent magnets, and magnetocaloric materials.

Prior to joining GE, Frank received was a Post-Doctoral Fellow in the Magnetic Materials Group, Metallurgy Division of the National Institute of Standards and Technology in Maryland. While at N.I.S.T. he worked on magnetocaloric materials, magnetic thin-films, and assisted in the development of magnetic Standard Reference Materials.

Frank received his PhD in Materials Science and Engineering from Carnegie Mellon University in 2003.. He received his MS in Materials Science and Engineering from the Massachusetts Institute of Technology (1999) and BS in Materials Science and Engineering from Carnegie Mellon (1996).

In-Ho Jung, PhD
Associate Professor,
William Dawson Scholar, Gerald Hatch Faculty Fellow Mining and Materials Engineering,
McGill University
CANADA
in-ho.jung@mcgill.ca

In-Ho joined the Department of Mining and Materials Engineering, McGill University in 2007 after his career as a senior researcher at RIST (Research Institute of Industrial Science and Technology), South Korea. His expertise is in computational thermodynamic database development and applications to material design and process design.

In-Ho has authored/co-authored more than 150 journal papers and conference papers, and invented over 20 patents. He is also co-developer of a thermo-chemical software, FactSage (www.factsage.com), which is one of the most well-known software packages in computational thermodynamics.

In-Ho is a member of Organizing Committee for the COM13's REE Symposium and also served as Organizing Committee for the inaugural REE Symposium at COM12.

Speakers Directory

Invited Speaker

Teak-Soo Kim, PhD
Executive Director, Professor
Korea Institute for Rare Metal
Korea Institute of Industrial Technology(KITECH)
University Of Science&Technology
KOREA
tskim@kitech.re.kr

Taek-Soo Kim, who earned his Ph.D. in Material Science, is a driving for rare materials development in both science and industry, contributing to the establishment of the KIRAM with KITECH and Korean Government in 2010.

Taek-Soo has published 120 scientific papers and holds 20 patents, many of which are related to rare metal issues. He runs various industry development programs within KIRAM. Since 2011, he has also contributed to global rare metals communities by organizing and chairing the Rare Material Committee, in conjunction with a series of annual International Symposia on Rare Metals and bi-lateral workshops with China, Japan, Germany, and the US.

Taek-Soo was also instrumental in installing the Department of Rare Metals at the University of Science and Technology (UST), Korea so as to systematically raise the profile of and educate students in rare metals.

Keynote Speaker

Alexander H. King D.Phil
Director
Critical Materials Institute
USA
alexking@ameslab.gov

Alex King is the Director of the Critical Materials Institute led by the Ames Laboratory, and also holds the Bergdahl Professorship of Materials Science at Iowa State University.

Alex worked as a post-doc at MIT before joining the faculty at Stony Brook. He then served as the Head of the School of Materials Engineering at Purdue University and became the Director of the Ames Laboratory in 2008, stepping down in 2013 to lead CMI. He has been the Chair of the University Materials Council, President of the Materials Research Society, a Visiting Fellow of the Japan Society for the Promotion of Science, and a Jefferson Science Fellow in the US Department of State, where he served as the Senior Science Advisor for the Bureau of African Affairs. He is a Fellow of IOM3, ASM International, and of MRS.

Alex earned his baccalaureate in Metallurgy at the University of Sheffield, and his doctorate at Oxford.

Anthony Y. Ku
Senior Engineer
GE Global Research
USA
kua@research.ge.com

Anthony Ku is a Senior Engineer in the Manufacturing and Materials Technologies organization at GE Global Research. Since joining GE in 2003, he has worked on a range of advanced materials development projects in support of GE's Water, Energy, Aviation, and Healthcare businesses. He is currently engaged in several projects centered on the themes of energy, water, and material sustainability, and is leading a corporate-level assessment to identify and address GE's supply chain exposure to critical materials.

Anthony received his PhD degree in chemical engineering from Princeton University and his BS in chemical engineering and M.S. in chemical engineering practice from MIT.

Deqian Li
Professor, RE Metallurgist
State Key Lab of Rare Earth Resource Utilization
Changchun Institute of Applied Chemistry
CHINA
ldq@ciac.jl.cn

Deqian Li graduated from Wuhan University in 1959, and has since been employed in the Changchun Institute of Applied Chemistry, Chinese Academy of Sciences. Li was appointed rare earth research director (1986-1992), and has been engaged in the study of separation chemistry and clean hydrometallurgical engineering of rare earths for over 50 years.

Li developed the separation process for rare earths using P507 (HEHEHP) and invented a technique to separate thorium and rare earths which has been applied across the rare earth hydrometallurgical industry. Li has established clean metallurgical processing of Baotou rare earth resource and bastnasite; and integrated separation and preparation technology which has first been used to produce nano-cerium fluoride with a purity of 99.999% at an industrial scale using solvent extraction.

Li's engineering and technological research has received numerous awards Li has published 330 scientific papers and been granted 23 patents, two of which have achieved National excellence Awards.

Speakers Directory

Xianping Luo, PhD
Professor, Faculty of Resource and Environmental Engineering,
Jiangxi University of Science and Technology
CHINA
lxp9491@163.com

Xianping Luo's main research interests are beneficiation theory and the technology of non-ferrous metals such as copper, zinc, lead, tungsten, rare earth, and precious metals such as gold and sliver; new beneficiation theory and technology for clean and effectively separate the complex lead-zinc-iron ore which was difficult to treat using traditional technology; synthesis and characterization of the property of highly effective collectors for copper-lead-zinc sulfide flotation; mine bioremediation and comprehensive utilization of solid wastes from mineral processing.

Luo earned his BSc and MSc Degrees in Ore Dressing Engineering degrees from Southern Institute of Metallurgy (Ganzhou, China) and his PhD in Mineral Processing Engineering from University of Science and Technology Beijing (Beijing, China).

Invited Speaker

Andries Meijerink, Prof. Dr.
Professor of Solid State Chemistry
Utrecht University
THE NETHERLANDS
a.meijerink@uu.nl

Andries Meijerink received his PhD in 1990 at the Utrecht University Afterwards he joined joined theUniversity of Wisconsin in Madison as a post-doctoral fellow. In 1996 he was appointed at the chair of Solid State Chemistry in the Debye Institute of the Utrecht University. Between 2003 and 2007 he served as Dean of the Department of Chemistry. He leads an active research group that focuses on the optical spectroscopy of lanthanide ions and of semiconductor quantum dots. His recent work involves fundamental research on new phosphors for white LEDs, up- and down-conversion materials and efficient scintillators, and unraveling the influence of quantum confinement and surface effects on the electronic structure of quantum dots through optical spectroscopy.

Andries has received several awards, including the DSM Award (1989), Shell Incentive Award (1995), Gold Medal of the Royal Dutch Chemical Society (1999) and ECS Centennial Award (2002). Since 2009 he has been a member of the Royal Dutch Academy of Sciences.

Patrick H.J. Mercier, PhD
Senior Research Officer
National Research Council Canada
Energy, Mining and Environment Portfolio
CANADA
patrick.mercier@nrc-cnrc.gc.ca

Patrick Mercier has recognized expertise in crystallography, mineralogy and materials science, with strong ties through his scientific advisory functions and contributions to the International Union of Crystallography (IUCr). He is a member or consultant on three materials-science related IUCr commissions (Inorganic and Mineral Structures; Structural Chemistry; Crystallographic Computing) and a representative in two IUCr Working Groups (Database Users; Diffraction Data Deposition).

Patrick's research interests are mainly in crystal chemistry -- the relationship between crystal structure, chemical composition and related physical properties. He uses materials informatics methods to combine *ab initio* density functional theory modeling of materials with experimental results (diffraction, spectroscopy, microscopy) in order to design materials with tailored physical and chemical properties.

Patrick holds MSc and PhD in Physics from the University of Ottawa and BEng in Physics from the Royal Military College.

Ghazaleh Nazari
Hydrometallurgical Process Engineer
Hatch
CANADA
GNazari@hatch.ca

Ghazaleh Nazari is a process engineer at Hatch, Mississauga, and has been working with the Non-Ferrous/Hydrometallurgy group since January 2012. She holds a BASc (2009) and a PhD (2012) in Materials Engineering, and a minor degree in Business and Engineering Management (2012) from the University of British Columbia. Ghazaleh's Ph.D. research focused on enhancing the kinetics of chalcopyrite leaching in the Galvanox™ process. She was the recipient of the Gordon Ritcey award from CIM in 2011, the NSERC Postgraduate Doctoral Scholarship in 2010, and the UBC Four Year Doctoral Fellowship in 2010.

In 2012, Ghazaleh received NSERC Industrial Research and Development Fellowship (IRDF) to study and evaluate various hydrometallurgical processes for extraction, recovery and separation of REE from the primary ore and develop a model to simulate the kinetics and thermodynamics of the complete flowsheet.

Speakers Directory

Henrie Notzl, MEng, MBA
Principal Process Engineer
Tenova Mining and Minerals
SOUTH AFRICA/CANADA
Henrie.Notzl@tenova.com

Henrie Notzl has been actively engaged with rare earth/rare metals processing for the past five years. Henrie currently serves as Technical Consultant to Avalon Rare Metals.

Henrie brings an extensive career in pilot plant and process development, engineering, commissioning and operations. Her 25^+ years of industry experience includes Manager of Technical Services for Fansteel (Ta, Nb, U, Th, Sc), President of Zlton Specialties as well as Technical Superintendent of Processing for conventional uranium/vanadium mills in the United States and Australia. Through Bateman Engineering, she has worked on a number of different rare earth projects which have progressed through the scoping study, prefeasibility and feasibility stages.

Henrie earned her Bachelor of Science from University of Waterloo (Co-Op), Masters of Engineering from University of Toronto, and an MBA from the University of Phoenix.

Ryan Ott
Scientist
Ames Laboratory (USDOE)
USA
rtott@ameslab.gov

Ryan Ott is a Principal Investigator in the Division of Materials Sciences and Engineering at Ames Laboratory and the Critical Materials Institute. Ryan's research interests include amorphous and nanostructured materials, synchrotron X-ray scattering and critical materials.

Ryan earned his BSc in Materials and Metallurgical Engineering from Michigan Technological University and his MS and PhD in Materials Science and Engineering from Johns Hopkins University.

Alexander Poscher, MSc
Ph.D. student
Chair of Nonferrous Metallurgy
University of Leoben
AUSTRIA
alexander.poscher@unileoben.ac.at

Alexander Poscher has worked on projects related to rare earths since his bachelor thesis on the recovery of rare earth elements from nickel metal hydride batteries in 2009.

In 2010 Alexander received his MSc with honors from the University of Leoben and has continued his research at the Chair of Nonferrous Metallurgy as a PhD student. Alexander's work mainly focuses on the extraction of rare earth elements from secondary resources, but also includes the recycling of other critical raw materials by hydro- and pyrometallurgical methods.

Invited Speaker

Jack Silver BSc, PhD, DSc, CChem, FRSC
Executive Director
Wolfson Centre for Materials Processing,
Brunel University
UK
Jack.silver@brunel.ac.uk

Jack Silver earned his BSc (1970) and PhD (1973) and D.Sc. (1992) from the University of London. He became a Chartered Chemist of the Royal Society of Chemistry in 1982 and a Fellow in 1987.

Jack's current research focuses on phosphors and display materials, lighting and photo-voltaics; biopolymer materials: polymer composites; and nanotechnology applications.

Jack's research has been featured in a number of soft science magazines including *New Scientist*, *Physics World* and *Electronics Weekly*. . He and his group have presented over 200 invited lectures/talks. Jack has published over 400 papers in refereed international journals and reviews. He has acted as a consultant to industry and as an expert witness.

Jack has been active in the fields of inorganic, organometallic chemistry and bioinorganic chemistry, holding more than twenty patents, including the only oral iron binding drug currently on the market for removing iron from the human body ("Desferiprone"), now used for treating patients in 90 countries.

Speakers Directory

Niraj K Singh, PhD
Senior Scientist
Aldrich Materials Science, Sigma-Aldrich Corporation
USA
Niraj.Singh@sial.com

Niraj has been a senior scientist with Sigma-Aldrich Corporation, USA since 2011.

Niraj received his doctoral degree from the Department of Physics, Indian Institute of Technology Bombay, Mumbai, India in 2007. From 2007 to early 2011 he worked as postdoctoral researcher at Ames Laboratory of US DOE at Iowa State University. Niraj's research focuses on functional materials suitable for various energy related applications. This includes intermetallic, ceramics, complex metal hydrides, and metal organic frameworks.

Karin Soldenhoff BSc (Hons), MSc, PhD
Manager Process Development & Research
Australian Nuclear Science & Technology Organisation Minerals
AUSTRALIA
khs@ansto.gov.au

Karin Soldenhoff graduated from the University of the Witwatersrand (South Africa) with a BSc (Hons) and from the University of Cape Town (South Africa) with a Masters degree in Chemistry. She was awarded a PhD in Chemical Engineering from the University of New South Wales, Australia.

Over a 28 year career in process development for the mining industry, Karin has led numerous projects commissioned by industry regarding various aspects of hydrometallurgical processing, with particular emphasis in separation technologies including solvent extraction and ion exchange.

She is currently the Manager – Process Development and Research for ANSTO Minerals at the Australian Nuclear Science and Technology Organisation. ANSTO Minerals specialises in processing of ores containing naturally occurring radioactivity, and specifically ores containing uranium and rare earths.

Ben Yu
Project Metallurgist
SGS Canada Inc.
CANADA
ben.yu@sgs.com

Ben Yu received his BASc and MASc degrees from the University of Toronto in the field of metallurgy and materials science. During his studies, Ben focused mainly in electrochemistry such as corrosion of nanocrystalline materials.

Ben joined SGS Lakefield in 2008 and developed into a project metallurgist. With SGS, Ben was responsible for beneficiation flowsheet development of sulphide and non-sulphide minerals. Recently, Ben has been involved with the flowsheet development of a number of rare earth projects.

Yavuz A. Topkaya, BMet, PhD
Professor
Middle East Technical University
TURKEY
topkaya@metu.edu.tr

Yavuz Topkaya obtained his Bachelor of Metallurgy degree from Sheffield University in England in 1969. He earned his PhD at McMaster University in Hamilton, Ontario, Canada.

Upon completing his doctorate in 1974, he worked at the Mineral Research and Exploration Institute in Turkey until 1979, following which he assumed the current position of Professor of Extractive Metallurgy at the Middle East Technical University, Metallurgical and Materials Engineering Department in Turkey.

Speakers Directory

Niels Verbaan
Principal Metallurgist
SGS Minerals Services, Lakefield
CANADA
niels.verbaan@sgs.com

Niels Verbaan joined SGS Minerals in 2000 and has worked on numerous projects involving hydrometallurgical processing of nickel laterites, silver/indium deposits, zinc oxides, secondary materials as well as rare earths. Since 2008 his primary focus has been on testing of various processing options of rare earth deposits. Niels specializes in the management of long term hydrometallurgical projects including flowsheet design and operation of complex integrated pilot plants.

Niels has a Master of Science degree in Raw Material Processing from Delft University in the Netherlands and a Master of Engineering degree in Hydrometallurgy from McGill University in Montreal.

Poster Session

Maria Estela De Vasconcellos
Professor/Researcher
Nuclear & Energy Research Institute - National Nuclear Energy Commission
BRAZIL
mariestelavasc@yahoo.com.br

Mari Estela de Vasconcellos is a professor and researcher at Nuclear and Energy Research Institute – National Nuclear Energy Commission - IPEN-CNEN/SP in São Paulo. She obtained her Ph.D. (2006) in the Nuclear Technology Field - Materials, at IPEN – University of São Paulo (IPEN-USP). Prior to that, she had participated in the Brazilian Nuclear Program (1986-1994).

De Vasconcellos is Professor of Rare Earths: Chemistry and Technology at IPEN-USP. Her body of work in the actinides and lanthanides field at IPEN/CNEN-SP dates back to 1986, and has been published numerous papers on the separation, purification and catalysis of rare earths. She is also member of a research group that produces high purity rare earths coupling fractional precipitation and ion exchange chromatography techniques in pilot plant. She utilizes her own high purity standards in research and development applications.

Yucong Wang, PhD, FASM
Manager, Department of Materials Technology
General Motors Company
USA
yucong.wang@gm.com

Yucong Wang leads GM’s materials technical specialist team developing and implementing materials technology strategies to support current and advanced product development and manufacturing. He also leads the materials laboratories within GM, responsible for product material environmental regulatory compliance.

Yucong has been working for GM in R&D, advanced manufacturing engineering, quality and product assurance and materials engineering since 1990. He received numerous honors and awards including Fellow of ASM International (2004), from the U.S. Department of Energy, the Herman H. Doehler Award (2005) and “Asian American Engineer of the Year” (2006).

Yucong has over 50 patents and authored or co-authored over 70 refereed technical publications. He obtained his BS and M.S. in Materials Science and Engineering from Shanghai Jiaotong University (China), his PhD in Materials Science and Engineering from Michigan Tech., and MBA from Central Michigan University.

Poster Session

Wenyuan Wu
Northeastern University,
CHINA
wuwy@smm.neu.edu.cn

Wenyuan Wu has been actively engaged in rare earth metallurgy for thirty years. Wu currently serves in the School of Materials and Metallurgy, Northeastern University, as a professor, specializing in non-ferrous metallurgy and rare earths metallurgy/rare earth metal.

Wu has hosted one “973” project, three National Natural Science Foundation programs, one Ministry of Science and Technology research project during the twelfth five-year plan, two Ministry of Education fund projects, one Liaoning Province Science Fund project, and received ten invention patents and published more than 100 academic papers. He also compiled 《Rare Earth Metallurgy》(Chemical Industry Press, 2005) and 《Rare Earth Metallurgy Technology》(Science Press, 2012).

Speakers Directory

Chen Xia, Ph.D.
Research scientist
CANMET Mining – Natural Resources Canada
CANADA
cxia@nrcan.gc.ca

Chen Xia graduated from Kunming Institute of Science and Technology in 1994 following which he worked as a project engineer at China Nonferrous Metals Industry Company. From 1998 to 2006, Chen studied at Queen's University in the Mining Engineering Department focusing on gold mineral processing and hydrometallurgy. He obtained MSc and PhD degrees in 2002 and 2008 respectively and has served as a research scientist in CANMET since 2006 on advanced cyanidation and innovative non-cyanide gold leaching technologies.

In 2012, Chen initiated his adventure in REE science and technology as the hydrometallurgy project leader. His main interest is on the decomposition of mixed type of RE ores or concentrate, as well as the removal of various impurities from acidic solutions of mixed REEs.

Zhigao Xu
Associate Professor
Wuhan Institute of Technology
CHINA
xuzhigaotc@126.com

Zhigao Xu served as a researcher at Hubei Tongji Huayue Pharmaceutical Co., Ltd from 2000 to 2004. Zhigao joined Wuhan Institute of Technology as lecturer in 2010 where he became an Associate Professor.

Xu has been actively engaged in separation science and technology for nearly ten years, undertaking several national research projects including 'Changjiang scholars and innovative team development', 'The early stage of the 973 research projects', and the 'Twelfth five year' national science and technology support plans. Zhigao has published 33 academic papers (12 catalogued by SCI and EI), and applied for 10 national invention patents (2 have been authorized. He received second prize at the Hubei Province Scientific and Technological Award Conference (2012).

Xu earned his Bachelors (2000) and Masters (2007) Chemical Engineering and Technology degrees from Wuhan Institute of Technology, and PhD in Nonferrous Metallurgy (2010) from General Research Institute for Nonferrous Metals.

Zhenghe Xu P.Eng, PhD, FCAE, FCIM
Teck Professor
University of Alberta
CANADA
zhenghe.xu@ualberta.ca

Zhenghe Xu's main research interest is interfacial sciences as applied to natural resources processing and utilization. He is Canada Research Chair in Mineral Processing and NSERC-Industry Research Chair in Oil Sands Engineering. Zhenghe has published more than 270 peer-reviewed scientific journal papers and 56 technical conference proceeding papers along with three US patents, one Canadian patent, two books and nine book chapters. He was elected to Canadian Academy of Engineering in 2008 and CIM fellow in 10.

Zhenghe earned his Minerals Engineering degrees (BSc and MSc) from Central South Institute of Mining and Metallurgy (Changsha, China) and Materials Science and Engineering degree from Virginia Polytechnic Institute and State University (Blacksburg, USA).

Bian Xue. Doctor,
Northeastern University,
CHINA
bianx@smm.neu.edu.cn

Poster Session

Dr. Bian Xue has been actively engaged in rare earth metallurgy for five years. Bian currently serves as a lecturer in the Nonferrous Metallurgy Institute, School of Materials and Metallurgy, Northeastern University. In recent years, he has published more than ten papers. Four research projects on rare earth minerals treatment are supported by National Foundation.

COM 2013
CONFERENCE OF METALLURGISTS
MET SOC
Hosted by MS&T13
October 27-31, 2013 | Montreal, Canada

Speakers Directory

Volha Yahorava, PhD
Chief Scientist
Mintek
SOUTH AFRICA
olgay@mintek.co.za

Volha (Olga) Yahorava is a Chief Scientist at Mintek and currently is leading rare earths (REE) development programme in Hydrometallurgy Division at Mintek which includes leaching, chemical upgrading, purification, and separation aspects.

Olga started at Mintek as a Post-doc fellow in 2007 and has been involved in a number of commercial and research projects dealing with base and precious metals, uranium and for the last 4 years – rare earths. Her main area of expertise is an ion exchange technology including traditional granular resins and fibrous ion exchangers.

Olga earned her BS Chem. Degree (chemist, chemist ecologist) from Belarusian State University and her PhD Chem. from The National Academy of Sciences of Belarus.

Invited Speaker

Janice Zinck
Research Manager
CANMET Mining - Natural Resources Canada
CANADA
janice.zinck@NRCan-RNCan.gc.ca

Janice Zinck is Manager of Natural Resources Canada’s Mine Waste Management and Processing Research Program; a key component of Canada’s Green Mining Initiative.

Janice has over twenty years of experience in environmental management and processing specifically in the areas of effluent treatment, sludge management, impurity control, and mine waste management. She has had conducted numerous research projects and has been involved in many national and international collaborations involving industry, other governments and universities. Currently her key research areas include critical and strategic metals, northern mineral resource development, water and waste management.

Janice holds several board positions in national organizations including, Secretary of the Canadian Mineral Processors, and Chair of CIM’s Environmental and Social Responsibility Society and is the Past Chair of MetSoc’s Environmental Section. Janice has degrees in Geology, Chemistry and Metallurgical Engineering.